

**The Coordination and Organometallic  
Chemistry of Bis( $\beta$ -diketonato)  
Ruthenium(II/III)**

A Thesis Submitted for the Degree of Doctor of Philosophy at the  
Australian National University



By

Matthew John Byrnes

Research School of Chemistry

Australian National University

Canberra

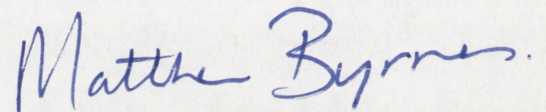
AUSTRALIA

July 2000



## DECLARATION

The work presented in this thesis is the original work of the candidate, except where due reference is made in the text.

A handwritten signature in blue ink that reads "Matthew Byrnes." The signature is written in a cursive style with a period at the end.

Matthew John Byrnes



## *Acknowledgements*

During the course of this thesis there are a great number of people I wish to thank during my time in Canberra. First of all, I would like to thank Professor Martin Bennett for accepting me as a PhD scholar and for the numerous discussions and ideas with regard to this project. I would also especially like to thank him for his patience in reading several drafts of this thesis. I would also like to thank Dr. Graham Heath for his helpful discussions with the electrochemical aspects of this project.

People I have to thank for proof reading this thesis at various stages include Lee Welling and Professor Alan Williams (University of Geneva). During the course of the research work there are the people I have associated with in the laboratories of the Bennett and Heath Groups which include (and not in any particular order) Lee Welling, Dr Eric Wenger, Horst Neumann, Joanne Smith, Dr Mike Kopp, Dr Rhodri Thomas, Dr Maria Contel-Fernandez, Matt Richmond, Richard Baldwin, Dr Chris Copley, Anja Heinemann, Stefan Lee, Nicholas Perkins, Dr Richard Webster, Dr Vincent Otieno-Alego and other past members of these groups. Other people within the RSC I would like to thank include Paul Gugger and other members of the Wild Group; Dr Nicola Brasch and her group; the staff of the UNMRC facility including Tin Cuhane, Peta Simmonds and Chris Blake; the X-ray facility staff of Dr Tony Willis, Dr Alison Edwards and Dr David Hockless for solving all of the structures presented in this thesis; and the ANU mass spectrometry service.

During my study here in Canberra I have taken up playing Rugby Union with the University's Rugby Club (formerly known as ANU Rugby) and wish to thank the many players and coaching staff there during the past several seasons. I have particularly enjoyed playing First Grade Monaro rugby and the associated "out of town" bus trips. In particular I would like to thank Peter "Branches" Bradley, Greg and Helen Corliss, Shayne Wilde,



Dom Bilby, Rob Krauss, Al Sands, Ben Stevens, Chris Jones, Scott Ellis, Dave "Mystery" Roberts, Rick Kimberely, John Lane, Tom McGorman, Steve White, Menasa Lesuma, Langi Eteuati, Dave Barratt, Gary Howell, Paul "Molly" Medwin and Des Amosa as well as many other players whose names escape me at this point.

I would also like to thank my godparents Phil and Donna Stuart, and their family for the hospitality over the years in particular in the last six months. Eric and Caroline Wenger also deserve thanks for letting me stay the last weeks of writing of this thesis. My former housemates Robert, Alison and Karen should also deserve thanks for putting up with me over the years, not always an easy thing at times. A special thanks is also due to my parents Tom and Judy Byrnes, my brother Nigel and my grandmother "Nan". There are also many aunts, uncles and cousins I also wish to thank collectively.

Last, but by no means least, I would like to thank my fiancée, Julie McMullen, whom I have known for over four years and has enriched my life enormously. Thank you Julie.



### Abstract

The ruthenium complex  $cis$ -[Ru(acac)<sub>2</sub>(η<sup>2</sup>-C<sub>2</sub>H<sub>4</sub>)<sub>2</sub>] has been isolated as an orange, slightly air-sensitive solid from the reduction of [Ru(acac)<sub>3</sub>] with freshly activated zinc dust in aqueous THF under an ethene atmosphere (*ca.* 3 bar) and has been characterized by elemental analysis, NMR spectroscopy and X-ray diffraction. In the solid state, the two C=C vectors of the ethene ligands are mutually orthogonal to each other and eclipse the Ru-O(acac) bonds. The ethene carbon atoms only show one resonance in the <sup>13</sup>C{<sup>1</sup>H} NMR spectrum at all accessible temperatures. Exchange between free and coordinated ethene could only be detected in the <sup>1</sup>H NMR spectrum at temperatures greater than *ca.* 80 °C, and probably occurs by a dissociative mechanism.

The complex  $cis$ -[Ru(acac)<sub>2</sub>(η<sup>2</sup>-C<sub>2</sub>H<sub>4</sub>)<sub>2</sub>] is a useful synthetic precursor. Reaction with ligands (L) to give  $cis$ -[Ru(acac)<sub>2</sub>(η<sup>2</sup>-C<sub>2</sub>H<sub>4</sub>)L] (L = NH<sub>3</sub>, C<sub>5</sub>H<sub>5</sub>N, MeCN, PPr<sup>*i*</sup><sub>3</sub>, PCy<sub>3</sub>, SbPh<sub>3</sub>) is also described; the complexes having L = NH<sub>3</sub>, C<sub>5</sub>H<sub>5</sub>N, PPr<sup>*i*</sup><sub>3</sub> and PCy<sub>3</sub> have been structurally characterized. In the case of the N-donors NH<sub>3</sub> and C<sub>5</sub>H<sub>5</sub>N, intermediate *trans*-isomers can be isolated or detected, which suggests that a *cis*- to *trans*-geometric rearrangement about the ruthenium metal centre occurs during the replacement of the first alkene via the square pyramidal five-coordinate species [Ru(acac)<sub>2</sub>(η<sup>2</sup>-C<sub>2</sub>H<sub>4</sub>)]. There is <sup>31</sup>P{<sup>1</sup>H} NMR spectroscopic evidence for a species which is either five-coordinate, [Ru(acac)<sub>2</sub>(PCy<sub>3</sub>)], or six-coordinate with weakly coordinated solvent, [Ru(acac)<sub>2</sub>(PCy<sub>3</sub>)(THF)]. The remaining ethene ligand is readily displaced from  $cis$ -[Ru(acac)<sub>2</sub>(η<sup>2</sup>-C<sub>2</sub>H<sub>4</sub>)L] (L = PPr<sup>*i*</sup><sub>3</sub>, PCy<sub>3</sub>) by CO to form *trans*-[Ru(acac)<sub>2</sub>(CO)L], by tertiary phosphines (PPr<sup>*i*</sup><sub>3</sub>, PCy<sub>3</sub>) to form [Ru(acac)<sub>2</sub>L<sub>2</sub>] and, in the case of the PPr<sup>*i*</sup><sub>3</sub> complex, N<sub>2</sub> to form  $cis$ -[[Ru(acac)<sub>2</sub>(PPr<sup>*i*</sup><sub>3</sub>)]<sub>2</sub>(μ-N<sub>2</sub>)]. The complex *trans*-[Ru(acac)<sub>2</sub>(PPr<sup>*i*</sup><sub>3</sub>)<sub>2</sub>] can be isolated at low temperatures, but isomerizes at room temperature to the *cis*-complex. Terminal alkynes, HC≡CR (R = Ph, SiMe<sub>3</sub>, Bu<sup>*t*</sup>) also replace the



ethene ligand to form vinylidene complexes  $cis$ -[Ru(acac)<sub>2</sub>(=C=C(H)R)L]. Reactions of the complexes  $cis$ - and  $trans$ -[Ru(acac)<sub>2</sub>(PPr<sup>*i*</sup>)<sub>2</sub>] and [Ru(acac)<sub>2</sub>(PCy<sub>3</sub>)<sub>2</sub>] are also described, although there is some ambiguity of the about whether the latter complex has  $cis$ - or  $trans$ -geometry in solution.

Fully reversible E<sub>1/2</sub>(Ru<sup>3+/2+</sup>) potentials for the ethene complexes  $cis$ -[Ru(acac)<sub>2</sub>(η<sup>2</sup>-C<sub>2</sub>H<sub>4</sub>)L] (L = C<sub>2</sub>H<sub>4</sub>, NH<sub>3</sub>, PPr<sup>*i*</sup>, PCy<sub>3</sub>, MeCN, SbPh<sub>3</sub>) and  $trans$ -[Ru(acac)<sub>2</sub>(η<sup>2</sup>-C<sub>2</sub>H<sub>4</sub>)L'] (L' = NH<sub>3</sub>, C<sub>5</sub>H<sub>5</sub>N) lie in the range +0.37 - +0.95 V (*vs* Ag/AgCl) at *ca.* -50 °C. The oxidation potentials of the carbonyl complexes [Ru(acac)<sub>2</sub>(PR<sub>3</sub>)(CO)] (R = Pr<sup>*i*</sup>, Cy) lie between +0.64 - +0.92 V (*vs* Ag/AgCl), whereas irreversible oxidation processes were found between +0.62 and +0.75 V (*vs* Ag/AgCl) for the vinylidene complexes  $cis$ -[Ru(acac)<sub>2</sub>(PR<sub>3</sub>)(=C=C(H)R)] (R = Ph, SiMe<sub>3</sub>) even at low temperatures. Two reversible redox processes were found at +0.30 and +0.90 V (*vs* Ag/AgCl) for  $cis$ -[Ru(acac)<sub>2</sub>(PPr<sup>*i*</sup>)<sub>2</sub>(μ-N<sub>2</sub>)], corresponding to the formation of Ru(II/III) and Ru(III/III) species.

Anodic oxidation of  $cis$ -[Ru(acac)<sub>2</sub>(η<sup>2</sup>-C<sub>2</sub>H<sub>4</sub>)L] (L = C<sub>2</sub>H<sub>4</sub>, NH<sub>3</sub>, SbPh<sub>3</sub>, PCy<sub>3</sub>) and  $trans$ -[Ru(acac)<sub>2</sub>(η<sup>2</sup>-C<sub>2</sub>H<sub>4</sub>)(NH<sub>3</sub>)] at *ca.* -50 °C gives the corresponding Ru(III) complexes  $cis$ -[Ru(acac)<sub>2</sub>(η<sup>2</sup>-C<sub>2</sub>H<sub>4</sub>)L]<sup>+</sup>, which have been characterized by UV-Vis and EPR spectroscopy. There is no evidence that either  $cis$ - or  $trans$ -[Ru(acac)<sub>2</sub>(η<sup>2</sup>-C<sub>2</sub>H<sub>4</sub>)(NH<sub>3</sub>)] undergo geometric isomerization during the oxidation and subsequent reduction under these conditions. Although these oxidized species are unstable at room temperature and cannot be isolated, chemical oxidation of  $trans$ -[Ru(acac)<sub>2</sub>(η<sup>2</sup>-C<sub>2</sub>H<sub>4</sub>)(NH<sub>3</sub>)] and  $cis$ -[Ru(acac)<sub>2</sub>(η<sup>2</sup>-C<sub>8</sub>H<sub>14</sub>)(SbPh<sub>3</sub>)] at *ca.* -70 °C with AgPF<sub>6</sub> affords blue solids which are believed to be the corresponding Ru(III)-alkene complexes. The mixed valence species  $cis$ -[Ru(acac)<sub>2</sub>(PPr<sup>*i*</sup>)<sub>2</sub>(μ-N<sub>2</sub>)]<sup>+</sup> shows a band in the near-IR at *ca.* 8900 cm<sup>-1</sup> which suggests some delocalization of the positive charge across both metal centres.

The reaction of neutral nucleophiles ( $\text{NC}_5\text{H}_5$ ,  $\text{PPh}_3$ ,  $\text{H}_2\text{O}$ ,  $\text{NHEt}_2$ ,  $\text{MeOH}$ ) with the chelate alkyne ruthenium(III) complex  $\text{cis-}[\text{Ru}(\text{acac})_2(o\text{-PhC}_\beta\equiv\text{C}_\alpha\text{C}_6\text{H}_4\text{NMe}_2)][\text{PF}_6]$  gives products derived by nucleophilic addition to the alkyne, which have been identified by X-ray crystallography and, in some cases, by EPR spectroscopy. However, triphenylphosphine reacts with the chelate alkene ruthenium(III) complex  $\text{cis-}[\text{Ru}(\text{acac})_2(o\text{-H}_2\text{C}=\text{C}(\text{H})\text{C}_6\text{H}_4\text{NMe}_2)][\text{PF}_6]$  in a more complicated manner with oxidation of an intermediate to form  $\text{cis-}[\text{Ru}^{\text{III}}(\text{acac})_2(o\text{-Me}_2\text{NC}_6\text{H}_4\text{C}(\text{O})\text{CHPPh}_3)][\text{PF}_6]$  which has been identified by X-ray crystallography.

The reaction of two equivalents of the alkynyldiphenylphosphines,  $\text{Ph}_2\text{PC}\equiv\text{CR}$  ( $\text{R} = \text{H}, \text{Me}, \text{Ph}$ ), with  $\text{cis-}[\text{Ru}(\text{acac})_2(\eta^2\text{-alkene})_2]$  (alkene =  $\text{C}_2\text{H}_4$ ,  $\text{C}_8\text{H}_{14}$ ) yields  $\text{trans-}[\text{Ru}(\text{acac})_2(\text{Ph}_2\text{PC}\equiv\text{CR})_2]$  as orange, air stable solids, which isomerize on heating (except in the case of  $\text{R} = \text{H}$ ) to the corresponding yellow *cis*-isomers. The electrochemical and chemical oxidation of these complexes has also been investigated. Addition of two equivalents of  $\text{Ph}_2\text{PC}\equiv\text{CPh}_2$  to  $\text{cis-}[\text{Ru}(\text{acac})_2(\eta^2\text{-C}_8\text{H}_{14})_2]$  forms an insoluble orange solid, which on heating in refluxing chlorobenzene, yields the yellow binuclear ruthenium(II) complex  $\text{cis-}[\{\text{Ru}(\text{acac})_2(\mu\text{-Ph}_2\text{PC}\equiv\text{CPh}_2)\}_2]$  in which the bridging alkynyl units are twisted in the solid state. There are two  $E_{1/2}(\text{Ru}^{3+/2+})$  potentials at +0.60 and +0.90 V (*vs*  $\text{Ag}/\text{AgCl}$ ) and the mixed-valence species, generated *in situ*, has a localised structure.



### Abbreviations

- acac<sup>-</sup> = 2,4-pentadionate (acetylacetonate) anion  
 (S)-BINAP = (S)-2,2'-bis(diphenylphosphino)1,1'-binaphthyl  
 br = broad  
 Bu<sup>n</sup> = normal butyl  
 Bu<sup>t</sup> = *tert*-butyl  
 COD = 1,5-cyclooctadiene  
 COT = 1,3,5,7-cyclooctatetraene  
 Cy = cyclohexyl  
 C<sub>2</sub>H<sub>4</sub> = ethene  
 C<sub>8</sub>H<sub>14</sub> = *cis*-cyclooctene  
 d = doublet  
 dd = doublet of doublets  
 DEPT = Dimensionless Enhanced Polarization Test  
 DIOP = (+)-2,3-*O*-isopropylidene-2,3-dihydroxy-1,4-bis(diphenylphosphino)butane  
 DMAD = dimethyl acetylenedicarboxylate  
 dppe = 1,2-bis(diphenylphosphino)ethane  
 dppm = 1,2-bis(diphenylphosphino)methane  
 dppp = 1,3-bis(diphenylphosphino)propane  
 dppz = dipyridophenazine  
 E<sub>1/2</sub>M<sup>(n+1)/n</sup> = electrode potential of a M<sup>(n+1)/n</sup> redox couple  
 E<sub>applied</sub> = applied potential  
 E<sub>L</sub>(L) = ligand electrochemical parameter  
 E<sub>Pa</sub> = anodic potential  
 E<sub>Pc</sub> = cathodic potential  
 EPR = electron paramagnetic resonance  
 Et = ethyl  
 FAB = Fast Atom Bombardment  
 HOMO = the highest occupied molecular orbital  
 i<sub>a</sub> = anodic current  
 i<sub>c</sub> = cathodic current  
 IR = infrared  
 J = coupling constant in Hz  
 k = rate constant  
 L = litre  
 LMCT = Ligand to Metal Charge Transfer  
 NHE = Normal Hydrogen Electrode  
 m = multiplet, or medium

M = a metal

$M^{n+1/n}$  = a redox couple

Me = methyl

MLCT = Metal to Ligand Charge Transfer

$M_s$  = a binding site

mol = moles

NBD = norbornadiene (bicyclo-[2,2,1]-hepta-2,5-diene)

NMR = nuclear magnetic resonance

OTTLE = optically transparent thin-layer electrode

*o* = ortho

*p* = para

Ph = phenyl

phen = 1,10-phenanthroline

ppm = parts per million

$Pr^i$  = isopropyl

py = pyridine

pyz = pyrazine

q = quartet

R = alkyl or aryl

RF = radio-frequency field

s = singlet, or strong

SCE = saturated calomel electrode

sh = shoulder

SKEW = (2S, 4S)-bis(diphenylphosphino)pentane

SP = 2-styryldiphenylphosphine

t = triplet

THF = tetrahydrofuran

TMPDA = N,N,N',N'-tetramethylphenylenediamine

TMS = tetramethylsilane

Tos<sup>-</sup> = *p*-toluenesulfonate anion

TPP = dianion of 5,10,15,20-tetraphenylporphyrin

UV = ultraviolet

Vis = visible

$\delta$  = chemical shift in ppm

$\epsilon$  = molar absorptivity in  $L mol^{-1} cm^{-1}$

$\omega_{1/2}$  = dynamic signal linewidth (in Hz)

$(\omega_{1/2})_o$  = signal linewidth (in Hz) in the absence of a dynamic process.



## Table of Contents

Title	i
Declaration	ii
Acknowledgments	iii
Abstract	v
Abbreviations	viii
Table of Contents	x
<b>Chapter 1 Chemistry of the Ru(II) and Ru(III) oxidation states</b>	
1.1 General Introduction	1
1.2 Ammine and Aqua Complexes of Ruthenium(II/III)	5
1.3 Acetylacetonato Complexes of Ruthenium(II/III)	15
1.4 Characterisation of <i>cis</i> - and <i>trans</i> -[Ru(acac) <sub>2</sub> L <sub>2</sub> ] complexes by NMR spectroscopy	26
1.5 Aims of this Study	27
1.6 References	28
<b>Chapter 2 Co-ordination and organometallic chemistry of <i>bis</i>-(β-diketonato)ruthenium(II) complexes</b>	
2.1 Synthesis, characterisation and properties of <i>cis</i> -[Ru(acac) <sub>2</sub> (η <sup>2</sup> -C <sub>2</sub> H <sub>4</sub> ) <sub>2</sub> ]	32
2.2 Reactions of <i>cis</i> -[Ru(acac) <sub>2</sub> (η <sup>2</sup> -C <sub>2</sub> H <sub>4</sub> ) <sub>2</sub> ] with SbPh <sub>3</sub> , CH <sub>3</sub> CN and other nitrogen donor ligands	38
2.3 Reactions of <i>cis</i> -[Ru(acac) <sub>2</sub> (η <sup>2</sup> -alkene) <sub>2</sub> ] (alkene = C <sub>2</sub> H <sub>4</sub> , C <sub>8</sub> H <sub>14</sub> ) with one equivalent of a tertiary phosphine	43
2.4 Solid State Structures of <i>trans</i> -[Ru(acac) <sub>2</sub> (η <sup>2</sup> -C <sub>2</sub> H <sub>4</sub> )(NC <sub>5</sub> H <sub>5</sub> ) and <i>cis</i> -[Ru(acac) <sub>2</sub> (η <sup>2</sup> -C <sub>2</sub> H <sub>4</sub> )L] (L = NH <sub>3</sub> , PPr <sup><i>i</i></sup> <sub>3</sub> , PCy <sub>3</sub> )	50
2.5 Variable temperature NMR spectroscopy of the complexes <i>cis</i> -[Ru(acac) <sub>2</sub> (η <sup>2</sup> -C <sub>2</sub> H <sub>4</sub> )L] (L = C <sub>2</sub> H <sub>4</sub> , SbPh <sub>3</sub> , PPr <sup><i>i</i></sup> <sub>3</sub> and PCy <sub>3</sub> )	57
2.6 Reactions of <i>cis</i> -[Ru(acac) <sub>2</sub> (η <sup>2</sup> -alkene) <sub>2</sub> ] with two equivalents of bulky tertiary phosphines	64
2.7 Reactions of [Ru(acac) <sub>2</sub> L <sub>2</sub> ] complexes with CO	74
2.8 Reactions of [Ru(acac) <sub>2</sub> L <sub>2</sub> ] complexes with alkynes	79
2.9 Reactions of <i>cis</i> -[Ru(acac) <sub>2</sub> (η <sup>2</sup> -C <sub>2</sub> H <sub>4</sub> )L] (L = NH <sub>3</sub> , SbPh <sub>3</sub> , PPr <sup><i>i</i></sup> <sub>3</sub> , PCy <sub>3</sub> ) complexes with tertiary phosphines, CO, alkynes and dinitrogen	83
2.10 Discussion	90
2.11 References	101

**Chapter 3 Co-ordination and organometallic chemistry of  
bis-( $\beta$ -diketonato)ruthenium(III) complexes**

3.1 Voltammetry	107
3.2 Electrolytic Oxidation	114
3.2.1 Spectrochemical Results	114
3.2.2 EPR Spectra	123
3.3 Chemical Oxidation of Monoethene Complexes <i>trans</i> - [Ru(acac) <sub>2</sub> ( $\eta^2$ -C <sub>2</sub> H <sub>4</sub> )(NH <sub>3</sub> )] and <i>cis</i> -[Ru(acac) <sub>2</sub> ( $\eta^2$ -alkene)L] (alkene = C <sub>2</sub> H <sub>4</sub> , L = PCy <sub>3</sub> ; alkene = C <sub>8</sub> H <sub>14</sub> , L = SbPh <sub>3</sub> )	127
3.4 Discussion	132
3.5 References	135

**Chapter 4 Reactivity of alkene and alkyne  
bis-( $\beta$ -diketonato)ruthenium(III) complexes**

4.1 Nucleophilic Addition Reactions	138
4.2 Reaction of <i>cis</i> -[Ru <sup>III</sup> (acac) <sub>2</sub> ( <i>o</i> -PhC $\equiv$ CC <sub>6</sub> H <sub>4</sub> NMe <sub>2</sub> )] [PF <sub>6</sub> ] with pyridine and diethylamine	139
4.3 Reaction of <i>cis</i> -[Ru <sup>III</sup> (acac) <sub>2</sub> ( <i>o</i> -PhC $\equiv$ CC <sub>6</sub> H <sub>4</sub> NMe <sub>2</sub> )] [PF <sub>6</sub> ] with H <sub>2</sub> O	146
4.4 Reactions of <i>cis</i> -[Ru <sup>III</sup> (acac) <sub>2</sub> ( <i>o</i> -PhC $\equiv$ CC <sub>6</sub> H <sub>4</sub> NMe <sub>2</sub> )] [PF <sub>6</sub> ] with PPh <sub>3</sub> and MeOH	149
4.5 Reaction of <i>cis</i> -[Ru(acac) <sub>2</sub> ( <i>o</i> -H <sub>2</sub> C=C(H)C <sub>6</sub> H <sub>4</sub> NMe <sub>2</sub> )] [PF <sub>6</sub> ] with PPh <sub>3</sub>	152
4.6 General Features of Crystal Structures	156
4.7 Discussion	156
4.8 References	164

**Chapter 5 Co-ordination chemistry of alkynyldiphenylphosphine  
bis-( $\beta$ -diketonato)ruthenium(II/III) complexes**

5.1 Reaction of <i>cis</i> -[Ru(acac) <sub>2</sub> ( $\eta^2$ -alkene) <sub>2</sub> ] with two equivalents of an alkynyl tertiary phosphine	168
5.2 Electrochemical Studies	186
5.3 Electronic Spectra	187
5.4 Chemical Oxidation	188
5.5 Discussion	194
5.6 References	196

**Chapter 6 Conclusions** 200

**Chapter 7 Experimental**

7.1 General Procedures	203
7.2.1 Preparation of <i>cis</i> -[Ru(acac) <sub>2</sub> ( $\eta^2$ -C <sub>2</sub> H <sub>4</sub> ) <sub>2</sub> ]	206
7.2.2 Preparation of <i>cis</i> -[Ru(acac) <sub>2</sub> ( $\eta^2$ -C <sub>2</sub> H <sub>4</sub> )(SbPh <sub>3</sub> )]	208
7.2.3 Preparation of <i>cis</i> -[Ru(acac) <sub>2</sub> ( $\eta^2$ -C <sub>2</sub> H <sub>4</sub> )(MeCN)]	209



7.2.4 Preparation of <i>trans</i> -[Ru(acac) <sub>2</sub> (η <sup>2</sup> -C <sub>2</sub> H <sub>4</sub> )(NH <sub>3</sub> )]	209
7.2.5 Preparation of <i>cis</i> -[Ru(acac) <sub>2</sub> (η <sup>2</sup> -C <sub>2</sub> H <sub>4</sub> )(NH <sub>3</sub> )]	210
7.2.6 <sup>31</sup> P{ <sup>1</sup> H} NMR Studies of the reaction of one equivalent of PR <sub>3</sub> (R = Ph, <i>p</i> -tolyl, Pr <sup>i</sup> , Cy and R' = Ph, R'' = Me) with <i>cis</i> -[Ru(acac) <sub>2</sub> (η <sup>2</sup> -alkene) <sub>2</sub> ] (alkene = C <sub>2</sub> H <sub>4</sub> , C <sub>8</sub> H <sub>14</sub> )	211
7.2.7 Preparation of <i>cis</i> -[Ru(acac) <sub>2</sub> (η <sup>2</sup> -C <sub>2</sub> H <sub>4</sub> )(PPr <sup>i</sup> <sub>3</sub> )]	211
7.2.8 Preparation of <i>cis</i> -[Ru(acac) <sub>2</sub> (η <sup>2</sup> -C <sub>2</sub> H <sub>4</sub> )(PCy <sub>3</sub> )]	212
7.2.9 Preparation of <i>trans</i> -[Ru(acac) <sub>2</sub> (PPr <sup>i</sup> <sub>3</sub> ) <sub>2</sub> ]	214
7.2.10 Preparation of [Ru(acac) <sub>2</sub> (PCy <sub>3</sub> ) <sub>2</sub> ] (assumed to be <i>trans</i> )	215
7.2.11 Attempted reaction of <i>cis</i> -[Ru(acac) <sub>2</sub> (η <sup>2</sup> -C <sub>8</sub> H <sub>14</sub> ) <sub>2</sub> ] with 2 equivalents of PBu <sup>t</sup> <sub>3</sub>	215
7.2.12 Preparation of <i>trans</i> -[Ru(acac) <sub>2</sub> (PPr <sup>i</sup> <sub>3</sub> )(CO)]	216
7.2.13 Preparation of <i>trans</i> -[Ru(acac) <sub>2</sub> (PCy <sub>3</sub> )(CO)]	217
7.2.14 Preparation of <i>cis</i> -[Ru(acac) <sub>2</sub> (PPr <sup>i</sup> <sub>3</sub> )(CO)]	218
7.2.15 Preparation of <i>cis</i> -[Ru(acac) <sub>2</sub> (PCy <sub>3</sub> )(CO)]	219
7.2.16 Preparation of <i>cis</i> -[Ru(acac) <sub>2</sub> (PPr <sup>i</sup> <sub>3</sub> )(=C=C(H)Ph)]	219
7.2.17 Preparation of <i>cis</i> -[Ru(acac) <sub>2</sub> (PPr <sup>i</sup> <sub>3</sub> )(=C=C(H)SiMe <sub>3</sub> )]	220
7.2.18 Preparation of <i>cis</i> -[Ru(acac) <sub>2</sub> (PPr <sup>i</sup> <sub>3</sub> )(=C=C(H)Bu <sup>t</sup> )]	221
7.2.19 Attempted reaction of HC≡CCO <sub>2</sub> Me with <i>cis</i> -[Ru(acac) <sub>2</sub> (PPr <sup>i</sup> <sub>3</sub> ) <sub>2</sub> ]	222
7.2.20 Attempted reaction of PhC≡CPh with <i>cis</i> -[Ru(acac) <sub>2</sub> (PPr <sup>i</sup> <sub>3</sub> ) <sub>2</sub> ]	222
7.2.21 Attempted reaction of 3-hexyne with <i>cis</i> -[Ru(acac) <sub>2</sub> (PPr <sup>i</sup> <sub>3</sub> ) <sub>2</sub> ]	222
7.2.22 Attempted reaction of 3-hexyne with <i>cis</i> -[Ru(acac) <sub>2</sub> (η <sup>2</sup> -C <sub>2</sub> H <sub>4</sub> )(PCy <sub>3</sub> )]	222
7.2.23 Attempted reaction of 2-butyne with <i>cis</i> -[Ru(acac) <sub>2</sub> (η <sup>2</sup> -C <sub>2</sub> H <sub>4</sub> )(PPr <sup>i</sup> <sub>3</sub> )]	223
7.2.24 Synthesis of <i>cis</i> -[Ru(acac) <sub>2</sub> (PCy <sub>3</sub> )(SbPh <sub>3</sub> )]	223
7.2.25 Attempted reaction of CO with <i>cis</i> -[Ru(acac) <sub>2</sub> (η <sup>2</sup> -C <sub>2</sub> H <sub>4</sub> )(SbPh <sub>3</sub> )]	224
7.2.26 Attempted reaction of PCy <sub>3</sub> with <i>cis</i> -[Ru(acac) <sub>2</sub> (η <sup>2</sup> -C <sub>2</sub> H <sub>4</sub> )(NH <sub>3</sub> )]	224
7.2.27 Reaction of dinitrogen with <i>cis</i> -[Ru(acac) <sub>2</sub> (η <sup>2</sup> -C <sub>2</sub> H <sub>4</sub> )(PPr <sup>i</sup> <sub>3</sub> )] to give <i>cis</i> -[Ru(acac) <sub>2</sub> (PPr <sup>i</sup> <sub>3</sub> ) <sub>2</sub> (μ-N <sub>2</sub> )]	224
7.2.28 Attempted oxidation of <i>cis</i> -[Ru(acac) <sub>2</sub> (η <sup>2</sup> -C <sub>2</sub> H <sub>4</sub> )(NH <sub>3</sub> )] with [Cp <sub>2</sub> Fe]PF <sub>6</sub>	226
7.2.29 Oxidation of <i>trans</i> -[Ru(acac) <sub>2</sub> (η <sup>2</sup> -C <sub>2</sub> H <sub>4</sub> )(NH <sub>3</sub> )] with AgPF <sub>6</sub>	226
7.2.30 Oxidation of <i>cis</i> -[Ru(acac) <sub>2</sub> (η <sup>2</sup> -C <sub>8</sub> H <sub>14</sub> )(SbPh <sub>3</sub> )] with AgPF <sub>6</sub>	226
7.2.31 Reaction of C <sub>5</sub> H <sub>5</sub> N with <i>cis</i> -[Ru(acac) <sub>2</sub> ( <i>o</i> -PhC≡CC <sub>6</sub> H <sub>4</sub> NMe <sub>2</sub> )] [PF <sub>6</sub> ]	227
7.2.32 Reaction of NEt <sub>2</sub> H with <i>cis</i> -[Ru(acac) <sub>2</sub> ( <i>o</i> -PhC≡CC <sub>6</sub> H <sub>4</sub> NMe <sub>2</sub> )] [PF <sub>6</sub> ]	227
7.2.33 Reaction of H <sub>2</sub> O with <i>cis</i> -[Ru(acac) <sub>2</sub> ( <i>o</i> -PhC≡CC <sub>6</sub> H <sub>4</sub> NMe <sub>2</sub> )] [PF <sub>6</sub> ]	228
7.2.34 Reaction of PPh <sub>3</sub> with <i>cis</i> -[Ru(acac) <sub>2</sub> ( <i>o</i> -PhC≡CC <sub>6</sub> H <sub>4</sub> NMe <sub>2</sub> )] [PF <sub>6</sub> ]	229
7.2.35 Reaction of dry MeOH with <i>cis</i> -[Ru(acac) <sub>2</sub> ( <i>o</i> -PhC≡CC <sub>6</sub> H <sub>4</sub> NMe <sub>2</sub> )] [PF <sub>6</sub> ]	229

7.2.36 Reaction of PPh <sub>3</sub> with	
<i>cis</i> -[Ru(acac) <sub>2</sub> ( <i>o</i> -H <sub>2</sub> C=C(H)C <sub>6</sub> H <sub>4</sub> NMe <sub>2</sub> )] [PF <sub>6</sub> ]	230
7.2.36 Preparation of <i>trans</i> -[Ru(acac) <sub>2</sub> (Ph <sub>2</sub> PC≡CH) <sub>2</sub> ]	230
7.2.38 Preparation of <i>trans</i> -[Ru(acac) <sub>2</sub> (Ph <sub>2</sub> PC≡CMe) <sub>2</sub> ]	231
7.2.39 Preparation of <i>trans</i> -[Ru(acac) <sub>2</sub> (Ph <sub>2</sub> PC≡CPh) <sub>2</sub> ]	232
7.2.40 Preparation of <i>trans</i> -[Ru(acac) <sub>2</sub> (Ph <sub>2</sub> PC≡CPh <sub>2</sub> ) <sub>n</sub> ]	233
7.2.41 Preparation of <i>cis</i> -[Ru(acac) <sub>2</sub> (Ph <sub>2</sub> PC≡CMe) <sub>2</sub> ]	233
7.2.42 Preparation of <i>cis</i> -[Ru(acac) <sub>2</sub> (Ph <sub>2</sub> PC≡CPh) <sub>2</sub> ]	234
7.2.43 Preparation of <i>cis</i> -[Ru(acac) <sub>2</sub> (Ph <sub>2</sub> PC≡CPh <sub>2</sub> ) <sub>2</sub> ]	235
7.2.44 Preparation of <i>trans</i> -[Ru(acac) <sub>2</sub> (Ph <sub>2</sub> PC≡CH) <sub>2</sub> ] [PF <sub>6</sub> ]	236
7.2.45 Preparation of <i>trans</i> -[Ru(acac) <sub>2</sub> (Ph <sub>2</sub> PC≡CMe) <sub>2</sub> ] [PF <sub>6</sub> ]	236
7.3 References	238
<b>Appendices</b>	
A.1 Structural parameters of <i>cis</i> -[Ru(acac) <sub>2</sub> (η <sup>2</sup> -C <sub>2</sub> H <sub>4</sub> ) <sub>2</sub> ]	239
A.2 Structural parameters of <i>trans</i> -[Ru(acac) <sub>2</sub> (η <sup>2</sup> -C <sub>2</sub> H <sub>4</sub> )(NC <sub>5</sub> H <sub>5</sub> )]	242
A.3 Structural parameters of <i>cis</i> -[Ru(acac) <sub>2</sub> (η <sup>2</sup> -C <sub>2</sub> H <sub>4</sub> )(NH <sub>3</sub> )]	245
A.4 Structural parameters of <i>cis</i> -[Ru(acac) <sub>2</sub> (η <sup>2</sup> -C <sub>2</sub> H <sub>4</sub> )(PPr <sup>i</sup> <sub>3</sub> )]	248
A.5 Structural parameters of <i>cis</i> -[Ru(acac) <sub>2</sub> (η <sup>2</sup> -C <sub>2</sub> H <sub>4</sub> )(PCy <sub>3</sub> )]	253
A.6 Structural parameters of <i>trans</i> -[Ru(acac) <sub>2</sub> (PCy <sub>3</sub> ) <sub>3</sub> ]	256
A.7 Structural parameters of <i>cis</i> -[Ru(acac) <sub>2</sub> (PPr <sup>i</sup> <sub>3</sub> ) <sub>2</sub> ]	259
A.8 Structural parameters of <i>cis</i> -[Ru(acac) <sub>2</sub> (PCy <sub>3</sub> )(SbPh <sub>3</sub> )]	262
A.9 Structural parameters of <i>cis</i> -[Ru(acac) <sub>2</sub> (SbPh <sub>3</sub> ) <sub>2</sub> ]	266
A.10 Structural parameters of <i>cis</i> -[Ru(acac) <sub>2</sub> (PPr <sup>i</sup> <sub>3</sub> ) <sub>2</sub> (μ-N <sub>2</sub> )]	270
A.11 Structural parameters of	
(E)- <i>cis</i> -[Ru <sup>III</sup> (acac) <sub>2</sub> ( <i>o</i> -Me <sub>2</sub> NC <sub>6</sub> H <sub>4</sub> C=C(NC <sub>5</sub> H <sub>5</sub> )Ph)] [PF <sub>6</sub> ]	273
A.12 Structural parameters of	
<i>cis</i> -[Ru <sup>III</sup> (acac) <sub>2</sub> ( <i>o</i> -Me <sub>2</sub> NC <sub>6</sub> H <sub>4</sub> C(H)C(=NET <sub>2</sub> )Ph)] [PF <sub>6</sub> ]	277
A.13 Structural parameters of	
<i>cis</i> -[Ru <sup>III</sup> (acac) <sub>2</sub> ( <i>o</i> -Me <sub>2</sub> NC <sub>6</sub> H <sub>4</sub> C(O)CH <sub>2</sub> Ph)] [PF <sub>6</sub> ]	281
A.14 Structural parameters of	
<i>cis</i> -[Ru <sup>III</sup> (acac) <sub>2</sub> ( <i>o</i> -Me <sub>2</sub> NC <sub>6</sub> H <sub>4</sub> C(O)CHPh <sub>3</sub> )] [PF <sub>6</sub> ]	285
A.15 Structural parameters of <i>trans</i> -[Ru(acac) <sub>2</sub> (Ph <sub>2</sub> PC≡CMe)].2CH <sub>2</sub> Cl <sub>2</sub>	289
A.16 Structural parameters of <i>cis</i> -[Ru(acac) <sub>2</sub> (Ph <sub>2</sub> PC≡CMe)].0.5CH <sub>2</sub> Cl <sub>2</sub>	291
A.17 Structural parameters of	
<i>trans</i> -[Ru(acac) <sub>2</sub> (Ph <sub>2</sub> PC≡CMe)] [PF <sub>6</sub> ].2CH <sub>2</sub> Cl <sub>2</sub>	297

*Chemistry of the Ru(II) and Ru(III)  
oxidation states*

*Chemistry of the Ru(II) and Ru(III) oxidation states.**1.1 General Introduction*

As a background to the work described in this thesis on acetylacetonato complexes of ruthenium, the relative affinity of Ru(II) and Ru(III) for unsaturated ligands will be discussed where the co-ligands are saturated and as a consequence will not compete for  $\pi$  back-donation of electrons. Although particular emphasis will be placed on the properties of the complexes  $[\text{Ru}(\text{NH}_3)_5\text{L}]^{2+/3+}$  and  $[\text{Ru}(\text{H}_2\text{O})_{6-x}\text{L}_x]^{2+/3+}$ , where L is an unsaturated ligand, the synthesis of these complexes will not be discussed. The second half of this chapter will deal with the synthesis and properties of  $[\text{Ru}(\text{acac})_2\text{L}_2]$  complexes, where L may be a saturated or unsaturated ligand. The chapter will conclude with the presentation of the aims of this thesis.

Although ruthenium displays almost the full range of oxidation states from -2 to +8, it is the oxidation states Ru(II) and Ru(III) that have received most attention. Both oxidation states display extensive chemistry with a range of ligands, including halide ions and oxygen, nitrogen, phosphorus and sulfur donors; ruthenium complexes containing N- donor ligands form perhaps the most numerous and important area for these two oxidation states.<sup>1-3</sup> Many ruthenium(II) and (III) complexes exist as configurationally stable, octahedral mononuclear species which differ only by one unit of charge. They are often interconvertible by a fully reversible one-electron process and electrochemical studies have been undertaken to probe the relative stabilities of the two oxidation states. The greater the positive potential, the more the Ru(II) oxidation state is stabilised relative to Ru(III).

The Ru(II) ion, unlike the Ru(III) ion, displays an unusual affinity for unsaturated ligands including N-heterocycles, alkenes and alkynes.<sup>4</sup> Perhaps the most striking example of the affinity for unsaturated ligands is



$[\text{Ru}(\text{NH}_3)_5(\text{N}_2)]^{2+}$ , which was the first dinitrogen complex to be isolated.<sup>5</sup> Since 1965, numerous synthetic routes have been devised for the formation of transition metal dinitrogen complexes and these have been extensively reviewed.<sup>6-9</sup> The poor affinity of the Ru(III) ion for  $\text{N}_2$  is shown by the fact that dinitrogen is liberated quantitatively when  $[\text{Ru}(\text{NH}_3)_5(\text{N}_2)]^{2+}$  is oxidised with Ce(IV), presumably via the unstable Ru(III) species.<sup>10</sup>

The unusual affinity of Ru(II) among the familiar dipositive ions for unsaturated ligands has been attributed to two factors. The first is the large radial extension of the  $d\pi$  orbitals from the metal to ligands in the first coordination sphere.<sup>11</sup> This allows for strong flow of electron density from the metal to the unoccupied  $\pi^*$  orbital of an unsaturated ligand. As the radial extension of the d electrons tends to decrease as the atomic number increases for a series of constant charge and it also tends to increase with period number,<sup>12</sup> no first row transition metal divalent ion would be expected to have a greater radial extension of the d electrons than Ru(II). Second, the electronic structure of the low-spin Ru(II) ( $t_{2g}^6$ ) ion has no  $d\sigma$  antibonding electrons, hence the metal to ligand separation will be smaller than for a high spin ion. The electrons of the Ru(II) will be more delocalised and available for back-donation.<sup>11</sup> Compared to the first transition series, ruthenium(II) is the only dipositive ion that has the full complement of  $d\pi$  electrons and no antibonding  $d\sigma$  electrons.<sup>11</sup>

On the basis of chemical behaviour, it has been concluded that the capacity of the  $d\pi$  electrons to participate in back-bonding is reduced when the oxidation number is increased from Ru(II) to Ru(III).<sup>11</sup> This loss of back-bonding ability has been interpreted as a contraction of the radial extension of the d-orbitals. A further contributing factor may be the loss of stabilisation energy by the removal of one electron from the full  $t_{2g}$  subshell of the parent Ru(II) ion.

Lever has used the change in the  $E_{1/2}(\text{Ru}^{3+/2+})$  couple as a function of ligand to generate the ligand parameterization parameters  $E_L$  for over 200 ligands.<sup>13</sup> The  $E_L$  parameter was defined as one-sixth of the  $E_{1/2}(\text{Ru}^{3+/2+})$  value *versus* NHE for the homoleptic complexes  $\text{RuL}_6$  (or  $\text{Ru}(\text{L-L})_3$  in the case of bidentate ligands). Assuming that the ligand parameters are additive, the redox potential of an octahedral metal complex  $\text{MX}_x\text{Y}_y\text{Z}_z$  may be calculated for any combination of the ligands using the equation:

$$E^\circ = S_M[\sum E_L(\text{L})] + I_M + C_{\text{ref}} \quad (\sum E_L(\text{L}) = xE_L(\text{X}) + yE_L(\text{Y}) + zE_L(\text{Z}))$$

where the parameters  $S_M$  and  $I_M$  depend upon both the metal and redox couple, as well as the spin state and stereochemistry. The term  $C_{\text{ref}}$  is a reference electrode correction factor (*ie.* difference between the reference electrode used and the NHE).

The validity of this approach to ruthenium complexes has been clearly demonstrated from the graph of the observed potentials against the calculated potentials for 103 mixed-ligand ruthenium complexes that are not part of the basis set used to derive the  $E_L$  parameters.<sup>13</sup> The observed potentials (measured in organic solvents *vs* NHE) of the redox couple  $\text{Ru}^{3+/2+}$  of various complexes were found to be related to the calculated values by the following expression<sup>13</sup>:

$$E_{1/2}(\text{Ru}^{3+/2+}) \text{ in Volts} = 0.97[\sum E_L(\text{L})] + 0.04 \quad \text{Eq. 1.1}$$

A similar relationship in water between the observed potentials of the redox couple  $\text{Ru}^{3+/2+}$  and the calculated values was found with the following expression<sup>13</sup>:

$$E_{1/2}(\text{Ru}^{3+/2+}) \text{ in Volts} = 1.14[\sum E_L(\text{L})] - 0.35 \quad \text{Eq. 1.2}$$

The predicted difference between potentials of the same complex in different media,  $\Delta E_{1/2}(\text{solvent})$ , *versus* a common reference electrode may be given by the following equation:

$$\Delta E_{1/2}(\text{solvent}) \text{ in Volts} = -0.17[\Sigma E_L(L)] + 0.39$$

As the term  $\Sigma E_L(L)$  varies by as much as two volts for different complexes, there will be a small but measurable difference between solvent potentials,  $\Delta E_{1/2}(\text{solvent})$ , according to the character of the ligands coordinated to the ruthenium centre.

Applying Lever's theory of ligand additivity, within reasonable limits, it is possible to predict the formal electrode potentials of the redox couple  $\text{Ru}^{3+/2+}$  for a wide range of hexacoordinated complexes as a simple summation of the contributions of the individual ligands. The utility<sup>14-16</sup> and limitations<sup>17</sup> of Lever's additivity have been recently examined. The effect of neutral and anionic ligands on the  $\text{Ru}^{3+/2+}$  couple for a series of homoleptic complexes is shown in Table 1.1.

**Table 1.1:** Comparison of measured and expected  $E_{1/2}(\text{Ru}^{3+/2+})$  values (in volts) of some homoleptic complexes  $\text{RuL}_6$  (or  $\text{Ru}(\text{L-L})_3$  in the case of bidentate ligands) in water and organic solvents.

Compound	$\Sigma E_L(L)$	$E_{1/2}(\text{Ru}^{3+/2+})$ vs NHE in $\text{H}_2\text{O}$		$E_{1/2}(\text{Ru}^{3+/2+})$ vs Ag/AgCl in organic solvent <sup>b</sup>	
		calculated <sup>a</sup>	observed	calculated <sup>c</sup>	observed
$[\text{Ru}(\text{NH}_3)_6]^{2+}$	+0.42	+0.13	+0.05 <sup>d</sup>	+0.25	-
$[\text{Ru}(\text{H}_2\text{O})_6]^{2+}$	+0.24	-0.08	+0.20 <sup>e</sup>	+0.07	-
$[\text{Ru}(\text{acac})_3]$	-0.48	-0.90	-	-0.63	-0.65 <sup>f</sup>
$[\text{RuCl}_6]^{3-}$	-1.36	-1.90	-	-1.55	-1.51 <sup>g</sup>

a) calculated by Eq. 1.1; b) calculated values are 0.2 V less positive than those vs NHE; c) calculated by Eq. 1.2; d) ref. 18 e) ref. 19; f) ref. 20; g) ref. 16

Examination of Table 1.1 indicates that the anionic ligands  $\text{acac}^-$  and  $\text{Cl}^-$  stabilise the  $\text{Ru}(\text{III})$  oxidation state relative to  $\text{Ru}(\text{II})$  more readily than the neutral ligands ammonia and water. The calculated effect of replacing two aqua or ammonia ligands around the  $\text{Ru}^{2+}$  ion by one bidentate  $\text{acac}^-$  anion is to reduce the oxidation potential by *ca.* 0.3 V. Therefore complexes

of the type  $[\text{Ru}(\text{acac})_2\text{L}_a\text{L}_b]$  would be expected to be more readily oxidised than the complexes  $[\text{Ru}(\text{NH}_3)_4\text{L}_a\text{L}_b]^{2+}$  or  $[\text{Ru}(\text{H}_2\text{O})_4\text{L}_a\text{L}_b]^{2+}$ .

### 1.2 Ammine and Aqua Complexes of Ruthenium(II/III)

This section deals with the properties and stability of ammine and aqua complexes of ruthenium(II/III) with unsaturated ligands. The dinitrogen complex  $[\text{Ru}(\text{NH}_3)_5(\text{N}_2)]^{2+}$ , obtained from  $[\text{Ru}(\text{NH}_3)_5(\text{H}_2\text{O})]^{2+}$  and dinitrogen, has been shown to react further with  $[\text{Ru}(\text{NH}_3)_5(\text{H}_2\text{O})]^{2+}$  to give the binuclear complex  $[\{\text{Ru}(\text{NH}_3)_5\}_2(\mu\text{-N}_2)]^{2+}$ .<sup>21,22</sup> The coordinated water molecule of  $[\text{Ru}(\text{NH}_3)_5(\text{H}_2\text{O})]^{2+}$  can also be replaced by aromatic nitrogen heterocycles,<sup>23</sup> nitriles<sup>24</sup>,  $\text{H}_2\text{S}$  and  $\text{R}_2\text{S}$ ,<sup>25</sup>  $\text{R}_2\text{Se}$ ,  $\text{R}_2\text{Te}$ ,  $\text{SnCl}_3^-$ ,<sup>4</sup>  $\text{SO}_2$ <sup>26</sup> and  $[\text{S}(\text{CH}_3)_3]^+$ .<sup>27</sup> In non-aqueous solvents,  $[\text{Ru}(\text{NH}_3)_5(\text{H}_2\text{O})]^{2+}$  will react with tertiary phosphines and phosphites to form the complexes *trans*- $[\text{Ru}(\text{NH}_3)_4(\text{PR}_3)_2]^{2+}$  and *trans*- $[\text{Ru}(\text{NH}_3)_4(\text{P}(\text{OR})_3)_2]^{2+}$ .<sup>28,29</sup>

The coordinated water molecule of  $[\text{Ru}(\text{NH}_3)_5(\text{H}_2\text{O})]^{2+}$  has been shown to be several orders of magnitude more labile towards substitution than the coordinated ammonia (see Table 1.2) and the replacement of ammonia ligands by other donors requires considerable effort. For this reason, the  $[\text{Ru}(\text{NH}_3)_5(\text{H}_2\text{O})]^{2+}$  complex is not a general starting material for the synthesis of complexes with the stoichiometry  $[\text{Ru}(\text{NH}_3)_x\text{L}_{6-x}]^{2+}$  ( $x < 5$ ).

**Table 1.2:** Substitution labilities of Ru-NH<sub>3</sub> and Ru-H<sub>2</sub>O at 25 °C expressed as rate constants ( $k$ , s<sup>-1</sup>) for the pseudo-first-order substitution process ( taken from ref. 30).

REACTION	Ru(II) (n = 2)	Ru(III) (n = 3)
$[\text{Ru}(\text{NH}_3)_6]^{n+} + \text{H}_2\text{O}$	$1.5 \times 10^{-6}$	$1.4 \times 10^{-10}$
$[\text{Ru}(\text{NH}_3)_5(\text{H}_2\text{O})]^{n+} + \text{H}_2\text{O}$	3	$5 \times 10^{-4}$
$[\text{Ru}(\text{H}_2\text{O})_6]^{n+} + \text{H}_2\text{O}$	$5 \times 10^{-2}$	$4 \times 10^{-6}$

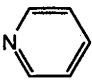
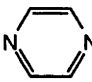
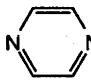
The reaction of  $[\text{Ru}(\text{H}_2\text{O})_6]^{2+}$  with various unsaturated ligands results in the formation of the aquaruthenium complexes  $[\text{Ru}(\text{H}_2\text{O})_x\text{L}_{6-x}]^{2+}$ , where



$x = 5$  ( $\text{N}_2$ ,<sup>31</sup>  $\text{H}_2$ ,<sup>32</sup>  $\text{CO}$ <sup>33</sup>) and  $x = 0, 2, 4$  (nitrogen heterocyclic ligands).<sup>34</sup> The stoichiometry of the isolated product depends upon the concentration of the incoming ligand.<sup>30</sup>

Semi-quantitative evidence for the strong back-bonding ability of Ru(II) can be seen in the comparison of the affinity of the metal centres  $\{\text{Ru}(\text{NH}_3)_5\}^{2+}$ ,  $\{\text{Ni}(\text{H}_2\text{O})_5\}^{2+}$  and  $\text{H}^+$  for unsaturated N-donor ligands shown in Table 1.3.

**Table 1.3** : Equilibrium quotients governing the substitution of coordinated water in the  $[\text{Ni}(\text{H}_2\text{O})_5(\text{H}_2\text{O})]^{2+}$  and  $[\text{Ru}(\text{NH}_3)_5(\text{H}_2\text{O})]^{2+}$  cations by unsaturated ligands (taken from ref. 4).

CENTRE	LIGAND			
	$\text{H}_2\text{O}$			
$\text{H}^+$	9.2	5.2	0.6	<0
$[\text{Ni}(\text{H}_2\text{O})_5]^{2+}$	2.8	1.8	1.0	-
$[\text{Ru}(\text{NH}_3)_5]^{2+}$	4.5	7.4	>8	>10 *

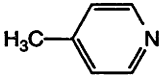
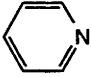
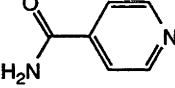
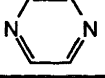
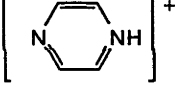
\*) from the change in the acidity of pyrazinium ion when  $\{\text{Ru}(\text{NH}_3)_5\}^{2+}$  is coordinated to it (vide infra), the affinity of pyrazinium ion for Ru(II) is known to be approximately  $10^2$  times that of pyrazine.

The trend in equilibrium quotients for  $\text{Ni}^{2+}_{(\text{aq})}$ , considered to be a representative of a divalent ion of the first transition series, is similar to those of  $\text{H}^+$ . Due to the lower ionic potential of  $\text{Ni}^{2+}_{(\text{aq})}$ , the magnitude of the equilibrium quotients changes much less markedly as the  $\sigma$ -basicity of the ligands decreases. In striking contrast, the affinity of Ru(II) for the ligands increases as the base strength decreases. In the series as selected, this is ascribed to the  $\pi$ -acidity increasing as the  $\sigma$ -base strength decreases.<sup>4</sup>

Further evidence for  $\pi$ -back-bonding in  $[\text{Ru}^{\text{II}}(\text{NH}_3)_5\text{L}]^{2+}$  is the presence of absorption bands attributed to the charge transfer or excitation of electrons from the  $d\pi$  metal orbitals to unoccupied  $\pi^*$  orbitals of the ligand

L. For N-heterocyclic ligands that are good  $\pi$ -acids, the bands occur in the visible region and have high extinction coefficients of the order  $10^4 \text{ M}^{-1} \text{ cm}^{-1}$ .<sup>23</sup> Absorption bands of similar intensity have also been observed for  $[\text{Ru}(\text{H}_2\text{O})_x\text{L}_{6-x}]^{2+}$  complexes with L being a  $\pi$ -acceptor ligand.<sup>30</sup> The wavelengths of absorption maxima for a series of complexes  $[\text{Ru}^{\text{II}}(\text{NH}_3)_5\text{L}]^{n+}$  ( $n = 2, 3$ ) are tabulated in Table 1.4.

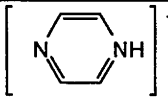
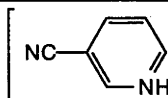
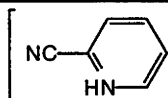
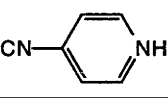
**Table 1.4:** Band maxima of metal-ligand charge transfer absorption of  $[\text{Ru}^{\text{II}}(\text{NH}_3)_5\text{L}]^{n+}$  ( $n = 2, 3$ ) complexes (taken from ref. 23).

LIGAND L	$\lambda$ (nm)
	398
	407
	479
	472
	529

As the electron-withdrawing power of the unsaturated ligand is increased, the  $d\pi-\pi^*$  absorption for the Ru(II) complexes moves to lower energies. This is to be expected if the ground state orbital is mainly metal centred, and the excited state is mainly ligand in character.

A further consequence of the coordination of bifunctional unsaturated N-heterocyclic ligands to Ru(II) or Ru(III) is the systematic change in their acid-base properties. This is illustrated in Table 1.5, which shows the affinity of bifunctional N-heterocycles for the hydrogen ion as free molecules and the same affinity after coordination of these molecules to Ru(II) and Ru(III).<sup>11</sup>

**Table 1.5:** Effect of Ru(II) and Ru(III) on the basicity of coordinated N-heterocycles in  $[\text{Ru}^{\text{II}}(\text{NH}_3)_5]^{n+}$  and  $[\text{Ru}^{\text{III}}(\text{NH}_3)_5]^{(n+1)+}$  complexes (taken from ref. 11).

ACID	pK <sub>a</sub>	ACID	pK <sub>a</sub>
	0.6		1.36
$[\text{Ru}^{\text{III}}(\text{NH}_3)_5\text{N} \begin{array}{c} \diagup \\ \text{pyrazine} \\ \diagdown \end{array}]^{4+}$	~ -0.8	$[\text{Ru}^{\text{II}}(\text{NH}_3)_5\text{NC} \begin{array}{c} \diagup \\ \text{4-cyanopyridine} \\ \diagdown \end{array}]^{3+}$	$1.75 \pm 0.05$
$[\text{Ru}^{\text{II}}(\text{NH}_3)_5\text{N} \begin{array}{c} \diagup \\ \text{pyrazine} \\ \diagdown \end{array}]^{3+}$	$2.5 \pm 0.1$		-0.26
$[\text{Ru}^{\text{II}}(\text{NH}_3)_5\text{N} \begin{array}{c} \diagup \\ \text{pyrazine} \\ \diagdown \end{array}]^{3+}$	7.3 *	$[\text{Ru}^{\text{II}}(\text{NH}_3)_5\text{NC} \begin{array}{c} \diagup \\ \text{2-cyanopyridine} \\ \diagdown \end{array}]^{3+}$	$0.80 \pm 0.10$
	1.90		
$[\text{Ru}^{\text{II}}(\text{NH}_3)_5\text{NC} \begin{array}{c} \diagup \\ \text{4-cyanopyridine} \\ \diagdown \end{array}]^{3+}$	$2.72 \pm 0.12$		

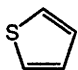
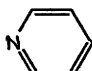
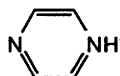
\* electronically excited by the  $d\pi \rightarrow \pi^*$  transition

The molecule pyrazine is much less basic than is pyridine (pK<sub>a</sub> for pyH<sup>+</sup> is 5.2). It seems reasonable that when the cationic species  $\{\text{Ru}(\text{NH}_3)_5\}^{3+}$  is attached to the free nitrogen of pyrazinium cation, the basicity of the uncoordinated nitrogen decreases, as is observed (more positive pK<sub>a</sub>), owing to the inductive effect of the "cationic metal site". By the same argument,  $\{\text{Ru}(\text{NH}_3)_5\}^{2+}$  would also be expected to increase the acidity of the heterocyclic cation, though not as much as  $\{\text{Ru}(\text{NH}_3)_5\}^{3+}$ . The measurements reveal, however, that the basicity of pyrazine is actually increased upon coordination to the dipositive ion.<sup>23</sup> The presumption is that electron density on the remote nitrogen atom is increased when  $\{\text{Ru}(\text{NH}_3)_5\}^{2+}$  coordinates to one end of pyrazine. The proposed mechanism by which electron density can be increased on the ligand is the donation of  $d\pi$  electrons by the electron-rich Ru(II) centre. The extent of this donation

must be great enough to more than compensate for the inductive effect exerted by Ru(II) on the nitrogen lone pair.

The chemical consequences of the diminished  $\pi$ -back-bonding of Ru(III) relative to Ru(II) have been mentioned previously (see p.1-2). The equilibrium quotients governing complex formation of Ru(III) compounds for a range of unsaturated ligands are lower than those of Ru(II) complexes. The ligands  $\text{NH}_3$  or  $\text{OH}^-$  show a preference for the Ru(III) ion (see Table 1.6).

**Table 1.6:** Comparisons of the equilibrium quotients governing complex formation with  $[\text{Ru}(\text{NH}_3)_5(\text{H}_2\text{O})]^{2+}$  and  $[\text{Ru}(\text{NH}_3)_5(\text{H}_2\text{O})]^{3+}$  in aqueous solution (taken from ref. 4).

Ligand	Ru(II)	Ru(III)	Ratio {Ru(II)/Ru(III)}
$\text{N}_2$	$3 \times 10^4$	$<4 \times 10^{-13}$	$> 10^{17}$
$\text{H}_2\text{S}$	$\sim 10$	$\sim 3 \times 10^{-8}$	$\sim 3 \times 10^8$
	$1.5 \times 10^3$	$\sim 2 \times 10^{-4}$	$\sim 8 \times 10^6$
	$2 \times 10^7$	$6 \times 10^3$	$3 \times 10^3$
	$3 \times 10^6$	$2 \times 10^6$	1.5
$\text{NH}_3$	$4 \times 10^4$	$2 \times 10^5$	$2 \times 10^{-1}$
$\text{OH}^-$	$6 \times 10^2$	$6 \times 10^{11}$	$10^{-9}$

The affinities of the ligands for Ru(III) follow the known or expected  $\sigma$ -base strengths of the ligands. With Ru(II) having a rather weak affinity for simple  $\sigma$ -bases such as  $\text{OH}^-$  and  $\text{NH}_3$ , but a relatively high affinity (compared with Ru(III)) for weak  $\sigma$ -bases such as  $\text{N}_2$  or thiophene if the  $\pi$ -acid strength is great enough, the ratios of the quotients governing complex formation for the two oxidation states cover a very wide range - from  $10^{-9}$  to  $10^{17}$  for the ligands shown.<sup>4</sup>

The average bond lengths, shown in Table 1.7, of Ru(II) and Ru(III) species  $[\text{Ru}(\text{NH}_3)_5(\text{pyrazine})]^{n+}$  ( $n = 2, 3$ )<sup>35</sup> and *cis*- $[\text{Ru}(\text{NH}_3)_4(\text{isonicotinamide})_2]^{n+}$  ( $n = 2, 3$ )<sup>36</sup> provide direct structural evidence for the reduced  $\pi$ -back-bonding ability of Ru(III) species with respect to Ru(II). The shorter Ru-NH<sub>3</sub> distances of both Ru(III) species follow the expected trend of an increase in metal charge. Due to the high affinity of  $\{\text{Ru}(\text{NH}_3)_n\}^{2+}$  for  $\pi$ -acceptor ligands, the Ru(II)-N(L) distances {N(L) is the nitrogen donor atom of the unsaturated ligand L} are shorter than the Ru(III)-N(L) distances as shown by the comparison bond lengths of  $[\text{Ru}(\text{NH}_3)_5(\text{pyz})]^{3+/2+}$  and *cis*- $[\text{Ru}(\text{NH}_3)_4(\text{isonicotinamide})]^{3+/2+}$ .

**Table 1.7:** Average metal-ligand distances (Å) of the species  $[\text{Ru}(\text{NH}_3)_5(\text{pyz})]^{n+}$  ( $n = 2, 3$ ; taken from ref. 35) and *cis*- $[\text{Ru}(\text{NH}_3)_4(\text{isonicotinamide})_2]^{n+}$  ( $n = 2, 3$ ; taken from ref. 36).

COMPLEX	Ru-NH <sub>3</sub> (trans)	Ru-NH <sub>3</sub> (cis)	Ru-N(L)*
$[\text{Ru}^{\text{II}}(\text{NH}_3)_5 \text{N} \begin{array}{c} \diagup \\ \diagdown \end{array} \text{N}]^{2+}$	2.166 (7)	2.153 (6)	2.006 (6)
$[\text{Ru}^{\text{III}}(\text{NH}_3)_5 \text{N} \begin{array}{c} \diagup \\ \diagdown \end{array} \text{N}]^{3+}$	2.125 (8)	2.106 (6)	2.076 (8)
<i>cis</i> - $[\text{Ru}^{\text{II}}(\text{NH}_3)_4 \left( \text{N} \begin{array}{c} \diagup \\ \diagdown \end{array} \text{C} \begin{array}{c} \text{O} \\ \parallel \\ \text{NH}_2 \end{array} \right)_2]^{2+}$	2.167 (6)	2.143 (6)	2.058 (14)
<i>cis</i> - $[\text{Ru}^{\text{III}}(\text{NH}_3)_4 \left( \text{N} \begin{array}{c} \diagup \\ \diagdown \end{array} \text{C} \begin{array}{c} \text{O} \\ \parallel \\ \text{NH}_2 \end{array} \right)_2]^{3+}$	2.133 (11)	2.118 (5)	2.099 (6)

\* N(L) is the nitrogen donor atom of the  $\pi$ -acid ligand L.

Various alkenes react with  $[\text{Ru}(\text{NH}_3)_5(\text{H}_2\text{O})]^{2+}$  to form the  $\pi$ -complexes  $[\text{Ru}(\text{NH}_3)_5(\text{L})]^{2+}$  (L = C<sub>2</sub>H<sub>4</sub>,<sup>37</sup> isobutene,<sup>37</sup> 1,4-cyclohexadiene,<sup>37</sup>



fumaric acid,<sup>37</sup> isobutylene,<sup>38</sup> propene,<sup>38</sup> 1,3-butadiene,<sup>38</sup> 1,4-pentadiene,<sup>38</sup> 1,4-hexadiene<sup>38</sup> and styrene<sup>39</sup>). Alkynes have also been shown to react with  $[\text{Ru}(\text{NH}_3)_5(\text{H}_2\text{O})]^{2+}$  to form the  $\pi$ -complexes  $[\text{Ru}(\text{NH}_3)_5(\text{L})]^{2+}$  ( $\text{L} = \text{C}_2\text{H}_2$ ,<sup>37</sup> phenylacetylene,<sup>37</sup> 3-hexyne<sup>37,40</sup> and dimethyl acetylenedicarboxylate {DMA D}<sup>41</sup>). Linear dienes react with the complex *cis*- $[\text{Ru}(\text{NH}_3)_4(\text{acetone})_2](\text{PF}_6)_2$  to form the  $\pi$ -complexes *cis*- $[\text{Ru}(\text{NH}_3)_4(\eta^4\text{-diene})](\text{PF}_6)_2$  (diene = 1,3-butadiene, 1,4-pentadiene and 1,5-hexadiene) complexes in which the coordinated diene displays an unusual *trans*-conformation.<sup>42</sup>

The reaction of ethene (60 bar) with  $[\text{Ru}(\text{H}_2\text{O})_6][\text{OTs}]_2$  results in the sequential formation of  $[\text{Ru}(\text{H}_2\text{O})_5(\text{C}_2\text{H}_4)]^{2+}$  and *cis*- $[\text{Ru}(\text{H}_2\text{O})_4(\text{C}_2\text{H}_4)_2]^{2+}$ . Both cations were characterised by <sup>1</sup>H, <sup>13</sup>C and <sup>17</sup>O NMR spectroscopy and isolated as their tosylate salts. After prolonged reaction, an organic phase formed which was shown to be a mixture of the isomeric butenes.<sup>43</sup> Various cyclic and acyclic functionalised alkenes also form complexes of the type  $[\text{Ru}(\text{H}_2\text{O})_5(\text{alkene})]^{2+}$  (alkene = 2,5-dihydrofuran<sup>19</sup> and 5,6-bis(methoxymethyl)-7-oxanorbornene<sup>44</sup>). Bidentate alkenes were also shown to form chelate complexes  $[\text{Ru}(\text{H}_2\text{O})_4(\text{LL}')][\text{OTs}]_2$  ( $\text{LL}' =$  diallyl ether, 3-buten-1-ol, 3-pentenoic acid). The 3-pentenoic acid mono-alkene complex,  $[\text{Ru}(\text{H}_2\text{O})_5(\text{CH}_2=\text{CHCH}_2\text{CH}_2\text{COOH})]^{2+}$  reacts slowly with excess alkene to form the bis(alkene) complex  $[\text{Ru}(\text{H}_2\text{O})_2(\text{C}_5\text{H}_7\text{O}_2)_2]^{2+}$ .<sup>19</sup>

The diene complex  $[\text{Ru}(\text{H}_2\text{O})_4(\text{COD})][\text{OTs}]_2$  (COD = 1,5-cyclooctadiene) was prepared from the reaction of  $[\text{Ru}(\text{H}_2\text{O})_6][\text{OTs}]_2$  in ethanol with excess COD.<sup>45</sup> Exchange reactions of  $[\text{Ru}(\text{H}_2\text{O})_4(\text{COD})][\text{OTs}]_2$  resulted in the exchange of one to four aqua ligands, depending upon the ligand. All the aqua ligands could be replaced by acetylacetonate anions to form the known complex  $[\text{Ru}(\text{acac})_2(\text{COD})]$ ,<sup>46</sup> whereas under a CO atmosphere (2 bar), only one aqua ligand is replaced to form the complex  $[\text{Ru}(\text{H}_2\text{O})_3(\text{COD})(\text{CO})]$ .<sup>45</sup>

Since the  $d\pi$ -orbitals of Ru(II) that participate in  $\pi$ -back-bonding are directly involved in the redox change Ru(II)  $\{t^6_{2g}\} \rightarrow$  Ru(III)  $\{t^5_{2g}\}$ , the redox potentials of Ru(II) complexes may be used to probe the extent of  $\pi$ -back-bonding present in the complex. Since  $\pi$ -back-bonding tends to stabilise the occupied  $\pi$ -orbitals (HOMO) and reduce interelectron repulsion in the metal ion, the stronger the back-bonding, the more the Ru(II) oxidation state is stabilised relative to Ru(III).

The data for the  $[\text{Ru}(\text{NH}_3)_5\text{L}]^{2+}$  series (see Table 1.8) show that charged ligands occupy the ends of the range of potentials  $E_{1/2}(\text{Ru}^{3+/2+})$  (with the exception of fumaric acid). The most negative oxidation potentials are found for complexes containing anionic ligands, such as chloride ion, which are strong  $\sigma$ - and  $\pi$ -donors and weak  $\pi$ -acceptors. The most positive oxidation potentials are found for ligands which have weak  $\pi$ -donor and strong  $\pi$ -acceptor ability, such as dinitrogen,  $[\text{SMe}_3]^+$  and fumaric acid (+1.12, +1.25 and +1.40 V respectively). The neutral non- $\pi$ -bonding ligands  $\text{NH}_3$  (+0.051 V) and  $\text{H}_2\text{O}$  (+0.066 V) occupy positions close to chloride ion. The oxidation potential of  $[\text{Ru}(\text{NH}_3)_6]^{2+}$  is less than that of  $[\text{Ru}(\text{NH}_3)_5(\text{H}_2\text{O})]^{2+}$ <sup>18</sup> as  $\text{NH}_3$  has a greater ligand field strength than  $\text{H}_2\text{O}$  and therefore stabilises Ru(III) better.<sup>47</sup>

**Table 1.8:** The oxidation potentials  $\{E_{1/2}Ru^{3+/2+}\}/V$  vs NHE, in Volts) of the complexes  $[Ru(NH_3)_5L]^{2+}$  and  $[Ru(H_2O)_xL_{6-x}]^{2+}$  measured in aqueous solution.

$[Ru(NH_3)_5L]^{2+}$			$[Ru(H_2O)_xL_{6-x}]^{2+}$			
Ligand	$E_{1/2}$	Ref.	Ligand	x	$E_{1/2}$	Ref.
Cl <sup>-</sup>	-0.042	18	H <sub>2</sub> O	5	+0.20	19
NH <sub>3</sub>	+0.051	18	allyl ethyl ether	5	+0.38	19
H <sub>2</sub> O	+0.066	18	pyridine ( <i>trans</i> -)	4	+0.42	34
pyridine	+0.305	18	pyrazine ( <i>trans</i> -)	4	+0.44	34
acetylene	+0.665	37	MeCN	5	+0.46	48
3-hexyne	+0.78	37	3-buten-1-ol <sup>a</sup>	4	+0.62	19
propylene	+0.83	38	Me <sub>2</sub> SO	5	+0.81	48
ethylene	+0.93	37	2,5-dihydrofuran	5	+0.83	19
1,4-pentadiene	+0.93	38	ethylene	5	+0.84	48
phenylacetylene	+0.95	37	N <sub>2</sub>	5	+0.92 <sup>b</sup>	48
styrene	+0.98	39	methyl acrylate	5	+0.94	19
DMAD <sup>c</sup>	+1.00	41	CO	5	+1.10	48
N <sub>2</sub>	+1.12 <sup>b</sup>	49	7-oxanorbornene	5	+1.33	19
[SMe <sub>3</sub> ] <sup>+</sup>	+1.25	27	diallyl ether <sup>a</sup>	4	>+1.5	19
fumaric acid <sup>d</sup>	+1.40	37	1,5-hexadiene	4	>+1.5	19

a) bidentate ligand; b) chemically irreversible process; c) DMAD = dimethylacetylenedicarboxylate; d) measured in MeCN

Further examination of Table 1.8 reveals the following important trends for a particular class of Ru(II) compounds: 1) the increase in  $E_{1/2}$  values reflects the increase in  $\pi$ -acidity in the order N-heterocycles < alkynes < alkenes < N<sub>2</sub> < CO; 2) the replacement of an alkene by an alkyne on a

particular binding site should stabilise the Ru(III) oxidation state by *ca.* 200 - 300 mV; 3) the introduction of electron-withdrawing groups on the alkene or alkyne carbon atoms stabilises the Ru(II) oxidation state by *ca.* 300 - 500 mV. This can be seen from the comparison of the oxidation potentials for  $[\text{Ru}(\text{NH}_3)_5(\eta^2\text{-C}_2\text{H}_4)]^{2+}$  (+0.93 V) and  $[\text{Ru}(\text{NH}_3)_5(\eta^2\text{-trans-HOOCCH=CHCOOH})]^{2+}$  (+1.4 V) as well as  $[\text{Ru}(\text{NH}_3)_5(\eta^2\text{-C}_2\text{H}_2)]^{2+}$  (+0.665 V) and  $[\text{Ru}(\text{NH}_3)_5(\eta^2\text{-DMAD})]^{2+}$  (+1.0 V).

Complexes of Ru(II) which contain strong  $\pi$ -acceptor ligands having large positive potentials yield only transitory ruthenium(III) species on oxidation which either decompose or rearrange to more stable Ru(III) complexes by ligand substitution. For example, dinitrogen is quantitatively released upon the chemical oxidation of  $[\text{Ru}(\text{NH}_3)_5(\text{N}_2)]\text{Cl}_2$  by Ce(IV).<sup>10</sup> This irreversible oxidation process of  $[\text{Ru}(\text{NH}_3)_5(\text{N}_2)]^{2+}$  was studied electrochemically and there was no evidence for the formation of  $[\text{Ru}(\text{NH}_3)_5(\text{N}_2)]^{3+}$  at scan rates of up to 100  $\text{Vs}^{-1}$ .<sup>49</sup> The forward scan on a graphite electrode gave an anodic peak ( $E_{\text{pa}} +0.81$  V *vs* SCE) whilst the return scan revealed a well displaced cathodic peak ( $E_{\text{pc}} = -0.33$  V) due to the reduction of  $[\text{Ru}^{\text{III}}(\text{NH}_3)_5\text{Cl}]^{2+}$  formed in the initial oxidation process.<sup>49</sup>

A similar observation was made for  $[\text{Ru}(\text{H}_2\text{O})_5(\text{N}_2)]^{2+}$  which showed a chemically irreversible process at  $E_{\text{pa}} = +0.72$  V (*vs* Ag/AgCl in 0.1M HOTf solution) and subsequent formation of  $[\text{Ru}(\text{H}_2\text{O})_6]^{3+}$ .<sup>48</sup> The carbonyl complexes  $[\text{Ru}(\text{H}_2\text{O})_5(\text{CO})]^{2+}$ <sup>48</sup> and *cis*- $[\text{Ru}(\text{acac})_2(\text{CO})_2]^{20}$  also display chemically irreversible behaviour in their cyclic voltammograms, as the strongly  $\pi$ -acidic CO ligands render the complex highly unstable at the Ru(III) level.

Similar substitution processes have been observed for the electrogenerated alkene complexes  $[\text{Ru}(\text{NH}_3)_5\text{L}]^{3+}$ . The cyclic voltammogram of  $[\text{Ru}(\text{NH}_3)_5(\eta^2\text{-1,3-butadiene})]^{2+}$  ( $E_{1/2} = 0.94$  *vs* NHE) in aqueous solution exhibits quasi-reversible behaviour. As the scan rate

decreases, the relative ratio of the peak heights for the cathodic and anodic current,  $i_c/i_a$ , also decreases, presumably because the alkene of the initially formed cation  $[\text{Ru}^{\text{III}}(\text{NH}_3)_5(\text{alkene})]^{3+}$  is replaced by a water molecule.<sup>38</sup> The complexes  $[\text{Ru}(\text{NH}_3)_5(\eta^2\text{-styrene})]^{2+39}$  and  $[\text{Ru}(\text{NH}_3)_5(\eta^2\text{-1,3-dimethyluracil})]^{2+50}$  ( $E_{\text{pa}} = +0.98 \text{ V vs NHE}$ ) show either a quasi-reversible or no reduction peak in their cyclic voltammograms due to similar ligand substitution processes. The wave for the Ru(II) oxidation implies an EC-type process in which electron-abstraction (process E) is followed by a rapid chemical reaction (aquation, process C) that prevents detection of the short-lived Ru(III) alkene complex.<sup>39,50</sup>

### 1.3 Acetylacetonato Complexes of Ruthenium(II/III)

Tris- $[\beta\text{-diketonato}]$  complexes of ruthenium  $[\text{Ru}(\beta\text{-diketonato})_3]$  have been the subject of extensive synthetic and electrochemical studies.<sup>1,2</sup> The complex  $[\text{Ru}(\text{acac})_3]$  has been prepared either by direct action of acetylacetonone on  $\text{RuCl}_3 \cdot 3\text{H}_2\text{O}$  in the presence of a base<sup>51-54</sup> or by treatment of reduced ruthenium(III) chloride (ruthenium blue) with acetylacetonone under basic conditions.<sup>55-59</sup> The relationship between the  $E_{1/2}(\text{Ru}^{3+/2+})$  potentials and the relative electron donating nature of the substituents of the  $\beta\text{-diketonato}$  moiety has been investigated.<sup>60-62</sup>

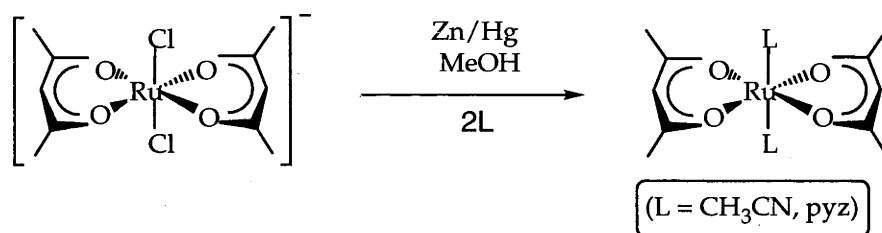
A general route for the synthesis of mononuclear bis- $(\beta\text{-diketonato})$ ruthenium(II) complexes was discovered by Kobayashi and coworkers, who reduced an ethanolic solution of  $[\text{Ru}(\text{acac})_3]$  by heating with zinc amalgam in the presence of acetonitrile to give the divalent ruthenium complex  $\text{cis-}[\text{Ru}(\text{acac})_2(\text{CH}_3\text{CN})_2]$  in 63% yield.<sup>63</sup> The only previously known bis(acetylacetonato)ruthenium(II) complexes  $\text{cis-}[\text{Ru}(\text{acac})_2\text{L}_2]$  were those with  $2\text{L} = 2\text{CO}$ <sup>64</sup>,  $2\text{PPh}_3$ <sup>65</sup>, COD,<sup>46</sup> phen,<sup>66</sup> dppz<sup>67</sup> and  $2\text{N}(\text{O})=\text{C}(\text{COCH}_3)_2$ .<sup>68</sup> The reported syntheses of these compounds required different precursors. A second synthetic route was also found which involved the direct action of



[Ru(acac)<sub>3</sub>] with acetonitrile in the presence of strong acids which forms *cis*-[Ru<sup>III</sup>(acac)<sub>2</sub>(CH<sub>3</sub>CN)<sub>2</sub>]<sup>+</sup>.<sup>69</sup>

The first reported *trans*-[Ru(acac)<sub>2</sub>L<sub>2</sub>]<sup>n+</sup> complex was *trans*-[Ph<sub>4</sub>As][Ru(acac)<sub>2</sub>Cl<sub>2</sub>], prepared from RuCl<sub>3</sub>·3H<sub>2</sub>O, acetylacetonone and aqueous KCl.<sup>70</sup> After subsequent addition of aqueous Ph<sub>4</sub>AsCl·xH<sub>2</sub>O and work up, the desired product was isolated in 20% yield. Zinc amalgam reduction of *trans*-[Ph<sub>4</sub>As][Ru(acac)<sub>2</sub>Cl<sub>2</sub>] in the presence of CH<sub>3</sub>CN or pyrazine at room temperature results in the formation of *trans*-[Ru(acac)<sub>2</sub>L<sub>2</sub>] (L = CH<sub>3</sub>CN, pyz) in yields *ca.* 80%.<sup>70</sup>

**Scheme 1.2:** Synthesis of *trans*-[Ru(acac)<sub>2</sub>L<sub>2</sub>] from *trans*-[Ph<sub>4</sub>As][Ru(acac)<sub>2</sub>Cl<sub>2</sub>].



The complex *cis*-[Ru(acac)<sub>2</sub>(SbPr<sup>*i*</sup><sub>3</sub>)<sub>2</sub>] has been isolated from the reaction of the  $\pi$ -allyl compound [Ru( $\eta^3$ -C<sub>3</sub>H<sub>5</sub>)<sub>2</sub>(SbPr<sup>*i*</sup><sub>3</sub>)<sub>2</sub>] with acetylacetonone in hot benzene.<sup>71</sup> One of the triisopropylstibine ligands is only weakly coordinated and readily displaced by a variety of ligands to form complexes of the type *cis*-[Ru(acac)<sub>2</sub>(SbPr<sup>*i*</sup><sub>3</sub>)L] (L = C<sub>2</sub>H<sub>4</sub>, PPr<sup>*i*</sup><sub>3</sub>, PCy<sub>3</sub>).<sup>71</sup> The complex *cis*-[Ru(acac)<sub>2</sub>(PPr<sup>*i*</sup><sub>3</sub>)<sub>2</sub>] can be isolated when an excess of PPr<sup>*i*</sup><sub>3</sub> is added to *cis*-[Ru(acac)<sub>2</sub>(SbPr<sup>*i*</sup><sub>3</sub>)<sub>2</sub>].<sup>71</sup>

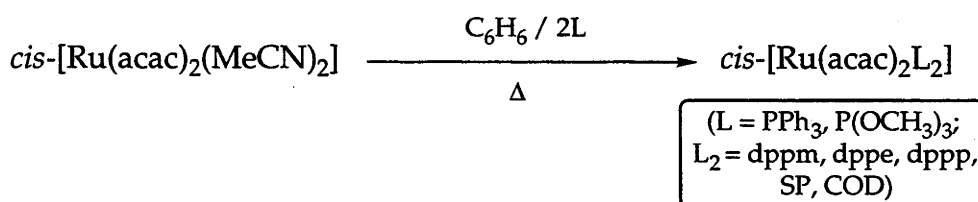
The chiral bidentate phosphine complexes *cis*-[Ru(acac)<sub>2</sub>(LL)] (LL = (S)-BINAP, SKEW and DIOP) were initially prepared by hydrogenation of methanolic solutions of [Ru(acac)<sub>3</sub>] in the presence of the appropriate phosphine.<sup>72</sup> The *cis*-[Ru(acac)<sub>2</sub>((S)-BINAP)] complex is also prepared by the reduction of [Ru(acac)<sub>3</sub>] by activated zinc dust in the presence of (S)-BINAP in hot ethanol in an almost quantitative yield.<sup>73</sup> The structures of *cis*-

[Ru(acac)<sub>2</sub>(LL)] complexes (LL = (S)-BINAP, DIOP) were confirmed by single crystal X-ray diffraction studies.<sup>72,73</sup> Addition of 2-(4-isobutylphenyl)propenoic acid to these chiral bidentate phosphine complexes, followed by hydrogenation, affords (S)-(+)-ibuprofen in various enantiomeric excesses.<sup>72</sup>

Radiolysis has also been used as an alternative to zinc or dihydrogen as a reducing agent for the synthesis of mononuclear [Ru(acac)<sub>2</sub>L<sub>2</sub>] complexes.<sup>74</sup> Alcoholic solutions of [Ru(acac)<sub>3</sub>] saturated with CO (1 bar) were exposed to  $\gamma$  radiation (<sup>60</sup>Co source) for two hours. The *trans*-[Ru(acac)<sub>2</sub>(CO)L] complexes (L = MeOH, EtOH or Pr<sup>i</sup>OH) were isolated as yellow solids in almost quantitative yield. Although a single crystal X-ray diffraction study of *trans*-[Ru(acac)<sub>2</sub>(CO)(MeOH)] confirmed the structure, the observation of numerous  $\nu(\text{CO})$  stretching bands in the IR spectrum<sup>74</sup> suggests that more than one species is present in solution.

The coordinated acetonitrile ligands of *cis*-[Ru(acac)<sub>2</sub>(CH<sub>3</sub>CN)<sub>2</sub>] can be replaced by various ligands in hot benzene to form complexes of the type *cis*-[Ru(acac)<sub>2</sub>L<sub>2</sub>] (L = PPh<sub>3</sub>, P(OMe)<sub>3</sub>; L<sub>2</sub> = dppe, dppe, dppp, SP, 1,5-COD).<sup>20</sup>

**Scheme 1.3:** Synthesis of *cis*-[Ru(acac)<sub>2</sub>L<sub>2</sub>] from *cis*-[Ru(acac)<sub>2</sub>(CH<sub>3</sub>CN)<sub>2</sub>] (from ref. 20).



The coordinated acetonitrile ligands may also be replaced by the ligand 3,3'-dithiobis(2,4-pentanedione) (H<sub>2</sub>dtba) to give either the mononuclear complex *cis*-[Ru(acac)<sub>2</sub>(topd-O,S)] (topd = 3-thioxo-2,4-pentanedione) or the binuclear complex *cis*-[Ru(acac)<sub>2</sub>]<sub>2</sub>(topd-O,S,O')

reaction conditions.<sup>75</sup> The complexes were characterised by a variety of techniques; in both cases there is some ambiguity as to the formal oxidation state of the ruthenium metal centre.

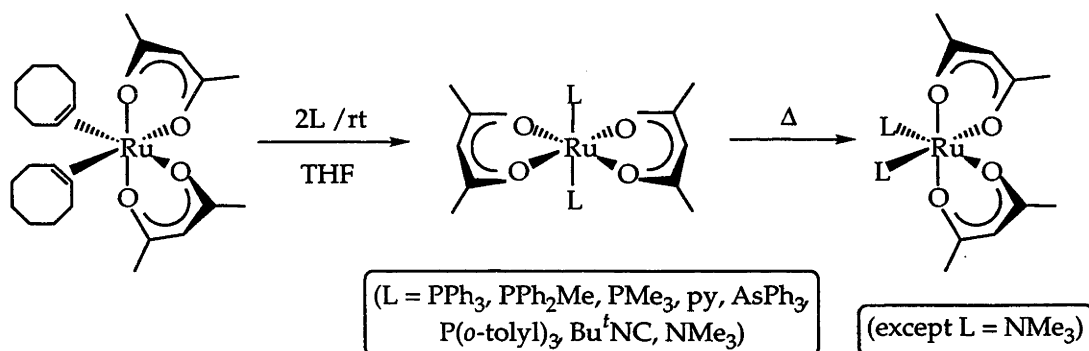
Kobayashi's methodology has been extended to the synthesis of the complexes  $[\text{Ru}(\text{acac})_2(\eta^2:\eta^2\text{-diene})]$  (diene = norbornadiene,<sup>76</sup> 1,5-cyclooctadiene,<sup>77</sup> 1,3,5,7-cyclooctatetraene,<sup>78</sup> 2,4-hexadiene,<sup>79</sup> 2,3-dimethyl-1,3-butadiene,<sup>79</sup> 1,3-cyclohexadiene,<sup>79</sup> 2,4-dimethyl-1,3-pentadiene,<sup>79</sup> 2,5-dimethyl-2,4-hexadiene,<sup>80</sup> isoprene,<sup>80</sup> 1,2,4,5-tetramethyl-1,4-cyclohexadiene<sup>80</sup>). The acyclic 1,3-dienes are coordinated to the ruthenium metal centre in a  $\eta^4$ -*trans*-diene conformation with two diastereomers present in various ratios.<sup>79</sup> The formation of these diastereomers is the result of the binding through the two enantiofaces of the dienes as shown by X-ray crystallographic studies on the complexes  $[\text{Ru}(\text{acac})_2(2,4\text{-dimethyl-1,3-pentadiene})]$  and  $[\text{Ru}(\text{acac})_2(2,5\text{-dimethyl-1,3-hexadiene})]$ .<sup>79,80</sup>

Reduction of an aqueous THF solution of  $[\text{Ru}(\text{acac})_3]$  by heating with zinc amalgam or freshly activated zinc dust in the presence of excess cyclooctene gives the bis(alkene) complex *cis*- $[\text{Ru}(\text{acac})_2(\eta^2\text{-C}_8\text{H}_{14})_2]$ .<sup>76</sup> This bis(alkene) complex is stable in aqueous THF but decomposes in the presence of ethanol to form ruthenium(III)-ethoxide complexes.<sup>77</sup> Although the cyclooctene complex *cis*- $[\text{Ru}(\text{acac})_2(\eta^2\text{-C}_8\text{H}_{14})_2]$  was not isolated as a pure compound, the stereochemical arrangement of the acetylacetonate ligands about the ruthenium centre and the coordination of cyclooctene were confirmed by <sup>1</sup>H NMR spectroscopy.<sup>76</sup>

The coordinated diene ligands of  $[\text{Ru}(\text{acac})_2(\eta^2:\eta^2\text{-diene})]$  (diene = 2,4-hexadiene, 2,3-dimethyl-1,3-butadiene) were reported to be readily displaced by either  $\text{PEt}_3$  or  $\text{P}(\text{OCH}_3)_3$  at room temperature to form a mixture of the complexes *trans*- and *cis*- $[\text{Ru}(\text{acac})_2\text{L}_2]$  (L =  $\text{PEt}_3$  or  $\text{P}(\text{OMe})_3$ ).<sup>79</sup> However, the coordinated cyclooctene ligands of *cis*- $[\text{Ru}(\text{acac})_2(\eta^2\text{-C}_8\text{H}_{14})_2]$  are readily displaced by a wide variety of ligands at room temperature to give red-

brown complexes of the general type *trans*-[Ru(acac)<sub>2</sub>L<sub>2</sub>] (L = NMe<sub>3</sub>, pyridine, *t*-butyl isocyanide, various tertiary phosphines and AsPh<sub>3</sub>).<sup>76</sup> The *cis*-[Ru(acac)<sub>2</sub>L<sub>2</sub>] (except L = NMe<sub>3</sub>) complexes were isolated only after heating the corresponding *trans*-[Ru(acac)<sub>2</sub>L<sub>2</sub>] isomers. The molecular structures of the *trans*- and *cis*-isomers of the complexes [Ru(acac)<sub>2</sub>L<sub>2</sub>] (L = PMe<sub>2</sub>Ph, CNBu<sup>t</sup>) have been confirmed by X-ray crystallography.<sup>76</sup>

**Scheme 1.4:** Replacement of both coordinated alkene ligands of *cis*-[Ru(acac)<sub>2</sub>(η<sup>2</sup>-C<sub>8</sub>H<sub>14</sub>)<sub>2</sub>] by ligands.

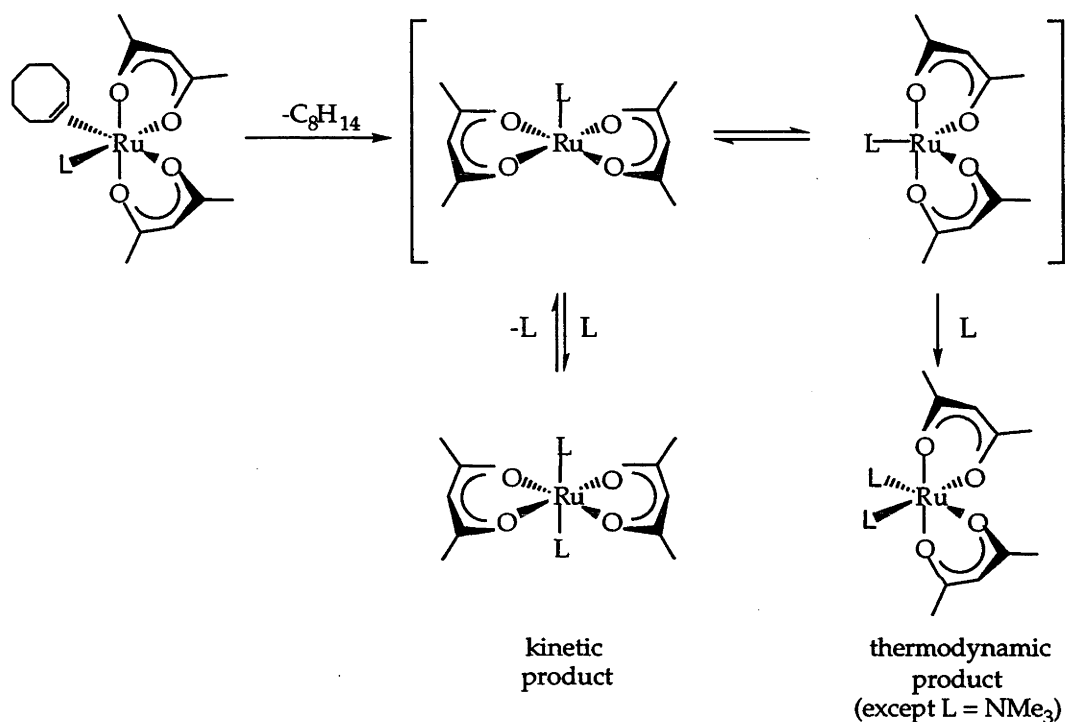


The reaction of *cis*-[Ru(acac)<sub>2</sub>(η<sup>2</sup>-C<sub>8</sub>H<sub>14</sub>)<sub>2</sub>] with acetonitrile or triphenylstibine affords the isolable yellow-brown complexes *cis*-[Ru(acac)<sub>2</sub>(η<sup>2</sup>-C<sub>8</sub>H<sub>14</sub>)L'] (L' = CH<sub>3</sub>CN, SbPh<sub>3</sub>).<sup>76</sup> The formation of the *cis*-[Ru(acac)<sub>2</sub>L<sub>2</sub>] can be achieved by refluxing the mono-substituted complex with excess L'. There is no evidence for the formation of the *trans*-isomers in either substitution step.<sup>76</sup>

The mechanism for the formation of *trans*-[Ru(acac)<sub>2</sub>L<sub>2</sub>] from *cis*-[Ru(acac)<sub>2</sub>(η<sup>2</sup>-C<sub>8</sub>H<sub>14</sub>)<sub>2</sub>] is not known but a suggested pathway involves the stepwise replacement of cyclooctene, probably via a dissociative process; the replacement of the second cyclooctene must occur more rapidly than the first for Group 15 donor ligands.<sup>76</sup> It is assumed that a square pyramidal five coordinate intermediate [Ru(acac)<sub>2</sub>L] is initially generated with preferential attack of the entering ligand L at the vacant site giving the kinetic product *trans*-[Ru(acac)<sub>2</sub>L<sub>2</sub>] (see Scheme 1.5). At higher temperatures, the trigonal

bipyramidal geometry for  $[\text{Ru}(\text{acac})_2\text{L}]$  may become accessible and with reversible dissociation of L from *trans*- $[\text{Ru}(\text{acac})_2\text{L}_2]$  results in the formation of the *cis* isomer.<sup>76</sup> The formation of *cis*- $[\text{Ru}(\text{acac})_2(\eta^2\text{-C}_8\text{H}_{14})\text{L}]$  in the first alkene substitution step is also thought to occur via a similar sequence via an undetected intermediate *trans*- $[\text{Ru}(\text{acac})_2(\eta^2\text{-C}_8\text{H}_{14})\text{L}]$ .

**Scheme 1.5:** Suggested pathway for formation of *trans*- and *cis*- $[\text{Ru}(\text{acac})_2\text{L}_2]$  from *cis*- $[\text{Ru}(\text{acac})_2(\eta^2\text{-C}_8\text{H}_{14})_2\text{L}]$  (taken from ref. 76).



The reaction of *cis*- $[\text{Ru}(\text{acac})_2(\eta^2\text{-C}_8\text{H}_{14})_2]$  with bidentate ditertiary phosphines has also been investigated.<sup>76</sup> The addition of two equivalents of dppm (diphenylphosphinomethane) initially forms *trans*- $[\text{Ru}(\text{acac})_2(\eta^1\text{-dppm})_2]$ . Facile loss of a coordinated dppm ligand results in the formation of *cis*- $[\text{Ru}(\text{acac})_2(\eta^2\text{-dppm})]$ . The chelate dppm complex may also be prepared by the addition of one equivalent of dppm to *cis*- $[\text{Ru}(\text{acac})_2(\eta^2\text{-C}_8\text{H}_{14})_2]$ . Reaction of the bidentate phosphines 1,2-bis(diphenylphosphino)ethane (dppe) or 1,3-bis(diphenylphosphino)propane (dppp) with *cis*- $[\text{Ru}(\text{acac})_2(\eta^2\text{-C}_8\text{H}_{14})_2]$  in a 1:1 molar ratio results in the formation of orange solids believed to be oligomeric  $[\text{Ru}(\text{acac})_2(\text{LL})]_n$  ( $\text{LL} = \text{dppe}, \text{dppp}$ ).<sup>76</sup> Heating of

these orange oligomeric solids affords the more soluble chelate complexes *cis*-[Ru(acac)<sub>2</sub>(LL)].<sup>76</sup>

Carbon monoxide (1 bar) readily reacts with *trans*-[Ru(acac)<sub>2</sub>(PPh<sub>3</sub>)<sub>2</sub>] to form the complex *trans*-[Ru(acac)<sub>2</sub>(PPh<sub>3</sub>)(CO)].<sup>76</sup> There is no observable reaction with *cis*-[Ru(acac)<sub>2</sub>(PPh<sub>3</sub>)<sub>2</sub>] under similar conditions. The *trans*-[Ru(acac)<sub>2</sub>(PPh<sub>3</sub>)(CO)] complex isomerises in refluxing toluene to form the corresponding *cis*-isomer.<sup>76</sup> The triphenylarsine complex *trans*-[Ru(acac)<sub>2</sub>(AsPh<sub>3</sub>)<sub>2</sub>] will also react with CO (4 bar) to give *cis*-[Ru(acac)<sub>2</sub>(AsPh<sub>3</sub>)(CO)], but there is no evidence for the formation of the *trans*-[Ru(acac)<sub>2</sub>(AsPh<sub>3</sub>)(CO)] as an intermediate.<sup>76</sup> The complex *trans*-[Ru(acac)<sub>2</sub>(NMe<sub>3</sub>)<sub>2</sub>] also readily reacts with CO to give *trans*-[Ru(acac)<sub>2</sub>(CO)(NMe<sub>3</sub>)].<sup>76</sup> The addition of PhC≡CH to *cis*-[Ru(acac)<sub>2</sub>(PPr<sup>*i*</sup><sub>3</sub>)<sub>2</sub>] or *cis*-[Ru(acac)<sub>2</sub>(SbPr<sup>*i*</sup><sub>3</sub>)L] (L = C<sub>2</sub>H<sub>4</sub>, SbPr<sup>*i*</sup><sub>3</sub>) in refluxing benzene gives the vinylidene complexes *cis*-[Ru(acac)<sub>2</sub>(PPr<sup>*i*</sup><sub>3</sub>)(=C=C(H)Ph)] and *cis*[Ru(acac)<sub>2</sub>(SbPr<sup>*i*</sup><sub>3</sub>)(=C=C(H)Ph)] respectively.<sup>71</sup> The supposed intermediate, [Ru(acac)<sub>2</sub>(PPr<sup>*i*</sup><sub>3</sub>)(η<sup>2</sup>-PhC≡CH)], could not be detected by NMR spectroscopy.

Hydrogenation of 2-(6'-methoxy-naphth-2'-yl)acrylic acid using an 'aged' sample of *cis*-[Ru(acac)<sub>2</sub>((S)-BINAP)] in methanol reportedly proceeds much faster than that catalysed by [Ru(OAc)<sub>2</sub>((S)-BINAP)].<sup>81</sup> A single crystal X-ray diffraction study of the 'aged' *cis*-[Ru(acac)<sub>2</sub>((S)-BINAP)] reveals that one of the acac ligands has been replaced by the *cis*-coordination of a solvent molecule and monodentate carboxyl coordination of the deprotonated acid.<sup>81</sup>

The oxidation potentials of the *cis*- and *trans*-complexes [Ru(acac)<sub>2</sub>(pyz)<sub>2</sub>] and [Ru(acac)<sub>2</sub>(CH<sub>3</sub>CN)<sub>2</sub>] show that the *trans*-isomer is easier to oxidise than the *cis*-isomer by up to 100 mV.<sup>70</sup> Later electrochemical studies<sup>20,82</sup> of *cis*- and *trans*-[Ru(acac)<sub>2</sub>L<sub>2</sub>] complexes reveal

that the difference between oxidation potentials may be as little as 50 mV and as high as 490 mV (see Table 1.9).

**Table 1.9:** Observed  $E_{1/2}(\text{Ru}^{3+/2+})$  potentials of  $[\text{Ru}(\text{acac})_2(\text{LL}')]$  for which both *cis* and *trans* isomers have been isolated (measured in  $\text{CH}_2\text{Cl}_2$ ).

L	L'	Geometric isomer	$E_{1/2}^\circ$ (vs Ag/AgCl)	$\Delta E_{1/2}^\circ$ (V)
$\text{C}_5\text{H}_5\text{N}$	$\text{C}_5\text{H}_5\text{N}$	<i>cis</i>	+0.01 <sup>a</sup>	0.05
		<i>trans</i>	-0.04 <sup>a</sup>	
MeCN	MeCN	<i>cis</i>	+0.24 <sup>b</sup>	0.12
		<i>trans</i>	+0.12 <sup>a</sup>	
PMe <sub>3</sub>	PMe <sub>3</sub>	<i>cis</i>	+0.26 <sup>a</sup>	0.26
		<i>trans</i>	0.00 <sup>a</sup>	
AsPh <sub>3</sub>	AsPh <sub>3</sub>	<i>cis</i>	+0.34 <sup>a</sup>	0.19
		<i>trans</i>	+0.15 <sup>a</sup>	
PPh <sub>3</sub>	PPh <sub>3</sub>	<i>cis</i>	+0.37 <sup>b</sup>	0.30
		<i>trans</i>	+0.07 <sup>b</sup>	
PMePh <sub>2</sub>	PMePh <sub>2</sub>	<i>cis</i>	+0.37 <sup>a</sup>	0.33
		<i>trans</i>	+0.04 <sup>a</sup>	
P(OMe) <sub>3</sub>	P(OMe) <sub>3</sub>	<i>cis</i>	+0.70 <sup>a</sup>	0.48
		<i>trans</i>	+0.22 <sup>a</sup>	
<sup>t</sup> BuNC	<sup>t</sup> BuNC	<i>cis</i>	+0.74 <sup>b</sup>	0.49
		<i>trans</i>	+0.25 <sup>b</sup>	
CO	PCy <sub>3</sub>	<i>cis</i>	+0.92 <sup>a</sup>	0.28
		<i>trans</i>	+0.64 <sup>a</sup>	
CO	PPh <sub>3</sub>	<i>cis</i>	+1.10 <sup>a</sup>	0.34
		<i>trans</i>	+0.76 <sup>b</sup>	
<i>cis</i> -[Ru(acac) <sub>2</sub> (η <sup>2</sup> -C <sub>8</sub> H <sub>14</sub> )L]				
NH <sub>3</sub>			+0.23 <sup>a</sup>	
SbPh <sub>3</sub>			+0.44 <sup>b</sup>	
MeCN			+0.44 <sup>b</sup>	
C <sub>8</sub> H <sub>14</sub>			+0.77 <sup>b</sup>	

a) ref. 82; b) ref. 20

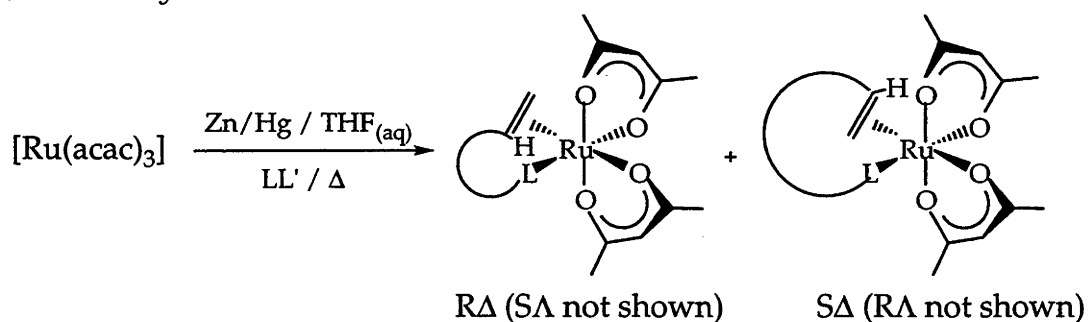
Whereas the  $[\text{Ru}(\text{NH}_3)_5(\eta^2\text{-alkene})]^{2+}$  complexes mentioned previously (see p.19) display either quasi-reversible or irreversible behaviour upon electrooxidation, the complexes *cis*-[Ru(acac)<sub>2</sub>(η<sup>2</sup>-C<sub>8</sub>H<sub>14</sub>)L] (L = NH<sub>3</sub>,<sup>20</sup> SbPh<sub>3</sub>,<sup>20</sup> CH<sub>3</sub>CN,<sup>82</sup> C<sub>8</sub>H<sub>14</sub><sup>20</sup>) display fully reversible behaviour in their cyclic voltammograms, even at room temperature. Under these conditions, where the  $E_{1/2}(\text{Ru}^{3+/2+})$  potentials have been lowered by 0.5 V



or more and a poorly coordinating solvent is present, the alkene in the products  $[\text{Ru}^{\text{III}}(\text{acac})_2(\eta^2\text{-C}_8\text{H}_{14})\text{L}]^+$  is not easily replaced on the electrochemical timescale. However, attempted chemical and electrochemical oxidation of the parent Ru(II) compounds has not led to isolable solid alkene complexes  $[\text{Ru}^{\text{III}}(\text{acac})_2(\eta^2\text{-C}_8\text{H}_{14})\text{L}]^+\text{X}^-$ , probably due to the weakened binding of the alkene to the Ru(III) centre.<sup>77</sup>

Zinc amalgam reduction of  $[\text{Ru}(\text{acac})_3]$  in the presence of the chelating alkene N- and O-donor ligands (LL' = 2-vinyl-N,N-dimethylaniline, 2-isopropenyl-N,N-dimethylaniline, 3-butenyldimethylamine, 2-allylpyridine, isomesityl oxide, 2-methoxystyrene, 3-butenylmethylether)<sup>83</sup> or the chelating acetylenic N-donor ligands *o*-RC≡CC<sub>6</sub>H<sub>4</sub>NMe<sub>2</sub> (R = Ph, SiMe<sub>3</sub>)<sup>84</sup> gives the corresponding  $[\text{Ru}(\text{acac})_2(\text{LL}')]$  complexes as either orange or brown solids. Coordination of the prochiral alkene of the LL' ligand to the chiral *cis*-{Ru(acac)<sub>2</sub>} fragment can give rise to a pair of diastereomers labelled **A** for the RΔ/SΛ pair and **B** for the SΔ/RΛ pair.<sup>83</sup> The molecular structures of both diastereoisomers of  $[\text{Ru}(\text{acac})_2(o\text{-H}_2\text{C}=\text{C}(\text{H})\text{C}_6\text{H}_4\text{NMe}_2)]$  have been determined by X-ray crystallography and the alkene has been shown to be coordinated by opposite enantiotropic faces.<sup>83</sup> The stabilisation gained from the chelate effect for the alkene N-donors was sufficient to prevent displacement of the coordinated alkene by CO, PMe<sub>3</sub> or pyridine.<sup>83</sup>

**Scheme 1.5:** *Synthesis of the chelated alkene complex  $[\text{Ru}(\text{acac})_2(2\text{-vinyl-N,N-dimethylaniline})]$ .*



Most of the chelated olefinic N- and O-donor complexes *cis*- $[\text{Ru}(\text{acac})_2(\text{LL}')]$  display a fully reversible oxidation potential in the range

+0.28 to 0.60 V(*vs* Ag/AgCl) (see Table 1.10). The voltammograms appear as a superposition of two peaks of different intensities arising from the diastereoisomers, the potentials of which differ by as much as 140 mV.<sup>83</sup> In agreement with the observation from Table 1.8 that the replacement of an alkene with an alkyne should lower the Ru(II) oxidation potential, the chelated acetylenic complexes have oxidation potentials 150 - 250 mV less than those of the couples measured for the diastereomeric alkene complexes (R $\Delta$ ,S $\Delta$ )- and (S $\Delta$ ,R $\Delta$ )-[Ru(acac)<sub>2</sub>(*o*-H<sub>2</sub>C=C(H)C<sub>6</sub>H<sub>4</sub>NMe<sub>2</sub>)].<sup>84</sup>

**Table 1.10:** The oxidation potentials {E<sub>1/2</sub>Ru<sup>3+/2+</sup>}/V *vs* Ag/AgCl, in Volts} of the complexes *cis*-[Ru(acac)<sub>2</sub>LL'] measured in CH<sub>2</sub>Cl<sub>2</sub>.

<i>cis</i> -[Ru(acac) <sub>2</sub> L <sub>2</sub> ]		
Ligand	E <sub>1/2</sub> (in Volts)	
acac <sup>-</sup>	-0.65 <sup>a</sup>	
TMEDA*	-0.35 <sup>b</sup>	
2,2'-bipyridine	-0.05 <sup>a</sup>	
2-(trimethylsilyl)ethynyl- -N,N-dimethylaniline	+0.19 <sup>b</sup>	
2-phenylethynyl- -N,N-dimethylaniline	+0.26 <sup>b</sup>	
3-butenyldimethylamine	isomer A	+0.28 <sup>c</sup>
	isomer B	+0.42 <sup>c</sup>
2-vinyl-N,N-dimethylaniline	isomer A	+0.42 <sup>c</sup>
	isomer B	+0.52 <sup>c</sup>
3-butenyl methyl ether	isomer A	+0.43 <sup>c</sup>
	isomer B	+0.53 <sup>c</sup>
3-butenyldiphenylphosphine	isomer A	+0.54 <sup>c</sup>
	isomer B	+0.54 <sup>c</sup>
SP*	+0.67 <sup>a</sup>	

a) ref. 20; b) ref. 83; c) ref. 84; \*) TMEDA = tetramethylethylenediamine; SP = 2-styryldiphenylphosphine

The chelating olefinic and acetylenic N- and O-donor ruthenium cations, [Ru<sup>III</sup>(acac)<sub>2</sub>(LL')]<sup>+</sup> (LL' = 2-vinyl-N,N-dimethylaniline, 2-isopropenyl-N,N-dimethylaniline, 3-butenyldimethylamine, 2-allylpyridine, isomesityl oxide, 2-methoxystyrene, 3-butenylmethylether, *o*-PhC≡CC<sub>6</sub>H<sub>4</sub>NMe<sub>2</sub>, *o*-(Me<sub>3</sub>SiC≡CC<sub>6</sub>H<sub>4</sub>NMe<sub>2</sub>) were isolated as deep blue,

paramagnetic  $\text{PF}_6$  or  $\text{SbF}_6$  salts by the oxidation of the ruthenium(II) precursors with  $\text{Ag}^+$  or  $[\text{FeCp}_2]^+$  salts. They are the first stable alkene and alkyne complexes of ruthenium(III).<sup>83,84</sup> The complexes were fully characterised and shown to be mononuclear by X-ray crystallography with the alkene or alkyne being coordinated to the metal centre.

#### 1.4 Characterisation of *cis* and *trans*- $[\text{Ru}(\text{acac})_2\text{L}_2]$ complexes by NMR spectroscopy

For future reference, certain spectroscopic features of the *cis*- and *trans*- $[\text{Ru}(\text{acac})_2\text{L}_2]$  complexes are noted here. The geometric isomers are readily identified by  $^1\text{H}$  and  $^{13}\text{C}\{^1\text{H}\}$  NMR spectroscopy. The complexes *trans*- $[\text{Ru}(\text{acac})_2\text{LL}']$  (where  $\text{L} = \text{L}'$  and  $\text{L} \neq \text{L}'$ ) display one methyl acac singlet and one methine acac singlet for both nuclei as well as one carbonyl acac resonance in the  $^{13}\text{C}\{^1\text{H}\}$  NMR spectrum. For the complex *cis*- $[\text{Ru}(\text{acac})_2\text{LL}']$  ( $\text{L} = \text{L}'$ ), there are two methyl singlets and one methine acac singlet for both the  $^1\text{H}$  and  $^{13}\text{C}\{^1\text{H}\}$  NMR spectra in addition to two carbonyl acac carbon singlets. The least symmetrical geometric complex, *cis*- $[\text{Ru}(\text{acac})_2\text{LL}']$  ( $\text{L} \neq \text{L}'$ ), shows four methyl acac singlets and two methine acac singlets for both nuclei as well as four carbonyl acac resonance in the  $^{13}\text{C}\{^1\text{H}\}$  NMR spectrum.

The  $^{31}\text{P}\{^1\text{H}\}$  NMR spectral data may also be used to determine the geometric arrangement of two tertiary phosphines as the chemical shift of the complexes *trans*- $[\text{Ru}(\text{acac})_2\text{L}_2]$  are about *ca.* 20 ppm more shielded than those of the corresponding *cis*-isomer.<sup>76</sup> For future reference, the  $^{31}\text{P}\{^1\text{H}\}$  NMR spectral data of the isolated phosphorus containing complexes are tabulated in Table 1.11.

**Table 1.11:**  $^{31}\text{P}\{^1\text{H}\}$  NMR spectral data for the phosphorus containing complexes of the type  $[\text{Ru}(\text{acac})_2\text{L}_2]$  reported in ref. 76.

Complex	$^{31}\text{P}\{^1\text{H}\}$ NMR				
	free	Complex		$\Delta\delta^a$	
		trans	cis	trans	cis
$[\text{Ru}(\text{acac})_2(\text{PMe}_3)_2]$	-62.0	+9.40	+31.7	+71.4	+93.7
$[\text{Ru}(\text{acac})_2(\text{PPhMe}_2)_2]$	-45.9	+17.7	+36.8	+63.6	+82.7
$[\text{Ru}(\text{acac})_2(\text{PMePh}_2)_2]$	-28.1	+24.7	+41.3	+52.8	+69.4
$[\text{Ru}(\text{acac})_2(\text{PEt}_3)_2]$	-19.2	+27.6	+46.3	+46.8	+65.5
$[\text{Ru}(\text{acac})_2(\text{P}(p\text{-tolyl})_3)_2]$	-8.6	+33.6	+52.6	+42.2	+58.8
$[\text{Ru}(\text{acac})_2(\text{PPh}_3)_2]$	-6.2	+33.9	+54.0	+40.1	+60.2
$[\text{Ru}(\text{acac})_2(\text{PPh}_2\text{Bu}^t)_2]^b$	+18.3	+40.3	+58.2	21.8	+39.9

a)  $\Delta\delta = \delta(\text{complex}) - \delta(\text{free})$ ; b) complex not published, ref. 77

### 1.5 Aims of this Study

The main aims of this study include i) the isolation of the ethene analogue of  $\text{cis}-[\text{Ru}(\text{acac})_2(\eta^2\text{-C}_8\text{H}_{14})_2]$ . Although the bis(ethene) complex had been detected in earlier unpublished work of C. Chung and H. Neumann by  $^1\text{H}$  NMR spectroscopy, attempts to isolate it were unsuccessful;<sup>85</sup> ii) an examination of the lability of the coordinated alkene ligands to gain some understanding of the mechanism of the replacement of the first alkene and of the stereochemical re-arrangements of the complexes in the presumably stepwise formation of  $\text{trans}-[\text{Ru}(\text{acac})_2\text{L}_2]$  from  $\text{cis}-[\text{Ru}(\text{acac})_2(\eta^2\text{-alkene})_2]$ ;<sup>76</sup> iii) an investigation of the electrochemical and chemical oxidation properties of these new complexes to see if stable, unchelated paramagnetic Ru(III)-alkene complexes of the type  $[\text{Ru}^{\text{III}}(\text{acac})_2(\eta^2\text{-alkene})\text{L}]\text{X}$  can be detected or isolated; and iv) an examination of the reactivity of the complexes  $[\text{Ru}^{\text{III}}(\text{acac})_2(\eta^2\text{-alkene})\text{L}]\text{X}$ .

## 1.6 References

- (1) Seddon, K. R.; Seddon, E. A. *The Chemistry of Ruthenium*; Elsevier Science: 1984, p 341.
- (2) Schröder, M.; Stephenson, T. A. In *Comprehensive Coordination Chemistry*; Gillard, R. D.; McCleverty, J. A., Eds.; Pergamon: Oxford, 1987; Vol. 4; p 277.
- (3) Cotton, F. A.; Wilkinson, G.; Murillo, C. A.; Bochmann, M. *Advanced Inorganic Chemistry*; 6th ed.; John Wiley and Sons, Inc.: 1999, p 1001.
- (4) Taube, H. *Pure and Appl. Chem.* **1979**, *51*, 901.
- (5) Allen, A. D.; Senoff, C. V. *Chem. Commun.* **1965**, 621.
- (6) Sellman, D. *Angew. Chem. Int. Ed. Engl.* **1974**, *13*, 639.
- (7) Allen, A. D.; Harris, R. O.; Loescher, B. R.; Stevens, J. R.; Whiteley, R. N. *Chem. Rev.* **1973**, *73*, 11.
- (8) Chatt, J.; Dilworth, J. R.; Richards, R. L. *Chem. Rev.* **1978**, *78*, 589.
- (9) Hidai, M.; Mizobe, Y. *Chem. Rev.* **1995**, *95*, 1115.
- (10) Harrison, D. E.; Taube, H. *J. Am. Chem. Soc.* **1967**, *89*, 5706.
- (11) Taube, H. In *Survey of Progress in Chemistry*; Scott, A. F., Ed.; Academic Press: 1973; Vol. 6; p 45.
- (12) Jørgensen, C. K. *Absorption Spectra and Chemical Bonding in Complexes*; Pergamon Press: Oxford: 1962.
- (13) Lever, A. B. P. *Inorg. Chem.* **1990**, *29*, 1271.
- (14) Lyons, L. J.; Pitz, S. L.; Boyd, D. C. *Inorg. Chem.* **1995**, *34*, 316.
- (15) Morris, R. H. *Inorg. Chem.* **1992**, *31*, 1471.
- (16) Duff, C. M.; Heath, G. A. *Inorg. Chem.* **1991**, *30*, 2528.
- (17) Heath, G. A.; Humphrey, D. G. *Chem. Commun.* **1991**, 1668.
- (18) Lim, H. S.; Barclay, D. J.; Anson, F. C. *Inorg. Chem.* **1972**, *11*, 1460.

- (19) McGrath, D. V.; Grubbs, R. H.; Ziller, J. W. *J. Am. Chem. Soc.* **1991**, *113*, 3611.
- (20) Wallace, L. PhD Thesis, ANU, 1991.
- (21) Armor, J. N.; Taube, H. *J. Am. Chem. Soc.* **1970**, *92*, 6170.
- (22) Harrison, D. E.; Weissberger, E.; Taube, H. *Science* **1968**, *159*, 320.
- (23) Ford, P.; Rudd, D. F. P.; Gaunder, R.; Taube, H. *J. Am. Chem. Soc.* **1968**, *90*, 11871194.
- (24) Clarke, R. E.; Ford, P. C. *Inorg. Chem.* **1970**, *1970*, 9.
- (25) Kuehn, C. G.; Taube, H. *J. Am. Chem. Soc.* **1976**, *98*, 689.
- (26) Allen, A. D.; Eliades, T.; Harris, R. O.; Reinsalu, P. *Can. J. Chem.* **1969**, *47*, 1605.
- (27) Stein, C. A.; Taube, H. *J. Am. Chem. Soc.* **1978**, *100*, 336.
- (28) Franco, D. W.; Taube, H. *Inorg. Chem.* **1978**, *17*, 571.
- (29) Franco, D. W. *Inorg. Chim. Acta* **1979**, *32*, 273.
- (30) Bernhard, P.; Lehmann, H.; Ludi, A. *Comments Inorg. Chem.* **1983**, *2*, 145.
- (31) Laurency, G.; Helm, L.; Merbach, A. E. *Inorg. Chim. Acta* **1991**, *189*, 131.
- (32) Aebischer, N.; Frey, U.; Merbach, A. E. *Chem. Commun.* **1998**, 2303.
- (33) Laurency, G.; Helm, L.; Ludi, A.; Merbach, A. E. *Helv. Chim. Acta* **1991**, *74*, 1236.
- (34) Bernhard, P.; Lehmann, H.; Ludi, A. *Chem. Commun.* **1981**, 1216.
- (35) Gress, M. E.; Creutz, C.; Quicksall, C. O. *Inorg. Chem.* **1981**, *20*, 1522.
- (36) Richardson, D. E.; Walker, D. D.; Sutton, J. E.; Hodgson, K. O.; Taube, H. *Inorg. Chem.* **1979**, *18*, 2216.
- (37) Lehmann, H.; Schenk, K. J.; Chapuis, G.; Ludi, A. *J. Am. Chem. Soc.* **1979**, *101*, 6197.
- (38) Elliott, M. G.; Shepherd, R. E. *Inorg. Chem.* **1988**, *27*, 3332.

- (39) Elliot, M. G.; Zhang, S.; Shepherd, R. E. *Inorg. Chem.* **1989**, *28*, 3036.
- (40) Hunziker, M.; Ludi, A. *J. Am. Chem. Soc.* **1977**, *99*, 7368.
- (41) Henderson, W. W.; Bancroft, B. T.; Shepherd, R. E.; Fackler, J. P., Jr. *Organometallics* **1986**, *5*, 506.
- (42) Sugaya, T.; Tomita, A.; Sago, H.; Sano, M. *Inorg. Chem.* **1996**, *35*, 2692.
- (43) Laurency, G.; Merbach, A. E. *Chem. Commun.* **1993**, 187.
- (44) Novak, B. M.; Grubbs, R. H. *J. Am. Chem. Soc.* **1988**, *110*, 7542.
- (45) Kölle, U.; Flunkert, G.; Görissen, R.; Schmidt, M. U.; Englert, U. *Angew. Chem. Int. Ed. Engl.* **1992**, *31*, 440.
- (46) Powell, P. J. *Organomet. Chem.* **1974**, *65*, 89.
- (47) Lever, A. B. P. *Inorganic Electronic Spectroscopy*; Elsevier: Amsterdam, 1968, p. 204.
- (48) Aebischer, N.; Sidorenkova, E.; Ravera, M.; Laurency, G.; Osella, D.; Weber, J.; Merbach, A. E. *Inorg. Chem.* **1997**, *36*, 6009.
- (49) Elson, C. M.; Gulens, J.; Itzkovitch, I. J.; Page, J. A. *Chem. Commun.* **1970**, 875.
- (50) Zhang, S.; Shepherd, R. E. *Inorg. Chim. Acta* **1989**, *163*, 237.
- (51) Barbieri, G. A. *Atti. accad. Lincei* **1914**, *23*, 334.
- (52) Wilkinson, G. *J. Am. Chem. Soc.* **1952**, *74*, 6146.
- (53) Grobelny, R.; Jezowska-Trzebiatowska, B.; Wojchiechowski, W. *J. Inorg. Nucl. Chem.* **1966**, *28*, 2715.
- (54) Gordon, J. G.; O'Connor, M. J.; Holm, R. H. *Inorg. Chim. Acta* **1971**, *5*, 381.
- (55) Endo, A.; Shimizu, K.; Satô, G. P.; Mukaida, M. *Chem. Lett.* **1984**, 437.
- (56) Endo, A.; Kajitani, M.; Mukaida, M.; Shimizu, K.; Satô, G. P. *Inorg. Chim. Acta* **1988**, *150*, 25.
- (57) Hoshino, Y.; Yukawa, Y.; Maruyama, T.; Endo, A.; Shimizu, K.; Satô, G. P. *Inorg. Chim. Acta* **1990**, *174*, 41.



- (58) Togano, T.; Nagao, N.; Tsuchida, M.; Kumakura, H.; Hisamatsu, K.; Howell, F. S.; Mukaida, M. *Inorg. Chim. Acta* **1992**, *195*, 221.
- (59) Knowles, T. S.; Howells, M. E.; Howlin, B. J.; Smith, G. W.; Amodio, C. A. *Polyhedron* **1994**, *13*, 2197.
- (60) Patterson, G. S.; Holm, R. H. *Inorg. Chem.* **1972**, *11*, 2285.
- (61) Takeuchi, Y.; Endo, A.; Shimizu, K.; Satô, G. P. *J. Electroanal. Chem.* **1985**, *185*, 185.
- (62) Endo, A.; Shimizu, K.; Satô, G. P. *Chem. Lett.* **1985**, 581.
- (63) Kobayashi, T.; Nishina, Y.; Shimizu, K.; Satô, G. P. *Chem. Lett.* **1988**, 1137.
- (64) Gilbert, J. D.; Wilkinson, G. J. *Chem. Soc. (A)* **1969**, 1749.
- (65) Queirós, M. A. M.; Robinson, S. D. *Inorg. Chem.* **1978**, *17*, 310.
- (66) Dwyer, F. P.; Goodwin, H. A.; Gyarfás, E. C. *Aust. J. Chem.* **1962**, *16*, 42.
- (67) Nair, R. B.; Yeung, L. K.; Murphy, C. J. *Inorg. Chem.* **1999**, *38*, 2536.
- (68) Mukaida, M.; Nomura, T.; Ishimori, T. *Bull. Chem. Soc. Jpn.* **1975**, *48*, 1443.
- (69) Kasahara, Y.; Hoshino, Y.; Shimizu, K.; Satô, G. P. *Chem. Lett.* **1990**, 381.
- (70) Hasegawa, T.; Lau, T. C.; Taube, H.; Schaefer, W. P. *Inorg. Chem.* **1991**, *30*, 2921.
- (71) Grünwald, G.; Laubender, M.; Wolf, J.; Werner, H. J. *Chem. Soc., Dalton Trans.* **1998**, 833.
- (72) Manimaran, T.; Wu, T.-C.; Klobucar, W. D.; Kolich, C. H.; Stahly, G. P. *Organometallics* **1993**, *12*, 1467.
- (73) Chan, A. S.; Laneman, S. A.; Day, C. X. *Inorg. Chim. Acta* **1995**, *228*, 159.
- (74) Remita, H.; Brik, M. E.; Daran, J. C.; Delcourt, M. O. *J. Organomet. Chem.* **1995**, *486*, 283.

- (75) Hashimoto, T.; Endo, A.; Nagao, N.; Satô, G. P. *Inorg. Chem.* **1998**, *37*, 5211.
- (76) Bennett, M. A.; Chung, G.; Hockless, D. C. R.; Neumann, H.; Willis, A. C. *J. Chem. Soc., Dalton Trans.* **1999**, 3451.
- (77) Bennett, M. A.; Neumann, H. *unpublished results*
- (78) Bennett, M. A.; Neumann, H.; Thomas, M.; Wang, X.; Pertici, P.; Salvadori, P.; Vitulli, G. *Organometallics* **1991**, *10*, 3237.
- (79) Ernst, R. D.; Melendez, E.; Stahl, L.; Ziegler, M. L. *Organometallics* **1991**, *10*, 3635.
- (80) Melendez, E.; Ilarraza, R.; Yap, G. P. A.; Rheingold, A. L. *J. Organomet. Chem.* **1996**, *522*, 1.
- (81) Chen, C.-C.; Huang, T.-T.; Lin, C.-W.; Cao, R.; Chan, A. S. C.; Wong, W. T. *Inorg. Chim. Acta* **1998**, *270*, 247.
- (82) Menglet, D. PhD Thesis, ANU, 1996.
- (83) Bennett, M. A.; Heath, G. A.; Hockless, D. C. R.; Kovacic, I.; Willis, A. *C. J. Am. Chem. Soc.* **1998**, *120*, 932.
- (84) Bennett, M. A.; Heath, G. A.; Hockless, D. C. R.; Kovacic, I.; Willis, A. *C. Organometallics* **1998**, *17*, 5867.
- (85) Bennett, M. A.; Chung, G.; Neumann, H. *unpublished results*,

*Co-ordination and organometallic  
chemistry of  
bis( $\beta$ -diketonato)ruthenium(II)  
complexes*

### 2.1 Synthesis, characterisation and properties of *cis*-[Ru(acac)<sub>2</sub>(η<sup>2</sup>-C<sub>2</sub>H<sub>4</sub>)<sub>2</sub>]

Treatment of [Ru(acac)<sub>3</sub>] in aqueous THF with freshly activated zinc dust under an ethene atmosphere (3 bar) results in an orange solution after heating to *ca.* 80 °C for one hour or less. Removal of THF *in vacuo* gives an orange sticky residue from which the required complex can be readily extracted with benzene or toluene. An orange crystalline solid is obtained after chromatographing a benzene solution and recrystallisation of the crude material from cold *n*-pentane. The solid may be handled for several hours in air with no visible signs of decomposition, but it changes to an uncharacterised violet solid after several weeks exposure to air. Using sodium amalgam (*ca.* 1.5%) under anhydrous conditions as the reducing agent instead of zinc dust leads to the formation of an unidentified brown insoluble material. The orange solid is formulated as *cis*-[Ru(acac)<sub>2</sub>(η<sup>2</sup>-C<sub>2</sub>H<sub>4</sub>)<sub>2</sub>] on the basis of analytical and spectroscopic data, and this formulation has been confirmed by X-ray structural analysis. The yield of the isolated solid is *ca.* 60%. The bis(ethene) complex forms stable, air-sensitive solutions in benzene, toluene and THF but decomposes in CH<sub>2</sub>Cl<sub>2</sub> at room temperature.

The <sup>1</sup>H and <sup>13</sup>C{<sup>1</sup>H} NMR spectra of the orange solid are shown in Figures 2.1 and 2.2, respectively. The NMR spectra show two methyl acac singlets [δ(<sup>1</sup>H) 1.82 and 1.86, δ(<sup>13</sup>C{<sup>1</sup>H}) 27.5 and 26.9], one methine acac singlet [δ(<sup>1</sup>H) 5.24, δ(<sup>13</sup>C{<sup>1</sup>H}) 98.0] and two carbonyl acac resonances [δ(<sup>13</sup>C{<sup>1</sup>H}) 185.1 and 186.6], consistent with the presence of the *cis*-[Ru(acac)<sub>2</sub>] moiety attached to two identical ligands (see p. 25). The <sup>1</sup>H NMR spectrum also displays a symmetrical eight proton multiplet between δ 3.70 - 3.85 which is assigned to the coordinated ethene. The *ca.* 2 ppm shift of the ethene protons to low frequency compared to free ethene (δ 5.24) is similar to that found for [Ru(NH<sub>3</sub>)<sub>5</sub>(η<sup>2</sup>-C<sub>2</sub>H<sub>4</sub>)<sub>2</sub>]<sup>2+</sup> (δ 3.57)<sup>1</sup> and *cis*-[Ru(H<sub>2</sub>O)<sub>4</sub>(η<sup>2</sup>-C<sub>2</sub>H<sub>4</sub>)<sub>2</sub>]<sup>2+</sup> (δ 3.81).<sup>2</sup> The singlet at δ 78.2 in the <sup>13</sup>C{<sup>1</sup>H} NMR spectrum (Figure

2.2), which splits into a triplet in the gated  $^{13}\text{C}$  NMR spectrum with a C-H coupling constant of 160 Hz, is assigned to the coordinated ethene carbon atoms. The chemical shift for the ethene carbon atoms is similar to that found for *cis*- $[\text{Ru}(\text{H}_2\text{O})_4(\eta^2\text{-C}_2\text{H}_4)_2]^{2+}$  ( $\delta$  76.6).<sup>2</sup> The slight increase observed in the C-H coupling constant from 156.4 Hz for free ethene<sup>3</sup> is also found for the complexes  $[\text{Ru}(\text{H}_2\text{O})_5(\eta^2\text{-C}_2\text{H}_4)]^{2+}$  ( $J_{\text{CH}} = 161.6$  Hz),<sup>2</sup>  $[(\eta^5\text{-C}_5\text{H}_5)\text{Rh}(\eta^2\text{-C}_2\text{H}_4)_2]$  ( $J_{\text{CH}} = 160$  Hz),<sup>4</sup>  $[\text{Rh}(\text{acac})(\eta^2\text{-C}_2\text{H}_4)_2]$  ( $J_{\text{CH}} = 158$  Hz),<sup>4</sup> and *trans*- $[\text{W}(\text{CO})_4(\eta^2\text{-C}_2\text{H}_4)_2]$  ( $J_{\text{CH}} = 161$  Hz).<sup>5</sup> The  $^1\text{H}$  NMR spectrum of *cis*- $[\text{Ru}(\text{acac})_2(\eta^2\text{-C}_2\text{H}_4)_2]$  recorded in the presence of free ethene shows no detectable broadening of the coordinated ethene signals, hence rapid exchange on the NMR timescale at room temperature does not occur. This contrasts with the rapid ethene exchange found for  $[\text{Rh}(\text{acac})(\eta^2\text{-C}_2\text{H}_4)_2]$  at 25 °C.<sup>6</sup> The rotation of the ethene ligands will be discussed later.

**Figure 2.1:** The  $^1\text{H}$  NMR spectrum of *cis*- $[\text{Ru}(\text{acac})_2(\eta^2\text{-C}_2\text{H}_4)_2]$  in  $d_6$ -benzene at 25 °C.

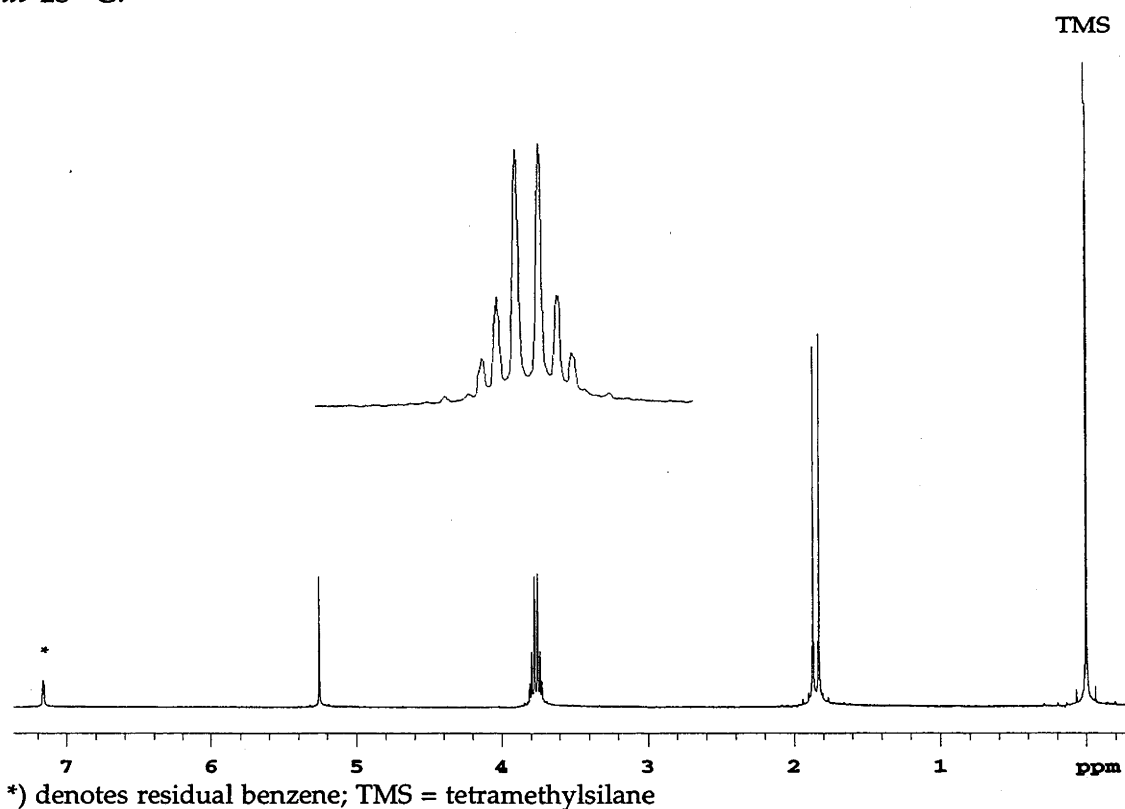
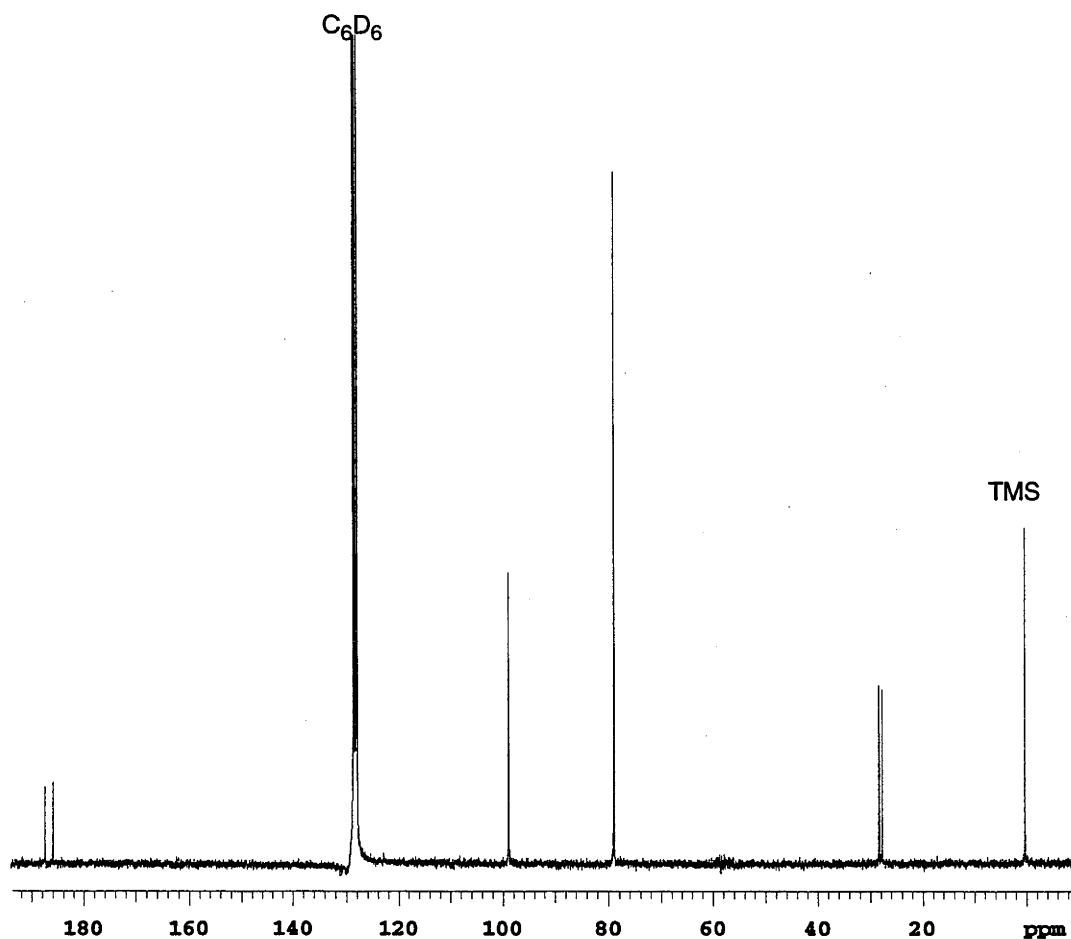


**Figure 2.2:** The  $^{13}\text{C}\{^1\text{H}\}$  NMR spectrum of *cis*- $[\text{Ru}(\text{acac})_2(\eta^2\text{-C}_2\text{H}_4)_2]$  in  $d_6$ -benzene at 25 °C.



TMS = tetramethylsilane

The strongest peak in the isotopic pattern of the orange solid was found at  $m/z$  356.0 in the FAB mass spectrum. Sequential loss of ethene results in the appearance of the ions  $\{\text{Ru}(\text{acac})_2(\eta^2\text{-C}_2\text{H}_4)\}^+$  and  $\{\text{Ru}(\text{acac})_2\}^+$ , the latter being the most abundant ion detected. The mass to charge ratio and relative abundance of these ions are shown in Table 2.1. The matrix used, in this case (3-nitrophenyl)octyl ether ( $\text{C}_{14}\text{H}_{21}\text{NO}_3$ ), also reacts with  $[\text{Ru}(\text{acac})_2(\eta^2\text{-C}_2\text{H}_4)_2]$ , either in solution or in the gas phase, to form the species  $\{\text{Ru}(\text{acac})_2(\eta^2\text{-C}_2\text{H}_4)(\text{C}_{14}\text{H}_{21}\text{NO}_3)\}^+$  and  $\{\text{Ru}(\text{acac})_2(\text{C}_{14}\text{H}_{21}\text{NO}_3)\}^+$ .

**Table 2.1:** FAB mass spectral data of the isolated orange solid *cis*-[Ru(acac)<sub>2</sub>(η<sup>2</sup>-C<sub>2</sub>H<sub>4</sub>)<sub>2</sub>].

m/z	Assignment	Relative Intensity (%)
579.1	{Ru(acac) <sub>2</sub> (C <sub>2</sub> H <sub>4</sub> )(C <sub>14</sub> H <sub>21</sub> NO <sub>3</sub> )} <sup>+</sup>	2
551.1	{Ru(acac) <sub>2</sub> (C <sub>14</sub> H <sub>21</sub> NO <sub>3</sub> )} <sup>+</sup>	20
356.0	{Ru(acac) <sub>2</sub> (C <sub>2</sub> H <sub>4</sub> ) <sub>2</sub> } <sup>+</sup>	10
328.0	{Ru(acac) <sub>2</sub> (C <sub>2</sub> H <sub>4</sub> )} <sup>+</sup>	23
299.9	{Ru(acac) <sub>2</sub> } <sup>+</sup>	100

The IR spectrum shows two strong bands at 1576 and 1515 cm<sup>-1</sup> characteristic of bidentate, O-bonded acac.<sup>7</sup> Since the coordination of an alkene to a metal centre typically lowers the ν(C=C) frequency by 70 - 170 cm<sup>-1</sup> compared to the free alkene,<sup>8</sup> the band due to coordinated ethene is likely to be hidden by the acac bands and cannot be observed. This situation is analogous to that found for the chelating alkene N- and O-donor ligand complexes [Ru(acac)<sub>2</sub>(LL')].<sup>9</sup>

The structure of *cis*-[Ru(acac)<sub>2</sub>(η<sup>2</sup>-C<sub>2</sub>H<sub>4</sub>)<sub>2</sub>] has been confirmed by an X-ray crystallographic study. The molecular structure and selected metrical parameters are shown in Figure 2.3 and Table 2.2, respectively. Crystal and refinement data, together with the full set of interatomic distances and angles, are given in Appendix A.1. The hydrogen atoms of the ethene groups were located in the difference maps and their coordinates were refined and are also given in Appendix A.1.

The solid state structure of *cis*-[Ru(acac)<sub>2</sub>(η<sup>2</sup>-C<sub>2</sub>H<sub>4</sub>)<sub>2</sub>] is that of a distorted octahedron with the metal atom at the centre and the two ethene ligands occupying mutually *cis* coordination sites. The Ru-O distances characterising the coordination of the acetylacetonato anion are in the range 2.055(1) - 2.080(1) Å. The Ru-C bond distances are 2.183(2) - 2.212(2) Å. The

C=C distances of the ethene ligands in each molecule were found to be 1.370(3) and 1.353(4) Å, *c.a.* 0.02 Å longer than the C=C bond length of free ethene [1.337(2) Å]. All of the ethene hydrogen atoms are symmetrically bent away from the ruthenium centre to form an angle,  $\alpha$ , of between 26 to 36°, where  $\alpha$  is defined as the angle between the normals to the H-C-H planes.<sup>10</sup>

The ethene ligands of *cis*-[Ru(acac)<sub>2</sub>( $\eta^2$ -C<sub>2</sub>H<sub>4</sub>)<sub>2</sub>] are mutually orthogonal in the solid state; the dihedral angle between the planes defined by the atoms Ru(1), C(11) and C(12), and Ru(1), C(13) and C(14) is 90°. The plane defined by the atoms Ru(1), C(11) and C(12) eclipses that defined by the atoms Ru(1), O(1) and O(4).

**Figure 2.3:** ORTEP diagram of the molecular structure of *cis*-[Ru(acac)<sub>2</sub>( $\eta^2$ -C<sub>2</sub>H<sub>4</sub>)<sub>2</sub>].

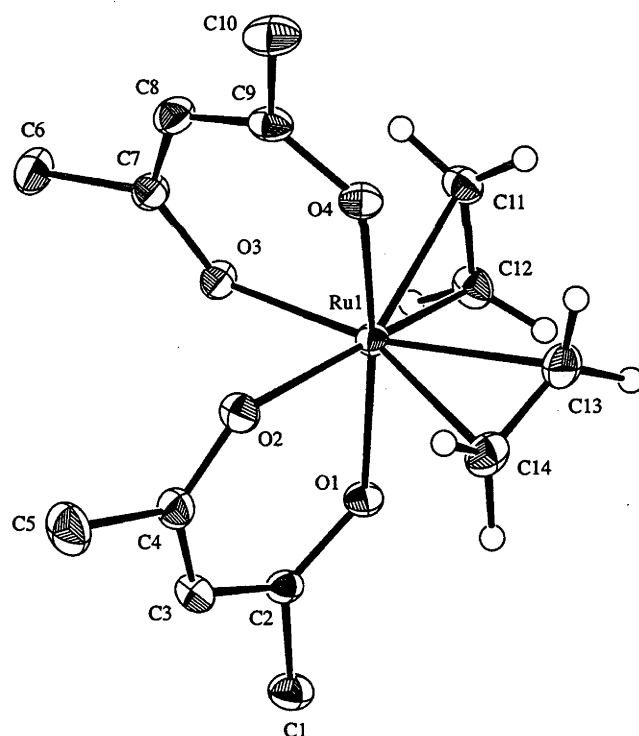




Table 2.2: Selected metrical parameters of *cis*-[Ru(acac)<sub>2</sub>( $\eta^2$ -C<sub>2</sub>H<sub>4</sub>)<sub>2</sub>]

Bond Distances (Å)			
Ru(1)-O(1)		2.080(1)	
Ru(1)-O(2)		2.068(1)	
Ru(1)-O(3)		2.061(1)	
Ru(1)-O(4)		2.055(1)	
Ru(1)-C(11)		2.205(2)	
Ru(1)-C(12)		2.209(2)	
Ru(1)-C(13)		2.212(2)	
Ru(1)-C(14)		2.183(2)	
C(11)-C(12)		1.370(3)	
C(13)-C(14)		1.353(4)	
C(11)-H(15)		0.90(3)	
C(11)-H(16)		0.89(3)	
C(12)-H(17)		0.98(2)	
C(12)-H(18)		0.90(3)	
C(13)-H(19)		0.88(3)	
C(13)-H(20)		1.04(3)	
C(14)-H(21)		0.98(3)	
C(14)-H(22)		0.95(3)	
Bond Angles (°)			
O(1)-Ru(1)-O(2)	90.32(6)	C(11)-Ru(1)-C(12)	36.17(8)
O(1)-Ru(1)-O(3)	85.87(6)	C(13)-Ru(1)-C(14)	35.85(9)
O(1)-Ru(1)-O(4)	170.05(5)	Ru(1)-C(11)-H(15)	103(2)
O(1)-Ru(1)-C(11)	111.64(7)	Ru(1)-C(11)-H(16)	108(2)
O(1)-Ru(1)-C(12)	75.63(7)	C(12)-C(11)-H(15)	121(2)
O(1)-Ru(1)-C(13)	98.47(8)	C(12)-C(11)-H(16)	123(2)
O(1)-Ru(1)-C(14)	85.18(8)	H(15)-C(11)-H(16)	115(2)
O(2)-Ru(1)-O(3)	81.56(6)	Ru(1)-C(12)-H(17)	103(1)
O(2)-Ru(1)-O(4)	79.86(6)	Ru(1)-C(12)-H(18)	110(2)
O(2)-Ru(1)-C(11)	152.77(8)	C(11)-C(12)-H(17)	121(2)
O(2)-Ru(1)-C(12)	160.95(8)	C(11)-C(12)-H(18)	120(2)
O(2)-Ru(1)-C(13)	112.26(8)	H(17)-C(12)-H(18)	117(2)
O(2)-Ru(1)-C(14)	79.25(8)	Ru(1)-C(13)-H(19)	105(2)
O(3)-Ru(1)-O(4)	94.21(6)	Ru(1)-C(13)-H(20)	116(1)
O(3)-Ru(1)-C(11)	84.11(7)	C(14)-C(13)-H(19)	117(2)
O(3)-Ru(1)-C(12)	84.60(8)	C(14)-C(13)-H(20)	126(2)
O(3)-Ru(1)-C(13)	165.35(8)	H(19)-C(13)-H(20)	112(2)
O(3)-Ru(1)-C(14)	158.74(9)	Ru(1)-C(14)-H(21)	101(2)
O(4)-Ru(1)-C(11)	78.24(7)	Ru(1)-C(14)-H(22)	109(2)
O(4)-Ru(1)-C(12)	114.29(7)	C(13)-C(14)-H(21)	123(2)
O(4)-Ru(1)-C(13)	83.92(8)	C(13)-C(14)-H(22)	118(2)
O(4)-Ru(1)-C(14)	91.35(8)	H(21)-C(14)-H(22)	117(2)

2.2 Reactions of *cis*-[Ru(acac)<sub>2</sub>(η<sup>2</sup>-C<sub>2</sub>H<sub>4</sub>)<sub>2</sub>] with SbPh<sub>3</sub>, and CH<sub>3</sub>CN and with other nitrogen donor ligands.

The coordinated ethene ligands of *cis*-[Ru(acac)<sub>2</sub>(η<sup>2</sup>-C<sub>2</sub>H<sub>4</sub>)<sub>2</sub>] are readily replaced upon addition of one equivalent of SbPh<sub>3</sub> or CH<sub>3</sub>CN to form yellow or brown, air-stable solid complexes *cis*-[Ru(acac)<sub>2</sub>(η<sup>2</sup>-C<sub>2</sub>H<sub>4</sub>)L] (L = SbPh<sub>3</sub>, CH<sub>3</sub>CN) in yields of 60 - 80%. The replacement of one ethene ligand in *cis*-[Ru(acac)<sub>2</sub>(η<sup>2</sup>-C<sub>2</sub>H<sub>4</sub>)<sub>2</sub>] by NH<sub>3</sub> in THF results in the isolation of the air stable orange solid *trans*-[Ru(acac)<sub>2</sub>(η<sup>2</sup>-C<sub>2</sub>H<sub>4</sub>)(NH<sub>3</sub>)] in yields of *ca.* 60%. The reaction of equimolar amounts of pyridine and *cis*-[Ru(acac)<sub>2</sub>(η<sup>2</sup>-C<sub>2</sub>H<sub>4</sub>)<sub>2</sub>] in benzene affords a mixture of *cis*- and *trans*-[Ru(acac)<sub>2</sub>(η<sup>2</sup>-C<sub>2</sub>H<sub>4</sub>)(NC<sub>5</sub>H<sub>5</sub>)] in the ratio of *ca.* 3:2 with a 70% yield. The complex *trans*-[Ru(acac)<sub>2</sub>(η<sup>2</sup>-C<sub>2</sub>H<sub>4</sub>)(NH<sub>3</sub>)] is insoluble in aromatic hydrocarbons, acetone and ether but is readily soluble in CH<sub>2</sub>Cl<sub>2</sub>. The pyridine complex *trans*-[Ru(acac)<sub>2</sub>(η<sup>2</sup>-C<sub>2</sub>H<sub>4</sub>)(NC<sub>5</sub>H<sub>5</sub>)] and the complexes *cis*-[Ru(acac)<sub>2</sub>(η<sup>2</sup>-C<sub>2</sub>H<sub>4</sub>)L] (L = SbPh<sub>3</sub>, CH<sub>3</sub>CN) are soluble in aromatic solvents and THF.

The benzene-soluble complex *cis*-[Ru(acac)<sub>2</sub>(η<sup>2</sup>-C<sub>2</sub>H<sub>4</sub>)(NH<sub>3</sub>)] may be isolated after several weeks from a CD<sub>2</sub>Cl<sub>2</sub> solution of *trans*-[Ru(acac)<sub>2</sub>(η<sup>2</sup>-C<sub>2</sub>H<sub>4</sub>)(NH<sub>3</sub>)] at room temperature or by passing a CH<sub>2</sub>Cl<sub>2</sub> solution of *trans*-[Ru(acac)<sub>2</sub>(η<sup>2</sup>-C<sub>2</sub>H<sub>4</sub>)(NH<sub>3</sub>)] through a neutral alumina (Activity III) column. The isomerization of the pyridine analogue *trans*-[Ru(acac)<sub>2</sub>(η<sup>2</sup>-C<sub>2</sub>H<sub>4</sub>)(NC<sub>5</sub>H<sub>5</sub>)] to the *cis*-isomer was found spectroscopically to be quantitative after heating overnight in d<sub>6</sub>-benzene. Attempts to obtain the pure *cis*-isomer by heating the mixture in toluene overnight caused partial decomposition with formation of *cis*-[Ru(acac)<sub>2</sub>(NC<sub>5</sub>H<sub>5</sub>)<sub>2</sub>].

The <sup>1</sup>H and <sup>13</sup>C{<sup>1</sup>H} NMR spectra of the complexes *trans*-[Ru(acac)<sub>2</sub>(η<sup>2</sup>-C<sub>2</sub>H<sub>4</sub>)L] (L = NH<sub>3</sub>, C<sub>5</sub>H<sub>5</sub>N) show the expected acac pattern (see p. 25) and are presented in Tables 2.3 and 2.4, respectively. A broad signal in the <sup>1</sup>H NMR spectrum for *trans*-[Ru(acac)<sub>2</sub>(η<sup>2</sup>-C<sub>2</sub>H<sub>4</sub>)(NH<sub>3</sub>)] at δ 3.05 is

assigned to the ammine protons. The pyridine protons and carbon atoms are found in the expected regions of the  $^1\text{H}$  and  $^{13}\text{C}\{^1\text{H}\}$  NMR spectra (see Table 2.3 and 2.4). The protons and carbon atoms of ethene for both complexes appear as a singlet in the  $^1\text{H}$  NMR and  $^{13}\text{C}\{^1\text{H}\}$  NMR spectra, respectively (see Table 2.3 and 2.4). The  $^{13}\text{C}$  NMR spectrum of *trans*-[Ru(acac) $_2$ ( $\eta^2$ -C $_2$ H $_4$ )(NH $_3$ )] shows a triplet at  $\delta$  72.2 due to the ethene carbon atoms with a C-H coupling constant of 160 Hz, similar to that found for *cis*-[Ru(acac) $_2$ ( $\eta^2$ -C $_2$ H $_4$ ) $_2$ ] (see p. 34). The two outside peaks of the triplet appear as doublets with a separation of 3 Hz, but the central peak is not split. The origin of this phenomenon is not known.

The  $^1\text{H}$  and  $^{13}\text{C}\{^1\text{H}\}$  NMR spectral data for the complexes *cis*-[Ru(acac) $_2$ ( $\eta^2$ -C $_2$ H $_4$ )L] (L = SbPh $_3$ , CH $_3$ CN, NH $_3$ , C $_5$ H $_5$ N) are shown in Tables 2.3 and 2.4, respectively and are similar to those reported for *cis*-[Ru(acac)( $\eta^2$ -C $_2$ H $_4$ )(SbPr $_3$ )].<sup>11</sup> The acac protons and carbon atoms show the expected pattern for the coordination of two different ligands to the *cis*-{Ru(acac) $_2$ } moiety (see p. 25). The resonance due to the nitrile carbon atom of CH $_3$ CN could not be detected. The ethene protons of *cis*-[Ru(acac) $_2$ ( $\eta^2$ -C $_2$ H $_4$ )L] (L = SbPh $_3$ , NH $_3$ , CH $_3$ CN) appear as symmetrical multiplets between  $\delta$  4.54 - 3.99. The  $^1\text{H}$  NMR ethene resonances of the complexes *cis*-[Ru(acac) $_2$ ( $\eta^2$ -C $_2$ H $_4$ )L] (L = NH $_3$ , MeCN, SbPh $_3$ ) at room temperature are very similar to the low temperature spectra found for [Rh(acac)( $\eta^2$ -C $_2$ H $_4$ ) $_2$ ]<sup>6</sup> and [RhCp( $\eta^2$ -C $_2$ H $_4$ )L] (L = C $_2$ H $_4$ ,<sup>6</sup> C $_2$ F $_4$ ,<sup>12</sup> SO $_2$ <sup>12</sup>). The ethene protons of *cis*-[Ru(acac) $_2$ ( $\eta^2$ -C $_2$ H $_4$ )(NC $_5$ H $_5$ )] appear as a singlet at  $\delta$  4.29 in  $d_6$ -benzene and in  $d_6$ -acetone. The ethene carbon atoms also appear as singlets in the  $^{13}\text{C}\{^1\text{H}\}$  NMR spectrum for all of the complexes. The gated  $^{13}\text{C}$  NMR spectra of *cis*-[Ru(acac) $_2$ ( $\eta^2$ -C $_2$ H $_4$ )L] (L = CH $_3$ CN, NH $_3$ ) each display a triplet at  $\delta$  65.9 and 72.5, respectively, due to the ethene carbon atoms with a C-H coupling constant of *ca.* 161 Hz, which is similar to that found for *cis*-[Ru(acac) $_2$ ( $\eta^2$ -C $_2$ H $_4$ ) $_2$ ] (see p. 33).

Table 2.3:  $^1\text{H}$  NMR spectral data of the mono-ethene complexes  $[\text{Ru}(\text{acac})_2(\eta^2\text{-C}_2\text{H}_4)(\text{L})]$ .

Compound	$^1\text{H}$ NMR <sup>a</sup>			Solvent
	$\text{CH}_3$ (acac)	CH (acac)	Other	
<i>cis</i> - $[\text{Ru}(\text{acac})_2(\eta^2\text{-C}_2\text{H}_4)(\text{CH}_3\text{CN})]$	1.81, 2.00, 2.01, 2.17	5.29, 5.50	0.59 (3H, $\text{CH}_3\text{CN}$ ) 4.44 - 4.37 (m, 4H, $\text{C}_2\text{H}_4$ );	$\text{C}_6\text{D}_6$
<i>cis</i> - $[\text{Ru}(\text{acac})_2(\eta^2\text{-C}_2\text{H}_4)(\text{SbPh}_3)]$	1.62, .169, 1.74, 2.02	5.15, 5.30	3.99 -4.26 (m, 4H, $\text{C}_2\text{H}_4$ ); 7.67 - 7.70 (m, 3H, $\rho\text{-SbC}_6\text{H}_5$ ); 7.00 - 7.13 (m, 12H, <i>m</i> - and <i>p</i> - $\text{SbC}_6\text{H}_5$ )	$\text{C}_6\text{D}_6$
<i>trans</i> - $[\text{Ru}(\text{acac})_2(\eta^2\text{-C}_2\text{H}_4)(\text{NH}_3)]$	1.91	5.38	3.05 (b, 3H, $\text{NH}_3$ ); 3.70 (4H, $\text{C}_2\text{H}_4$ )	$\text{CD}_2\text{Cl}_2$
<i>cis</i> - $[\text{Ru}(\text{acac})_2(\eta^2\text{-C}_2\text{H}_4)(\text{NH}_3)]$	1.97, 2.02, 2.18, 2.35	5.14, 5.28	1.52 (br, 3H, $\text{NH}_3$ ) 4.1 - 4.3 (m, 4H, $\text{C}_2\text{H}_4$ );	$\text{C}_6\text{D}_6$
<i>trans</i> - $[\text{Ru}(\text{acac})_2(\eta^2\text{-C}_2\text{H}_4)(\text{C}_5\text{H}_5\text{N})]$	1.80	5.05	4.29 (4H, $\text{C}_2\text{H}_4$ ); 8.85 (d, 1H, $J_{\text{HH}}$ 5 Hz, <i>o</i> - $\text{C}_5\text{H}_5\text{N}$ ); 6.82 (d, 2H, $J_{\text{HH}}$ 7 Hz, <i>p</i> - $\text{C}_5\text{H}_5\text{N}$ ); 6.66 (d, 2H, $J_{\text{HH}}$ 7 Hz, <i>m</i> - $\text{C}_5\text{H}_5\text{N}$ );	$\text{C}_6\text{D}_6$
<i>cis</i> - $[\text{Ru}(\text{acac})_2(\eta^2\text{-C}_2\text{H}_4)(\text{C}_5\text{H}_5\text{N})]$	1.88, 1.90, 1.94, 1.96	5.32, 5.33	4.29 (4H, $\text{C}_2\text{H}_4$ ); 6.38 (d, 2H, $J_{\text{HH}}$ 7 Hz, <i>m</i> - $\text{C}_5\text{H}_5\text{N}$ ); 6.64 (d, 2H, $J_{\text{HH}}$ 7 Hz, <i>p</i> - $\text{C}_5\text{H}_5\text{N}$ ); 8.53 (d, 1H, $J_{\text{HH}}$ 5 Hz, <i>o</i> - $\text{C}_5\text{H}_5\text{N}$ )	$\text{C}_6\text{D}_6$

a) singlets unless otherwise indicated.

**Table 2.4:**  $^{13}\text{C}\{^1\text{H}\}$  NMR spectral data of the mono-ethene complexes  $[\text{Ru}(\text{acac})_2(\eta^2\text{-C}_2\text{H}_4)(\text{L})]$ .

Compound	$^{13}\text{C}\{^1\text{H}\}$ NMR <sup>a</sup>				Solvent
	CH <sub>3</sub> (acac)	CH (acac)	CO (acac)	Other	
<i>cis</i> -[Ru(acac) <sub>2</sub> (η <sup>2</sup> -C <sub>2</sub> H <sub>4</sub> )(CH <sub>3</sub> CN)]	27.3, 27.7, 27.9, 28.2	99.0, 99.1	185.5, 186.1, 186.2, 187.8	2.2 (CH <sub>3</sub> CN); 72.5 (C <sub>2</sub> H <sub>4</sub> )	C <sub>6</sub> D <sub>6</sub>
<i>cis</i> -[Ru(acac) <sub>2</sub> (η <sup>2</sup> -C <sub>2</sub> H <sub>4</sub> )(SbPh <sub>3</sub> )]	27.4, 27.7, 27.9, 28.0	98.6, 100.2	185.3, 185.8, 186.8, 188.7	57.9 (C <sub>2</sub> H <sub>4</sub> ); 128.9, 129.6, 132.0, 136.6 (SbC <sub>6</sub> H <sub>5</sub> )	C <sub>6</sub> D <sub>6</sub>
<i>trans</i> -[Ru(acac) <sub>2</sub> (η <sup>2</sup> -C <sub>2</sub> H <sub>4</sub> )(NH <sub>3</sub> )]	27.8	99.6	186.9	72.2 (C <sub>2</sub> H <sub>4</sub> )	CD <sub>2</sub> Cl <sub>2</sub>
<i>cis</i> -[Ru(acac) <sub>2</sub> (η <sup>2</sup> -C <sub>2</sub> H <sub>4</sub> )(NH <sub>3</sub> )]	27.4, 27.7, 28.0, 28.1	98.9, 99.1	184.0, 185.5, 185.6, 189.1	65.9 (C <sub>2</sub> H <sub>4</sub> )	C <sub>6</sub> D <sub>6</sub>
<i>trans</i> -[Ru(acac) <sub>2</sub> (η <sup>2</sup> -C <sub>2</sub> H <sub>4</sub> )(C <sub>5</sub> H <sub>5</sub> N)]	27.7	99.5	186.0	75.4 (C <sub>2</sub> H <sub>4</sub> ); 123.6, 136.7, 151.9 (C <sub>5</sub> H <sub>5</sub> N);	C <sub>6</sub> D <sub>6</sub>
<i>cis</i> -[Ru(acac) <sub>2</sub> (η <sup>2</sup> -C <sub>2</sub> H <sub>4</sub> )(C <sub>5</sub> H <sub>5</sub> N)]	27.6, 27.9, 28.1, 28.4	99.2, 99.3	185.0, 185.8, 186.4, 187.6	73.1 (C <sub>2</sub> H <sub>4</sub> ); 123.3, 134.3, 153.6 (C <sub>5</sub> H <sub>5</sub> N)	C <sub>6</sub> D <sub>6</sub>

a) all singlets

Table 2.5: IR and MS data of the isolated mono-ethene complexes  $[\text{Ru}(\text{acac})_2(\eta^2\text{-C}_2\text{H}_4)\text{L}]$ .

Compound	Infrared Data (KBr) ( $\text{cm}^{-1}$ )		FAB MS		
	$\nu(\text{acac})$	Other	m/z	Relative Abundance	Assignment
<i>cis</i> - $[\text{Ru}(\text{acac})_2(\eta^2\text{-C}_2\text{H}_4)(\text{CH}_3\text{CN})]$	1571, 1518	2262 $\nu(\text{C}\equiv\text{N})$	369.0	23	$[\text{Ru}(\text{acac})_2(\eta^2\text{-C}_2\text{H}_4)(\text{CH}_3\text{CN})]^+$
			340.9	54	$\{\text{Ru}(\text{acac})_2(\text{CH}_3\text{CN})\}^+$
			299.9	100	$\{\text{Ru}(\text{acac})_2\}^+$
<i>cis</i> - $[\text{Ru}(\text{acac})_2(\eta^2\text{-C}_2\text{H}_4)(\text{SbPh}_3)]$	1568, 1514		1005.9	8	$\{\text{Ru}(\text{acac})_2(\text{SbPh}_3)_2\}^+$
			679.9	19	$[\text{Ru}(\text{acac})_2(\eta^2\text{-C}_2\text{H}_4)(\text{SbPh}_3)]^+$
			653.9	100	$\{\text{Ru}(\text{acac})_2(\text{SbPh}_3)\}^+$
			552.9	25	$[\text{Ru}(\text{acac})(\text{SbPh}_3)]^+$
			299.9	97	$\{\text{Ru}(\text{acac})_2\}^+$
<i>trans</i> - $[\text{Ru}(\text{acac})_2(\eta^2\text{-C}_2\text{H}_4)(\text{NH}_3)]$	1567, 1510	3335 $\nu(\text{NH})$	345.0	45	$[\text{Ru}(\text{acac})_2(\eta^2\text{-C}_2\text{H}_4)(\text{NH}_3)]^+$
			317.0	77	$\{\text{Ru}(\text{acac})_2(\text{NH}_3)\}^+$
			299.9	100	$\{\text{Ru}(\text{acac})_2\}^+$
<i>cis</i> - $[\text{Ru}(\text{acac})_2(\eta^2\text{-C}_2\text{H}_4)(\text{NH}_3)]$	1566, 1510	3334 $\nu(\text{NH})$	345.0	92	$[\text{Ru}(\text{acac})_2(\eta^2\text{-C}_2\text{H}_4)(\text{NH}_3)]^+$
			317.0	100	$\{\text{Ru}(\text{acac})_2(\text{NH}_3)\}^+$
			300.0	87	$\{\text{Ru}(\text{acac})_2\}^+$
<i>trans</i> - $[\text{Ru}(\text{acac})_2(\eta^2\text{-C}_2\text{H}_4)(\text{C}_5\text{H}_5\text{N})]$	1565, 1515	1547 $\nu(\text{NC}_5\text{H}_5)$	407.1	9	$[\text{Ru}(\text{acac})_2(\eta^2\text{-C}_2\text{H}_4)(\text{NC}_5\text{H}_5)]^+$
			379.1	100	$\{\text{Ru}(\text{acac})_2(\text{NC}_5\text{H}_5)\}^+$
			300.1	85	$\{\text{Ru}(\text{acac})_2\}^+$

All the isolated complexes  $[\text{Ru}(\text{acac})_2(\eta^2\text{-C}_2\text{H}_4)\text{L}]$  ( $\text{L} = \text{SbPh}_3, \text{CH}_3\text{CN}, \text{NH}_3, \text{C}_5\text{H}_5\text{N}$ ) display parent ion molecular peaks in the FAB mass spectra. Ion peaks corresponding to the species  $\{\text{Ru}(\text{acac})_2\text{L}\}^+$  and  $\{\text{Ru}(\text{acac})_2\}^+$  were also found, in higher relative abundance (see Table 2.5). The IR spectra of the complexes display strong bands in the region  $1571 - 1510 \text{ cm}^{-1}$ , characteristic of bidentate, O-bonded acac (see Table 2.5).<sup>7</sup> The acetonitrile complex displays a medium intensity band at  $2262 \text{ cm}^{-1}$  assigned to the  $\nu(\text{C}\equiv\text{N})$  stretch of an aliphatic nitrile coordinated to a metal via the nitrogen atom.<sup>7</sup> Both  $[\text{Ru}(\text{acac})_2(\eta^2\text{-C}_2\text{H}_4)(\text{NH}_3)]$  complexes display a medium band at *ca.*  $3335 \text{ cm}^{-1}$  due to the antisymmetric  $\nu(\text{NH})$  mode and in the case of the *cis*-isomer, a band of medium intensity was found at  $1626 \text{ cm}^{-1}$  due to the degenerate  $\text{NH}_3$  deformation  $\delta_a(\text{HNH})$ .<sup>7</sup> The isolated pyridine complex shows a band at  $1547 \text{ cm}^{-1}$  which is presumably due to a "breathing" vibration of the coordinated pyridine since free pyridines have four such vibrations in the region  $1610 - 1400 \text{ cm}^{-1}$ .<sup>13</sup>

### 2.3 Reactions of *cis*- $[\text{Ru}(\text{acac})_2(\eta^2\text{-alkene})_2]$ (alkene = $\text{C}_2\text{H}_4, \text{C}_8\text{H}_{14}$ ) with one equivalent of a tertiary phosphine

The reactions of one equivalent of various tertiary phosphines with *cis*- $[\text{Ru}(\text{acac})_2(\eta^2\text{-alkene})_2]$  (alkene =  $\text{C}_2\text{H}_4, \text{C}_8\text{H}_{14}$ ) in THF, containing a small amount of *d*<sub>8</sub>-toluene, were investigated by  $^{31}\text{P}\{^1\text{H}\}$  NMR spectroscopy at *ca.*  $-35 \text{ }^\circ\text{C}$ . The first detectable signals in the case of the tertiary phosphines  $\text{PPhMe}_2$ ,  $\text{PPh}_3$  and  $\text{P}(p\text{-tolyl})_3$  were singlets at  $\delta$  17.3, 34.8 and 32.8, respectively, which correspond to *trans*- $[\text{Ru}(\text{acac})_2\text{L}_2]$  ( $\text{L} = \text{PPhMe}_2, \text{PPh}_3$  and  $\text{P}(p\text{-tolyl})_3$ ).<sup>14</sup> Warming the  $\text{PPhMe}_2$  reaction solution to room temperature results in the isomerization of *trans*- $[\text{Ru}(\text{acac})_2(\text{PPhMe}_2)_2]$  to *cis*- $[\text{Ru}(\text{acac})_2(\text{PPhMe}_2)_2]$ . No other product was detected by  $^{31}\text{P}\{^1\text{H}\}$  NMR spectroscopy apart from free  $\text{PPhMe}_2$  still present in solution. On warming the  $\text{PPh}_3$  or  $\text{P}(p\text{-tolyl})_3$  mixtures to room temperature a singlet at *ca.*  $\delta$  +54.7, probably due to either *cis*- $[\text{Ru}(\text{acac})_2\text{L}_2]$ <sup>14</sup> or *cis*- $[\text{Ru}(\text{acac})_2(\eta^2\text{-C}_2\text{H}_4)\text{L}]$  [ $\text{L} =$

$\text{PPh}_3$ ,  $\text{P}(p\text{-tolyl})_3$ ] (see below), and a weak singlet at *ca.*  $\delta$  +83.9 are observed. The latter peak was the only signal observed when a large excess (ten equivalents) of *cis*- $[\text{Ru}(\text{acac})_2(\eta^2\text{-C}_8\text{H}_{14})_2]$  was added to a solution of  $\text{PPh}_3$  in THF at room temperature. It may be due to a square-pyramidal five-coordinate species  $[\text{Ru}(\text{acac})_2\text{L}]$  in which the phosphorus atom occupies the apical position or, perhaps more likely, a six-coordinate solvento-complex *trans*- $[\text{Ru}(\text{acac})_2\text{L}(\text{THF})]$ . Similarly deshielded  $^{31}\text{P}\{^1\text{H}\}$  chemical shifts were found for the apical phosphine of the five-coordinate complexes  $[\text{RuX}(\text{NN}'\text{N})(\text{PPh}_3)][\text{OTf}]$  ( $\text{X} = \text{Cl}, \text{OTf}$ ;  $\text{NN}'\text{N} = 2,6\text{-bis}[(\text{dimethylamino})\text{-methyl}]\text{pyridine}$ ),<sup>15</sup>  $[\text{Ru}(\text{N}(\text{S}(\text{PR}_2)_2)(\text{PPh}_3)]$  ( $\text{R} = \text{Ph}, \text{Pr}^i$ ),<sup>16</sup> the square pyramidal complexes  $[\text{RuCl}_2(\text{PR}_3)_3]$  ( $\text{R} = \text{Ph}$ ,<sup>17</sup> *p*-tolyl<sup>18</sup>) and for the  $\text{PPh}_3$  of  $[\text{RuCl}_2(\text{PPh}_3)\text{L}]$  ( $\text{L} = \text{dppm}, \text{dppe}$  and  $\text{dppp}$ ).<sup>19</sup>

The behaviour of *cis*- $[\text{Ru}(\text{acac})_2(\eta^2\text{-C}_2\text{H}_4)_2]$  with one equivalent of the sterically more demanding tertiary phosphines  $\text{PPr}^i_3$  and  $\text{PCy}_3$  was also followed by  $^{31}\text{P}\{^1\text{H}\}$  NMR spectroscopy under the conditions outlined above *i.e.* in THF. The first detectable product from the reaction of *cis*- $[\text{Ru}(\text{acac})_2(\eta^2\text{-C}_2\text{H}_4)_2]$  with one equivalent of  $\text{PPr}^i_3$  corresponds to *trans*- $[\text{Ru}(\text{acac})_2(\text{PPr}^i_3)_2]$  ( $\delta = 29.6$ , see p. 64). Warming the solution to *ca.* 10 °C results in the loss of the peak due to *trans*- $[\text{Ru}(\text{acac})_2(\text{PPr}^i_3)_2]$  and the generation a singlet at  $\delta$  +87.3 possibly due to  $[\text{Ru}(\text{acac})_2(\text{PPr}^i_3)(\text{THF})]$  (see above and p. 66),  $\delta$  +50.5 presumably due to *cis*- $[\text{Ru}(\text{acac})_2(\eta^2\text{-C}_2\text{H}_4)(\text{PPr}^i_3)]$  (see below), a peak at  $\delta$  +47.7 due to small amount of *cis*- $[\text{Ru}(\text{acac})_2(\text{PPr}^i_3)_2]$ , and a peak at  $\delta$  +19.2 due to free  $\text{PPr}^i_3$ .

On addition of one equivalent of  $\text{PCy}_3$  to *cis*- $[\text{Ru}(\text{acac})_2(\eta^2\text{-C}_2\text{H}_4)_2]$  in THF at *ca.* -35 °C singlets at  $\delta$  +21.0 due to an unknown species and at +8.9 due to free  $\text{PCy}_3$  still present are observed. Warming the solution to *ca.* 0 °C causes the almost quantitative formation after 30 minutes of a P-containing species giving rise to a singlet at *ca.*  $\delta$  +74.7. This species may be the corresponding square pyramidal five-coordinate species  $[\text{Ru}(\text{acac})_2(\text{PCy}_3)]$  or



the six-coordinate *trans*-[Ru(acac)<sub>2</sub>(PCy<sub>3</sub>)(THF)] (see p. 67). Further warming of the sample to *ca.* +25 °C forms a new species which gives a singlet at *ca.* δ +39.7 which is probably to *cis*-[Ru(acac)<sub>2</sub>(η<sup>2</sup>-C<sub>2</sub>H<sub>4</sub>)(PCy<sub>3</sub>)] (see below).

To study the effect of solvent, the reaction of one equivalent of a tertiary phosphine (PPh<sub>3</sub>, PPr<sup>*i*</sup><sub>3</sub> and PCy<sub>3</sub>) with *cis*-[Ru(acac)<sub>2</sub>(η<sup>2</sup>-C<sub>2</sub>H<sub>4</sub>)<sub>2</sub>] in d<sub>6</sub>-benzene was also followed by <sup>31</sup>P{<sup>1</sup>H} and <sup>1</sup>H NMR spectroscopy at room temperature. Replacement of the coordinated ethene ligands appears to be slower in aromatic solvents than in THF. Under these conditions, the only resonances observed in the <sup>31</sup>P{<sup>1</sup>H} NMR spectra are singlets at δ +54.7, +50.5 and +40.0 for PPh<sub>3</sub>, PPr<sup>*i*</sup><sub>3</sub> and PCy<sub>3</sub>, respectively. The <sup>1</sup>H NMR spectrum of the product isolated from the reaction of *cis*-[Ru(acac)<sub>2</sub>(η<sup>2</sup>-C<sub>2</sub>H<sub>4</sub>)<sub>2</sub>] and PPr<sup>*i*</sup><sub>3</sub> is shown in Figure 2.4. The <sup>1</sup>H NMR spectral data for these mixtures are almost the same as for the isolated solids (see p. 46) shown in Table 2.6. All these mixtures exhibit the expected acac pattern in the <sup>1</sup>H NMR spectrum for two different ligands coordinated to the *cis*-[Ru(acac)<sub>2</sub>] moiety. A four proton symmetrical multiplet was observed between δ(<sup>1</sup>H) 3.7 - 4.8 which in each case is assigned to the ethene protons, the splitting pattern being similar to that previously observed for the isolated complexes *cis*-[Ru(acac)<sub>2</sub>(η<sup>2</sup>-C<sub>2</sub>H<sub>4</sub>)L] (L = NH<sub>3</sub>, CH<sub>3</sub>CN, SbPh<sub>3</sub>). Thus, the products from the reaction of one equivalent of the tertiary phosphines (PPh<sub>3</sub>, PPr<sup>*i*</sup><sub>3</sub> and PCy<sub>3</sub>) with *cis*-[Ru(acac)<sub>2</sub>(η<sup>2</sup>-C<sub>2</sub>H<sub>4</sub>)<sub>2</sub>] in d<sub>6</sub>-benzene are the mono-alkene complexes *cis*-[Ru(acac)<sub>2</sub>(η<sup>2</sup>-C<sub>2</sub>H<sub>4</sub>)(PR<sub>3</sub>)] (R = Ph, Pr<sup>*i*</sup>, Cy).

The formation of *trans*-[Ru(acac)<sub>2</sub>L<sub>2</sub>] from the reaction of one equivalent of a tertiary phosphine L with *cis*-[Ru(acac)<sub>2</sub>(η<sup>2</sup>-alkene)<sub>2</sub>] (alkene = C<sub>2</sub>H<sub>4</sub>, C<sub>8</sub>H<sub>14</sub>) in THF at low temperatures indicates that the second alkene is replaced more rapidly than the first. Stabilisation of the square planar five-coordinate intermediate [Ru(acac)<sub>2</sub>L] by THF allows a second equivalent of L to react to form *trans*-[Ru(acac)<sub>2</sub>L<sub>2</sub>], which generally precipitates from solution. This five coordinate intermediate is not stabilised in non-

Table 2.6:  $^1\text{H}$  NMR spectral data of the mono-ethene phosphine complexes *cis*-[Ru(acac) $_2$ ( $\eta^2$ -C $_2$ H $_4$ )L].

Compound	$^1\text{H}$ NMR <sup>a</sup>		
	CH $_3$ (acac)	CH (acac)	Other
<i>cis</i> -[Ru(acac) $_2$ ( $\eta^2$ -C $_2$ H $_4$ )(PPh $_3$ )]	1.62, 1.64, 1.88, 1.96	5.07, 6.45	3.63 - 4.33 (4H, m, C $_2$ H $_4$ ); 7.62 - 7.68 (m, 3H, <i>o</i> -C $_6$ H $_5$ ); 7.04 - 7.06 (m, 12H, <i>m,p</i> -C $_6$ H $_5$ )
<i>cis</i> -[Ru(acac) $_2$ ( $\eta^2$ -C $_2$ H $_4$ )(PPt $_3$ )]	1.84, 1.86, 1.88, 1.94	5.30, 5.35	1.08, 1.23 (both dd, 18H, <i>J</i> <sub>PH</sub> 12 Hz, <i>J</i> <sub>HH</sub> 7.2 Hz, CHCH $_3$ ); 2.45 (m, 3H, CHCH $_3$ ); 4.00 - 4.60 (m, 4H, C $_2$ H $_4$ )
<i>cis</i> -[Ru(acac) $_2$ ( $\eta^2$ -C $_2$ H $_4$ )(PCy $_3$ )]	1.83, 1.86, 1.87, 1.98	5.30, 5.40	2.25 - 1.10 (b, 33H, C $_6$ H $_11$ ); 3.78 - 4.38 (m, 4H, C $_2$ H $_4$ )

a) measured in  $d_6$ -benzene; singlets unless otherwise indicated.

Table 2.7: IR and MS data of the isolated mono-ethene complexes  $[\text{Ru}(\text{acac})_2(\eta^2\text{-C}_2\text{H}_4)\text{L}]$ .

Compound	Infrared Data (KBr) ( $\text{cm}^{-1}$ ) v(acac)	FAB MS		
		m/z	Relative Abundance	Assignment
<i>cis</i> - $[\text{Ru}(\text{acac})_2(\eta^2\text{-C}_2\text{H}_4)(\text{PPr}^i_3)]$	1583, 1514	460.1	100	$\{\text{Ru}(\text{acac})_2(\text{PPr}^i_3)\}^+$
		359.1	10	-
		300.0	17	$\{\text{Ru}(\text{acac})_2\}^+$
<i>cis</i> - $[\text{Ru}(\text{acac})_2(\eta^2\text{-C}_2\text{H}_4)(\text{PCy}_3)]$	1585, 1512	860.5	2	$\{\text{Ru}(\text{acac})_2(\text{PCy}_3)_2\}^+$
		580.3	100	$\{\text{Ru}(\text{acac})_2(\text{PCy}_3)\}^+$
		479.2	19	-
		375.1	18	-

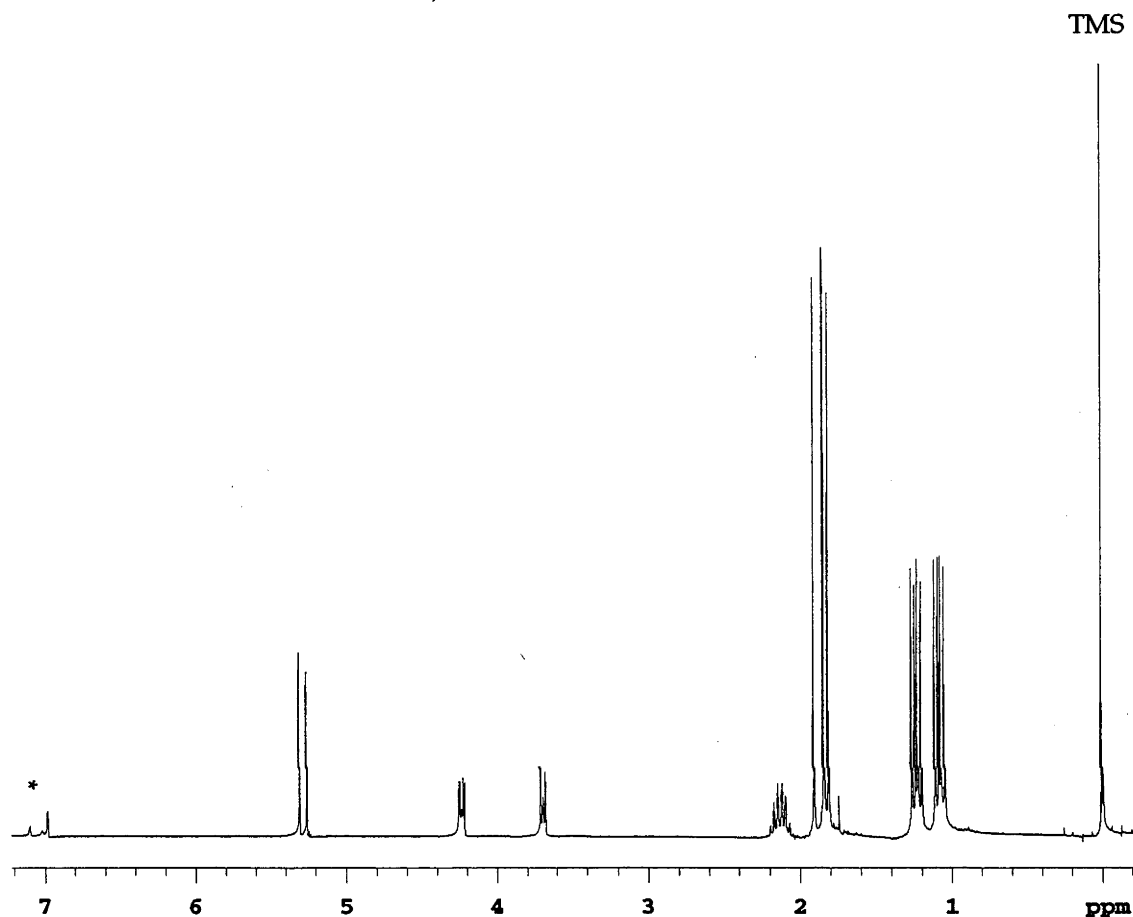
Table 2.8:  $^{13}\text{C}\{^1\text{H}\}$  and  $^{31}\text{P}\{^1\text{H}\}$  NMR spectral data of the mono-ethene phosphine complexes  $\text{cis-}[\text{Ru}(\text{acac})_2(\eta^2\text{-C}_2\text{H}_4)\text{L}]$ .

Compound	$^{13}\text{C}\{^1\text{H}\}$ NMR <sup>a</sup>				$^{31}\text{P}\{^1\text{H}\}$ NMR <sup>a</sup>
	$\text{CH}_3$ (acac)	CH (acac)	CO (acac)	Other	
$\text{cis-}[\text{Ru}(\text{acac})_2(\eta^2\text{-C}_2\text{H}_4)(\text{PPh}_3)]$	27.3, 28.0, 28.2, 28.3 (d, $J_{\text{PC}}$ 6.0 Hz)	98.9, 99.2	184.2, 185.8, 186.0, 186.8	69.3 ( $\text{C}_2\text{H}_4$ )	+54.7
$\text{cis-}[\text{Ru}(\text{acac})_2(\eta^2\text{-C}_2\text{H}_4)(\text{PPr}^i_3)]$	27.2, 27.5, 28.1 (d, $J_{\text{PC}}$ 5.6 Hz), 28.3	98.1, 99.8	184.7, 185.0, 185.5 (d, $J_{\text{PC}}$ 2.2 Hz), 187.7	19.4, 19.0 ( $\text{PCHCH}_3$ ); 24.8 (d, $J_{\text{PC}}$ 19 Hz, $\text{PCHCH}_3$ ); 69.6 ( $\text{C}_2\text{H}_4$ )	+50.5
$\text{cis-}[\text{Ru}(\text{acac})_2(\eta^2\text{-C}_2\text{H}_4)(\text{PCy}_3)]$	27.6, 27.7, 28.1 (d, $J_{\text{PC}}$ 5.6 Hz), 28.4	98.2, 99.8	184.5, 184.9, 185.6 (d, $J_{\text{PC}}$ 2.2 Hz), 187.7	27.2, 28.5, 28.6, 28.7, 28.9, 29.2 ( $\text{PCH}(\text{CH}_2)_5$ ); 35.4 (d, $J_{\text{PC}}$ 19 Hz, $\text{PCH}(\text{CH}_2)_5$ ); 69.5 ( $\text{C}_2\text{H}_4$ )	+40.0

a) measured in  $d_6$ -benzene; singlets unless otherwise indicated.

coordinating solvents, such as benzene or toluene, and presumably re-coordinates ethene to form *cis*-[Ru(acac)<sub>2</sub>(η<sup>2</sup>-C<sub>2</sub>H<sub>4</sub>)L].

**Figure 2.4:** <sup>1</sup>H NMR spectrum of the isolated complex *cis*-[Ru(acac)<sub>2</sub>(η<sup>2</sup>-C<sub>2</sub>H<sub>4</sub>)(PPr<sup>i</sup><sub>3</sub>)] (*d*<sub>8</sub>-toluene).



On a preparative scale, the addition of one equivalent of the tertiary phosphines PPh<sub>3</sub>, PPr<sup>i</sup><sub>3</sub> and PCy<sub>3</sub> to a solution of *cis*-[Ru(acac)<sub>2</sub>(η<sup>2</sup>-C<sub>2</sub>H<sub>4</sub>)<sub>2</sub>] in benzene (or toluene) resulted in a colour change from yellow to orange after several hours. In the case of the reaction of PPh<sub>3</sub>, the orange solid *trans*-[Ru(acac)<sub>2</sub>(PPh<sub>3</sub>)<sub>2</sub>] precipitated from solution, presumably having been formed as a result of disproportionation of initially formed *cis*-[Ru(acac)<sub>2</sub>(η<sup>2</sup>-C<sub>2</sub>H<sub>4</sub>)(PPh<sub>3</sub>)]. The reaction with the phosphines PPr<sup>i</sup><sub>3</sub> and PCy<sub>3</sub> affords the mono-ethene complexes as red crystalline and yellow microcrystalline solids, respectively, in yields of *ca.* 65 - 70%.

The most abundant ion peak detected in FAB mass spectra of the isolated complexes *cis*-[Ru(acac)<sub>2</sub>(η<sup>2</sup>-C<sub>2</sub>H<sub>4</sub>)(PR<sub>3</sub>)] (R= Pr<sup>i</sup>, Cy) corresponds to the molecular fragment [Ru(acac)<sub>2</sub>(PR<sub>3</sub>)]<sup>+</sup> (m/z 580.3 for R=Cy and 460.1 for R= Pr<sup>i</sup>). The peaks associated with the parent compound [Ru(acac)<sub>2</sub>(η<sup>2</sup>-C<sub>2</sub>H<sub>4</sub>)(PR<sub>3</sub>)] were not detected and peaks associated with the complexes [Ru(acac)<sub>2</sub>(PR<sub>3</sub>)<sub>2</sub>] were either not detected or were in very low abundance (see Table 2.7). For these complexes, it appears that the ethene ligand is only weakly coordinated to the metal centre. The IR spectra (KBr disc) of the solids display two strong broad bands in the region *ca.* 1583 and *ca.* 1514 cm<sup>-1</sup>, characteristic of bidentate, O-bonded acac.<sup>7</sup> The band due to the ν(C=C) frequency could not be detected, presumably being hidden by the intense bands of the acac ligands (see p. 35).

The <sup>1</sup>H and <sup>31</sup>P{<sup>1</sup>H} NMR spectra of the isolated solids were identical with those of *cis*-[Ru(acac)<sub>2</sub>(η<sup>2</sup>-C<sub>2</sub>H<sub>4</sub>)(PR<sub>3</sub>)] (R= Pr<sup>i</sup>, Cy) measured *in situ* (see p. 46 and 48). The <sup>13</sup>C{<sup>1</sup>H} NMR spectral data for the complexes *cis*-[Ru(acac)<sub>2</sub>(η<sup>2</sup>-C<sub>2</sub>H<sub>4</sub>)(PR<sub>3</sub>)] (R= Pr<sup>i</sup>, Cy) are shown in Table 2.8. A triplet at δ 69.6 in the gated <sup>13</sup>C NMR spectrum for *cis*-[Ru(acac)<sub>2</sub>(η<sup>2</sup>-C<sub>2</sub>H<sub>4</sub>)(PPr<sup>i</sup><sub>3</sub>)] has a C-H coupling constant of 160 Hz in the proton coupled spectrum and is assigned to the ethene carbon atoms. The <sup>31</sup>P{<sup>1</sup>H} NMR spectrum of *cis*-[Ru(acac)<sub>2</sub>(η<sup>2</sup>-C<sub>2</sub>H<sub>4</sub>)(PCy<sub>3</sub>)] in THF shows two singlets of equal intensity at δ 39.8 and 75.1 after *ca.* 48 hours (see p. 44 and 67).

#### 2.4 Solid State Structures of *trans*-[Ru(acac)<sub>2</sub>(η<sup>2</sup>-C<sub>2</sub>H<sub>4</sub>)(NC<sub>5</sub>H<sub>5</sub>)] and *cis*-[Ru(acac)<sub>2</sub>(η<sup>2</sup>-C<sub>2</sub>H<sub>4</sub>)L] (L = NH<sub>3</sub>, PPr<sup>i</sup><sub>3</sub>, PCy<sub>3</sub>)

The molecular structures of the complexes *trans*-[Ru(acac)<sub>2</sub>(η<sup>2</sup>-C<sub>2</sub>H<sub>4</sub>)(NC<sub>5</sub>H<sub>5</sub>)] and *cis*-[Ru(acac)<sub>2</sub>(η<sup>2</sup>-C<sub>2</sub>H<sub>4</sub>)L] (L = NH<sub>3</sub>, PPr<sup>i</sup><sub>3</sub>, PCy<sub>3</sub>) were confirmed by single crystal X-ray crystallography and are shown in Figures 2.5 - 2.8. In each case, the metal atom occupies the centre of a distorted octahedron. Selected metrical parameters for these complexes are shown in Tables 2.9 - 2.12. Crystal and refinement data of *trans*-[Ru(acac)<sub>2</sub>(η<sup>2</sup>-

$C_2H_4)(NC_5H_5)]$  and *cis*-[Ru(acac) $_2(\eta^2-C_2H_4)L]$  ( $L = NH_3, PPr^i_3, PCy_3$ ), together with the full set of interatomic distances and angles, are given in Appendices A.2 - A.5. Two crystallographically different molecules were found in the unit cell of *cis*-[Ru(acac) $_2(\eta^2-C_2H_4)(PPr^i_3)$ ].

The complexes *trans*-[Ru(acac) $_2(\eta^2-C_2H_4)(NC_5H_5)]$  and *cis*-[Ru(acac) $_2(\eta^2-C_2H_4)(PCy_3)]$  show disorder arising from two different orientations of the coordinated ethene in the crystal.

The Ru-O distances characterising the coordination of the acetylacetonato anion were usually found in the expected range of 2.05 - 2.08 Å, although a slight lengthening of up to *ca.* 0.03 Å was found for the Ru-O distances *trans* to the ethene ligand of *cis*-[Ru(acac) $_2(\eta^2-C_2H_4)(NH_3)]$  and the phosphorus atoms of *cis*-[Ru(acac) $_2(\eta^2-C_2H_4)(PR_3)]$  ( $R = Pr^i, Cy$ ). The Ru-N distances of *trans*-[Ru(acac) $_2(\eta^2-C_2H_4)(NC_5H_5)]$  and *cis*-[Ru(acac) $_2(\eta^2-C_2H_4)(NH_3)]$  were *ca.* 2.10 Å; the Ru-P distances of *cis*-[Ru(acac) $_2(\eta^2-C_2H_4)(PR_3)]$  ( $R = Pr^i, Cy$ ) were *ca.* 2.33 Å and differed by *ca.* 0.03 Å between the two complexes.

For all four structures, the carbon-carbon bond length of the coordinated ethene is only *ca.* 0.02 Å longer than the C=C bond length of free ethene (1.337(2) Å). The C=C vector for the ethene group of *cis*-[Ru(acac) $_2(\eta^2-C_2H_4)(NH_3)]$  eclipses the plane defined by the atoms Ru(1), O(2) and N(1), whereas for *cis*-[Ru(acac) $_2(\eta^2-C_2H_4)(PPr^i_3)]$ , the C=C vector eclipses the plane defined by the atoms Ru(1), O(1) and O(3). In the structures *trans*-[Ru(acac) $_2(\eta^2-C_2H_4)(NC_5H_5)]$  and *cis*-[Ru(acac) $_2(\eta^2-C_2H_4)(PCy_3)]$ , the C=C vectors for the mutually orthogonal orientations of the ethene groups eclipse the Ru-O bonds and, in the case of the tricyclohexylphosphine complex, the minor ethene conformation eclipses the plane defined by atoms Ru(1), P(1) and O(2). The Ru-C distances for these mono-ethene complexes range from *ca.* 2.15 Å for the ammine complex to *ca.* 2.19 Å for the minor conformer of the tricyclohexylphosphine complex.

**Figure 2.5:** ORTEP diagram of the molecular structure of *trans*-[Ru(acac)<sub>2</sub>(η<sup>2</sup>-C<sub>2</sub>H<sub>4</sub>)(C<sub>5</sub>H<sub>5</sub>N)] showing only the major conformation of the disordered ethene group.

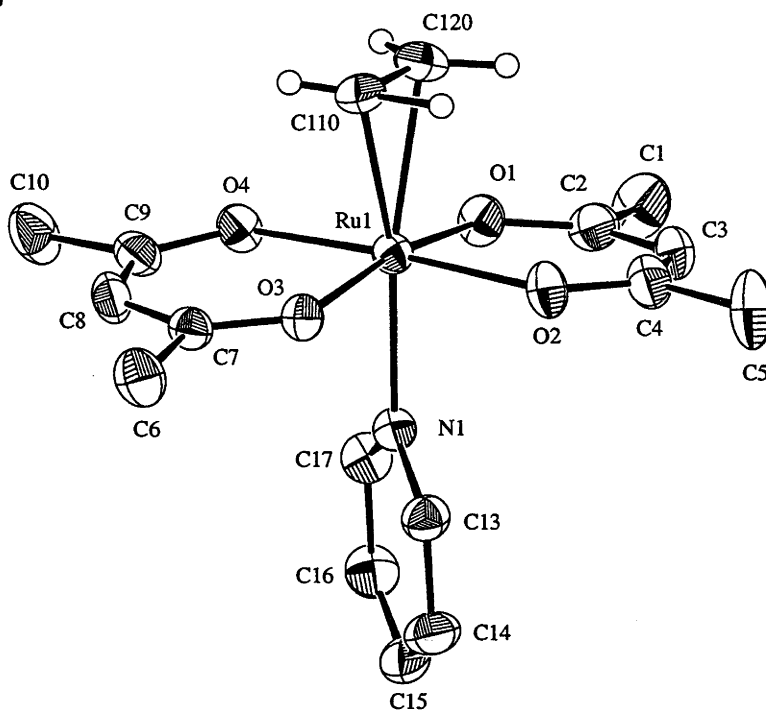


**Figure 2.6:** ORTEP diagram of the molecular structure of *cis*-[Ru(acac)<sub>2</sub>(η<sup>2</sup>-C<sub>2</sub>H<sub>4</sub>)(NH<sub>3</sub>)].

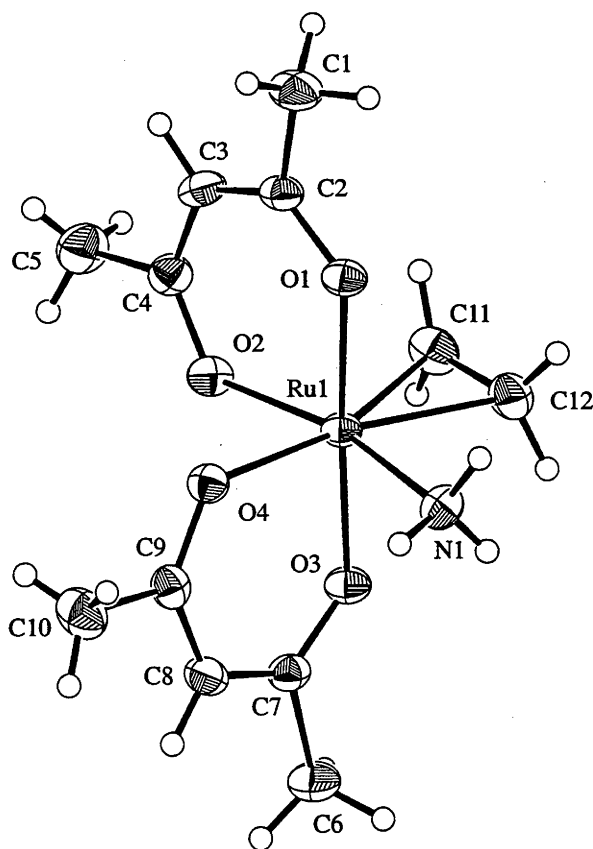




**Table 2.9:** Selected metrical parameters of *trans*-[Ru(acac)<sub>2</sub>(η<sup>2</sup>-C<sub>2</sub>H<sub>4</sub>)(C<sub>5</sub>H<sub>5</sub>N)].

Bond Distances (Å)			
Ru(1)-O(1)	2.054(2)	Ru(1)-C(111)	2.164(8)*
Ru(1)-O(2)	2.046(2)	Ru(1)-C(120)	2.179(5)
Ru(1)-O(3)	2.063(2)	Ru(1)-C(121)	2.179(8)*
Ru(1)-O(4)	2.051(2)	C(110)-C(111)	0.73(2)
Ru(1)-N(1)	2.095(3)	C(110)-C(120)	1.35(1)
Ru(1)-C(110)	2.171(5)	C(111)-C(121)	1.39(3)
Bond Angles (°)			
O(1)-Ru(1)-O(2)	93.58(9)	O(3)-Ru(1)-N(1)	85.78(9)
O(1)-Ru(1)-O(3)	169.72(9)	O(4)-Ru(1)-N(1)	88.2(1)
O(1)-Ru(1)-O(4)	85.65(9)	C(110)-Ru(1)-C(120)	36.1(3)
O(1)-Ru(1)-N(1)	83.96(9)	C(111)-Ru(1)-C(121)	37.3(7)
O(2)-Ru(1)-O(3)	86.76(8)	N(1)-Ru(1)-C(110)	163.2(2)
O(2)-Ru(1)-O(4)	176.22(9)	N(1)-Ru(1)-C(111)	165.8(5)
O(2)-Ru(1)-N(1)	88.0(1)	N(1)-Ru(1)-C(120)	160.6(2)
O(3)-Ru(1)-O(4)	93.34(8)	N(1)-Ru(1)-C(121)	156.7(5)

\*) restrained during refinement.

**Table 2.10:** Selected metrical parameters of *cis*-[Ru(acac)<sub>2</sub>(η<sup>2</sup>-C<sub>2</sub>H<sub>4</sub>)(NH<sub>3</sub>)].

Bond Distances (Å)			
Ru(1)-O(1)	2.052(2)	Ru(1)-C(12)	2.151(3)
Ru(1)-O(2)	2.066(2)	C(11)-C(12)	1.356(4)
Ru(1)-O(3)	2.048(2)	C(11)-H(18)	0.94(3)
Ru(1)-O(4)	2.092(2)	C(11)-H(19)	1.06(3)
Ru(1)-N(1)	2.108(2)	C(12)-H(20)	0.96(3)
Ru(1)-C(11)	2.147(3)	C(12)-H(21)	0.97(3)
Bond Angles (°)			
O(1)-Ru(1)-O(2)	93.07(6)	N(1)-Ru(1)-C(12)	79.2(1)
O(1)-Ru(1)-O(3)	176.67(6)	Ru(1)-C(11)-H(18)	110(2)
O(1)-Ru(1)-O(4)	88.28(6)	Ru(1)-C(11)-H(19)	110(2)
O(1)-Ru(1)-N(1)	89.74(8)	C(12)-C(11)-H(18)	121(2)
O(2)-Ru(1)-O(3)	90.18(6)	C(12)-C(11)-H(19)	119(1)
O(2)-Ru(1)-O(4)	83.68(6)	H(18)-C(11)-H(19)	115(2)
O(2)-Ru(1)-N(1)	165.43(8)	Ru(1)-C(12)-H(20)	113(2)
O(3)-Ru(1)-O(4)	92.79(6)	Ru(1)-C(12)-H(21)	109(2)
O(3)-Ru(1)-N(1)	87.29(7)	C(11)-C(12)-H(20)	125(2)
O(4)-Ru(1)-N(1)	82.12(8)	C(11)-C(12)-H(21)	118(2)
C(11)-Ru(1)-C(12)	36.8(1)	H(20)-C(12)-H(21)	111(3)
N(1)-Ru(1)-C(11)	116.0(1)		

Figure 2.7: ORTEP diagram of *cis*-[Ru(acac)<sub>2</sub>(η<sup>2</sup>-C<sub>2</sub>H<sub>4</sub>)(PPri<sub>3</sub>)].

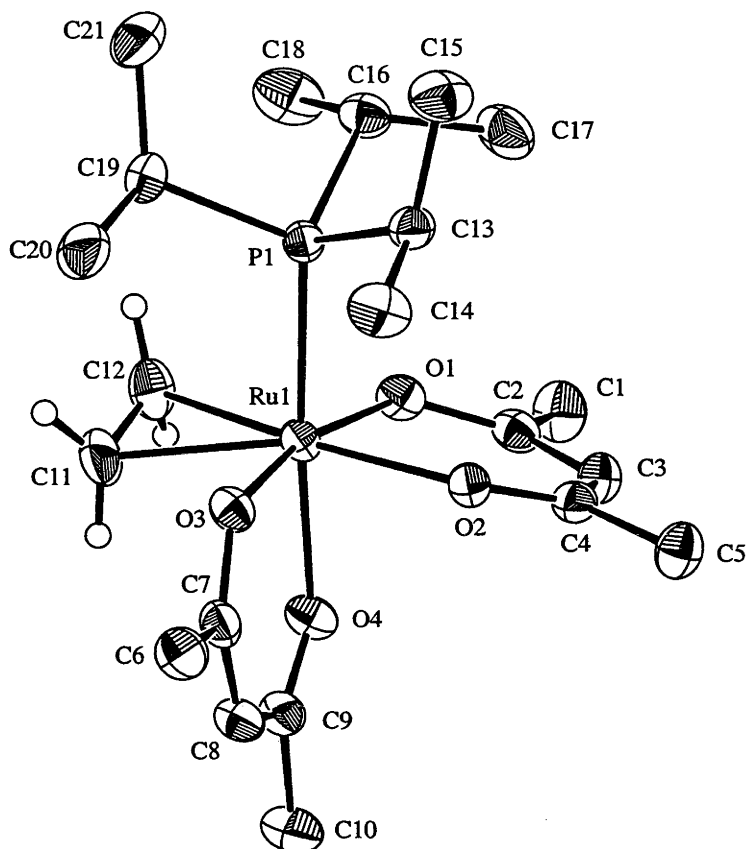
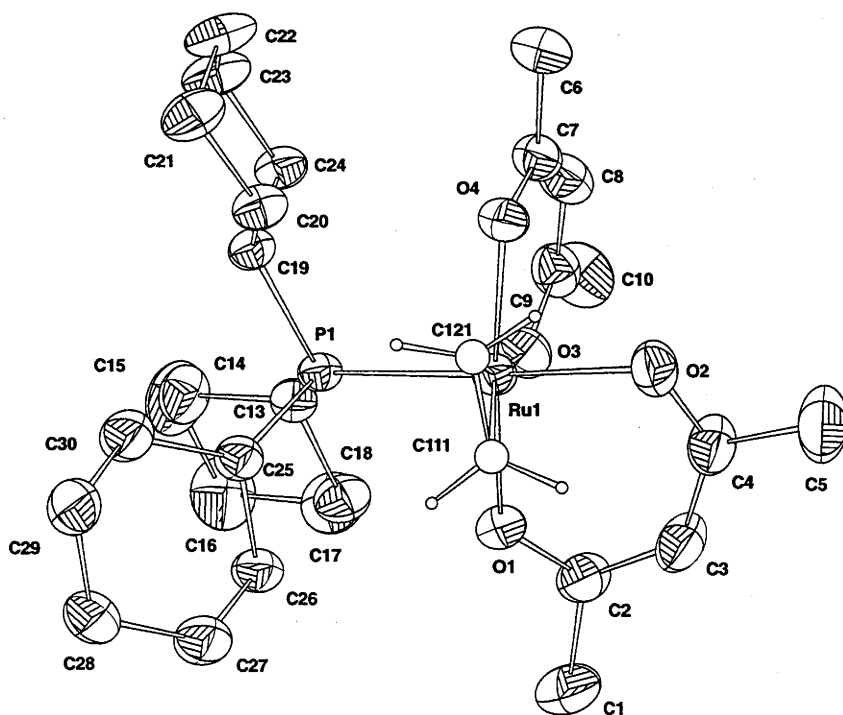


Figure 2.8: ORTEP diagram of the molecular structure of *cis*-[Ru(acac)<sub>2</sub>(η<sup>2</sup>-C<sub>2</sub>H<sub>4</sub>)(PCy<sub>3</sub>)] showing only the major conformation of the disordered ethene group.



**Table 2.11:** Selected metrical parameters of *cis*-[Ru(acac)<sub>2</sub>(η<sup>2</sup>-C<sub>2</sub>H<sub>4</sub>)(PPri<sub>3</sub>)]

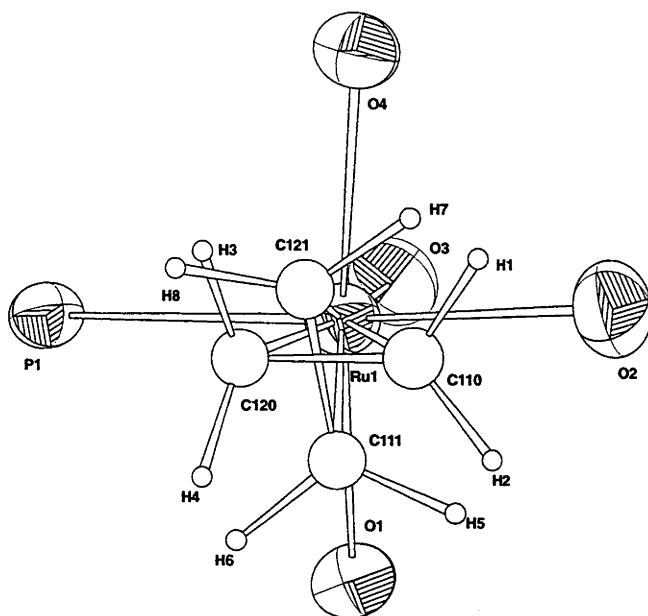
Bond Distances (Å)			
Ru(1)-O(1)	2.079(3)	Ru(2)-O(5)	2.082(3)
Ru(1)-O(2)	2.077(3)	Ru(2)-O(6)	2.079(3)
Ru(1)-O(3)	2.071(3)	Ru(2)-O(7)	2.064(3)
Ru(1)-O(4)	2.094(3)	Ru(2)-O(8)	2.089(3)
Ru(1)-P(1)	2.321(1)	Ru(2)-P(2)	2.322(1)
Ru(1)-C(11)	2.172(5)	Ru(2)-C(32)	2.180(6)
Ru(1)-C(12)	2.181(5)	Ru(2)-C(33)	2.185(5)
C(11)-C(12)	1.350(9)	C(32)-C(33)	1.350(9)
Bond Angles (°)			
O(1)-Ru(1)-O(2)	89.1(1)	O(5)-Ru(2)-O(6)	89.5(1)
O(1)-Ru(1)-O(3)	167.4(1)	O(5)-Ru(2)-O(7)	168.1(1)
O(1)-Ru(1)-O(4)	81.4(1)	O(5)-Ru(2)-O(8)	81.4(1)
O(1)-Ru(1)-P(1)	95.68(9)	O(5)-Ru(2)-P(2)	95.93(9)
O(2)-Ru(1)-O(3)	79.9(1)	O(6)-Ru(2)-O(7)	80.3(1)
O(2)-Ru(1)-O(4)	85.4(1)	O(6)-Ru(2)-O(8)	84.7(1)
O(2)-Ru(1)-P(1)	91.63(9)	O(6)-Ru(2)-P(2)	91.14(9)
O(3)-Ru(1)-O(4)	91.6(1)	O(7)-Ru(2)-O(8)	91.5(1)
O(3)-Ru(1)-P(1)	90.70(9)	O(7)-Ru(2)-P(2)	90.48(9)
O(4)-Ru(1)-P(1)	175.9(1)	O(8)-Ru(2)-P(2)	175.01(9)
C(11)-Ru(1)-C(12)	36.1(2)	C(32)-Ru(2)-C(33)	36.0(2)
P(1)-Ru(1)-C(11)	99.7(2)	P(2)-Ru(2)-C(32)	100.5(2)
P(1)-Ru(1)-C(12)	91.3(2)	P(2)-Ru(2)-C(33)	91.0(2)

**Table 2.12:** Selected metrical parameters of *cis*-[Ru(acac)<sub>2</sub>(η<sup>2</sup>-C<sub>2</sub>H<sub>4</sub>)(PCy<sub>3</sub>)]

Bond Distances (Å)			
Ru(1)-O(1)	2.06(2)	Ru(1)-C(121)	2.148(2)
Ru(1)-O(2)	2.10(2)	C(110)-C(111)*	1.005
Ru(1)-O(3)	2.07(2)	C(110)-C(120)*	1.344
Ru(1)-O(4)	2.074(18)	C(110)-C(121)*	0.987
Ru(1)-P(1)	2.356(7)	C(111)-(C120)*	1.097
Ru(1)-C(110)	2.167(2)	C(111)-C(121)*	1.356
Ru(1)-C(120)	2.151(2)	C(120)-C(121)*	0.738
Ru(1)-C(111)	2.190(2)		
Bond Angles (°)			
O(1)-Ru(1)-O(2)	90.9(7)	O(3)-Ru(1)-P(1)	89.2(5)
O(1)-Ru(1)-O(3)	89.2(5)	O(4)-Ru(1)-P(1)	94.4(5)
O(1)-Ru(1)-O(4)	173.1(7)	C(110)-Ru(1)-C(120)	35.93(3)
O(1)-Ru(1)-P(1)	90.2(5)	P(1)-Ru(1)-C(110)	116.33(15)
O(2)-Ru(1)-O(3)	82.9(7)	P(1)-Ru(1)-C(120)	80.40(15)
O(2)-Ru(1)-O(4)	83.9(7)	C(111)-Ru(1)-C(121)	36.78(3)
O(2)-Ru(1)-P(1)	172.0(6)	P(1)-Ru(1)-C(111)	99.29(15)
O(3)-Ru(1)-O(4)	90.2(7)	P(1)-Ru(1)-C(121)	93.92(15)

\*) the atoms C(110), C(111), C(120) and C(121) were restrained during refinement.

**Figure 2.9:** ORTEP diagram of *cis*-[Ru(acac)<sub>2</sub>(η<sup>2</sup>-C<sub>2</sub>H<sub>4</sub>)(PCy<sub>3</sub>)] showing both conformations of the ethene ligand.



The hydrogen atoms of the ethene groups for the complexes *cis*-[Ru(acac)<sub>2</sub>(η<sup>2</sup>-C<sub>2</sub>H<sub>4</sub>)(NH<sub>3</sub>)] and *cis*-[Ru(acac)<sub>2</sub>(η<sup>2</sup>-C<sub>2</sub>H<sub>4</sub>)(PPr<sup>*i*</sup><sub>3</sub>)] were located in the difference maps and are included in the full crystallographic data in Appendices A.3 and A.4. As the ethene ligands of *trans*-[Ru(acac)<sub>2</sub>(η<sup>2</sup>-C<sub>2</sub>H<sub>4</sub>)(NC<sub>5</sub>H<sub>5</sub>)] and *cis*-[Ru(acac)<sub>2</sub>(η<sup>2</sup>-C<sub>2</sub>H<sub>4</sub>)(PCy<sub>3</sub>)] are disordered the ethene hydrogen atoms have been restrained during the refinement and have not been included.

The ethene ligands of the complexes *trans*-[Ru(acac)<sub>2</sub>(η<sup>2</sup>-C<sub>2</sub>H<sub>4</sub>)(NC<sub>5</sub>H<sub>5</sub>)] and *cis*-[Ru(acac)<sub>2</sub>(η<sup>2</sup>-C<sub>2</sub>H<sub>4</sub>)(PCy<sub>3</sub>)] occupy two mutually orthogonal orientations which eclipse the remaining bonds about the metal. The relative occupancies for the two ethene conformations defined by the atoms C(110) - C(120) and C(111) - C(121) are *ca.* 0.735(6) and 0.265(6) for *trans*-[Ru(acac)<sub>2</sub>(η<sup>2</sup>-C<sub>2</sub>H<sub>4</sub>)(NC<sub>5</sub>H<sub>5</sub>)] and *ca.* 0.44(4) and 0.55(4) for *cis*-[Ru(acac)<sub>2</sub>(η<sup>2</sup>-C<sub>2</sub>H<sub>4</sub>)(PCy<sub>3</sub>)], respectively.

X-ray diffraction is not a suitable technique to determine whether the disorder of the ethene ligand in *cis*-[Ru(acac)<sub>2</sub>(η<sup>2</sup>-C<sub>2</sub>H<sub>4</sub>)(PCy<sub>3</sub>)] is static or

dynamic in nature. Possible dynamic processes include a full rotation ( $180^\circ$  jumps) of the ethene ligand or a half rotation ( $90^\circ$  jumps) followed by another half rotation in either direction to give the original conformation or the equivalent of a full rotation. Ethene rotation has been observed for the complex  $[\text{Rh}(\text{acac})(\eta^2\text{-C}_2\text{H}_4)_2]$  and  $[\text{Rh}(\text{acac})(\eta^2\text{-C}_2\text{D}_4)_2]$  in the solid state by  $^1\text{H}$ ,  $^{13}\text{C}\{^1\text{H}\}$  and  $^2\text{H}$  NMR spectroscopic techniques.<sup>20</sup>

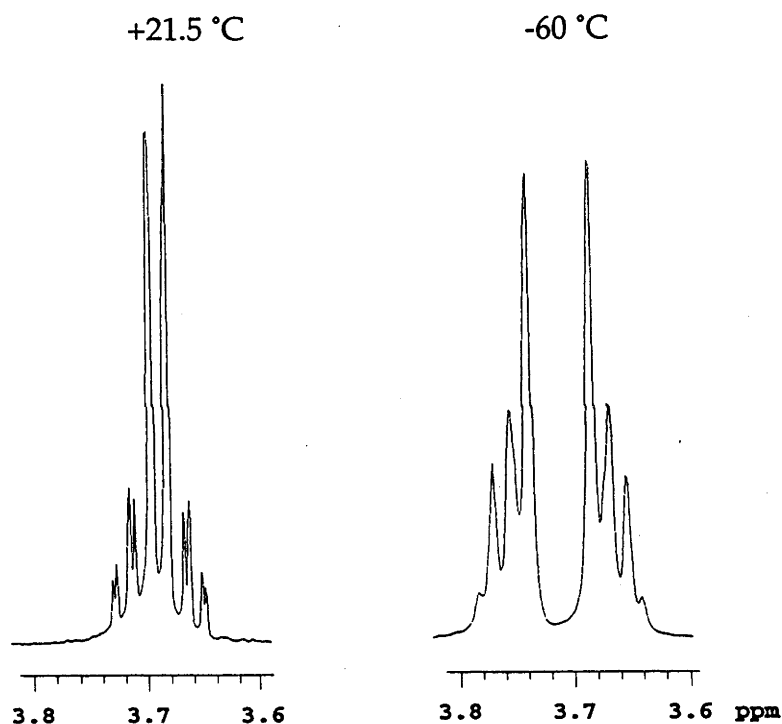
### 2.5 Variable temperature NMR spectroscopy of the complexes *cis*- $[\text{Ru}(\text{acac})_2(\eta^2\text{-C}_2\text{H}_4)\text{L}]$ ( $\text{L} = \text{C}_2\text{H}_4, \text{SbPh}_3, \text{PPr}^i_3$ and $\text{PCy}_3$ )

The  $^1\text{H}$  and  $^{13}\text{C}\{^1\text{H}\}$  NMR spectra of coordinated ethene in solutions of the complexes *cis*- $[\text{Ru}(\text{acac})_2(\eta^2\text{-C}_2\text{H}_4)\text{L}]$  ( $\text{L} = \text{C}_2\text{H}_4, \text{SbPh}_3, \text{PPr}^i_3, \text{PCy}_3$  at room temperature are less complicated than would be expected on the basis of the static structures shown in Figures 2.3 and 2.6–2.8. For the mono-ethene complexes, if rotation about the  $\text{Ru}\text{-C}_2\text{H}_4$  axis were slow, one would expect four  $^1\text{H}$  and two  $^{13}\text{C}\{^1\text{H}\}$  NMR resonances, and these numbers could be doubled for the bis(ethene) complex.

The  $^1\text{H}$  NMR spectrum of *cis*- $[\text{Ru}(\text{acac})_2(\eta^2\text{-C}_2\text{H}_4)_2]$  at room temperature shows an 8 H-resonance for the ethene protons in the form of a symmetrical AA'BB' multiplet. The non-equivalence is presumably induced by the chiral *cis*- $[\text{Ru}(\text{acac})_2]$  moiety, since a similar pattern has been reported for the ethene protons of the chiral platinum(II) complexes  $[\text{Pt}(\eta^2\text{-C}_2\text{H}_4)\{\textit{cis}\text{-}1\text{-(N=CHC}_6\text{H}_4\text{)-}2\text{-(N=CHPh)C}_6\text{H}_{10}\}][\text{BF}_4]$  and  $[\text{Pt}(\eta^2\text{-C}_2\text{H}_4)\{\textit{trans}\text{-}1\text{-(N=CHC}_6\text{H}_4\text{)-}2\text{-(N=CHPh)C}_6\text{H}_{10}\}][\text{BF}_4]$ .<sup>21</sup> The two halves of the multiplet move apart and broaden slightly on cooling to  $-60^\circ\text{C}$ , as illustrated in Figure 2.10. The variation in the chemical shift (in Hz) between the inner lines of the ethene multiplet between  $-90^\circ\text{C}$  and  $+50^\circ\text{C}$  is shown in Table 2.13 and represented graphically in Figure 2.11. The appearance of the spectrum is unaffected by the presence of free ethene (*ca.* 1 bar) at room temperature. In the  $^{13}\text{C}\{^1\text{H}\}$  NMR

there is a single, sharp resonance due to coordinated ethene between  $-95\text{ }^{\circ}\text{C}$  and  $21.5\text{ }^{\circ}\text{C}$ . The observations are consistent with rapid rotation of the ethene ligands about the Ru-C<sub>2</sub>H<sub>4</sub> axis, which equilibrates, separately, the mutually *trans*-protons and the two carbon atoms in each ethene unit. Thus, the two ethene multiplets are assigned to the inner and outer protons, as in the cases of [Rh(acac)( $\eta^2$ -C<sub>2</sub>H<sub>4</sub>)<sub>2</sub>],<sup>6,22</sup> [CpRh( $\eta^2$ -C<sub>2</sub>H<sub>4</sub>)<sub>2</sub>],<sup>12</sup> and the platinum(II) complexes mentioned above.<sup>21</sup>

**Figure 2.10:** The temperature dependence of the ethene multiplet in the <sup>1</sup>H NMR spectrum of *cis*-[Ru(acac)<sub>2</sub>( $\eta^2$ -C<sub>2</sub>H<sub>4</sub>)<sub>2</sub>] in *d*<sub>8</sub>-toluene.



The <sup>1</sup>H and <sup>13</sup>C{<sup>1</sup>H} NMR spectra of *cis*-[Ru(acac)<sub>2</sub>( $\eta^2$ -C<sub>2</sub>H<sub>4</sub>)L] (L = SbPh<sub>3</sub>, PPr<sup>i</sup><sub>3</sub>, PCy<sub>3</sub>) are generally similar to those of the bis(ethene) complex except that at low temperature the <sup>1</sup>H multiplets broaden into two featureless peaks. The isopropyl methyl and methine carbon resonances of the PPr<sup>i</sup><sub>3</sub> complex also broaden considerably at low temperature, possibly owing to slowed rotation of the isopropyl groups.

Gradual heating of a d<sub>8</sub>-toluene solution of *cis*-[Ru(acac)<sub>2</sub>(η<sup>2</sup>-C<sub>2</sub>H<sub>4</sub>)<sub>2</sub>] to *ca.* +95 °C, under an argon atmosphere, results in the convergence of both ethene multiplets to a broad singlet at δ(<sup>1</sup>H) 3.64. Some decomposition occurs at temperatures higher than *ca.* +60 °C as shown by the appearance of several new peaks of low intensity in the <sup>1</sup>H NMR spectrum at δ 5.40, 5.24, 4.99, 2.32, 1.73 and 1.55. These resonances remain when the sample is allowed to cool to room temperature. The nature of the species giving rise to these new signals has not been investigated.

In the presence of free ethene, however, no decomposition of *cis*-[Ru(acac)<sub>2</sub>(η<sup>2</sup>-C<sub>2</sub>H<sub>4</sub>)<sub>2</sub>] was observed. Both ethene multiplets again slowly converge to a broad singlet with a coalescence temperature of 80 ± 5 °C; the signal due to free ethene remains sharp at δ 5.24 at this temperature, which suggests that exchange with coordinated ethene is not occurring rapidly on the NMR timescale. A full line-shape analysis would be required to obtain rate data for the process that equilibrates the ethene resonances. The complexity of the spin system does not allow use of the standard equation  $k_r = \pi(\Delta\nu)/(2)^{1/2}$  <sup>23</sup> at coalescence, where Δν is the chemical shift difference (in Hz) between the resonances in the absence of a dynamic process. Also, this approximate equation assumes that the line-width of the exchanging resonances is negligible compared to the chemical shift separation, which is not the case here.

At *ca.* 90 °C broadening of the <sup>1</sup>H NMR resonances of the ethene and methyl acac resonances becomes evident and this effect continues to the highest accessible temperature of *ca.* 105 °C (probe). The broadening of the methyl acac proton resonances is shown in Figure 2.12. The signal due to free

ethene also broadens and shifts upfield, which suggests that exchange between free and coordinated ethene is now occurring rapidly on the NMR timescale.

**Table 2.13:** Variation in the chemical shift (in Hertz) between the inner lines of the ethene multiplet for *cis*-[Ru(acac)<sub>2</sub>(η<sup>2</sup>-C<sub>2</sub>H<sub>4</sub>)<sub>2</sub>] with temperature (K).

Temperature (K)	Δν (Hertz)
183.0	26.4
213.0	16.5
240.5	11.1
268.0	7.8
294.5	4.5
304.5	3.6
324.0	2.7

**Figure 2.11:** Plot of Temperature (K) *vs* the difference in the chemical shift of the inner most lines for *cis*-[Ru(acac)<sub>2</sub>(η<sup>2</sup>-C<sub>2</sub>H<sub>4</sub>)<sub>2</sub>] (in Hertz).

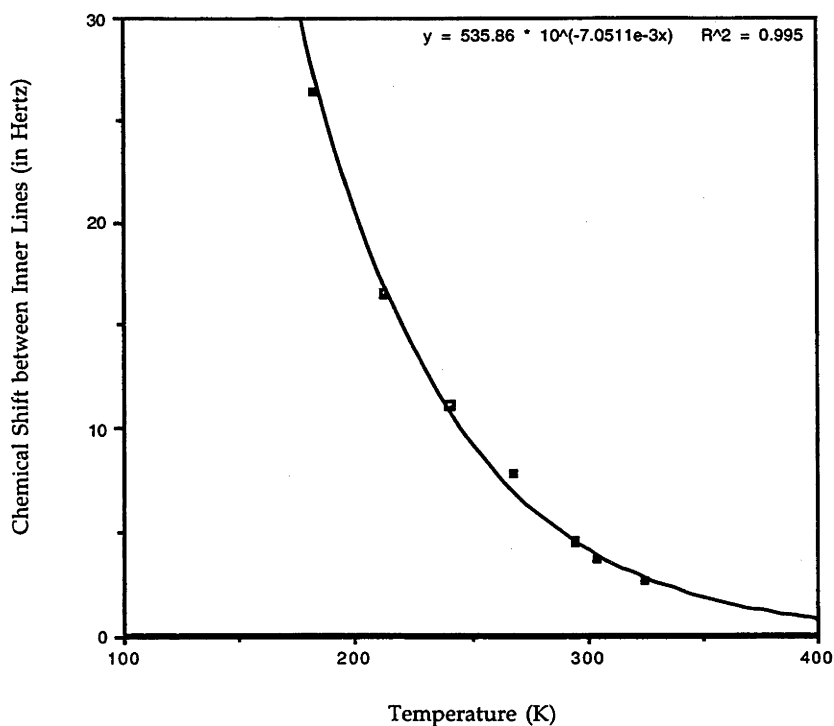
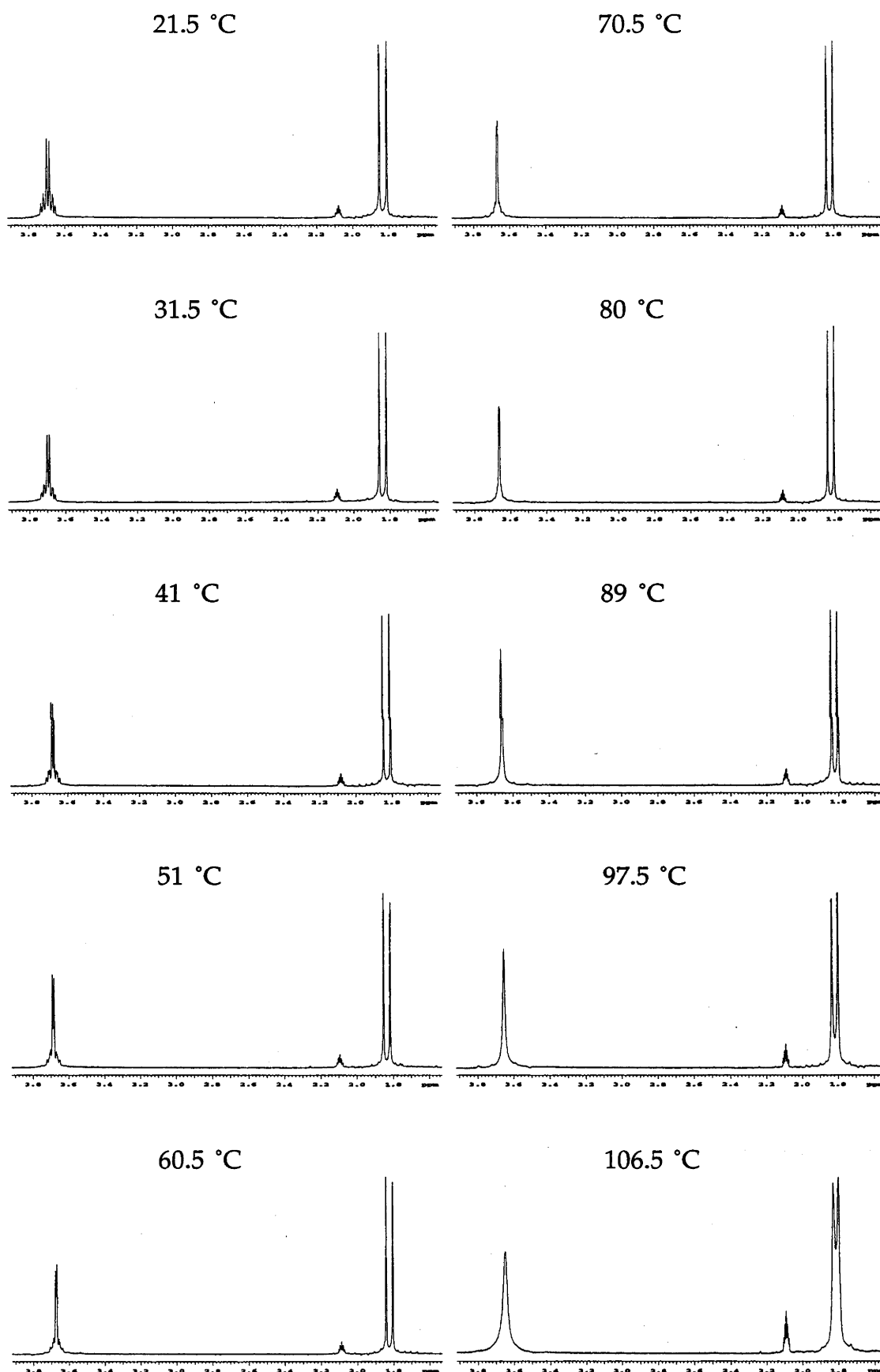




**Figure 2.12:** Variable temperature  $^1\text{H}$  NMR spectra for the ethene and methyl acac resonances of *cis*-[Ru(acac) $_2$ ( $\eta^2$ -C $_2$ H $_4$ ) $_2$ ] in *d* $_8$ -toluene.\*



\*) the multiplet at  $\delta$  2.09 is due to the residual methyl proton resonances of *d* $_8$ -toluene

The exchange between free and coordinated ethene is probably dissociative and takes place via the five-coordinate species  $[\text{Ru}(\text{acac})_2(\eta^2\text{-C}_2\text{H}_4)]$  (see discussion). The rate of exchange for this process may be estimated from the linewidths of the acac methyl resonances by the use of the equation<sup>21</sup>:

$$k_r = \pi[\omega_{1/2} - (\omega_{1/2})_0] \text{ (in Hertz) Eq. 2.4}$$

where  $\omega_{1/2}$  is the linewidth of the resonance at the onset of the dynamic process and  $(\omega_{1/2})_0$  is the linewidth of the same resonance in the absence of the dynamic process. For the methyl acac resonances in *cis*- $[\text{Ru}(\text{acac})_2(\eta^2\text{-C}_2\text{H}_4)_2]$ ,  $(\omega_{1/2})_0$  was estimated to be 1.18 Hz whereas  $\omega_{1/2}$  has a value of 2.52 Hz at *ca.* 80 °C. From Eq. 2.1, the rate for this process was calculated to be 4.2 Hz with an activation energy of *ca.* 83 kJ mol<sup>-1</sup> at 80 °C. One condition for the use of Eq. 2.4 is that the observed broadening of the signals is in the slow exchange range.<sup>21</sup> Thus, this equation is valid only for the early stages of broadening of the resonance and cannot be used at or near the coalescence temperature where exchange is fast. Large errors are to be expected in the measurement of two rather small linewidths and in addition to the previously mentioned errors associated with temperature (see p. 58).<sup>21</sup>

It seems likely that the process causing the broadening of the acac proton signals is also responsible for the coalescence of the ethene multiplets. It must be emphasised here that the calculated value for the free energy of activation is only a crude estimate and is associated with probable errors of *ca.* 2–3 kJ mol<sup>-1</sup>; more precise measurements have not been undertaken. The most likely explanation for the dynamic behaviour observed is that one of the coordinated ethene ligands dissociates reversibly at higher temperatures. The ethene signals coalesce because their chemical shift difference is less than that of the methyl acac resonances. Evidence for ethene dissociation was found for  $[\text{Rh}(\text{2'-acetylphenoxy-O,O}')(\eta^2\text{-C}_2\text{H}_4)_2]$ <sup>24</sup>, and the same process may also

No page 63

account for the observed broadening of the acac resonances at high temperatures for  $[\text{Rh}(\text{acac})(\eta^2\text{-C}_2\text{H}_4)(\eta^2\text{-C}_2(\text{OMe})_4)]$  and  $[\text{Rh}(\text{acac})(\eta^2\text{-cis-C}_2\text{H}_2(\text{OMe})_2)]$ .<sup>22</sup> The  $\Delta G^\ddagger$  value for ethene dissociation varies between 41 and 58 kJ mol<sup>-1</sup> for a series of  $[\text{Rh}(\beta\text{-diketonato})(\eta^2\text{-C}_2\text{H}_4)(\eta^2\text{-alkene})]$  (alkene = C<sub>2</sub>H<sub>4</sub>, 2,4-dimethoxy-2-butene).<sup>22,24</sup>

### 2.6 Reactions of *cis*- $[\text{Ru}(\text{acac})_2(\eta^2\text{-alkene})_2]$ with two equivalents of bulky tertiary phosphines

The addition of two equivalents of triisopropylphosphine, PPr<sup>*i*</sup><sub>3</sub>, to a THF solution of *cis*- $[\text{Ru}(\text{acac})_2(\eta^2\text{-alkene})_2]$  (alkene = C<sub>2</sub>H<sub>4</sub>, C<sub>8</sub>H<sub>14</sub>) at room temperature leads to the formation of the complex *cis*- $[\text{Ru}(\text{acac})_2(\text{PPr}^i_3)_2]$ , which has been prepared previously from the reaction of two equivalents of PPr<sup>*i*</sup><sub>3</sub> with *cis*- $[\text{Ru}(\text{acac})_2(\text{SbPr}^i_3)_2]$  or by the reduction of  $[\text{Ru}(\text{acac})_3]$  with Zn/Hg in the presence of PPr<sup>*i*</sup><sub>3</sub>.<sup>11</sup> The <sup>1</sup>H, <sup>13</sup>C{<sup>1</sup>H} and <sup>31</sup>P{<sup>1</sup>H} NMR spectral data obtained here agree with the reported spectral data (see Table 2.14 and 2.15). There was no reaction between PBu<sup>*t*</sup><sub>3</sub> and *cis*- $[\text{Ru}(\text{acac})_2(\eta^2\text{-alkene})_2]$  (alkene = C<sub>2</sub>H<sub>4</sub>, C<sub>8</sub>H<sub>14</sub>) in hot THF detected by <sup>31</sup>P{<sup>1</sup>H} NMR spectroscopy. However, the reaction of *cis*- $[\text{Ru}(\text{acac})_2(\eta^2\text{-C}_8\text{H}_{14})_2]$  in cold THF (*ca.* -40 to -25 °C) with PPr<sup>*i*</sup><sub>3</sub> results in the formation of the moderately air-stable, rust-red complex *trans*- $[\text{Ru}(\text{acac})_2(\text{PPr}^i_3)_2]$  in a yield of *ca.* 40 - 60%. Under the same conditions, the bis(ethene) complex *cis*- $[\text{Ru}(\text{acac})_2(\eta^2\text{-C}_2\text{H}_4)_2]$  does not afford a solid on treatment with PPr<sup>*i*</sup><sub>3</sub> in cold THF after one hour, indicating that ethene is less easily displaced than cyclooctene. Warming a solution of

**Table 2.14:**  $^1\text{H}$  and  $^{13}\text{C}\{^1\text{H}\}$  NMR spectral parameters for the  $[\text{Ru}(\text{acac})_2]$  moiety in the bulky bis(phosphine) complexes  $[\text{Ru}(\text{acac})_2(\text{L})_2]$ .

Complex	$^1\text{H}$ NMR <sup>a</sup>		$^{13}\text{C}\{^1\text{H}\}$ NMR <sup>a</sup>		Solvent	
	$\delta\text{CH}_3$	$\delta\text{CH}$	$\delta\text{CH}_3$	$\delta\text{CH}$		$\delta\text{CO}$
<i>trans</i> - $[\text{Ru}(\text{acac})_2(\text{PPr}^i_3)_2]$	1.75	5.10	27.4	100.5	184.1	$\text{C}_6\text{D}_5\text{CD}_3^b$
<i>cis</i> - $[\text{Ru}(\text{acac})_2(\text{PPr}^i_3)_2]$	1.78, 1.91	5.30	27.8, 27.9	99.8	183.6, 186.8	$\text{C}_6\text{D}_6$
$[\text{Ru}(\text{acac})_2(\text{PCy}_3)_2]$	1.82, 1.94	5.28	27.7 (d, $J_{\text{PC}} = 2.2$ Hz), 28.0	100.3	183.5, 186.7	$\text{C}_6\text{D}_5\text{CD}_3$

a) singlets unless otherwise indicated.

**Table 2.15:**  $^1\text{H}$ ,  $^{13}\text{C}\{^1\text{H}\}$  and  $^{31}\text{P}\{^1\text{H}\}$  NMR spectral parameters for the tertiary phosphines in the bulky bis(phosphine) complexes  $[\text{Ru}(\text{acac})_2\text{L}_2]$ .

Complex	$^1\text{H}$ NMR <sup>a</sup>		$^{13}\text{C}\{^1\text{H}\}$ NMR <sup>a</sup>		$^{31}\text{P}\{^1\text{H}\}$ NMR <sup>a</sup>	Solvent
	$\delta$	Assignment	$\delta$	Assignment		
<i>trans</i> - $[\text{Ru}(\text{acac})_2(\text{PPr}^i_3)_2]$	1.32 (br)	$\text{CHCH}_3$	20.0 (br)	$\text{CHCH}_3$	+29.6	$\text{C}_6\text{D}_5\text{CD}_3^b$
	2.30 (br)	$\text{CHCH}_3$	24.8 (br)	$\text{CHCH}_3$		
<i>cis</i> - $[\text{Ru}(\text{acac})_2(\text{PPr}^i_3)_2]$	1.24, 1.37 (36 H, both dd, $J_{\text{PH}} 11$ Hz, $J_{\text{HH}} 7.2$ Hz)	$\text{CHCH}_3$	27.6 (d, $J_{\text{PC}} = 9$ Hz)	$\text{CHCH}_3$	+47.7	$\text{C}_6\text{D}_6$
	2.46 (6 H, m)	$\text{CHCH}_3$	38.0 (br)	$\text{CHCH}_3$		
$[\text{Ru}(\text{acac})_2(\text{PCy}_3)_2]$	1.15 - 1.45, 1.60 - 2.10, 2.20 - 2.40	$\text{CH}_2$ , $\text{CH}$	27.5, 29.1 (m), 30.2 (br)	$\text{CH}_2$	+38.5 (vb)	$\text{C}_6\text{D}_5\text{CD}_3$
			38.0 (br)	$\text{CH}$		

a) singlets unless otherwise indicated; b) recorded at  $-40$  °C to prevent *trans* to *cis* isomerisation.

*trans*-[Ru(acac)<sub>2</sub>(PPr<sup>*i*</sup><sub>3</sub>)<sub>2</sub>] in d<sub>8</sub>-toluene from *ca.* -35 °C to *ca.* -5 °C forms *cis*-[Ru(acac)<sub>2</sub>(PPr<sup>*i*</sup><sub>3</sub>)<sub>2</sub>] as shown by <sup>31</sup>P{<sup>1</sup>H} and <sup>1</sup>H NMR spectroscopy. A similar facile *trans*- to *cis*-isomerization has been recently observed for the complex [Ru(acac)<sub>2</sub>(PPh<sub>2</sub><sup>*t*</sup>Bu)<sub>2</sub>].<sup>28</sup>

The <sup>1</sup>H, <sup>13</sup>C{<sup>1</sup>H} and <sup>31</sup>P{<sup>1</sup>H} NMR spectral data of *trans*-[Ru(acac)<sub>2</sub>(PPr<sup>*i*</sup><sub>3</sub>)<sub>2</sub>], recorded at *ca.* -35 °C, are shown in Tables 2.14 - 15. The resonances assigned to the methyl and methine protons of the isopropyl groups are broad at this temperature.

The <sup>31</sup>P{<sup>1</sup>H} NMR spectrum of *cis*-[Ru(acac)<sub>2</sub>(PPr<sup>*i*</sup><sub>3</sub>)<sub>2</sub>] in THF shows three singlets at δ +87.2, +47.6 and +19.9, the latter two peaks are clearly due to *cis*-[Ru(acac)<sub>2</sub>(PPr<sup>*i*</sup><sub>3</sub>)<sub>2</sub>] and free PPr<sup>*i*</sup><sub>3</sub>. The peak at δ +87.2, which is almost equal in intensity to that found for free PPr<sup>*i*</sup><sub>3</sub>, has been previously detected in the reaction of one equivalent of PPr<sup>*i*</sup><sub>3</sub> with *cis*-[Ru(acac)<sub>2</sub>(η<sup>2</sup>-C<sub>2</sub>H<sub>4</sub>)<sub>2</sub>] in THF at *ca.* 10 °C (see p. 44). This peak is not observed in d<sub>6</sub>-benzene or d<sub>8</sub>-toluene. It is therefore concluded that the P-species giving rise to the highly deshielded peak at δ +87.2 is a six-coordinate solvento-species [Ru(acac)<sub>2</sub>(PPr<sup>*i*</sup><sub>3</sub>)(THF)]. A similar situation exists for [Ru(acac)<sub>2</sub>(PCy<sub>3</sub>)<sub>2</sub>] in THF (see p. 67).

The reaction of *cis*-[Ru(acac)<sub>2</sub>(η<sup>2</sup>-alkene)<sub>2</sub>] (alkene = C<sub>2</sub>H<sub>4</sub>, C<sub>8</sub>H<sub>14</sub>) with two equivalents of PCy<sub>3</sub> has provided contradictory results that at present cannot be fully interpreted. Addition of two equivalents of PCy<sub>3</sub> to a THF solution of *cis*-[Ru(acac)<sub>2</sub>(η<sup>2</sup>-alkene)<sub>2</sub>] (alkene = C<sub>2</sub>H<sub>4</sub>, C<sub>8</sub>H<sub>14</sub>) at room temperature gives a rust red solid in 80% yield whose elemental analysis corresponds to the formula [Ru(acac)<sub>2</sub>(PCy<sub>3</sub>)<sub>2</sub>].

The IR spectra of *trans*-[Ru(acac)<sub>2</sub>(PPr<sup>*i*</sup><sub>3</sub>)<sub>2</sub>] and [Ru(acac)<sub>2</sub>(PCy<sub>3</sub>)<sub>2</sub>] have two strong bands between 1564 and 1507 cm<sup>-1</sup> characteristic of bidentate, O-bonded acac.<sup>7</sup> The FAB mass spectra of *trans*-[Ru(acac)<sub>2</sub>(PPr<sup>*i*</sup><sub>3</sub>)<sub>2</sub>] and [Ru(acac)<sub>2</sub>(PCy<sub>3</sub>)<sub>2</sub>] do not show the parent molecular ion peak, the highest

mass peak corresponding to  $\{\text{Ru}(\text{acac})_2\text{L}\}^+$ ; in contrast,  $\text{cis-}[\text{Ru}(\text{acac})_2(\text{PPr}^i_3)_2]$  shows the parent molecular ion (see Table 2.16).

**Table 2.16:** IR and MS spectra of the isolated bulky phosphine complexes  $[\text{Ru}(\text{acac})_2\text{L}_2]$ .

Complex	$\nu(\text{acac})$ ( $\text{cm}^{-1}$ )	FAB MS		
		$m/z$	Relative Abundance	Assignment
$\text{cis-}[\text{Ru}(\text{acac})_2(\text{PPr}^i_3)_2]$	1576,	620.0	12	$\{\text{Ru}(\text{acac})_2(\text{PPr}^i_3)_2\}^+$
	1511	519.0	7	$\{\text{Ru}(\text{acac})_2(\text{PPr}^i_3)_2\}^+$
		459.9	100	$\{\text{Ru}(\text{acac})_2(\text{PPr}^i_3)\}^+$
$\text{trans-}[\text{Ru}(\text{acac})_2(\text{PPr}^i_3)_2]$	1564,	460.2	100	$\{\text{Ru}(\text{acac})_2(\text{PPr}^i_3)\}^+$
	1507			
$[\text{Ru}(\text{acac})_2(\text{PCy}_3)_2]$	1563,	860.5	6	$\{\text{Ru}(\text{acac})_2(\text{PCy}_3)_2\}^+$
	1506	580.2	100	$\{\text{Ru}(\text{acac})_2(\text{PCy}_3)\}^+$

The rust red solid  $[\text{Ru}(\text{acac})_2(\text{PCy}_3)_2]$  is almost insoluble in aromatic solvents and partially soluble in THF at room temperature; on warming it dissolves completely in both solvents forming orange brown solutions. On cooling a red-brown solid crystallises from the toluene solution; the spectral properties of these two solids in solution are identical and the slight difference in colour may be due to crystal size effects or the presence of different crystal forms.

The  $^{31}\text{P}\{^1\text{H}\}$  NMR spectrum in THF at room temperature shows sharp signals at  $\delta +75.6$  and  $+10.5$  of equal intensity. The latter is clearly due to free  $\text{PCy}_3$  and the former is presumably due to the same species that was observed in the reaction of  $\text{PCy}_3$  (one equivalent) with  $\text{cis-}[\text{Ru}(\text{acac})_2(\eta^2\text{-C}_2\text{H}_4)_2]$  in THF and assigned to either a five-coordinate species  $[\text{Ru}(\text{acac})_2(\text{PCy}_3)]$  or a six-coordinate solvento-species  $[\text{Ru}(\text{acac})_2(\text{PCy}_3)(\text{THF})]$  (see p. 44). A solution obtained by warming a suspension of the solid in THF shows an additional broad peak at  $\delta +38.5$  ( $\omega_{1/2}$  145 Hz), which is more intense than the other two peaks (intensity ratio of the peaks at  $\delta +38.5$  and

$\delta +75.6$  is *ca.* 1.5 : 1). This spectrum remains unchanged when the solution is cooled to room temperature. The  $^1\text{H}$  NMR spectrum of the solution in THF at room temperature shows two singlets at  $\delta$  1.75 and 5.20, consistent with the presence of a species having mutually *trans* acac groups. There is also a broad signal at  $\delta +2.49$ , whose assignment is uncertain; it could be due to the residual protons of coordinated THF. The  $^{13}\text{C}\{^1\text{H}\}$  NMR spectrum in THF at room temperature shows singlets at  $\delta$  27.4 (methyl acac), 100.2 (methine acac) and 183.8 (carbonyl acac) which supports the *trans* assignment. The cyclohexyl proton resonances appear as broad resonances between  $\delta$  2.00 - 1.00. In THF, therefore, it appears that there is an equilibrium:



A solution of  $[\text{Ru}(\text{acac})_2(\text{PCy}_3)_2]$  in  $d_8$ -toluene shows in the  $^{31}\text{P}\{^1\text{H}\}$  NMR spectrum a broad resonance at  $\delta +38.5$ , similar to that observed in hot THF. This peak sharpens when the solution is heated to *ca.* 100 °C in the NMR spectrometer. A similar observation was made by Werner and coworkers<sup>11</sup> for the bis(acetato) complex  $[\text{Ru}(\text{O}_2\text{CCH}_3)_2(\text{PCy}_3)_2]$  but no interpretation was given. The  $^1\text{H}$  NMR spectrum of this solution, at room temperature, shows two singlets of equal intensity at  $\delta$  1.94 and 1.82, and a singlet at  $\delta$  5.28, assigned to the methyl acac and methine acac protons, respectively. There are broad resonances between  $\delta$  2.40 and 1.15 due to the cyclohexyl protons. This pattern is consistent with the presence of a species having *cis* acac groups, for example *cis*- $[\text{Ru}(\text{acac})_2(\text{PCy}_3)_2]$ . The  $^{13}\text{C}\{^1\text{H}\}$  NMR spectral data (see Table 2.14) also seemingly support this conclusion.

However, a crystal selected from solid obtained by cooling a hot toluene solution shows that this contains *trans*- $[\text{Ru}(\text{acac})_2(\text{PCy}_3)_2]$  (see later). Moreover, the  $^{31}\text{P}\{^1\text{H}\}$  chemical shift of  $\delta +38.5$  seems more consistent with the *trans*-formulation, on the basis of the following argument. The  $^{31}\text{P}\{^1\text{H}\}$  chemical shifts for *cis*- and *trans*- $[\text{Ru}(\text{acac})_2(\text{PCy}_3)_2]$  can be predicted by the same methodology that Shaw and coworkers used for the prediction of



$^{31}\text{P}\{^1\text{H}\}$  chemical shifts for *trans*-[PdCl<sub>2</sub>L<sub>2</sub>] (L = tertiary phosphine).<sup>29</sup> A plot of the  $^{31}\text{P}\{^1\text{H}\}$  chemical shift of the free tertiary phosphine *versus* the change in  $^{31}\text{P}\{^1\text{H}\}$  chemical shift on coordination for the complexes *trans*-[Ru(acac)<sub>2</sub>L<sub>2</sub>] and *cis*-[Ru(acac)<sub>2</sub>L<sub>2</sub>] based on the data in Table 1.11 (see p. 26) is shown in Figure 2.14. A reasonable linear relationship was found for both isomers of [Ru(acac)<sub>2</sub>L<sub>2</sub>] (L = tertiary phosphine):

$$y = 50.3 - 0.73x \quad (\text{cis}) \quad \text{Eq. 2.5}$$

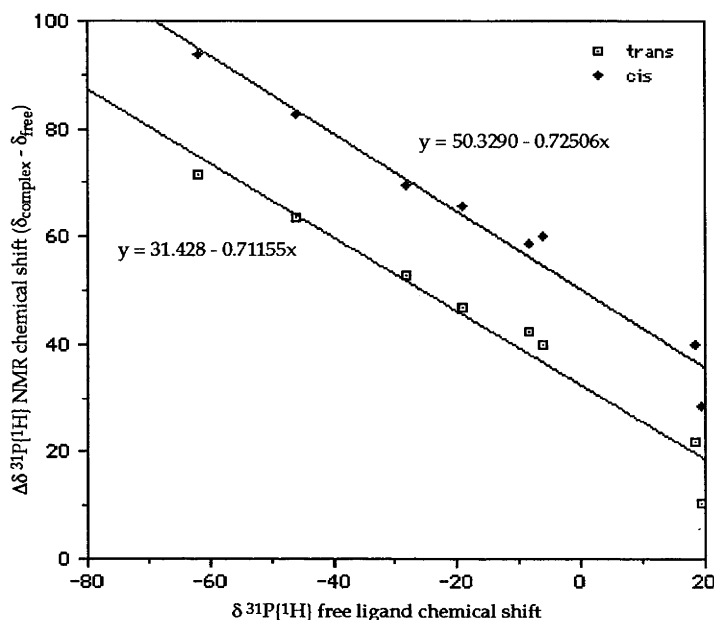
$$y = 31.4 - 0.71x \quad (\text{trans}) \quad \text{Eq. 2.6}$$

(where  $y$  = change in  $^{31}\text{P}\{^1\text{H}\}$  chemical shift and  $x$  =  $^{31}\text{P}\{^1\text{H}\}$  chemical shift of free tertiary phosphine)

On this basis, the predicted  $^{31}\text{P}\{^1\text{H}\}$  chemical shifts of *trans*-[Ru(acac)<sub>2</sub>(PCy<sub>3</sub>)<sub>2</sub>] and *cis*-[Ru(acac)<sub>2</sub>(PCy<sub>3</sub>)<sub>2</sub>] are *ca.*  $\delta$  +34.4 and + 53.2. Thus, the broad peak at  $\delta$  +38.5 observed in toluene at room temperature and in hot THF seems more likely to be due to the *trans*-isomer, in apparent contradiction with the  $^1\text{H}$  and  $^{13}\text{C}\{^1\text{H}\}$  NMR spectral data. Further support for this argument is that the  $\delta_{\text{P}}$  values for *cis*-[Ru(acac)<sub>2</sub>(PCy<sub>3</sub>)(CO)] and *cis*-[Ru(acac)<sub>2</sub>(PCy<sub>3</sub>)(SbPh<sub>3</sub>)] (see p. 67 and 77) are 52.3 and 53.2, respectively, close to the value predicted for *cis*-[Ru(acac)<sub>2</sub>(PCy<sub>3</sub>)<sub>2</sub>]. The  $\delta_{\text{P}}$  values for *cis*-[Ru(acac)<sub>2</sub>(PPh<sub>3</sub>)<sub>2</sub>] (54.0)<sup>14</sup> and *cis*-[Ru(acac)<sub>2</sub>(PPh<sub>3</sub>)(CO)] (53.4)<sup>14</sup> are also very similar. However, the values for *cis*-[Ru(acac)<sub>2</sub>(PPr<sup>*i*</sup><sub>3</sub>)<sub>2</sub>] (47.7) (see p. 65) and *cis*-[Ru(acac)<sub>2</sub>(PPr<sup>*i*</sup><sub>3</sub>)(CO)] (61.5) (see p. 76) differ significantly.

A further complication is that on cooling a *d*<sub>8</sub>-toluene solution to *ca.* -65 °C the broad peak at  $\delta$  +38.5 resolves into two peaks of unequal intensity at  $\delta$  +37.7 and +36.9. Identification of the species present could not be achieved by either  $^1\text{H}$  or  $^{13}\text{C}\{^1\text{H}\}$  NMR spectroscopy due to the broadness of the cyclohexyl proton and carbon resonances at these low temperatures. The reversibility of the dynamic process was confirmed when the sample was warmed back to *ca.* +25 °C and the broad resonance at  $\delta$  +38.5 was obtained. Clearly in the toluene solution there are equilibria between at least two species.

**Figure 2.13:** Plot of the  $^{31}\text{P}\{^1\text{H}\}$  NMR chemical shift of the free tertiary phosphine ( $\delta$ ) vs the change in  $^{31}\text{P}\{^1\text{H}\}$  chemical shift on coordination ( $\Delta\delta$ ) for the complexes *trans*-[Ru(acac) $_2$ L $_2$ ] (black) and *cis*-[Ru(acac) $_2$ L $_2$ ] (blue).



In the remainder of this thesis, the complex will be referred to as *trans*-[Ru(acac) $_2$ (PCy $_3$ ) $_2$ ] on the basis of the crystallographic and  $^{31}\text{P}\{^1\text{H}\}$  NMR spectral evidence as well as the poor solubility, which is typical of the *trans* isomers in the [Ru(acac) $_2$ L $_2$ ] series.<sup>14</sup>

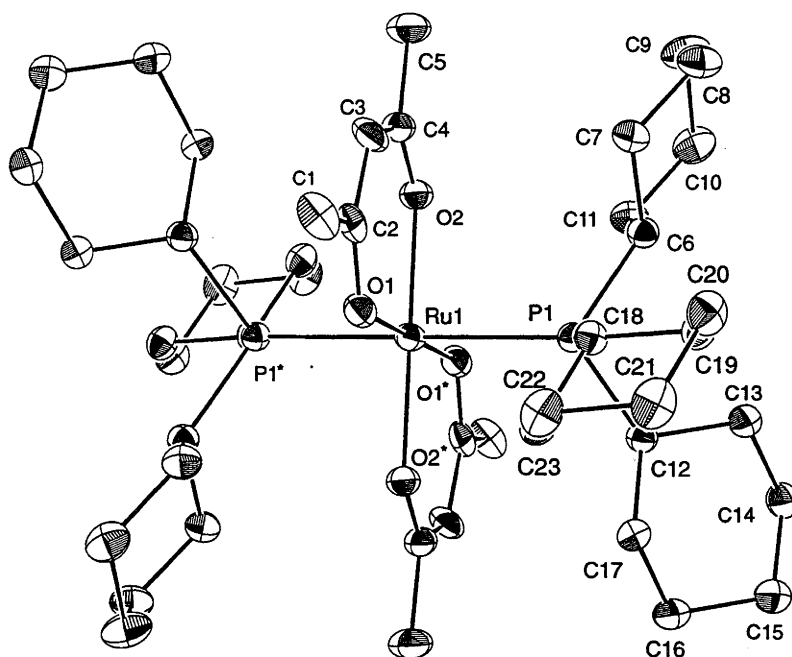
Heating a sample of *trans*-[Ru(acac) $_2$ (PCy $_3$ ) $_2$ ] at *ca.* 120 °C in  $d_8$ -toluene for two days results in the gradual loss of the species associated with the peak at  $\delta$  +38.7 and the formation of singlets at  $\delta$  +70.7 and +70.2 as well as a peak at  $\delta$  +8.6 due to free PCy $_3$  in the  $^{31}\text{P}\{^1\text{H}\}$  NMR spectrum. The corresponding  $^1\text{H}$  NMR spectrum has two interesting features. First, the residual aromatic proton signals at  $\delta$  +7.10 and 7.02 of  $d_8$ -toluene have increased considerably in intensity compared to the methyl signal, suggesting that H/D exchange has occurred.<sup>30</sup> Second, there are no methine acac signals above  $\delta$  5.00; however, four multiplets between  $\delta$  +4.8 - 3.5 are

now present, possibly due to  $\pi$ -coordination of toluene. This behaviour has not been studied further.

The molecular structures of *trans*-[Ru(acac)<sub>2</sub>(PCy<sub>3</sub>)<sub>2</sub>] and *cis*-[Ru(acac)<sub>2</sub>(PPr<sup>*i*</sup><sub>3</sub>)<sub>2</sub>] are shown in Figures 2.14 - 2.15; selected metrical parameters are in Tables 2.17 -18, respectively. Crystal and refinement data, together with the full set of interatomic distances and angles, are given in Appendices A.6 and A.7.

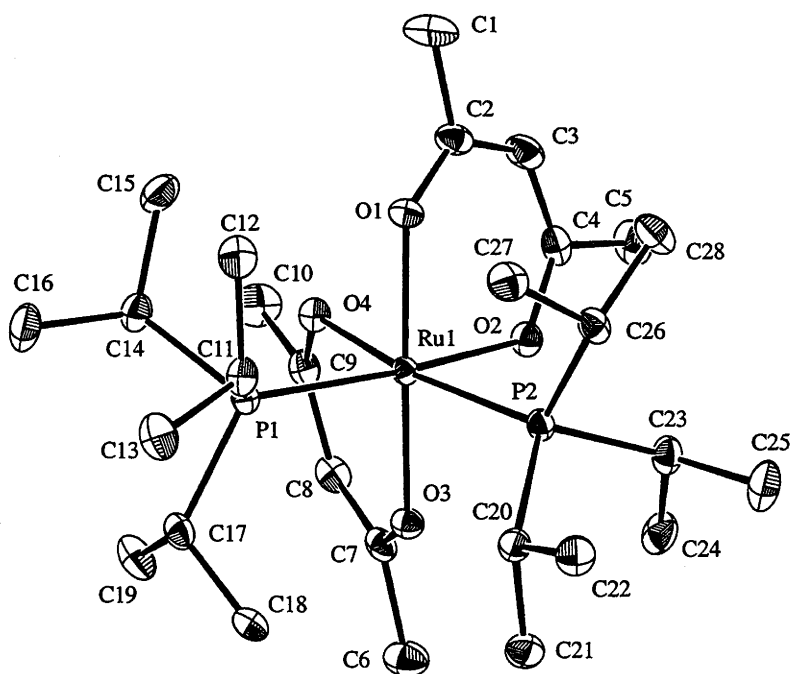
The Ru-O distances *trans* to the oxygen acac atoms are as expected, but the Ru-O distances *trans* to the phosphorus atoms were found to be significantly longer (see Table 2.17). The Ru-P bond length for *trans*-[Ru(acac)<sub>2</sub>(PCy<sub>3</sub>)<sub>2</sub>] was found to be 2.4268(3) Å which is significantly longer than in *trans*-[Ru(acac)<sub>2</sub>(PMePh<sub>2</sub>)<sub>2</sub>] (2.343(1) and 2.346(1) Å); for *cis*-[Ru(acac)<sub>2</sub>(PPr<sup>*i*</sup><sub>3</sub>)<sub>2</sub>], the Ru-P distances are also significantly longer than those found for *cis*-[Ru(acac)<sub>2</sub>(PMePh<sub>2</sub>)<sub>2</sub>] (2.2765(9) Å).<sup>14</sup> The P-Ru-P angle of *cis*-[Ru(acac)<sub>2</sub>(PPr<sup>*i*</sup><sub>3</sub>)<sub>2</sub>] is 105°, which is the same, within experimental error, as the P-Rh-P angles of the complexes [Rh(acac)(PCy<sub>3</sub>)<sub>2</sub>] (105°)<sup>31</sup> and [Rh( $\eta^2$ -O<sub>2</sub>CCH<sub>3</sub>)(PPr<sup>*i*</sup><sub>3</sub>)<sub>2</sub>] (106°),<sup>32</sup> and the P-Mo-P angles of the complexes *cis*-[Mo(CO)<sub>4</sub>(PPh<sub>3</sub>)<sub>2</sub>] (105°)<sup>33</sup> and *cis*-[Mo(CO)<sub>4</sub>(PCy<sub>3</sub>)<sub>2</sub>] (105°).<sup>34</sup>

Figure 2.14: ORTEP diagram of the molecular structure of *trans*- $[\text{Ru}(\text{acac})_2(\text{PCy}_3)_2]$ .



\*) atom generated by the symmetry operation (1-x, 1-y, 1-z)

Figure 2.15: ORTEP diagram of the molecular structure of *cis*- $[\text{Ru}(\text{acac})_2(\text{PPr}^i_3)_2]$ .



**Table 2.17:** Selected metrical parameters of *trans*-[Ru(acac)<sub>2</sub>(PCy<sub>3</sub>)<sub>2</sub>].

Bond Distances (Å)			
Ru(1)-O(1)		2.0707(10)	
Ru(1)-O(2)		2.0646(10)	
Ru(1)-P(1)		2.4268(3)	
Bond Angles (°)			
P(1)-Ru(1)-P(1)*	180.0	P(1)-Ru(1)-O(2)*	88.90(1)
P(1)-Ru(1)-O(1)	91.00(10)	O(1)-Ru(1)-O(1)*	180.0
P(1)-Ru(1)-O(1)*	89.00(10)	O(1)-Ru(1)-O(2)	91.90(10)
P(1)-Ru(1)-O(2)	91.10(10)	O(2)-Ru(1)-O(2)*	180.0

\*) atom generated by the symmetry operation (1-x, 1-y, 1-z)

**Table 2.18:** Selected metrical parameters of *cis*-[Ru(acac)<sub>2</sub>(PPr<sup>i</sup><sub>3</sub>)<sub>2</sub>]

Bond Distances (Å)			
Ru(1)-O(1)		2.068(2)	
Ru(1)-O(2)		2.088(2)	
Ru(1)-O(3)		2.059(2)	
Ru(1)-O(4)		2.104(2)	
Ru(1)-P(1)		2.3525(9)	
Ru(1)-P(2)		2.3467(8)	
Bond Angles (°)			
O(1)-Ru(1)-O(2)	90.46(8)	O(2)-Ru(1)-P(2)	87.25(6)
O(1)-Ru(1)-O(3)	174.02(7)	O(3)-Ru(1)-O(4)	90.50(8)
O(1)-Ru(1)-O(4)	79.77(8)	O(3)-Ru(1)-P(1)	93.86(6)
O(1)-Ru(1)-P(1)	90.20(6)	O(3)-Ru(1)-P(2)	88.73(6)
O(1)-Ru(1)-P(2)	94.43(6)	O(4)-Ru(1)-P(1)	87.57(6)
O(2)-Ru(1)-O(3)	84.62(8)	O(4)-Ru(1)-P(2)	167.01(6)
O(2)-Ru(1)-O(4)	79.77(8)	P(1)-Ru(1)-P(2)	105.42(3)
O(2)-Ru(1)-P(1)	167.23(6)		

### 2.7 Reactions of $[\text{Ru}(\text{acac})_2\text{L}_2]$ complexes with CO.

The red complexes  $\text{trans-}[\text{Ru}(\text{acac})_2(\text{PR}_3)_2]$  ( $\text{R} = \text{Pr}^i, \text{Cy}$ ) readily react with CO (1 bar) in aromatic solvents to form the yellow complexes  $\text{trans-}[\text{Ru}(\text{acac})_2\text{L}(\text{CO})]$  ( $\text{L} = \text{PPr}^i_3, \text{PCy}_3$ ) in yields of between 50 - 70%. The carbonylation reaction of  $\text{trans-}[\text{Ru}(\text{acac})_2(\text{PPr}^i_3)_2]$  was carried out at *ca.* -20 °C to prevent competing formation of  $\text{cis-}[\text{Ru}(\text{acac})_2(\text{PPr}^i_3)_2]$ . The  $\text{cis-}[\text{Ru}(\text{acac})_2(\text{PPr}^i_3)_2]$  complex also reacts with CO (3 bar) at room temperature over several days to form  $\text{trans-}[\text{Ru}(\text{acac})_2(\text{PPr}^i_3)(\text{CO})]$ . There is no evidence for the replacement of  $\text{PPh}_3$  by CO (1-3 bar) from  $\text{cis-}[\text{Ru}(\text{acac})_2(\text{PPh}_3)_2]$  under similar conditions. The complexes  $\text{trans-}[\text{Ru}(\text{acac})_2\text{L}(\text{CO})]$  ( $\text{L} = \text{PPr}^i_3, \text{PCy}_3$ ) isomerise on heating in benzene to form the corresponding *cis*-isomers in yields of 50 - 60%.

The  $^1\text{H}$ ,  $^{13}\text{C}\{^1\text{H}\}$  and  $^{31}\text{P}\{^1\text{H}\}$  NMR spectral data for the complexes *cis*- and *trans*- $[\text{Ru}(\text{acac})_2\text{L}(\text{CO})]$  ( $\text{L} = \text{PPr}^i_3, \text{PCy}_3$ ) are shown in Tables 2.19 - 2.20. The coordination of CO was confirmed by the synthesis of *trans-}[\text{Ru}(\text{acac})\_2(^{13}\text{CO})(\text{PCy}\_3)] using  $^{13}\text{CO}$ ; this complex showed a very intense doublet in the  $^{13}\text{C}\{^1\text{H}\}$  NMR spectrum at  $\delta$  206.9 ( $J_{\text{PC}} = 120$  Hz) and a doublet in  $^{31}\text{P}\{^1\text{H}\}$  NMR spectrum at  $\delta$  8.4 ( $J_{\text{PC}} = 121$  Hz).*

The highest identifiable peak in the isotopic pattern in the FAB mass spectra of the complexes *trans-}[\text{Ru}(\text{acac})\_2\text{L}(\text{CO})] ( $\text{L} = \text{PPr}^i_3, \text{PCy}_3$ ) corresponds to the loss of the carbonyl ligand, *i.e.*  $\{\text{Ru}(\text{acac})_2\text{L}\}^+$  ( $\text{L} = \text{PPr}^i_3, \text{PCy}_3$ ), whereas the highest observed ion peak for *cis-}[\text{Ru}(\text{acac})\_2\text{L}(\text{CO})] ( $\text{L} = \text{PPr}^i_3, \text{PCy}_3$ ) corresponds to the parent ion (see Table 2.21. The IR spectra of the complexes *cis* and *trans-}[\text{Ru}(\text{acac})\_2\text{L}(\text{CO})] ( $\text{L} = \text{PPr}^i_3, \text{PCy}_3$ ) show one strong absorption in the region 1950 - 1928  $\text{cm}^{-1}$  due to  $\nu(\text{C}\equiv\text{O})$ ; the frequency is almost the same for the isomeric pairs. The *trans*-complexes show two strong acac bands between 1572 - 1510  $\text{cm}^{-1}$  whereas the***

Table 2.19:  $^1\text{H}$  and  $^{13}\text{C}\{^1\text{H}\}$  NMR spectral parameters of the  $\{\text{Ru}(\text{acac})_2\}$  moiety of the complexes  $[\text{Ru}(\text{acac})_2\text{LL}']$ .

L	L'	Geometry	$^1\text{H}$ NMR <sup>a</sup>		$^{13}\text{C}\{^1\text{H}\}$ NMR <sup>a</sup>		
			$\delta\text{CH}_3$	$\delta\text{CH}$	$\delta\text{CH}_3$	$\delta\text{CH}$	$\delta\text{CO}$
$\text{PPri}_3$	CO	<i>trans</i>	1.70	5.08	27.0	100.8	189.1
$\text{PPri}_3$	CO	<i>cis</i>	1.91, 1.85, 1.79, 1.71	5.34, 5.16	28.0, 27.8, 27.7, 27.2	100.2, 99.1	189.1, 187.8, 186.5, 186.0
$\text{PCy}_3$	CO	<i>trans</i>	1.73	5.09	27.0	100.6	188.9
$\text{PCy}_3$	CO	<i>cis</i>	1.98, 1.86, 1.86, 1.73	5.40, 5.17	28.1, 27.9, 27.8 (d, $J_{\text{PC}}$ = 5.4 Hz), 27.3	100.3, 99.2	189.0, 187.9, 186.4, 186.0
$\text{PCy}_3$	SbPh <sub>3</sub>	<i>cis</i>	2.00, 1.93, 1.80, 1.68	5.46, 5.02	28.0 <sub>4</sub> , 28.0 <sub>0</sub> , 27.9	100.4, 99.6	186.8, 186.2, 184.7, 184.0

a) measured in  $d_6$ -benzene; singlets unless otherwise indicated.

**Table 2.20:**  $^1\text{H}$ ,  $^{13}\text{C}\{^1\text{H}\}$  and  $^{31}\text{P}\{^1\text{H}\}$  NMR spectral parameters of the ligands of the complexes  $[\text{Ru}(\text{acac})_2\text{LL}']$ .

L	L'	Geometry	$^1\text{H}$ NMR <sup>a</sup>		$^{13}\text{C}\{^1\text{H}\}$ NMR <sup>a</sup>		$^{31}\text{P}\{^1\text{H}\}$ NMR
			$\delta$	Assignment	$\delta$	Assignment	
PPr <sub>3</sub>	CO	<i>trans</i>	2.25 (3H, m)	PCHCH <sub>3</sub>	206.5 (d, $J_{\text{PC}} = 120$ Hz)	$\text{C}\equiv\text{O}$	+18.9
			1.23 (18H, dd, $J_{\text{PH}} = 12$ Hz, $J_{\text{HH}} = 7.1$ Hz)	PCHCH <sub>3</sub>	23.1 (d, $J_{\text{PC}} = 20$ Hz)	PCHCH <sub>3</sub> PCHCH <sub>3</sub>	
PPr <sub>3</sub>	CO	<i>cis</i>	2.25 (3H, m)	PCHCH <sub>3</sub>	209.4 (d, $J_{\text{PC}} = 18$ Hz)	$\text{C}\equiv\text{O}$	+61.5
			1.25, 1.13 (18H, both dd, $J_{\text{PH}} = 13$ Hz, $J_{\text{HH}} = 7.0$ Hz)	PCHCH <sub>3</sub>	24.7 (d, $J_{\text{PC}} = 22$ Hz)	PCHCH <sub>3</sub> PCHCH <sub>3</sub>	
PCy <sub>3</sub>	CO	<i>trans</i>	2.30 - 1.50, 1.40 - 1.05 (33H, broad m)	PCHCH <sub>2</sub> and PCHCH <sub>2</sub>	206.8 (d, $J_{\text{PC}} = 120$ Hz)	$\text{C}\equiv\text{O}$	+8.4
					33.3 (d, $J_{\text{PC}} = 10$ Hz)	PCHCH <sub>2</sub> PCHCH <sub>2</sub>	
PCy <sub>3</sub>	CO	<i>cis</i>	2.30 - 2.10, 2.00 - 1.50, 1.30 - 1.10 (33H, broad m)	PCHCH <sub>2</sub> and PCHCH <sub>2</sub>	29.1, 28.6 (d, $J_{\text{PC}} = 8.8$ Hz), 27.1	$\text{C}\equiv\text{O}$	+52.1
					209.6 (d, $J_{\text{PC}} = 18$ Hz)	PCHCH <sub>2</sub> PCHCH <sub>2</sub>	

a) measured in  $d_6$ -benzene; singlets unless otherwise indicated.



Table 2.20 (cont.):  $^1\text{H}$ ,  $^{13}\text{C}\{^1\text{H}\}$  and  $^{31}\text{P}\{^1\text{H}\}$  NMR spectral parameters of the ligands of the complexes  $[\text{Ru}(\text{acac})_2\text{LL}']$ .

L	L'	Geometry	$^1\text{H}$ NMR <sup>a</sup>		$^{13}\text{C}\{^1\text{H}\}$ NMR <sup>a</sup>		$^{31}\text{P}\{^1\text{H}\}$ NMR
			$\delta$	Assignment	$\delta$	Assignment	
PCy <sub>3</sub>	SbPh <sub>3</sub>	<i>cis</i>	7.80 - 7.77 (6H, m) 7.13 - 7.06 (9H, m)  2.30 - 1.00 (33H, broad m)	o-C <sub>6</sub> H <sub>5</sub> m- and p-C <sub>6</sub> H <sub>5</sub> PCHCH <sub>2</sub> and PCHCH <sub>2</sub>	137.1 136.5 129.0 128.4  38.8 (d, $J_{\text{PC}} = 19$ Hz) 29.8, 29.1, 28.6 (d, $J_{\text{PC}} = 4$ Hz), 28.5 (d, $J_{\text{PC}} = 4$ Hz), 27.4	o-C <sub>6</sub> H <sub>5</sub> ipso-C <sub>6</sub> H <sub>5</sub> p-C <sub>6</sub> H <sub>5</sub> m-C <sub>6</sub> H <sub>5</sub> PCHCH <sub>2</sub> PCHCH <sub>2</sub>	+53.5

a) measured in *d*<sub>6</sub>-benzene; singlets unless otherwise indicated.

Table 2.21: IR and MS data of the isolated mixed ligand complexes  $[\text{Ru}(\text{acac})_2\text{LL}]^+$ .

Compound	Infrared Data (KBr) ( $\text{cm}^{-1}$ )		FAB MS		
	$\nu(\text{acac})$	Other	$m/z$	Relative Abundance	Assignment
<i>trans</i> - $[\text{Ru}(\text{acac})_2(\text{PPr}^i_3)(\text{CO})]$	1566, 1517	1931 $[\nu(\text{C}\equiv\text{O})]$	460.1	100	$\{\text{Ru}(\text{acac})_2(\text{PPr}^i_3)\}^+$
<i>cis</i> - $[\text{Ru}(\text{acac})_2(\text{PPr}^i_3)(\text{CO})]$	1588, 1573, 1516	1928 $[\nu(\text{C}\equiv\text{O})]$	488.2	45	$\{\text{Ru}(\text{acac})_2(\text{PPr}^i_3)(\text{CO})\}^+$
			460.2	100	$\{\text{Ru}(\text{acac})_2(\text{PPr}^i_3)\}^+$
<i>trans</i> - $[\text{Ru}(\text{acac})_2(\text{PCy}_3)(\text{CO})]$	1572, 1510	1950 $[\nu(\text{C}\equiv\text{O})]$	389.1	24	$\{\text{Ru}(\text{acac})(\text{PPr}^i_3)(\text{CO})\}^+$
			580.1	53	$\{\text{Ru}(\text{acac})_2(\text{PCy}_3)\}^+$
<i>cis</i> - $[\text{Ru}(\text{acac})_2(\text{PCy}_3)(\text{CO})]$	1589, 1575, 1520	1944 $[\nu(\text{C}\equiv\text{O})]$	297.1	50	$\{\text{Ru}(\text{acac})_2\}^+$
			608.3	62	$\{\text{Ru}(\text{acac})_2(\text{PCy}_3)(\text{CO})\}^+$
			580.2	100	$\{\text{Ru}(\text{acac})_2(\text{PCy}_3)\}^+$
<i>cis</i> - $[\text{Ru}(\text{acac})_2(\text{PCy}_3)(\text{SbPh}_3)]$	1568, 1510		509.2	31	$\{\text{Ru}(\text{acac})(\text{PCy}_3)(\text{CO})\}^+$
			932.4	4	$\{\text{Ru}(\text{acac})_2(\text{PCy}_3)(\text{SbPh}_3)\}^+$
			580.3	100	$\{\text{Ru}(\text{acac})_2(\text{PCy}_3)\}^+$

*cis* analogues show three strong bands between 1589 - 1516  $\text{cm}^{-1}$  (see Table 2.21), characteristic of bidentate O-bonded acac ligands bands.<sup>7</sup>

### 2.8 Reactions of $[\text{Ru}(\text{acac})_2\text{L}_2]$ complexes with alkynes.

Addition of the terminal alkynes  $\text{PhC}\equiv\text{CH}$ ,  $\text{Bu}^t\text{C}\equiv\text{CH}$  and  $\text{Me}_3\text{SiC}\equiv\text{CH}$  to *cis*- $[\text{Ru}(\text{acac})_2(\text{PPr}^i_3)_2]$  in hot benzene results in the isolation of the red vinylidene complexes *cis*- $[\text{Ru}(\text{acac})_2(\text{PPr}^i_3)\{\text{=C=C}(\text{H})\text{R}\}]$  ( $\text{R} = \text{Ph}, \text{Bu}^t, \text{SiMe}_3$ ) in yields of 55 - 65%. The Ph and  $\text{SiMe}_3$  derivatives have been made independently of this work.<sup>11</sup>

The reaction of *cis*- $[\text{Ru}(\text{acac})_2(\text{PPr}^i_3)_2]$  with terminal alkynes was also found to proceed at *ca.* +25°C, albeit slowly, to form the vinylidene complexes. The expected intermediate,  $[\text{Ru}(\text{acac})_2(\text{PPr}^i_3)(\eta^2\text{-HC}\equiv\text{CR})]$ , was not detected by NMR spectroscopy at ambient conditions. There was no detectable reaction after two days between *cis*- $[\text{Ru}(\text{acac})_2(\text{PPr}^i_3)_2]$  and  $\text{PhC}\equiv\text{CPh}$ , 3-hexyne or the electron-deficient alkyne  $\text{HC}\equiv\text{CCO}_2\text{CH}_3$  in hot benzene. As expected from the lack of reactivity with CO,<sup>14</sup> no reaction was observed between *cis*- $[\text{Ru}(\text{acac})_2(\text{PPh}_3)_2]$  or *cis*- $[\text{Ru}(\text{acac})_2(\text{SbPh}_3)_2]$  and  $\text{PhC}\equiv\text{CH}$  in hot benzene.

The  $^1\text{H}$ ,  $^{13}\text{C}\{^1\text{H}\}$  and  $^{31}\text{P}\{^1\text{H}\}$  NMR spectral data of the complexes *cis*- $[\text{Ru}(\text{acac})_2(\text{PPr}^i_3)\{\text{=C=C}(\text{H})\text{R}\}]$  ( $\text{R} = \text{Ph}, \text{Bu}^t, \text{SiMe}_3$ ) are shown in Tables 2.22 and 2.23. The presence of the vinylidene group  $\text{Ru}=\text{C}_\alpha\text{C}_\beta(\text{H})\text{R}$  was confirmed by the low field signals in the  $^{13}\text{C}\{^1\text{H}\}$  spectrum between 338.5 and 356.4 (d,  $J_{\text{PC}} = 20$  Hz) and 93.4 - 121.2 which are assigned to the  $\alpha$ - and  $\beta$ -carbon atoms, respectively.<sup>11</sup> The vinylidene protons were found as a doublet in the range  $\delta(^1\text{H})$  3.67 - 5.24 (d,  $J_{\text{PH}} = 4$  Hz) (see Table 2.23).

The complex *trans*- $[\text{Ru}(\text{acac})_2(\text{PCy}_3)_2]$  also reacts with  $\text{Me}_3\text{SiC}\equiv\text{CH}$  in hot benzene to give exclusively a species believed to be the vinylidene complex *cis*- $[\text{Ru}(\text{acac})_2(\text{PCy}_3)\{\text{=C=C}(\text{H})\text{SiMe}_3\}]$  on the basis of its NMR spectra. However, all attempts to purify the compound by chromatography

**Table 2.22:**  $^1\text{H}$  and  $^{13}\text{C}\{^1\text{H}\}$  NMR spectral parameters of the  $\{\text{Ru}(\text{acac})_2\}$  moiety of the isolated mononuclear vinylidene complexes  $\text{cis-}[\text{Ru}(\text{acac})_2(\text{PR}_3)\{\text{C}=\text{C}(\text{H})\text{R}'\}]$  ( $\text{R} = \text{Pr}^i, \text{Cy}$ ).

Complex	$^1\text{H}$ NMR <sup>a</sup>		$^{13}\text{C}\{^1\text{H}\}$ NMR <sup>a</sup>			Solvent
	$\delta\text{CH}_3$	$\delta\text{CH}$	$\delta\text{CH}_3$	$\delta\text{CH}$	$\delta\text{CO}$	
<i>cis</i> - $[\text{Ru}(\text{acac})_2(\text{PPr}^i_3)\{\text{C}=\text{C}(\text{H})\text{Ph}\}]$						$\text{C}_6\text{D}_6$
<i>cis</i> - $[\text{Ru}(\text{acac})_2(\text{PPr}^i_3)\{\text{C}=\text{C}(\text{H})\text{Bu}^t\}]$	1.77, 1.80, 1.93, 1.97	5.18, 5.35	24.3, 24.6, 27.1, 28.0	98.8, 99.7	184.7, 186.8, 187.6, 188.3	$\text{C}_6\text{D}_6$
<i>cis</i> - $[\text{Ru}(\text{acac})_2(\text{PPr}^i_3)\{\text{C}=\text{C}(\text{H})\text{SiMe}_3\}]$	1.79, 1.84, 1.94	5.20, 5.35	27.7, 28.4, 28.5, 28.6	99.5, 100.2	185.0, 186.8, 187.4, 188.2	$\text{C}_6\text{D}_6$
<i>cis</i> - $[\text{Ru}(\text{acac})_2(\text{PCy}_3)\{\text{C}=\text{C}(\text{H})\text{SiMe}_3\}]$	1.80, 1.85, 1.93, 1.96	5.16, 5.34				$\text{C}_6\text{D}_5\text{CD}_3$

a) singlets unless otherwise indicated.

**Table 2.23:**  $^1\text{H}$ ,  $^{13}\text{C}\{^1\text{H}\}$  and  $^{31}\text{P}\{^1\text{H}\}$  NMR spectral parameters of the vinylidene and phosphine groups of the isolated mononuclear vinylidene complexes  $\text{cis-}[\text{Ru}(\text{acac})_2(\text{PR}_3)_2(\text{C}=\text{C}(\text{H})\text{R}')] ]$  ( $\text{R} = \text{Pr}^i, \text{Cy}$ ).

L	R	$^1\text{H}$ NMR <sup>a</sup>		$^{13}\text{C}\{^1\text{H}\}$ NMR <sup>a</sup>		$^{31}\text{P}\{^1\text{H}\}$ NMR	Solvent
		$\delta$	Assignment	$\delta$	Assignment		
$\text{PPr}^i_3$	But	4.10 (d, $J_{\text{PH}} = 4$ Hz); 2.47 (m);	$=\text{C}=\text{C}(\underline{\text{H}})\text{C}(\text{CH}_3)_3$ PCHCH <sub>3</sub>	356.4 (d, $J_{\text{PC}} = 20$ Hz);	$=\underline{\text{C}}=\text{C}(\text{H})\text{C}(\text{CH}_3)_3$	+55.5	$\text{C}_6\text{D}_6$
		1.21, 1.29 (both dd, $J_{\text{PH}} =$ 12.8 Hz $J_{\text{HH}} = 7.2$ Hz); 1.26	PCHCH <sub>3</sub> $=\text{C}=\text{C}(\text{H})\text{C}(\underline{\text{C}}\text{H}_3)_3$	121.2; 33.1; 30.1;	$=\text{C}=\underline{\text{C}}(\text{H})\text{C}(\text{CH}_3)_3$ $=\text{C}=\text{C}(\text{H})\text{C}(\underline{\text{C}}\text{H}_3)_3$ $=\text{C}=\text{C}(\text{H})\underline{\text{C}}(\text{CH}_3)_3$ PCHCH <sub>3</sub> PCHCH <sub>3</sub>		
$\text{PPr}^i_3$	SiMe <sub>3</sub>	3.67 (d, $J_{\text{PH}} = 4.2$ Hz); 2.47 (m);	$=\text{C}=\text{C}(\underline{\text{H}})\text{Si}(\text{CH}_3)_3$ PCHCH <sub>3</sub>	338.5 (d, $J_{\text{PC}} = 19$ Hz);	$=\underline{\text{C}}=\text{C}(\text{H})\text{Si}(\text{CH}_3)_3$	+56.9	$\text{C}_6\text{D}_6$
		1.21, 1.29 (both dd, $J_{\text{PH}} =$ 12.9 Hz $J_{\text{HH}} = 7.4$ Hz); 0.29	PCHCH <sub>3</sub> $=\text{C}=\text{C}(\text{H})\text{Si}(\underline{\text{C}}\text{H}_3)_3$	93.4; 24.9 (d, $J_{\text{PC}} = 22$ Hz); 19.4, 19.7;	$=\text{C}=\underline{\text{C}}(\text{H})\text{Si}(\text{CH}_3)_3$ PCHCH <sub>3</sub> PCHCH <sub>3</sub> $=\text{C}=\text{C}(\text{H})\text{Si}(\underline{\text{C}}\text{H}_3)_3$		
$\text{PCy}_3$	SiMe <sub>3</sub>			2.3		+47.7	$\text{C}_6\text{D}_5\text{CD}_3$

a) singlets unless otherwise indicated.

Table 2.24: IR and MS data of the isolated mixed ligand complexes  $[\text{Ru}(\text{acac})_2\text{LL}]^+$ .

Compound	Infrared Spectra		FAB MS		
	$\nu(\text{acac})$ (KBr) ( $\text{cm}^{-1}$ )	Other (KBr) ( $\text{cm}^{-1}$ )	$m/z$	Relative Abundance	Assignment
<i>cis</i> - $[\text{Ru}(\text{acac})_2(\text{PPr}^i_3)(=\text{C}=\text{C}(\text{H})\text{Bu}^t)]$	1580, 1514 <sup>†</sup>	1638 (C=C) <sup>†</sup>	542.1	5	$[\text{Ru}(\text{acac})_2(\text{PPr}^i_3)(=\text{C}=\text{C}(\text{H})\text{Bu}^t)]^+$
			460.1	100	$\{\text{Ru}(\text{acac})_2(\text{PPr}^i_3)\}^+$
			300.0	8	$\{\text{Ru}(\text{acac})_2\}^+$
<i>cis</i> - $[\text{Ru}(\text{acac})_2(\text{PPr}^i_3)(=\text{C}=\text{C}(\text{H})\text{SiMe}_3)]$	1589, 1538, 1519	1610 (C=C)	1058.4	16	-
			972.3	29	-
			546.1	9	$\{\text{Ru}(\text{acac})_2(\text{PPr}^i_3)(=\text{C}(\text{H})\text{SiMe}_3)\}^+$
			488.1	19	$\{\text{Ru}(\text{acac})_2(\text{PPr}^i_3)\text{Si}\}^+$
			460.1	100	$\{\text{Ru}(\text{acac})_2(\text{PPr}^i_3)\}^+$
			300.0	8	$\{\text{Ru}(\text{acac})_2\}^+$

† recorded in  $\text{C}_6\text{H}_6$ .

led to decomposition. The  $^1\text{H}$  NMR spectral data of this complex are as expected for a *cis*-[Ru(acac) $_2$ LL'] complex with two different ligands (see Table 2.22 and p. 25). A doublet found at  $\delta$  3.60 ( $J_{\text{PH}} = 5$  Hz) is assigned to the vinylidene proton. The  $^{31}\text{P}\{^1\text{H}\}$  NMR spectrum shows a sharp singlet at  $\delta$  +47.7.

The parent molecular ion was found in the FAB mass spectra for *cis*-[Ru(acac) $_2$ (PPr $^i$  $_3$ )(=C=C(H)Bu $^t$ )] at  $m/z$  542.1 with the most abundant ion due to {Ru(acac) $_2$ (PPr $^i$  $_3$ )} $^+$  at  $m/z$  460.1 (see Table 2.24). The parent molecular ion was not detected for *cis*-[Ru(acac) $_2$ (PPr $^i$  $_3$ )(=C=C(H)SiMe $_3$ )], though {Ru(acac) $_2$ (PPr $^i$  $_3$ )} $^+$  was detected as the most abundant ion present. Ion peaks corresponding to unknown species were detected at  $m/z$  >546.1 and are probably related to the reaction of 3-nitrobenzylalcohol with the vinylidene unit (see Table 2.24). The IR spectrum shows strong absorptions between 1589 and 1519  $\text{cm}^{-1}$ , characteristic of bidentate, O-bonded acac (see Table 2.24).<sup>7</sup> A strong band at 1610  $\text{cm}^{-1}$  and 1638  $\text{cm}^{-1}$  was also observed for *cis*-[Ru(acac) $_2$ (PPr $^i$  $_3$ )(=C=C(H)SiMe $_3$ )] and *cis*-[Ru(acac) $_2$ (PPr $^i$  $_3$ )(=C=C(H)Bu $^t$ )], respectively, and is assigned to the C=C stretching vibration as it lies within the range of 1650 - 1600  $\text{cm}^{-1}$  typically found for ruthenium vinylidene complexes.<sup>35,36</sup>

### 2.9 Reactions of *cis*-[Ru(acac) $_2$ ( $\eta^2$ -C $_2$ H $_4$ )L] (L = NH $_3$ , SbPh $_3$ , PPr $^i$ $_3$ , PCy $_3$ ) complexes with tertiary phosphines, CO, alkynes and dinitrogen.

The complex *cis*-[Ru(acac) $_2$ (PCy $_3$ )(SbPh $_3$ )] is formed in yields of *ca.* 80% by the reaction of *cis*-[Ru(acac) $_2$ ( $\eta^2$ -C $_2$ H $_4$ )(SbPh $_3$ )] with one equivalent of PCy $_3$  or of *cis*-[Ru(acac) $_2$ ( $\eta^2$ -C $_2$ H $_4$ )(PCy $_3$ )] with one equivalent of SbPh $_3$  in aromatic solvents. In contrast, there was no detectable reaction between *cis*-[Ru(acac) $_2$ ( $\eta^2$ -C $_2$ H $_4$ )(NH $_3$ )] and PCy $_3$  in  $d_6$ -benzene even after two weeks at room temperature. The  $^1\text{H}$  and  $^{13}\text{C}\{^1\text{H}\}$  NMR spectra of *cis*-[Ru(acac) $_2$ (PCy $_3$ )(SbPh $_3$ )] show the expected acac patterns (see p. 25). The aromatic protons and carbon atoms were found in the expected region, as

were the cyclohexyl protons and carbon atoms (see Table 2.19 and 2.20). The  $^{31}\text{P}\{^1\text{H}\}$  NMR spectrum reveals one sharp singlet at  $\delta$  53.5.

The highest ion peak detected in FAB mass spectrum corresponds to  $\{\text{Ru}(\text{acac})_2(\text{PCy}_3)(\text{SbPh}_3)\}^+$ . Ions were also detected which correspond to  $\{\text{Ru}(\text{acac})_2(\text{PCy}_3)\}^+$  (see Table 2.20). The IR spectrum shows two strong absorptions at 1568 and 1510  $\text{cm}^{-1}$ , characteristic of bidentate, O-bonded acac.<sup>7</sup>

The structures of *cis*- $[\text{Ru}(\text{acac})_2(\text{SbPh}_3)\text{L}]$  ( $\text{L} = \text{SbPh}_3, \text{PCy}_3$ ) have been confirmed by X-ray crystallographic studies (see Appendices A.8 and A.9). The Ru-O distances characterising the coordination of the acetylacetonato anion for both complexes were found to lie between 2.05 - 2.12 Å. The Ru-O bond *trans* to  $\text{PCy}_3$  in *cis*- $[\text{Ru}(\text{acac})_2(\text{PCy}_3)(\text{SbPh}_3)]$  is only *ca.* 0.06 Å longer than the Ru-O bonds opposite to antimony or oxygen acac atoms. The Ru-P bond was found to be 2.309(1) Å in length, which is *ca.* 0.04 Å shorter than the Ru-P bond length found for the complexes *cis*- $[\text{Ru}(\text{acac})_2(\text{PPr}^i_3)_2]$  (see Table 2.19), *cis*- $[\text{Ru}(\text{acac})_2(\eta^2\text{-C}_2\text{H}_4)(\text{PPr}^i_3)]$  (see Table 2.11) and *cis*- $[\text{Ru}(\text{acac})_2(\eta^2\text{-C}_2\text{H}_4)(\text{PCy}_3)]$  (see Table 2.12). The Ru-Sb distances are between 2.54 - 2.58 Å. The P-Ru-Sb angle was found to be 100°, whereas the Sb-Ru-Sb angle was found to be 97°, similar to that found for the P-Ru-P angle for the complex *cis*- $[\text{Ru}(\text{acac})_2(\text{PPh}_2\text{Me})_2]$  (96°).<sup>14</sup>

The complex *cis*- $[\text{Ru}(\text{acac})_2(\eta^2\text{-C}_2\text{H}_4)(\text{PPr}^i_3)]$  readily reacts with one equivalent of  $\text{PPr}^i_3$  to form *cis*- $[\text{Ru}(\text{acac})_2(\text{PPr}^i_3)_2]$  in  $\text{d}_6$ -benzene at room temperature. The reaction is believed to take place via the complex *trans*- $[\text{Ru}(\text{acac})_2(\text{PPr}^i_3)_2]$ , which readily isomerises to the more stable *cis*-isomer (see p. 59). The mono-ethene complexes *cis*- $[\text{Ru}(\text{acac})_2(\eta^2\text{-C}_2\text{H}_4)(\text{PPr}^i_3)]$  and *cis*- $[\text{Ru}(\text{acac})_2(\eta^2\text{-C}_2\text{H}_4)(\text{PCy}_3)]$  readily react with CO (1 bar) at room temperature in  $\text{d}_6$ -benzene to form exclusively the corresponding complexes *trans*- $[\text{Ru}(\text{acac})_2(\text{CO})\text{L}]$  ( $\text{L} = \text{PPr}^i_3, \text{PCy}_3$ ), as shown by  $^1\text{H}$  and  $^{31}\text{P}\{^1\text{H}\}$  NMR spectroscopy. In contrast, there is no detectable reaction between *cis*-



$[\text{Ru}(\text{acac})_2(\eta^2\text{-alkene})(\text{SbPh}_3)]$  (alkene =  $\text{C}_2\text{H}_4$ ,  $\text{C}_8\text{H}_{14}$ ) and CO (1-3 bar) in benzene after several days at room temperature.

The complex  $\text{cis-}[\text{Ru}(\text{acac})_2(\eta^2\text{-C}_2\text{H}_4)(\text{PPr}^i_3)]$  readily reacts with  $\text{PhC}\equiv\text{CH}$  in  $\text{d}_6$ -benzene at room temperature to form quantitatively  $\text{cis-}[\text{Ru}(\text{acac})_2(\text{PPr}^i_3)(=\text{C}=\text{C}(\text{H})\text{Ph})]$ , as shown by NMR spectroscopy. The presumed intermediate  $\text{cis-}[\text{Ru}(\text{acac})_2(\text{PPr}^i_3)(\eta^2\text{-HC}\equiv\text{CPh})]$  was not detected. No detectable reaction occurs between the complexes  $\text{cis-}[\text{Ru}(\text{acac})_2(\eta^2\text{-C}_2\text{H}_4)\text{L}]$  ( $\text{L} = \text{PPr}^i_3, \text{PCy}_3$ ) and excess 2-butyne or 3-hexyne, even on heating.

The yellow, crystalline binuclear complex  $\text{cis-}[\{\text{Ru}(\text{acac})_2(\text{PPr}^i_3)\}_2(\mu\text{-N}_2)]$  was isolated in *ca.* 90% yield after heating a benzene solution of  $\text{cis-}[\text{Ru}(\text{acac})_2(\eta^2\text{-C}_2\text{H}_4)(\text{PPr}^i_3)]$  to 50 - 60 °C for 3 days under an atmosphere of industrial grade hydrogen (3 bar). The product presumably arises from the presence of a small amount of  $\text{dinitrogen}$  <sup>(*ca.* 100 ppm, see experimental)</sup> in the hydrogen gas. There was no detectable loss of ethene when a benzene solution of  $\text{cis-}[\text{Ru}(\text{acac})_2(\eta^2\text{-C}_2\text{H}_4)(\text{PPr}^i_3)]$  was heated either *in vacuo* or under high purity argon (3 bar). The dinitrogen complex was also isolated after attempting to recrystallise a *n*-pentane solution of  $\text{cis-}[\text{Ru}(\text{acac})_2(\eta^2\text{-C}_2\text{H}_4)(\text{PPr}^i_3)]$  in a nitrogen-filled dry box over a period of several weeks.  $^{31}\text{P}\{^1\text{H}\}$  NMR experiments indicate that the product formed under a dinitrogen atmosphere (3 bar) is identical with that isolated from the reaction of impure dihydrogen.

The presence of nitrogen in the isolated yellow solid was confirmed by elemental analysis and an X-ray structural study (see below). The Raman spectrum also shows a strong band due to a N-N stretching vibration at 2089  $\text{cm}^{-1}$ , very close to the values of 2100 and 2080  $\text{cm}^{-1}$  found for the binuclear complexes  $[\{\text{Ru}(\text{NH}_3)_5\}_2(\mu\text{-N}_2)]^{4+}$ <sup>37</sup> and  $[\{\text{Ru}(\text{H}_2\text{O})_5\}_2(\mu\text{-N}_2)]^{4+}$ ,<sup>38</sup> respectively. No band in this region is observed in the IR spectrum either in benzene or in the solid state, which is consistent with the presence of  $\mu\text{-N}_2$  coordination in both phases. The IR spectrum shows two strong bands at 1582 and 1512  $\text{cm}^{-1}$  characteristic of bidentate, O-bonded acac.<sup>7</sup> The most abundant ion detected at  $m/z$  460.2 in the FAB mass spectrum corresponds to

the species  $\{\text{Ru}(\text{acac})_2(\text{PPr}^i_3)\}^+$ . The molecular parent ion  $[\{\text{Ru}(\text{acac})_2(\text{PPr}^i_3)\}_2(\mu\text{-N}_2)]^+$  was found at  $m/z$  948.2, though there is also an unidentified peak at  $m/z$  950.2.

The solid state structure of *cis*- $[\{\text{Ru}(\text{acac})_2(\text{PPr}^i_3)\}_2(\mu\text{-N}_2)]$  is shown in Figure 2.16 and selected metrical parameters are given in Table 2.25. The complex is binuclear with each ruthenium atom at the centre of a distorted octahedron with the phosphorus and nitrogen atoms *cis* to each other. Only the homochiral ( $\Delta\Delta/\Lambda\Lambda$ ) isomer was found in the crystal. Crystal and refinement data of the isomers, together with the full set of interatomic distances and angles, are given in Appendix A.10. The Ru-O distances characterising the coordination of the acetylacetonato anion were in the expected range, though the Ru-O distances *trans* to  $\text{PPr}^i_3$  were *ca.* 0.06 Å longer than the Ru-O distances opposite to the dinitrogen and oxygen acac atoms.

The Ru-P bond lengths (2.312(2) Å) are *ca.* 0.04 Å shorter than those in *cis*- $[\text{Ru}(\text{acac})_2(\text{PPr}^i_3)_2]$  (see Table 2.19) but almost equal to that found for *cis*- $[\text{Ru}(\text{acac})_2(\eta^2\text{-C}_2\text{H}_4)(\text{PPr}^i_3)]$  (see Table 2.11). The Ru-N distance for *cis*- $[\{\text{Ru}(\text{acac})_2(\text{PPr}^i_3)\}_2(\mu\text{-N}_2)]$  is (1.919(4) Å) is similar to that found for the binuclear structure  $[\{\text{Ru}(\text{NH}_3)_5\}_2(\mu\text{-N}_2)]^{4+}$  (1.928(6) Å).<sup>39</sup> The Ru-N $\equiv$ N-Ru unit shows a slight deviation from linearity, the Ru-N-N angle being 174°. The N-N distance is 1.135(8) Å (*cf* N-N = 1.0977 Å for free N<sub>2</sub>),<sup>40</sup> consistent with backdonation of electron density from Ru(II) to N<sub>2</sub>.<sup>41</sup> Similar lengthening of the N $\equiv$ N distance is found for  $[\{\text{Ru}(\text{NH}_3)_5\}_2(\mu\text{-N}_2)]^{4+}$  (1.124(15) Å)<sup>39</sup> and  $[\{\textit{mer,trans}\text{-RuCl}_2(\text{NN}'\text{N})_2\}_2(\mu\text{-N}_2)]$  (NN'N = 2,6-bis[(dimethylamino)methyl]pyridine) (1.110(3) Å).<sup>15</sup>

**Figure 2.16:** ORTEP diagram of the molecular structure of the homochiral *cis*-[ $\{\text{Ru}(\text{acac})_2(\text{PPr}^i_3)\}_2(\mu\text{-N}_2)$ ].

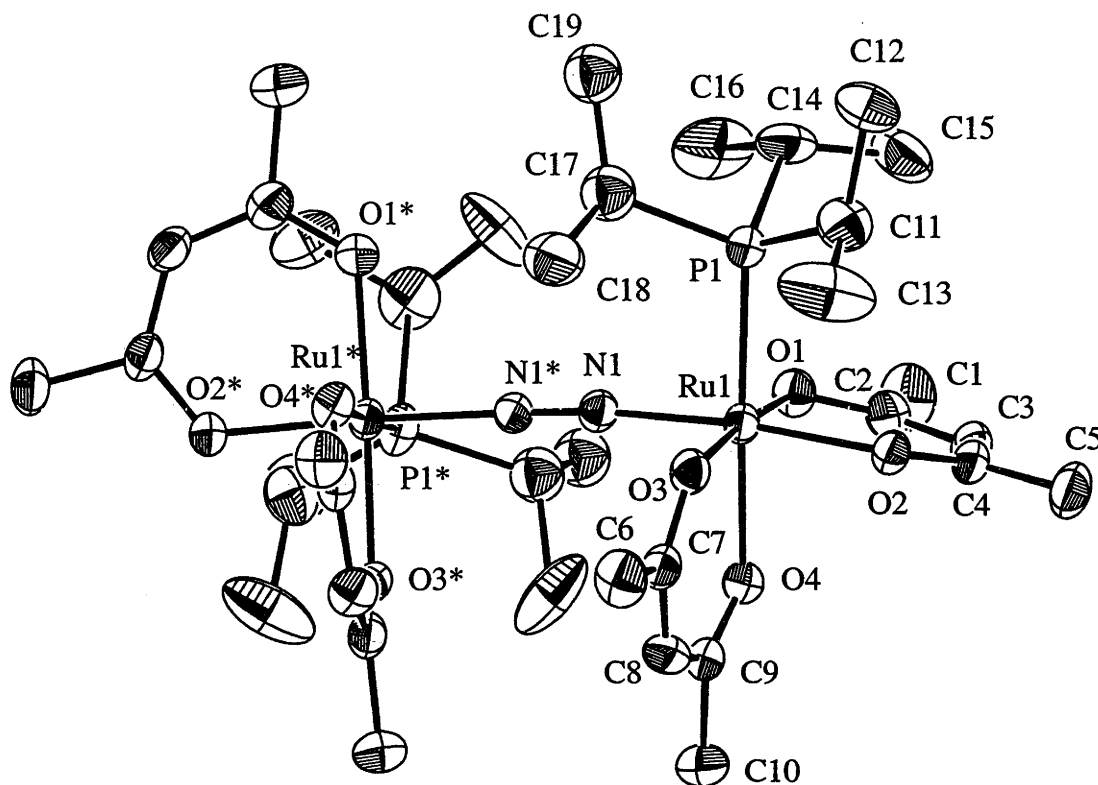


**Table 2.25:** Selected metrical parameters of *cis*-[ $\{\text{Ru}(\text{acac})_2(\text{PPr}^i_3)\}_2(\mu\text{-N}_2)$ ].

Bond Distances (Å)			
Ru(1)-O(1)		2.046(4)	
Ru(1)-O(2)		2.035(4)	
Ru(1)-O(3)		2.050(4)	
Ru(1)-O(4)		2.107(4)	
Ru(1)-P(1)		2.312(2)	
Ru(1)-N(1)		1.919(4)	
N(1)-N(1) <sup>a</sup>		1.135(8)	
Bond Angles (°)			
O(1)-Ru(1)-O(2)	92.4(2)	O(2)-Ru(1)-N(1)	174.2(2)
O(1)-Ru(1)-O(3)	173.8(2)	O(3)-Ru(1)-O(4)	91.3(2)
O(1)-Ru(1)-O(4)	82.5(2)	O(3)-Ru(1)-P(1)	90.2(1)
O(1)-Ru(1)-P(1)	96.0(1)	O(3)-Ru(1)-N(1)	90.0(2)
O(1)-Ru(1)-N(1)	92.6(1)	O(4)-Ru(1)-P(1)	177.9(1)
O(2)-Ru(1)-O(3)	86.8(1)	O(4)-Ru(1)-N(1)	88.9(2)
O(2)-Ru(1)-O(4)	86.4(1)	P(1)-Ru(1)-N(1)	92.6(1)
O(2)-Ru(1)-P(1)	92.3(1)	Ru(1)-N(1)-N(1) <sup>a</sup>	174.2(4)

a) indicates atom generated by the symmetry operation (2-x, y, 3/2-z).

Viewing the binuclear structure  $cis-[{\text{Ru}(\text{acac})_2(\text{PPr}^i_3)}_2(\mu\text{-N}_2)]$  along the Ru(1)-N(1)-N(2)-Ru(2) axis reveals that the two Ru-PPr<sup>i</sup><sub>3</sub> vectors are almost perpendicular to each other. A similar orientation of the two NN'N ligand systems found for  $[{\text{mer,trans-RuCl}_2(\text{NN}'\text{N})_2}_2(\mu\text{-N}_2)]$  (NN'N = 2,6-bis[(dimethylamino)methyl]pyridine)<sup>15</sup> and the *trans*-PPr<sup>i</sup><sub>3</sub> groups of  $cis,trans,cis-[{\text{RuH}_2(\text{PPr}^i_3)_2(\text{N}_2)}_2(\mu\text{-N}_2)]$ <sup>42</sup> may be accounted for by the following simple orbital argument. Since Ru(II) is a low spin d<sup>6</sup>-electron ion in an octahedral environment, the t<sub>2g</sub> set of orbitals is filled. Therefore, π-back-donation of electron density from ruthenium t<sub>2g</sub> orbitals will occur into two orthogonal sets of empty π\* antibonding orbitals of the nitrogen. By perpendicular twisting of the [Ru] moieties, this back-donation will be maximised.<sup>15</sup>

The <sup>1</sup>H NMR spectrum of  $cis-[{\text{Ru}(\text{acac})_2(\text{PPr}^i_3)}_2(\mu\text{-N}_2)]$  reveals the presence of two isomers in solution, which are likely the homochiral complex (ΔΔ/ΛΛ) and the heterochiral complex (ΔΛ/ΛΔ) arising from the chirality of the *cis*-[Ru(acac)<sub>2</sub>] groups. The <sup>1</sup>H, <sup>13</sup>C{<sup>1</sup>H} and <sup>31</sup>P{<sup>1</sup>H} NMR spectral data for  $cis-[{\text{Ru}(\text{acac})_2(\text{PPr}^i_3)}_2(\mu\text{-N}_2)]$  are shown in Table 2.26. When the complex was first isolated, the major isomer displayed four methyl acac singlets and two methine acac singlets, whereas the minor isomer showed three methyl acac singlets (presumably due to accidental overlap) and two methine singlets. In the <sup>13</sup>C{<sup>1</sup>H} NMR spectrum, there are seven detectable methyl acac resonances, four methine acac singlets and seven C≡O acac resonances; the odd number of resonances is presumably due to accidental overlap. The ratio of the major and minor isomers *ca.* 10 minutes after dissolution in C<sub>6</sub>D<sub>6</sub> at room temperature is *ca.* 4:1, after 14 hours *ca.* 2:1 and after 62 hours *ca.* 3:2. The <sup>31</sup>P{<sup>1</sup>H} NMR spectrum reveals two peaks at δ 60.6 and 60.5 also in a ratio of *ca.* 3:2 in d<sub>6</sub>-benzene after 62 hours. The <sup>1</sup>H NMR spectrum of  $cis-[{\text{Ru}(\text{acac})_2(\text{PPr}^i_3)}_2(\mu\text{-N}_2)]$  measured *in situ* from the reaction solution indicates that the isomers are in a ratio of *ca.* 1:1. This isomerization of  $cis-[{\text{Ru}(\text{acac})_2(\text{PPr}^i_3)}_2(\mu\text{-N}_2)]$  probably occurs via

**Table 2.26:**  $^1\text{H}$ ,  $^{13}\text{C}\{^1\text{H}\}$  and  $^{31}\text{P}\{^1\text{H}\}$  NMR spectral parameters of the  $[\text{Ru}(\text{acac})_2]$  moiety of the complex  $\text{cis}-[(\text{Ru}(\text{acac})_2(\text{PPri}_3)_2(\mu\text{-N}_2))]_2$  in  $d_6$ -benzene at room temperature.

$^1\text{H}$ NMR <sup>a</sup>		$^{13}\text{C}\{^1\text{H}\}$ NMR <sup>a</sup>			$^{31}\text{P}\{^1\text{H}\}$ NMR <sup>a</sup>		
acac		acac					
$\text{CH}_3$	CH	$\text{PPri}_3$	$\text{CH}_3$	CH	$\text{C}=\text{O}$		
1.81, 1.83, 1.85, 2.03	5.26, 5.33	2.47 (6H, m) 1.29, 1.40 (dd, $J_{\text{PC}} = 12.5$ Hz, $J_{\text{PH}} = 7.5$ Hz)	28.3 ( $J_{\text{PC}} = 5.6$ Hz), 27.8, 27.6, 27.2	98.5, 100.3	187.5, 186.4, 185.7, 184.6	19.2, 19.5 24.6 (d, $J_{\text{PC}} = 20$ Hz)	+60.6
1.80, 1.87, 2.08	5.29, 5.35	2.47 (6H, m) 1.29, 1.40 (dd, $J_{\text{PC}} = 12.5$ Hz, $J_{\text{PH}} = 7.5$ Hz)	28.4 ( $J_{\text{PC}} = 5.6$ Hz), 27.6, 27.2	98.6, 100.3	187.6, 185.8, 184.5	19.1, 19.4 24.6 (d, $J_{\text{PC}} = 20$ Hz)	+60.5

a) singlets unless otherwise indicated.

the undetected mononuclear complex  $cis\text{-}[\text{Ru}(\text{acac})_2(\text{PPr}^i_3)(\text{N}_2)]$  and the coordinatively unsaturated species  $[\text{Ru}(\text{acac})_2(\text{PPr}^i_3)]$ . Similar dissociation of bridging dinitrogen was observed for  $[\{\text{Ni}(\text{PCy}_3)_2\}_2(\mu\text{-N}_2)]$ .<sup>43</sup> Diastereoisomers were also detected by  $^1\text{H}$  NMR spectroscopy for the binuclear osmium(II) complex  $cis\text{-}[\{\text{Os}(\text{bpy})_2\text{Cl}\}_2(\mu\text{-N}_2)][\text{PF}_6]_2$ .<sup>44</sup>

The binuclear complex  $cis\text{-}[\{\text{Ru}(\text{acac})_2(\text{PPr}^i_3)\}_2(\mu\text{-N}_2)]$  readily reacts with  $\text{C}_2\text{H}_4$  (1 bar) in  $\text{C}_6\text{D}_6$  at  $25^\circ\text{C}$  to re-form  $cis\text{-}[\text{Ru}(\text{acac})_2(\eta^2\text{-C}_2\text{H}_4)(\text{PPr}^i_3)]$ . The reaction is quantitative according to  $^{31}\text{P}\{^1\text{H}\}$  and  $^1\text{H}$  NMR spectroscopy. The dinitrogen complex also readily reacts with  $\text{PhC}\equiv\text{CH}$  or  $\text{CO}$  (1 bar) at  $25^\circ\text{C}$  to form the complexes  $cis\text{-}[\text{Ru}(\text{acac})_2(\text{PPr}^i_3)(=\text{C}=\text{C}(\text{H})\text{Ph})]$  and  $trans\text{-}[\text{Ru}(\text{acac})_2(\text{PPr}^i_3)(\text{CO})]$ , respectively. For both reactions, the yields were quantitative as shown by  $^{31}\text{P}\{^1\text{H}\}$  NMR spectroscopy.

## 2.10 Discussion

The affinity of the Ru(II) ion for unsaturated ligands such as alkenes, CO and  $\text{N}_2$  as previously discussed in Chapter 1, is also shown by the number of  $[\text{Ru}(\text{acac})_2\text{LL}']$  complexes isolated in which either L or L' is an unsaturated ligand. The reduction of  $[\text{Ru}(\text{acac})_3]$  by activated zinc dust in the presence of cyclooctene to form  $cis\text{-}[\text{Ru}(\text{acac})_2(\eta^2\text{-C}_8\text{H}_{14})_2]$ <sup>14</sup> has been extended to ethene and probably could include other alkenes. Unlike the complex  $cis\text{-}[\text{Ru}(\text{acac})_2(\eta^2\text{-C}_8\text{H}_{14})_2]$ , which is only stable in solution in the presence of free alkene,<sup>14</sup> the ethene analogue can be isolated as a crystalline solid which is indefinitely stable under an argon atmosphere. Although numerous ruthenium(II) ethene complexes have been isolated, most of these complexes contain only one ethene group together with Cp, CO and tertiary phosphines. Examples of isolated ethene complexes include  $[\text{Ru}(\text{NH}_3)_5(\eta^2\text{-C}_2\text{H}_4)][\text{S}_2\text{O}_6]$ ,<sup>1</sup>  $[\text{Ru}(\text{H}_2\text{O})_{6-x}(\eta^2\text{-C}_2\text{H}_4)_x][\text{OTf}]_2$  ( $x = 1, 2$ ),<sup>2</sup>  $[\text{RuCl}_2(\text{CO})(\eta^2\text{-C}_2\text{H}_4)(\text{PPhMe}_2)]$ ,<sup>45</sup>  $[\text{CpRu}(\text{PMe}_3)_2(\eta^2\text{-C}_2\text{H}_4)][\text{PF}_6]$ ,<sup>46</sup>  $[\text{CpRu}(\text{PPh}_3)_2(\eta^2\text{-C}_2\text{H}_4)][\text{BF}_4]$ ,<sup>47</sup>  $[\text{CpRu}(\eta^2\text{-C}_2\text{H}_4)_3][\text{BF}_4]$ ,<sup>48</sup>  $[\text{CpRu}(\text{CO})_2(\eta^2\text{-C}_2\text{H}_4)]$

$C_2H_4)] [BF_4]$ ,<sup>49</sup>  $[(\eta^6-C_6H_6)RuCl(PMe_3)(\eta^2-C_2H_4)] [PF_6]$ ,<sup>50</sup>  $[(\eta^6-C_6H_6)Ru(PMe_3)_2(\eta^2-C_2H_4)] [PF_6]_2$ ,<sup>51</sup>  $[Ru(\text{porphyrinato})(\eta^2-C_2H_4)]$  (porphyrinato = 5,10,15,20-tetra-*p*-tolylporphyrinato dianion or 2,3,7,8,12,13,17,18-octaethyl-porphyrinato dianion),<sup>52</sup> *mer,trans*- $[RuCl_2(\eta^3-NN'N)(\eta^2-C_2H_4)]$  (NN'N = 2,6-bis[dimethylamino)methyl]pyridine),<sup>53</sup>  $[Ru(\text{tmtaa})(\eta^2-C_2H_4)(THF)]$  (tmtaa = dibenzotetramethyltetraza[14]annulene dianion),<sup>54</sup>  $[Cp^*Ru(CO)_2(\eta^2-C_2H_4)] [PF_6]$ ,<sup>55</sup> and  $[RuH\{(\eta^3-C_6H_8)PCy_2\}(PCy_3)(\eta^2-C_2H_4)]$ .<sup>56</sup> Ruthenium(II) ethene complexes which have been detected in solution but not isolated owing to easy loss of ethene include  $[Cp^*Ru(\eta^2-C_2H_4)(\eta^1-O_2CCH_3)(PPh_3)]$ ,<sup>57</sup> *trans*- $[Ru(PPh_3)_2Cl(NO)(\eta^2-C_2H_4)]$ ,<sup>58</sup> *cis*- $[Ru(\text{acac})_2(\eta^2-C_2H_4)(SbPr^i_3)]$ ,<sup>11</sup>  $[Cp^*Ru(PPr^i_3)(\eta^2-C_2H_4)Cl]$ ,<sup>59</sup>  $[Cp^*Ru(PPr^i_2Ph)(\eta^2-C_2H_4)(OCH_2CF_3)]$ <sup>60</sup> and  $[CpRu(\text{tmeda})(\eta^2-C_2H_4)] [BAr'_4]$  [tmeda = N,N,N',N'-tetramethylethylenediamine; Ar' = 3,5-C<sub>6</sub>H<sub>3</sub>(CF<sub>3</sub>)<sub>2</sub>].<sup>61</sup>

The relative stabilities of *cis*- $[Ru(\text{acac})_2(\eta^2-C_2H_4)_2]$  and *cis*- $[Ru(\text{acac})_2(\eta^2-C_8H_{14})_2]$  reflect the observed trend in the metal-alkene stability constants, K, for rhodium(I),<sup>62</sup> nickel(0)<sup>63</sup> and Ag(I).<sup>64,65</sup> In all three cases the values of K decrease as the number of alkyl substituents on the C=C bond increases; the stereochemistry about the C=C bond also has an effect on K. For example, the stability constants of ethene and *cis*-cyclooctene with silver(I) at 40 °C are 22.3 and 14.4, respectively.<sup>64</sup> Since the replacement of hydrogen atoms at the C=C bond by electron donating groups increases the energy of the  $\pi$  and  $\pi^*$  orbitals,<sup>66</sup>  $\pi$ -back-donation from the metal to the alkene will be reduced and the metal-alkene bond will be destabilised.

The two ethene ligands of *cis*- $[Ru(\text{acac})_2(\eta^2-C_2H_4)_2]$  are mutually orthogonal and eclipse the *trans* O-Ru-O and O-Ru-( $\eta^2-C_2H_4$ ) vectors. This conformation is probably the result of electronic and steric effects. Similar bis(ethene) conformations have been observed for the octahedral complexes *trans*- $[Mo(\eta^2-C_2H_4)_2(PMe_3)_4]$ ,<sup>67</sup> *trans*- $[W(\eta^2-C_2H_4)_2(PMe_3)_4]$ ,<sup>68</sup> *trans*- $[W(CO)_4(\eta^2-C_2H_4)_2]$ ,<sup>5</sup> *cis,mer*- $[OsH(\eta^2-C_2H_4)_2(PMe_2Ph)_3]^+{}^{23}$  and *cis*-

$[\text{ReHCl}_2(\eta^2\text{-C}_2\text{H}_4)_2(\text{PMe}_2\text{Ph})_2]$ .<sup>69</sup> The bonding and conformational preferences for the molybdenum and tungsten complexes have been subject of a number theoretical studies.<sup>66,70,71</sup> In particular, Veillard and coworkers<sup>70</sup> have discussed the relative energies of the different conformations for the model complex *trans*- $[\text{Mo}(\eta^2\text{-C}_2\text{H}_4)_2(\text{PH}_3)_4]$  and found that the staggered-eclipsed (the first term applies to the relative orientation of the ethene ligands while the second defines the position of the axial ethene groups relative to the *trans* P-Mo-P vectors) was the most stable on the basis of electronic and steric effects. This result agrees well with the observed conformation for *trans*- $[\text{Mo}(\eta^2\text{-C}_2\text{H}_4)_2(\text{PMe}_3)_4]$ , which allows  $\pi$ -back donation of electron density from two mutually orthogonal metal  $t_{2g}$  orbitals to the ethene  $\pi^*$  orbitals instead of one and thus reduces the competition for  $\pi$ -back donation.<sup>67</sup>

In the closely related  $d^8$  complexes  $[\text{Rh}(\text{acac})(\eta^2\text{-C}_2\text{H}_4)_2]$ <sup>72</sup> and  $[\text{CpRh}(\eta^2\text{-C}_2\text{H}_4)_2]$ ,<sup>73</sup> however, both ethene ligands are parallel. A similar situation was found for the seven-coordinate complex  $[\text{ReH}_3(\eta^2\text{-C}_2\text{H}_4)_2(\text{PPhPr}^i_2)_2]$ .<sup>74</sup> The ethene conformations for the  $d^8$  complexes in which the ethene ligands are *cis* are readily rationalised by consideration of the electronic interactions. Since there are no ligands on the z-axis for a  $d^8$ -square planar complex, the energy of the  $d_{z^2}$  orbital decreases whereas the energy of the  $d_{x^2-y^2}$  orbital increases, relative to the triply degenerate  $t_{2g}$  orbitals of a regular octahedron. The  $t_{2g}$  orbitals are also affected with the  $d_{xy}$  orbital increasing in energy and the  $d_{xz}, yz$  orbitals decreasing in energy. It is this decrease in energy which affords a greater overlap with the ethene  $\pi^*$  orbitals than for the  $d_{xy}$  orbital and results in greater  $\pi$ -backdonation.

The reason for the adoption of the orthogonal ethene conformation in the octahedral complexes *cis*- $[\text{Ru}(\text{acac})_2(\eta^2\text{-C}_2\text{H}_4)_2]$ , *cis,mer*- $[\text{OsH}(\eta^2\text{-C}_2\text{H}_4)_2(\text{PMe}_2\text{Ph})_3]$ <sup>74a</sup> and *cis*- $[\text{Re}(\eta^2\text{-C}_2\text{H}_4)_2(\text{H})(\text{PMe}_2\text{Ph})_2\text{Cl}_2]$ <sup>69</sup> is less clear. For a regular octahedron, the metal  $t_{2g}$  orbitals available for  $\pi$ -back donation



are triply degenerate for  $d^4$  and  $d^6$  ions. Therefore, neither conformation will be significantly preferred and steric effects may well come into play. Calculations performed on *cis,mer*-[OsH( $\eta^2$ -C<sub>2</sub>H<sub>4</sub>)<sub>2</sub>(PMe<sub>2</sub>Ph)<sub>3</sub>]<sup>+</sup> indicate that the energy difference between the parallel and orthogonal ethene conformations is less than 10 kJ mol<sup>-1</sup>.<sup>23</sup> Since the complexes *cis*-[Ru(acac)<sub>2</sub>( $\eta^2$ -C<sub>2</sub>H<sub>4</sub>)(NH<sub>3</sub>)] and *cis*-[Ru(acac)<sub>2</sub>( $\eta^2$ -C<sub>2</sub>H<sub>4</sub>)(PPr<sup>*i*</sup>)<sub>3</sub>] show different orientations of the ethene ligand, and *cis*-[Ru(acac)<sub>2</sub>( $\eta^2$ -C<sub>2</sub>H<sub>4</sub>)(PCy<sub>3</sub>)] shows both orientations of the ethene vectors (see p. 51), the energy difference between conformations must be small. A third ethene conformation exists in which the C=C vectors are linear but this was calculated to be *ca.* 84 kJ mol<sup>-1</sup> higher in energy than the ground state for *cis,mer*-[OsH( $\eta^2$ -C<sub>2</sub>H<sub>4</sub>)<sub>2</sub>(PMe<sub>2</sub>Ph)<sub>3</sub>]<sup>+</sup>.<sup>23</sup> This destabilisation was attributed to the fact that only one metal d orbital has the proper symmetry to overlap with two ethene  $\pi^*$  orbitals and also to strong ethene/ethene steric repulsion.

The metrical data for the coordinated ethene ligands of *cis*-[Ru(acac)<sub>2</sub>( $\eta^2$ -C<sub>2</sub>H<sub>4</sub>)<sub>2</sub>] are very similar to those found for [Rh(acac)( $\eta^2$ -C<sub>2</sub>H<sub>4</sub>)<sub>2</sub>] and Zeise's salt, K[PtCl<sub>3</sub>( $\eta^2$ -C<sub>2</sub>H<sub>4</sub>)] *i.e.* the C=C bond lengths are almost equal and only slightly greater than those in free ethene,<sup>40</sup> and the bend-back angles for the ethene protons are also similar (see p. 35 - 36). On the basis of this crystallographic evidence, the Dewar-Chat-Duncanson model<sup>75,76</sup> is probably more appropriate than the metallacycle description<sup>36</sup> of the metal-alkene bond for all *trans*- and *cis*-[Ru(acac)<sub>2</sub>( $\eta^2$ -C<sub>2</sub>H<sub>4</sub>)L] complexes. A metallacyclic description of the metal-alkene bond would require the C-C distance to be closer to that of a single bond (1.54 Å) and a bend-back angle  $\alpha$  approaching 60°.<sup>73</sup> Further evidence for the Dewar-Chat-Duncanson model of bonding for ethene in these complexes are the coordinated ethene C-H coupling constants (*ca.* 155 - 160 Hz), which are very close to that of free ethene (156.4 Hz).<sup>3</sup>

Unfortunately, the observed equivalence of the carbon atoms of the coordinated  $C_2H_4$  ligands in solution, even at the lowest accessible temperature, precludes an estimate of the alkene rotation barrier. This observation implies either that the rotation is very rapid on the NMR timescale, even at *ca.*  $-95\text{ }^\circ\text{C}$ , or that the inequivalence induced by *cis*- $[Ru(acac)_2]$  is unobservably small. The  $\Delta G^\ddagger$  value for ethene rotation in *cis*- $[Ru(acac)_2(\eta^2-C_2H_4)_2]$  would not be expected to be substantially different from those measured for comparable Pt(II) and Rh(I) complexes (*ca.*  $50 - 55\text{ kJ mol}^{-1}$ ),<sup>22,25-27</sup> given the similarity of C=C and M-C bond lengths, and in the fact for  $[Rh(acac)(\eta^2-C_2H_4)_2]$  there are two mutually *cis*-alkenes. In fact, the for other ruthenium(II)-ethene complexes which includes  $[CpRu(\eta^2-C_2H_4)LL']^{n+}$  ( $n = 0$ ,  $L = Me$ ,  $L' = CO$ ;<sup>77</sup>  $n = 1$ ,  $L = L' = CO$ <sup>78</sup>) and  $[CpRu(\eta^2-C_2H_4)L_2][OTf]$  ( $L_2 =$  diisopropyl-1,4-diaza-1,3-butadiene, bis-*p*-tolyl-1,4-diaza-1,3-butadiene),<sup>79</sup> the  $\Delta G^\ddagger$  value for rotation lies between *ca.*  $30 - 40\text{ kJ mol}^{-1}$ . The close similarity between the crude estimates of  $\Delta G^\ddagger$  for *cis*- $[Ru(acac)_2(\eta^2-C_2H_4)_2]$  suggests that the same process, *viz* reversible ethene dissociation, is responsible for the coalescence of the ethene proton multiplets and the broadening of the acac methyl resonances. If rotation is very rapid, the most likely mechanism for the observed equivalence is rotation about the Ru- $\eta^2-C_2H_4$  axis rather than about the C=C bond, since the latter process requires the ethene protons to point directly at the metal centre during the rotation.<sup>6,26</sup> Direct experimental evidence exists for the former process exists in the chiral complexes  $[CpCr(\eta^2-C_2H_4)(CO)(NO)]$ <sup>80</sup> and  $[Os(\eta^2-C_2H_4)(CO)(NO)(PPh_3)_2][PF_6]$ .<sup>81</sup> The variation of the proton chemical shift of the ethene protons with temperature is probably due to the relative populations of ethene rotamers since various halogen substituted ethanes also show a chemical shift temperature dependence with different nuclei.<sup>82</sup>

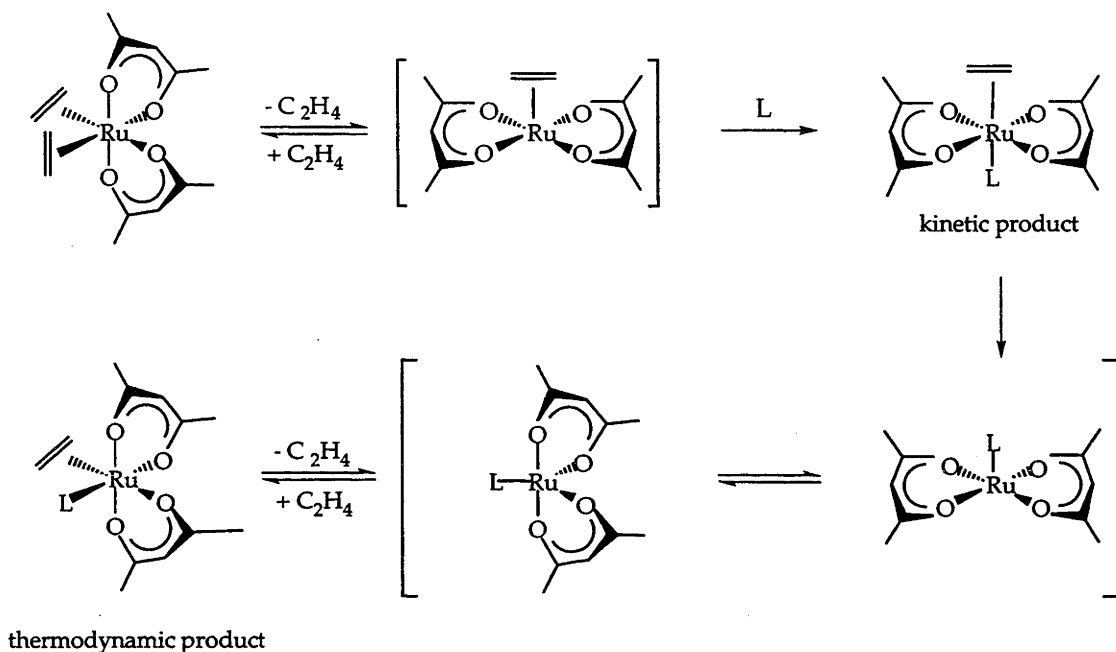
The occurrence of reversible ethene dissociation for *cis*- $[Ru(acac)_2(\eta^2-C_2H_4)_2]$  is not surprising since *cis*- $[Ru(acac)_2(\eta^2-C_8H_{14})_2]$  is only stable in the presence of free  $C_8H_{14}$ <sup>14</sup> and since ethene is also readily replaced by various

monodentate ligands at room temperature. Ethene exchange is slow on the NMR timescale at room temperature, whereas fast ethene exchange is found for  $[\text{Rh}(\text{acac})(\eta^2\text{-C}_2\text{H}_4)_2]$  under similar conditions.<sup>6</sup> An associative mechanism is proposed for the rhodium(I) complex, which has 16 valence electrons and two free coordination sites, to form a five-coordinated species  $[\text{Rh}(\text{acac})(\eta^2\text{-C}_2\text{H}_4)_3]$ .<sup>6</sup> However, coordination of a third ethene ligand to *cis*- $[\text{Ru}(\text{acac})_2(\eta^2\text{-C}_2\text{H}_4)_2]$  is unfavourable as the Ru(II) ion is co-ordinatively saturated and the complex has 18 valence electrons. There is also no detectable ethene exchange for the rhodium(I) complex  $[\text{CpRh}(\eta^2\text{-C}_2\text{H}_4)_2]$  at room temperature or above 100 °C, presumably due to the fact that this complex also has 18 valence electrons.<sup>6</sup>

Initial loss of the alkene from *cis*- $[\text{Ru}(\text{acac})_2(\eta^2\text{-C}_2\text{H}_4)_2]$  is believed to occur with the formation of a five-coordinate square-pyramidal intermediate  $[\text{Ru}(\text{acac})_2(\eta^2\text{-C}_2\text{H}_4)]$  in which ethene occupies the apical position. Preferential attack of the incoming ligand L at the vacant site will give *trans*- $[\text{Ru}(\text{acac})_2(\eta^2\text{-C}_2\text{H}_4)\text{L}]$ . Subsequent loss of ethene from this complex may give the square pyramidal five-coordinate intermediate  $[\text{Ru}(\text{acac})_2\text{L}]$  (see p. 21) which then isomerises to a trigonal bi-pyramidal five-coordinate intermediate. Coordination with ethene forms *cis*- $[\text{Ru}(\text{acac})_2(\eta^2\text{-C}_2\text{H}_4)\text{L}]$ , the thermodynamic product. This sequence is shown in Scheme 2.1. Evidence supporting this pathway is the isolation of the complexes *trans*- $[\text{Ru}(\text{acac})_2(\eta^2\text{-C}_2\text{H}_4)\text{L}]$  (L = NH<sub>3</sub>, C<sub>5</sub>H<sub>5</sub>N), both of which slowly isomerise to their *cis* analogues. The isolation (or detection) of the monosubstituted complexes *cis*- $[\text{Ru}(\text{acac})_2(\eta^2\text{-C}_2\text{H}_4)\text{L}]$  (L = PPh<sub>3</sub>, PPr<sup>*i*</sup><sub>3</sub>, PCy<sub>3</sub>) in an aromatic solvent provides the first evidence for the stepwise replacement of alkenes by a tertiary phosphine in this series of complexes. Weakly coordinating solvents, such as THF, appear to stabilise the square-pyramidal five coordinate species  $[\text{Ru}(\text{acac})_2\text{L}]$  by occupying the vacant coordination site and thus allow a second equivalent of L to react with this intermediate to form *trans*- $[\text{Ru}(\text{acac})_2\text{L}_2]$ , which usually precipitates from

solution. In non-coordinating solvents such as benzene however, this five-coordinate intermediate is not stabilised and thus re-coordinates ethene.

**Scheme 2.1:** Suggested pathway for formation of *trans*- and *cis*-[Ru(acac)<sub>2</sub>(η<sup>2</sup>-C<sub>2</sub>H<sub>4</sub>)L] from *cis*-[Ru(acac)<sub>2</sub>(η<sup>2</sup>-C<sub>2</sub>H<sub>4</sub>)<sub>2</sub>].



Square-pyramidal geometry for a five-coordinate d<sup>6</sup>-metal complex is to be expected on the basis of theoretical calculations.<sup>83,84</sup> Spectroscopic evidence also exists for dilute solutions of *trans*-[Ru(acac)<sub>2</sub>(PCy<sub>3</sub>)<sub>2</sub>] and solutions of *cis*-[Ru(acac)<sub>2</sub>(η<sup>2</sup>-C<sub>2</sub>H<sub>4</sub>)(PCy<sub>3</sub>)] in THF to dissociate to give either the square-pyramidal five-coordinate [Ru(acac)<sub>2</sub>(PCy<sub>3</sub>)] species or, more likely, a six-coordinate *trans*-[Ru(acac)<sub>2</sub>(PCy<sub>3</sub>)(THF)] complex in which the solvent is weakly coordinated. Moreover, spectroscopic evidence exists for the formation of [Ru(acac)<sub>2</sub>(PR<sub>3</sub>)(THF)] (R = Ph, Pr<sup>i</sup>), although the stereochemistry about the ruthenium atom is not known for either example. A similar dissociation reaction has been reported for [Ru(OEP)(PPh<sub>3</sub>)<sub>2</sub>] (OEP = octaethylporphyrinato dianion),<sup>85</sup> although no <sup>31</sup>P{<sup>1</sup>H} NMR spectral data were reported. Other square-pyramidal ruthenium(II) complexes which have been either characterised structurally or spectroscopically include [RuCl<sub>2</sub>(PPh<sub>3</sub>)<sub>3</sub>],<sup>17</sup>

[RuCl(NN'N)(PPh<sub>3</sub>)]OTf and [Ru(OTf)(NN'N)(PPh<sub>3</sub>)]OTf (NN'N = 2,6-bis[(dimethylamino)-methyl]pyridine),<sup>15</sup> [Ru{N(SPh<sub>2</sub>)<sub>2</sub>}(PPh<sub>3</sub>)] and [Ru{N(SPr<sup>i</sup>)<sub>2</sub>}(PPh<sub>3</sub>)](N(SR<sub>2</sub>)<sub>2</sub> = bis(dialkylthiophosphoryl)amides).<sup>16</sup>

The formation of *cis*-[Ru(acac)<sub>2</sub>(η<sup>2</sup>-C<sub>2</sub>H<sub>4</sub>)L] (L = PPh<sub>3</sub>, PPr<sup>i</sup><sub>3</sub>, PCy<sub>3</sub>) is believed to occur via the undetected intermediate *trans*-[Ru(acac)<sub>2</sub>(η<sup>2</sup>-C<sub>2</sub>H<sub>4</sub>)L]. As tertiary phosphines have a stronger *trans*-influence than either NH<sub>3</sub> or pyridine, the metal-η<sup>2</sup>-C<sub>2</sub>H<sub>4</sub> bond in *trans*-[Ru(acac)<sub>2</sub>(η<sup>2</sup>-C<sub>2</sub>H<sub>4</sub>)L] is expected to be weaker for L = tertiary phosphine than for L = NH<sub>3</sub> or pyridine.<sup>86</sup> The thermodynamic instability of the complexes *trans*-[Ru(acac)<sub>2</sub>L<sub>2</sub>] presumably arises from the electronic effects of two π-acceptor ligands, even if relatively weak, competing for electron density from the same d-orbital on ruthenium(II).<sup>14</sup> By rearranging to the corresponding *cis*-complexes, the π-acceptor ligands are now *trans* to an π-donor oxygen acac atom and no longer compete with each other for electron density.

The carbonyl complexes *trans*-[Ru(acac)<sub>2</sub>(CO)(PR<sub>3</sub>)] (R = Pr<sup>i</sup>, Cy) readily form from *trans*-[Ru(acac)<sub>2</sub>(PR<sub>3</sub>)<sub>2</sub>] in the presence of CO; the complex *cis*-[Ru(acac)<sub>2</sub>(PPr<sup>i</sup><sub>3</sub>)<sub>2</sub>] also reacts with CO, albeit more slowly, to form *trans*-[Ru(acac)<sub>2</sub>(CO)(PPr<sup>i</sup><sub>3</sub>)]. The *cis*- to *trans*-stereochemical rearrangement about the ruthenium atom is similar to that found during the replacement of the coordinated alkenes from *cis*-[Ru(acac)<sub>2</sub>(η<sup>2</sup>-alkene)<sub>2</sub>] and presumably also occurs via the square pyramidal five-coordinate species [Ru(acac)<sub>2</sub>(PR<sub>3</sub>)] (R = Pr<sup>i</sup>, Cy). Heating these *trans*-[Ru(acac)<sub>2</sub>(CO)(PR<sub>3</sub>)] (R = Pr<sup>i</sup>, Cy) complexes results in the isolation of the corresponding *cis*-isomers. This *trans*- to *cis*-isomerization probably occurs via phosphine dissociation to form a carbonyl five-coordinate species [Ru(acac)<sub>2</sub>(CO)].

Terminal alkynes, HC≡CR (R = Ph, SiMe<sub>3</sub>, Bu<sup>t</sup>), also react with *cis*-[Ru(acac)<sub>2</sub>(PPr<sup>i</sup><sub>3</sub>)<sub>2</sub>] and *cis*-[Ru(acac)<sub>2</sub>(η<sup>2</sup>-C<sub>2</sub>H<sub>4</sub>)(PPr<sup>i</sup><sub>3</sub>)] to form the vinylidene complexes *cis*-[Ru(acac)<sub>2</sub>(PPr<sup>i</sup><sub>3</sub>)<sub>2</sub>]=C=C(H)R]. There are several possible mechanisms for the formation of a vinylidene ligand within the

coordination sphere of a metal atom. The first mechanism involves a 1,2-hydrogen shift in a metal- $\eta^2$ -HC $\equiv$ CR intermediate and <sup>the</sup>second the involves oxidative addition of the alkyne to form an alkynyl(hydrido) complex which subsequently re-arranges to form the vinylidene complex.<sup>35,87-89</sup> The former mechanism is preferred for the d<sup>6</sup> Ru(II) ion on the basis of experimental and calculated results.<sup>36,87-90</sup> The second mechanism appears to be favoured in the case of the d<sup>8</sup> Rh(I) ion; several alkynyl(hydrido) complexes of rhodium(III) which subsequently re-arrange to form the vinylidene-rhodium(I) complexes have been isolated.<sup>91-93</sup> Calculations also show that this mechanism is favoured for rhodium complexes.<sup>94</sup> A third possible mechanism involves the insertion of the alkyne into a metal-hydride bond to form a  $\sigma$ -vinyl, which undergoes an  $\alpha$ -hydrogen migration to give a hydrido/vinylidene complex.<sup>94a</sup> This mechanism can be excluded as there is no evidence for ruthenium-hydride complexes in this work. Disubstituted alkynes do not displace ethene from *cis*-[Ru(acac)<sub>2</sub>( $\eta^2$ -C<sub>2</sub>H<sub>4</sub>)L] (L = PPr<sup>i</sup><sub>3</sub>, PCy<sub>3</sub>), an observation that may correlate with the reduced stability constants found for disubstituted alkynes with Ag(I) (*e.g.* the stability constant K for 3-hexyne is 2.6 which is less than for ethene, K = 22.2).<sup>64</sup>

The strong affinity of the Ru(II) ion for dinitrogen (see p. 1 - 2) is also shown by the formation of the binuclear complex *cis*-[Ru(acac)<sub>2</sub>(PPr<sup>i</sup><sub>3</sub>)<sub>2</sub>( $\mu$ -N<sub>2</sub>)] by heating a solution of *cis*-[Ru(acac)<sub>2</sub>( $\eta^2$ -C<sub>2</sub>H<sub>4</sub>)(PPr<sup>i</sup><sub>3</sub>)] under industrial grade dihydrogen (3 bar) containing *ca.* 100 ppm N<sub>2</sub>. The reaction of *cis*-[Ru(acac)<sub>2</sub>( $\eta^2$ -C<sub>2</sub>H<sub>4</sub>)(PPr<sup>i</sup><sub>3</sub>)] with N<sub>2</sub> (3 bar) also gives the dinuclear complex, as judged by the <sup>31</sup>P{<sup>1</sup>H} NMR chemical shift, not a mononuclear complex [Ru(acac)<sub>2</sub>(PPr<sup>i</sup><sub>3</sub>)(N<sub>2</sub>)]. Since there is a slight but significant difference in the <sup>31</sup>P{<sup>1</sup>H} NMR chemical shifts of comparable mono- and binuclear N<sub>2</sub> complexes *e.g.* *mer,trans*-[IrH<sub>3</sub>(PPr<sup>i</sup><sub>3</sub>)<sub>2</sub>(N<sub>2</sub>)] ( $\delta$  +44.8) and *mer,trans*-[IrH<sub>3</sub>(PPr<sup>i</sup><sub>3</sub>)<sub>2</sub>( $\mu$ -N<sub>2</sub>)] ( $\delta$  +47.7)<sup>95</sup> as well as *cis,cis,trans*-[RuH<sub>2</sub>(N<sub>2</sub>)<sub>2</sub>(PPr<sup>i</sup><sub>3</sub>)<sub>2</sub>] ( $\delta$  +73.6) and *cis,trans,cis*-[RuH<sub>2</sub>(PPr<sup>i</sup><sub>3</sub>)<sub>2</sub>(N<sub>2</sub>)<sub>2</sub>( $\mu$ -N<sub>2</sub>)] ( $\delta$  +76.3),<sup>42</sup> a similar difference would also be expected between *cis*-[Ru(acac)<sub>2</sub>(PPr<sup>i</sup><sub>3</sub>)(N<sub>2</sub>)] and *cis*-[Ru(acac)<sub>2</sub>(PPr<sup>i</sup><sub>3</sub>)<sub>2</sub>( $\mu$ -N<sub>2</sub>)]. However, there is no evidence for the formation of *cis*-[Ru(acac)<sub>2</sub>(PPr<sup>i</sup><sub>3</sub>)(N<sub>2</sub>)], which is presumed to be an intermediate in the formation of the binuclear complex and the interconversion of the diastereoisomers.

The mild conditions required for the isomerization of *trans*-[Ru(acac)<sub>2</sub>(PPr<sup>*i*</sup><sub>3</sub>)<sub>2</sub>] contrast with those for *trans*-[Ru(acac)<sub>2</sub>(PPh<sub>3</sub>)<sub>2</sub>] and *trans*-[Ru(acac)<sub>2</sub>(PMe<sub>3</sub>)<sub>2</sub>], which isomerise in refluxing benzene and mesitylene, respectively.<sup>14</sup> As the phosphine cone angle increases,<sup>96</sup> the reactivity of the isolated complexes increases. Nolan and coworkers have measured the Ru-PR<sub>3</sub> bond energy for the complexes [(*p*-cymene)RuCl<sub>2</sub>L]<sup>97</sup> and [Cp'RuCIL] (L = tertiary phosphine; Cp' = Cp<sup>98</sup> or Cp\*<sup>99</sup>) and found that trimethylphosphine forms relatively stronger Ru-P bonds by *ca.* 45 kJ mol<sup>-1</sup> than either triisopropyl phosphine or tricyclohexylphosphine. The Ru-PR<sub>3</sub> bond energy appears to increase as the Tolman cone angle<sup>96</sup> decreases although electronic factors are also involved in determining the magnitude.<sup>97,99</sup>

The Ru-O (acac) bond lengths in the complexes *cis*-[Ru(acac)<sub>2</sub>(η<sup>2</sup>-C<sub>2</sub>H<sub>4</sub>)L] (L = C<sub>2</sub>H<sub>4</sub>, NH<sub>3</sub>, PPr<sup>*i*</sup><sub>3</sub> and PCy<sub>3</sub>), *trans*-[Ru(acac)<sub>2</sub>(η<sup>2</sup>-C<sub>2</sub>H<sub>4</sub>)(NC<sub>5</sub>H<sub>5</sub>)], *cis*-[Ru(acac)<sub>2</sub>(PPr<sup>*i*</sup><sub>3</sub>)<sub>2</sub>] and *trans*-[Ru(acac)<sub>2</sub>(PCy<sub>3</sub>)<sub>2</sub>] are generally in the range 2.05 - 2.07 Å, similar to those in the complexes [Ru(acac)<sub>2</sub>L<sub>2</sub>] (L = PPh<sub>2</sub>Me, CNBu<sup>*t*</sup>, dppm)<sup>14</sup> and in the {Ru<sup>II</sup>(acac)<sub>2</sub>} chelate complexes of *o*-CH<sub>2</sub>=CHC<sub>6</sub>H<sub>4</sub>NMe<sub>2</sub><sup>9</sup> and *o*-PhC≡CC<sub>6</sub>H<sub>4</sub>NMe<sub>2</sub>.<sup>100</sup> In complexes containing a tertiary phosphine, however, the Ru-O distances opposite to the phosphorus atom are significantly longer (*ca.* 0.02 - 0.06 Å) than those *trans* to the acac oxygen atoms, consistent with the higher *trans* influence of the tertiary phosphine. The Ru-P bond distances range from 2.312(2) to 2.4268 (3) Å with the longest distance belonging to *trans*-[Ru(acac)<sub>2</sub>(PCy<sub>3</sub>)<sub>2</sub>]. This distance is similar to that found for [Ru(OEP)(PPh<sub>3</sub>)<sub>2</sub>] (OEP = octaethylporphyrinato dianion) (2.438 (<1) Å) which dissociates in dilute solution to a five-coordinate complex with the phosphine in the apical position.<sup>85</sup>

The steric repulsion between the *cis*-PPr<sup>*i*</sup><sub>3</sub> groups in *cis*-[Ru(acac)<sub>2</sub>(PPr<sup>*i*</sup><sub>3</sub>)<sub>2</sub>] is presumably responsible for the large P-Ru-P bond angle of 105 ° and for the Ru-P bond lengths of *ca.* 2.35 Å, which are *ca.* 0.07 Å

longer than those found in *cis*-[Ru(acac)<sub>2</sub>(PPh<sub>2</sub>Me)<sub>2</sub>] (P-Ru-P bond angle of 93°).<sup>14</sup> Similar P-M-P angles were found for the complexes [Rh(acac)(PCy<sub>3</sub>)<sub>2</sub>],<sup>31</sup> *cis*-[Mo(CO)<sub>4</sub>(PR<sub>3</sub>)<sub>2</sub>] (R = Ph, Cy) (both 105°)<sup>33,34</sup> and *cis*-[Mo(CO)<sub>4</sub>(PPh<sub>2</sub>Me)<sub>2</sub>] (93°).<sup>33</sup> The average Mo-P bond distance for *cis*-[Mo(CO)<sub>4</sub>(PCy<sub>3</sub>)<sub>2</sub>] (2.654 Å) was found to be *ca.* 0.08 Å longer than that for the PPh<sub>3</sub> complex and *ca.* 0.1 Å longer than that for the PPh<sub>2</sub>Me complex; the longer Mo-P distances for the phosphines with a larger cone angle<sup>96</sup> appears to be the main method for relieving steric strain in these complexes. On this basis, it is not surprising that *cis*-[Ru(acac)<sub>2</sub>(PCy<sub>3</sub>)<sub>2</sub>] does not readily form. Steric repulsion between adjacent PCy<sub>3</sub> groups may destabilise the corresponding *cis*-isomer, although, as previously stated, complexes which contain *cis*-PCy<sub>3</sub> groups do exist and crystal structures have been determined.<sup>31,34</sup>

The Ru-C (C<sub>2</sub>H<sub>4</sub>) bond lengths for the complexes *cis*-[Ru(acac)<sub>2</sub>(η<sup>2</sup>-C<sub>2</sub>H<sub>4</sub>)L] (L = C<sub>2</sub>H<sub>4</sub>, NH<sub>3</sub>, PPr<sup>*i*</sup><sub>3</sub> and PCy<sub>3</sub>) range from 2.157(3) to 2.212(2) Å. Steric interaction between the ethene protons and the co-ligand may result in the adoption of different conformations in the complexes *cis*-[Ru(acac)<sub>2</sub>(η<sup>2</sup>-C<sub>2</sub>H<sub>4</sub>)(NH<sub>3</sub>)] and *cis*-[Ru(acac)<sub>2</sub>(η<sup>2</sup>-C<sub>2</sub>H<sub>4</sub>)(PPr<sup>*i*</sup><sub>3</sub>)] (see p. 51). The ethene protons having a greater interaction with the isopropyl protons than with the ammine protons. A slight increase in the Ru-P bond length for *cis*-[Ru(acac)<sub>2</sub>(η<sup>2</sup>-C<sub>2</sub>H<sub>4</sub>)(PCy<sub>3</sub>)] may reduce this steric interaction between the ethene protons and the cyclohexyl protons so that both orientations are observed. The Ru-C distances fall in the range 2.15 - 2.21 Å, with *cis*-[Ru(acac)<sub>2</sub>(η<sup>2</sup>-C<sub>2</sub>H<sub>4</sub>)(NH<sub>3</sub>)] at the lower end of the range and *cis*-[Ru(acac)<sub>2</sub>(η<sup>2</sup>-C<sub>2</sub>H<sub>4</sub>)<sub>2</sub>] at the upper end. Presumably, the range of Ru-C distances reflects the ease of replacement of the ethene ligand. Additional evidence for this statement can be derived from the comparison of the E<sub>1/2</sub>(Ru<sup>3+/2+</sup>) potentials (see Chapter 3).



## 2.11 References

- (1) Lehmann, H.; Schenk, K. J.; Chapuis, G.; Ludi, A. *J. Am. Chem. Soc.* **1979**, *101*, 6197.
- (2) Laurency, G.; Merbach, A. E. *Chem. Commun.* **1993**, 187.
- (3) Levy, G. C.; Lichter, R. L.; Nelson, G. L. *Carbon-13 Nuclear Magnetic Resonance Spectroscopy*; 2nd ed.; Wiley: New York, 1980, p 89.
- (4) Bodner, G. M.; Stornoff, B. N.; Doddrell, D.; Todd, L. J. *Chem. Commun.* **1970**, 1530.
- (5) Szymanska-Buzar, T.; Kern, K.; Downs, A. J.; Green, T. M.; Morris, L. J.; Parsons, S. *New J. Chem.* **1999**, 407.
- (6) Cramer, R. *J. Am. Chem. Soc.* **1964**, *86*, 217.
- (7) Nakamoto, K. *Infrared and Raman Spectra of Inorganic and Coordination Compounds*; 4th ed.; Wiley: New York, 1986.
- (8) Pruchnik, F. P. *Organometallic Chemistry of the Transition Elements*; Fackler Jr., J. P., Ed.; Plenum Press: New York and London, 1990.
- (9) Bennett, M. A.; Heath, G. A.; Hockless, D. C. R.; Kovacic, I.; Willis, A. *C. J. Am. Chem. Soc.* **1998**, *120*, 932.
- (10) Ricci, J. S.; Ibers, J. A. *J. Am. Chem. Soc.* **1970**, *92*, 5333.
- (11) Grünwald, G.; Laubender, M.; Wolf, J.; Werner, H. *J. Chem. Soc., Dalton Trans.* **1998**, 833.
- (12) Cramer, R.; Kline, J. B.; Roberts, J. D. *J. Am. Chem. Soc.* **1969**, *91*, 2519.
- (13) Bellamy, L. J. *The Infrared Spectra of Complex Molecules*; 3rd ed.; Chapman and Hall: London, 1975.
- (14) Bennett, M. A.; Chung, G.; Hockless, D. C. R.; Neumann, H.; Willis, A. *C. J. Chem. Soc., Dalton Trans.* **1999**, 3451.
- (15) Abbenhius, R. A. T. M.; del Río, I.; Bergshoef, M. M.; Boersma, J.; Veldman, N.; Spek, A. L.; van Koten, G. *Inorg. Chem.* **1998**, *37*, 1749.
- (16) Leung, W. H.; Zheng, H.; Chim, J. L. C.; Chan, J.; Wong, W. T.; Williams, I. D. *J. Chem. Soc., Dalton Trans.* **2000**, 423.
- (17) Hoffman, P. R.; Caulton, K. G. *J. Am. Chem. Soc.* **1975**, *97*, 4221.

- (18) Armit, P. W.; Sime, W. J.; Stephenson, T. A.; Scott, L. J. *Organomet. Chem.* **1978**, *161*, 391.
- (19) Jung, C. W.; Garrou, P. E.; Hoffman, P. R.; Caulton, K. G. *Inorg. Chem.* **1984**, *23*, 726.
- (20) Vierkötter, S. A.; Barnes, C. E.; Garner, G. L.; Butler, L. G. *J. Am. Chem. Soc.* **1994**, *116*, 7445.
- (21) Baar, C. A.; Jenkins, H. A.; Jennings, M. C.; Yap, G. P. A.; Puddephatt, R. *J. Organometallics* **2000**, *19*, 4870.
- (22) Herberhold, M.; Kreiter, C. G.; Wiedersatz, G. O. *J. Organomet. Chem.* **1976**, *120*, 103.
- (23) Sandström, J. *Dynamic NMR Spectroscopy*; Academic Press: London, 1982, p 76.
- (24) Wickenheiser, E. B.; Cullen, W. R. *Inorg. Chem.* **1990**, *29*, 4671.
- (25) Holloway, C. E.; Hulley, G.; Johnson, B. F. G.; Lewis, J. J. *Chem. Soc. (A)* **1969**, 53.
- (26) Holloway, C. E.; Hulley, G.; Johnson, B. F. G.; Lewis, J. J. *Chem. Soc. (A)* **1970**, 1653.
- (27) Ashley-Smith, J.; Douek, I.; Johnson, B. F. G.; Lewis, J. J. *Chem. Soc., Dalton Trans.* **1972**, 1776.
- (28) Bennett, M. A.; Neumann, H. *unpublished results*.
- (29) Mann, B. E.; Masters, C.; Shaw, B. L.; Slade, R. M.; Stainbank, R. E. *Inorg. Nucl. Chem. Letters* **1971**, *7*, 881.
- (30) Chaudret, B. *J. Organomet. Chem.* **1984**, *268*, C33.
- (31) Esteruelas, M. A.; Lahoz, F. J.; Oñate, E.; Oro, L. A.; Rodríguez, L.; Steinert, P.; Werner, H. *Organometallics* **1996**, *15*, 3436.
- (32) Werner, H.; Schäfer, M.; Nürnberg, O.; Wolf, J. *Chem. Ber.* **1994**, *127*, 27.
- (33) Cotton, F. A.; Darenbourg, D. J.; Klein, S.; Kolthammer, B. W. S. *Inorg. Chem.* **1982**, *21*, 294.

- (34) Watson, M.; Woodward, S.; Conole, G.; Kessler, M.; Sykara, G. *Polyhedron* **1994**, *13*, 2455.
- (35) Antonova, A. B.; Ioganson, A. A. *Russ. Chem. Rev.* **1989**, *58*, 693.
- (36) Puerta, M. C.; Valerga, P. *Coord. Chem. Rev.* **1999**, *193-195*, 977.
- (37) Chatt, J.; Nikolsky, A. B.; Richards, R. L.; Sanders, J. R. *Chem. Commun.* **1969**, 154.
- (38) Creutz, C.; Taube, H. *Inorg. Chem.* **1971**, *10*, 2664.
- (39) Treitel, I. M.; Flood, M. T.; March, R. E.; Gray, H. B. *J. Am. Chem. Soc.* **1969**, *91*, 6512.
- (40) Lide, R. D. *Handbook of Chemistry and Physics*; 76th ed.; CRC Press: New York, 1998, Section 9, p 20.
- (41) Ondrechen, M. J.; Ratner, M. J.; Ellis, D. E. *J. Am. Chem. Soc.* **1981**, *103*, 1656.
- (42) Abdur-Rashid, K.; Gusev, D. G.; Lough, A. J.; Morris, R. H. *Organometallics* **2000**, *19*, 1652.
- (43) Jolly, P. W.; Jonas, K.; Krüger, C.; Tsay, Y. H. *J. Organomet. Chem.* **1971**, *33*, 109.
- (44) Coia, G. M.; Demadis, K. D.; Meyer, T. J. *Inorg. Chem.* **2000**, *39*, 2212.
- (45) Brown, L. D.; Barnard, C. F. J.; Daniels, J. A.; Mawby, R. J.; Ibers, J. A. *Inorg. Chem.* **1978**, *17*, 2932.
- (46) Bruce, M. I.; Wong, F. S. *J. Organomet. Chem.* **1981**, *210*, C5.
- (47) Mynott, R.; Lehkuhl, H.; Kreuzer, E.-M.; Jousen, E. *Angew. Chem. Int. Ed. (Engl)* **1990**, *29*, 289.
- (48) Crocker, M.; Green, M.; Orpen, A. G.; Thomas, D. M. *Chem. Commun.* **1984**, 1141.
- (49) Faller, J. W.; Johnson, B. V. *J. Organomet. Chem.* **1975**, *88*, 101.
- (50) Werner, R.; Werner, H. *Chem. Ber.* **1983**, *116*, 2074.
- (51) Werner, H.; Werner, R. *Chem. Ber.* **1985**, *118*, 4543.
- (52) Collman, J. P.; Brothers, P. J.; McElwee-White, L.; Rose, E.; Wright, L. J. *J. Am. Chem. Soc.* **1985**, *107*, 4570.

- (53) del Río, I.; Gossage, R. A.; Hannu, M. S.; Lutz, M.; Spek, A. L.; van Koten, G. *Organometallics* **1999**, *18*, 1097.
- (54) Hesschenbrouck, J.; Solari, E.; Scopelliti, R.; Floriani, C.; Re, N. J. *Organomet. Chem.* **2000**, *596*, 77.
- (55) Guerchais, V.; Lapinte, C.; Thépot, J. *Organometallics* **1988**, *7*, 604.
- (56) Borowski, A. F.; Sabo-Etienne, S.; Christ, M. L.; Donnadiou, B.; Chaudret, B. *Organometallics* **1996**, *15*, 1427.
- (57) Werner, H.; Braun, T.; Daniel, T.; Gevert, O.; Schulz, M. J. *Organomet. Chem.* **1997**, *541*, 127.
- (58) Burrell, A. K.; Clark, G. R.; Rickard, C. E. F.; Roper, W. R.; Wright, A. H. *J. Chem. Soc., Dalton Trans.* **1991**, 609.
- (59) Campion, B. K.; Heyn, R. H.; Tilley, T. D. *Chem. Commun.* **1988**, 278.
- (60) Johnson, T. J.; Huffman, J. C.; Caulton, K. G. *J. Am. Chem. Soc.* **1992**, *114*, 2725.
- (61) Gemel, C.; Huffman, J. C.; Caulton, K. G.; Mauthner, K.; Kirchner, K. J. *Organomet. Chem.* **2000**, *593-594*, 342.
- (62) Cramer, R. *J. Am. Chem. Soc.* **1967**, *89*, 4621.
- (63) Tolman, C. *J. Am. Chem. Soc.* **1974**, *96*, 2780.
- (64) Muhs, M. A.; Weiss, F. T. *J. Am. Chem. Soc.* **1962**, *84*, 4697.
- (65) Cvetanović, R. J.; Duncan, F. J.; Falconer, W. E.; Irwin, R. S. *J. Am. Chem. Soc.* **1965**, *87*, 1827.
- (66) Albright, T. A.; Hoffmann, R.; Thibeault, J. C.; Thorn, D. L. *J. Am. Chem. Soc.* **1979**, *101*, 3801.
- (67) Carmona, E.; Marin, J. M.; Poveda, M. L.; Atwood, J. L.; Rogers, R. D. *J. Am. Chem. Soc.* **1983**, *105*, 3104.
- (68) Carmona, E.; Galindo, A.; Poveda, M. L.; Rogers, R. D. *Inorg. Chem.* **1985**, *24*, 4033.
- (69) Komiya, S.; Baba, A. *Organometallics* **1991**, *10*, 3105.
- (70) Bachmann, C.; Demuyneck, J.; Veillard, A. *J. Am. Chem. Soc.* **1978**, *100*, 2366.

- (71) Burdett, J. K.; Albright, T. A. *Inorg. Chem.* **1979**, *18*, 2112.
- (72) Evans, J. A.; Russell, D. R. *Chem. Commun.* **1971**, 197.
- (73) Blom, R.; Rankin, D. W. H.; Robertson, H. E.; Perutz, R. N. *J. Chem. Soc., Dalton Trans.* **1993**, 1983.
- (74) Hazel, N. J.; Howard, J. A. K.; Spencer, J. L. *Chem. Commun.* **1984**, 1663.
- (74a) Johnson, T. J.; Huffman, J. C.; Caulton, K. G.; Jackson, S. A.; Eisenstein, O. *Organometallics* **1989**, *8*, 2073.
- (75) Chatt, J.; Duncanson, L. A. *J. Chem. Soc.* **1953**, 2939.
- (76) Dewar, M. J. S. *Bull. Soc. Chim. France* **1951**, *18*, C79.
- (77) Mahmoud, K. A.; Rest, A. J.; Alt, H. G. *J. Chem. Soc., Dalton Trans.* **1985**, 1365.
- (78) Faller, J. W.; Johnson, B. V. *J. Organomet. Chem.* **1975**, *88*, 101.
- (79) de Klerk-Engels, B.; Delis, J. G. P.; Ernsting, J.; Elsevier, C. J.; Frühauf, H.; Stufkens, D. J.; Vrieze, K.; Goubitz, K.; Fraanje, J. *Inorg. Chim. Acta* **1995**, *240*, 273.
- (80) Alt, H.; Herberhold, M.; Kreiter, C. G.; Strack, H. *J. Organomet. Chem.* **1974**, *77*, 353.
- (81) Segal, J. A.; Johnson, B. F. G. *J. Chem. Soc., Dalton Trans.* **1975**, 677.
- (82) Gutowsky, H. S.; Belford, G. G.; McMahan, P. E. *J. Chem. Phys.* **1962**, *36*, 3353.
- (83) Elian, M.; Hoffmann, R. *Inorg. Chem.* **1975**, *14*, 1058.
- (84) Burdett, J. K. *J. Chem. Soc., Faraday Trans. 2* **1974**, *70*, 1599.
- (85) Ariel, S.; Dolphin, D.; Domazetis, G.; James, B. R.; Leung, T. W.; Rettig, S. J.; Trotter, J.; Williams, G. M. *Can. J. Chem.* **1984**, *62*, 755.
- (86) Appleton, T. G.; Clark, H. C.; Manzer, L. E. *Coord. Chem. Rev.* **1973**, *10*, 335.
- (87) Bruneau, C.; Dixneuf, P. H. *Acc. Chem. Res.* **1999**, *32*, 311.
- (88) Bruce, M. I. *Chem. Rev.* **1991**, *91*, 197.
- (89) Naota, T.; Takaya, H.; Murahashi, S.-I. *Chem. Rev.* **1998**, *98*, 2599.
- (90) Wakatsuki, Y.; Koga, N.; Yamazaki, H.; Morokuma, K. *J. Am. Chem. Soc.* **1994**, *116*, 8105.

- (91) Werner, H.; Baum, B.; Schneider, D.; Windmüller, B. *Organometallics* **1994**, *13*, 1089.
- (92) Rappert, T.; Nürnberg, O.; Mahr, N.; Wolf, J.; Werner, H. *Organometallics* **1992**, *11*, 4156.
- (93) Wolf, J.; Werner, H.; Serhadli, O.; Ziegler, M. L. *Angew. Chem. Int. Ed. Engl.* **1983**, *22*, 414.
- (94) Wakatsuki, Y.; Koga, N.; Werner, H.; Morokuma, K. *J. Am. Chem. Soc.* **1997**, *119*, 360.
- (94a) Oliván, M.; Clot, E.; Eisenstein, O.; Caulton, K. G. *Organometallics* **1998**, *17*, 3091.
- (95) Goldman, A. S.; Halpern, J. J. *Organomet. Chem.* **1990**, *382*, 237.
- (96) Tolman, C. A. *Chem. Rev.* **1977**, *77*, 313.
- (97) Serron, S. A.; Nolan, S. P. *Organometallics* **1995**, *14*, 4611.
- (98) Cucullu, M. E.; Luo, L.; Nolan, S. P. *Organometallics* **1995**, *14*, 289.
- (99) Luo, L.; Nolan, S. P. *Organometallics* **1994**, *13*, 4781.
- (100) Bennett, M. A.; Heath, G. A.; Hockless, D. C. R.; Kovacic, I.; Willis, A. C. *Organometallics* **1998**, *17*, 5867.

*Co-ordination and organometallic  
chemistry of  
bis( $\beta$ -diketonato)ruthenium(III)  
complexes*

As mentioned in the Introduction, the  $\text{Ru}^{3+/2+}$  redox potentials for  $[\text{Ru}(\text{NH}_3)_5\text{L}]^{2+}$ ,  $[\text{Ru}(\text{H}_2\text{O})_x\text{L}_{6-x}]^{2+}$  and  $[\text{Ru}(\text{acac})_2\text{L}_2]$  (where L = monodentate ligand) have been extensively studied to determine the relative stability of the two oxidation states. This chapter deals with the redox properties of the new complexes mentioned in the preceding chapter. Various electrochemical methods, often coupled with spectroscopic techniques, have been used in this work in order to determine the stability of the oxidised products and whether the Ru(III) oxidation state is chemically accessible. As a consequence, the chapter is divided into the following sections: voltammetry, electrolytic oxidation, chemical oxidation and discussion.

### 3.1 Voltammetry

The cyclic and AC (alternating current) voltammograms of *cis*- $[\text{Ru}(\text{acac})_2(\eta^2\text{-C}_2\text{H}_4)_2]$  show a quasi-reversible electron transfer process at +0.95 V (*vs* Ag/AgCl) at *ca.* -50 °C in  $\text{CH}_2\text{Cl}_2$  (see Figure 3.1). Although the observed couple is symmetrical, the difference between the potentials of the oxidation and reduction processes,  $\Delta E_p$ , varies with scan rate (see Table 3.1).<sup>1</sup> Ferrocene was also measured under these non-standard conditions and its  $\Delta E_p$  varies little at low scan rates but increases at a scan rate of 500  $\text{mV s}^{-1}$ . The AC trace of a mixture of *cis*- $[\text{Ru}(\text{acac})_2(\eta^2\text{-C}_2\text{H}_4)_2]$  and ferrocene at *ca.* -50 °C shows two symmetric peaks with a peak width at half-height of 105 mV and 85 mV, respectively.

At room temperature, a non-symmetric cyclic voltammogram trace was found for *cis*- $[\text{Ru}(\text{acac})_2(\eta^2\text{-C}_2\text{H}_4)_2]$  at slow scan rates (*ca.* 50  $\text{mVs}^{-1}$ ). A second complex, whose reversibility was not investigated, was also detected during the reduction process at  $E_{pc} = +0.40$  V (*vs* Ag/AgCl).



**Figure 3.1:** CV and AC voltammograms of  $cis-[Ru(acac)_2(\eta^2-C_2H_4)_2]$  measured at *ca.*  $-50\text{ }^\circ\text{C}$  in  $CH_2Cl_2$ .

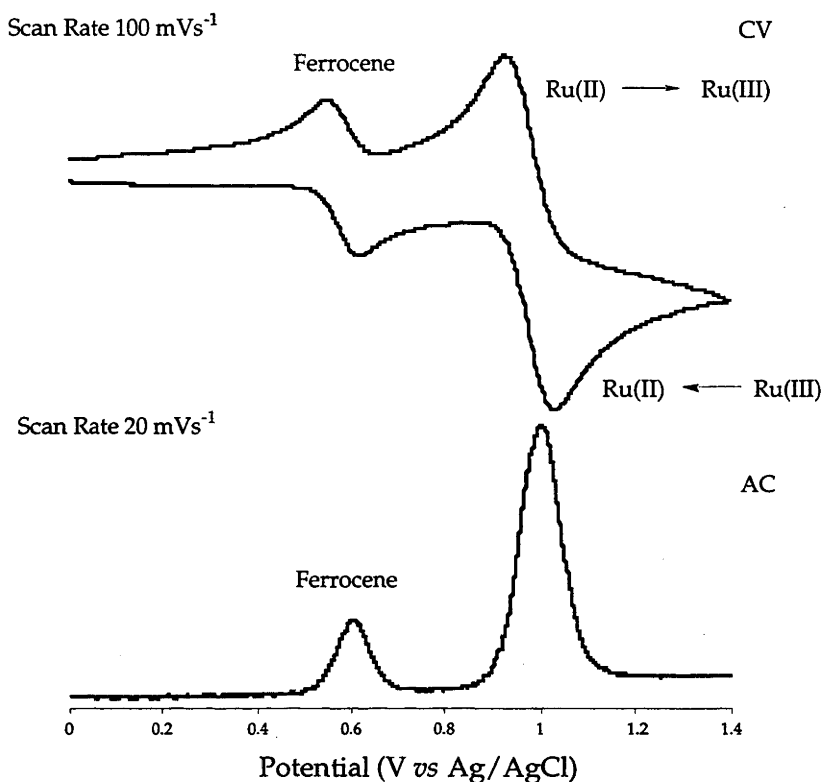


**Table 3.1:** Variation of  $\Delta E_P$  with scan rate for  $cis-[Ru(acac)_2(\eta^2-C_2H_4)_2]$  and  $Cp_2Fe$  at *ca.*  $-50\text{ }^\circ\text{C}$  in  $CH_2Cl_2$ .

Scan Rate ( $mV\ s^{-1}$ )	$\Delta E_P$ (mV)	
	$cis-[Ru(acac)_2(\eta^2-C_2H_4)_2]$	$Cp_2Fe$
50	90	62
100	106	64
200	122	66
500	160	85

The replacement of one ethene ligand by a ligand L to form  $cis-[Ru(acac)_2(\eta^2-C_2H_4)L]$  ( $L = NH_3, MeCN, SbPh_3, C_5H_5N, PPr^i_3, PCy_3$ ) lowers the  $E_{1/2}(Ru^{3+/2+})$  potentials to between +0.37 and +0.59 V (*vs* Ag/AgCl); all of the isolated monoethene complexes show fully reversible voltammograms at *ca.*  $-50\text{ }^\circ\text{C}$  at a scan rate of  $100\text{ mVs}^{-1}$ . The lowest oxidation potential found for the monoethene complexes corresponds to

both geometric isomers of  $[\text{Ru}(\text{acac})_2(\eta^2\text{-C}_2\text{H}_4)(\text{NH}_3)]$  (+0.37 V *vs* Ag/AgCl); the highest potential found is shown by *cis*- $[\text{Ru}(\text{acac})_2(\eta^2\text{-C}_2\text{H}_4)(\text{SbPh}_3)]$  (see Table 3.2).

**Table 3.2:** The oxidation potentials  $E_{1/2}(\text{Ru}^{3+/2+})$  (*vs* Ag/AgCl) of the complexes  $[\text{Ru}(\text{acac})_2(\eta^2\text{-alkene})\text{L}]$  measured in  $\text{CH}_2\text{Cl}_2$  at *ca.* -50 °C.

Complex	Geometric isomer	$E_{1/2}(\text{Ru}^{3+/2+})$ (V <i>vs</i> Ag/AgCl)
$[\text{Ru}(\text{acac})_2(\eta^2\text{-C}_2\text{H}_4)(\text{NH}_3)]$	<i>trans</i>	+0.37
	<i>cis</i>	+0.37
$[\text{Ru}(\text{acac})_2(\eta^2\text{-C}_2\text{H}_4)(\text{NC}_5\text{H}_5)]$	<i>trans</i>	+0.38
$[\text{Ru}(\text{acac})_2(\eta^2\text{-C}_2\text{H}_4)(\text{PPr}^i_3)]$	<i>cis</i>	+0.42
$[\text{Ru}(\text{acac})_2(\eta^2\text{-C}_2\text{H}_4)(\text{PCy}_3)]$	<i>cis</i>	+0.43
$[\text{Ru}(\text{acac})_2(\eta^2\text{-C}_2\text{H}_4)(\text{MeCN})]$	<i>cis</i>	+0.56
$[\text{Ru}(\text{acac})_2(\eta^2\text{-C}_2\text{H}_4)(\text{SbPh}_3)]$	<i>cis</i>	+0.59
$[\text{Ru}(\text{acac})_2(\eta^2\text{-C}_2\text{H}_4)_2]$	<i>cis</i>	+0.95
$[\text{Ru}(\text{acac})_2(\eta^2\text{-C}_8\text{H}_{14})(\text{NH}_3)]$	<i>cis</i>	+0.23 <sup>a</sup>
$[\text{Ru}(\text{acac})_2(\eta^2\text{-C}_8\text{H}_{14})(\text{SbPh}_3)]$	<i>cis</i>	+0.44 <sup>b</sup>
$[\text{Ru}(\text{acac})_2(\eta^2\text{-C}_8\text{H}_{14})(\text{MeCN})]$	<i>cis</i>	+0.44 <sup>b</sup>
$[\text{Ru}(\text{acac})_2(\eta^2\text{-C}_8\text{H}_{14})_2]$	<i>cis</i>	+0.77 <sup>b</sup>

a) ref. 2; b) ref. 3.

In most cases, the geometric isomers of previously isolated  $[\text{Ru}(\text{acac})_2\text{LL}']$  ( $\text{L} = \text{L}, \text{L} \neq \text{L}'$ ) complexes show different  $E_{1/2}(\text{Ru}^{3+/2+})$  potentials, the difference  $\Delta E_{1/2}$  ranging from 50 mV for  $[\text{Ru}(\text{acac})_2(\text{NC}_5\text{H}_5)_2]$  to 490 mV for  $[\text{Ru}(\text{acac})_2(\text{Bu}^t\text{NC})_2]$  (see Table 1.9). The lower  $E_{1/2}$  values of the complexes *trans*- $[\text{Ru}(\text{acac})_2\text{L}_2]$  presumably arise from the electronic effects of two  $\pi$ -acceptor ligands, even if relatively weak, competing for electron density from the same d-orbital on ruthenium(II). This is the same argument that has been proposed to account for the thermodynamic instability of the *trans*-complexes.<sup>4</sup> In the corresponding *cis*-complexes, the  $\pi$ -acceptor ligands are now *trans* to a  $\pi$ -donor oxygen acac atom and no longer compete with each other for electron density, thus stabilising the metal centre at the Ru(II) level. Since  $\text{NH}_3$  is a saturated ligand and has no

$\pi$ -acceptor ability, it will not compete for electron density from the metal (see p. 1). The acac anion is also a good  $\pi$ -donor and therefore the ethene ligand has no competition for  $\pi$ -back-donation from either ligand.

Whereas each isomer of  $[\text{Ru}(\text{acac})_2(\eta^2\text{-C}_2\text{H}_4)(\text{NH}_3)]$  shows a fully reversible redox process at room temperature, the complex *trans*- $[\text{Ru}(\text{acac})_2(\eta^2\text{-C}_2\text{H}_4)(\text{NC}_5\text{H}_5)]$  exhibits quasi-reversible behaviour at low scan rates, probably due to the loss of the ethene ligand. The measured  $E_{1/2}(\text{Ru}^{3+/2+})$  values of the three isolated mixed nitrogen-donor/ethene complexes lie within the range found for the chelated bidentate N-donor alkene complexes  $[\text{Ru}(\text{acac})_2(\text{LL}')] (LL' = 2\text{-vinyl-N,N-dimethylaniline, 3-butenyldimethylamine, 2-allylpyridine, 2-isopropenylaniline, 2-isopropenyl-N,N-dimethylaniline, allyldimethylamine, 3-butenyldimethylamine}) [+0.28 - +0.52 \text{ V (vs Ag/AgCl)}]$ .<sup>5,6</sup>

Although fully reversible cyclic and AC voltammograms are found for the complexes *cis*- $[\text{Ru}(\text{acac})_2(\eta^2\text{-C}_2\text{H}_4)(\text{PR}_3)] (R = \text{Pr}^i, \text{Cy})$  at  $-50^\circ\text{C}$ , at room temperature both complexes also show *irreversible* behaviour with the formation in each case of an unidentified daughter product, which has not been investigated further. Increasing the scan rate to  $2 \text{ Vs}^{-1}$  results in quasi-reversible behaviour, which suggests that the oxidised species is undergoing a chemical reaction after the electron transfer step. The CV traces for *cis*- $[\text{Ru}(\text{acac})_2(\eta^2\text{-C}_2\text{H}_4)(\text{PCy}_3)]$  at both  $-50^\circ\text{C}$  and  $+25^\circ\text{C}$  are shown in Figure 3.2. As was the case for the nitrogen donor ligands, the  $E_{1/2}(\text{Ru}^{3+/2+})$  potentials measured for *cis*- $[\text{Ru}(\text{acac})_2(\eta^2\text{-C}_2\text{H}_4)(\text{PR}_3)] (R = \text{Pr}^i, \text{Cy})$  are close to the oxidation potential measured for the analogous chelated complex *cis*- $[\text{Ru}(\text{acac})_2(\text{Me}_2\text{PCH}_2\text{CH}_2\text{CH}=\text{CH}_2)] (+0.46 \text{ V vs Ag/AgCl})$ .<sup>6</sup>

The  $E_{1/2}$  potential found for *cis*- $[\text{Ru}(\text{acac})_2(\eta^2\text{-C}_2\text{H}_4)_2]$  is *ca.*  $0.5 - 0.6 \text{ V}$  less than the calculated values for  $[\text{Ru}(\text{H}_2\text{O})_4(\text{C}_2\text{H}_4)_2]^{2+}$  and  $[\text{Ru}(\text{NH}_3)_4(\eta^2\text{-C}_2\text{H}_4)_2]^{2+}$  in an organic solvent (see Table 3.3). This result is in agreement with the predicted lowering caused by replacement of two ammine or aqua

ligands by an acac ligand at the  $\text{Ru}^{2+}$  ion (see p. 4). The oxidation potential found for  $\text{cis}[\text{Ru}(\text{acac})_2(\eta^2\text{-C}_2\text{H}_4)_2]$  is similar to the calculated potentials for the monoethene complexes  $[\text{Ru}(\text{NH}_3)_5(\eta^2\text{-C}_2\text{H}_4)]^{2+}$  and  $[\text{Ru}(\text{H}_2\text{O})_5(\eta^2\text{-C}_2\text{H}_4)]^{2+}$  in an organic solvent (see Table 3.3), but *ca.* 0.2 V higher than for  $\text{cis}[\text{Ru}(\text{acac})_2(\eta^2\text{-C}_8\text{H}_{14})_2]$ .<sup>2</sup> A comparison of the  $E_{1/2}$  values of the ethene complexes  $\text{cis}[\text{Ru}(\text{acac})_2(\eta^2\text{-C}_2\text{H}_4)\text{L}]$  ( $\text{L} = \text{C}_2\text{H}_4, \text{NH}_3, \text{SbPh}_3, \text{CH}_3\text{CN}$ ) with those of their cyclooctene analogues (see Table 1.9) also shows that the mono-ethene complexes are harder to oxidise by up to *ca.* 140 mV. These results correlate with the expected degree (or extent) of  $\pi$ -back-donation from the metal to the alkene. As was mentioned previously (see p. 92), the replacement of the hydrogen atoms at the  $\text{C}=\text{C}$  bond by alkyl substituents increases the energy of the  $\pi$  and  $\pi^*$  orbitals,<sup>7</sup> thus  $\pi$ -backdonation from the metal to the cyclooctene will be reduced compared to that for ethene. Hence, the  $\text{Ru}(\text{III})$  centre will be more stable in the case of cyclooctene.

**Figure 3.2:** Cyclic voltammograms of  $\text{cis}[\text{Ru}(\text{acac})_2(\eta^2\text{-C}_2\text{H}_4)(\text{PCy}_3)]$  measured at a scan rate of  $100 \text{ mVs}^{-1}$  in  $\text{CH}_2\text{Cl}_2$ .

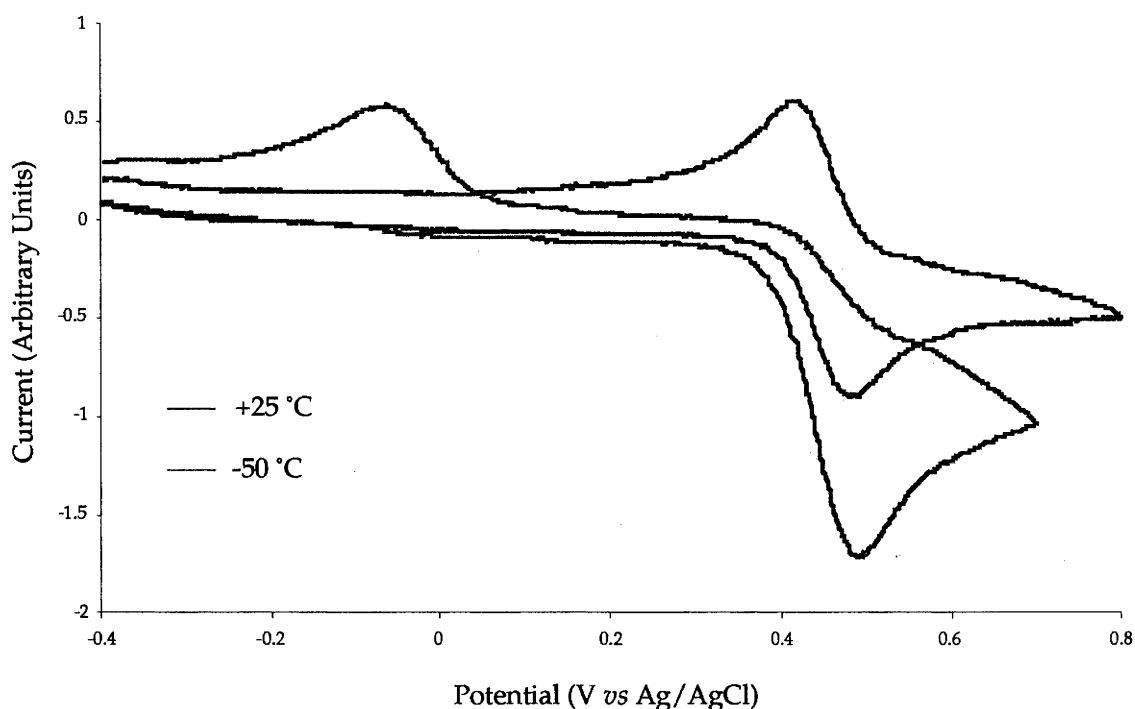


**Table 3.3:** Comparison of measured and expected  $E_{1/2}(\text{Ru}^{3+/2+})$  values (in volts) of some Ru(II)-ethene complexes using Lever's electrochemical ligand parameters (from ref. 8).

Compound	$\Sigma E_L(L)$	$E_{1/2}(\text{Ru}^{3+/2+})$ <i>vs</i> NHE in $\text{H}_2\text{O}$		$E_{1/2}(\text{Ru}^{3+/2+})$ <i>vs</i> Ag/AgCl in organic solvent <sup>b</sup>	
		calc. <sup>a</sup>	found	calc. <sup>c</sup>	found
$[\text{Ru}(\text{NH}_3)_5(\eta^2\text{-C}_2\text{H}_4)]^{2+}$	+1.11	+0.91	+0.93 <sup>e</sup>	+0.92	-
$[\text{Ru}(\text{NH}_3)_4(\eta^2\text{-C}_2\text{H}_4)_2]^{2+}$	+1.80	+1.70	-	+1.59	-
$[\text{Ru}(\text{H}_2\text{O})_5(\eta^2\text{-C}_2\text{H}_4)]^{2+}$	+0.96	+0.74	+0.84 <sup>e</sup>	+0.77	-
$[\text{Ru}(\text{H}_2\text{O})_4(\eta^2\text{-C}_2\text{H}_4)_2]^{2+}$	+1.68	+1.57	>1.5 <sup>f</sup>	+1.47	-
<i>cis</i> - $[\text{Ru}(\text{acac})_2(\eta^2\text{-C}_2\text{H}_4)_2]$	+1.20	+1.02	-	+1.01	+0.95
<i>cis</i> - $[\text{Ru}(\text{acac})_2(\eta^2\text{-C}_2\text{H}_4)(\text{NH}_3)]$	+0.51	+0.23	-	+0.33	+0.37
<i>trans</i> - $[\text{Ru}(\text{acac})_2(\eta^2\text{-C}_2\text{H}_4)(\text{NH}_3)]$	+0.51	+0.23	-	+0.33	+0.37
<i>trans</i> - $[\text{Ru}(\text{acac})_2(\eta^2\text{-C}_2\text{H}_4)(\text{NC}_5\text{H}_5)]$	+0.69	+0.44	-	+0.51	+0.38
<i>cis</i> - $[\text{Ru}(\text{acac})_2(\eta^2\text{-C}_2\text{H}_4)(\text{MeCN})]$	+0.78	+0.54	-	+0.60	+0.56
<i>cis</i> - $[\text{Ru}(\text{acac})_2(\eta^2\text{-C}_2\text{H}_4)(\text{SbPh}_3)]$	+0.82	+0.58	-	+0.64	+0.59

a) calculated by Eq. 1.2; b) calculated values are 0.2 V less positive than those *vs* NHE; c) calculated by Eq. 1.1; d) ref. 9; e) ref. 10; f) value for *cis*- $[\text{Ru}(\text{H}_2\text{O})_4(\text{diallylether})]$ , ref. 11.

The complex *trans*- $[\text{Ru}(\text{acac})_2(\text{PPr}^i_3)_2]$  shows a fully reversible  $E_{1/2}(\text{Ru}^{3+/2+})$  couple at -0.14 V (*vs* Ag/AgCl) which is similar to the values for *trans*- $[\text{Ru}(\text{acac})_2(\text{PEt}_3)_2]$  (-0.13 V *vs* Ag/AgCl)<sup>3</sup> and *trans*- $[\text{Ru}(\text{acac})_2(\text{NMe}_3)_2]$  (-0.18 V *vs* Ag/AgCl),<sup>3</sup> but *ca.* 140 mV and *ca.* 210 mV less than those found for *trans*- $[\text{Ru}(\text{acac})_2(\text{PMe}_3)_2]$ <sup>3</sup> and *trans*- $[\text{Ru}(\text{acac})_2(\text{PPh}_3)_2]$ ,<sup>2</sup> respectively (see Table 1.9). A fully reversible oxidation couple was also found for *cis*- $[\text{Ru}(\text{acac})_2(\text{PPr}^i_3)_2]$  at +0.02 V (*vs* Ag/AgCl). The difference in oxidation potentials between the geometric isomers,  $\Delta E_{1/2}$ , for  $[\text{Ru}(\text{acac})_2(\text{PPr}^i_3)_2]$  is 160 mV, which is similar to those found for  $[\text{Ru}(\text{acac})_2(\text{MeCN})_2]$  ( $\Delta E_{1/2} = 120$  mV) and  $[\text{Ru}(\text{acac})_2(\text{AsPh}_3)_2]$  ( $\Delta E_{1/2} = 190$  mV) (see Table 1.9). The oxidation potential of *cis*- $[\text{Ru}(\text{acac})_2(\text{PPr}^i_3)_2]$  is *ca.* 240 mV less than that for *cis*- $[\text{Ru}(\text{acac})_2(\text{PMe}_3)_2]$  (+0.26 V *vs* Ag/AgCl, see Table 1.9), which may arise from the greater electron-donating ability of  $\text{PPr}^i_3$  relative to that of  $\text{PMe}_3$ . Due to the poor solubility of *trans*-

[Ru(acac)<sub>2</sub>(PCy<sub>3</sub>)<sub>2</sub>], the E<sub>1/2</sub>(Ru<sup>3+/2+</sup>) potential could not be measured; however, *cis*-[Ru(acac)<sub>2</sub>(PCy<sub>3</sub>)(SbPh<sub>3</sub>)] has a fully reversible E<sub>1/2</sub>(Ru<sup>3+/2+</sup>) couple at +0.19 V (*vs* Ag/AgCl).

The cyclic and AC voltammograms of the isolated carbonyl phosphine complexes show fully reversible E<sub>1/2</sub>(Ru<sup>3+/2+</sup>) couples at room temperature in the range +0.64 - +0.92 V (*vs* Ag/AgCl) (see Table 3.4). These values indicate the stabilizing effect of CO on the Ru(II) oxidation state relative to tertiary phosphines. The oxidation potential for *trans*-[Ru(acac)<sub>2</sub>(CO)(PCy<sub>3</sub>)] indicates that this complex is easier to oxidise by 250 mV than its *cis*-isomer. Both isolated vinylidene complexes *cis*-[Ru(acac)<sub>2</sub>(PPr<sup>*i*</sup><sub>3</sub>){=C=C(H)R}](R = SiMe<sub>3</sub>, Ph) show irreversible oxidation potentials due to irreversible oxidation processes, E<sub>pa</sub>, at +0.62 V (*vs* Ag/AgCl) (R = SiMe<sub>3</sub>) and +0.75 V (*vs* Ag/AgCl) (R = Ph) at scan rates up to 500 mVs<sup>-1</sup> and at *ca.* -50 °C. An irreversible oxidation process is also found for *cis*-[Ru(acac)<sub>2</sub>(CO)<sub>2</sub>] under similar conditions;<sup>2</sup> this irreversibility was explained<sup>2</sup> on the basis that the CO ligands are strong π-acceptors and the complex is very unstable in the Ru(III) oxidation state. The complex *cis*-[Ru(acac)<sub>2</sub>(PPr<sup>*i*</sup><sub>3</sub>)(CO)] is harder to oxidise than either vinylidene complex by up to 300 mV (see Table 3.4), which suggests that the mono-substituted vinylidene ligands are weaker π-acids than CO. A similar evaluation of π-acid strength was made for the diphenylvinylidene ligand |C=CPh<sub>2</sub> on rhodium(I).<sup>12</sup>

The cyclic and AC voltammograms of the binuclear complex *cis*-[Ru(acac)<sub>2</sub>(PPr<sup>*i*</sup><sub>3</sub>)<sub>2</sub>](μ-N<sub>2</sub>) show two reversible oxidation potentials at +0.30 and +0.90 V (*vs* Ag/AgCl) at -50 °C in CH<sub>2</sub>Cl<sub>2</sub>. All previously studied mononuclear complexes of the type [Ru(acac)<sub>2</sub>LL'] (L = L'; L ≠ L') containing chelated alkenes and alkynes<sup>5,6,13</sup> or π-acceptor ligands<sup>2,3</sup> show only one one-electron oxidation in the potential range 0 - +1.5 V from the Ru(II) to Ru(III) oxidation state and show no Ru(III) to Ru(IV) oxidation. Thus, the two oxidation couples for the dinitrogen complex are believed to correspond

to the sequential oxidation of the two ruthenium metal centres *i.e.* Ru(II/II)  $\rightarrow$  Ru(II/III) and Ru(II/III)  $\rightarrow$  Ru(III/III). At room temperature, the initial oxidation process is fully reversible whereas the second oxidation process is irreversible. The difference in potential between the oxidation couples is similar to that found for the related complex  $[\{\text{Ru}(\text{NH}_3)_5\}_2(\mu\text{-N}_2)]^{4+}$ , which undergoes a reversible one-electron oxidation potential at +0.73 V (*vs* NHE) and a second irreversible oxidation process at  $\sim 1.2$  V (*vs* NHE).<sup>14</sup>

**Table 3.4:** Oxidation potentials of mixed phosphine complexes in  $\text{CH}_2\text{Cl}_2$  (*ca.* 20 °C unless otherwise stated).

Complex	Geometric isomer	$E_{1/2}(\text{Ru}^{3+}/2+)$ (V <i>vs</i> Ag/AgCl)
[Ru(acac) <sub>2</sub> (PPr <sup><i>i</i></sup> ) <sub>2</sub> ]	<i>trans</i>	-0.14 <sup>a</sup>
	<i>cis</i>	+0.02
[Ru(acac) <sub>2</sub> (PPr <sup><i>i</i></sup> )(CO)]	<i>trans</i>	-
	<i>cis</i>	+0.92
[Ru(acac) <sub>2</sub> (PCy <sub>3</sub> )(CO)]	<i>trans</i>	+0.64 <sup>b</sup>
	<i>cis</i>	+0.89 <sup>b</sup>
[Ru(acac) <sub>2</sub> (PCy <sub>3</sub> )(SbPh <sub>3</sub> )]	<i>cis</i>	+0.19
[Ru(acac) <sub>2</sub> (PPr <sup><i>i</i></sup> )(=C=C(H)SiMe <sub>3</sub> )]	<i>cis</i>	+0.62 <sup>a,c</sup>
[Ru(acac) <sub>2</sub> (PPr <sup><i>i</i></sup> )(=C=C(H)Ph)]	<i>cis</i>	+0.75 <sup>a,c</sup>
[[Ru(acac) <sub>2</sub> (PPr <sup><i>i</i></sup> )] <sub>2</sub> ( $\mu\text{-N}_2$ )]	<i>cis</i>	+0.30, +0.90 <sup>a</sup>

a) measured at *ca.* -50 °C; b) values agree  $\pm 30$  mV with those reported in ref. 3; c) irreversible oxidation process.

### 3.2 Electrolytic Oxidation

#### 3.2.1 Spectroelectrochemical Results

The electronic (UV-Vis) spectra for numerous *cis*- and *trans*-[Ru(acac)<sub>2</sub>L<sub>2</sub>]<sup>*n*+</sup> (L = monodentate ligand) (*n* = 0, 1),<sup>2,3</sup> and the chelate alkene complexes *cis*-[Ru(acac)<sub>2</sub>LL']<sup>*n*+</sup> (LL' = 2-vinyl-N,N-dimethylaniline, 2-allylpyridine, 3-butenyldimethylamine, 3-butenyldimethylphosphine) (*n* = 0, 1)<sup>5,6</sup> have been recorded and show characteristic bands for each oxidation state. Unstable ruthenium(III) complexes, such as *cis*-[Ru(acac)<sub>2</sub>( $\eta^2\text{-C}_8\text{H}_{14}$ )L]<sup>+</sup> (L = NH<sub>3</sub>, MeCN and SbPh<sub>3</sub>) have also been generated electrochemically and

characterised *in situ* in an optically transparent thin layer electrode (OTTLE) cell.<sup>3</sup>

The electronic (UV-Vis) spectrum of the complex *cis*-[Ru(acac)<sub>2</sub>(η<sup>2</sup>-C<sub>2</sub>H<sub>4</sub>)<sub>2</sub>] exhibits a broad band at 32700 cm<sup>-1</sup> (ε = 9400 L M<sup>-1</sup> cm<sup>-1</sup>) and a slightly stronger absorption near 38800 cm<sup>-1</sup> (ε = 12400 L M<sup>-1</sup> cm<sup>-1</sup>) (see Figure 3.3). Applying a potential of +1.20 V (*vs* Ag/AgCl) to the solution at *ca* -50 °C causes the gradual loss of these bands and the formation of new bands at 13300 cm<sup>-1</sup> (ε = 2600 M<sup>-1</sup> cm<sup>-1</sup>), 16000 (ε = 2200 L M<sup>-1</sup> cm<sup>-1</sup>) and 34100 cm<sup>-1</sup> (ε = 9400 L M<sup>-1</sup> cm<sup>-1</sup>). After the solution had been exhaustively oxidized, the original Ru(II) spectrum was regenerated after applying a potential of +0.70 V (*vs* Ag/AgCl). During both the oxidation and reduction process, isosbestic points were observed, as shown in Figure 3.3, indicating that only two absorbing species are present in solution. The bands found in the spectra of *cis*-[Ru(acac)<sub>2</sub>(η<sup>2</sup>-C<sub>2</sub>H<sub>4</sub>)<sub>2</sub>] and of the electrogenerated species are similar in both position and intensity to those of the previously studied complexes *cis*-[Ru<sup>II/III</sup>(acac)<sub>2</sub>L<sub>2</sub>]<sup>0/+1</sup> (L = monodentate ligand)<sup>2,3</sup> and the chelate complexes *cis*-[Ru<sup>II/III</sup>(acac)<sub>2</sub>(LL')]<sup>0/+1</sup> (LL' = 2-vinyl-N,N-dimethylaniline, 2-allylpyridine, 2-isopropenyl-N,N-dimethylaniline, allyldimethylamine, 3-butenyldimethylamine, 3-butenyldimethylphosphine, 3-butenyldiphenylphosphine and isomesityl oxide)<sup>5,6</sup> A direct comparison can be made with the electronic spectra recorded for *cis*-[Ru(acac)<sub>2</sub>(COD)]<sup>0/+</sup> (COD = 1,5-cyclooctadiene),<sup>2</sup> which are shown in Figure 3.4. No *cis*- to *trans*-isomerization is believed to be occurring for the bis(ethene) complex during the oxidation process since such isomerization for the COD complex is highly improbable. Thus, the one electron oxidation of *cis*-[Ru(acac)<sub>2</sub>(η<sup>2</sup>-C<sub>2</sub>H<sub>4</sub>)<sub>2</sub>] results in the formation of the ruthenium(III)-bis(ethene) cation *cis*-[Ru<sup>III</sup>(acac)<sub>2</sub>(η<sup>2</sup>-C<sub>2</sub>H<sub>4</sub>)<sub>2</sub>]<sup>+</sup> at low temperatures. The broadness of the bands may be attributed to a vibrational broadening phenomenon caused by distortion of the equilibrium geometry in the excited state.<sup>15</sup>



**Figure 3.3:** Electronic spectra recorded during the one-electron oxidation of *cis*- $[\text{Ru}(\text{acac})_2(\eta^2\text{-C}_2\text{H}_4)_2]$  in 0.5 M  $[\text{Bu}^n_4\text{N}][\text{PF}_6]/\text{CH}_2\text{Cl}_2$  at ca  $-50^\circ\text{C}$  [ $E_{\text{appl}} = +1.20\text{ V}$  (vs  $\text{Ag}/\text{AgCl}$ )].

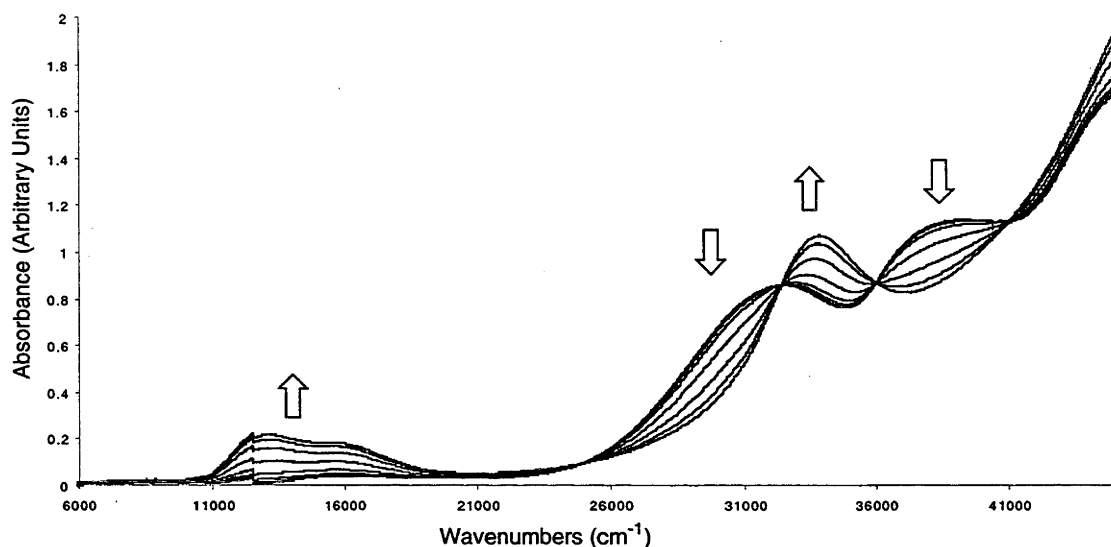
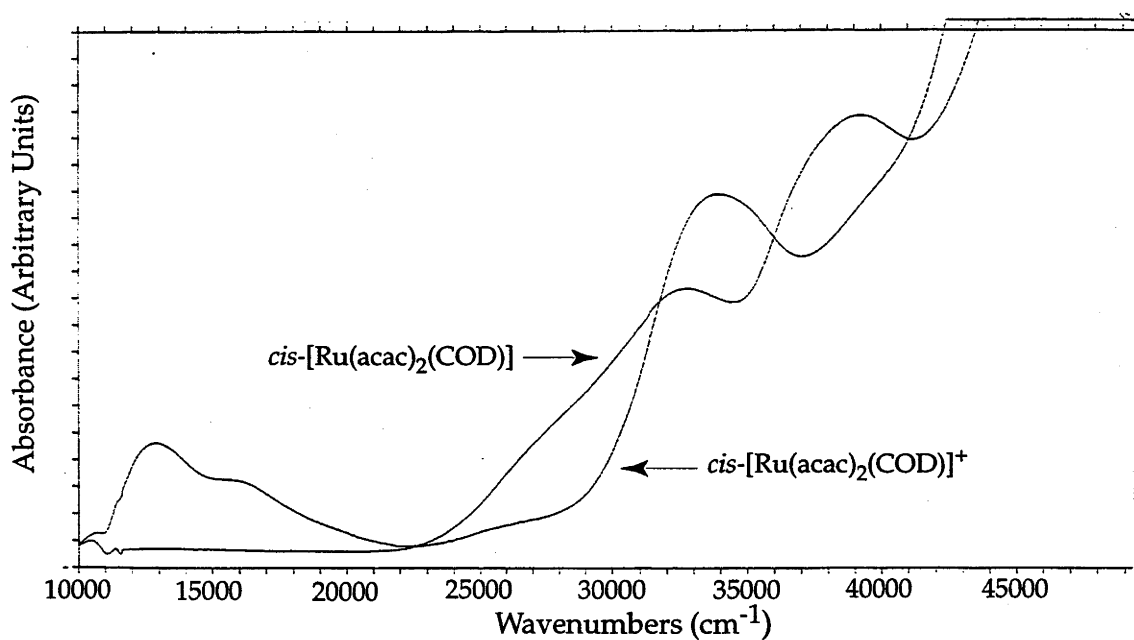


**Figure 3.4:** Electronic spectra recorded for  $[\text{Ru}(\text{acac})_2(\text{COD})]^{n+}$  (COD = 1,5-cyclooctadiene) in 0.1 M  $[\text{Bu}^n_4\text{N}][\text{PF}_6]/\text{MeCN}$  at ca  $-40^\circ\text{C}$  (taken from ref. 2).



The electronic spectra recorded at *ca.* -50 °C for the oxidation process in the complexes *cis*-[Ru(acac)<sub>2</sub>(η<sup>2</sup>-C<sub>2</sub>H<sub>4</sub>)L] (L = NH<sub>3</sub>, PCy<sub>3</sub>, SbPh<sub>3</sub>), *trans*-[Ru(acac)<sub>2</sub>(η<sup>2</sup>-C<sub>2</sub>H<sub>4</sub>)(NH<sub>3</sub>)] and *cis*-[Ru(acac)<sub>2</sub>(PPri<sub>3</sub>)<sub>2</sub>(μ-N<sub>2</sub>)] show the same general features as observed for the bis(ethene) complex (see Tables 3.6 and 3.7). Above *ca.* 30000 cm<sup>-1</sup> aromatic π → π\* transitions of the phenyl rings of *cis*-[Ru(acac)<sub>2</sub>(η<sup>2</sup>-C<sub>2</sub>H<sub>4</sub>)(SbPh<sub>3</sub>)] significantly broaden the electronic spectrum. The electronic spectra for the oxidised complexes of *cis*-[Ru(acac)<sub>2</sub>(η<sup>2</sup>-C<sub>2</sub>H<sub>4</sub>)L] (L = NH<sub>3</sub>, SbPh<sub>3</sub>) are also similar to those of the previously reported cyclooctene analogues.<sup>3</sup> Spectra recorded during the reduction of the electrogenerated Ru(III) species were found to be identical with those of the initial Ru(II) complex, indicating that the oxidation process is fully reversible. The electronic spectra of *cis*- and *trans*-[Ru(acac)<sub>2</sub>(η<sup>2</sup>-C<sub>2</sub>H<sub>4</sub>)(NH<sub>3</sub>)] are very similar as shown in Figures 3.3 and 3.4, except for the ν<sub>2</sub> vibronic component of the Ru(II) → acac π\* MLCT transition (see Table 3.6). For the *cis*-complex ν<sub>2</sub> is located at *ca.* 32000 cm<sup>-1</sup>, whereas for the *trans*-isomer it is at 28500 cm<sup>-1</sup>. Similar differences in the electronic spectra of geometric isomers were found for *cis*- and *trans*-[Co(NH<sub>3</sub>)<sub>4</sub>(H<sub>2</sub>O)F][ClO<sub>4</sub>], although the bands in these complexes are due to d-d transitions.<sup>16</sup> The electronic spectra of the oxidised products of *cis*- and *trans*-[Ru(acac)<sub>2</sub>(η<sup>2</sup>-C<sub>2</sub>H<sub>4</sub>)(NH<sub>3</sub>)] however, are almost indistinguishable from each other (see Tables 3.5 and 3.6).

The transitions for both oxidation states have been previously assigned, using the spectra of the species [Ru<sup>II/III</sup>(acac)<sub>3</sub>]<sup>0,-1</sup> as a basis.<sup>2</sup> The electronic spectrum of [Ru<sup>III</sup>(acac)<sub>3</sub>] consists of three well-defined bands due to a ligand-centred transition (acac π → π\*) at 36700 cm<sup>-1</sup> (ε = 16800 M<sup>-1</sup> cm<sup>-1</sup>), a Ru(III) → acac π\* MLCT (metal to ligand charge transfer transition) at 28800 cm<sup>-1</sup> (ε = 7500 M<sup>-1</sup> cm<sup>-1</sup>) and an acac π → Ru(III) LMCT (ligand to metal charge transfer transition) at 20000 cm<sup>-1</sup> (ε = 1500 M<sup>-1</sup> cm<sup>-1</sup>). The electronic spectrum of the electrogenerated [Ru<sup>II</sup>(acac)<sub>3</sub>]<sup>-</sup> anion, measured *in situ*, shows two main bands due to a ligand acac π → acac π\* transitions at 36300

**Figure 3.5:** Electronic spectra recorded during the one-electron oxidation of *cis*-[Ru(acac)<sub>2</sub>(η<sup>2</sup>-C<sub>2</sub>H<sub>4</sub>)(NH<sub>3</sub>)] in CH<sub>2</sub>Cl<sub>2</sub> at *ca.* -50 °C.

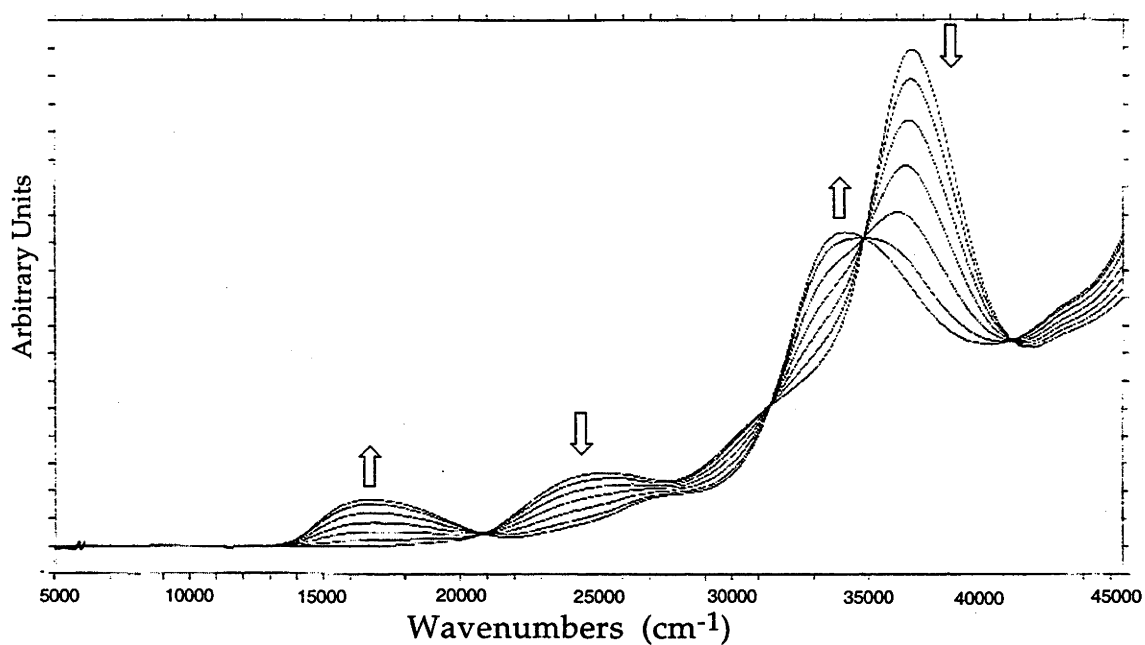


**Figure 3.6:** Electronic spectra recorded during the one-electron oxidation of *trans*-[Ru(acac)<sub>2</sub>(η<sup>2</sup>-C<sub>2</sub>H<sub>4</sub>)(NH<sub>3</sub>)] in CH<sub>2</sub>Cl<sub>2</sub> at *ca.* -50 °C.

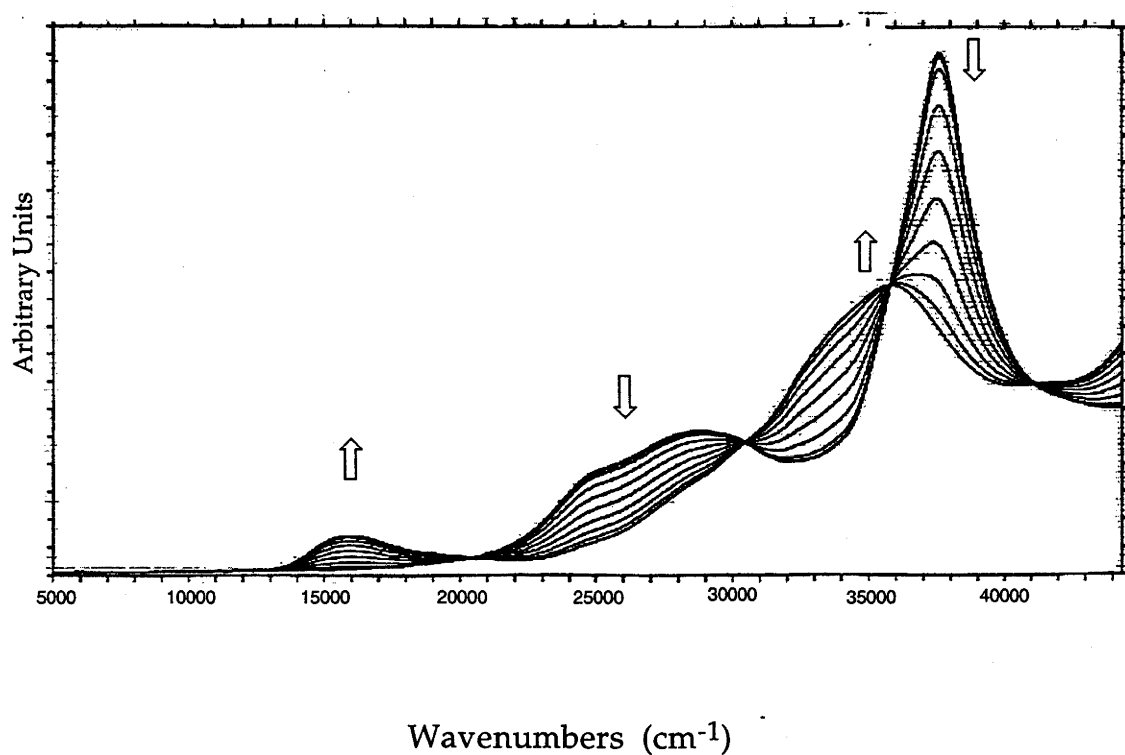


**Table 3.5:** Principal electronic band maxima (in  $\text{cm}^{-1}$ ) for the isolated ethene complexes  $[\text{Ru}^{\text{II}}(\text{acac})_2(\eta^2\text{-C}_2\text{H}_4)\text{L}]$  and  $\text{cis-}[\{\text{Ru}(\text{acac})_2(\text{PPr}^i_3)\}_2(\mu\text{-N}_2)]$  (figures in brackets are the molar absorptivities in  $\text{M}^{-1} \text{cm}^{-1} \text{L}^{-1}$ ).

COMPLEX	MLCT		acac $\pi \rightarrow$ acac $\pi^*$	$E_{1/2}(\text{Ru}^{3+/2+})$ (V vs Ag/AgCl)
	$\nu_1$	$\nu_2$		
<i>cis</i> - $[\text{Ru}(\text{acac})_2(\eta^2\text{-C}_2\text{H}_4)(\text{NH}_3)]$	25500 (3100)	31000 (4900)	36700 (15100)	+0.37
<i>trans</i> - $[\text{Ru}(\text{acac})_2(\eta^2\text{-C}_2\text{H}_4)(\text{NH}_3)]$	25000 (2700)	28500 (4000)	37700 (14500)	+0.37
<i>cis</i> - $[\text{Ru}(\text{acac})_2(\eta^2\text{-C}_2\text{H}_4)(\text{PCy}_3)]$	29600 (6500)	-	36700 (14600)	+0.43
<i>cis</i> - $[\text{Ru}(\text{acac})_2(\eta^2\text{-C}_2\text{H}_4)(\text{SbPh}_3)]$	26200 (2800)		38800 (12600)	+0.59
<i>cis</i> - $[\text{Ru}(\text{acac})_2(\eta^2\text{-C}_2\text{H}_4)_2]$	32700 (6000)		38800 (8000)	+0.95
<i>cis</i> - $[\{\text{Ru}(\text{acac})_2(\text{PPr}^i_3)\}_2(\mu\text{-N}_2)]$	27500 (16900)		37400 (53500)	+0.30 / +0.90

**Table 3.6:** Principal electronic band maxima (in  $\text{cm}^{-1}$ ) for the isolated ethene complexes  $[\text{Ru}^{\text{III}}(\text{acac})_2(\eta^2\text{-C}_2\text{H}_4)\text{L}]^+$  and  $\text{cis-}[\{\text{Ru}(\text{acac})_2(\text{PPr}^i_3)\}_2(\mu\text{-N}_2)]^{2+}$  (figures in brackets are the molar absorptivities in  $\text{M}^{-1} \text{cm}^{-1} \text{L}^{-1}$ )\*.

COMPLEX	MLCT		MLCT	acac ( $\pi \rightarrow \pi^*$ )
	$\nu_3$	$\nu_4$		
<i>cis</i> - $[\text{Ru}(\text{acac})_2(\eta^2\text{-C}_2\text{H}_4)(\text{NH}_3)]$	16800 (2200)	-	27000 (sh)	34000 (9800)
<i>trans</i> - $[\text{Ru}(\text{acac})_2(\eta^2\text{-C}_2\text{H}_4)(\text{NH}_3)]$	16000 (1000)	-	-	36000 (8000)
<i>cis</i> - $[\text{Ru}(\text{acac})_2(\eta^2\text{-C}_2\text{H}_4)(\text{PCy}_3)]$	14700 (1300)	17600 (1300)	29400 (4700)	36600 (12700)
<i>cis</i> - $[\text{Ru}(\text{acac})_2(\eta^2\text{-C}_2\text{H}_4)(\text{SbPh}_3)]$	13900 (1300)	16900 (1200)	-	-
<i>cis</i> - $[\text{Ru}(\text{acac})_2(\eta^2\text{-C}_2\text{H}_4)_2]$	13300 (2100)	16000 (1800)	-	34100 (8000)
<i>cis</i> - $[\{\text{Ru}(\text{acac})_2(\text{PPr}^i_3)\}_2(\mu\text{-N}_2)]$	13900 (3000)	17800 (3000)	30300 (16700)	37600 (35700)
<i>cis</i> - $[\text{Ru}(\text{acac})_2(\eta^2\text{-C}_8\text{H}_{14})(\text{NH}_3)]^{\text{a}}$	17200	-	-	34600
<i>cis</i> - $[\text{Ru}(\text{acac})_2(\eta^2\text{-C}_8\text{H}_{14})(\text{SbPh}_3)]^{\text{a}}$	14600	-	-	35000

a) ref. 3.

$\text{cm}^{-1}$  and a  $\text{Ru(II)} \rightarrow \text{acac } \pi^*$  MLCT transition at  $19800 \text{ cm}^{-1}$  (a shoulder at *ca.*  $21000 \text{ cm}^{-1}$  is very likely a higher vibronic component of the same band).<sup>2</sup>

The spectra of the complexes *cis*- $[\text{Ru}^{\text{II}}(\text{acac})_2\text{L}_2]$  and the chelate alkene and alkyne complexes *cis*- $[\text{Ru}^{\text{II}}(\text{acac})_2(\text{LL}')] ]$  are similar to that of  $[\text{Ru}^{\text{II}}(\text{acac})_3]^-$ , dominated by just two bands belonging to the  $\text{acac } \pi \rightarrow \text{acac } \pi^*$  transition and  $\text{Ru(II)} \rightarrow \text{acac } \pi^*$  (MLCT) transition.<sup>2,6</sup> The latter transition has two components labelled  $\nu_1$  and  $\nu_2$ ; the latter component appears as a weak shoulder to lower energy. The energies of these components, which fall in the range  $20000$  to  $34000 \text{ cm}^{-1}$  depending on the ligands, have been found to vary linearly with the  $E_{1/2}(\text{Ru}^{3+/2+})$  values, which span a potential range of  $-0.65 \text{ V}$  to  $+0.87 \text{ V}$ .<sup>2,3,6</sup> In contrast with  $[\text{Ru}^{\text{III}}(\text{acac})_3]$ , the electronic spectra of the complexes *cis*- $[\text{Ru}^{\text{III}}(\text{acac})_2\text{L}_2]^+$  and the alkene chelate complexes *cis*- $[\text{Ru}^{\text{III}}(\text{acac})_2(\text{LL}')]^+$  generally show just two bands assigned to the  $\text{acac } \pi \rightarrow \text{Ru(III)} \text{ LMCT}$ , generally found in the range  $12700 - 20000 \text{ cm}^{-1}$ , and an  $\text{acac } \pi \rightarrow \text{acac } \pi^*$  transition usually at  $33700 - 35000 \text{ cm}^{-1}$ .<sup>2,6</sup> The  $\text{acac } \pi \rightarrow \text{Ru(III)} \text{ LMCT}$  usually appears as a single, broad band or as a double feature with higher ( $\nu_3$ ) and lower energy ( $\nu_4$ ) components. These two components are usually found between  $13000$  and  $18000 \text{ cm}^{-1}$  (see Table 3.6).

The electronic spectrum of *cis*- $[\{\text{Ru}(\text{acac})_2(\text{PPr}^i_3)\}_2(\mu\text{-N}_2)]$  is very similar to the spectra of other isolated complexes that have similar  $E_{1/2}(\text{Ru}^{3+/2+})$  values, as shown in Table 3.6. After applying a potential of *ca.*  $+1.2 \text{ V}$  (*vs*  $\text{Ag}/\text{AgCl}$ ) at *ca.*  $-50 \text{ }^\circ\text{C}$ , the electrogenerated spectra are consistent with the presence of the doubly oxidised species *cis*- $[\{\text{Ru}^{\text{III}}(\text{acac})_2(\text{PPr}^i_3)\}_2(\mu\text{-N}_2)]^{2+}$ , see Table 3.6 for band positions. Spectra recorded during the reduction of the electrogenerated  $\text{Ru(III/III)}$  complex were found to be identical with those of the initial  $\text{Ru(II/II)}$  complex, indicating that the two-electron oxidation process is fully reversible.

The electronic spectrum of the mixed-valence species *cis*- $[\{\text{Ru}(\text{acac})_2(\text{PPr}^i_3)\}_2(\mu\text{-N}_2)]^+$  displays a broad, weak, asymmetric near-IR band

**Figure 3.7:** Electronic spectra recorded during the one-electron oxidation of *cis*-[[Ru(acac)<sub>2</sub>(PPR<sup>i</sup>)<sub>2</sub>(μ-N<sub>2</sub>)]<sub>2</sub> in 0.5 M [Bu<sup>n</sup>]<sub>4</sub>[PF<sub>6</sub>]/CH<sub>2</sub>Cl<sub>2</sub> at ca -50 °C [*E*<sub>appl</sub> = +0.60 V (vs Ag/AgCl)].

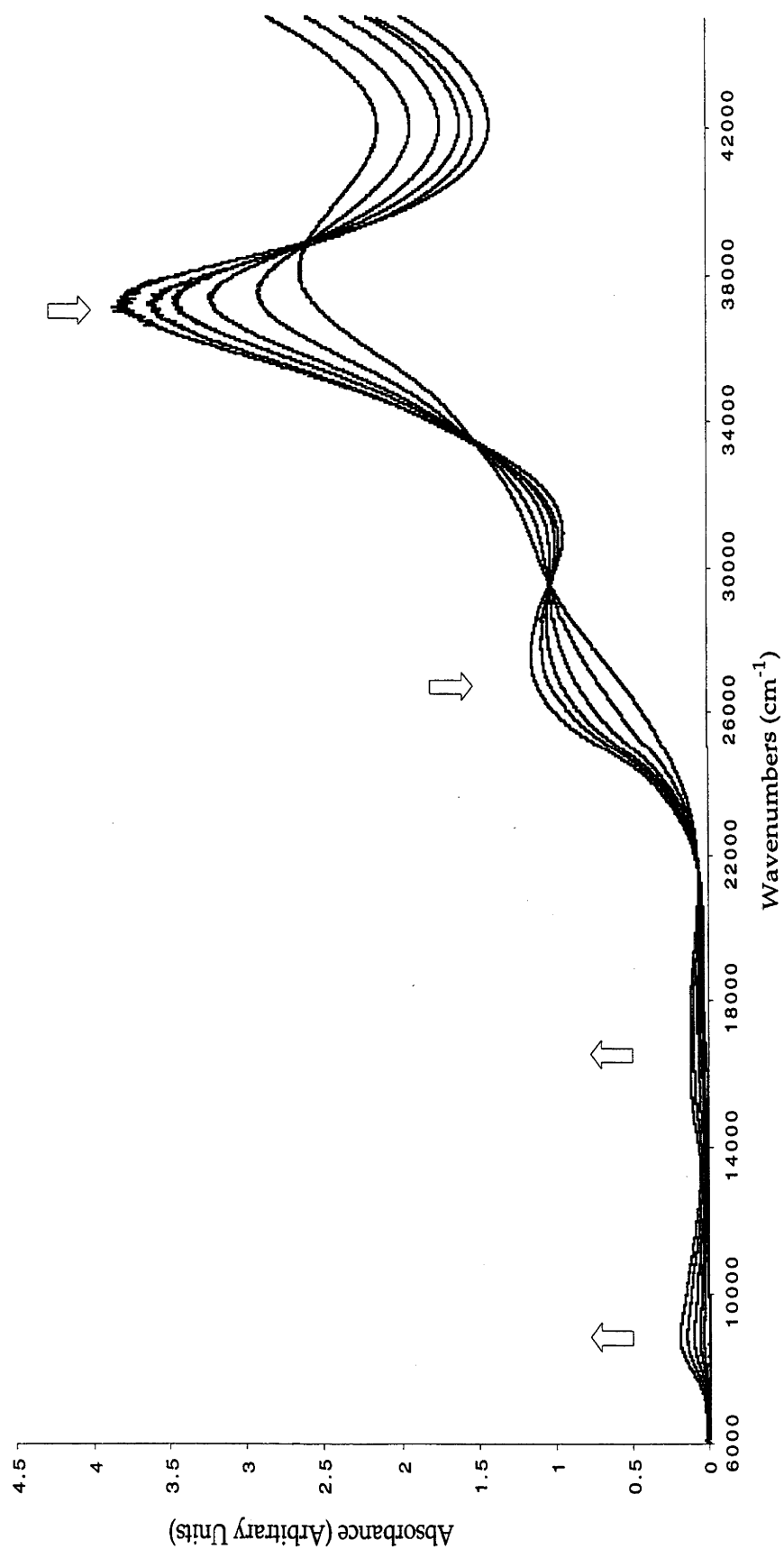


**Figure 3.8** The near-IR band for the mixed valence complex *cis*- $[[\text{Ru}(\text{acac})_2(\text{PPr}^i_3)]_2(\mu\text{-N}_2)]^+$  in a standard  $\text{CH}_2\text{Cl}_2$  electrolyte solution at *ca.*  $-50^\circ\text{C}$ .

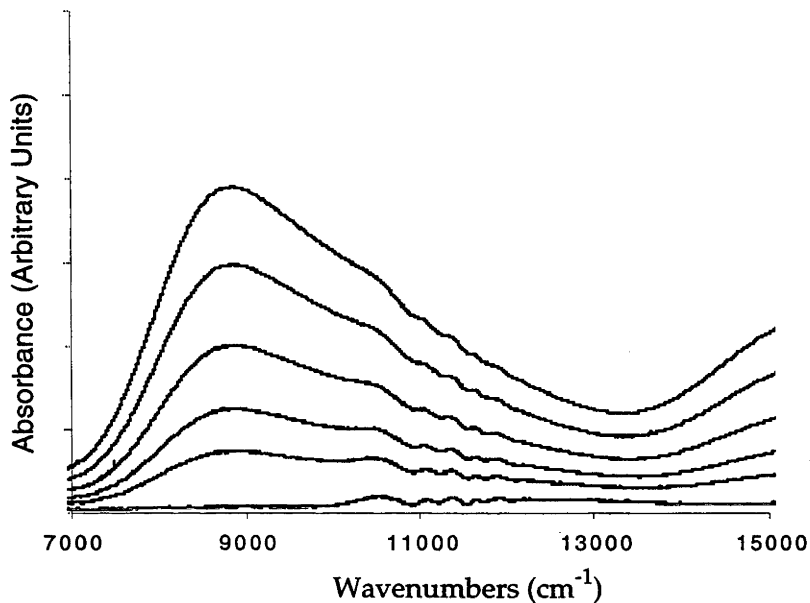
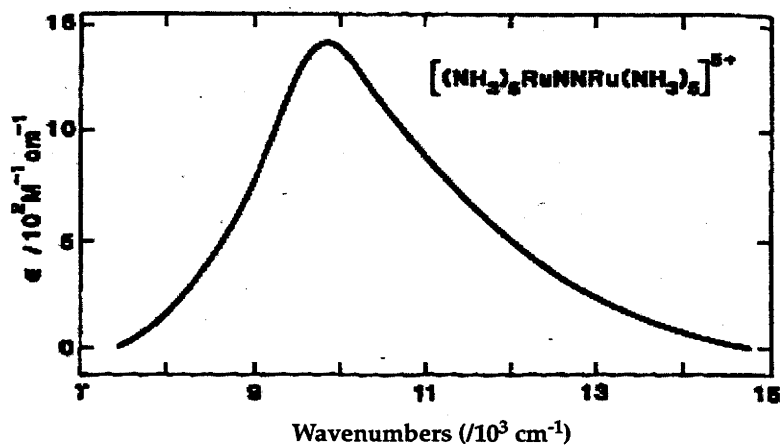


**Figure 3.9** The near-IR band for the mixed valence complex  $[(\text{Ru}(\text{NH}_3)_5)_2(\mu\text{-N}_2)]^{5+}$  (taken from ref. 14).



at *ca.* 8900  $\text{cm}^{-1}$  which is not present in either the Ru(II/II) or Ru(III/III) oxidation states (see Figures 3.7 and 3.8). Similar near-IR bands have been reported for the mixed-valence species  $[\{\text{Ru}(\text{NH}_3)_5\}_2(\mu\text{-N}_2)]^{5+14}$  (see Figure 3.9) and the Creutz-Taube ion  $[\{\text{Ru}(\text{NH}_3)_5\}_2(\mu\text{-pyz})]^{5+}$  (pyz = pyrazine).<sup>17,18</sup> Although this band is broader for  $[\{\text{Ru}(\text{acac})_2(\text{PPr}^i_3)\}_2(\mu\text{-N}_2)]^+$  ( $\omega_{1/2}$  *ca.* 3700  $\text{cm}^{-1}$ ) than for  $[\{\text{Ru}(\text{NH}_3)_5\}_2(\mu\text{-N}_2)]^{5+}$  ( $\omega_{1/2}$  *ca.* 2630  $\text{cm}^{-1}$ ),<sup>14</sup> the half-width is less than the value of *ca.* 4750  $\text{cm}^{-1}$  predicted by the Hush theory<sup>19</sup> for localized mixed-valence systems. Hush has also suggested that delocalized systems will show asymmetric bands.<sup>20</sup> These observations suggest that *cis*- $[\{\text{Ru}(\text{acac})_2(\text{PPr}^i_3)\}_2(\mu\text{-N}_2)]^+$  is valence delocalized, but probably not to the same extent as either the Creutz-Taube ion or  $[\{\text{Ru}(\text{NH}_3)_5\}_2(\mu\text{-N}_2)]^{5+}$ .<sup>14</sup>

### 3.2.2 EPR Spectra

As mentioned earlier, many configurationally stable Ru(III) complexes only differ from the corresponding Ru(II) complexes by one unit of charge (see p. 1). The Ru(III) ion is low-spin  $4d^5$  with one unpaired electron. The majority of its complexes are paramagnetic and, in principle, should show electron paramagnetic resonance (EPR) spectra. EPR spectroscopy may provide important information about the electronic structure of paramagnetic systems. EPR studies have been carried out on numerous Ru(III) complexes including  $[\text{Ru}(\text{acac})_3]$ ,<sup>21</sup>  $[\text{Ru}(\text{NH}_3)_6]^{3+22}$  and  $[\text{Ru}(\text{en})_3]^{3+}$ .<sup>23</sup>

There are two possible spin-states for a single electron ( $s = 1/2$ ) which are degenerate in the absence of zero-field splitting. This degeneracy is lifted in the presence of an external magnetic field and transitions between these levels are now possible. The difference in energy between these two levels which is measured in an EPR spectrum is related to the spectroscopic splitting factor  $g$ . For a free electron  $g$  is 2.0023; however,  $g$  is a tensor quantity and has inherent direction. The magnitude of  $g$  depends on the orientation of the system with respect to the magnetic field, except when the system is cubic Isotropic

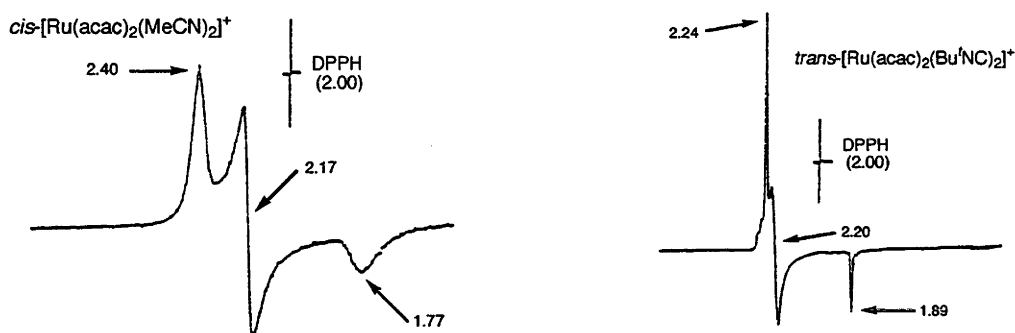


behaviour is observed for a perfect cubic system since  $g$  will have a value independent of orientation. Anisotropic behaviour is found for systems which have lower electronic symmetry and will usually have non-equivalent components along the  $x$ ,  $y$  and  $z$  axes. In the case of a complex which shows rhombic symmetry, e.g. *cis*- $\text{MX}_4\text{L}_2$  (where L and X are monodentate ligands), all three components are indeed inequivalent,  $g_x \neq g_y \neq g_z$ , which gives rise to three absorptions. One example is *cis*- $[\text{W}(\text{CO})_4(\eta^2\text{-alkene})_2]^+$  (alkene = 1-pentene, 1-hexene, cyclopentene, cyclohexene, cycloheptene, cyclooctene).<sup>18</sup> For a frozen solution it is not possible to assign these peaks to  $g_x$ ,  $g_y$  and  $g_z$ . If the complex shows overall axial symmetry, as is usually found for *trans*- $\text{MX}_4\text{L}_2$  (where L and X are monodentate ligands), then  $g$  will have one component ( $g_z$ ) parallel to the principal symmetry axis, known as  $g_{\parallel}$ . The components along the  $x$  and  $y$  axes ( $g_x$  and  $g_y$ ) are equivalent and give rise to a single resonance labelled  $g_{\perp}$ . Examples of Ru(III) complexes with axial spectra include *trans*- $[\text{Ru}(\text{NH}_3)_4\{\text{P}(\text{OEt})_3(\text{H}_2\text{O})\}][\text{CF}_3\text{SO}_3]_3$ <sup>24</sup> and *trans*- $[\text{Ru}(\text{NH}_3)_4\{\text{P}(\text{OEt})_3\}_2][\text{CF}_3\text{SO}_3]_3$ .<sup>25</sup>

However, complexes which contain bidentate ligands, eg. acac and bipy, usually show three resonances in the EPR spectrum regardless of whether the complex has overall axial or rhombic symmetry. The two donor atoms of one ligand are not completely electronically independent of each other as are the donor atoms of two monodentate ligands. This is known as the Orgel effect<sup>26,27</sup> and will become manifest in a slight rhombic distortion of *cis* or *trans*- $\text{MX}_4\text{L}_2$  when chelating ligands (AA) replace X, giving  $\text{M}(\text{AA})_2\text{L}_2$ .<sup>28</sup> In the case of *trans*- $[\text{Ru}^{\text{III}}(\text{acac})_2\text{L}_2][\text{PF}_6]$  (L =  $\text{Bu}^t\text{NC}$ ,  $\text{PPh}_3$ ), the spectra may be regarded as pseudo-axial with two relatively close resonances,  $g_1$  and  $g_2$ , between 2.28 and 2.20 (see Table 3.7). For the complexes *cis*- $[\text{Ru}^{\text{III}}(\text{acac})_2\text{L}_2][\text{PF}_6]$  (L = MeCN,  $\text{PPh}_3$ ,  $\text{Bu}^t\text{NC}$ ;  $\text{L}_2$  = dppe, dppp, 1,5-cyclooctadiene and 2-styryldiphenylphosphine) the difference between the  $g$ -values of these absorptions is greater than 0.13 (see Table 3.7). Thus, it

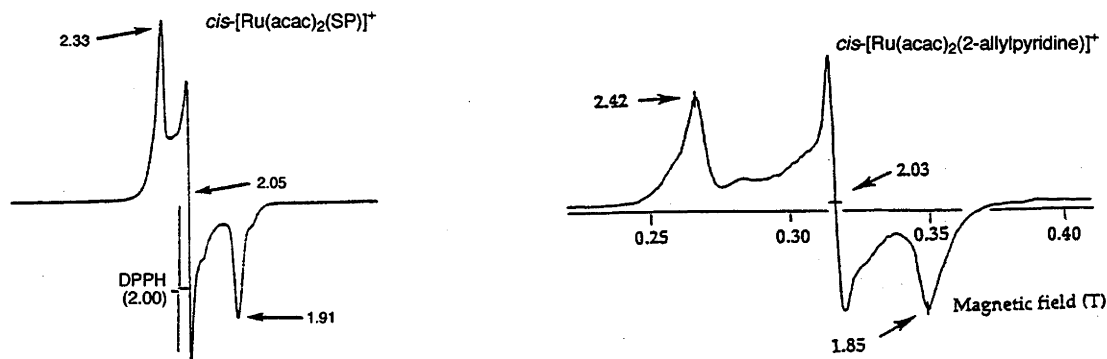
appears to be possible, in principle, to discriminate between Ru(III) geometric isomers on the basis of their EPR spectra, but it must be noted that several complexes such as *cis*-[Ru<sup>III</sup>(bipy)L<sub>2</sub>][ClO<sub>4</sub>] (L = MeOC(S)S<sup>-</sup>, Et<sub>2</sub>NC(S)S<sup>-</sup>) also show only two *g*-values<sup>29</sup> and *trans*-Cs[Ru(acac)<sub>2</sub>Cl<sub>2</sub>] shows three well separated resonances (see Table 3.7).

**Figure 3.10:** EPR spectra for complexes of the type [Ru<sup>III</sup>(acac)<sub>2</sub>L<sub>2</sub>][PF<sub>6</sub>] (L = monodentate ligand) (taken from ref. 2).\*



\*) DPPH = diphenylpicrylhydrazyl ( $g_0 = 2.0037$ ).

**Figure 3.11:** EPR spectra for complexes of the type [Ru<sup>III</sup>(acac)<sub>2</sub>LL'] [PF<sub>6</sub>] (LL' = 2-styryldiphenylphosphine, 2-allylpyridine) (taken from ref. 2 and 6).\*



\*) DPPH = diphenylpicrylhydrazyl ( $g_0 = 2.0037$ ).

Bulk anodic electrolysis of *trans*-[Ru(acac)<sub>2</sub>(η<sup>2</sup>-C<sub>2</sub>H<sub>4</sub>)(NH<sub>3</sub>)] at -40 °C results in a colour change from yellow to blue; a small aliquot of the solution was frozen and the EPR spectrum recorded. The spectrum is shown in Figure 3.12 and appears to be consistent with the presence of an axially distorted ruthenium(III) complex. Since *trans*-[Ru(acac)<sub>2</sub>(η<sup>2</sup>-C<sub>2</sub>H<sub>4</sub>)(NH<sub>3</sub>)] is axially distorted (neglecting the bridging backbone of the acac ligands), one

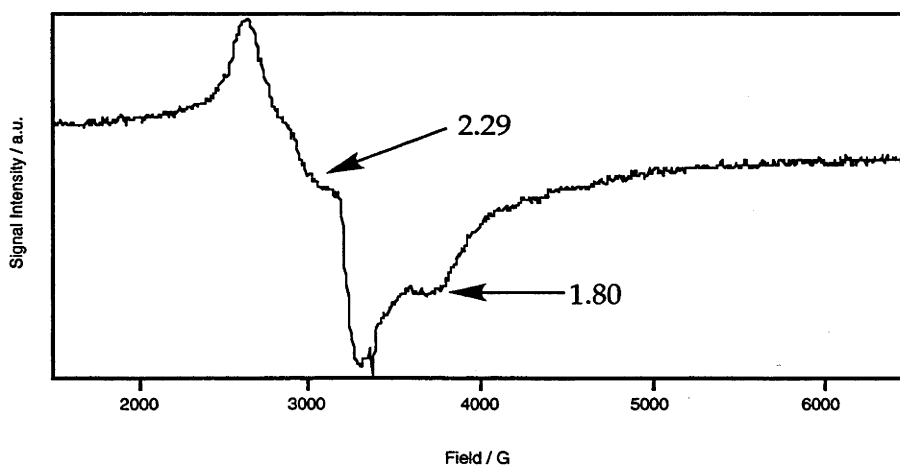
interpretation is that isomerization has not occurred during oxidation (see the reservation above). This conclusion agrees with those drawn from the spectroelectrochemical results.

**Table 3.7:** *g*-Values for various  $[Ru(acac)_2L_2][PF_6]$  and  $[Ru(acac)_2LL'][PF_6]$  complexes.

Complex	Geometric Isomer	$g_1$	$g_2$	$g_3$
$Cs[Ru^{III}(acac)_2Cl_2]^a$	<i>trans</i>	2.67	2.16	1.28
$[Ru^{III}(acac)_2(MeCN)_2][PF_6]^b$	<i>cis</i>	2.40	2.17	1.77
$[Ru^{III}(acac)_2(dppe)][PF_6]^b$	<i>cis</i>	2.29	2.14	1.92
$[Ru^{III}(acac)_2(dppp)][PF_6]^b$	<i>cis</i>	2.40	2.12	1.86
$[Ru^{III}(acac)_2(PPh_3)_2][PF_6]^b$	<i>trans</i>	2.28	2.23	1.84
	<i>cis</i>	2.40	2.08	1.84
$[Ru^{III}(acac)_2(Bu^tNC)_2][PF_6]^b$	<i>trans</i>	2.24	2.20	1.89
	<i>cis</i>	2.28	2.10	1.91
$[Ru^{III}(acac)_2(COD)][PF_6]^{b,c}$	<i>cis</i>	2.23	2.10	1.94
$[Ru^{III}(acac)_2(SP)][PF_6]^{b,c}$	<i>cis</i>	2.33	2.05	1.91
$[Ru^{III}(acac)_2(o-H_2C=C(H)CH_2C_5H_4N)][PF_6]^d$	<i>cis</i>	2.42	2.03	1.85
$[Ru^{III}(acac)_2(o-PhC\equiv CC_6H_4NMe_2)][PF_6]^e$	<i>cis</i>	2.22	2.05	1.92

a) ref. 30; b) ref. 2; c) COD = 1,5-cyclooctadiene, SP = 2-styryldiphenylphosphine; d) ref. 5; e) ref. 13.

**Figure 3.12:** The EPR spectrum of the species isolated from the anodic oxidation of  $trans-[Ru(acac)_2(\eta^2-C_2H_4)(NH_3)]$  at ca. -40 °C.



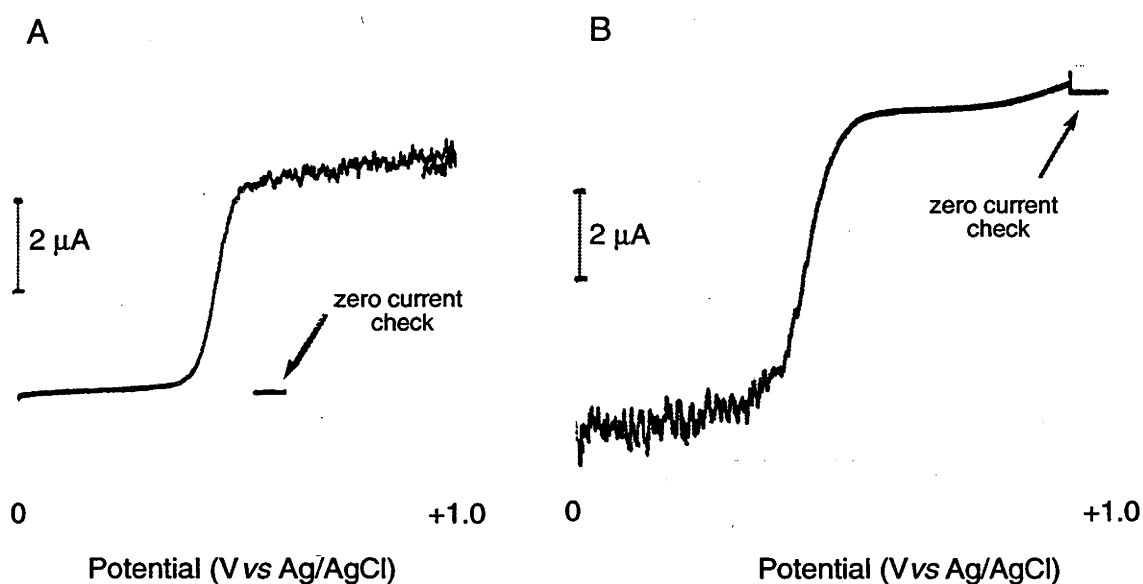
Anodic oxidation of *cis*-[Ru(acac)<sub>2</sub>(η<sup>2</sup>-C<sub>2</sub>H<sub>4</sub>)<sub>2</sub>] under the same conditions outlined for *trans*-[Ru(acac)<sub>2</sub>(η<sup>2</sup>-C<sub>2</sub>H<sub>4</sub>)(NH<sub>3</sub>)] also results in the formation of a deep blue solution. However, *in situ* cyclic voltammetric experiments show that a second species is present in solution, the same as that previously detected when the CV traces were recorded at room temperature (see p. 107). The EPR spectrum of this frozen solution shows several resonances which are also typical of ruthenium(III) complexes but the identity of the species responsible for them is unknown.

**3.3 Chemical oxidation of monoethene complexes *trans*-[Ru(acac)<sub>2</sub>(η<sup>2</sup>-C<sub>2</sub>H<sub>4</sub>)(NH<sub>3</sub>)] and *cis*-[Ru(acac)<sub>2</sub>(η<sup>2</sup>-alkene)L] (alkene = C<sub>2</sub>H<sub>4</sub>, L = PCy<sub>3</sub>; alkene = C<sub>8</sub>H<sub>14</sub>, L = SbPh<sub>3</sub>)**

As the electronic and EPR spectra of the products arising from the anodic electrolysis of the complexes *trans*-[Ru(acac)<sub>2</sub>(η<sup>2</sup>-C<sub>2</sub>H<sub>4</sub>)(NH<sub>3</sub>)] and *cis*-[Ru(acac)<sub>2</sub>(η<sup>2</sup>-C<sub>2</sub>H<sub>4</sub>)L] (L = C<sub>2</sub>H<sub>4</sub>, NH<sub>3</sub>, SbPh<sub>3</sub> and PCy<sub>3</sub>) were obtained at *ca.* -50 °C over a timescale of tens of minutes and did not show any change at this temperature, attempts were made to isolate these new species. The addition of one equivalent of AgPF<sub>6</sub> to a chilled standard electrolyte solution containing *cis*-[Ru(acac)<sub>2</sub>(η<sup>2</sup>-C<sub>2</sub>H<sub>4</sub>)(PCy<sub>3</sub>)] in a jacketed electrochemical cell gave a deep blue solution, whose CV traces (Ru<sup>III</sup> → Ru<sup>II</sup>) were superimposable on those previously recorded before the addition of the oxidant (Ru<sup>II</sup> → Ru<sup>III</sup>). Hydrodynamic voltammetric results show that for *cis*-[Ru(acac)<sub>2</sub>(η<sup>2</sup>-C<sub>2</sub>H<sub>4</sub>)(PCy<sub>3</sub>)] no current is detected between 0 and +0.4 V (*vs* Ag/AgCl), as shown in Figure 3.13A. As the potential passes between +0.4 and +0.5 V (*vs* Ag/AgCl), however, a positive current passes through the solution which corresponds to the oxidation of the complex; above +0.5 V a limiting current is reached. The potential at half the current height is *ca.* +0.45 V (*vs* Ag/AgCl) which agrees with the value measured previously by cyclic voltammetry (see p. 109). After the addition of a slight excess of AgPF<sub>6</sub>, a negative current is found between 0 and +0.4 V; above

+0.5 V there is no current passing through the solution as shown in Figure 3.13B. The potential at half the current height is also *ca.* +0.45 V which indicates that the oxidised species  $\text{cis-}[\text{Ru}^{\text{III}}(\text{acac})_2(\eta^2\text{-C}_2\text{H}_4)(\text{PCy}_3)][\text{PF}_6]$  is present in solution. The current is slightly greater after the addition of the oxidant but this may be due to a slight concentration of the solution owing to loss of  $\text{CH}_2\text{Cl}_2$  by evaporation, the presence of colloidal silver on the electrodes or the slight excess of  $\text{Ag}(\text{I})$ .

**Figure 3.13:** Hydrodynamic voltammograms for A)  $\text{cis-}[\text{Ru}(\text{acac})_2(\eta^2\text{-C}_2\text{H}_4)(\text{PCy}_3)]$  (scan rate  $20 \text{ mV s}^{-1}$ ) and B) after the addition of  $\text{AgPF}_6$  (scan rate  $10 \text{ mV s}^{-1}$ ) starting from 0 V (*vs*  $\text{Ag}/\text{AgCl}$ ).

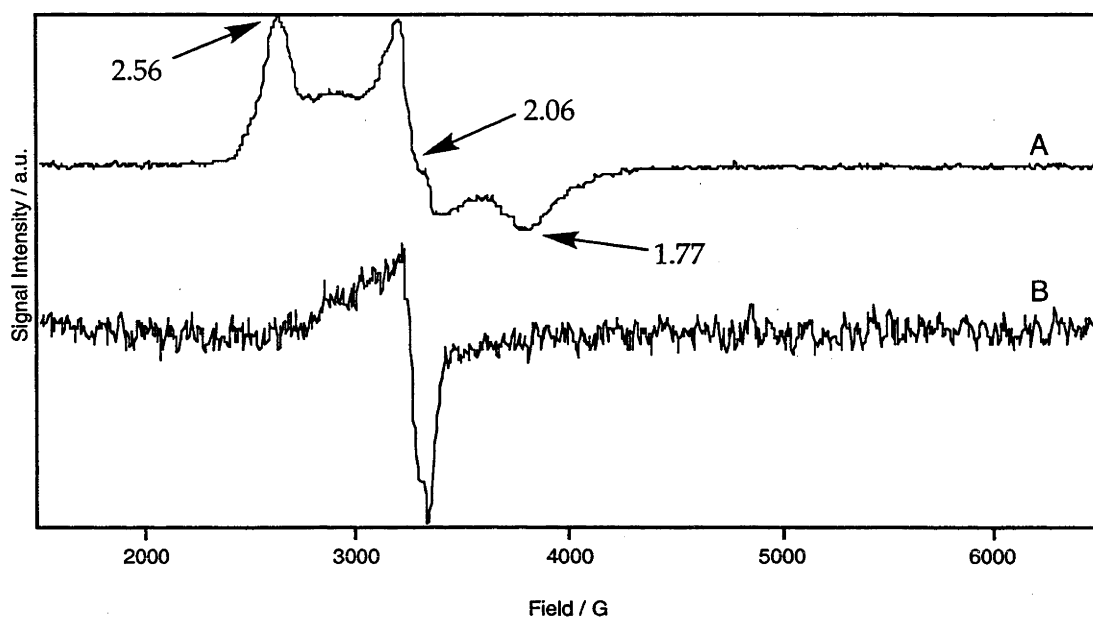


From the chemical oxidation of  $\text{trans-}[\text{Ru}(\text{acac})_2(\eta^2\text{-C}_2\text{H}_4)(\text{NH}_3)]$  with  $[\text{Cp}_2\text{Fe}][\text{PF}_6]$  (0.9 equivalents) in  $\text{CH}_2\text{Cl}_2$  at room temperature a red solid can be isolated. CV studies of this red solid show that this is a mixture of species, including ferrocene,  $[\text{Ru}(\text{acac})_3]$ , and an unidentified species which gives an electrochemically irreversible wave at  $-0.21 \text{ V}$  (*vs*  $\text{Ag}/\text{AgCl}$ ). This solid has not been studied further. The oxidation of  $\text{trans-}[\text{Ru}(\text{acac})_2(\eta^2\text{-C}_2\text{H}_4)(\text{NH}_3)]$  with  $\text{AgPF}_6$  (1.3 equivalents) at *ca.*  $-70^\circ\text{C}$ , however, results in the formation of a deep blue solution from which a deep blue solid may be obtained. Dissolving this blue solid in  $\text{CH}_2\text{Cl}_2$  at room temperature results in a red solution after several minutes. Storage of the blue solid at *ca.*  $-20^\circ\text{C}$  also results in a slow colour change to red after several weeks. The IR spectrum

of the blue solid (KBr disc) shows a very strong absorption at  $1521\text{ cm}^{-1}$  and a weak absorption at  $2964\text{ cm}^{-1}$ , both bands characteristic of  $\nu(\text{C}=\text{O})$  and  $\nu(\text{C}=\text{C})$  in coordinated O-bonded bidentate acac and N-H deformation of coordinated  $\text{NH}_3$ , respectively.<sup>31</sup> The presence of the  $\text{PF}_6$  anion was confirmed by the presence of strong bands at  $847$  and  $558\text{ cm}^{-1}$ .<sup>31</sup>

The EPR spectrum of a solution obtained by *in situ* chemical oxidation of  $\text{trans-}[\text{Ru}(\text{acac})_2(\eta^2\text{-C}_2\text{H}_4)(\text{NH}_3)]$  with  $\text{AgPF}_6$  at *ca.*  $-70\text{ }^\circ\text{C}$  shows three resonances at  $g_1 = 2.56$ ,  $g_2 = 2.06$  and  $g_3 = 1.77$  (see Figure 3.14A). As previously mentioned (see p. 124), a large separation between  $g_1$  and  $g_2$  is consistent with a *cis*-complex. However, this spectrum differs from that obtained by anodic electrolysis (see p. 126) in the presence of a signal at  $g$  2.06 which at first sight, might suggest that *trans*- to *cis*-isomerization has occurred during chemical oxidation. A similar EPR spectrum has also been recorded for the solid isolated from the chemical oxidation of  $\text{cis-}[\text{Ru}(\text{acac})_2(\eta^2\text{-C}_8\text{H}_{14})(\text{SbPh}_3)]$  (see below). The result for the ethene complex appears to contrast with the conclusion drawn from the spectroelectrochemical results for *cis*- and *trans*- $[\text{Ru}(\text{acac})_2(\eta^2\text{-C}_2\text{H}_4)(\text{NH}_3)]$  (see p. 117). However, the EPR spectrum of  $\text{AgPF}_6$  shows a resonance which is believed to be due to a small amount of colloidal silver (see Figure 3.14B). Since the valence electronic configuration for  $\text{Ag}(0)$  is  $4d^{10}5s^1$  with one unpaired electron, an EPR signal is expected. Thus, the resonance at slightly lower field than  $g$  2.10 in the spectrum shown in Figure 3.14A may be due to colloidal silver. Since no attempt was made to filter the solution at *ca.*  $-70\text{ }^\circ\text{C}$ , the amount of colloidal silver must be equal to that of the ruthenium complex. If this peak at  $g$  2.06 is subtracted, the appearance of the spectrum is much closer to that of the solution obtained by bulk electrolysis. However, further EPR studies on  $\text{trans-}[\text{Ru}(\text{acac})_2(\eta^2\text{-C}_2\text{H}_4)(\text{NH}_3)]$ , as well as  $\text{cis-}[\text{Ru}(\text{acac})_2(\eta^2\text{-C}_2\text{H}_4)(\text{NH}_3)]$  and other available complexes are required to clarify this situation.

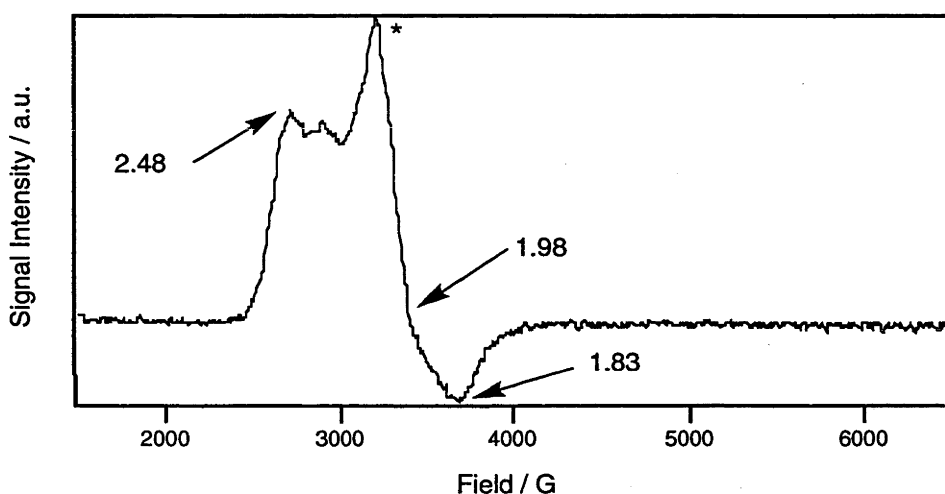
**Figure 3.14:** EPR spectra of A) *in situ* chemical oxidation of *trans*-[Ru(acac)<sub>2</sub>(η<sup>2</sup>-C<sub>2</sub>H<sub>4</sub>)(NH<sub>3</sub>)] chemical oxidation and B) AgPF<sub>6</sub> as a frozen solution of 0.5 M [Bu<sup>n</sup><sub>4</sub>N][PF<sub>6</sub>]/CH<sub>2</sub>Cl<sub>2</sub> at 4.7 K.



Chemical oxidation of a cold solution of *cis*-[Ru(acac)<sub>2</sub>(η<sup>2</sup>-C<sub>8</sub>H<sub>14</sub>)(SbPh<sub>3</sub>)]<sup>4</sup> with AgPF<sub>6</sub> also gives a deep blue solid which, unlike the corresponding compound made from *trans*-[Ru(acac)<sub>2</sub>(η<sup>2</sup>-C<sub>2</sub>H<sub>4</sub>)(NH<sub>3</sub>)], appears to be indefinitely stable at room temperature; a sample has been kept for over one year. The elemental analysis of the solid was consistent with the formulation [Ru<sup>III</sup>(acac)<sub>2</sub>(η<sup>2</sup>-C<sub>8</sub>H<sub>14</sub>)(SbPh<sub>3</sub>)] [PF<sub>6</sub>] containing *ca.* 10% of AgPF<sub>6</sub>. The +ve FAB mass spectrum shows the presence of the parent cation at *m/z* 762.2 and ions corresponding to {Ru(acac)<sub>2</sub>(SbPh<sub>3</sub>)}<sup>+</sup>; the IR spectrum shows two absorptions at 1552 and 1518 cm<sup>-1</sup>, consistent with O-bonded bidentate acac coordination and a strong absorptions at 840 and 557 cm<sup>-1</sup> indicating the presence of the [PF<sub>6</sub>] anion.<sup>31</sup> Cyclic and AC voltammetric studies at *ca.* -45 °C show that the isolated blue solid has a fully reversible E<sub>1/2</sub>(Ru<sup>3+/2+</sup>) couple at +0.48 V (*vs* Ag/AgCl), which is very close to the reported potential of *cis*-[Ru(acac)<sub>2</sub>(η<sup>2</sup>-C<sub>8</sub>H<sub>14</sub>)(SbPh<sub>3</sub>)] (see Table 1.10).

The EPR spectrum of  $[\text{Ru}^{\text{III}}(\text{acac})_2(\eta^2\text{-C}_8\text{H}_{14})(\text{SbPh}_3)][\text{PF}_6]$  shown in Figure 3.15 is similar to that of the 2-allylpyridine complex  $\text{cis-}[\text{Ru}(\text{acac})_2(o\text{-H}_2\text{C}=\text{CHCH}_2\text{C}_5\text{H}_4\text{N})]$  (see p. 125). The largest absorption at slightly lower field than *ca.*  $g$  1.98 probably has a small contribution from  $\text{Ag}(0)$  present in the solid (see above). However, the magnitude of the difference between  $g_1$  (2.48) and  $g_2$  (1.98) suggests that a  $\text{cis-}[\text{Ru}(\text{acac})_2\text{L}_2]$  species is present in solution.

**Figure 3.15:** EPR Spectrum of the blue solid isolated from the oxidation of  $\text{cis-}[\text{Ru}(\text{acac})_2(\eta^2\text{-C}_8\text{H}_{14})(\text{SbPh}_3)]$  with  $\text{AgPF}_6$  in 0.5 M  $[\text{Bu}^n_4\text{N}][\text{PF}_6]/\text{CH}_2\text{Cl}_2$  at 4.7 K.



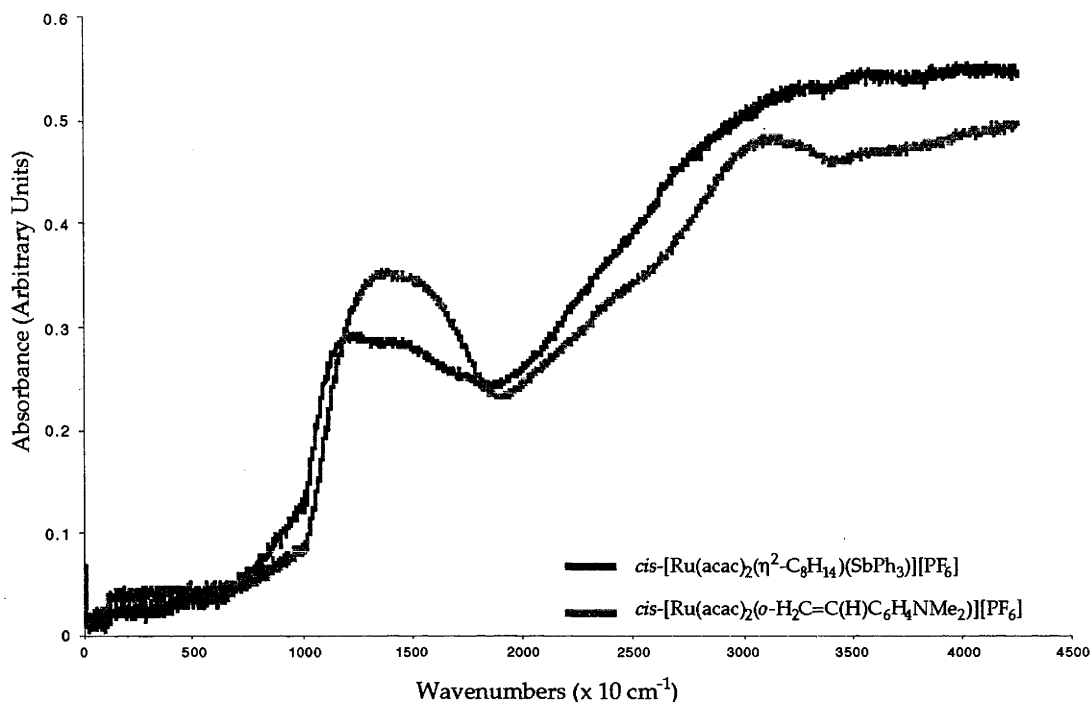
\*) absorption which probably contains a small contribution from  $\text{Ag}$  present.

The complexes  $[\text{Ru}^{\text{III}}(\text{acac})_2\text{L}_2]^+$  show a characteristic  $\text{acac } \pi \rightarrow \text{Ru(III)}$  LMCT between  $12000 - 20000 \text{ cm}^{-1}$  in solution (see Table 3.6). For comparison, the electronic spectrum of the blue solid was therefore recorded by solid state reflectance UV-Vis spectroscopy. It shows a broad band between  $12000 - 18000 \text{ cm}^{-1}$  in either a matrix of  $\text{KCl}$  or  $[\text{Bu}^n_4\text{N}][\text{BF}_4]$ , as shown in Figure 3.16. This transition is also present in the spectrum of the isolated solid  $\text{cis-}[\text{Ru}^{\text{III}}(\text{acac})_2(o\text{-H}_2\text{C}=\text{C}(\text{H})\text{C}_6\text{H}_4\text{NMe}_2)][\text{PF}_6]$  but is absent for  $\text{cis-}[\text{Ru}^{\text{II}}(\text{acac})_2(\eta^2\text{-C}_2\text{H}_4)(\text{SbPh}_3)]$  in both matrices. The spectrum of  $[\text{Ru}^{\text{III}}(\text{acac})_2(\eta^2\text{-C}_8\text{H}_{14})(\text{SbPh}_3)][\text{PF}_6]$  in  $\text{MgO}$  does not show this transition, possibly because traces of water in  $\text{MgO}$  may form hydroxide ions which can



reduce the Ru(III) species to Ru(II) complexes in a similar manner found for ethoxide ions and *cis*-[Ru(acac)<sub>2</sub>(*o*-H<sub>2</sub>C=C(H)C<sub>6</sub>H<sub>4</sub>NMe<sub>2</sub>)] [PF<sub>6</sub>].<sup>6</sup>

**Figure 3.16** Solid state electronic spectra in KCl matrix.



On the basis of the available evidence, the blue solid isolated from the oxidation of *cis*-[Ru(acac)<sub>2</sub>(η<sup>2</sup>-C<sub>8</sub>H<sub>14</sub>)(SbPh<sub>3</sub>)] with AgPF<sub>6</sub> at low temperatures is *cis*-[Ru<sup>III</sup>(acac)<sub>2</sub>(η<sup>2</sup>-C<sub>8</sub>H<sub>14</sub>)(SbPh<sub>3</sub>)] [PF<sub>6</sub>].

### 3.4 Discussion

There are relatively few well-characterised mononuclear paramagnetic transition metal alkene and alkyne complexes and most contain either early transition metals or 3d-elements. They include [(N<sub>3</sub>N)Mo(η<sup>2</sup>-C<sub>2</sub>H<sub>4</sub>)] [(N<sub>3</sub>N)<sup>3-</sup> = [(Me<sub>3</sub>SiNCH<sub>2</sub>CH<sub>2</sub>)<sub>3</sub>N]<sup>3-</sup>],<sup>32</sup> [Tp<sup>*t*-Bu,Me</sup>Co(η<sup>2</sup>-C<sub>2</sub>H<sub>4</sub>)] (Tp<sup>*t*-Bu,Me</sup> = hydridotris(3-*t*-Bu-5-methyl-pyrazolyl)borate),<sup>33</sup> [(η<sup>5</sup>:η<sup>1</sup>-C<sub>5</sub>H<sub>4</sub>(CH<sub>2</sub>)<sub>2</sub>Ni-Pr)V(η<sup>4</sup>-C<sub>6</sub>H<sub>10</sub>)],<sup>34</sup> [CpV<sup>I</sup>(L)(PMe<sub>3</sub>)<sub>2</sub>] (L = C<sub>2</sub>H<sub>4</sub>, PhC≡CPh),<sup>35</sup> [V(CO)<sub>4</sub>(LL')] (LL' = *o*-CH<sub>2</sub>=CHCH<sub>2</sub>C<sub>6</sub>H<sub>4</sub>PPh<sub>2</sub>, *E*-*o*-CH<sub>3</sub>CH=CHC<sub>6</sub>H<sub>4</sub>PPh<sub>2</sub>),<sup>36</sup> [Cp<sub>2</sub>V(*E*-MeO<sub>2</sub>CH=CHCO<sub>2</sub>Me)],<sup>37-39</sup> [Fe(η<sup>2</sup>-C<sub>2</sub>H<sub>4</sub>)<sub>2</sub>(PEt<sub>3</sub>)<sub>2</sub>],<sup>40</sup> [Co<sup>I</sup>(η<sup>2</sup>-H<sub>2</sub>C=CHCN)(PMe<sub>3</sub>)<sub>3</sub>][BF<sub>4</sub>],<sup>41</sup> [Co<sup>I</sup>(η<sup>2</sup>-C<sub>2</sub>H<sub>4</sub>)(PR<sub>3</sub>)<sub>3</sub>] (R = Me,<sup>42-44</sup> Ph<sup>45</sup>), [Co<sup>I</sup>(COD)(PMe<sub>3</sub>)<sub>2</sub>] (COD = 1,5-cyclooctadiene),<sup>44</sup> [(η<sup>5</sup>-C<sub>5</sub>H<sub>4</sub>SiMe<sub>3</sub>)<sub>2</sub>Nb(η<sup>2</sup>-

$\text{RC}\equiv\text{CR}'$ )] ( $\text{R} = \text{R}' = \text{Ph}, \text{Me}, \text{CO}_2\text{Me}$ ;  $\text{R} = \text{Me}, \text{R}' = \text{CO}_2\text{Me}$ ),<sup>46</sup>  $[\eta^6\text{-C}_6\text{Me}_6)\text{Cr}^{\text{I}}(\eta^2\text{-Me}_3\text{SiC}\equiv\text{CSiMe}_3)(\text{CO})_2][\text{PF}_6]^{47}$  and  $[\eta^6\text{-C}_6\text{Me}_{6-x}\text{H}_x)\text{Cr}(\eta^2\text{-PhC}\equiv\text{CPh})][\text{PF}_6]$  ( $x = 0, 1$ ).<sup>48</sup>

Examples of paramagnetic alkene and alkyne complexes for a later transition metal are the complexes *cis*- $[\text{Ru}^{\text{III}}(\text{acac})_2(\text{LL}')][\text{PF}_6]$  ( $\text{LL}' = 2\text{-vinyl-N,N-dimethylaniline}, 2\text{-isopropenyl-N,N-dimethylaniline}, 3\text{-butenyldimethylamine}, 2\text{-allylpyridine}, \text{isomesityl oxide}, 2\text{-methoxystyrene}, 3\text{-butenylmethylether}, 2\text{-phenylethynyl-N,N-dimethylaniline}, 2\text{-trimethylsilylethynyl-N,N-dimethylaniline}$ )<sup>5,13</sup> which make use of the chelate effect to increase stability. The work described in this Chapter shows that non-chelated alkene-ruthenium(III) complexes  $[\text{Ru}^{\text{III}}(\text{acac})_2(\eta^2\text{-alkene})\text{L}][\text{X}]$  (alkene =  $\text{C}_2\text{H}_4$ , L =  $\text{C}_2\text{H}_4, \text{NH}_3, \text{PCy}_3, \text{MeCN}, \text{SbPh}_3$ ; alkene =  $\text{C}_8\text{H}_{14}$ <sup>3</sup>, L =  $\text{NH}_3, \text{MeCN}, \text{SbPh}_3$ ) can be generated electrochemically at low temperature. Unlike the related chelated alkene complexes however, these oxidised species decompose in  $\text{CH}_2\text{Cl}_2$  at room temperature. Presumably decomposition occurs by alkene dissociation as a direct result of the reduced  $\pi$ -backbonding of the Ru(III) ion (see p. 2), although the possibility that the oxidised species are reacting with the solvent cannot be discounted.

However, chemical oxidation of the complexes *trans*- $[\text{Ru}(\text{acac})_2(\eta^2\text{-C}_2\text{H}_4)(\text{NH}_3)]$  and *cis*- $[\text{Ru}(\text{acac})_2(\eta^2\text{-C}_8\text{H}_{14})(\text{SbPh}_3)]$  with a suitable oxidant at low temperatures affords the corresponding salts *trans*- $[\text{Ru}^{\text{III}}(\text{acac})_2(\eta^2\text{-C}_2\text{H}_4)(\text{NH}_3)][\text{PF}_6]$  and *cis*- $[\text{Ru}^{\text{III}}(\text{acac})_2(\eta^2\text{-C}_8\text{H}_{14})(\text{SbPh}_3)][\text{PF}_6]$ ; the latter solid appears to be indefinitely stable at room temperature. Spectroelectrochemical results suggest that the complexes retain their geometric configuration during oxidation, although attempts to confirm this conclusion by EPR spectroscopy have been inconclusive. Further studies with these very sensitive oxidised alkene complexes are required to establish this point. Other alkenes which have electron-donating substituents attached to the C=C bond could also be expected to stabilise the Ru(III)

oxidation state as well, whereas alkenes with electron-withdrawing substituents would be expected to give more reactive and unstable species than that found for ethene.

The oxidation potential of  $cis$ -[Ru(acac)<sub>2</sub>( $\eta^2$ -C<sub>8</sub>H<sub>14</sub>)(SbPh<sub>3</sub>)] is *ca.* 200 mV higher than  $trans$ -[Ru(acac)<sub>2</sub>( $\eta^2$ -C<sub>2</sub>H<sub>4</sub>)(NH<sub>3</sub>)], yet, qualitatively, the oxidised triphenylstibine complex appears to be much more stable than the oxidised ammine complex. Oxidation of  $cis$ -[Ru(acac)<sub>2</sub>( $\eta^2$ -C<sub>2</sub>H<sub>4</sub>)(SbPh<sub>3</sub>)] under similar conditions would presumably result in a species which is more stable than the ammine complex but less stable than the cyclooctene analogue. The reason for the greater stability at the Ru(III) level when triphenylstibine is co-ligand is not known.

Although non-chelated mono- or di-substituted alkyne complexes [Ru(acac)<sub>2</sub>( $\eta^2$ -RC $\equiv$ CR)L] (L = co-ligand) have not been isolated (see Chapter 2), the oxidation potentials for such complexes can be predicted to lie 200 to 300 mV lower than those found for the corresponding ethene complexes (see Table 1.8). The chemical oxidation of these compounds may also be expected to yield isolable ruthenium(III)-alkyne complexes [Ru<sup>III</sup>(acac)<sub>2</sub>( $\eta^2$ -RC $\equiv$ CR)L][X]. Structural studies of redox-active alkyne complexes  $cis$ -[Ru(acac)<sub>2</sub>(*o*-PhC $\equiv$ CC<sub>6</sub>H<sub>4</sub>NMe<sub>2</sub>)]<sup>n+</sup> (n = 0, 1),<sup>13</sup> [( $\eta^6$ -C<sub>6</sub>HMe<sub>5</sub>)Cr( $\eta^2$ -PhC $\equiv$ CPh)(CO)<sub>2</sub>]<sup>n+</sup> and [(Tp')Mo( $\eta^2$ -PhC $\equiv$ CPh)(CO)<sub>2</sub>]<sup>n+</sup> [Tp' = HB(3,5-dimethylpyrazolyl)<sub>3</sub>] (n = 0, 1)<sup>49</sup> appear to indicate that the alkyne-binding affinities for both oxidation states do not differ greatly, unlike the alkene redox pair  $cis$ -[Ru(acac)<sub>2</sub>(*o*-H<sub>2</sub>C=C(H)C<sub>6</sub>H<sub>4</sub>NMe<sub>2</sub>)]<sup>n+</sup> (n = 0, 1).<sup>5</sup>

## 3.5 References

- (1) Astruc, D. *Electron Transfer and Radical Processes in Transition Metal Chemistry*; VCH: New York, 1995, p 98.
- (2) Wallace, L. PhD Thesis, ANU, 1991.
- (3) Menglet, D. PhD Thesis, ANU, 1996.
- (4) Bennett, M. A.; Chung, G.; Hockless, D. C. R.; Neumann, H.; Willis, A. *C. J. Chem. Soc., Dalton Trans.* **1999**, 3451.
- (5) Bennett, M. A.; Heath, G. A.; Hockless, D. C. R.; Kovacik, I.; Willis, A. *C. J. Am. Chem. Soc.* **1998**, *120*, 932.
- (6) Kovacik, I. PhD Thesis, ANU, 1995.
- (7) Albright, T. A.; Hoffmann, R.; Thibeault, J. C.; Thorn, D. L. *J. Am. Chem. Soc.* **1979**, *101*, 3801.
- (8) Lever, A. B. P. *Inorg. Chem.* **1990**, *29*, 1271.
- (9) Lehmann, H.; Schenk, K. J.; Chapuis, G.; Ludi, A. *J. Am. Chem. Soc.* **1979**, *101*, 6197.
- (10) Aebischer, N.; Sidorenkova, E.; Ravera, M.; Laurency, G.; Osella, D.; Weber, J.; Merbach, A. E. *Inorg. Chem.* **1997**, *36*, 6009.
- (11) McGrath, D. V.; Grubbs, R. H.; Ziller, J. W. *J. Am. Chem. Soc.* **1991**, *113*, 3611.
- (12) Kovacik, I.; Gevert, O.; Werner, H.; Schmittel, M.; Söllner, R. *Inorg. Chim. Acta* **1998**, *275-276*, 435.
- (13) Bennett, M. A.; Heath, G. A.; Hockless, D. C. R.; Kovacik, I.; Willis, A. *C. Organometallics* **1998**, *17*, 5867.
- (14) Richardson, D. E.; Sen, J. P.; Buhr, J. D.; Taube, H. *Inorg. Chem.* **1982**, *21*, 3136.
- (15) Dodsworth, E. S.; Lever, A. B. P. *Chem. Phys. Lett.* **1986**, *124*, 152.
- (16) Lever, A. B. P. *Inorganic Electronic Spectroscopy*; Elsevier: Amsterdam, 1968, p 306.

- (17) Creutz, C.; Taube, H. *J. Am. Chem. Soc.* **1969**, *91*, 3988.
- (18) Creutz, C.; Taube, H. *J. Am. Chem. Soc.* **1973**, *95*, 1086.
- (19) Hush, N. *Prog. Inorg. Chem.* **1967**, *8*, 391.
- (20) Hush, N. In *Mixed-Valence Compounds*; Brown, D. B., Ed.; Reidel Publishing Co.: Dordrecht, Holland, 1980; p 151.
- (21) Simone, R. E. D. *J. Am. Chem. Soc.* **1973**, *95*, 6238.
- (22) Griffiths, J. H. E.; Owen, J.; Ward, I. M. *Proc. Roy. Soc., Ser. A* **1963**, *219*, 526.
- (23) Stanko, J. A.; Peresie, H. J.; Bernstein, R. A.; Wang, R.; Wang, P. S. *Inorg. Chem.* **1973**, *12*, 634.
- (24) de Rezende, N. M. S.; de Martins, S.; Marinho, L. A.; Santos, J. A. V. d.; Tabak, M.; Perussi, J. R.; Franco, D. W. *Inorg. Chim. Acta* **1991**, *182*, 87.
- (25) Mazzetto, S. E.; Rodrigues, E.; Franco, D. W. *Polyhedron* **1993**, *12*, 971.
- (26) Orgel, L. E. *J. Chem. Soc.* **1961**, 3683.
- (27) Ceulemans, A.; Dendooven, M.; Vanquickenborne, L. G. *Inorg. Chem.* **1985**, *24*, 1153.
- (28) Sugano, S.; Tanabe, Y.; Kamimura, H. *Multiplets of Transition Metal Ions in Crystals*; Academic Press: New York, 1970.
- (29) Kulkarni, S. S.; Santra, B. K.; Munshi, P.; Lahiri, G. K. *Polyhedron* **1998**, *17*, 4365.
- (30) Heath, G. A.; Webster, R. *unpublished results*
- (31) Nakamoto, K. *Infrared and Raman Spectra of Inorganic and Coordination Compounds*; 4th ed.; Wiley: New York, 1986.
- (32) Greco, G. E.; O'Donoghue, M. B.; Seidel, S. W.; Davis, W. M.; Schrock, R. R. *Organometallics* **2000**, *19*, 1132.
- (33) Jewson, J. D.; Liable-Sands, L. M.; Yap, G. P. A.; Rheingold, A. L.; Theopold, K. H. *Organometallics* **1999**, *18*, 300.
- (34) Witte, P. T.; Meetsma, A.; Hessen, B. *Organometallics* **1999**, *18*, 2944.

- (35) Hessen, B.; Auke, M.; Bolhuis, F. V.; Teuben, J. H.; Helgesson, G.; Jagner, S. *Organometallics* **1990**, *9*, 1925.
- (36) Interrante, L. V.; Nelson, G. V. *J. Organomet. Chem.* **1970**, *25*, 153.
- (37) Fachinetti, G.; Nero, S. D.; Floriani, C. *J. Chem. Soc., Dalton Trans.* **1976**, 1046.
- (38) Fachinetti, G.; Floriani, C.; Chiesi-Villa, A.; Guastini, C. *Inorg. Chem.* **1979**, *18*, 2282.
- (39) Morán, M.; Santos-Garcia, J. J.; Masaguer, J. R.; Fernández, V. J. *Organomet. Chem.* **1985**, *295*, 327.
- (40) Hoberg, H.; Jenni, K.; Angermund, K.; Krüger, C. *Angew. Chem. Int. Ed. Engl.* **1987**, *26*, 153.
- (41) Peres, Y.; Dartiguenave, M.; Devillers, J. *Nouv. J. Chim.* **1986**, *10*, 149.
- (42) Klein, H.-F. *Angew. Chem., Int. Ed. Engl.* **1985**, *26*, 153.
- (43) Klein, H.-F.; Gross, J.; Bassett, J.-M.; Schubert, U. *Z. Naturforsch. B* **1980**, *35*, 614.
- (44) Klein, H.-F.; Gross, J.; Witty, H.; Neugebauer, D. *Z. Naturforsch. B* **1984**, *39*, 643.
- (45) Kubo, Y.; Pu, L.-S.; Yamamoto, A.; Ikeda, S. *J. Organomet. Chem.* **1975**, *84*, 369.
- (46) Antinolo, A.; Otero, A.; Fajardo, M.; Garcia-Yebra, C.; Lopez-Mardomingo, C.; Martin, A.; Gomez-Sal, P. *Organometallics* **1997**, *16*, 2601.
- (47) Connelly, N. G.; Orpen, A. G.; Rieger, A. L.; Rieger, P. H.; Scott, C. J.; Rosair, G. M. *Chem. Commun.* **1992**, 1293.
- (48) Connelly, N. G.; Johnson, G. A. *J. Organomet. Chem.* **1974**, *77*, 341.
- (49) Bartlett, I. M.; Connelly, N. G.; Orpen, A. G.; Quayle, M. J.; Rankin, J. C. *Chem. Commun.* **1996**, 2583.

*Reactivity of alkene and alkyne  
bis( $\beta$ -diketonato)ruthenium(III)  
complexes*

### 4.1 Nucleophilic Addition Reactions

The complexation of alkenes or alkynes to a metal atom which is in a high oxidation state (II to IV) and has either a full formal positive charge or remote electron-withdrawing ligands such as CO usually renders the unsaturated hydrocarbons susceptible to nucleophilic attack.<sup>1-3</sup> Such changes in reactivity are generally attributed to the net withdrawal of electron density from the unsaturated carbon atoms, although theoretical calculations suggest that alkene slippage from  $\eta^2$ - to  $\eta^1$ -coordination is required for external nucleophilic attack.<sup>4</sup> The addition of neutral or charged nitrogen and oxygen nucleophiles to mono-alkenes, chelating alkenes or dienes that are coordinated to Pd(II),<sup>5-10</sup> Pt(II)<sup>8-19</sup> and Fe(II)<sup>20-25</sup> has been extensively studied and many of these reactions are synthetically or industrially important. In most cases, attack of the nucleophile on a coordinated alkene occurs *exo* to the metal centre.<sup>1</sup> Even tertiary phosphines can behave as nucleophiles rather than ligands *e.g.* dimethylphenylphosphine PPhMe<sub>2</sub> reacts with the coordinated ethene of [RuCl<sub>2</sub>( $\eta^2$ -C<sub>2</sub>H<sub>4</sub>)(CO)(PPhMe<sub>2</sub>)<sub>2</sub>] at low temperatures to give nucleophilic addition products instead of ethene displacement.<sup>26</sup> The addition of nucleophiles to alkynes coordinated to Pt(II),<sup>27-30</sup> Fe(II),<sup>31-34</sup> W(II) and Mo(II)<sup>35-39</sup> has also been studied.

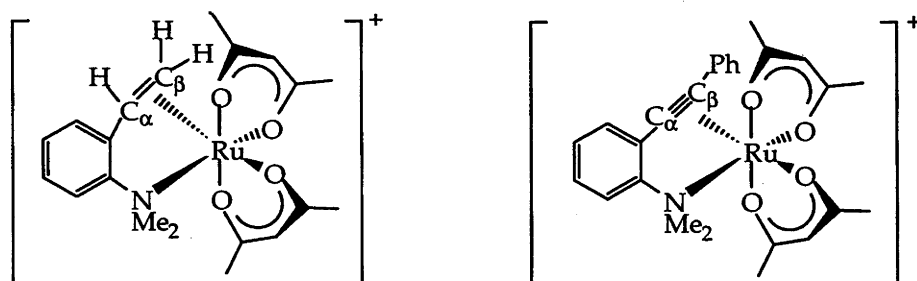
The fact that alkenes and alkynes can coordinate to ruthenium(III), a relatively high oxidation state, suggested the possibility that they might be susceptible to nucleophilic attack. There is a report that ruthenium(III) chloride catalyses the hydration of various alkynes to ketones via an undetected Ru(III)-vinyl alcohol complex.<sup>40</sup> However, because the coordination is generally weak, especially for alkenes, the work described in this Chapter is restricted to systems stabilised by chelation, *i.e.* *cis*-[Ru<sup>III</sup>(acac)<sub>2</sub>(LL')][PF<sub>6</sub>] (LL' = 2-vinyl-N,N'-dimethylaniline,<sup>41</sup> 2-phenylethynyl-N,N'-dimethylaniline<sup>42</sup>). Preliminary studies were described



in the PhD thesis of Kováčik.<sup>43</sup> He made the following observations: neutral nucleophiles do not add to the alkene in the Ru(II) starting materials nor do they displace the coordinated alkene or alkyne; addition of ethoxide ions to these Ru(III) salts results in the one-electron reduction to the corresponding Ru(II) compounds; a similar one-electron reduction of *cis*-[Ru<sup>III</sup>(acac)<sub>2</sub>(*o*-H<sub>2</sub>C=C(H)C<sub>6</sub>H<sub>4</sub>NMe<sub>2</sub>)] [PF<sub>6</sub>] to the Ru(II) compound is observed with pyridine; *cis*-[Ru<sup>III</sup>(acac)<sub>2</sub>(*o*-PhC≡CC<sub>6</sub>H<sub>4</sub>NMe<sub>2</sub>)] [PF<sub>6</sub>] reacts with water and pyridine, and in the case of *cis*-[Ru<sup>III</sup>(acac)<sub>2</sub>(*o*-H<sub>2</sub>C=C(H)C<sub>6</sub>H<sub>4</sub>NMe<sub>2</sub>)] [PF<sub>6</sub>] with excess PMe<sub>3</sub>, to form red solids whose structures were unknown.<sup>43</sup>

In this subsequent discussion, the label C<sub>α</sub> refers to the carbon atom attached to the N,N-dimethylaniline unit and C<sub>β</sub> to the next carbon atom (see Figure 4.1).

**Figure 4.1:** Labelling of the chelate alkene and alkyne carbon atoms for the complexes *cis*-[Ru<sup>III</sup>(acac)<sub>2</sub>(*o*-PhC≡CC<sub>6</sub>H<sub>4</sub>NMe<sub>2</sub>)] [PF<sub>6</sub>] and *cis*-[Ru<sup>III</sup>(acac)<sub>2</sub>(*o*-H<sub>2</sub>C=C(H)C<sub>6</sub>H<sub>4</sub>NMe<sub>2</sub>)] [PF<sub>6</sub>].



#### 4.2 Reaction of *cis*-[Ru<sup>III</sup>(acac)<sub>2</sub>(*o*-PhC≡CC<sub>6</sub>H<sub>4</sub>NMe<sub>2</sub>)] [PF<sub>6</sub>] with pyridine and diethylamine.

The addition of excess pyridine or diethylamine to *cis*-[Ru<sup>III</sup>(acac)<sub>2</sub>(*o*-PhC≡CC<sub>6</sub>H<sub>4</sub>NMe<sub>2</sub>)] [PF<sub>6</sub>]<sup>42</sup> in CH<sub>2</sub>Cl<sub>2</sub> results in a red solution almost immediately from which red to black crystals of 1:1 adducts can be isolated in yields of *ca.* 50-75%. Although satisfactory elemental analyses were not obtained for either solid, the amount of nitrogen detected is consistent with the presence of only two nitrogen atoms per ruthenium atom. The +ve FAB

mass spectral data for these isolated solids show parent molecular ion peaks which correspond to  $\{\text{Ru}(\text{acac})_2(\text{Me}_2\text{NC}_6\text{H}_4\text{C}\equiv\text{CPh.NC}_5\text{H}_5)\}^+$  and  $\{\text{Ru}(\text{acac})_2(\text{Me}_2\text{NC}_6\text{H}_4\text{C}\equiv\text{CPh.NEt}_2)\}^+$  (see Table 4.1).

**Table 4.1:** +ve FAB mass spectral data for the isolated solids from the reaction of pyridine or diethylamine with *cis*- $[\text{Ru}(\text{acac})_2(o\text{-PhC}\equiv\text{CC}_6\text{H}_4\text{NMe}_2)][\text{PF}_6]$ .

Nucleophile	m/z	Assignment	Relative Intensity (%)
C <sub>5</sub> H <sub>5</sub> N	600.2	$\{\text{Ru}(\text{acac})_2(\text{Me}_2\text{NC}_6\text{H}_4\text{C}\equiv\text{CPh.NC}_5\text{H}_5)\}^+$	30
	521.1	$\{\text{Ru}(\text{acac})_2(\text{Me}_2\text{NC}_6\text{H}_4\text{C}\equiv\text{CPh})\}^+$	100
Et <sub>2</sub> NH	593.2	$\{\text{Ru}(\text{acac})_2(\text{Me}_2\text{NC}_6\text{H}_4\text{C}\equiv\text{CPh.NEt}_2)\}^+$	100
	522.1	$\{\text{Ru}(\text{acac})_2(\text{Me}_2\text{NC}_6\text{H}_4\text{C}\equiv\text{CPh.H})\}^+$	8
	495.1	$\{\text{Ru}(\text{acac})(\text{Me}_2\text{NC}_6\text{H}_4\text{C}\equiv\text{CPh.NEt}_2\text{H})\}^+$	10

Electrochemical studies show a fully reversible  $E_{1/2}(\text{Ru}^{3+/2+})$  process at -0.50 V (*vs* Ag/AgCl) for the pyridine adduct, which is considerably more negative than that previously found for *cis*- $[\text{Ru}(\text{acac})_2(\text{TMPDA})]$  (TMPDA = N,N,N',N'-tetramethyl-1,2-phenylenediamine) (-0.29 V *vs* Ag/AgCl),<sup>43</sup> *trans*- $[\text{Ru}(\text{acac})_2(\text{NC}_5\text{H}_5)_2]$  (-0.04 V *vs* Ag/AgCl),<sup>44</sup> *cis*- $[\text{Ru}(\text{acac})_2(\text{NC}_5\text{H}_5)_2]$  (+0.01 V *vs* Ag/AgCl)<sup>44</sup> and *cis*- $[\text{Ru}(\text{acac})_2(o\text{-PhC}\equiv\text{CC}_6\text{H}_4\text{NMe}_2)]$  (+0.26 V *vs* Ag/AgCl).<sup>42</sup> This electrochemical evidence strongly suggests that the product is not simply a coordination compound of pyridine, *e.g.*  $[\text{Ru}(\text{acac})_2(\text{NC}_5\text{H}_5)_2][\text{PF}_6]$  or *cis*- $[\text{Ru}(\text{acac})_2(o\text{-PhC}\equiv\text{CC}_6\text{H}_4\text{NMe}_2)(\text{NC}_5\text{H}_5)][\text{PF}_6]$  formed by complete or partial displacement of the alkyne ligand. By contrast, there is no detectable redox ( $\text{Ru}^{3+/2+}$ ) process between -1.0 and +1.0 V (*vs* Ag/AgCl) for the solid obtained from the diethylamine reaction. The EPR spectrum for the pyridine adduct as a frozen solution, is shown in Figure 4.2. It has three resonances at  $g_1 = 2.35$ ,  $g_2 = 2.29$ ,  $g_3 = 1.76$  as well as some fine structure, and is typical for a ruthenium(III) complex (see p. 123 - 125).

The IR spectra (KBr disc) for both solids show two strong bands at 1580 and 1510  $\text{cm}^{-1}$ , characteristic of O-bonded bidentate acac<sup>45</sup> and strong bands

at *ca.* 842 and 557  $\text{cm}^{-1}$  due to the  $\text{PF}_6$  anion (see Table 4.2).<sup>45</sup> There are no absorptions in the region of *ca.* 1970  $\text{cm}^{-1}$  and *ca.* 2200  $\text{cm}^{-1}$  due to the  $\nu(\text{C}\equiv\text{C})$  of the coordinated and free alkyne, respectively.<sup>42</sup> A band detected in the spectrum at 1547  $\text{cm}^{-1}$  in the pyridine adduct is presumably due to a "breathing" vibration of the coordinated pyridine.<sup>46</sup>

**Figure 4.2:** EPR Spectra of the isolated solid from the reaction of pyridine with *cis*- $[\text{Ru}(\text{acac})_2(o\text{-PhC}\equiv\text{CC}_6\text{H}_4\text{NMe}_2)][\text{PF}_6]$  as a frozen solution of 0.5 M  $[\text{Bu}^n_4\text{N}][\text{PF}_6]/\text{CH}_2\text{Cl}_2$  at 4.7 K.

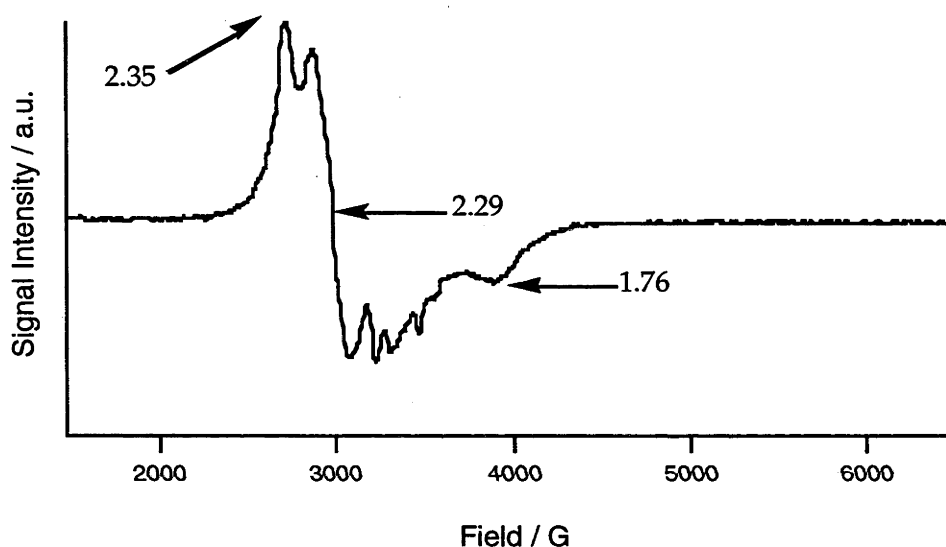


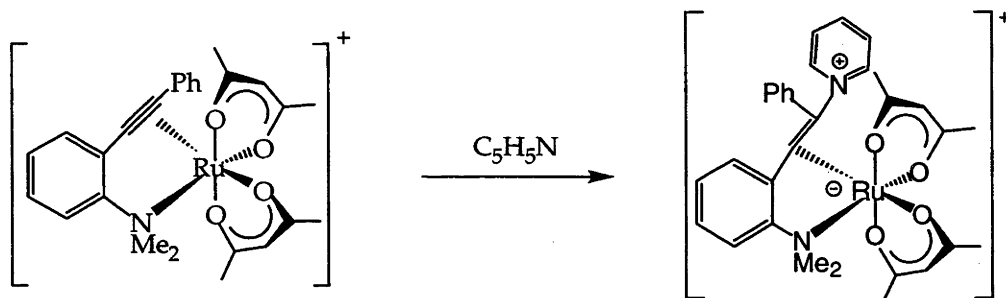
**Table 4.2:** IR spectral data for the isolated solids from the reaction of pyridine and diethylamine with *cis*- $[\text{Ru}(\text{acac})_2(o\text{-PhC}\equiv\text{CC}_6\text{H}_4\text{NMe}_2)][\text{PF}_6]$  (KBr disc).

Nucleophile	$\nu(\text{acac})$	$\nu(\text{PF}_6)$	Other
$\text{C}_5\text{H}_5\text{N}$	1569, 1519	841, 558	1547
$\text{NHEt}_2$	1578, 1518	842, 557	-

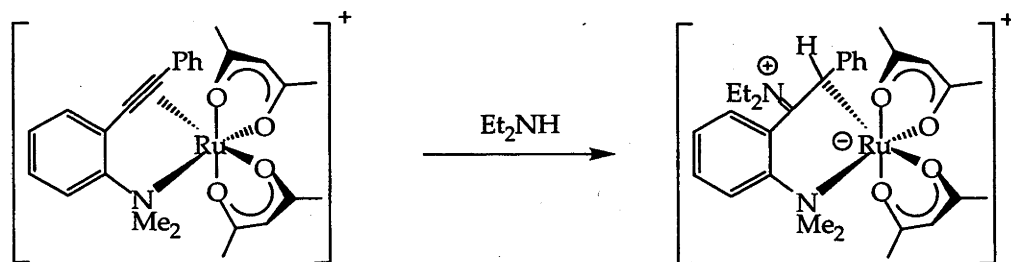
The structures of the pyridine and diethylamine adducts were identified by X-ray crystallography as (E)- $\text{cis}-[\text{Ru}^{\text{III}}(\text{acac})_2\{o\text{-Me}_2\text{NC}_6\text{H}_4\text{C}=\text{C}(\text{NC}_5\text{H}_5)\text{Ph}\}][\text{PF}_6]$  and  $\text{cis}-[\text{Ru}^{\text{III}}(\text{acac})_2\{o\text{-Me}_2\text{NC}_6\text{H}_4\text{C}(\text{H})\text{C}(\text{NEt}_2)\text{Ph}\}][\text{PF}_6]$  respectively. In both cases, addition to the coordinated alkyne has occurred as shown in

Equations 4.1 and 4.2, respectively. The structures are best regarded as zwitterionic with a formal positive charge on the nitrogen atom and a negative charge on the metal atom. In both cases, the ruthenium complex has an overall positive charge.

**Equation 4.1:** Formation of (E)- $cis-[Ru^{III}(acac)_2\{o-Me_2NC_6H_4C=C(NC_5H_5)Ph\}][PF_6]$  from the reaction of pyridine with  $cis-[Ru(acac)_2(o-PhC\equiv CC_6H_4NMe_2)][PF_6]$ .



**Equation 4.2:** Formation of  $cis-[Ru^{III}(acac)_2\{o-Me_2NC_6H_4C(=NEt_2)C(H)Ph\}][PF_6]$  from the reaction of diethylamine with  $cis-[Ru(acac)_2(o-PhC\equiv CC_6H_4NMe_2)][PF_6]$ .



The molecular structures of the cations are shown in Figures 4.3 and 4.4.; selected metrical data are presented in Tables 4.3 and 4.4. Crystal and refinement data, together with the full set of interatomic distances and angles, are given in Appendix A.11 and 12.

In the pyridine adduct, the nitrogen atom of the pyridine is bound to the  $\beta$ -carbon atom of the alkyne and forms a five-membered ring containing a substituted vinyl group via a single N-C bond [N(2) - C(8) atom (*ca.* 1.49 Å)]. The pyridine group is *endo* to the ruthenium atom about the C=C bond.

The distance between the alkene carbon atoms C(7) and C(8) (*ca.* 1.35 Å) is characteristic of a C=C bond (see Chapter 2). A single bond is also evident between the Ru atom and the C $_{\alpha}$  atom of the vinyl group [Ru - C(7) *ca.* 2.03 Å], whereas there is no interaction between the Ru and C(8) atoms, the separation being *ca.* 3.06 Å.

In contrast, the diethylamine adduct contains a six-membered ring, the secondary amine nitrogen atom, N(2), being attached to the  $\alpha$ -carbon atom by a double bond (*ca.* 1.33 Å), a distance *ca.* 0.04 Å longer than in other iminium salts.<sup>47-50</sup> A single bond is also evident between the Ru atom and the C $_{\alpha}$  atom [Ru - C(8) *ca.* 2.19 Å], although this distance is significantly greater than that in the pyridine adduct. Moreover, the distance between the Ru and the  $\beta$ -carbon atom C(7) atoms is *ca.* 2.73 Å, <sup>although non-bonding,</sup> which is substantially shorter than the corresponding non-bonding distance in the pyridine adduct. Also the C(7) - C(8) bond distance of the vinyl group (*ca.* 1.43 Å), which is midway between the expected values for a C=C bond (*ca.* 1.33 Å) and a C-C bond (*ca.* 1.53 Å), suggests the possibility of delocalization of the N-C  $\pi$ -electrons into the adjacent C-C bond. The hydrogen atom on the  $\beta$ -carbon atom was clearly located in the difference maps and there was no peak adjacent to N(2).

A possible resonance structure, an enamine, is shown in Scheme 4.1B in which there is partial double bond character in the bond between atoms C(7) and C(8) and a lone pair of electrons at N(2). The distance between  $\alpha$ -carbon and N(2) atoms is *ca.* 0.07 Å shorter than those typically found for an enamine.<sup>50-52</sup> A resonance contribution of this type does not always lead to pyramidalization at the nitrogen atom, as several enamines<sup>50-52</sup> show N trigonal planar geometry: in this case the three bond angles about N(2) add up to *ca.* 360°. However, the enamine resonance form probably does not contribute much to the observed structure because the difference in the Ru-

**Figure 4.3:** ORTEP diagram of the cation of (E)-  
 $\overline{cis-[Ru^{III}(acac)_2(o-Me_2NC_6H_4C=C(NC_5H_5)Ph)] [PF_6]}$ .

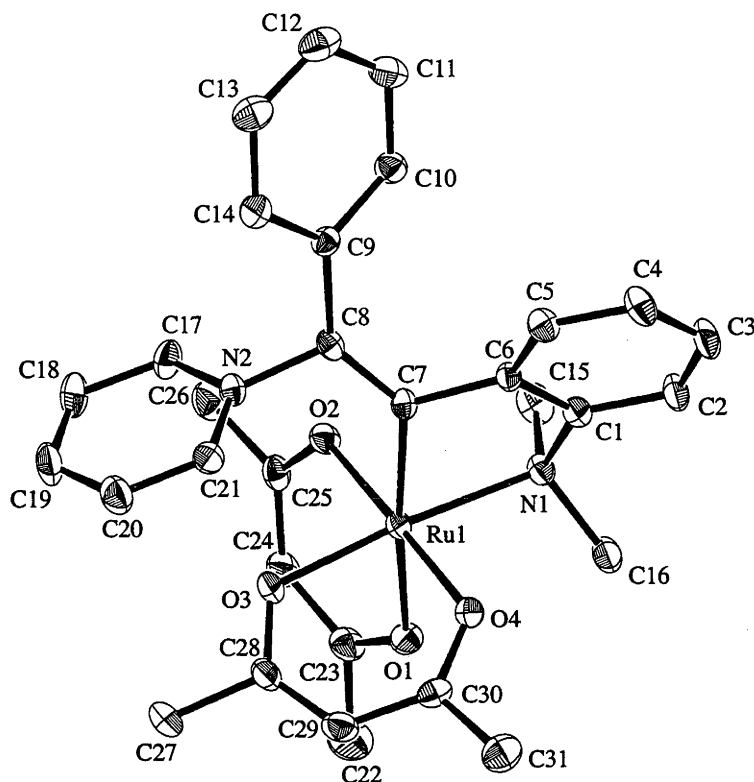


**Table 4.3:** Selected metrical parameters of  
 $\overline{cis-[Ru^{III}(acac)_2(o-Me_2NC_6H_4C=C(NC_5H_5)Ph)] [PF_6]}$ .

Bond Distances (Å)			
Ru(1)-O(1)	2.116(5)	Ru(1)-C(7)	2.031(7)
Ru(1)-O(2)	2.018(5)	N(2)-C(8)	1.488(8)
Ru(1)-O(3)	2.018(5)	C(7)-C(8)	1.348(9)
Ru(1)-O(4)	2.002(5)	N(2)-C(8)	1.488(8)
Ru(1)-N(1)	2.152(5)	C(8)-C(9)	1.475(9)
Bond Angles (°)			
O(1)-Ru(1)-O(2)	89.4(2)	O(3)-Ru(1)-N(1)	175.5(2)
O(1)-Ru(1)-O(3)	84.2(2)	O(3)-Ru(1)-C(7)	103.1(2)
O(1)-Ru(1)-O(4)	90.5(2)	O(4)-Ru(1)-N(1)	86.7(2)
O(1)-Ru(1)-N(1)	91.7(2)	O(4)-Ru(1)-C(7)	103.1(2)
O(1)-Ru(1)-C(7)	87.4(2)	N(1)-Ru(1)-C(7)	81.1(2)
O(2)-Ru(1)-O(3)	86.7(2)	Ru(1)-C(7)-C(6)	110.0(5)
O(2)-Ru(1)-O(4)	178.1(2)	Ru(1)-C(7)-C(8)	128.4(5)
O(2)-Ru(1)-N(1)	95.2(2)	C(6)-C(7)-C(8)	121.0(6)
O(2)-Ru(1)-C(7)	87.4(2)	C(7)-C(8)-C(9)	133.4(6)
O(3)-Ru(1)-O(4)	91.4(2)	C(7)-C(8)-N(2)	116.1(6)

Figure 4.4: ORTEP diagram of the cation of

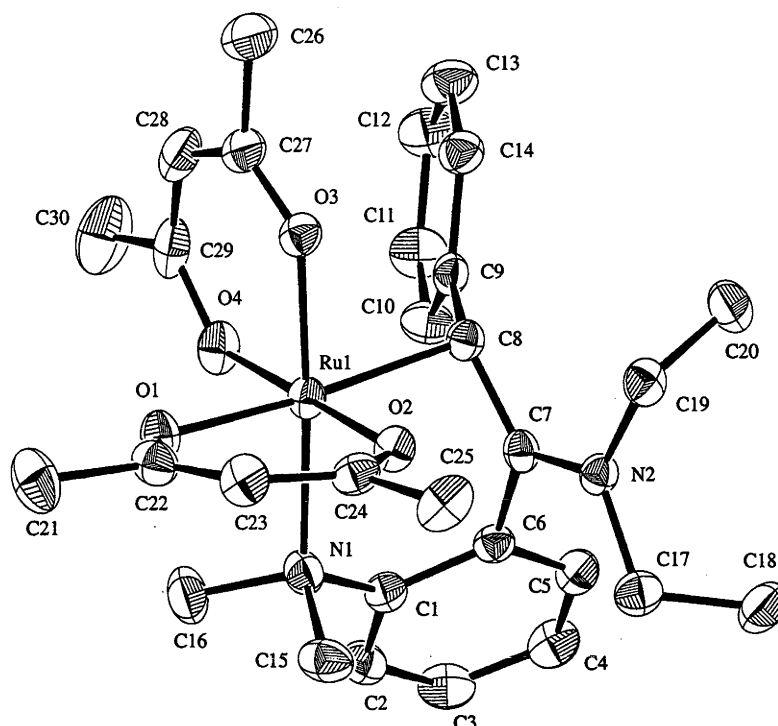
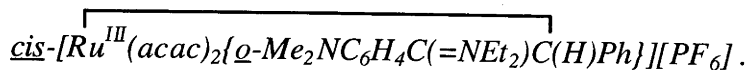
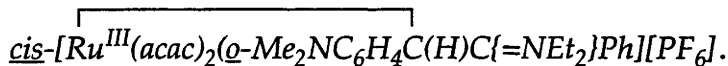


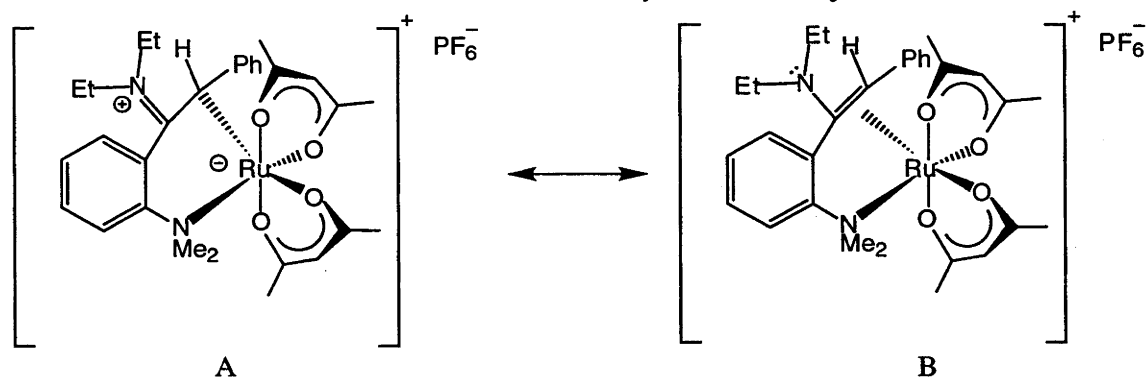
Table 4.4: Selected metrical parameters of



Bond Distances (Å)			
Ru(1)-O(1)	2.081(2)	Ru(1)-C(7)	2.729(3)
Ru(1)-O(2)	2.004(2)	C(7)-C(8)	1.426(4)
Ru(1)-O(3)	2.019(2)	C(7)-N(2)	1.331(4)
Ru(1)-O(4)	1.990(2)	N(2)-C(17)	1.477(4)
Ru(1)-N(1)	2.181(3)	N(2)-C(19)	1.483(4)
Ru(1)-C(8)	2.194(3)		
Bond Angles (°)			
O(1)-Ru(1)-O(2)	89.47(9)	O(4)-Ru(1)-N(1)	86.3(1)
O(1)-Ru(1)-O(3)	88.43(9)	O(4)-Ru(1)-C(8)	92.6(1)
O(1)-Ru(1)-O(4)	90.1(1)	N(1)-Ru(1)-C(8)	97.5(1)
O(1)-Ru(1)-N(1)	88.9(1)	Ru(1)-C(8)-C(7)	95.5(2)
O(1)-Ru(1)-C(8)	173.1(1)	Ru(1)-C(8)-C(9)	113.9(2)
O(2)-Ru(1)-O(3)	88.28(9)	C(7)-C(8)-C(9)	123.7(3)
O(2)-Ru(1)-O(4)	179.5(1)	C(6)-C(7)-C(8)	119.2(3)
O(2)-Ru(1)-N(1)	93.4(1)	C(6)-C(7)-N(2)	118.1(3)
O(2)-Ru(1)-C(8)	87.9(1)	C(8)-C(7)-N(2)	122.7(3)
O(3)-Ru(1)-O(4)	92.0(1)	C(7)-N(2)-C(17)	123.5(3)
O(3)-Ru(1)-N(1)	176.9(1)	C(7)-N(2)-C(19)	121.9(3)
O(3)-Ru(1)-C(8)	85.1(1)	C(17)-N(2)-C(19)	114.3(3)

C bond lengths to the  $\alpha$  and  $\beta$  carbon atoms (*ca.* 2.14, 2.73 Å) is far greater than those to the alkene carbon atoms in the Ru(III) chelate complex *cis*-[Ru<sup>III</sup>(acac)<sub>2</sub>(*o*-H<sub>2</sub>C=C(H)C<sub>6</sub>H<sub>4</sub>NMe<sub>2</sub>)] [SbF<sub>6</sub>] (both 2.24 Å).<sup>41</sup>

**Scheme 4.1:** Possible resonance structures for the diethylamine adduct.



#### 4.3 Reaction of *cis*-[Ru<sup>III</sup>(acac)<sub>2</sub>(*o*-PhC≡CC<sub>6</sub>H<sub>4</sub>NMe<sub>2</sub>)] [PF<sub>6</sub>] with H<sub>2</sub>O.

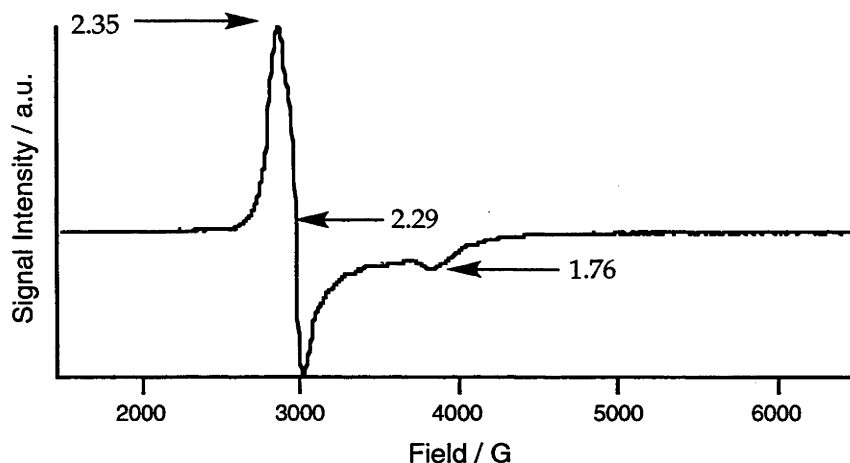
Red crystals of a 1:1 adduct can be isolated in *ca.* 70 % yield from a red solution obtained by stirring *cis*-[Ru<sup>III</sup>(acac)<sub>2</sub>(*o*-PhC≡CC<sub>6</sub>H<sub>4</sub>NMe<sub>2</sub>)] [PF<sub>6</sub>]<sup>42</sup> in aqueous THF overnight. Satisfactory elemental analyses were obtained. The +ve FAB mass spectrum shows the parent molecular ion at  $m/z$  539.0 (100% relative abundance) and is assigned to [Ru(acac)<sub>2</sub>(Me<sub>2</sub>NC<sub>6</sub>H<sub>4</sub>C≡CPh.H<sub>2</sub>O)]<sup>+</sup>. An ion peak at  $m/z$  299.1 (47% relative abundance) is due to [Ru(acac)<sub>2</sub>]<sup>+</sup>. The IR spectrum of this solid (KBr disc) shows a strong broad absorption at 1523 cm<sup>-1</sup>, characteristic of bidentate O-bonded acac,<sup>45</sup> as well as strong bands at 843 and 558 cm<sup>-1</sup> due to the presence of the PF<sub>6</sub> anion.<sup>45</sup> A medium-intensity peak at 1594 cm<sup>-1</sup> can be assigned to  $\nu$ (C=O) of a coordinated keto group. No absorptions assignable to free or coordinated alkyne were detected.

A fully reversible Ru<sup>3+/2+</sup> couple was found at +0.05 V (*vs* Ag/AgCl), which is *ca.* 0.5 V more positive than that found for the pyridine adduct and is similar to the values found for coordination complexes of the type [Ru(acac)<sub>2</sub>L<sub>2</sub>] (see Chapter 3). The EPR spectrum for water adduct as a frozen



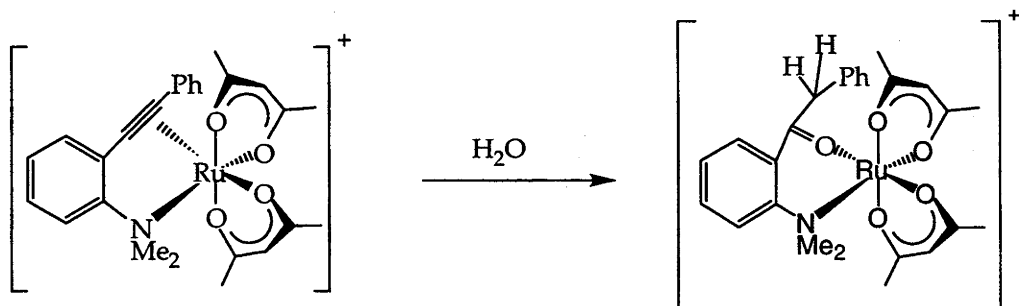
glass, shown in Figure 4.5, has three resonances at  $g_1 = 2.35$ ,  $g_2 = 2.29$  and  $g_3 = 1.76$ , and is typical for a ruthenium(III) complex (see p. 123 - 125).

**Figure 4.5:** EPR Spectra of the isolated solid from the reaction of water with *cis*-[Ru(acac)<sub>2</sub>(*o*-PhC≡CC<sub>6</sub>H<sub>4</sub>NMe<sub>2</sub>)] [PF<sub>6</sub>] as a frozen solution of 0.5 M [Bu<sup>n</sup><sub>4</sub>N][PF<sub>6</sub>]/CH<sub>2</sub>Cl<sub>2</sub> at 4.7 K.



An X-ray crystallographic study identified the red solid as the benzyl ketone complex  $\text{cis-[Ru}^{\text{III}}(\text{acac})_2(\textit{o}\text{-Me}_2\text{NC}_6\text{H}_4\text{C}(\text{O})\text{CH}_2\text{Ph})]\text{[PF}_6\text{]}$  formed by addition of water to the coordinated alkyne, as shown in Equation 4.3. The molecular structure is shown in Figure 4.6; selected metrical data are presented in Table 4.5. Crystal and refinement data, together with the full set of interatomic distances and angles, are given in Appendix A.13.

**Equation 4.3:** Formation of  $\text{cis-[Ru}^{\text{III}}(\text{acac})_2(\textit{o}\text{-Me}_2\text{NC}_6\text{H}_4\text{C}(\text{O})\text{CH}_2\text{Ph})]\text{[PF}_6\text{]}$  from the reaction of water with *cis*-[Ru(acac)<sub>2</sub>(*o*-PhC≡CC<sub>6</sub>H<sub>4</sub>NMe<sub>2</sub>)] [PF<sub>6</sub>].



The oxygen atom from the water molecule is attached to the C<sub>α</sub> atom and the distance between these atoms (*ca.* 1.24 Å) is typical of a C=O bond.

The bond distance between the  $C_{\alpha}$  and  $C_{\beta}$  carbon atoms is *ca.* 1.53 Å, which is typical of a C-C single bond. The distance between the ruthenium atom and the coordinated keto oxygen atom [Ru-O(5)] was found to be *ca.* 2.02 Å, similar to that found for Ru<sup>III</sup>-O acac bond lengths (see later). The alternative tautomeric enol structure (see Scheme 4.2) can be rejected on the basis of the structural evidence.

**Scheme 4.2:** Possible benzyl ketone and enol tautomeric structures.

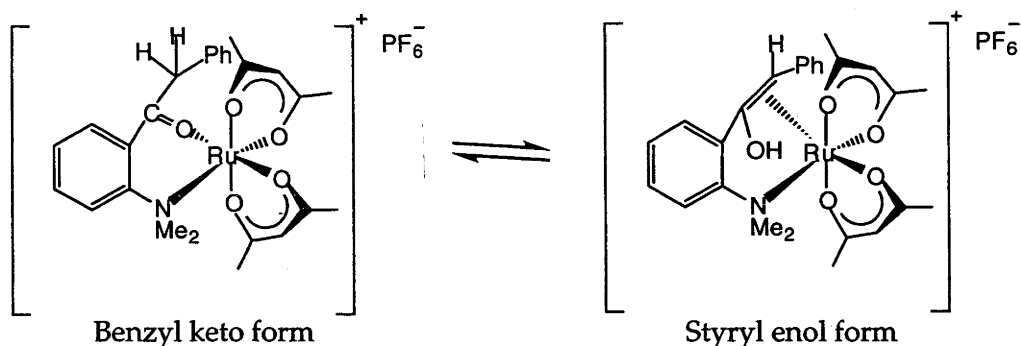


**Figure 4.6:** ORTEP diagram of the cation of  $\text{cis-}[\text{Ru}^{\text{III}}(\text{acac})_2(\text{o-Me}_2\text{NC}_6\text{H}_4\text{C}(\text{O})\text{CH}_2\text{Ph})][\text{PF}_6]$ .

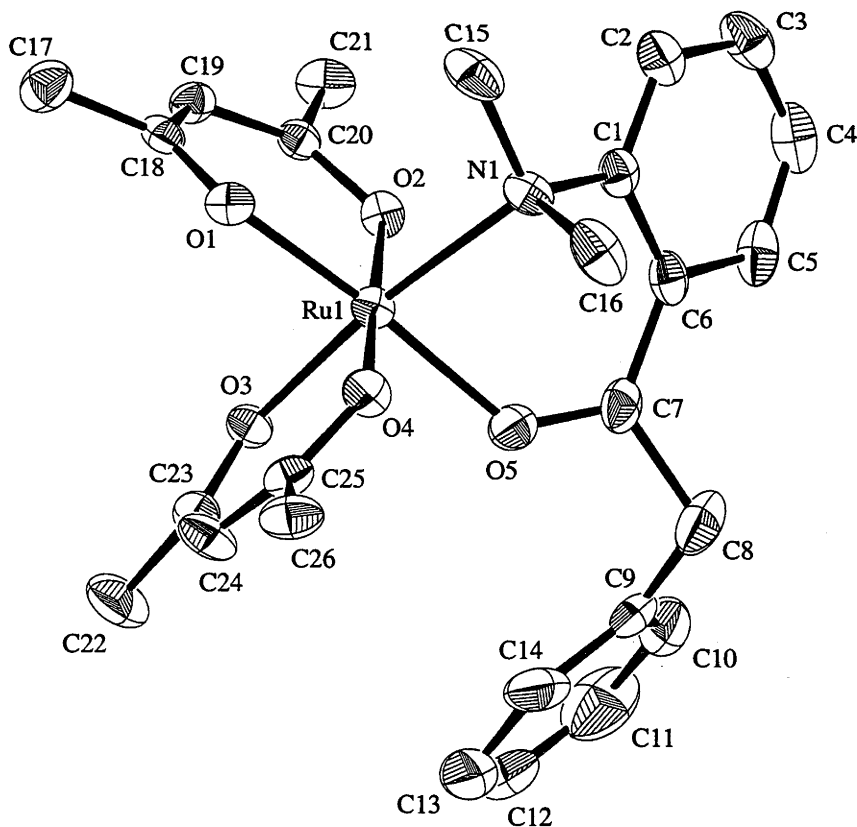


**Table 4.5:** Selected metrical parameters of*cis*-[Ru<sup>III</sup>(acac)<sub>2</sub>(*o*-Me<sub>2</sub>NC<sub>6</sub>H<sub>4</sub>C(O)CH<sub>2</sub>Ph)][PF<sub>6</sub>].

Bond Distances (Å)			
Ru(1)-O(1)	1.978(7)	Ru(1)-N(1)	2.148(9)
Ru(1)-O(2)	2.003(6)	O(5)-C(7)	1.24(1)
Ru(1)-O(3)	1.989(7)	C(6)-C(7)	1.46(2)
Ru(1)-O(4)	1.995(7)	C(7)-C(8)	1.53(1)
Ru(1)-O(5)	2.016(7)		
Bond Angles (°)			
O(1)-Ru(1)-O(2)	92.2(3)	O(3)-Ru(1)-O(5)	87.8(3)
O(1)-Ru(1)-O(3)	89.0(3)	O(3)-Ru(1)-N(1)	171.6(3)
O(1)-Ru(1)-O(4)	86.8(3)	O(4)-Ru(1)-O(5)	89.2(3)
O(1)-Ru(1)-O(5)	174.8(3)	O(4)-Ru(1)-N(1)	90.2(3)
O(1)-Ru(1)-N(1)	99.0(3)	O(5)-Ru(1)-N(1)	84.3(3)
O(2)-Ru(1)-O(3)	90.1(3)	Ru(1)-O(5)-C(7)	130.0(8)
O(2)-Ru(1)-O(4)	177.0(3)	O(5)-C(7)-C(6)	122(1)
O(2)-Ru(1)-O(5)	92.(3)	O(5)-C(7)-C(8)	115(1)
O(2)-Ru(1)-N(1)	87.1(3)	C(6)-C(7)-C(8)	123(1)
O(3)-Ru(1)-O(4)	92.7(3)	C(7)-C(8)-C(9)	114(1)

#### 4.4 Reactions of *cis*-[Ru<sup>III</sup>(acac)<sub>2</sub>(*o*-PhC≡CC<sub>6</sub>H<sub>4</sub>NMe<sub>2</sub>)] [PF<sub>6</sub>] with PPh<sub>3</sub> and with MeOH

The addition of excess PPh<sub>3</sub> to *cis*-[Ru(acac)<sub>2</sub>(*o*-PhC≡CC<sub>6</sub>H<sub>4</sub>NMe<sub>2</sub>)] [PF<sub>6</sub>]<sup>42</sup> in CH<sub>2</sub>Cl<sub>2</sub> immediately gave a red solution from which a red solid, believed to be a 1:1 adduct, was isolated in *ca.* 62% yield. Similarly, a red crystalline solid was isolated from a red solution obtained by stirring a THF solution of *cis*-[Ru(acac)<sub>2</sub>(*o*-PhC≡CC<sub>6</sub>H<sub>4</sub>NMe<sub>2</sub>)] [PF<sub>6</sub>]<sup>42</sup> with dry methanol overnight. The yield of this solid is *ca.* 86% on the basis of addition of one methanol ligand per ruthenium cation. Although satisfactory elemental analyses were not obtained for either product, they were consistent with the formation of a 1:1 adduct in each case. The parent molecular ions for a 1:1 adduct were detected in the +ve FAB mass spectra of both compounds, but the elemental analyses were not satisfactory.

**Table 4.6:** +ve FAB mass spectral data for the isolated solids from the reaction of PPh<sub>3</sub> or methanol with *cis*-[Ru(acac)<sub>2</sub>(*o*-PhC≡CC<sub>6</sub>H<sub>4</sub>NMe<sub>2</sub>)] [PF<sub>6</sub>].

Nucleophile	m/z	Assignment	Relative Intensity (%)
PPh <sub>3</sub>	783.1	{Ru(acac) <sub>2</sub> (Me <sub>2</sub> NC <sub>6</sub> H <sub>4</sub> C≡CPh.PPh <sub>3</sub> )} <sup>+</sup>	17
	684.0	{Ru(acac)(Me <sub>2</sub> NC <sub>6</sub> H <sub>4</sub> C≡CPh.PPh <sub>3</sub> )} <sup>+</sup>	3
	5210	{Ru(acac) <sub>2</sub> (Me <sub>2</sub> NC <sub>6</sub> H <sub>4</sub> C≡CPh)} <sup>+</sup>	100
MeOH	553.0	{Ru(acac) <sub>2</sub> (Me <sub>2</sub> NC <sub>6</sub> H <sub>4</sub> C≡CPh.MeOH)} <sup>+</sup>	35
	538.0	{Ru(acac) <sub>2</sub> (Me <sub>2</sub> NC <sub>6</sub> H <sub>4</sub> C≡CPh.OH)} <sup>+</sup>	100
	522.0	{Ru(acac)(Me <sub>2</sub> NC <sub>6</sub> H <sub>4</sub> C≡CPh.H)} <sup>+</sup>	50

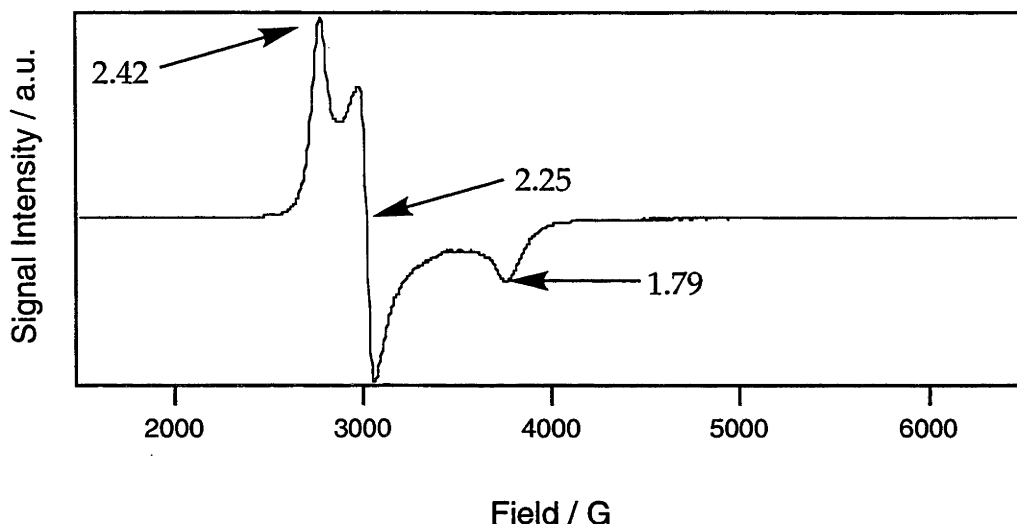
The IR spectra of both products show two strong bands between 1570 and 1510 cm<sup>-1</sup>, characteristic of bidentate O-coordinated acac;<sup>45</sup> the presence of the [PF<sub>6</sub>] anion was confirmed by the strong absorptions 843 and 558 cm<sup>-1</sup>.<sup>45</sup> As was previously found for the pyridine and diethylamine adducts, there were no detectable absorption bands corresponding to the alkyne. A band of medium intensity at 1632 cm<sup>-1</sup> in the methanol adduct may be assigned to ν(C=C).

**Table 4.7:** IR spectral data for the isolated solids from the reaction of PPh<sub>3</sub> or methanol with *cis*-[Ru(acac)<sub>2</sub>(*o*-PhC≡CC<sub>6</sub>H<sub>4</sub>NMe<sub>2</sub>)] [PF<sub>6</sub>] (KBr disc).

Nucleophile	ν(acac)	ν(PF <sub>6</sub> )	Other
PPh <sub>3</sub>	1567, 1517	843, 558	-
MeOH	1564, 1521	843, 558	1632

The EPR spectrum for PPh<sub>3</sub> adduct is shown in Figure 4.7 as a frozen solution. There are three resonances at g<sub>1</sub> = 2.42, g<sub>2</sub> = 2.25 and g<sub>3</sub> = 1.79, and is typical for a ruthenium(III) complex (see p. 123 - 125). The electrochemical behaviour of these complexes has not been investigated.

**Figure 4.7:** EPR Spectra of the isolated solid from the reaction of  $\text{PPh}_3$  with  $\text{cis-}[Ru(\text{acac})_2(\text{o-PhC}\equiv\text{CC}_6\text{H}_4\text{NMe}_2)][\text{PF}_6]$  as a frozen solution of 0.5 M  $[\text{Bu}^n_4\text{N}][\text{PF}_6]/\text{CH}_2\text{Cl}_2$  at 4.7 K.



The structures of both products are not known since X-ray quality crystals could not be obtained. Possible structures for the  $\text{PPh}_3$  adduct, a phosphonium ylid, and the methanol adduct, a vinyl ether, are shown in Figures 4.8 and 4.9, respectively. These proposed structures are not unreasonable given that a phosphonium ylid complex  $(\text{E})\text{-}[\text{CpMn}(\text{CO})_2(\text{C}\{\text{CO}_2\text{Me}\}=\text{C}(\text{H})\text{PPh}_3)]^{53}$  and several vinyl ether complexes<sup>33,54,55</sup> have been isolated from alkyne complexes.

**Figure 4.8:** Possible structures of the red compound isolated from the addition of  $\text{PPh}_3$  to  $\text{cis-}[Ru(\text{acac})_2(\text{o-PhC}\equiv\text{CC}_6\text{H}_4\text{NMe}_2)][\text{PF}_6]$  in  $\text{CH}_2\text{Cl}_2$ .

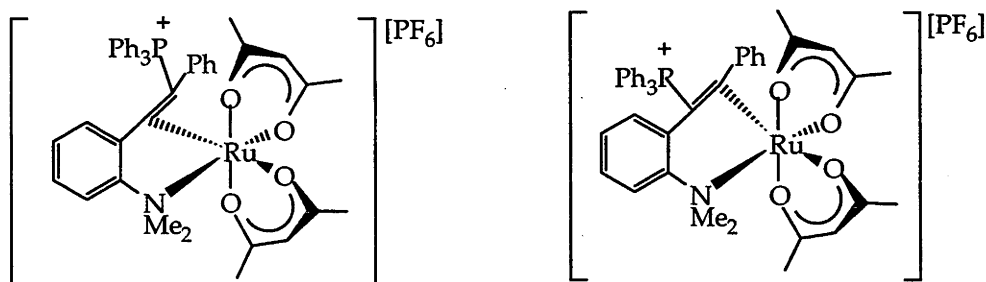
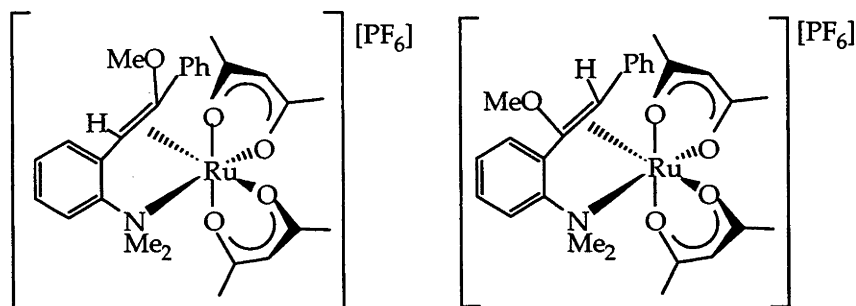


**Figure 4.9:** Possible structures of the red compound isolated from the addition of methanol to  $cis$ -[Ru(acac)<sub>2</sub>(*o*-PhC≡CC<sub>6</sub>H<sub>4</sub>NMe<sub>2</sub>)] [PF<sub>6</sub>] in THF.



#### 4.5 Reaction of $cis$ -[Ru(acac)<sub>2</sub>(*o*-H<sub>2</sub>C=C(H)C<sub>6</sub>H<sub>4</sub>NMe<sub>2</sub>)] [PF<sub>6</sub>] with PPh<sub>3</sub>.

A red solution forms almost immediately upon adding excess PPh<sub>3</sub> to a CH<sub>2</sub>Cl<sub>2</sub> solution of  $cis$ -[Ru<sup>III</sup>(acac)<sub>2</sub>(*o*-H<sub>2</sub>C=C(H)C<sub>6</sub>H<sub>4</sub>NMe<sub>2</sub>)] [PF<sub>6</sub>]<sup>41</sup> or  $cis$ -[Ru<sup>III</sup>(acac)<sub>2</sub>(*o*-H<sub>2</sub>C=C(H)C<sub>6</sub>H<sub>4</sub>NMe<sub>2</sub>)] [BF<sub>4</sub>] at room temperature under an inert atmosphere. The isolated [BF<sub>4</sub>] salt gave an elemental analysis (C, H, N, P) in apparent agreement with the formulation as a 1:1 adduct and on this basis the yield was *ca.* 50 - 60%. The [PF<sub>6</sub>] salt did not analyse satisfactorily. The <sup>31</sup>P{<sup>1</sup>H} NMR spectrum in CD<sub>2</sub>Cl<sub>2</sub> revealed the presence of the [PF<sub>6</sub>] anion and the [PO<sub>2</sub>F<sub>2</sub>] anion as a septet at  $\delta_P$  -143.8 ( $J_{PF}$  = 710 Hz) and a triplet at  $\delta$  -16.4 ( $J_{PF}$  = 950 Hz), respectively. The spectroscopic data for the difluorophosphate anion are similar to data previously reported in the literature.<sup>56,57</sup> Hydrolysis of AgPF<sub>6</sub> in CH<sub>2</sub>Cl<sub>2</sub> is known<sup>57</sup> and may be occurring here as a slight excess of this silver salt was used to oxidise  $cis$ -[Ru(acac)<sub>2</sub>(*o*-H<sub>2</sub>C=C(H)C<sub>6</sub>H<sub>4</sub>NMe<sub>2</sub>)]. However, the hydrolysis of the [PF<sub>6</sub>] anion may also be catalysed by the presence of a transition metal.<sup>56</sup>

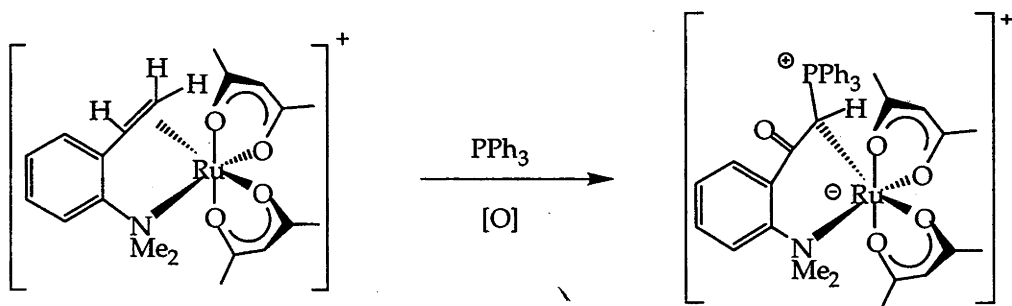
The +ve FAB mass spectrum of the red solid isolated from the reaction involving the [PF<sub>6</sub>] anion shows the highest mass peak, presumably due to the parent ion, at  $m/z$  723.1 (15% relative abundance) which is assigned to {Ru(acac)<sub>2</sub>(Me<sub>2</sub>NC<sub>6</sub>H<sub>4</sub>C<sub>2</sub>H.OPPh<sub>3</sub>)<sup>+</sup>. Ion peaks at  $m/z$  706.1 (63% relative abundance) and 406.1 (100% relative abundance) are assigned to {Ru(acac)<sub>2</sub>(Me<sub>2</sub>NC<sub>6</sub>H<sub>4</sub>C<sub>2</sub>.PPh<sub>3</sub>)<sup>+</sup> and {Me<sub>2</sub>NC<sub>6</sub>H<sub>4</sub>C<sub>2</sub>.PPh<sub>3</sub>)<sup>+</sup>, respectively.

The IR spectrum of the solid (KBr disc) shows strong absorptions at 1549 and 1520  $\text{cm}^{-1}$ , characteristic of O-bonded, bidentate acac;<sup>45</sup> strong absorptions at 840 and 558  $\text{cm}^{-1}$  confirmed the presence of the  $[\text{PF}_6]$  anion.<sup>45</sup> A medium absorption at 1307  $\text{cm}^{-1}$  may be due to  $\nu(\text{PO})$  of the  $[\text{PO}_2\text{F}_2]$  anion.<sup>57</sup> The  $E_{1/2}(\text{Ru}^{3+/2+})$  value for red crystals isolated from this reaction was -0.45 V (*vs* Ag/AgCl), similar to that found for the pyridine adduct (see p. 140).

The structure of the 1:1 adduct isolated from the reaction of  $\text{PPh}_3$  and  $\text{cis-}[\text{Ru}^{\text{III}}(\text{acac})_2(\text{o-H}_2\text{C}=\text{C}(\text{H})\text{C}_6\text{H}_4\text{NMe}_2)][\text{PF}_6]$ <sup>41</sup> was identified by X-ray crystallography as the triphenylphosphonium-ylid complex  $\text{cis-}[\text{Ru}^{\text{III}}(\text{acac})_2\{\text{o-Me}_2\text{NC}_6\text{H}_4\text{C}(\text{O})\text{C}(\text{H})(\text{PPh}_3)\}][\text{PF}_6]$  as shown in Equation 4.4.

There was no difluorophosphate anion detected in the crystal. This structure may also be regarded a zwitterion with a formal positive charge on the phosphorus atom and a negative charge on the metal atom. The  $\text{PPh}_3$  unit is attached to the  $\beta$ -carbon atom to give a six-membered chelate ring and, unexpectedly, the  $\alpha$ -carbon atom carries an oxygen atom. Thus, the attack by the nucleophile  $\text{PPh}_3$  is accompanied by the loss of two hydrogen atoms and the gain of one oxygen atom. The analytical data for this formulation does not differ significantly from that for the expected 1:1 adduct for both the  $[\text{BF}_4]$  or  $[\text{PF}_6]$  salts.

**Equation 4.4:** Formation of  $\text{cis-}[\text{Ru}^{\text{III}}(\text{acac})_2\{\text{o-Me}_2\text{NC}_6\text{H}_4\text{C}(\text{O})\text{C}(\text{H})(\text{PPh}_3)\}][\text{PF}_6]$  from the reaction of triphenylphosphine with  $\text{cis-}[\text{Ru}(\text{acac})_2(\text{o-H}_2\text{C}=\text{C}(\text{H})\text{CC}_6\text{H}_4\text{NMe}_2)][\text{PF}_6]$ .

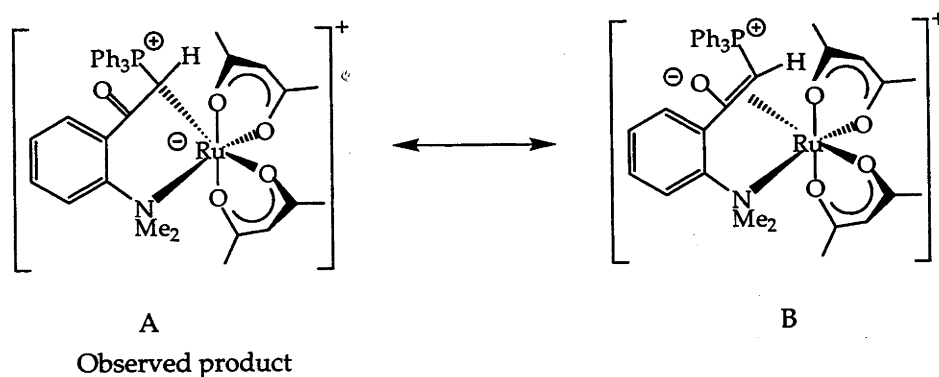


The molecular structure is shown in Figure 4.10 and selected metrical data is presented in Table 4.8. Crystal and refinement data, together with the full set of interatomic distances and angles, are given in Appendix A.14.

The distance separating the P and the  $\alpha$ -carbon atoms is *ca.* 1.79 Å and is typical for phosphorus ylid complexes which contain bulky substituents on the carbanion.<sup>58</sup> The phosphorus atom is also *exo* to the ruthenium atom. A single bond is also evident between the Ru atom and the C $\beta$  atom [Ru - C(20) *ca.* 2.16 Å] which is similar to that found in the diethylamine adduct. The distance between the Ru atom and  $\alpha$ -carbon atom, C(19), (*ca.* 2.81 Å), indicates little or no interaction.

The keto group points away from and is not coordinated to the metal atom. The distance between the atoms O(5) and C(19) (*ca.* 1.23 Å) is slightly longer than those typically found for a C=O bond. The distance between  $\alpha$  and  $\beta$ -carbon atoms [C(19) and C(20)] is *ca.* 1.46 Å, which is similar to that found for the diethylamine adduct (see p. 143). The metrical data are consistent with a contribution from a zwitterionic resonance form B, as shown in Scheme 4.3, in which there is a

**Scheme 4.3:** Proposed resonance structures for the phosphonium adduct.



double bond between atoms C(19) and C(20) and a negative charge on oxygen atom O(5). However, as the hydrogen atom on the  $\beta$ -carbon atom, C(20), was



Figure 4.10: ORTEP diagram of the cation of

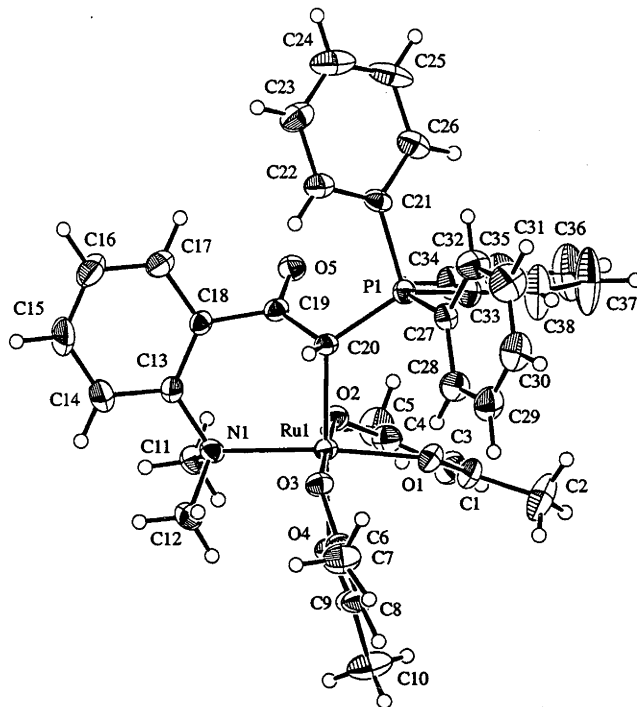
$$\text{cis-[Ru}^{\text{III}}(\text{acac})_2(\text{o-Me}_2\text{NC}_6\text{H}_4\text{C(O)CHPh}_3\text{)][PF}_6\text{]}.$$


Table 4.8: Selected metrical parameters of

$$\text{cis-[Ru}^{\text{III}}(\text{acac})_2(\text{o-Me}_2\text{NC}_6\text{H}_4\text{C(O)CHPh}_3\text{)][PF}_6\text{]}.$$

Bond Distances (Å)			
Ru(1)-O(1)	1.999(3)	O(5)-C(19)	1.227(5)
Ru(1)-O(2)	1.996(3)	P(1)-C(20)	1.794(5)
Ru(1)-O(3)	1.999(3)	P(1)-C(21)	1.799(5)
Ru(1)-O(4)	2.043(3)	P(1)-C(27)	1.814(5)
Ru(1)-N(1)	2.204(4)	P(1)-C(33)	1.795(5)
Ru(1)-C(20)	2.160(4)	C(19)-C(20)	1.459(6)
Ru(1)-C(19)	2.810(5)	C(20)-H(25)	0.92(4)
Bond Angles (°)			
O(1)-Ru(1)-O(2)	90.3(1)	C(20)-P(1)-C(21)	108.4(2)
O(1)-Ru(1)-O(3)	88.1(1)	C(20)-P(1)-C(27)	108.4(2)
O(1)-Ru(1)-O(4)	85.5(1)	C(20)-P(1)-C(33)	119.0(2)
O(1)-Ru(1)-N(1)	174.3(1)	C(21)-P(1)-C(27)	105.6(2)
O(1)-Ru(1)-C(20)	92.3(2)	C(21)-P(1)-C(33)	106.1(2)
O(2)-Ru(1)-O(3)	177.2(1)	C(27)-P(1)-C(33)	108.6(2)
O(2)-Ru(1)-O(4)	86.3(1)	Ru(1)-C(20)-P(1)	124.0(5)
O(2)-Ru(1)-N(1)	92.0(1)	Ru(1)-C(20)-C(19)	100.0(3)
O(2)-Ru(1)-C(20)	95.8(2)	P(1)-C(20)-C(19)	111.5(3)
O(3)-Ru(1)-O(4)	91.2(1)	C(20)-C(19)-O(5)	123.8(5)
O(3)-Ru(1)-N(1)	89.4(1)	C(18)-C(19)-O(5)	119.5(4)
O(3)-Ru(1)-C(20)	86.6(2)	C(18)-C(19)-C(20)	116.5(4)
O(4)-Ru(1)-N(1)	89.4(1)	Ru(1)-C(20)-H(25)	100(3)
O(4)-Ru(1)-C(20)	177.0(2)	P(1)-C(20)-H(25)	108(3)
N(1)-Ru(1)-C(20)	92.6(2)	C(19)-C(20)-H(25)	113(3)

clearly located in the difference maps and refined, it was possible to sum the bond angles about C(20) ( $657^\circ$ ); this value suggests  $sp^3$ -hybridization ( $6 \times 109.5^\circ = 657^\circ$ ) at this carbon atom. Additional evidence for the zwitterionic structure shown in Scheme 4.6A is that the  $Ru^{3+/2+}$  redox couple is similar to that found for the similarly formulated pyridine adduct (see p. 140) rather than that for an alkene complex (see p. 109).

#### 4.6 General Features of Crystal Structures.

For all four structures, the metal atom occupies the centre of a distorted octahedron. The Ru-O distances are typically *ca.* 1.98 - 2.02 Å, except for the Ru-O bonds *trans* to the Ru-C  $\sigma$ -bonded carbon atoms, which are between *ca.* 0.04 and 0.10 Å longer than those *trans* to an acac oxygen atom (see Tables 4.3 - 4.4 and 4.8). These distances are *ca.* 0.02 Å shorter than those found in *cis*-[Ru(acac)<sub>2</sub>(*o*-PhC $\equiv$ CC<sub>6</sub>H<sub>4</sub>NMe<sub>2</sub>)] [PF<sub>6</sub>],<sup>42</sup> but similar to those found in *cis*-[Ru(acac)<sub>2</sub>(*o*-H<sub>2</sub>C=C(H)C<sub>6</sub>H<sub>4</sub>NMe<sub>2</sub>)] [PF<sub>6</sub>].<sup>41</sup>

#### 4.7 Discussion

As was expected, nucleophiles such as NR<sub>2</sub>H, pyridine and H<sub>2</sub>O react with *cis*-[Ru<sup>III</sup>(acac)<sub>2</sub>(*o*-PhC $\equiv$ CC<sub>6</sub>H<sub>4</sub>NMe<sub>2</sub>)] [PF<sub>6</sub>] to form products derived by attack at the unsaturated carbon atoms. Similarly PPh<sub>3</sub> attacks the  $\beta$ -carbon atom of *cis*-[Ru<sup>III</sup>(acac)<sub>2</sub>(*o*-H<sub>2</sub>C=C(H)C<sub>6</sub>H<sub>4</sub>NMe<sub>2</sub>)] [PF<sub>6</sub>], although this process is complicated by oxidation of the aliphatic carbon atom. The structures of these nucleophilic addition products could only be reliably determined by X-ray crystallography because the paramagnetism of the complexes prevented routine NMR studies. It is believed that methanol and PPh<sub>3</sub> also add to the alkyne carbon atoms in a similar manner, but the products of these reactions have not been structurally characterized. This situation is unusual; most nucleophilic addition reactions with alkenes and alkynes involve diamagnetic complexes. There are relatively few Ru<sup>III</sup>-C  $\sigma$ -bonded complexes known which include [Ru(TPP)Ph] (TPP = dianion of 5,10,15,20-

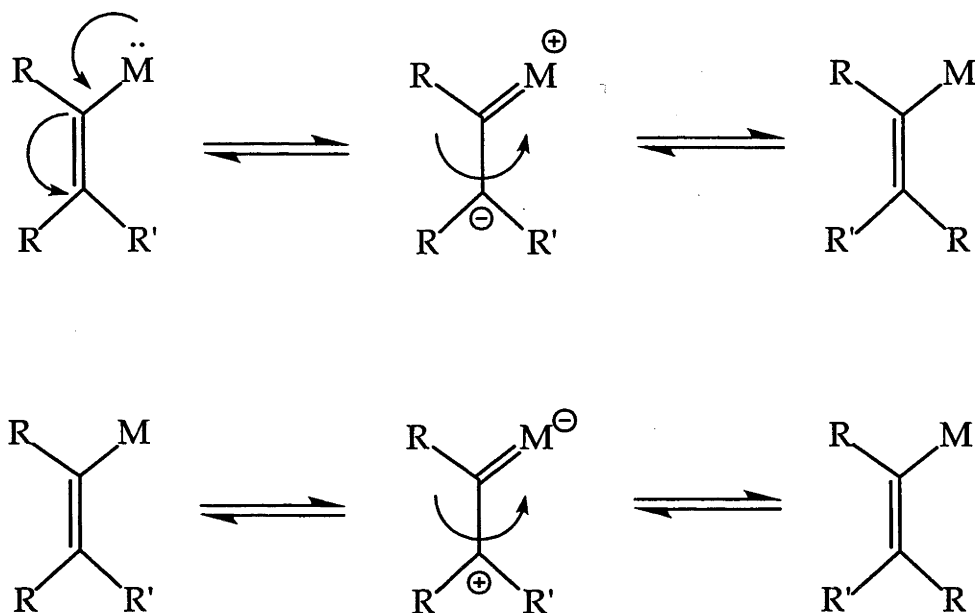
tetraphenylporphyrin) and several cyclometallated Schiff base complexes such as  $[\text{Ru}^{\text{III}}\text{Br}(\text{PPh}_3)_2(2\text{-(phenylazo)phenolato-C}^2, \text{N}, \text{O})]^{59}$  in which the Ru-C distance is *ca.* 2.03 Å.

Nucleophilic attack on coordinated alkenes and alkynes usually results in products in which the nucleophile is *exo* to the metal (see p. 138) and this is the case for the structurally characterized diethylamine and the triphenylphosphine adducts. However, for the pyridine and water adducts, the heteroatom of the nucleophile is *endo* to the ruthenium atom. An alternative possible mode of attack is initial displacement of the alkyne, coordination of the nucleophile to the metal, followed by insertion of the alkene or alkyne into the metal-nucleophile bond.<sup>1</sup> This would cause the nucleophile to occupy an *endo*-position relative to the metal atom.

However, the stereochemistry of the product isolated from the addition of a nucleophile to a coordinated alkyne need not necessarily define the mode of addition. For example, the reaction of dimethyl acetylenedicarboxylate to  $[\text{CpRuH}(\text{PPh}_3)_2]^{60}$  and  $[\text{RhH}(\text{CO})(\text{PPh}_3)_3]^{61}$  affords  $[\text{CpRu}(\text{PPh}_3)_2\{\textit{trans}\text{-MeO}_2\text{CC}=\text{C}(\text{H})\text{CO}_2\text{Me}\}]$  and  $[\text{Rh}(\text{CO})(\text{PPh}_3)_2\{\textit{trans}\text{-MeO}_2\text{CC}=\text{C}(\text{H})\text{CO}_2\text{Me}\}]$ , respectively. In a similar fashion, the reaction of  $\text{PhC}\equiv\text{CPh}$  to  $[\text{Ni}(\text{acac})(\text{Me})(\text{PPh}_3)]$  results in the formation of the vinyl complex  $[\text{Ni}(\text{acac})(\text{PPh}_3)(\textit{trans}\text{-PhC}=\text{C}(\text{Me})\text{Ph})]^{62}$ . In all three cases, it is believed that the metal-H or metal-alkyl bond adds *endo* to the coordinated alkyne, followed by *cis*- to *trans*-isomerization of the vinyl groups. Schwartz and Hart<sup>63</sup> were able to show that *cis*- $\text{MeCO}_2\text{C}(\text{Me})\text{C}=\text{C}(\text{H})\text{CCO}_2\text{Me}$  is exclusively formed from the pyrolysis of a freshly prepared solution of  $[\text{RhI}(\text{Me})(\text{CO})(\text{PPh}_3)_2\{\text{MeCO}_2\text{C}=\text{C}(\text{H})\text{CO}_2\text{Me}\}]$ , whereas as a mixture of *cis*- and *trans*- $\text{MeCO}_2\text{C}(\text{Me})\text{C}=\text{C}(\text{H})\text{CCO}_2\text{Me}$  is detected after allowing the same rhodium solution to stir for 24 hours before heating. This *cis*- to *trans*-isomerization can be rationalized by postulating rotation about the C=C double bond via a dipolar intermediate, as shown in Scheme 4.4; the formation of a double bond

between the metal and carbon atom and a single bond between the vinyl carbon atoms allows the rotation to occur. The sign and the location of the charge will probably depend on the metal, the oxidation state of the metal and the substituents of the vinyl group.

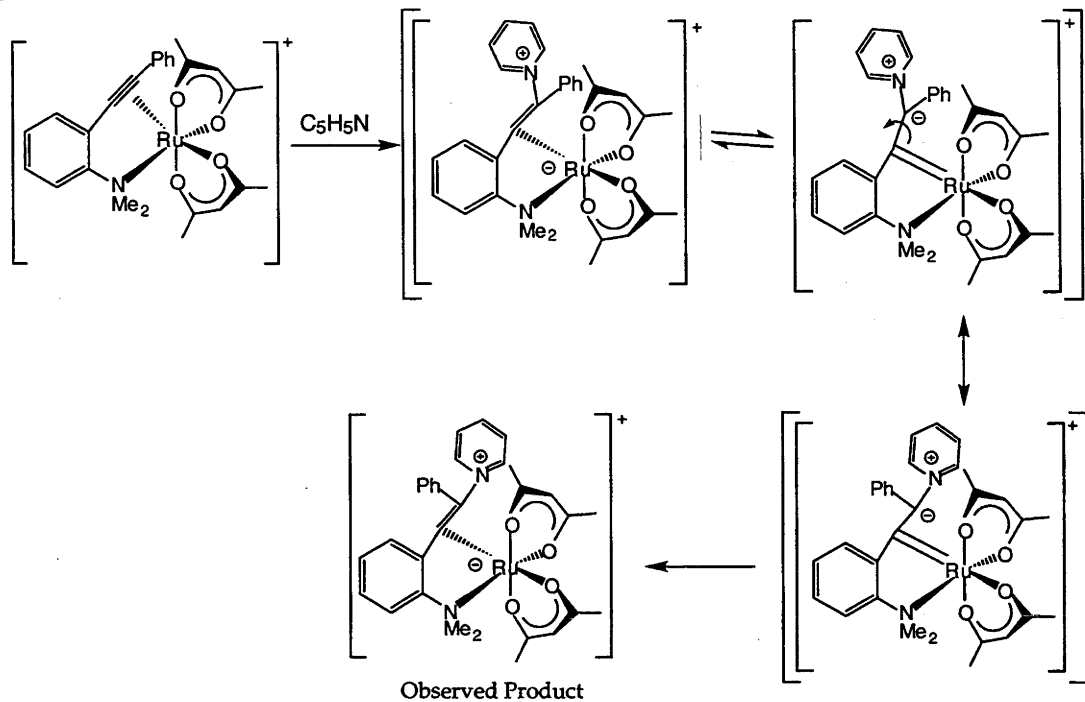
**Scheme 4.4:** Possible dipole mechanisms for the rotation of the substituents about the C=C bond.



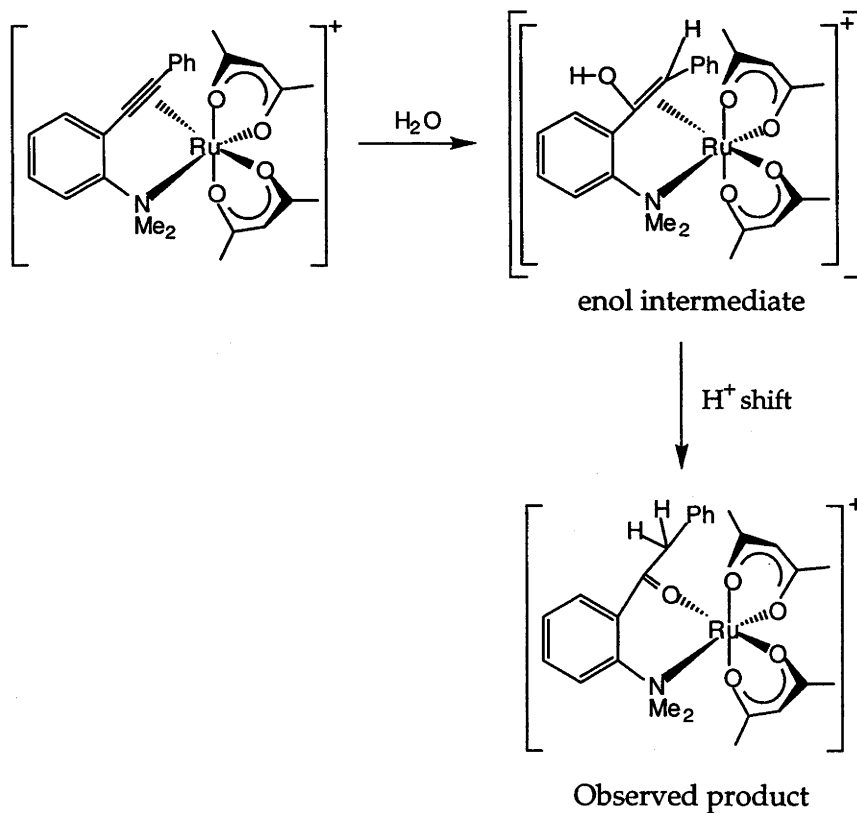
Therefore, initial coordination of pyridine to the ruthenium complex may be *exo* giving a (Z)-vinyl species. Rotation of the phenyl and pyridine substituents probably also occurs via a resonance structure to form the observed (E)-vinyl complex, as shown in Scheme 4.5. The reasons for this *trans* to *cis* isomerization are not known.

The benzyl ketone complex is probably formed by initial *exo*-attack of water on the  $\alpha$ -carbon atom to give a vinyl alcohol intermediate, as shown in Scheme 4.6. As for most organic aliphatic enols, the equilibrium for this keto-enol tautomer would be expected to be heavily in favour of the ketone,<sup>64</sup> which is the observed product. The ketone oxygen atom can now coordinate to the ruthenium atom after rotation about a C-C bond. An iron (1-benzoyl)ethyl complex, [CpFe(CO){P(OPh)<sub>3</sub>}(CH(Me)C(=O)Ph)], and an iron vinyl ether complex, (E)-[CpFe(CO){P(OPh)<sub>3</sub>}(C(Me)=C(OMe)Ph)] have been

**Scheme 4.5:** Proposed pathway for the formation of  $cis-[Ru^{III}(acac)_2(o-Me_2NC_6H_4C=C(NC_5H_5)Ph)][PF_6]$  via initial trans addition of pyridine to  $cis-[Ru^{III}(acac)_2(o-PhC\equiv CC_6H_4NMe_2)][PF_6]$ .



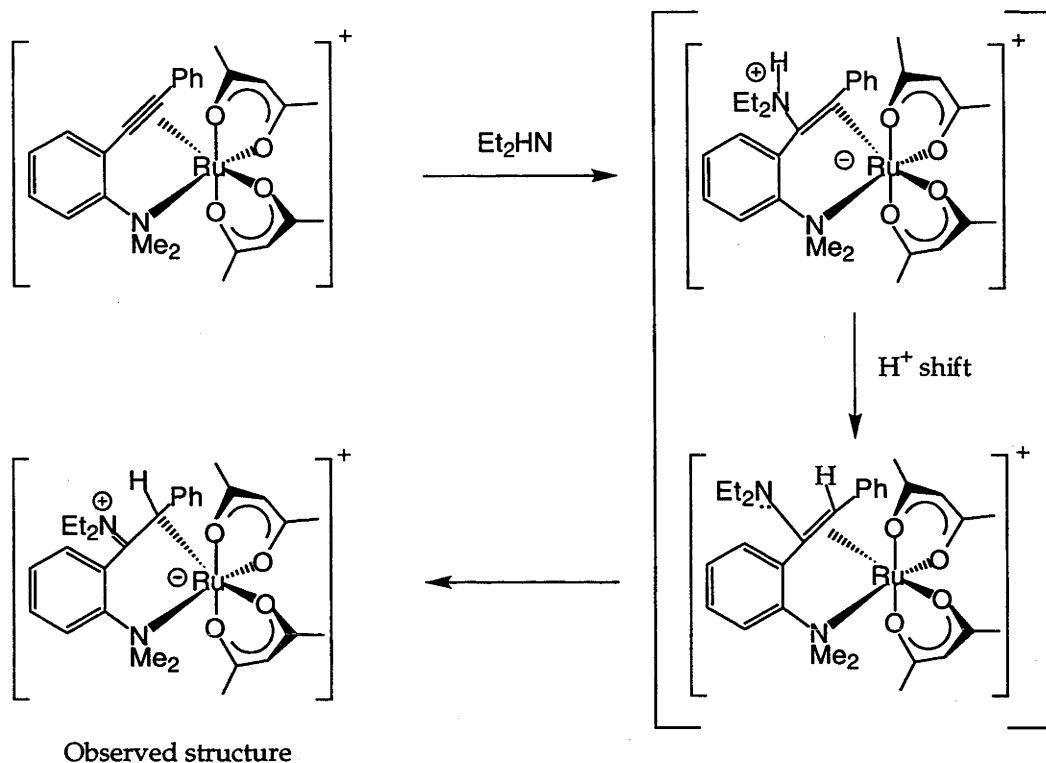
**Scheme 4.6:** Proposed reaction pathway for the formation of  $cis-[Ru^{III}(acac)_2(o-Me_2NC_6H_4C(O)CH_2Ph)][PF_6]$



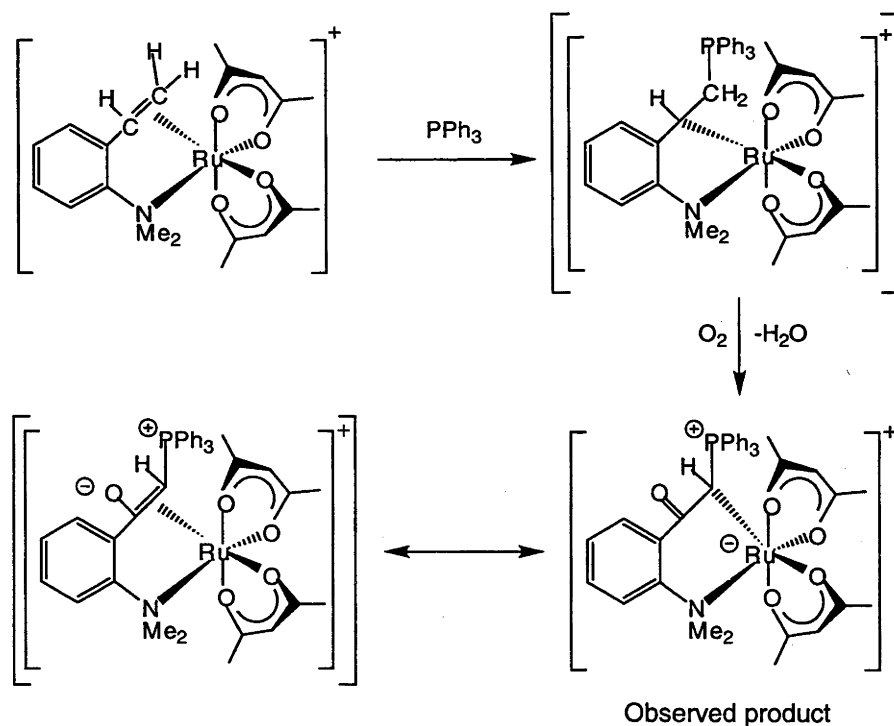
isolated by passing a solution of  $[\text{CpFe}(\text{CO})\{\text{P}(\text{OPh})_3\}(\eta^2\text{-MeC}\equiv\text{CPh})][\text{BF}_4]$  through neutral alumina and reacting the alkyne complex with methanol in the presence of a base, respectively.<sup>33</sup> Presumably, the first product arises by attack of water adsorbed on the alumina on the alkyne to give an enolate, which then undergoes a keto-enol tautomerism. Taube and coworkers<sup>55</sup> have shown that water and methanol will add to  $[\text{Os}(\text{NH}_3)_5(\eta^2\text{-MeC}\equiv\text{CMe})][\text{OTf}]_2$  to form  $[\text{Os}(\text{NH}_3)_5(\text{cis-}\eta^2\text{-MeHC}=\text{C}(\text{OH})\text{Me})][\text{OTf}]_2$  and  $[\text{Os}(\text{NH}_3)_5(\text{cis-}\eta^2\text{-MeHC}=\text{C}(\text{OMe})\text{Me})][\text{OTf}]_2$ , respectively. Oxidation of  $[\text{Os}(\text{NH}_3)_5(\text{cis-}\eta^2\text{-MeHC}=\text{C}(\text{OH})\text{Me})][\text{OTf}]_2$  results in the formation of the tautomeric 2-butanone complex,<sup>55</sup> similar to the ruthenium(III) keto-complex isolated here; one electron reduction of the latter might be expected to form the enol tautomer.

The formation of  $\text{cis-}[\text{Ru}^{\text{III}}(\text{acac})_2(o\text{-Me}_2\text{NC}_6\text{H}_4\text{C}(\text{H})\text{C}(\text{=N}\text{Et}_2)\text{Ph})][\text{PF}_6]$  probably occurs in a similar manner as that proposed for water *viz trans*-attack of  $\text{NEt}_2\text{H}$  on the  $\alpha$ -carbon atom followed by the transfer of the proton from the quaternary nitrogen atom to the  $\beta$ -carbon atom. This results in the formation of an enamine, the nitrogen analogue of an enol. The lone pair of electrons on the nitrogen atom in the enamine may be used to form the alkenyl iminium complex. The iminium complex *trans*- $[\text{CpFe}(\text{CO})\{\text{P}(\text{OPh})_3\}(\text{C}(\text{H})\text{MeC}(\text{=N}\text{HPh})\text{Me})][\text{BF}_4]$  has been isolated from the reaction of phenylamine with  $[\text{CpFe}(\text{CO})\{\text{P}(\text{OPh})_3\}(\eta^2\text{-MeC}\equiv\text{CMe})][\text{BF}_4]$ .<sup>33</sup> Evidence for the enamine proposed in Scheme 4.7 exists in the structural characterization of *trans*-(Z)- $[\text{PtCl}_2(\text{NHEt}_2)(o\text{-NC}_5\text{H}_4\text{C}(\text{H})=\text{C}(\text{NEt}_2)\text{Ph})]$ , isolated from the reaction of excess diethylamine with the non-coordinated alkyne in *trans*- $[\text{PtCl}_2(\text{SEt}_2)(o\text{-NC}_5\text{H}_4\text{C}\equiv\text{CPh})]$ .<sup>65</sup> The amine nitrogen atom in the platinum complex is attached to  $\beta$ -carbon atom, opposite to that for ruthenium(III). The reasons for this difference in reactivity are not clear but may be related to the fact that the alkyne is not coordinated to the platinum(II) atom.

**Scheme 4.7:** Proposed pathway for the addition of  $\text{NEt}_2\text{H}$  to *cis*- $[\text{Ru}^{\text{III}}(\text{acac})_2(\text{o-PhC}\equiv\text{CC}_6\text{H}_4\text{NMe}_2)][\text{PF}_6]$ .



**Scheme 4.8:** Proposed mechanism for the addition of  $\text{PPh}_3$  to *cis*- $[\text{Ru}^{\text{III}}(\text{acac})_2(\text{o-H}_2\text{C}=\text{C}(\text{H})\text{C}_6\text{H}_4\text{NMe}_2)][\text{PF}_6]$ .



The addition of  $\text{PPh}_3$  to  $\text{cis-}[\text{Ru}^{\text{III}}(\text{acac})_2(o\text{-H}_2\text{C}=\text{C}(\text{H})\text{C}_6\text{H}_4\text{NMe}_2)][\text{PF}_6]$  probably occurs via direct attack on the alkene  $\text{C}_\beta$  atom to form a phosphonium-ylid complex  $\text{cis-}[\text{Ru}^{\text{III}}(\text{acac})_2\{o\text{-NMe}_2\text{C}_6\text{H}_4\text{C}(\text{H})\text{CH}_2\text{PPh}_3\}][\text{PF}_6]$  containing a five-membered ring, as shown in Scheme 4.8.

Anionic oxygen nucleophiles, such as methoxide ions, also attack the  $\beta$ -carbon atom of  $\text{cis-}[\text{PtCl}_2(\text{H}_2\text{C}=\text{C}(\text{H})\text{CH}_2\text{CH}_2\text{PPh}_2)]^9$  and  $\text{cis-}[\text{PtCl}_2(o\text{-H}_2\text{C}=\text{C}(\text{H})\text{C}_6\text{H}_4\text{AsPh}_2)]^{12,13,15}$  to form similar methoxyethyl platinum(II) complexes. The five-membered ring ruthenium complex is then oxidised presumably by a process in which water is eliminated and oxygen is added to the  $\alpha$ -carbon atom to form the six-membered ring  $\text{cis-}[\text{Ru}^{\text{III}}(\text{acac})_2(o\text{-NMe}_2\text{C}_6\text{H}_4\text{C}(\text{O})\text{CHPPh}_3)][\text{PF}_6]$ . The exact nature of this oxidation has not been elucidated. The added oxygen atom could come from the atmosphere or from water. The observed reactivity of triphenylphosphine with  $\text{cis-}[\text{Ru}^{\text{III}}(\text{acac})_2(o\text{-H}_2\text{C}=\text{C}(\text{H})\text{C}_6\text{H}_4\text{NMe}_2)][\text{PF}_6]$  differs to that found for the platinum(II) complex  $\text{cis-}[\text{PtCl}_2(\text{H}_2\text{C}=\text{C}(\text{H})\text{CH}_2\text{CH}_2\text{PPh}_2)]$  where  $\text{PPh}_3$  displaces the alkene and attacks the metal.<sup>9</sup> This result may suggest that alkenes coordinated to Ru(III) may be more susceptible to nucleophilic attack than Pt(II).

There is much synthetic and industrial interest in the addition of heteroatoms across  $\text{C}=\text{C}$  and  $\text{C}\equiv\text{C}$  bonds. However, most interest has been for alkenes as stable metal-alkyne complexes are inert to nucleophilic attack whereas unstable metal-alkyne oligomerize.<sup>66</sup> Oxygen nucleophiles, such as water and alcohols, catalytically react with alkenes and alkynes to give aldehydes or ketones in the presence of Pd(II).<sup>1,3,66-68</sup> Stoichiometric hydroamination reactions of unsaturated hydrocarbons promoted by transition metals are known, but there are few catalytic intermolecular aminations, mainly because of the strong affinity of amines for the metal centre.<sup>1,3,66,69</sup>

However, intramolecular amination reactions, especially those involving



aromatic amines, are much more common and have been used to form N-heterocycles catalytically.<sup>1,3,66,69,70</sup> Although the nucleophilic reactions presented in this Chapter are stoichiometric, they do suggest that Ru(III) complexes may have some potential for the addition of heteroatoms to unsaturated hydrocarbons. The reactivity of *cis*-[Ru<sup>III</sup>(acac)<sub>2</sub>(*o*-H<sub>2</sub>C=C(H)C<sub>6</sub>H<sub>4</sub>NMe<sub>2</sub>)] [PF<sub>6</sub>] and [Ru<sup>III</sup>(acac)<sub>2</sub>(η<sup>2</sup>-alkene)L] [PF<sub>6</sub>] with nitrogen nucleophiles under anhydrous conditions should also be investigated. The reduction of <sup>the</sup>chelate <sup>complex</sup>alkene from Ru(III) to Ru(II) by pyridine<sup>43</sup> may have been the result of traces of water present to form hydroxide ions which probably react in a similar manner to that found for ethoxide ions.<sup>43</sup>

The factors that determine the direction and regioselectivity of nucleophilic attack for these ruthenium(III) complexes are not yet understood. Reactions with nitrogen and phosphorus nucleophiles which differ in steric requirements and basicity from those used here should be studied in an effort to identify these factors. Important information may also be gained from varying the alkyne substituents by using the known complex *cis*-[Ru<sup>III</sup>(acac)<sub>2</sub>(*o*-Me<sub>3</sub>SiC≡CC<sub>6</sub>H<sub>4</sub>NMe<sub>2</sub>)] [PF<sub>6</sub>].<sup>42</sup> Similar information may be gained *e.g.* by using tertiary phosphines which have different electronic and steric properties from those of PPh<sub>3</sub> in the case of *cis*-[Ru<sup>III</sup>(acac)<sub>2</sub>(*o*-H<sub>2</sub>C=C(H)C<sub>6</sub>H<sub>4</sub>NMe<sub>2</sub>)] [PF<sub>6</sub>]. The effect of alkyl substitution of the alkene could also be investigated by using the 2-isopropenyl-*N,N*-dimethylaniline analogue.<sup>41</sup>

## 4.8 References

- (1) Collman, J. P.; Hegedus, L. S.; Norton, J. R.; Finke, R. G. *Principles and Applications of Organotransition Metal Chemistry*; University Science Books: California, 1987.
- (2) Pruchnik, F. P. *Organometallic Chemistry of the Transition Elements*; Fackler Jr., J. P., Ed.; Plenum Press: New York and London, 1990.
- (3) Hegedus, L. S. In *Organometallics in Synthesis - A Manual*; Schlosser, M., Ed.; John Wiley and Sons: 1994; p 385.
- (4) Eisenstein, O.; Hoffmann, R. J. *Am. Chem. Soc.* **1981**, *103*, 4308.
- (5) Hahn, C.; Vitagliano, A.; Giordano, F.; Taube, R. *Organometallics* **1998**, *17*, 2060.
- (6) Stille, J. K.; Morgan, R. A. *J. Am. Chem. Soc.* **1966**, *88*, 5135.
- (7) Cope, A. C.; Kliegman, J. M.; Friedrich, E. C. *J. Am. Chem. Soc.* **1967**, *89*, 287.
- (8) Palumbo, R.; Renzi, A. D.; Panunzi, A.; Paiaro, G. *J. Am. Chem. Soc.* **1969**, *91*, 3874.
- (9) Haszeldine, R. N.; Hunt, R. J.; Parish, R. V. *J. Chem. Soc. (A)* **1971**, 3705.
- (10) Nyholm, R. S. *Pure and Appl. Chem.* **1971**, *27*, 127.
- (11) Maresca, L.; Natile, G. *Comments Inorg. Chem.* **1994**, *16*, 95.
- (12) Cooper, M. K.; Guernsey, P. J.; McPartlin, M. *J. Chem. Soc., Dalton Trans.* **1980**, 349.
- (13) Cooper, M. K.; Guernsey, P. J.; Donaldson, P.; McPartlin, M. *J. Organomet. Chem.* **1977**, *131*, C11.
- (14) Hewertson, W.; Taylor, I. C. *Chem. Commun.* **1970**, 428.
- (15) Cooper, M. K.; Guernsey, P. J.; Ling, J. H.; Nyholm, R. S. *J. Organomet. Chem.* **1975**, *91*, 117.
- (16) Al-Najjar, I. M.; Green, M.; Kerrison, S. J. S.; Sadler, P. J. *J. Chem. Research (S)* **1979**, 206.

- (17) Natile, G.; Maresca, L.; Cattalini, L. *J. Chem. Soc., Dalton Trans.* **1977**, 651.
- (18) Panunzi, A.; Renzi, A. D.; Palumbo, R.; Paiaro, G. *J. Am. Chem. Soc.* **1969**, *91*, 3879.
- (19) Hollings, D.; Green, M.; Claridge, D. V. *J. Organomet. Chem.* **1973**, *54*, 399.
- (20) Giering, W. P.; Rosenblum, M. *J. Organomet. Chem.* **1970**, *25*, C71.
- (21) Giering, W. P.; Rosenblum, M. *Chem. Commun.* **1971**, 441.
- (22) Berryhill, S. R.; Rosenblum, M. *J. Org. Chem.* **1980**, *45*, 1984.
- (23) Berryhill, S. R.; Price, T.; Rosenblum, M. *J. Org. Chem.* **1983**, *48*, 158.
- (24) Kaplan, P. D.; Schmidt, P.; Orchin, M. *J. Am. Chem. Soc.* **1968**, *90*, 4175.
- (25) Sarhan, J. K. K.; Green, M.; Al-Najjar, I. M. *J. Chem. Soc., Dalton Trans.* **1984**, 771.
- (26) Stephenson, M.; Mawby, R. J. *J. Chem. Soc., Dalton Trans.* **1981**, 2112.
- (27) Chisholm, M. H.; Clark, H. C. *Chem. Commun.* **1970**, 763.
- (28) Chisholm, M. H.; Clark, H. C. *Inorg. Chem.* **1971**, *10*, 1711.
- (29) Chisholm, M. H.; Clark, H. C. *Inorg. Chem.* **1971**, *10*, 2557.
- (30) Chisholm, M. H.; Clark, H. C. *Acc. Chem. Res.* **1973**, *6*, 202.
- (31) Reger, D. L.; Belmore, K. A.; Mintz, E.; Charles, N. G.; Griffith, E. A. H.; Amma, E. L. *Organometallics* **1983**, *2*, 101.
- (32) Reger, D. L.; Belmore, K. A.; Mintz, E.; McElligott, P. J. *Organometallics* **1984**, *3*, 134.
- (33) Reger, R. L.; Klaeren, S. A.; Lebioda, L. *Organometallics* **1986**, *5*, 1072.
- (34) Akita, M.; Kakuta, S.; Sugimoto, S.; Terada, M.; Moro-oka, Y. *Chem. Commun.* **1992**, 451.
- (35) Davidson, J. L.; Vasapollo, G.; Manojlović-Muir, L.; Muir, K. W. *Chem. Commun.* **1982**, 1025.
- (36) Allen, S. R.; Baker, P.; Barnes, S. G.; Bottrill, M.; Green, M.; Orpen, A. G.; Williams, I. D.; Welch, A. J. *J. Chem. Soc., Dalton Trans.* **1983**, 927.

- (37) Feng, S. G.; White, P. S.; Templeton, J. L. *J. Am. Chem. Soc.* **1992**, *114*, 2951.
- (38) Feng, S. G.; Templeton, J. L. *Organometallics* **1992**, *11*, 2168.
- (39) Morrow, J. R.; Tonker, T. L.; Templeton, J. L.; Kenan Jr., W. R. *J. Am. Chem. Soc.* **1985**, *107*, 6956.
- (40) Halpern, J.; James, B. R.; Kemp, A. L. W. *J. Am. Chem. Soc.* **1961**, *83*, 4097.
- (41) Bennett, M. A.; Heath, G. A.; Hockless, D. C. R.; Kovacic, I.; Willis, A. C. *J. Am. Chem. Soc.* **1998**, *120*, 932.
- (42) Bennett, M. A.; Heath, G. A.; Hockless, D. C. R.; Kovacic, I.; Willis, A. C. *Organometallics* **1998**, *17*, 5867.
- (43) Kovacic, I. PhD Thesis, ANU, 1995.
- (44) Menglet, D. PhD Thesis, ANU, 1996.
- (45) Nakamoto, K. *Infrared and Raman Spectra of Inorganic and Coordination Compounds*; 4th ed.; Wiley: New York, 1986.
- (46) Bellamy, L. J. *The Infrared Spectra of Complex Molecules*; 3rd ed.; Chapman and Hall: London, 1975.
- (47) Trefonas, L. M.; R. L. Flurry, J.; Majeste, R.; Meyers, E. A.; Copland, R. F. *J. Am. Chem. Soc.* **1966**, *88*, 2145.
- (48) Childs, R. F.; Dickie, B. D.; Faggiani, R.; Fyfe, C. A.; Lock, C. J. L.; Wasylishen, R. E. *J. Crystallogr. Spectrosc. Res.* **1985**, *15*, 73.
- (49) Knop, O.; Cameron, T. S.; Bakshi, P. K.; Kwiatkowski, W.; Choi, S. C.; Adhikesavalu, D. *Can. J. Chem.* **1993**, *71*, 1495.
- (50) Knüppel, S.; Fauré, J.; Erker, G.; Kehr, G.; Nissinen, M.; Fröhlich, R. *Organometallics* **2000**, *19*, 1262.
- (51) Cook, A. G. In *Enamines: Synthesis, Structure and Reactions*; 2nd ed.; Cook, A. G., Ed.; Marcel Dekker: New York, 1988; p 1.
- (52) Kowalski, D.; Fröhlich, R.; Erker, G. *Z. Naturforsch.* **1996**, *51b*, 1053.
- (53) Kolobova, N. E.; Ivanov, L. L.; Zhvanko, O. S.; Chechulina, I. N.; Batsanov, A. S.; Struchkov, Yu. T. *J. Organomet. Chem.* **1982**, *238*, 223.

- (54) Chisholm, M. H.; Clark, H. C.; Hunter, D. H. *Chem. Commun.* **1971**, 809.
- (55) Harman, W. D.; Dobson, J. C.; Taube, H. J. *Am. Chem. Soc.* **1989**, *111*, 3061.
- (56) Thompson, S. J.; Bailey, P. M.; White, C.; Maitlis, P. M. *Angew. Chem. Int. Ed. Engl.* **1976**, *15*, 490.
- (57) Fernández-Galán, R.; Manzano, B. R.; Otero, A.; Lanfranchi, M.; Pellinghelli, M. A. *Inorg. Chem.* **1994**, *33*, 2309.
- (58) Johnson, A. W. *Ylides and Imines of Phosphorus*; John Wiley and Sons: New York, 1993, p 47.
- (59) Lahiri, G. K.; Bhattacharya, S.; Mukherjee, M.; Mukherjee, A. K.; Chakravorty, A. *Inorg. Chem.* **1987**, *26*, 3359.
- (60) Blackmore, T.; Bruce, M. I.; Stone, F. G. *A. J. Chem. Soc., Dalton Trans.* **1974**, 106.
- (61) Booth, B. L.; Lloyd, A. D. *J. Organomet. Chem.* **1972**, *35*, 195.
- (62) Huggins, J. M.; Bergman, R. G. *J. Am. Chem. Soc.* **1981**, *103*, 3002.
- (63) Hart, D. W.; Schwartz, J. J. *Organomet. Chem.* **1975**, *87*, C11.
- (64) March, J. *Advanced Organic Chemistry*; 3rd ed.; John Wiley and Sons: New York, 1985, p 66.
- (65) Dupont, J.; Casagrande, O. L.; Aiub, A. C.; Beck, J.; Hoerner, M.; Bortoluzzi, A. *Polyhedron* **1994**, *13*, 2583.
- (66) Hegedus, L. S. In *Comprehensive Organic Syntheses*; Trost, B. M.; Fleming, I., Eds.; Pergamon: New York, 1991; Vol. 4; p 551.
- (67) Jira, R. In *Applied Homogenous Catalysis with Organometallic Compounds*; Cornils, B.; Herrmann, W. A., Eds.; Weinheim, VCH: **1996**; Vol. 1; p 374.
- (68) Henkelmann, J. In *Applied Homogenous Catalysis with Organometallic Compounds*; Cornils, B.; Herrmann, W. A., Eds.; Weinheim, VCH: **1996**; Vol. 1; p 275.
- (69) Müller, T. E.; Beller, M. *Chem. Rev.* **1998**, *98*, 675.
- (70) Cardillo, G.; Orena, M. *Tetrahedron* **1990**, *46*, 3321.

*Co-ordination chemistry of  
alkynyldiphenylphosphine  
bis( $\beta$ -diketonato)ruthenium(II)  
complexes*

### 5.1 Reactivity of *cis*-[Ru(acac)<sub>2</sub>(η<sup>2</sup>-alkene)<sub>2</sub>] with two equivalents of an alkynyl tertiary phosphine

The co-ordination and reactivity of alkynyldiphenylphosphines, Ph<sub>2</sub>PC≡CR, has been of some interest. Alkynylphosphines are potential difunctional ligands with the capacity to co-ordinate as simple phosphines,<sup>1-13</sup> or disubstituted alkynes<sup>8,14,15</sup> or to use both the phosphine lone pair and the alkynyl π orbitals in a multidentate bonding fashion.<sup>8,9,11,15-19</sup> Bis(diphenylphosphino)acetylene, Ph<sub>2</sub>PC≡CPh<sub>2</sub>, has also been the subject of much attention in both P-monodentate<sup>20,21</sup> and bridging<sup>10,13,19-28</sup> co-ordination modes. An electrochemical investigation of [{Ru<sub>3</sub>(CO)<sub>11</sub>]<sub>2</sub>(μ-Ph<sub>2</sub>PC≡CPh<sub>2</sub>)] led to the conclusion that there was no detectable electronic communication between the two {Ru<sub>3</sub>(CO)<sub>11</sub>} units but due to chemical complications the possibility of a weak interaction could not be excluded.<sup>29</sup> The aims of the study described in this Chapter are to investigate the reactivity of various alkynyldiphenylphosphines with the bis(alkene) complexes *cis*-[Ru(acac)<sub>2</sub>(η<sup>2</sup>-C<sub>2</sub>H<sub>4</sub>)<sub>2</sub>] and examine the properties and reactivity of the isolated complexes.

The addition of two equivalents of the alkynyldiphenylphosphines, Ph<sub>2</sub>PC≡CR (R = H, Me, Ph), to a solution of *cis*-[Ru(acac)<sub>2</sub>(η<sup>2</sup>-alkene)<sub>2</sub>] (alkene = C<sub>2</sub>H<sub>4</sub>, C<sub>8</sub>H<sub>14</sub>) in THF at room temperature results in the isolation of orange, air stable solids *trans*-[Ru(acac)<sub>2</sub>(Ph<sub>2</sub>PC≡CR)<sub>2</sub>] in yields *ca.* 60 - 98%. These orange solids are virtually insoluble in THF, benzene or toluene but readily form air-stable solutions in CH<sub>2</sub>Cl<sub>2</sub> and chlorobenzene. Heating a solution of *trans*-[Ru(acac)<sub>2</sub>(Ph<sub>2</sub>PC≡CR)<sub>2</sub>] (R = Me, Ph) in chlorobenzene at reflux causes quantitative isomerization to the air-stable yellow complexes *cis*-[Ru(acac)<sub>2</sub>(Ph<sub>2</sub>PC≡CR)<sub>2</sub>], which were isolated in yields of *ca.* 65%. These solids are readily soluble in aromatic solvents and CH<sub>2</sub>Cl<sub>2</sub> forming yellow, air-stable solutions. The behaviour of *trans*-[Ru(acac)<sub>2</sub>(Ph<sub>2</sub>PC≡CH)<sub>2</sub>] is more complex as shown by monitoring of the <sup>31</sup>P{<sup>1</sup>H} NMR spectra. After heating,

a  $C_6D_6$  solution of  $trans$ - $[Ru(acac)_2(Ph_2PC\equiv CH)_2]$  at  $85\text{ }^\circ C$  for 45 minutes, the main peak observed, at  $\delta$  24.2, is due to unchanged starting material; there are also smaller peaks of equal intensity at  $\delta$  32.0 (d, 43 Hz) and  $\delta$  -14.3 (d, 43 Hz). The latter resonance suggests the presence of uncoordinated phosphorus atoms. The  $^{31}P\{^1H\}$  NMR chemical shift for free  $Ph_2PC\equiv CH$  has been reported as a singlet at  $\delta$  -33.3 in  $C_6D_6$ .<sup>30</sup> Prolonged heating of this solution results in singlets at  $\delta$  -17.1, -16.2, 42.5 and several peaks between 47.7 - 49.7. This reaction has not been investigated further.

The addition of two equivalents of the bidentate ditertiary phosphine  $Ph_2PC\equiv CPh_2$  to  $cis$ - $[Ru(acac)_2(\eta^2-C_8H_{14})_2]$  in THF initially results in a clear orange solution. However, stirring the solution overnight gives an orange red precipitate which is insoluble in benzene, toluene,  $CH_2Cl_2$  and chlorobenzene. The elemental analysis corresponds approximately to the formula  $trans$ - $[Ru(acac)_2(\mu-Ph_2PC\equiv CPh_2)]$  and the orange solid is presumed to be an oligomeric or polymeric material, similar to those isolated from the reaction of  $cis$ - $[Ru(acac)_2(\eta^2-C_8H_{14})_2]$  with 1,2-bis(diphenylphosphino)ethane and 1,3-bis(diphenylphosphino)propane.<sup>31</sup> The IR spectrum does not show any bands in the region 2300 and  $1600\text{ cm}^{-1}$  due to  $\nu(C\equiv C)$ . The absence of such bands has been suggested by Carty and co-workers<sup>22,24,25</sup> to indicate that there has been no lowering of the symmetry of the ligand due to coordination of the  $C\equiv C$  bond. A suspension of this orange red material  $trans$ - $[Ru(acac)_2(Ph_2PC\equiv CPh_2)]$  in refluxing chlorobenzene gives the yellow, air-stable complex  $cis$ - $[Ru(acac)_2(\mu-Ph_2PC\equiv CPh_2)]_2$  in *ca.* 40% yield.

The  $^1H$ ,  $^{13}C\{^1H\}$  and  $^{31}P\{^1H\}$  NMR spectral data for the complexes  $trans$ - $[Ru(acac)_2(Ph_2PC\equiv CR)_2]$  ( $R = H, CH_3, Ph$ ),  $cis$ - $[Ru(acac)_2(Ph_2PC\equiv CR)_2]$  ( $R = Me, Ph$ ) and  $cis$ - $[Ru(acac)_2]_2(\mu-Ph_2PC\equiv CPh_2)_2$  are shown in Tables 5.1 - 5.4. Resonances due to the aromatic protons and carbon atoms were found in the expected regions. Due to the tendency for these complexes to crystallise out of solution, it was difficult to obtain the signals due to the



carbon atoms of the alkynyl unit in the  $^{13}\text{C}\{^1\text{H}\}$  NMR spectrum. The  $\text{C}_\alpha$  atoms of the  $\text{Ph}_2\text{PC}_\alpha\equiv\text{C}_\beta\text{-R}$  ( $\text{R} = \text{Me, Ph}$ ) functional groups were detected as a triplets for the *trans*- $[\text{Ru}(\text{acac})_2(\text{Ph}_2\text{PC}\equiv\text{CR})_2]$  complexes, whereas in the *cis*-isomers, the same atoms appear as a six line symmetrical multiplet. In both cases the carbon atom  $\text{C}_\alpha$  is part of an AA'X system ( $\text{A} = ^{31}\text{P}$ ;  $\text{X} = ^{13}\text{C}$ ) and the different patterns probably arise from the differing magnitude of  $J(\text{AA}')$  in the *trans*- and *cis*-isomers. Since the values for the resonances of the alkynyl carbon atoms change little upon co-ordination compared to the free ligands,<sup>30</sup> the alkynyl moieties are probably not co-ordinated to the ruthenium atom. However, this evidence is not clear-cut because for the chelated alkyne complexes *cis*- $[\text{Ru}(\text{acac})_2(o\text{-RC}\equiv\text{C}_6\text{H}_4\text{NMe}_2)]$  ( $\text{R} = \text{H, Ph, SiMe}_3$ ), the  $^{13}\text{C}\{^1\text{H}\}$  chemical shifts of the alkynyl carbon atoms differ only slightly from those of the free ligand.<sup>32</sup>

**Table 5.1:**  $^1\text{H}$  and  $^{13}\text{C}\{^1\text{H}\}$  NMR spectral parameters of the  $\{\text{Ru}(\text{acac})_2\}$  moiety of the bis(alkynyl)diphenylphosphine complexes  $\text{trans-}[\text{Ru}(\text{acac})_2\text{L}_2]$ .

Ligand	$^1\text{H}$ NMR <sup>a</sup>		$^{13}\text{C}\{^1\text{H}\}$ NMR <sup>a</sup>	
	$\delta\text{CH}_3$	$\delta\text{CH}$	$\delta\text{CH}_3$	$\delta\text{CH}$
$\text{Ph}_2\text{PC}\equiv\text{CH}$	1.39	4.36	27.2	100.3
$\text{Ph}_2\text{PC}\equiv\text{CCH}_3$	1.42	4.43	27.4	99.9
$\text{Ph}_2\text{PC}\equiv\text{CPh}$	1.37	4.50	27.5	100.3
				$\delta\text{CO}$
				185.5
				185.6
				186.0

**Table 5.2:**  $^1\text{H}$ ,  $^{13}\text{C}\{^1\text{H}\}$  and  $^{31}\text{P}\{^1\text{H}\}$  NMR spectral parameters of the tertiary phosphines of the bis(alkynyl)diphenylphosphine complexes  $\text{trans-}[\text{Ru}(\text{acac})_2\text{L}_2]$ .

Ligand	$^1\text{H}$ NMR <sup>a</sup>		$^{13}\text{C}\{^1\text{H}\}$ NMR <sup>a</sup>		$^{31}\text{P}\{^1\text{H}\}$ NMR <sup>a</sup>
	$\delta$	Assignment	$\delta$	Assignment	
$\text{Ph}_2\text{PC}\equiv\text{CH}$	3.49 (1H, t, $J_{\text{PH}} = 2.4$ Hz)	C $\equiv$ CH aromatic	79.0 (t, $J_{\text{PC}} = 30$ Hz)	C $\equiv$ CH	+22.8
	7.26 - 7.73 (10H, m)		97.7 (d, $J_{\text{PC}} = 4.2$ Hz)	C $\equiv$ CH	
			128.1 (t, $J_{\text{PC}} = 4.5$ Hz)	<i>m</i> -C $_6$ H $_5$	
			129.6	<i>p</i> -C $_6$ H $_5$	
			132.0 (t, $J_{\text{PC}} = 20$ Hz)	<i>ipso</i> -C $_6$ H $_5$	
			132.7 (t, $J_{\text{PC}} = 6.6$ Hz)	<i>o</i> -C $_6$ H $_5$	

a) measured in  $\text{CD}_2\text{Cl}_2$ , all singlets unless otherwise indicated.

**Table 5.2 (cont):**  $^1\text{H}$ ,  $^{13}\text{C}\{^1\text{H}\}$  and  $^{31}\text{P}\{^1\text{H}\}$  NMR spectral parameters of the tertiary phosphines of the bis(alkynyl)diphenylphosphine complexes *trans*-[Ru(acac)<sub>2</sub>L<sub>2</sub>].

Ligand	$^1\text{H}$ NMR <sup>a</sup>		Assignment	$^{13}\text{C}\{^1\text{H}\}$ NMR <sup>a</sup>		$^{31}\text{P}\{^1\text{H}\}$ NMR <sup>a</sup>
	$\delta$	Assignment		$\delta$	Assignment	
Ph <sub>2</sub> PC≡CCH <sub>3</sub>	2.20 (3H)	C≡CCH <sub>3</sub>	5.96	C≡CCH <sub>3</sub>	+21.9	
	7.32 - 7.77 (10H)	aromatic	72.4 (t, J <sub>PC</sub> = 35 Hz)	C≡CCH <sub>3</sub>		
			107.5	C≡CCH <sub>3</sub>		
			127.9 (t, J <sub>PC</sub> = 4.1 Hz)	<i>m</i> -C <sub>6</sub> H <sub>5</sub>		
			129.2	<i>p</i> -C <sub>6</sub> H <sub>5</sub>		
Ph <sub>2</sub> PC≡CPh	7.30 - 7.84 (15H)	aromatic	132.7 (t, J <sub>PC</sub> = 6.3 Hz)	<i>o</i> -C <sub>6</sub> H <sub>5</sub>	+22.1	
			133.4 (t, J <sub>PC</sub> = 20 Hz)	<i>ipso</i> -C <sub>6</sub> H <sub>5</sub>		
			83.6 (m)	C≡CPh		
			108.9 (m)	C≡CPh		
			128.1 (t, J <sub>PC</sub> = 4.4 Hz)	<i>m</i> -C <sub>6</sub> H <sub>5</sub>		
			128.8	<i>o</i> -C <sub>6</sub> H <sub>5</sub>		
	129.5	<i>p</i> -C <sub>6</sub> H <sub>5</sub>				
	129.6	<i>p</i> -C <sub>6</sub> H <sub>5</sub>				
	132.1	<i>ipso</i> -C <sub>6</sub> H <sub>5</sub>				
	132.9 (t, J <sub>PC</sub> = 6.5 Hz)	<i>o</i> -C <sub>6</sub> H <sub>5</sub>				

a) measured in CD<sub>2</sub>Cl<sub>2</sub>, singlets unless otherwise indicated.

**Table 5.3:**  $^1\text{H}$  and  $^{13}\text{C}\{^1\text{H}\}$  NMR spectral parameters of the  $[\text{Ru}(\text{acac})_2]$  moiety of the bis(phosphine) complexes  $\text{cis-}[\text{Ru}(\text{acac})_2\text{L}_2]$ .

Ligand	$^1\text{H}$ NMR <sup>a</sup>		$^{13}\text{C}\{^1\text{H}\}$ NMR <sup>a</sup>	
	$\delta\text{CH}_3$	$\delta\text{CH}$	$\delta\text{CH}_3$	$\delta\text{CH}$
$\text{Ph}_2\text{PC}\equiv\text{CCH}_3$	1.32, 2.07	5.33	27.2, 28.6	99.5
$\text{Ph}_2\text{PC}\equiv\text{CPh}$	1.38, 2.02	5.23	27.3, 28.5	99.5
$\text{Ph}_2\text{PC}\equiv\text{CPh}_2$	1.45, 1.65	5.02	27.6, 27.7	99.6
				$\delta\text{CO}$
				185.4, 187.2
				185.4, 187.3
				184.6, 187.4

a) measured in  $\text{CD}_2\text{Cl}_2$ , all singlets.

**Table 5.4:**  $^1\text{H}$ ,  $^{13}\text{C}\{^1\text{H}\}$  and  $^{31}\text{P}\{^1\text{H}\}$  NMR spectral parameters of the tertiary phosphines of the bis(alkynyl)diphenylphosphine complexes  $\text{cis-}[\text{Ru}(\text{acac})_2\text{L}_2]$ .

Ligand	$^1\text{H}$ NMR <sup>a</sup>		$^{13}\text{C}\{^1\text{H}\}$ NMR <sup>a</sup>		$^{31}\text{P}\{^1\text{H}\}$ NMR <sup>a</sup>
	$\delta$	Assignment	$\delta$	Assignment	
$\text{Ph}_2\text{PC}\equiv\text{CCH}_3$	2.02 (6H, vt $J_{\text{PH}} 1.2$ Hz)	-C $\equiv$ CCH $_3$ aromatic	5.82	-C $\equiv$ CCH $_3$	+39.8
	7.10 - 7.90 (20 H, m)		72.8 (a symmetrical six line multiplet, spacing between lines 17.6, 38.4, 6.9, 37.0 and 18.7 Hz)	-C $\equiv$ CCH $_3$	
			107.9 (t, $J_{\text{PC}} = 5.5$ Hz)	-C $\equiv$ CCH $_3$	
			127.2 (t, $J_{\text{PC}} = 5$ Hz)	<i>m</i> -C $_6$ H $_5$	
			127.6 (t, $J_{\text{PC}} = 5$ Hz)	<i>m</i> -C $_6$ H $_5$	
			128.7	<i>p</i> -C $_6$ H $_5$	
			132.1 (t, $J_{\text{PC}} = 5.5$ Hz)	<i>o</i> -C $_6$ H $_5$	
			132.5 (t, $J_{\text{PC}} = 5.5$ Hz)	<i>o</i> -C $_6$ H $_5$	
			136.7 (t, $J_{\text{PC}} = 22$ Hz)	<i>ipso</i> -C $_6$ H $_5$	
			137.5 (t, $J_{\text{PC}} = 26$ Hz)	<i>ipso</i> -C $_6$ H $_5$	

**Table 5.4 (cont):**  $^1\text{H}$ ,  $^{13}\text{C}\{^1\text{H}\}$  and  $^{31}\text{P}\{^1\text{H}\}$  NMR spectral parameters of the tertiary phosphines of the bis(alkynylidiphenylphosphine) complexes *cis*-[Ru(acac) $_2$ L $_2$ ].

Ligand	$^1\text{H}$ NMR <sup>a</sup>		$^{13}\text{C}\{^1\text{H}\}$ NMR <sup>a</sup>		$^{31}\text{P}\{^1\text{H}\}$ NMR <sup>a</sup>
	$\delta$	Assignment	$\delta$	Assignment	
Ph $_2$ PC $\equiv$ CPh	7.08 - 7.94 (30 H, m)	aromatic	84.3 (a six line multiplet, spacing between lines 18.6, 34.0, 7.7, 34.0 and 17.6 Hz)	-C $\equiv$ CPh	+40.3
			109.1 (d, $J_{\text{PC}} = 5$ Hz)	-C $\equiv$ CPh	
			127.7 (t, $J_{\text{PC}} = 5$ Hz)	<i>m</i> -C $_6$ H $_5$	
			128.8	<i>p</i> -C $_6$ H $_5$	
			128.9	<i>p</i> -C $_6$ H $_5$	
			129.5	<i>ipso</i> -C $_6$ H $_5$	
			131.9 (t, $J_{\text{PC}} = 5.7$ Hz)	<i>o</i> -C $_6$ H $_5$	
			132.0	<i>o</i> -C $_6$ H $_5$	
			132.5 (t, $J_{\text{PC}} = 5.5$ Hz)	<i>o</i> -C $_6$ H $_5$	
			136.4 (t, $J_{\text{PC}} = 22.9$ Hz)	<i>ipso</i> -C $_6$ H $_5$	
137.2 (t, $J_{\text{PC}} = 26.2$ Hz)	<i>ipso</i> -C $_6$ H $_5$				

a) measured in CD $_2$ Cl $_2$ , all singlets unless otherwise indicated.

**Table 5.4 (cont):**  $^1\text{H}$ ,  $^{13}\text{C}\{^1\text{H}\}$  and  $^{31}\text{P}\{^1\text{H}\}$  NMR spectral parameters of the tertiary phosphines of the bis(alkynyl)diphenylphosphine complexes *cis*-[Ru(acac)<sub>2</sub>L<sub>2</sub>].

Ligand	$^1\text{H}$ NMR <sup>a</sup>		$^{13}\text{C}\{^1\text{H}\}$ NMR <sup>a</sup>		$^{31}\text{P}\{^1\text{H}\}$ NMR <sup>a</sup>
	$\delta$	Assignment	$\delta$	Assignment	
Ph <sub>2</sub> PC≡CPh <sub>2</sub>	8.10 - 8.16 (m, 16 H)	o-C <sub>6</sub> H <sub>5</sub> m- and p-C <sub>6</sub> H <sub>5</sub>	104.8 (a symmetrical six line multiplet, spacing between lines 19.0, 30.8, 7.7, 27.0 and 19.2 Hz)	-C≡CPh <sub>2</sub>	+43.1
	6.99 - 7.25 (m, 24 H)		127.5 (t, <i>J</i> <sub>PC</sub> = 4 Hz)	m-C <sub>6</sub> H <sub>5</sub>	
			127.6 (t, <i>J</i> <sub>PC</sub> = 4 Hz)	m-C <sub>6</sub> H <sub>5</sub>	
			128.6	p-C <sub>6</sub> H <sub>5</sub>	
			129.6	p-C <sub>6</sub> H <sub>5</sub>	
			132.0 (t, <i>J</i> <sub>PC</sub> = 5.2 Hz)	o-C <sub>6</sub> H <sub>5</sub>	
			133.9 (t, <i>J</i> <sub>PC</sub> = 24 Hz)	<i>ipso</i> -C <sub>6</sub> H <sub>5</sub>	
	135.4 (t, <i>J</i> <sub>PC</sub> = 5.5 Hz)	o-C <sub>6</sub> H <sub>5</sub>			
		135.9 (t, <i>J</i> <sub>PC</sub> = 24 Hz)	<i>ipso</i> -C <sub>6</sub> H <sub>5</sub>		

a) measured in CD<sub>2</sub>Cl<sub>2</sub>, all singlets unless otherwise indicated.

The IR spectra of the isolated complexes exhibit two intense bands, characteristic of bidentate O-bonded acac (see Table 5.6).<sup>33</sup> A strong absorption was also found in the region 2200 - 2035 cm<sup>-1</sup>, except for *cis*-[Ru(acac)<sub>2</sub>(μ-Ph<sub>2</sub>PC≡CPh<sub>2</sub>)<sub>2</sub>], which corresponds to the uncoordinated ν(C≡C) band. The ν(C≡C) values are *ca.* 12 cm<sup>-1</sup> higher than those of the ligands (see Table 5.6), as has also been observed for the complexes [(η<sup>5</sup>-C<sub>5</sub>H<sub>5</sub>)<sub>2</sub>Rh<sub>2</sub>(CO)(μ-η<sup>1</sup>:η<sup>1</sup>-CF<sub>3</sub>C≡CCF<sub>3</sub>)(η<sup>1</sup>-Ph<sub>2</sub>PC≡CR)] (R = H, Me, Ph),<sup>10</sup> *cis*-[PtX<sub>2</sub>(Ph<sub>2</sub>PC≡CPh)<sub>2</sub>] (X = I, CF<sub>3</sub>, C<sub>6</sub>F<sub>5</sub>, Me),<sup>34</sup> [AuCl(Ph<sub>2</sub>PC≡CH)],<sup>35</sup> [(η<sup>6</sup>-C<sub>6</sub>Me<sub>6</sub>)RuCl<sub>2</sub>(Ph<sub>2</sub>PC≡CH)]<sup>4</sup> and [PdCl<sub>2</sub>(Ph<sub>2</sub>PC≡CMe)]<sub>2</sub>.<sup>12</sup> The Raman spectrum of *cis*-[Ru(acac)<sub>2</sub>(μ-Ph<sub>2</sub>PC≡CPh<sub>2</sub>)<sub>2</sub>] shows a medium absorption at 2131 cm<sup>-1</sup> which is assigned to the symmetrical C≡C stretching vibration and is within the range 2143 to 2109 cm<sup>-1</sup> found for the bridged Ph<sub>2</sub>PC≡CPh<sub>2</sub> binuclear complexes of Cu(I), Ag(I), Au(I), Pt(II), Pd(II), Hg(II), Rh(I) and Ni(0).<sup>19,22,24,25,36</sup> Calculations suggest that the π\*<sub>C≡C</sub> occupancy is higher in the free ligand than in the coordinated systems, because of delocalization of the phosphorus lone pair of electrons, thus accounting for the trend in ν(C≡C) values.

**Table 5.6:** IR spectral data for the complexes *trans*-[Ru(acac)<sub>2</sub>(Ph<sub>2</sub>PC≡CR)<sub>2</sub>] (R = H, CH<sub>3</sub>, Ph) and *cis*-[Ru(acac)<sub>2</sub>(Ph<sub>2</sub>PC≡CR)<sub>2</sub>] (R = CH<sub>3</sub>, Ph).

Complex	ν(acac) (cm <sup>-1</sup> ) (solid)	ν(C≡C) (cm <sup>-1</sup> ) (solid)	Δν(C≡C) (cm <sup>-1</sup> ) <sup>a</sup>
Ph <sub>2</sub> PC≡CH <sup>b</sup>	-	2032	-
<i>trans</i> -[Ru(acac) <sub>2</sub> (Ph <sub>2</sub> PC≡CH) <sub>2</sub> ]	1568, 1511	2035	3
Ph <sub>2</sub> PC≡CMe <sup>b</sup>	-	2186	-
<i>trans</i> -[Ru(acac) <sub>2</sub> (Ph <sub>2</sub> PC≡CMe) <sub>2</sub> ]	1568, 1512	2198	12
<i>cis</i> -[Ru(acac) <sub>2</sub> (Ph <sub>2</sub> PC≡CMe) <sub>2</sub> ]	1574, 1514	2200	14
Ph <sub>2</sub> PC≡CPh <sup>b</sup>	-	2158	-
<i>trans</i> -[Ru(acac) <sub>2</sub> (Ph <sub>2</sub> PC≡CPh) <sub>2</sub> ]	1567, 1512	2172	14
<i>cis</i> -[Ru(acac) <sub>2</sub> (Ph <sub>2</sub> PC≡CPh) <sub>2</sub> ]	1574, 1515	2171	13
<i>cis</i> -[Ru(acac) <sub>2</sub> (μ-Ph <sub>2</sub> PC≡CPh <sub>2</sub> ) <sub>2</sub> ]	1573, 1514	2131 <sup>c</sup>	34 <sup>c,d</sup>

a) Δν(C≡C) = ν(C≡C)<sub>complex</sub> - ν(C≡C)<sub>free</sub>; b) ref. 37; c) Raman spectrum; d) ref. 22



The FAB mass spectra of *trans*-[Ru(acac)<sub>2</sub>(Ph<sub>2</sub>PC≡CR)<sub>2</sub>] (R = H, CH<sub>3</sub>, Ph), *cis*-[Ru(acac)<sub>2</sub>(Ph<sub>2</sub>PC≡CR)<sub>2</sub>] (R = CH<sub>3</sub>, Ph) and *cis*-[Ru(acac)<sub>2</sub>(μ-Ph<sub>2</sub>PC≡CPh<sub>2</sub>)<sub>2</sub>] display the parent molecular ion peak, with the most abundant ion present corresponding to the species {Ru(acac)<sub>2</sub>(Ph<sub>2</sub>PC≡CR)}<sup>+</sup> (see Table 5.7). Also detected were the ions corresponding to the loss of one acac ligand from the parent ion.

**Table 5.7:** FAB mass spectral data of the isolated alkynylidiphosphine complexes [Ru(acac)<sub>2</sub>(Ph<sub>2</sub>PC≡CR)<sub>2</sub>] and [Ru(acac)<sub>2</sub>(μ-Ph<sub>2</sub>PC≡CPh<sub>2</sub>)<sub>2</sub>].

Phosphine	Geometric isomer	m/z	Assignment	Relative Intensity (%)
Ph <sub>2</sub> PC≡CH	<i>trans</i>	720.2	{Ru(acac) <sub>2</sub> (Ph <sub>2</sub> PC≡CH) <sub>2</sub> } <sup>+</sup>	65
		621.3	{Ru(acac)(Ph <sub>2</sub> PC≡CH) <sub>2</sub> } <sup>+</sup>	10
		510.2	{Ru(acac) <sub>2</sub> (Ph <sub>2</sub> PC≡CH)} <sup>+</sup>	100
Ph <sub>2</sub> PC≡CMe	<i>trans</i>	748.4	{Ru(acac) <sub>2</sub> (Ph <sub>2</sub> PC≡CMe) <sub>2</sub> } <sup>+</sup>	50
		649.3	{Ru(acac)(Ph <sub>2</sub> PC≡CMe) <sub>2</sub> } <sup>+</sup>	10
		523.2	{Ru(acac) <sub>2</sub> (Ph <sub>2</sub> PC≡CMe)} <sup>+</sup>	100
Ph <sub>2</sub> PC≡CPh	<i>trans</i>	872.2	{Ru(acac) <sub>2</sub> (Ph <sub>2</sub> PC≡CPh) <sub>2</sub> } <sup>+</sup>	20
		773.1	{Ru(acac)(Ph <sub>2</sub> PC≡CPh) <sub>2</sub> } <sup>+</sup>	5
		586.1	{Ru(acac) <sub>2</sub> (Ph <sub>2</sub> PC≡CPh)} <sup>+</sup>	100
Ph <sub>2</sub> PC≡CMe	<i>cis</i>	748.1	{Ru(acac) <sub>2</sub> (Ph <sub>2</sub> PC≡CMe) <sub>2</sub> } <sup>+</sup>	100
		649.1	{Ru(acac)(Ph <sub>2</sub> PC≡CMe) <sub>2</sub> } <sup>+</sup>	25
		524.1	{Ru(acac) <sub>2</sub> (Ph <sub>2</sub> PC≡CMe)} <sup>+</sup>	35
Ph <sub>2</sub> PC≡CPh	<i>cis</i>	872.2	{Ru(acac) <sub>2</sub> (Ph <sub>2</sub> PC≡CPh) <sub>2</sub> } <sup>+</sup>	35
		774.2	{Ru(acac)(Ph <sub>2</sub> PC≡CPh) <sub>2</sub> } <sup>+</sup>	5
		586.1	{Ru(acac) <sub>2</sub> (Ph <sub>2</sub> PC≡CPh)} <sup>+</sup>	12
Ph <sub>2</sub> PC≡CPh <sub>2</sub>	<i>cis</i>	1387.8	{Ru <sub>2</sub> (acac) <sub>4</sub> (Ph <sub>2</sub> PC≡CPh <sub>2</sub> ) <sub>2</sub> } <sup>+</sup>	75
		1288.7	{Ru <sub>2</sub> (acac) <sub>3</sub> (Ph <sub>2</sub> PC≡CPh <sub>2</sub> ) <sub>2</sub> } <sup>+</sup>	23

The structures of both geometric isomers of [Ru(acac)<sub>2</sub>(Ph<sub>2</sub>PC≡CMe)<sub>2</sub>] and of *cis*-[Ru(acac)<sub>2</sub>(μ-Ph<sub>2</sub>PC≡CPh<sub>2</sub>)<sub>2</sub>] have been confirmed by single crystal X-ray crystallography. The molecular structures and selected metrical parameters are shown in Figures 5.1 - 5.3 and Tables 5.8 - 5.10, respectively. Crystal and refinement data of both complexes, together with the full set of

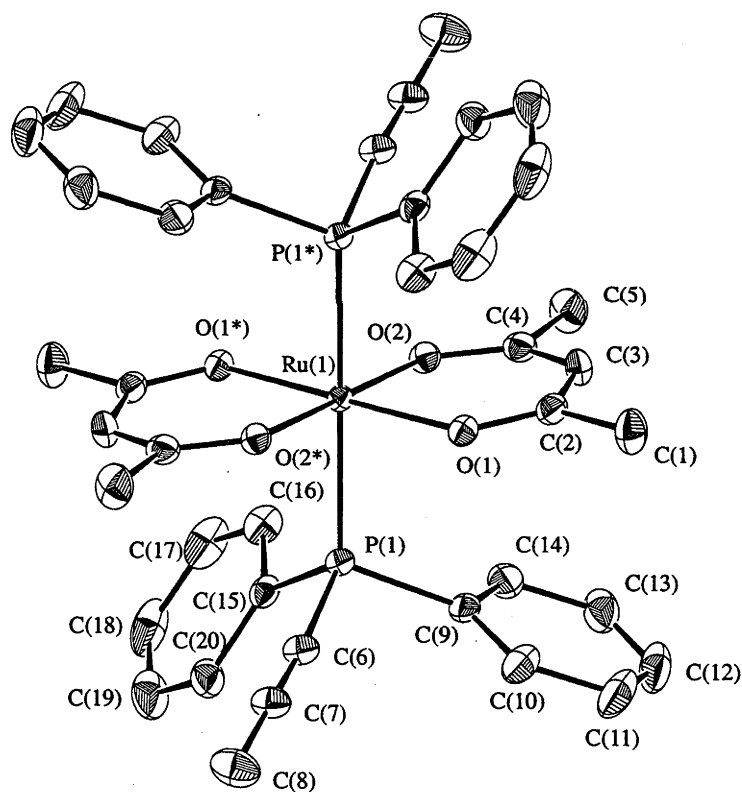
interatomic distances and angles, are given in Appendices A.15 - A.17. In the crystal structure of *cis*-[Ru(acac)<sub>2</sub>(Ph<sub>2</sub>PC≡CMe)<sub>2</sub>] there are two independent molecules in the unit cell with one alkynyl group of the second molecule showing some disorder. The unit cell of *cis*-[Ru(acac)<sub>2</sub>(μ-Ph<sub>2</sub>PC≡CPh)<sub>2</sub>] contains solvent molecules which could not be refined, the most likely species being CH<sub>2</sub>Cl<sub>2</sub>, n-hexane or water. At present, the atom sites are modelled to resemble the contoured electron density map of this area, but the molecules responsible for it have not been identified.

The Ru-O distances in *trans*-[Ru(acac)<sub>2</sub>(Ph<sub>2</sub>PC≡CMe)<sub>2</sub>], *cis*-[Ru(acac)<sub>2</sub>(Ph<sub>2</sub>PC≡CMe)<sub>2</sub>] and *cis*-[Ru(acac)<sub>2</sub>(Ph<sub>2</sub>PC≡CPh)<sub>2</sub>] are as expected, the Ru-O distances *trans* to the phosphorus atoms being *ca.* 0.03 Å longer than those *trans* to acac oxygen atoms (see Table 5.8 - 5.10). The Ru-P distances vary between 2.249(1) to 2.3330(7) Å, shorter distances being found in the *cis* complex (see Table 5.8 - 5.10); the Ru-P distance of *trans*-[Ru(acac)<sub>2</sub>(Ph<sub>2</sub>PC≡CMe)<sub>2</sub>] is similar to those of *trans*-[Ru(acac)<sub>2</sub>(PPh<sub>2</sub>Me)<sub>2</sub>].<sup>31</sup> The P-Ru-P angles of *cis*-[Ru(acac)<sub>2</sub>(Ph<sub>2</sub>PC≡CMe)<sub>2</sub>] (two independent molecules, both 94°) and *cis*-[Ru(acac)<sub>2</sub>(Ph<sub>2</sub>PC≡CPh)<sub>2</sub>] (92 and 94° for the one molecule) are the same as that found for *cis*-[Ru(acac)<sub>2</sub>(PPh<sub>2</sub>Me)<sub>2</sub>] (96°).<sup>31</sup> For the propynyldiphenylphosphine complexes, the C≡C bond length is *ca.* 1.18 Å which is similar to those found for [CpFe(CO)<sub>2</sub>(PPh<sub>2</sub>C≡CPh)][BF<sub>4</sub>] (1.202(5) Å),<sup>7</sup> [Ru<sub>3</sub>(CO)<sub>11</sub>(Ph<sub>2</sub>PC≡CPh)] (1.182 Å),<sup>16</sup> *trans*-[Pd(SCN)<sub>2</sub>(Ph<sub>2</sub>PC≡CBu<sup>t</sup>)<sub>2</sub>] (1.167(16) Å),<sup>1</sup> *cis*-[Pt(NCS)(SCN)(Ph<sub>2</sub>PC≡CBu<sup>t</sup>)<sub>2</sub>] (1.220(4) Å),<sup>2</sup> [(Bu<sup>t</sup>C≡CPh<sub>2</sub>P)<sub>2</sub>Pt(μ-η<sup>1</sup>:η<sup>2</sup>-C≡CPh)<sub>2</sub>]Pd(C<sub>6</sub>F<sub>5</sub>)<sub>2</sub>] (1.177(5) and 1.189(5) Å),<sup>11</sup> [Fe<sub>3</sub>(CO)<sub>8</sub>(μ<sub>2</sub>-CO)(μ<sub>3</sub>-S)(Ph<sub>2</sub>PC≡CPr<sup>i</sup>)] (1.171(9) Å)<sup>3</sup> and [Ru<sub>3</sub>(CO)<sub>8</sub>(μ<sub>3</sub>-S)(Ph<sub>2</sub>PC≡CBu<sup>t</sup>)] (1.192(6) Å).<sup>3</sup>

The alkynyl units in *trans*-[Ru(acac)<sub>2</sub>(Ph<sub>2</sub>PC≡CMe)<sub>2</sub>] are slightly distorted from linearity, the P(1)-C(6)-C(7) angle being *ca.* 174°. A similar bending of the alkynyl carbon atoms occurs for *cis*-[Ru(acac)<sub>2</sub>(Ph<sub>2</sub>PC≡CMe)<sub>2</sub>] with bond angles varying between 173 - 177°.

Similar bending of the P-C≡C moiety has been observed in the complexes *trans*-[Pd(SCN)<sub>2</sub>(Ph<sub>2</sub>PC≡CBu<sup>t</sup>)<sub>2</sub>] (174°),<sup>1</sup> *cis*-[Pt(NCS)(SCN)(Ph<sub>2</sub>PC≡CBu<sup>t</sup>)<sub>2</sub>] (168 and 176°),<sup>2</sup> [(Bu<sup>t</sup>C≡CPh<sub>2</sub>P)<sub>2</sub>Pt(μ-η<sup>1</sup>:η<sup>2</sup>-C≡CPh)<sub>2</sub>]Pd(C<sub>6</sub>F<sub>5</sub>)<sub>2</sub>] (166 and 175°),<sup>11</sup> [Fe<sub>3</sub>(CO)<sub>6</sub>(Ph<sub>2</sub>PC≡CPh)<sub>3</sub>(μ<sub>3</sub>-P<sup>t</sup>Bu)(μ<sub>3</sub>-Se)] (168 - 175°),<sup>5</sup> [Ph<sub>2</sub>MePC≡CBPh<sub>3</sub>] (169°).<sup>38</sup> These deviations have been attributed to non-bonding interactions between the alkyne and the groups attached to the phosphorus atoms,<sup>27,39</sup> to crystal packing forces<sup>40</sup> or to a contribution from a resonance form with a lone pair of electrons on the α-carbon atom of the alkynyl moiety as proposed for [Mn(CO)<sub>5</sub>Br(C≡CPh<sub>3</sub>)].<sup>41</sup>

**Figure 5.1:** ORTEP diagram of the molecular structure of *trans*-[Ru(acac)<sub>2</sub>(Ph<sub>2</sub>PC≡CMe)<sub>2</sub>].



\*) atom generated by the symmetry operation (1-x, 1-y, 1-z)

**Figure 5.2:** ORTEP diagram of the molecular structure for one of the independent molecules of *cis*-[Ru(acac)<sub>2</sub>(Ph<sub>2</sub>PC≡CMe)<sub>2</sub>].

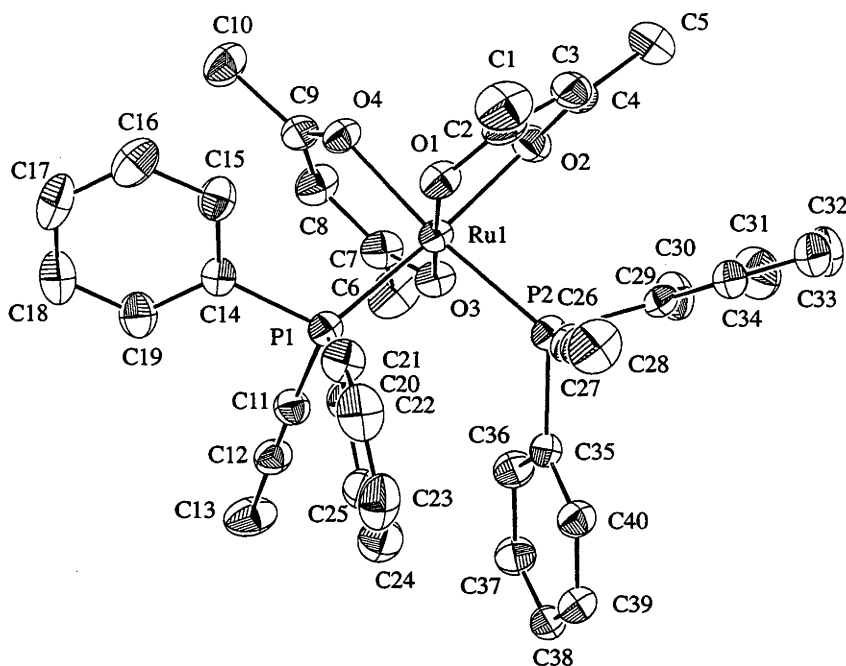


**Figure 5.3:** ORTEP diagram of the molecular structure of *cis*-[[Ru(acac)<sub>2</sub>(Ph<sub>2</sub>PC≡CPh<sub>2</sub>)<sub>2</sub>]<sub>2</sub>.

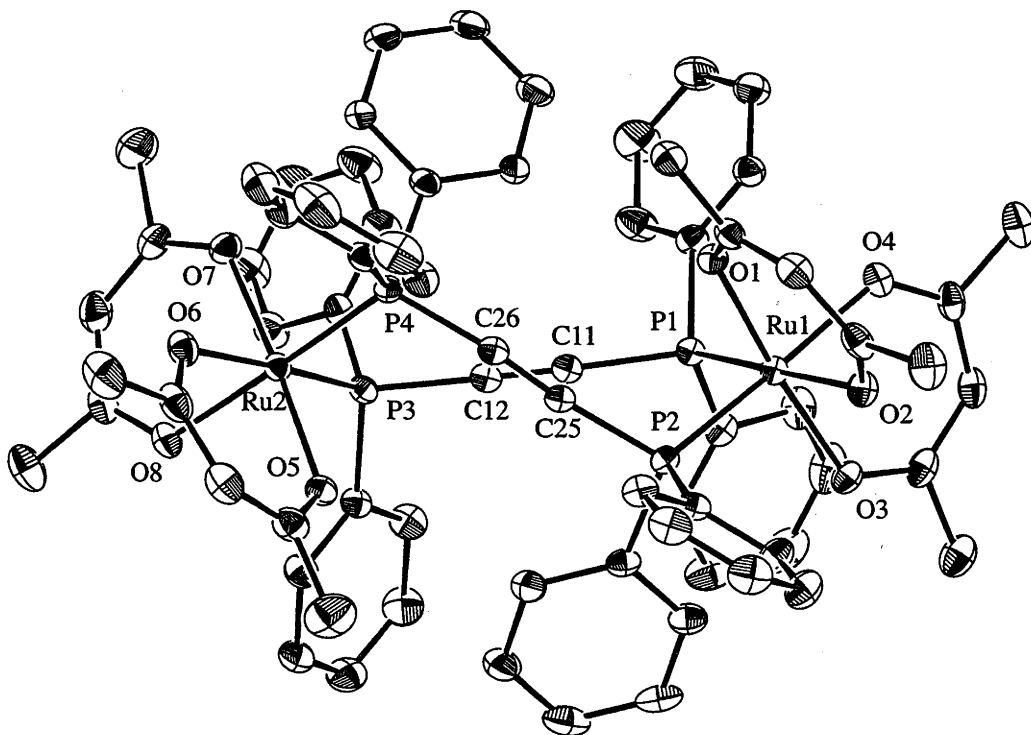


**Table 5.8:** Selected metrical parameters of *trans*-[Ru(acac)<sub>2</sub>(Ph<sub>2</sub>PC≡CMe)<sub>2</sub>].

Bond Distances (Å)			
Ru(1)-P(1)		2.3330(7)	
Ru(1)-O(1)		2.060(2)	
Ru(1)-O(2)		2.063(2)	
Bond Angles (°)			
P(1)-Ru(1)-P(1) <sup>a</sup>	180.0	O(1)-Ru(1)-O(1) <sup>a</sup>	180.0
P(1)-Ru(1)-O(1) <sup>a</sup>	91.27(6)	O(1)-Ru(1)-O(2)	93.34(7)
P(1)-Ru(1)-O(1)	88.73(6)	O(1)-Ru(1)-O(2) <sup>a</sup>	86.66(7)
P(1)-Ru(1)-O(2)	90.22(6)	O(2)-Ru(1)-O(2) <sup>a</sup>	180.0
P(1)-Ru(1)-O(2) <sup>a</sup>	89.78(6)		

a) atom generated by the symmetry operation (1-x, 1-y, 1-z)

**Table 5.9:** Selected metrical parameters of *cis*-[Ru(acac)<sub>2</sub>(Ph<sub>2</sub>PC≡CMe)<sub>2</sub>].

Bond Distances (Å)			
Ru(1)-P(1)	2.249(1)	Ru(2)-P(3)	2.259(1)
Ru(1)-P(2)	2.265(1)	Ru(2)-P(4)	2.254(2)
Ru(1)-O(1)	2.063(3)	Ru(2)-O(5)	2.056(3)
Ru(1)-O(2)	2.088(3)	Ru(2)-O(6)	2.095(3)
Ru(1)-O(3)	2.059(3)	Ru(2)-O(7)	2.069(3)
Ru(1)-O(4)	2.098(3)	Ru(2)-O(8)	2.104(4)
Bond Angles (°)			
P(1)-Ru(1)-P(2)	94.20(5)	P(3)-Ru(2)-P(4)	94.30(5)
P(1)-Ru(1)-O(1)	91.3(1)	P(3)-Ru(2)-O(5)	90.6(1)
P(1)-Ru(1)-O(2)	174.3(1)	P(3)-Ru(2)-O(6)	176.8(1)
P(1)-Ru(1)-O(3)	93.5(1)	P(3)-Ru(2)-O(7)	92.0(1)
P(1)-Ru(1)-O(4)	90.1(1)	P(3)-Ru(2)-O(8)	92.6(1)
P(2)-Ru(1)-O(1)	89.91(9)	P(4)-Ru(2)-O(5)	92.4(1)
P(2)-Ru(1)-O(2)	91.0(1)	P(4)-Ru(2)-O(6)	88.8(1)
P(2)-Ru(1)-O(3)	92.82(9)	P(4)-Ru(2)-O(7)	91.8(1)
P(2)-Ru(1)-O(4)	174.2(1)	P(4)-Ru(2)-O(8)	172.8(1)
O(1)-Ru(1)-O(2)	91.2(1)	O(5)-Ru(2)-O(6)	90.0(1)
O(1)-Ru(1)-O(3)	174.3(1)	O(5)-Ru(2)-O(7)	174.9(1)
O(1)-Ru(1)-O(4)	86.0(1)	O(5)-Ru(2)-O(8)	85.5(1)
O(2)-Ru(1)-O(3)	83.8(1)	O(6)-Ru(2)-O(7)	87.2(1)
O(2)-Ru(1)-O(4)	85.0(1)	O(6)-Ru(2)-O(8)	84.3(1)
O(3)-Ru(1)-O(4)	90.9(1)	O(7)-Ru(2)-O(8)	89.9(1)

**Table 5.10:** Selected metrical parameters of *cis*-[Ru(acac)<sub>2</sub>(Ph<sub>2</sub>PC≡CPh<sub>2</sub>)<sub>2</sub>].

Bond Distances (Å)			
Ru(1)-P(1)	2.265(1)	Ru(2)-P(3)	2.269(1)
Ru(1)-P(2)	2.253(1)	Ru(2)-P(4)	2.261(1)
Ru(1)-O(1)	2.051(3)	Ru(2)-O(5)	2.065(3)
Ru(1)-O(2)	2.090(3)	Ru(2)-O(6)	2.088(3)
Ru(1)-O(3)	2.068(3)	Ru(2)-O(7)	2.056(3)
Ru(1)-O(4)	2.091(3)	Ru(2)-O(8)	2.097(3)
C(11)-C(12)	1.179(6)	C(25)-C(26)	1.190(6)
Bond Angles (°)			
P(1)-Ru(1)-P(2)	92.04(4)	P(3)-Ru(2)-P(4)	94.43(4)
P(1)-Ru(1)-O(1)	91.82(9)	P(3)-Ru(2)-O(5)	91.61(9)
P(1)-Ru(1)-O(2)	173.97(9)	P(3)-Ru(2)-O(6)	172.26(9)
P(1)-Ru(1)-O(3)	91.10(9)	P(3)-Ru(2)-O(7)	90.7(1)
P(1)-Ru(1)-O(4)	95.85(9)	P(3)-Ru(2)-O(8)	91.93(9)
P(2)-Ru(1)-O(1)	88.94(9)	P(4)-Ru(2)-O(5)	92.06(9)
P(2)-Ru(1)-O(2)	92.60(9)	P(4)-Ru(2)-O(6)	92.64(9)
P(2)-Ru(1)-O(3)	95.36(9)	P(4)-Ru(2)-O(7)	91.15(9)
P(2)-Ru(1)-O(4)	170.26(9)	P(4)-Ru(2)-O(8)	173.51(9)
O(1)-Ru(1)-O(2)	92.1(1)	O(5)-Ru(2)-O(6)	91.3(1)
O(1)-Ru(1)-O(3)	174.7(1)	O(5)-Ru(2)-O(7)	175.9(1)
O(1)-Ru(1)-O(4)	85.1(1)	O(5)-Ru(2)-O(8)	86.5(1)
O(2)-Ru(1)-O(3)	84.6(1)	O(6)-Ru(2)-O(7)	86.0(1)
O(2)-Ru(1)-O(4)	79.9(1)	O(6)-Ru(2)-O(8)	81.1(1)
O(3)-Ru(1)-O(4)	90.2(1)	O(7)-Ru(2)-O(8)	90.1(1)
Ru(1)-P(1)-C(11)	119.7(1)	Ru(2)-P(3)-C(12)	121.9(1)
Ru(1)-P(2)-C(25)	112.4(2)	Ru(2)-P(4)-C(26)	114.1(1)
P(1)-C(11)-C(12)	178.3(4)	P(2)-C(25)-C(26)	170.1(4)
P(3)-C(12)-C(11)	177.9(4)	P(4)-C(26)-C(25)	169.7(4)

In *cis*-[Ru(acac)<sub>2</sub>(μ-Ph<sub>2</sub>PC≡CPh<sub>2</sub>)<sub>2</sub>] each ruthenium atom is at the centre of a distorted octahedron with the phosphorus atoms *cis* to each other. Only the homochiral (ΔΔ/ΛΛ) isomer was found in the crystal. The two octahedra have different orientations as shown by a dihedral angle of *ca.* 46° between the planes defined by the atoms Ru(1), P(1) and P(2), and Ru(2), P(3) and P(4), respectively (see Figure 5.3). Similar angles between the two co-ordination planes were found for [Pt<sub>2</sub>Cl<sub>4</sub>(μ-Ph<sub>2</sub>PC≡CPh<sub>2</sub>)<sub>2</sub>] (*ca.* 33°) and [Pt<sub>2</sub>I<sub>4</sub>(μ-Ph<sub>2</sub>PC≡CPh<sub>2</sub>)<sub>2</sub>] (*ca.* 43°) whereas for [Pd<sub>2</sub>Cl<sub>4</sub>(μ-Ph<sub>2</sub>PC≡CPh<sub>2</sub>)<sub>2</sub>] (*ca.* 0°) the 10-membered ring is planar.<sup>19</sup> Presumably the tilting of the two co-ordination planes in *cis*-[Ru(acac)<sub>2</sub>(μ-Ph<sub>2</sub>PC≡CPh<sub>2</sub>)<sub>2</sub>] partially releases the

strain of the 10-membered ring as was found for  $[\text{Pt}_2\text{X}_4(\mu\text{-Ph}_2\text{PC}\equiv\text{CPh}_2)_2]$  ( $\text{X} = \text{Cl, I}$ ) but there is more strain imposed upon the ruthenium complex as the P-Ru-P angles are almost  $90^\circ$  where as the P-M-P angles are close to  $95^\circ$  for  $[\text{Pt}_2\text{X}_4(\mu\text{-Ph}_2\text{PC}\equiv\text{CPh}_2)_2]$  ( $\text{X} = \text{Cl, I}$ )<sup>19</sup> and  $105^\circ$  for *cis*- $[\text{Pd}_2\text{Cl}_4(\mu\text{-Ph}_2\text{PC}\equiv\text{CPh}_2)_2]$ .<sup>19</sup>

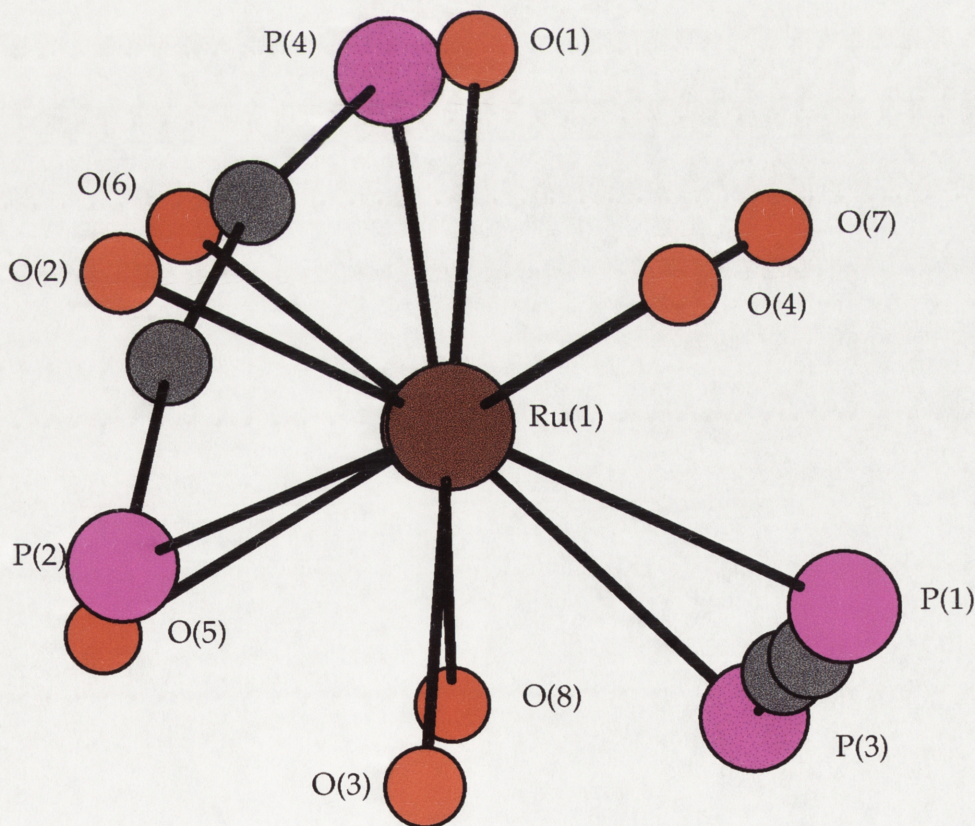
The bridging  $\text{Ph}_2\text{PC}\equiv\text{CPh}_2$  ligand defined by the P(1) and P(3) atoms of *cis*- $[\{\text{Ru}(\text{acac})_2(\mu\text{-Ph}_2\text{PC}\equiv\text{CPh}_2)\}_2]$  lies almost parallel to the Ru-Ru axis and is essentially linear [P(1)-C(11)-C(12) and P(3)-C(12)-C(11) both  $178^\circ$ ]. However, the second bridging  $\text{Ph}_2\text{PC}\equiv\text{CPh}_2$  ligand shows a slight concave bowing shown by the angles P(2)-C(25)-C(26) and P(4)-C(26)-C(25) ( $170^\circ$  each). This deviation from linearity of the alkyne fragment may be best viewed along the Ru-Ru axis as shown in Figure 5.4. Similar small deviations from linearity are observed in  $\text{Ph}_2\text{PC}\equiv\text{CPh}_2$ <sup>39</sup> and many of its complexes.<sup>13,19,26-28</sup> The bond angles about the P atoms with the Ru atom and the carbon atom of the alkyne unit varies between  $120 - 122^\circ$  for atoms P(1) and P(3), and  $112 - 114^\circ$  for atoms P(2) and P(4). Thus, the linear bridging  $\text{Ph}_2\text{PC}\equiv\text{CPh}_2$  ligand shows the greatest strain about the phosphorus atoms



with angles *ca.* 10° greater than an ideal tetrahedron whilst the non-linear bridging Ph<sub>2</sub>PC≡CPh<sub>2</sub> ligand has less strain with angles *ca.* 5° greater.

The C≡C bond lengths found in *cis*-[Ru(acac)<sub>2</sub>(μ-Ph<sub>2</sub>PC≡CPh<sub>2</sub>)<sub>2</sub>] (1.179(6) - 1.190(6) Å) are similar to those found in *cis*-[Mo(CO)<sub>4</sub>]<sub>2</sub>(μ-Ph<sub>2</sub>PC≡CPh<sub>2</sub>)<sub>2</sub>] (1.188(6) and 1.192(6) Å),<sup>26</sup> [Os<sub>3</sub>(CO)<sub>11</sub>]<sub>2</sub>(μ-Ph<sub>2</sub>PC≡CPh<sub>2</sub>)<sub>2</sub>] (1.22(2) Å),<sup>27</sup> [CpMn(CO)<sub>2</sub>]<sub>2</sub>(μ-Ph<sub>2</sub>PC≡CPh<sub>2</sub>) (1.199(5) Å),<sup>13</sup> [Pd<sub>2</sub>Cl<sub>4</sub>(μ-Ph<sub>2</sub>PC≡CPh<sub>2</sub>)<sub>2</sub>] (1.199(4) Å)<sup>19</sup> and [Pt<sub>2</sub>Cl<sub>4</sub>(μ-Ph<sub>2</sub>PC≡CPh<sub>2</sub>)<sub>2</sub>] (1.16(2) and 1.22(2) Å)<sup>19</sup> but differ slightly from [Pt<sub>2</sub>I<sub>4</sub>(μ-Ph<sub>2</sub>PC≡CPh<sub>2</sub>)<sub>2</sub>] (1.13(2) and 1.21(2) Å),<sup>19</sup> [Fe<sub>3</sub>(CO)<sub>9</sub>(μ<sub>3</sub>-CMe)](Ph<sub>2</sub>PC≡CPh<sub>2</sub>)[CpFe(CO)<sub>2</sub>] (1.210(4) and 1.250(5) Å)<sup>20</sup> and [Ru<sub>3</sub>(μ-H)(μ<sub>3</sub>-C≡CBu<sup>t</sup>)(CO)<sub>8</sub>]<sub>2</sub>(μ-Ph<sub>2</sub>PC≡CPh<sub>2</sub>)<sub>2</sub>].<sup>28</sup>

**Figure 5.4:** Chem3D diagram of *cis*-[Ru(acac)<sub>2</sub>(μ-Ph<sub>2</sub>PC≡CPh<sub>2</sub>)<sub>2</sub>] viewed down the Ru - Ru axis (acac and phenyl carbon atoms have been omitted for clarity).





## 5.2 Electrochemical Studies

The cyclic and AC voltammograms of the complexes *trans*-[Ru(acac)<sub>2</sub>(Ph<sub>2</sub>PC≡CR)<sub>2</sub>] (R = H, Me, Ph) and *cis*-[Ru(acac)<sub>2</sub>(Ph<sub>2</sub>PC≡CR)<sub>2</sub>] (R = Me, Ph) show fully reversible E<sub>1/2</sub>(Ru<sup>3+/2+</sup>) couples between +0.09 and +0.49 V (*vs* Ag/AgCl) in CH<sub>2</sub>Cl<sub>2</sub> at room temperature (see Table 5.11). The measured potentials for the *trans* analogues are similar to those of *trans*-[Ru(acac)<sub>2</sub>(PPh<sub>2</sub>Me)<sub>2</sub>] (+0.04 V, see Table 1.9), *trans*-[Ru(acac)<sub>2</sub>(PPh<sub>3</sub>)<sub>2</sub>] (+0.07 V, see Table 1.9) and *trans*-[Ru(acac)<sub>2</sub>(P(OCH<sub>3</sub>)<sub>3</sub>)<sub>2</sub>] (+0.22 V, see Table 1.9). The *cis* complexes are more difficult to oxidise than the *trans* by *ca.* 0.3 V, the potentials being similar to those of *cis*-[Ru(acac)<sub>2</sub>L<sub>2</sub>] (L = PPh<sub>2</sub>Me, PPh<sub>3</sub>) (see Table 1.9). The cyclic and AC voltammograms of the binuclear complex *cis*-[Ru(acac)<sub>2</sub>(Ph<sub>2</sub>PC≡CPh<sub>2</sub>)<sub>2</sub>] show two reversible oxidation potentials at +0.60 and +0.90V(*vs* Ag/AgCl), attributable to the sequential oxidation of the two metal centres Ru(II/II) → Ru(II/III) and Ru(II/III) → Ru(III/III) (see Chapter 3). The Ru(II/II) → Ru(II/III) potential is *ca.* 150 mV higher than that of the Ru(II) → Ru(III) potentials of *cis*-[Ru(acac)<sub>2</sub>(Ph<sub>2</sub>PC≡CR)<sub>2</sub>], indicative of the electron-withdrawing influence of the adjacent [Ru(acac)<sub>2</sub>(PPh<sub>2</sub>)<sub>2</sub>] centre.

**Table 5.11:** Oxidation potentials of bis(alkynylphosphine) complexes measured at a scan rate of 100 mVs<sup>-1</sup> and +20 °C in CH<sub>2</sub>Cl<sub>2</sub>.

Complex	Geometric isomer	E <sub>1/2</sub> (Ru <sup>3+/2+</sup> ) (V <i>vs</i> Ag/AgCl)
[Ru(acac) <sub>2</sub> (Ph <sub>2</sub> PC≡CH) <sub>2</sub> ]	<i>trans</i>	+0.16
[Ru(acac) <sub>2</sub> (Ph <sub>2</sub> PC≡CMe) <sub>2</sub> ]	<i>trans</i>	+0.09
	<i>cis</i>	+0.45
[Ru(acac) <sub>2</sub> (Ph <sub>2</sub> PC≡CPh) <sub>2</sub> ]	<i>trans</i>	+0.12
	<i>cis</i>	+0.49
[Ru(acac) <sub>2</sub> (Ph <sub>2</sub> PC≡CPh <sub>2</sub> ) <sub>2</sub> ]	<i>cis</i>	+0.60 (II/III), +0.90 (III/III)

## 5.3 Electronic Spectra

The electronic (UV-Vis) spectra of the complexes *cis* and *trans*-[Ru(acac)<sub>2</sub>(Ph<sub>2</sub>PC≡CMe)<sub>2</sub>] and the binuclear complex *cis*-[Ru(acac)<sub>2</sub>(Ph<sub>2</sub>PC≡CPh)<sub>2</sub>]<sub>2</sub>, dissolved in a standard electrolyte solution, show the expected bands due to the Ru(II) → acac π\* transition as well as the acac π → acac π\* transition (see Table 5.12). Above *ca.* 30000 cm<sup>-1</sup> the π → π\* transitions of the phenyl rings broaden or hide the acac transitions.<sup>12,42</sup> Applying a potential of *ca.* 300 mV greater than the previously measured E<sub>1/2</sub>(Ru<sup>3/2+</sup>) values results in the loss of these bands and the appearance of new bands consistent with the presence of a ruthenium (III) species (see Table 5.13). After the complexes had been exhaustively oxidised, the original spectra were re-generated after applying a potential of *ca.* 300 mV lower than the corresponding E<sub>1/2</sub>(Ru<sup>3/2+</sup>) values.

The one-electron anodic electrolysis (E<sub>applied</sub> = +0.75 V *vs* Ag/AgCl) of the binuclear complex *cis*-[Ru(acac)<sub>2</sub>(Ph<sub>2</sub>PC≡CPh)<sub>2</sub>]<sub>2</sub> resulted in the formation of *cis*-[Ru<sup>II/III</sup>(acac)<sub>2</sub>(Ph<sub>2</sub>PC≡CPh)<sub>2</sub>]<sub>2</sub><sup>+</sup>. This mixed valence species shows the characteristic Ru(III) → acac π\* transition MLCT [13800<sub>Λ</sub> cm<sup>-1</sup> (ε = 4400 L mol<sup>-1</sup> cm<sup>-1</sup>) and 16200 cm<sup>-1</sup> (ε = 4400 L mol<sup>-1</sup> cm<sup>-1</sup>)]; however, no intervalence band between 6000 - 10000 cm<sup>-1</sup> was detected suggesting that the mixed valence species has a localised structure.<sup>43</sup> This was confirmed by the second one-electron oxidation (E<sub>applied</sub> = +1.10 V *vs* Ag/AgCl) of the mixed-valence complex formed *in situ*, which caused the intensity of the Ru(III) → acac π\* transition MLCT to double (see Table 5.13). Changes in the band positions above 30000 cm<sup>-1</sup> were also observed, probably reflecting the fact that only one chromophore was present for the Ru(III/III) species. The changes in the electronic spectrum after both anodic electrolytic processes were found to be reversible when the species were reduced.

**Table 5.12:** Principal electronic band maxima (in  $\text{cm}^{-1}$ ) for both isomers of  $[\text{Ru}^{\text{II}}(\text{acac})_2(\text{Ph}_2\text{PC}\equiv\text{CMe})_2]$  and  $\text{cis}-\{[\text{Ru}^{\text{II}}(\text{acac})_2(\text{Ph}_2\text{PC}\equiv\text{CPh}_2)]_2\}$  (figures in brackets are the molar absorptivity in  $\text{L mol}^{-1} \text{cm}^{-1}$ ).

COMPLEX	MLCT		acac $\pi \rightarrow$ acac $\pi^*$	$E_{1/2}(\text{Ru}^{3+/2+})$ (V vs Ag/AgCl)
	$\nu_1$	$\nu_2$		
<i>trans</i> - $[\text{Ru}(\text{acac})_2(\text{Ph}_2\text{PC}\equiv\text{CMe})_2]$	28100 (5900)	27000	35900 (15500)	+0.09
<i>cis</i> - $[\text{Ru}(\text{acac})_2(\text{Ph}_2\text{PC}\equiv\text{CMe})_2]$	30000 (6900)	-	36700 (14400)	+0.45
<i>cis</i> - $\{[\text{Ru}(\text{acac})_2(\text{Ph}_2\text{PC}\equiv\text{CPh}_2)]_2\}$	31700 (12700)	-	36300 (23400)	+0.60

**Table 5.13:** Principal electronic band maxima (in  $\text{cm}^{-1}$ ) for both isomers of  $[\text{Ru}^{\text{III}}(\text{acac})_2(\text{Ph}_2\text{PC}\equiv\text{CMe})_2]$  and  $\text{cis}-\{[\text{Ru}^{\text{III}}(\text{acac})_2(\text{Ph}_2\text{PC}\equiv\text{CPh}_2)]_2\}$  (figures in brackets are the molar absorptivity in  $\text{L mol}^{-1} \text{cm}^{-1}$ ).

COMPLEX	MLCT		MLCT	acac $\pi$ $\rightarrow$ acac $\pi^*$	$E_{1/2}$ ( $\text{Ru}^{3+/2+}$ ) (V vs Ag/AgCl)
	$\nu_3$	$\nu_4$			
<i>trans</i> - $[\text{Ru}^{\text{III}}(\text{acac})_2(\text{Ph}_2\text{PC}\equiv\text{CMe})_2]$	14900 (1300)	-	32100 (21700)	34200 (19500)	+0.09
<i>cis</i> - $[\text{Ru}^{\text{III}}(\text{acac})_2(\text{Ph}_2\text{PC}\equiv\text{CMe})_2]$	15000 (2300)	-	33500 (8500)		+0.45
<i>cis</i> - $\{[\text{Ru}^{\text{III}}(\text{acac})_2(\text{Ph}_2\text{PC}\equiv\text{CPh}_2)]_2\}$	13800 (4400)	16200 (4400)	33300 (16500)		+0.90

#### 5.4 Chemical Oxidation

Addition of a slight excess of  $\text{AgPF}_6$  to an orange solution of *trans*- $[\text{Ru}^{\text{II}}(\text{acac})_2(\text{Ph}_2\text{PC}\equiv\text{CR})_2]$  ( $\text{R} = \text{H}, \text{Me}$ ) at room temperature results in the formation of the green complexes *trans*- $[\text{Ru}^{\text{III}}(\text{acac})_2(\text{Ph}_2\text{PC}\equiv\text{CR})_2][\text{PF}_6]$  ( $\text{R} = \text{H}, \text{Me}$ ) in yields of *ca.* 90%. These green solids were characterised by elemental

analysis, cyclic and AC voltammetric studies, IR spectroscopy, mass spectroscopy, EPR spectroscopy and in the case of *trans*-[Ru<sup>III</sup>(acac)<sub>2</sub>(Ph<sub>2</sub>PC≡CMe)<sub>2</sub>][PF<sub>6</sub>], an X-ray crystallographic study (see below). The chemical oxidation of *trans*-[Ru<sup>II</sup>(acac)<sub>2</sub>(Ph<sub>2</sub>PC≡CPh)<sub>2</sub>] has not been investigated. Addition of approximately one equivalent of AgPF<sub>6</sub> to a yellow solution of *cis*-[Ru<sup>II</sup>(acac)<sub>2</sub>(Ph<sub>2</sub>PC≡CR)<sub>2</sub>] (R = Me, Ph) under analogous conditions results in the formation of deep blue solutions. However, neither of these complexes have been isolated as pure crystalline solids.

The highest detectable ion in the +ve FAB mass spectra is due to the parent cation [Ru<sup>III</sup>(acac)<sub>2</sub>(Ph<sub>2</sub>PC≡CR)<sub>2</sub>]<sup>+</sup> and ions associated with the loss of one phosphine (see Table 5.14). The IR spectra of *trans*-[Ru<sup>III</sup>(acac)<sub>2</sub>(Ph<sub>2</sub>PC≡CR)<sub>2</sub>][PF<sub>6</sub>] (R = H, Me) shows either two strong bands or one strong band with a shoulder on the high-energy side between 1560 - 1510 cm<sup>-1</sup>, whose position and intensity are characteristic of bidentate, O-bonded acac for the chelated N-donor alkene and alkyne complexes *cis*-[Ru(acac)<sub>2</sub>LL'].<sup>32,44</sup> The presence of the [PF<sub>6</sub>]<sup>-</sup> anion for both isolated Ru(III) compounds was confirmed by the bands belonging to the IR active ν<sub>3</sub> and ν<sub>4</sub> valence vibrations of the anion found at *ca.* 840 and 558 cm<sup>-1</sup>, respectively.<sup>33</sup> A strong absorption between 2201 - 2059 cm<sup>-1</sup> corresponds to the uncoordinated ν(C≡C) band (see Table 5.15).

**Table 5.14:** Positive FAB mass spectral data of the complexes *trans*-[Ru(acac)<sub>2</sub>L<sub>2</sub>][PF<sub>6</sub>].

Complex	m/z	Assignment	Rel. Int. (%)
[Ru <sup>III</sup> (acac) <sub>2</sub> (Ph <sub>2</sub> PC≡CH) <sub>2</sub> ] <sup>+</sup>	720.2	{Ru(acac) <sub>2</sub> (Ph <sub>2</sub> PC≡CH) <sub>2</sub> } <sup>+</sup>	25
	510.2	{Ru(acac) <sub>2</sub> (Ph <sub>2</sub> PC≡CH)} <sup>+</sup>	100
[Ru <sup>III</sup> (acac) <sub>2</sub> (Ph <sub>2</sub> PC≡CMe) <sub>2</sub> ] <sup>+</sup>	748.2	{Ru(acac) <sub>2</sub> (Ph <sub>2</sub> PC≡CMe) <sub>2</sub> } <sup>+</sup>	30
	649.1	{Ru(acac)(Ph <sub>2</sub> PC≡CMe) <sub>2</sub> } <sup>+</sup>	10
	524.1	{Ru(acac) <sub>2</sub> (Ph <sub>2</sub> PC≡CMe)} <sup>+</sup>	100

**Table 5.15:** IR spectral data (in  $\text{cm}^{-1}$ ) for the complexes *trans*- $[\text{Ru}^{\text{III}}(\text{acac})_2(\text{Ph}_2\text{PC}\equiv\text{CR})_2][\text{PF}_6]$  ( $R = \text{H}, \text{Me}$ ) (KBr).

Complex	$\nu(\text{acac})$	$\nu(\text{C}\equiv\text{C})$	$\nu(\text{PF}_6)$	
			$\nu_3$	$\nu_4$
$[\text{Ru}^{\text{III}}(\text{acac})_2(\text{Ph}_2\text{PC}\equiv\text{CH})_2]^+$	1538, 1520	2059	841	558
$[\text{Ru}^{\text{III}}(\text{acac})_2(\text{Ph}_2\text{PC}\equiv\text{CMe})_2]^+$	1520	2201	840	558

Cyclic and AC voltammograms of the green complexes indicate that *trans* to *cis* isomerisation has not occurred during the chemical oxidation process as the measured  $E_{1/2}(\text{Ru}^{3+/2+})$  potentials do not differ from those of the starting complexes (see Table 5.11). The EPR spectra recorded as frozen solutions in 0.5 M  $[\text{Bu}^n_4\text{N}][[\text{PF}_6]/\text{CH}_2\text{Cl}_2]$  show three  $g$  values (see Figure 5.4 and Table 5.16).

The features of the EPR spectra are consistent with axial symmetry  $C_{4v}$ . Since *trans*- $[\text{Ru}(\text{acac})_2(\text{Ph}_2\text{PC}\equiv\text{CH}_3)_2]$  belongs to the  $C_{4v}$  point group (ignoring the bidentate ligand backbone), the EPR spectra also suggest that the coordination sphere has remained unchanged during the oxidation process. These results indicate that the cations generated by oxidation are typical of ruthenium(III) and are not ruthenium(II) complexes which contain a cationic ligand radical, for which a  $g$ -value close to the free-electron value (2.00) would be expected.<sup>44</sup>

Although three resonances were found in the EPR spectra, tetragonal distortion is thought to have occurred with the  $g_{\parallel}$  occupying the lowest value and two closely resonances corresponding to  $g_{\perp}$  (see Chapter 3). Similar spectra were recorded for *trans*- $[\text{Ru}(\text{acac})_2\text{L}_2]^+$  ( $\text{L} = \text{PPh}_3, \text{CNBu}^t$ ).<sup>45</sup> The measurable splitting of  $g_{\perp}$  implies that there is also a slight rhombic distortion, most likely due to the Orgel effect of bidentate ligands.<sup>46-48</sup> The Orgel effect allows for the fact that the two donor atoms on one ligand are not completely independent of each other and expressed in a rhombic distortion of *trans*- or *cis*- $\text{MX}_4\text{L}_2$  when the chelating ligands (AA) replace X

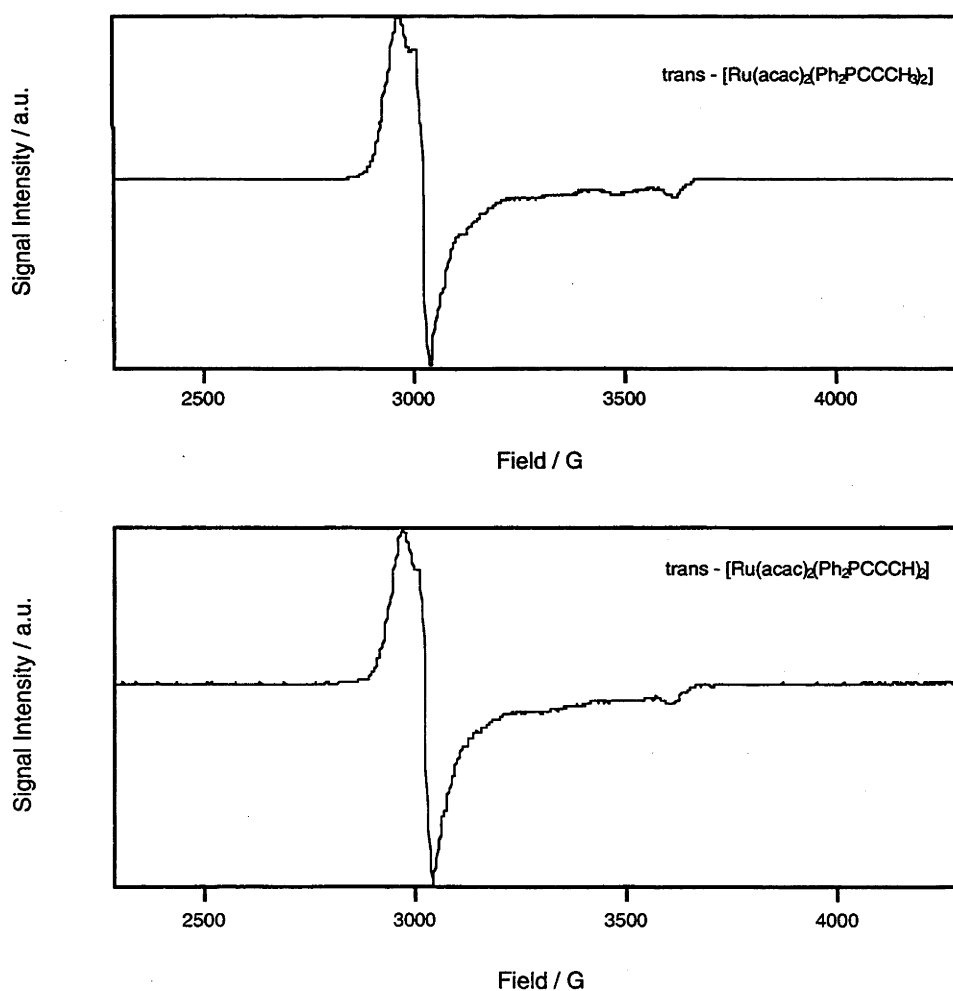
to give  $M(AA)_2L_2$ . EPR spectra recorded for the complexes *trans*- $[Ru(NH_3)_4\{P(OEt)_3\}(H_2O)][CF_3SO_3]_3$ <sup>49</sup> and *trans*- $[Ru(NH_3)_4\{P(OEt)_3\}_2][CF_3SO_3]_3$ <sup>50</sup> show a similar tetragonal distortion but there was no splitting of the  $g_{\perp}$  resonance.

**Table 5.16:** *g*-Values for some *trans*- $[Ru^{III}(acac)_2L_2][PF_6]$  complexes.

COMPLEX	$g_1$	$g_2$	$g_3$
<i>trans</i> - $[Ru^{III}(acac)_2(PPh_2PC\equiv CH)_2]^+$	2.27	2.23	1.86
<i>trans</i> - $[Ru^{III}(acac)_2(PPh_2PC\equiv CMe)_2]^+$	2.26	2.22	1.86
<i>trans</i> - $[Ru^{III}(acac)_2(PPh_3)_2]^+$ a	2.28	2.23	1.84
<i>trans</i> - $[Ru^{III}(acac)_2(Bu^tNC)_2]^+$ a	2.24	2.20	1.89

a) recorded in 1:1  $CH_2Cl_2$ /toluene at 120 K, taken from ref. 45.

**Figure 5.4:** EPR Spectra of the complexes *trans*- $[Ru^{III}(acac)_2(PPh_2PC\equiv CR)_2][PF_6]$  ( $R = H, Me$ ) recorded as a frozen glass in 0.5 M  $[Bu^t_4N][PF_6]/CH_2Cl_2$  at 4.7 K.



The structure of *trans*-[Ru<sup>III</sup>(acac)<sub>2</sub>(Ph<sub>2</sub>PC≡CMe)<sub>2</sub>][PF<sub>6</sub>] was confirmed by an X-ray crystallographic study. The molecular structure and selected metrical parameters are shown in Figure 5.5 and Table 5.17, respectively. Crystal and refinement data of the isomers, together with the full set of interatomic distances and angles, are given in Appendix A.18. Two molecules of CH<sub>2</sub>Cl<sub>2</sub> co-crystallised in the unit cell per molecule of ruthenium.

The Ru-O distances characterising the coordination of the acetylacetonato anion are 2.003(3) and 2.011(3) Å. These distances, which are very similar to the analogous ones (*ca.* 2.00 Å) in the orthorhombic and monoclinic forms of the [Ru<sup>III</sup>(acac)<sub>3</sub>],<sup>51,52</sup> are *ca.* 0.05 Å shorter than in the parent *trans*-[Ru(acac)<sub>2</sub>(Ph<sub>2</sub>PC≡CMe)<sub>2</sub>]. They confirm the stronger coordination of acac- anions to Ru(III) than to Ru(II). The Ru-P(1) bond distance was found to be 2.393(1) Å which is *ca.* 0.06 Å longer than in the parent Ru(II) complex and may reflect the reduction in π-back-bonding ability of the Ru(III) ion.<sup>53</sup>

**Figure 5.5:** ORTEP diagram of the cation of *trans*- $[\text{Ru}^{\text{III}}(\text{acac})_2(\text{Ph}_2\text{PC}\equiv\text{CMe})_2][\text{PF}_6]$ .

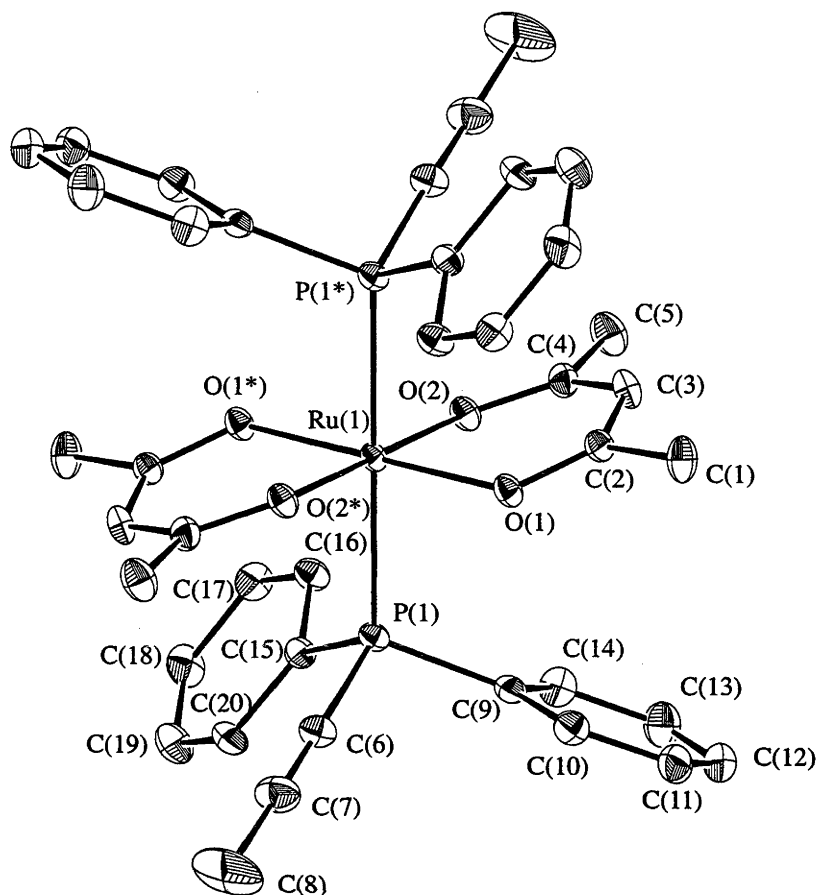


**Table 5.17:** Selected metrical parameters of *trans*- $[\text{Ru}^{\text{III}}(\text{acac})_2(\text{Ph}_2\text{PC}\equiv\text{CMe})_2][\text{PF}_6]$ .

Bond Distances (Å)			
Ru(1)-O(1)		2.011(3)	
Ru(1)-O(2)		2.003(3)	
Ru(1)-P(1)		2.393(1)	
Bond Angles (°)			
O(1)-Ru(1)-O(1) <sup>a</sup>	180.0	O(1)-Ru(1)-P(1)	89.64(8)
O(1)-Ru(1)-O(2)	90.3(1)	O(1) <sup>a</sup> -Ru(1)-P(1)	90.36(8)
O(1)-Ru(1)-O(2) <sup>a</sup>	89.7(1)	O(2)-Ru(1)-P(1)	88.88(9)
O(2)-Ru(1)-O(2) <sup>a</sup>	180.0	O(2) <sup>a</sup> -Ru(1)-P(1)	91.12(9)
P(1)-Ru(1)-P(1) <sup>a</sup>	180.0		



## 5.5 Discussion

The ligands  $\text{Ph}_2\text{PC}\equiv\text{CR}$  ( $\text{R} = \text{H}, \text{Me}, \text{Ph}$ ) form the complexes  $[\text{Ru}(\text{acac})_2(\text{Ph}_2\text{PC}\equiv\text{CR})_2]$  similar to those formed by other monodentate P-donors.<sup>31</sup> In most cases these exist as *trans*- and *cis*-isomers, the latter being, as usual, thermodynamically the more stable. In no case was evidence found for coordination of the triple bond.

The complexes show a reversible  $\text{Ru}^{3+}/2+$  couple at room temperature. The  $E_{1/2}$ -values, are in the range  $+0.09 - +0.16 \text{ V}$  (*vs*  $\text{Ag}/\text{AgCl}$ ) (*trans*) and  $+0.45 - +0.49 \text{ V}$  (*vs*  $\text{Ag}/\text{AgCl}$ ) (*cis*), these values being consistently *ca.* 100 mV more positive than the values for the corresponding  $\text{PPh}_3$  and  $\text{PMePh}_2$  complexes. This trend indicates that there may be an electron-withdrawing influence of the alkynyl substituent that slightly stabilizes the  $\text{Ru}(\text{II})$  relative to the  $\text{Ru}(\text{III})$  oxidation state. As in the case of the complexes with other monodentate P-donors, the redox process occurs with retention of the geometrical configuration at the metal atom.

The trends in the M-O and M-P distances in *trans*- and *cis*- $[\text{Ru}(\text{acac})_2(\text{Ph}_2\text{PC}\equiv\text{CMe})_2]$  are similar to those in *trans*- and *cis*- $[\text{Ru}(\text{acac})_2(\text{PPh}_2\text{Me})_2]$ .<sup>31</sup> Likewise, the M-O and M-P distances in *trans*- $[\text{Ru}(\text{acac})_2(\text{Ph}_2\text{PC}\equiv\text{CMe})_2][\text{PF}_6]$  are similar to those in the chelating alkene and alkyne N-donor ligand complexes *cis*- $[\text{Ru}(\text{acac})_2(\text{LL}')][\text{SbF}_6]$ ,<sup>32,44</sup> and in the orthorhombic and monoclinic modifications of  $[\text{Ru}(\text{acac})_3]$ .<sup>51,54</sup>

The complex *cis*- $[\{\text{Ru}(\text{acac})_2(\mu\text{-Ph}_2\text{PC}\equiv\text{CPh}_2)\}_2]$  shows two fully reversible couples at room temperature separated by *ca.* 300 mV. However, the electronic spectra recorded during these oxidation processes indicate that the mixed-valence complex displays the properties found for the isolated redox centers  $\text{Ru}(\text{II})$  and  $\text{Ru}(\text{III})$ . Therefore, the mixed-valence complex *cis*- $[\{\text{Ru}^{\text{II/III}}(\text{acac})_2(\text{Ph}_2\text{PC}\equiv\text{CPh}_2)\}_2]^+$  is a Class II compound according to the Robin-Day classification<sup>55</sup> *i.e.* there is no electronic communication between

the metal centres and the observed separation of the  $E_{1/2}$ -values is probably due to electrostatic effects. The mixed valence complex is not a Class I compound for which the electronic interactions are so weak that only the properties of the isolated redox centres are observed and only the only one  $E_{1/2}(\text{Ru}^{3+/2+})$  potential would be anticipated. Similar results were found for  $[\{\text{Ru}_3(\text{CO})_{11}\}_2(\mu\text{-Ph}_2\text{PC}\equiv\text{CPh}_2)]$ ,<sup>29</sup> except that fast chemical decomposition of the reduced species occurred so the cyclic voltammograms were irreversible and any weak interactions could not be detected.

## 5.6 References

- (1) Berau, G.; Carty, A. J.; Chieh, P. C.; Patel, H. A. *J. Chem. Soc., Dalton Trans.* **1973**, 488.
- (2) Wong, Y. S.; Jacobson, S.; Chieh, P. C.; Carty, A. J. *Inorg. Chem.* **1974**, *13*, 284.
- (3) Hogarth, G.; Taylor, N. J.; Carty, A. J.; Meyer, A. *Chem. Commun.* **1988**, 834.
- (4) Gaye, M.; Demerseman, B.; Dixneuf, P. H. *J. Organomet. Chem.* **1992**, *424*, 65.
- (5) Imhof, W.; Eber, B.; Huttner, G.; Emmerich, C. *J. Organomet. Chem.* **1993**, *447*, 21.
- (6) Moldes, I.; de la Encarnación, E.; Ros, J.; Alaverz-Larena, A.; Piniella, J. F. *J. Organomet. Chem.* **1998**, *566*, 165.
- (7) Louattani, E.; Lledós, A.; Suades, J.; Alvarez-Larena, A.; Piniella, J. F. *Organometallics* **1995**, *14*, 1053.
- (8) Carty, A. J.; Paik, H. N.; Ng, T. W. *J. Organomet. Chem.* **1974**, *74*, 279.
- (9) Sappa, E.; Predieri, G.; Tiripicchio, A.; Camellini, M. T. *J. Organomet. Chem.* **1985**, *297*, 103.
- (10) Dickson, R. S.; Simone, T. D.; Parker, R. J.; Fallon, G. D. *Organometallics* **1997**, *16*, 1531.
- (11) Ara, I.; Falvello, L. R.; Fernández, S.; Fornés, J.; Lalinde, E.; Martín, A.; Moreno, M. T. *Organometallics* **1997**, *16*, 5923.
- (12) Wheelock, K. S.; Nelson, J. H.; Jonassen, H. B. *Inorg. Chim. Acta.* **1970**, *4*, 399.
- (13) Orama, O. *J. Organomet. Chem.* **1986**, *314*, 273.
- (14) Ward, B. C.; Templeton, J. L. *J. Am. Chem. Soc.* **1980**, *102*, 1532.
- (15) Powell, A. K.; Went, M. J. *J. Chem. Soc., Dalton Trans.* **1992**, 439.
- (16) Jacobson, S.; Carty, A. J.; Mathew, M.; Palenik, G. J. *J. Am. Chem. Soc.* **1974**, *96*, 4330.

- (17) Carty, A. J.; Smith, W. F.; Taylor, N. J. J. *Organomet. Chem.* **1978**, *146*, C1.
- (18) Hota, N. K.; Patel, H. A.; Carty, A. J.; Mathew, M.; Palenik, G. J. J. *Organomet. Chem.* **1971**, *32*, C55.
- (19) Oberhauser, W.; Bachmann, C.; Stampfl, T.; Brüggeller, P. *Inorg. Chim. Acta* **1997**, *256*, 223.
- (20) Louattani, E.; Suades, J.; Urtiaga, K.; Arriortua, M. I.; Solans, X. *Organometallics* **1996**, *15*, 468.
- (21) Adams, C. J.; Bruce, M. I.; Skelton, B. W.; White, A. H. J. *Organomet. Chem.* **1993**, *447*, 91.
- (22) Carty, A. J.; Efraty, A. *Chem. Commun.* **1968**, 1559.
- (23) Carty, A. J.; Ng, T. W. *Chem. Commun.* **1970**, 149.
- (24) Anderson, W. A.; Carty, A. J.; Efraty, A. *Can. J. Chem.* **1969**, *47*, 3361.
- (25) Carty, A. J.; Efraty, A. *Can. J. Chem.* **1968**, *46*, 1598.
- (26) Hogarth, G.; Norman, T. *Polyhedron* **1996**, *15*, 2859.
- (27) Amoroso, A. J.; Johnson, B. F. G.; Lewis, J.; Massey, A. D.; Raithby, P. R.; Wong, W. T. J. *Organomet. Chem.* **1992**, *440*, 219.
- (28) Bruce, M. I.; Humphrey, P. A.; Skelton, B. W.; White, A. H. *Aust. J. Chem.* **1997**, *50*, 535.
- (29) Osella, D.; Hanzlík, J. *Inorg. Chim. Acta* **1993**, *213*, 311.
- (30) Bennett, M. A.; Coble, C. J.; Rae, A. D.; Wenger, E.; Willis, A. C. *Organometallics* **2000**, *19*, 1522.
- (31) Bennett, M. A.; Chung, G.; Hockless, D. C. R.; Neumann, H.; Willis, A. C. *J. Chem. Soc., Dalton Trans.* **1999**, 3451.
- (32) Bennett, M. A.; Heath, G. A.; Hockless, D. C. R.; Kovacic, I.; Willis, A. C. *Organometallics* **1998**, *17*, 5867.
- (33) Nakamoto, K. *Infrared and Raman Spectra of Inorganic and Coordination Compounds*; 4th ed.; Wiley: New York, 1986.

- (34) Johnson, D. K.; Rukachaisirikul, J.; Sun, Y.; Taylor, N. J.; Carty, A. J.; Carty, A. J. *Inorg. Chem.* **1993**, *32*, 5544.
- (35) Jia, G.; Puddephatt, R. J.; Vittal, J. J. *J. Organomet. Chem.* **1993**, *449*, 211.
- (36) Carty, A. J.; Efraty, A. *Inorg. Chem.* **1969**, *8*, 543.
- (37) Mathais, R.; Mathis, M. B. E. F. *J. Mol. Structure* **1968**, *1*, 481.
- (38) Bestmann, H. J.; Behl, H.; Bremer, M. *Angew. Chem. Int. Ed. Engl.* **1989**, *28*, 1219.
- (39) Bart, J. C. J. *Acta Crystallogr., Sect. B* **1969**, *25*, 489.
- (40) Yuan, Z.; Taylor, N. J.; Sun, Y.; Marder, T. B.; Williams, I. D.; Cheng, L. *J. Organomet. Chem.* **1993**, *449*, 27.
- (41) Goldberg, S. Z.; Duesler, E. N.; Raymond, K. N. *Inorg. Chem.* **1972**, *11*, 1397.
- (42) Silverstein, R. M.; Bassler, G. C.; Morrill, T. C. *Spectrometric Identification of Organic Compounds*; 5th ed.; John Wiley and Sons: New York, 1991, p 306.
- (43) Astruc, D. *Electron Transfer and Radical Processes in Transition Metal Chemistry*; VCH: New York, 1995, p 98.
- (44) Bennett, M. A.; Heath, G. A.; Hockless, D. C. R.; Kovacic, I.; Willis, A. C. *J. Am. Chem. Soc.* **1998**, *120*, 932.
- (45) Wallace, L. PhD Thesis, ANU, 1991.
- (46) Orgel, L. E. *J. Chem. Soc.* **1961**, 3683.
- (47) Sugano, S.; Tanabe, Y.; Kamimura, H. *Multiplets of Transition Metal Ions in Crystals*; Academic Press: New York, 1970.
- (48) Ceulemans, A.; Dendooven, M.; Vanquickenborne, L. G. *Inorg. Chem.* **1985**, *24*, 1153.
- (49) de Rezende, N. M. S.; Martins, S. d. C.; Marinho, L. A.; Santos, J. A. V. d.; Tabak, M.; Perussi, J. R.; Franco, D. W. *Inorg. Chim. Acta* **1991**, *182*, 87.
- (50) Mazzetto, S. E.; Rodrigues, E.; Franco, D. W. *Polyhedron* **1993**, *12*, 971.

- (51) Knowles, T. S.; Howlin, B. J.; Jones, J. R.; Povey, D. C.; Amodio, C. A. *Polyhedron* **1993**, *12*, 2921.
- (52) Knowles, T. S.; Howells, M. E.; Howlin, B. J.; Smith, G. W.; Amodio, C. A. *Polyhedron* **1994**, *13*, 2197.
- (53) Taube, H. In *Survey of Progress in Chemistry*; Scott, A. F., Ed.; Academic Press: 1973; Vol. 6; p 45.
- (54) Matsuzawa, H.; Ohashi, Y.; Kaizu, Y.; Kobayashi, H. *Inorg. Chem.* **1988**, *27*, 2981.
- (55) Robin, M. B.; Day, P. *Adv. Inorg. Chem. Radiochem.* **1967**, *10*, 247.

## *Conclusions*

## 6.1 Conclusions

All of the aims of this study have been met with varying degrees of success, although there many areas which need to be investigated<sup>8</sup> further. The complex *cis*-[Ru(acac)<sub>2</sub>(η<sup>2</sup>-C<sub>2</sub>H<sub>4</sub>)<sub>2</sub>] has been isolated and characterised, and its structure in the solid state has been established. This result provides support for the formulation of the much more labile *cis*-cyclooctene analogue, which can only be made *in situ*. Apart from ethene or cyclooctene, various other alkenes and disubstituted alkynes probably can be coordinated to ruthenium using this methodology. Depending on the reaction conditions used, one ethene ligand may be replaced by certain monodentate ligands (L) to form complexes of the type *cis*-[Ru(acac)<sub>2</sub>(η<sup>2</sup>-C<sub>2</sub>H<sub>4</sub>)L] (L = NH<sub>3</sub>, MeCN, C<sub>5</sub>H<sub>5</sub>N, SbPh<sub>3</sub>, PPr<sup>*i*</sup><sub>3</sub>, PCy<sub>3</sub>). These complexes are probably formed via the complexes *trans*-[Ru(acac)<sub>2</sub>(η<sup>2</sup>-C<sub>2</sub>H<sub>4</sub>)L], which can only be detected or isolated in the case of L = NH<sub>3</sub>, C<sub>5</sub>H<sub>5</sub>N. Isolation of the kinetic products *trans*-[Ru(acac)<sub>2</sub>(η<sup>2</sup>-C<sub>2</sub>H<sub>4</sub>)L] (L = NH<sub>3</sub>, C<sub>5</sub>H<sub>5</sub>N) provides important information about the likely course of the replacement reaction of *cis*-[Ru(acac)<sub>2</sub>(η<sup>2</sup>-alkene)<sub>2</sub>] (alkene = C<sub>2</sub>H<sub>4</sub>, C<sub>8</sub>H<sub>14</sub>). In the first step, alkene dissociation forms the five-coordinate, square pyramidal species [Ru(acac)<sub>2</sub>(η<sup>2</sup>-alkene)] and ligand L then adds preferentially to the vacant coordination site. Isomerization of *trans*-[Ru(acac)<sub>2</sub>(η<sup>2</sup>-C<sub>2</sub>H<sub>4</sub>)L] to the corresponding *cis*-complexes also occurs with initial loss of the alkene to reform the five-coordinate species square pyramidal [Ru(acac)<sub>2</sub>L], which rearranges to a trigonal bipyramidal species; re-coordination of the alkene results in the formation of the thermodynamically favoured *cis*-isomer. There is spectroscopic evidence for the five-coordinate species [Ru(acac)<sub>2</sub>PCy<sub>3</sub>], which is formed when *trans*-[Ru(acac)<sub>2</sub>(PCy<sub>3</sub>)<sub>2</sub>] or *cis*-[Ru(acac)<sub>2</sub>(η<sup>2</sup>-C<sub>2</sub>H<sub>4</sub>)(PCy<sub>3</sub>)] are dissolved in THF, although the possibility that it is a six-coordinate solvento species *trans*-[Ru(acac)<sub>2</sub>(PCy<sub>3</sub>)(THF)] cannot be excluded.



Since the coordinated ethene of *cis*-[Ru(acac)<sub>2</sub>(η<sup>2</sup>-C<sub>2</sub>H<sub>4</sub>)(PR<sub>3</sub>)] (R = Pr<sup>i</sup>, Cy) is quite labile, these complexes may also prove to be useful starting materials. The complexes *cis*-[Ru(acac)<sub>2</sub>(PR<sub>3</sub>)<sub>2</sub>] (R = Pr<sup>i</sup>, Cy) are also potential starting materials as one PR<sub>3</sub> ligand may be replaced by 1-alkynes or CO to form *cis*-[Ru(acac)<sub>2</sub>(PR<sub>3</sub>)<sub>2</sub>]{=C=C(H)R'}] (R' = Ph, SiMe<sub>3</sub>) and *trans*-[Ru(acac)<sub>2</sub>(PR<sub>3</sub>)(CO)], respectively. Disubstituted alkynes do not displace ethene from these complexes with heating, but dinitrogen reversibly displaces ethene from *cis*-[Ru(acac)<sub>2</sub>(η<sup>2</sup>-C<sub>2</sub>H<sub>4</sub>)(PPr<sup>i</sup><sub>3</sub>)] to form the binuclear complex *cis*-[Ru(acac)<sub>2</sub>(PPr<sup>i</sup><sub>3</sub>)<sub>2</sub>](μ-N<sub>2</sub>).

Although the Ru(III) ion undoubtedly has a lower π-back-bonding ability than Ru(II), Ru(III)-η<sup>2</sup>-ethene complexes including the parent bis(ethene) complex *cis*-[Ru<sup>III</sup>(acac)<sub>2</sub>(η<sup>2</sup>-C<sub>2</sub>H<sub>4</sub>)<sub>2</sub>][PF<sub>6</sub>], have been detected in *ca.* -50 °C. The effect of the two acac ligands is to reduce the Ru<sup>3+/2+</sup> oxidation potentials for the ethene complexes to between +0.4 and +1.0 V (*vs* Ag/AgCl) relative to [Ru(NH<sub>3</sub>)<sub>5</sub>(η<sup>2</sup>-C<sub>2</sub>H<sub>4</sub>)]<sup>2+</sup>, [Ru(H<sub>2</sub>O)<sub>4</sub>(η<sup>2</sup>-C<sub>2</sub>H<sub>4</sub>)<sub>2</sub>]<sup>2+</sup>. These oxidised ethene complexes show no signs of isomerization by UV-Vis or EPR spectroscopy and although these species appear to be indefinitely stable at low temperatures, decomposition occurs at ambient temperatures. Despite this instability, the first Ru<sup>III</sup>-alkene complex that is not stabilised by chelation, *cis*-[Ru(acac)<sub>2</sub>(η<sup>2</sup>-C<sub>8</sub>H<sub>14</sub>)(SbPh<sub>3</sub>)][PF<sub>6</sub>], has been isolated as a deep blue solid at low temperatures. Thus, it appears that at low temperature and with a suitable choice of alkene, a range of Ru<sup>III</sup>-alkene complexes should be capable of isolation.

The last aim of this work was to investigate the reactivity of the paramagnetic ruthenium(III)-alkene and -alkyne complexes with nucleophiles. Because of the instability of most the unchelated alkene-ruthenium(III) complexes at room temperature and the lack of analogous alkyne complexes, studies have been restricted to the isolable complexes *cis*-[Ru(acac)<sub>2</sub>(*o*-H<sub>2</sub>C=C(H)C<sub>6</sub>H<sub>4</sub>NMe<sub>2</sub>)][PF<sub>6</sub>] and *cis*-[Ru(acac)<sub>2</sub>(*o*-

$\text{PhC}\equiv\text{CC}_6\text{H}_4\text{NMe}_2$ ][ $\text{PF}_6$ ] originally prepared by Kováčik in this group. These react with various neutral nucleophiles, including  $\text{PPh}_3$ ,  $\text{C}_5\text{H}_5\text{N}$ ,  $\text{Et}_2\text{HN}$  and  $\text{H}_2\text{O}$ , without displacement of the alkene or alkyne. The crystal structures of the pyridine and diethylamine adducts show that these nucleophiles have attacked one of the unsaturated carbon atoms with formation of a Ru-C  $\sigma$  bond. The reasons for the preferential attack of the nucleophile with one unsaturated carbon atom over another are not understood. However, if the synthetic difficulties in the synthesis of  $\text{Ru}^{\text{II}}$ -alkyne complexes could be overcome, nucleophilic addition reactions with these oxidised species would probably present a rich area of chemistry.

# *Experimental*

## Experimental

### 7.1 General Procedures

All operations were carried out under an argon atmosphere, unless otherwise stated using standard Schlenk techniques. Solvents were purified by standard methods. Pentane, hexane, THF, diethyl ether, benzene and toluene were pre-dried over sodium wire and distilled from sodium/benzophenone/tetraglyme under nitrogen. Dichloromethane was dried over  $\text{CaH}_2$  and distilled under nitrogen. Chlorobenzene was washed successively with concentrated  $\text{H}_2\text{SO}_4$ , aqueous  $\text{Na}_2\text{CO}_3$  and water, pre-dried over  $\text{CaSO}_4$  and distilled from  $\text{P}_2\text{O}_5$  under nitrogen.<sup>1</sup> Dried solvents were stored under nitrogen or argon in Schlenk flasks fitted with Young's taps.

Zinc dust was washed successively with dilute  $\text{H}_2\text{SO}_4$ , water and THF immediately before use. Liquid zinc amalgam (2 - 3% Zn),<sup>2</sup>  $[\text{Ru}(\text{acac})_3]$ ,<sup>3-6</sup>  $[\text{Cp}_2\text{Fe}][\text{PF}_6]$ ,<sup>7</sup> *cis*- $[\text{Ru}(\text{acac})_2(\eta^2\text{-C}_8\text{H}_{14})(\text{SbPh}_3)]$ ,<sup>8</sup> *cis*- $[\text{Ru}(\text{acac})_2(o\text{-H}_2\text{C}=\text{C}(\text{H})\text{C}_6\text{H}_4\text{NMe}_2)][\text{PF}_6]$ <sup>9</sup> and *cis*- $[\text{Ru}(\text{acac})_2(o\text{-PhC}\equiv\text{CC}_6\text{H}_4\text{NMe}_2)][\text{PF}_6]$ <sup>10</sup> were prepared according to the literature methods. The (alkynyl)diphenylphosphines  $\text{Ph}_2\text{PC}\equiv\text{CR}$  ( $\text{R} = \text{H}$ ,<sup>11</sup>  $\text{Me}$ ,<sup>12</sup>  $\text{Ph}$ <sup>12</sup>) were prepared by Dr. C. Copley (RSC); bis(diphenylphosphino)acetylene was obtained from Fluka and <sup>used</sup> as received. Industrial grade ethene (Gas Code 090), dihydrogen (Gas Code 135) and anhydrous ammonia (Gas Code 178) were used as received from BOC Gases. CO (C.P. Grade, Gas Code 156, 99.0% minimum purity) was also used as received from BOC Gases.

All reactions which involved ethene were carried out in a Lab Crest medium pressure vessel (90 mm height x 50 mm width) in a well ventilated room behind a safety screen. Reactions involving CO or dihydrogen were carried out in a fumehood and behind a safety screen if the vessel was pressurised higher than 1 bar.

Nuclear magnetic resonance spectra were recorded at 20.5 °C (unless otherwise indicated) on a Varian Gemini 300 BB or on <sup>instruments</sup> Varian VXR 300/ (1H at 300 MHz, 13C at 75.4 MHz, 31P at 121.4 MHz). Variable temperature

NMR spectra were recorded on the Varian VXR 300 instrument. The chemical shifts ( $\delta$ ) for  $^1\text{H}$  and  $^{13}\text{C}$  are given in ppm referenced to the residual protons and the carbon atoms of the deuterated solvents. The  $^{31}\text{P}$  chemical shifts are referenced to external 85%  $\text{H}_3\text{PO}_4$ . The coupling constants ( $J$ ) are given in Hertz (Hz). Infrared spectra were recorded on either a Perkin-Elmer 1800 Fourier Transform Infrared Spectrophotometer or a Perkin-Elmer Spectrum One infrared spectrometer using KBr discs or 0.1 mm path length KBr cells for the mid-IR range (4000 - 400  $\text{cm}^{-1}$ ). Fast Atom Bombardment (FAB) mass spectra were measured on a VG ZAB2-SEQ mass spectrometer using either 3-nitrobenzyl alcohol or (3-nitrophenyl)octyl ether as the matrix. The mass spectral data are presented in the relevant chapters. Microanalyses were performed by the staff of the Australian National University Analytical Services Unit, Canberra.

Cyclic voltammetry (CV) and alternating current voltammetry (ACV) measurements were performed using a PAR-170 system, linked to a Macintosh LC630 computer *via* an AD Instruments MacLab interface system. A standard three-electrode configuration was used. Standard electrolyte solutions consisted of 0.5 M  $[\text{Bu}^n_4\text{N}][\text{PF}_6]$  in  $\text{CH}_2\text{Cl}_2$ . The working electrode was a platinum disc and the auxiliary electrode was a platinum bar. The reference electrode was a Ag/AgCl electrode.<sup>13</sup> Under these conditions ferrocene was oxidised at +0.55 V. Typical scan rates for CV were 50 to 500  $\text{mVs}^{-1}$  and 20  $\text{mVs}^{-1}$  for ACV. The electrochemical vessel was a jacketted glass cell (*ca.* 5 mL). The electrolyte solutions were purged with  $\text{N}_2$  and the cell maintained under an inert atmosphere. Low-temperature measurements were performed with the jacketted glass cell connected to a Lauda RL6 cooling bath with circulating methanol. The temperature was monitored by a digital thermometer with the probe placed in the electrochemical solution. The potentials of the complexes were recorded in standard electrolyte solutions of 0.5 M  $[\text{Bu}^n_4\text{N}][\text{PF}_6]$  in  $\text{CH}_2\text{Cl}_2$  at ambient temperatures unless otherwise indicated and referenced to a Ag/AgCl

electrode. The ferrocene couple was recorded under these non-standard conditions to assess electrochemical reversibility.

The electronic spectra in the range 6000 - 45000  $\text{cm}^{-1}$  were collected from a cryogenically controlled, optically transparent thin-layer electrode (OTTLE) cell placed in the beam of either a Perkin-Elmer  $\lambda 9$  or a Cary 5E UV-Vis-NIR spectrophotometer, as described previously.<sup>13</sup> The sample solution was prepared and transferred into the sample cell in an Argon-filled M-BRAUN Labmaster 130 dry-box. The electrolysis was carried out at a potential typically 300 mV past the relevant  $E_{1/2}(\text{Ru}^{3+/2+})$  value, and continued until the spectrum ceased to change and the current decayed to a constant minimum. After completion, the potential was reset and the spectrum of the starting complex was regenerated. The observation of sharply defined isosbestic points and the full regeneration of the starting spectra were taken as evidence for chemical reversibility for the observed process.

Solid state reflectance spectra were collected with a Harrick Praying Mantis Diffuse Reflection Attachment installed in a Cary 5 UV-Vis-NIR spectrophotometer. The sample was diluted in either MgO, KCl or  $[\text{Bu}^n_4\text{N}][\text{BF}_4]$ .

Continuous wave X-band EPR spectra were collected by Dr. R. Webster (RSC, ANU) on a Bruker ESP 300e (with a frequency counter for accurate g-value measurements) spectrometer employing a rectangular TE102 cavity. The modulation frequency was set at 50-100 kHz, the microwave power to 2.0 mW (sufficiently low to avoid sample saturation), the modulation amplitude set at 5 Gauss, the time constant to 0.33 s and the sweep time 330 s. The temperature was lowered to 4.8 K using liquid He and an Oxford Instruments cryostat. The EPR spectral data are presented in chapters 3, 4 and 5.

Raman spectra were collected by Dr. V. Otieno-Alego (University of Canberra) on a Renishaw Raman system 2000 (Renishaw Plc) configured with an external Olympus BH-2 microscope and Peltier cooled (-70 °C.) CCD detector comprising ca. 400 x 600 pixels. A holographic notch filter was used as a beam splitter. The excitation source was either an air cooled 25 mW helium neon (HeNe) laser (Spectra-Physics Lasers, Inc., model 127) emitting at 632.8 nm or a Renishaw near infrared (NIR) laser diode (Renishaw Plc Transducer Systems) emitting at 780 nm. The system was set to give 3-4 cm<sup>-1</sup> spectral resolution (determined by measuring the FWHM of the laser line by curve fitting. Typically, the laser was focussed onto the sample using a x50 microscope objective and the spectra were collected using integration times ranging between 10 and 20 seconds, with 2 to 5 accumulations.

Crystal and molecular structures of the ruthenium complexes were collected and solved by Dr A. Edwards, Dr. D. C. R. Hockless and Dr. A. C. Willis (RSC ANU Canberra). The experimental conditions and methods used are described in the appendices.

### 7.2.1 Preparation of *cis*-[Ru(acac)<sub>2</sub>(C<sub>2</sub>H<sub>4</sub>)<sub>2</sub>]

Freshly activated zinc dust (2.4 g, 36.7 mmol) was mixed with [Ru(acac)<sub>3</sub>] (930 mg, 2.34 mmol) in a medium pressure vessel which was evacuated and backfilled with ethene (1 bar) three times. Freshly distilled THF (20 mL) and ca. 12 drops of deoxygenated, distilled H<sub>2</sub>O were added to the mixture via syringe. The flask was then heated to ca. 80 °C with magnetic stirring under 3 bar of ethene pressure (safety shield used when pressure of the vessel was higher than 1 bar). Within one hour, the colour of the solution changed from cherry-red to dark brown then finally orange.

After allowing the reaction vessel to cool to room temperature and reducing the ethene pressure (1 bar), the heterogenous reaction mixture was allowed to stand for ca. 10 minutes. The zinc dust quickly settled on the

bottom of the flask and the cloudy orange solution was carefully decanted into a Schlenk flask under an ethene atmosphere (1 bar). The solvent was removed *in vacuo*, leaving an orange residue. Addition of n-pentane (10 mL) resulted in an orange solution with a white colloidal suspension, presumably containing zinc(II) by-products. Filtration through a short column (*ca.* 5 x 2 cm) of neutral alumina (Activity III) under  $C_2H_4$  (1 bar) with n-pentane and then benzene gave a clear orange solution. The solvent was removed *in vacuo* and the minimum amount of n-pentane (*ca.* 5 mL) was added to re-dissolve the residue. After 2 days at  $-20^\circ C$ , 500 mg (60%) of the orange microcrystalline solid *cis*-[Ru(acac) $_2(\eta^2-C_2H_4)_2$ ] was isolated. The solid was carefully washed with cold n-pentane. Crystals suitable for X-ray diffraction studies were obtained from the slow evaporation of the supernatant.

The orange solid appears to be stable indefinitely under an argon atmosphere at *ca.* 25 °C and may also be handled for several hours in the air without any visible signs of decomposition. However, after two weeks' exposure of a sample to air a change in colour from orange to violet had occurred. The bis(ethene) complex *cis*-[Ru(acac) $_2(\eta^2-C_2H_4)_2$ ] forms stable, air-sensitive solutions in THF, benzene and toluene, but slowly decomposes in  $CH_2Cl_2$ .

Microanalysis: (Found: C, 47.06 H 5.89%.  $C_{14}H_{22}O_4Ru$  requires C, 47.31; H 6.24%). IR (KBr):  $\nu(\text{acac})$  1576 and 1515  $cm^{-1}$ . NMR ( $C_6D_5CD_3$ ):  $\delta_H$  (300 MHz) 5.24 [2 H, s, C(O)CH]; 3.85 - 3.70 [8 H, m,  $C_2$ H $_4$ ]; 1.86, 1.82 [6 H each, s, C(O)CH $_3$ ];  $\delta_C$  (75.43 MHz) 186.6, 185.1 [both s, C(O)CH $_3$ ]; 98.0 [s, C(O)CH]; 78.2 [s, C $_2$ H $_4$ ]; 27.5, 26.9 [s, C(O)CH $_3$ ].  $E_{1/2}(Ru^{3+/2+})$ : +0.95V ( $-45^\circ C$ ;  $\Delta E_p = 100$  mV).



For the following syntheses, a solution of *cis*-[Ru(acac)<sub>2</sub>(η<sup>2</sup>-C<sub>2</sub>H<sub>4</sub>)<sub>2</sub>] was prepared immediately before as outlined above and the yield was assumed to be quantitative.

### 7.2.2 Preparation of *cis*-[Ru(acac)<sub>2</sub>(η<sup>2</sup>-C<sub>2</sub>H<sub>4</sub>)(SbPh<sub>3</sub>)]

A solution of SbPh<sub>3</sub> (412 mg, 1.17 mmol) in THF (40 mL) was added dropwise to a THF solution (ca. 40 mL) of *cis*-[Ru(acac)<sub>2</sub>(η<sup>2</sup>-C<sub>2</sub>H<sub>4</sub>)<sub>2</sub>] (prepared from 500 mg [Ru(acac)<sub>3</sub>], 1.26 mmol) and stirred overnight at room temperature to give a brown solution. The solvent was removed *in vacuo*, leaving a brown residue. A yellow band was eluted first when the brown residue was chromatographed on a neutral alumina column (Activity III) with benzene or toluene. The yellow solution collected was immediately pumped to dryness to give a brownish oil. A yellow solid (537mg, 63%) that formed after stirring the brown oil in n-pentane (150 mL) for 45 minutes was isolated by filtration. An orange fraction from the chromatography was collected and discarded; a brown ring remained at the top of the column.

The <sup>1</sup>H NMR spectrum of the isolated yellow complex *cis*-[Ru(acac)<sub>2</sub>(η<sup>2</sup>-C<sub>2</sub>H<sub>4</sub>)(SbPh<sub>3</sub>)] showed the presence of a small amount of [Ru(acac)<sub>2</sub>(SbPh<sub>3</sub>)<sub>2</sub>], which could not be removed. The solid *cis*-[Ru(acac)<sub>2</sub>(η<sup>2</sup>-C<sub>2</sub>H<sub>4</sub>)(SbPh<sub>3</sub>)] appears to be very stable when exposed to air, but forms air-sensitive solutions in THF, benzene and toluene.

Microanalysis: (Found: C, 53.36; H 4.79%. C<sub>30</sub>H<sub>33</sub>O<sub>4</sub>RuSb requires C, 52.96; H 4.89%). IR (KBr): ν(acac) 1568 and 1514 cm<sup>-1</sup>. NMR (C<sub>6</sub>D<sub>6</sub>): δ<sub>H</sub> (300 MHz) 7.70-7.67 [6 H, m, *o*-SbC<sub>6</sub>H<sub>5</sub>]; 7.13-7.00 [9 H, m, *m*- and *p*-SbC<sub>6</sub>H<sub>5</sub>]; 5.30, 5.15 [1 H each, s, C(O)CH]; 4.26 - 3.99 [4 H, m, C<sub>2</sub>H<sub>4</sub>]; 2.02, 1.74, 1.69, 1.62 [3 H each, s, C(O)CH<sub>3</sub>]. δ<sub>C</sub> (75.43 MHz) 188.7, 186.8, 185.8, 185.3 [all s, C(O)CH<sub>3</sub>]; 136.6, 132.0, 129.6, 128.9 [all s, SbC<sub>6</sub>H<sub>5</sub>]; 100.2, 98.6 [both s, C(O)CH]; 57.9 [s, C<sub>2</sub>H<sub>4</sub>], 28.0, 27.9, 27.7, 27.4 [all s, C(O)CH<sub>3</sub>]. E<sub>1/2</sub>(Ru<sup>3+/2+</sup>): +0.59 V (ca. -50 °C)

### 7.2.3 Preparation of *cis*-[Ru(acac)<sub>2</sub>(η<sup>2</sup>-C<sub>2</sub>H<sub>4</sub>)(MeCN)]

A solution of *cis*-[Ru(acac)<sub>2</sub>(η<sup>2</sup>-C<sub>2</sub>H<sub>4</sub>)<sub>2</sub>] (prepared from 360 mg [Ru(acac)<sub>3</sub>], 0.90 mmol) in THF (20 mL) was stirred with acetonitrile (0.2 mL, 4.1 mmol) at room temperature overnight and the mixture evaporated to dryness. The yellow brown solid *cis*-[Ru(acac)<sub>2</sub>(η<sup>2</sup>-C<sub>2</sub>H<sub>4</sub>)(MeCN)] was isolated by filtration (250 mg, 75%) after the residue had been stirred with n-hexane (ca. 10 mL) for 20 minutes and filtered.

Solid *cis*-[Ru(acac)<sub>2</sub>(η<sup>2</sup>-C<sub>2</sub>H<sub>4</sub>)(MeCN)] appears to be stable when stored in air for several months at room temperature and readily forms yellow solutions in THF, benzene and toluene.

Microanalysis: (Found: C, 45.39; H, 5.99; N, 3.43%. C<sub>14</sub>H<sub>21</sub>NO<sub>4</sub>Ru requires C, 45.65; H, 5.75; N, 3.80%). IR (KBr): ν(N≡C) 2262 cm<sup>-1</sup>; ν(acac) 1571 and 1518 cm<sup>-1</sup>. NMR (C<sub>6</sub>D<sub>6</sub>): δ<sub>H</sub> (300 MHz) 5.50, 5.29 [1 H each, s, C(O)CH]; 4.44 - 4.37 [4 H, m, C<sub>2</sub>H<sub>4</sub>]; 2.17, 2.01, 2.00, 1.81 [3 H each, s, C(O)CH<sub>3</sub>]; 0.59 [3H, s, CH<sub>3</sub>CN]. δ<sub>C</sub> (75.43 MHz) 187.8, 186.8, 185.8, 185.3 [all s, C(O)CH<sub>3</sub>]; 99.1, 99.0 [both s, CHC(O)]; 72.5 [s, C<sub>2</sub>H<sub>4</sub>]; 28.2, 27.9, 27.7, 27.3 [all s, C(O)CH<sub>3</sub>]. E<sub>1/2</sub>(Ru<sup>3+/2+</sup>): +0.56 V (ca. -50 °C).

### 7.2.4 Preparation of *trans*-[Ru(acac)<sub>2</sub>(η<sup>2</sup>-C<sub>2</sub>H<sub>4</sub>)(NH<sub>3</sub>)]

Bubbling NH<sub>3</sub> through a solution of *cis*-[Ru(acac)<sub>2</sub>(η<sup>2</sup>-C<sub>2</sub>H<sub>4</sub>)<sub>2</sub>] (prepared from 1.254 g [Ru(acac)<sub>3</sub>], 3.15 mmol) in THF for 20 minutes formed an orange precipitate. The solvent was removed *in vacuo*. 670mg (62%) of *trans*-[Ru(acac)<sub>2</sub>(η<sup>2</sup>-C<sub>2</sub>H<sub>4</sub>)(NH<sub>3</sub>)] was isolated after the orange brown solid had been washed several times with n-hexane.

The complex *trans*-[Ru(acac)<sub>2</sub>(η<sup>2</sup>-C<sub>2</sub>H<sub>4</sub>)(NH<sub>3</sub>)] is very stable when exposed to air as a solid; the solid is insoluble in THF, benzene, toluene and n-hexane, but readily dissolves in CH<sub>2</sub>Cl<sub>2</sub>.

Microanalysis: (Found: C, 41.73; H, 6.07%. N, 4.13; C<sub>12</sub>H<sub>21</sub>NO<sub>4</sub>Ru requires C, 41.85; H, 6.15; N, 4.07%). IR (KBr): ν(NH) 3335 cm<sup>-1</sup>; ν(acac) 1568 and 1509 cm<sup>-1</sup>. NMR (CD<sub>2</sub>Cl<sub>2</sub>): δ<sub>H</sub> (300 MHz) 5.38 [2 H, s, C(O)CH]; 3.70 [4 H, s, C<sub>2</sub>H<sub>4</sub>]; 3.05 [3 H, br, NH<sub>3</sub>]; 1.91 [12 H, s, C(O)CH<sub>3</sub>]. δ<sub>C</sub> (75.43 MHz) 186.9 [s, C(O)CH<sub>3</sub>]; 99.6 [s, CHC(O)]; 72.2 [s, C<sub>2</sub>H<sub>4</sub>]; 27.8 [s, C(O)CH<sub>3</sub>]. E<sub>1/2</sub>(Ru<sup>3+/2+</sup>): +0.37 V.

### 7.2.5 Preparation of *cis*-[Ru(acac)<sub>2</sub>(η<sup>2</sup>-C<sub>2</sub>H<sub>4</sub>)(NH<sub>3</sub>)]

Bubbling NH<sub>3</sub> through a solution of *cis*-[Ru(acac)<sub>2</sub>(η<sup>2</sup>-C<sub>2</sub>H<sub>4</sub>)<sub>2</sub>] (prepared from 607 mg [Ru(acac)<sub>3</sub>], 1.52 mmol) in THF for 20 minutes results in the formation of an orange precipitate. The mixture was evaporated to dryness and the orange brown residue dissolved in CH<sub>2</sub>Cl<sub>2</sub> (ca. 2 mL) and then chromatographed on a neutral alumina column (Activity III) with CH<sub>2</sub>Cl<sub>2</sub>. A red fraction was collected first and discarded. An orange fraction was then collected and the solvent removed *in vacuo* leaving a yellow residue. Stirring the residue in n-pentane (20 mL) precipitated the required compound as a yellow brown micro-crystalline solid (230 mg, 45%). Crystals suitable for X-ray diffraction studies were obtained from the slow evaporation of the supernatant.

The yellow brown solid *cis*-[Ru(acac)<sub>2</sub>(η<sup>2</sup>-C<sub>2</sub>H<sub>4</sub>)(NH<sub>3</sub>)] is stable for several months when exposed to air at room temperature, and is also soluble in THF, benzene and toluene forming moderately air-sensitive yellow solutions.

Microanalysis: (Found: C, 41.76; H, 5.90; N, 4.07;  $C_{12}H_{21}NO_4Ru$  requires C, 41.85; H, 6.15; N, 4.07). IR (KBr):  $\nu(NH)$  3334  $cm^{-1}$ ;  $\nu(acac)$  1566 and 1509  $cm^{-1}$ . NMR ( $C_6D_6$ ):  $\delta_H$  (300 MHz) 5.28, 5.14 [1 H each, s,  $C(O)CH$ ]; 4.30 - 4.10 [4 H, m,  $C_2H_4$ ]; 2.35, 2.18, 2.02, 1.97 [3 H each, s,  $C(O)CH_3$ ]; 1.52 [3 H, br,  $NH_3$ ].  $\delta_C$  (75.43 MHz) 189.1, 185.6, 185.5, 184.0 [all s,  $C(O)CH_3$ ]; 99.1, 98.9 [both s,  $CHC(O)$ ]; 65.9 [s,  $C_2H_4$ ]; 28.1, 28.0, 27.7, 27.4 [all s,  $C(O)CH_3$ ].  $E_{1/2}(Ru^{3+/2+})$ : +0.37 V.

**7.2.6  $^{31}P\{^1H\}$  NMR Studies of the reaction of one equivalent of  $PR_3$  ( $R = Ph$ ,  $p$ -tolyl,  $Pr^i$ ,  $Cy$  and  $R' = Ph$ ,  $R'' = Me$ ) with  $cis$ - $[Ru(acac)_2(\eta^2\text{-alkene})_2]$  (alkene =  $C_2H_4$ ,  $C_8H_{14}$ )**

A typical experiment involved the preparation of fresh solutions of  $Ru(acac)_2(alkene)_2$  (alkene =  $C_2H_4$ ,  $C_8H_{14}$ ) in THF, of which aliquots were injected into a NMR tube under an inert atmosphere. These tubes were then sealed after the addition of a small amount of  $C_6D_5CD_3$ . A standard solution of  $PR_3$  in  $C_6D_5CD_3$  was also prepared. The solutions were then cooled in a dry ice/acetone slush bath. After mixing the solutions, the sample were then immediately placed into a pre-cooled NMR probe ( $-40\text{ }^\circ C$ ) and  $^{31}P\{^1H\}$  NMR spectra were recorded immediately.

**7.2.7 Preparation of  $cis$ - $[Ru(acac)_2(\eta^2-C_2H_4)(PPr^i_3)]$**

To a magnetically stirred solution of freshly prepared  $cis$ - $[Ru(acac)_2(\eta^2-C_2H_4)_2]$  (prepared from 1.0 g  $[Ru(acac)_3]$ , 2.51 mmol) in benzene (40 mL) was added  $PPr^i_3$  (0.48 mL, 2.51 mmol) at room temperature. After stirring overnight, the solution had changed colour from yellow to orange. The solvent was removed *in vacuo* and the orange residue was redissolved in *n*-pentane (*ca.* 5mL). The solution was cooled to  $-20\text{ }^\circ C$  and a red crystalline solid formed. The supernatant liquid was carefully decanted from the solid which was washed with cold *n*-pentane. The volume of supernatant was reduced to obtain a second crop of the red crystalline

material. The total amount of the solid *cis*-[Ru(acac)<sub>2</sub>(η<sup>2</sup>-C<sub>2</sub>H<sub>4</sub>)(PPr<sup>i</sup><sub>3</sub>)] isolated was 676 mg (55 %). Crystals suitable for X-ray diffraction studies were obtained from the first crystallisation.

The solid red complex *cis*-[Ru(acac)<sub>2</sub>(η<sup>2</sup>-C<sub>2</sub>H<sub>4</sub>)(PPr<sup>i</sup><sub>3</sub>)] appears to be stable indefinitely under an argon atmosphere at *ca.* 25 °C and is very soluble in benzene and toluene to form yellow solutions. Exposure of these solutions to air results in the formation of a green solution.

Microanalysis: (Found: C, 51.10 H, 7.61%. C<sub>30</sub>H<sub>51</sub>O<sub>4</sub>PRu requires C, 51.73; H, 8.06). IR (KBr): ν(acac) 1583 and 1514 cm<sup>-1</sup>. NMR (C<sub>6</sub>D<sub>6</sub>): δ<sub>H</sub> (300 MHz) 5.35, 5.30 [1 H each, s, C(O)CH]; 4.60 - 4.00 [4 H, m, C<sub>2</sub>H<sub>4</sub>]; 2.45 [3 H, m, CHCH<sub>3</sub>]; 1.94, 1.88, 1.86, 1.84 [3 H each, s, C(O)CH<sub>3</sub>]; 1.23, 1.08 (9 H each, both dd, J<sub>PH</sub> = 12 Hz, J<sub>HH</sub> = 7.2 Hz, PCHCH<sub>3</sub>). δ<sub>C</sub> (75.43 MHz) 187.7(s), 185.5 (d, J<sub>PC</sub> = 2.2 Hz), 184.7(s), 185.5(s) [C(O)CH<sub>3</sub>]; 99.8, 98.1 [both s, C(O)CH]; 69.6 [s, C<sub>2</sub>H<sub>4</sub>]; 28.3(s), 28.1 (d, J<sub>PC</sub> = 5.6 Hz), 27.5(s), 27.2(s) [C(O)CH<sub>3</sub>]; 24.8 (d, J<sub>PC</sub> = 19 Hz, PCHCH<sub>3</sub>); 19.4, 19.0 [both s, PCHCH<sub>3</sub>]. δ<sub>P</sub> (121.5 MHz) +50.6 (s). E<sub>1/2</sub>(Ru<sup>3+/2+</sup>): +0.42 V (-50 °C).

### 7.2.8 Preparation of *cis*-[Ru(acac)<sub>2</sub>(η<sup>2</sup>-C<sub>2</sub>H<sub>4</sub>)(PCy<sub>3</sub>)]

A freshly prepared solution of *cis*-[Ru(acac)<sub>2</sub>(η<sup>2</sup>-C<sub>2</sub>H<sub>4</sub>)<sub>2</sub>] (prepared from 420 mg [Ru(acac)<sub>3</sub>], 1.05 mmol) in benzene (40 mL) was treated dropwise with a solution of PCy<sub>3</sub> (292 mg, 1.04 mmol) in benzene (10 mL) at room temperature and the mixture was stirred overnight. After one hour the solution had changed colour from yellow to orange. Removal of the solvent in *in vacuo* resulted in an orange residue which was re-dissolved in n-pentane (20 mL) with magnetic stirring. Reducing the volume of solution gave a yellow micro-crystalline solid which was washed with cold n-pentane. The mother liquor was reduced again in volume, cooled to *ca.* -20

°C and allowed to stand overnight. A second crop of the yellow microcrystalline solid was obtained. Slow evaporation of the supernatant resulted in yellow crystals suitable for X-ray diffraction studies. The total yield of solid isolated was 641 mg (68%).

The solid yellow complex *cis*-[Ru(acac)<sub>2</sub>(η<sup>2</sup>-C<sub>2</sub>H<sub>4</sub>)(PCy<sub>3</sub>)] appears to be stable indefinitely under an argon atmosphere at *ca.* 25 °C, but slowly turns green when exposed to air after 3-4 weeks. It also readily dissolves in benzene and toluene to form yellow, air-sensitive solutions. Exposure of these solutions to air gives a green solution.

Microanalysis: (Found: C, 57.78; H, 8.11%. C<sub>30</sub>H<sub>51</sub>O<sub>4</sub>PRu requires C, 59.29; H, 8.46%). IR (KBr): ν(acac) 1585 and 1512 cm<sup>-1</sup>. NMR (C<sub>6</sub>D<sub>6</sub>): δ<sub>H</sub> (300 MHz) 5.40, 5.29 [1 H each, s, C(O)CH]; 4.38 - 3.78 [4 H, m, C<sub>2</sub>H<sub>4</sub>]; 1.98, 1.87, 1.86, 1.83 [3 H each, s, C(O)CH<sub>3</sub>]; 2.25 - 1.10 (33H, br m, C<sub>6</sub>H<sub>11</sub>). δ<sub>C</sub> (75.43 MHz) 187.7(s), 185.6 (d, J<sub>PC</sub> = 2.2 Hz), 185.0(s), 184.6(s) [C(O)CH<sub>3</sub>]; 99.8, 98.2 [both s, C(O)CH]; 69.5 [s, C<sub>2</sub>H<sub>4</sub>]; 35.4 [d, J<sub>PC</sub> = 19 Hz, PCH(CH<sub>2</sub>)<sub>5</sub>]; 28.4(s), 28.1 (d, J<sub>PC</sub> = 5.6 Hz), 27.7(s), 27.6(s) [C(O)CH<sub>3</sub>]; 29.2, 28.9, 28.7, 28.6, 28.5, 27.2 (all s, PCH(CH<sub>2</sub>)<sub>5</sub>). δ<sub>P</sub> (121.5 MHz) +40.0 (s). E<sub>1/2</sub>(Ru<sup>3+/2+</sup>): +0.43 V (-50 °C).

The C and H elemental analyses are in good agreement with the formula C<sub>28</sub>H<sub>47</sub>O<sub>4</sub>PRu, corresponding to the loss of ethene from *cis*-[Ru(acac)<sub>2</sub>(η<sup>2</sup>-C<sub>2</sub>H<sub>4</sub>)(PCy<sub>3</sub>)]. Although the compound does not appear to lose ethene at room temperature in an inert atmosphere, it is possible that ethene is lost as the temperature of the analytical oven is raised before combustion occurs. The compound appears to be spectroscopically pure.

7.2.9 Preparation of *trans*-[Ru(acac)<sub>2</sub>(PPr<sup>i</sup><sub>3</sub>)<sub>2</sub>]

A solution of *cis*-[Ru(acac)<sub>2</sub>(η<sup>2</sup>-C<sub>8</sub>H<sub>14</sub>)<sub>2</sub>] (prepared from 800 mg [Ru(acac)<sub>3</sub>], *ca.* 2.0 mmol) in THF (30 mL) was cooled to *ca.* <-25 °C and PPr<sup>i</sup><sub>3</sub> (0.78 mL, 4.08 mmol) was added via a gas-tight syringe. After stirring for one hour, a fine rust-red solid was observed. The volume of solvent was reduced *in vacuo* by half and cold n-hexane was cannulated into the flask. The mixture was stirred for *ca.* 5 minutes and then allowed to settle. The supernatant was decanted from the solid and cold n-pentane was cannulated into the flask. The above process was repeated until supernatant was almost colourless. The rust-red solid *trans*-[Ru(acac)<sub>2</sub>(PPr<sup>i</sup><sub>3</sub>)<sub>2</sub>] (0.58 g, *ca.* 45%) was isolated after filtration.

The isolated solid is stable under an inert atmosphere and at *ca.* -20 °C; slow decomposition occurs when exposed to air at room temperature. The solid readily dissolves in cold toluene and isomerises to *cis*-[Ru(acac)<sub>2</sub>(PPr<sup>i</sup><sub>3</sub>)<sub>2</sub>] at room temperature in solution. This compound has been prepared independently by Werner and coworkers<sup>14</sup> by addition of an excess of PPr<sup>i</sup><sub>3</sub> to *cis*-[Ru(acac)<sub>2</sub>(SbPr<sup>i</sup><sub>3</sub>)<sub>2</sub>] or by reduction of [Ru(acac)<sub>3</sub>] with Zn/Hg in the presence of excess PPr<sup>i</sup><sub>3</sub>.

Microanalysis (Found: C, 53.32; H 8.38%. C<sub>28</sub>H<sub>56</sub>O<sub>4</sub>P<sub>2</sub>Ru requires C, 54.26; H 8.38%). IR (KBr): ν(acac) 1565 and 1507 cm<sup>-1</sup>. NMR (d<sub>8</sub>-toluene -35 °C): δ<sub>H</sub> (300 MHz) 5.10 [2 H, s, C(O)CH]; 2.30 [6H, br m, PCH(CH<sub>3</sub>)<sub>2</sub>]; 1.75 [12H, s, C(O)CH<sub>3</sub>], 1.32 [36H, br m, PCH(CH<sub>3</sub>)<sub>2</sub>]. δ<sub>C</sub> (75.43 MHz) 184.1 [s, C(O)CH<sub>3</sub>]; 100.5 [s, C(O)CH]; 27.4 [s, C(O)CH<sub>3</sub>]; 24.8 [br, PCH(CH<sub>3</sub>)<sub>2</sub>]; 20.0 [br, PCH(CH<sub>3</sub>)<sub>2</sub>]. δ<sub>P</sub> (121.5 MHz) +29.6 (s). E<sub>1/2</sub>(Ru<sup>3+</sup>/2+): -0.14 V (-45 °C).

### 7.2.10 Preparation of $[\text{Ru}(\text{acac})_2(\text{PCy}_3)_2]$ (assumed to be *trans*)

A solution of *cis*- $[\text{Ru}(\text{acac})_2(\eta^2\text{-C}_2\text{H}_4)_2]$  (prepared from 300 mg  $[\text{Ru}(\text{acac})_3]$ , 0.75 mmol) in THF (15 mL) was stirred with  $\text{PCy}_3$  (500 mg, 1.78 mmol) at room temperature and within approximately 30 minutes a fine brown solid had formed. The mixture was stirred for another 6 hours and then allowed to stand overnight. The supernatant was carefully decanted off and the solid washed with *n*-pentane. 530 mg of a brown solid was isolated (82%).

The isolated solid is air-stable and insoluble in benzene and toluene but dissolves in hot aromatic solvents. The solid appears to be partially soluble in THF at room temperature. The solid appears to decompose in  $\text{CH}_2\text{Cl}_2$ .

Microanalysis (Found: C, 64.23; H 9.57; P 6.93%.  $\text{C}_{46}\text{H}_{80}\text{O}_4\text{P}_2\text{Ru}$  requires C, 64.23; H 9.37; P 7.20%). IR (KBr):  $\nu(\text{acac})$  1563 and 1506  $\text{cm}^{-1}$ . NMR (*d*<sub>8</sub>-toluene):  $\delta_{\text{H}}$  (300 MHz) 5.3 [2 H, s, C(O)CH]; 2.40 - 2.20, 2.10 - 1.60, 1.45 - 1.15 [66H, br m,  $\text{PC}_6\text{H}_{11}$ ]; 1.94, 1.82 [6 H each, s, C(O)CH<sub>3</sub>].  $\delta_{\text{C}}$  (75.43 MHz) 186.7, 183.5 [both s, C(O)CH<sub>3</sub>]; 100.3 [s, C(O)CH]; 38.0 [br, PCH(CH<sub>2</sub>)<sub>5</sub>]; 30.2 [br, PCH(CH<sub>2</sub>)<sub>5</sub>]; 29.1, 27.5 (m, PCH(CH<sub>2</sub>)<sub>5</sub>); 28.0 (s), 27.7 (d,  $J_{\text{PC}} = 2.2$  Hz) [C(O)CH<sub>3</sub>].  $\delta_{\text{P}}$  (121.5 MHz) +38.5 (vb s).

### 7.2.11 Attempted reaction of *cis*- $[\text{Ru}(\text{acac})_2(\text{C}_8\text{H}_{14})_2]$ with 2 equivalents of $\text{PBu}^t_3$

To a stirred solution of *cis*- $[\text{Ru}(\text{acac})_2(\eta^2\text{-C}_8\text{H}_{14})_2]$  (prepared from 260 mg  $[\text{Ru}(\text{acac})_3]$ , 0.65 mmol) in THF (20 mL),  $\text{PBu}^t_3$  (250  $\mu\text{L}$ ) was added via syringe. After 7 days an aliquot of the solution was removed. The  $^{31}\text{P}\{^1\text{H}\}$  NMR spectrum showed only one singlet due to  $\text{PBu}^t_3$  at  $\delta +62.5$ , hence no reaction had taken place.



7.2.12 Preparation of *trans*-[Ru(acac)<sub>2</sub>(PPr<sup>i</sup><sub>3</sub>)(CO)]

A cold solution (-70 °C) of *trans*-[Ru(acac)<sub>2</sub>(PPr<sup>i</sup><sub>3</sub>)<sub>2</sub>] (246 mg, 0.40 mmol) in toluene (2 mL) and n-hexane (5 mL) was slowly warmed to room temperature under a CO atmosphere (1 bar). When the temperature of the solution had reached *ca.* -15 °C, a yellow solution had formed. Removal of the solvent *in vacuo* left a yellow residue. The residue was stirred with pentane (5 mL) and the solution was reduced in volume (*ca.* 2 mL). The yellow solution was cooled to -20 °C for two days during which a yellow solid crystallised. The solid was filtered from the solution and washed with a small amount of cold pentane (2 mL). 105mg of the required compound was isolated as a yellow solid (52%).

It appears to be stable towards air, but after several months the solid has a green tinge. The complex is readily soluble in THF, benzene and toluene.

Microanalysis (Found: C, 49.10; H, 7.25; P, 6.36%. C<sub>20</sub>H<sub>35</sub>O<sub>5</sub>PRu requires C, 49.27; H, 7.24; P, 6.35%). IR (KBr):  $\nu(\text{CO})$  1931 cm<sup>-1</sup>;  $\nu(\text{acac})$  1566 and 1517 cm<sup>-1</sup>. NMR (C<sub>6</sub>D<sub>6</sub>):  $\delta_{\text{H}}$  (300 MHz) 5.08 [2 H, C(O)CH]; 2.27 [3 H, m PCHCH<sub>3</sub>]; 1.70 [12H, C(O)CH<sub>3</sub>]; 1.23 (18 H, dd,  $J_{\text{PH}} = 12$  Hz,  $J_{\text{HH}} = 7.1$  Hz, PCHCH<sub>3</sub>).  $\delta_{\text{C}}$  (75.43 MHz) 206.5 [d,  $J_{\text{PC}} = 120$  Hz, C≡O]; 189.1 [C(O)CH<sub>3</sub>]; 100.8 [C(O)CH]; 27.0 [C(O)CH<sub>3</sub>]; 23.1 [d,  $J_{\text{PC}} = 20$  Hz, PCHCH<sub>3</sub>]; 19.1 [PCHCH<sub>3</sub>].  $\delta_{\text{P}}$  (121.5 MHz) +18.9 (s).

A solution of *cis*-[Ru(acac)<sub>2</sub>(PPr<sup>i</sup><sub>3</sub>)<sub>2</sub>] (197 mg, 0.32 mmol) was dissolved in benzene (*ca.* 10 mL) and stirred for 3 days under a CO atmosphere (3 bar) in a medium pressure vessel behind a safety shield. The reaction was followed by <sup>31</sup>P{<sup>1</sup>H} NMR spectroscopy and free PPr<sup>i</sup><sub>3</sub>, *trans*-

[Ru(acac)<sub>2</sub>(PPr<sup>i</sup><sub>3</sub>)(CO)] and a small amount *cis*-[Ru(acac)<sub>2</sub>(PPr<sup>i</sup><sub>3</sub>)(CO)] were detected.

CO (1 bar) was gently bubbled through a solution of *cis*-[Ru(acac)<sub>2</sub>(η<sup>2</sup>-C<sub>2</sub>H<sub>4</sub>)(PPr<sup>i</sup><sub>3</sub>)] (*ca.* 15 mg, 0.03 mmol) in C<sub>6</sub>D<sub>6</sub> (0.4 mL) for 30 minutes. The <sup>1</sup>H and <sup>31</sup>P{<sup>1</sup>H} NMR spectra were checked periodically over several hours and showed that *trans*-[Ru(acac)<sub>2</sub>(PPr<sup>i</sup><sub>3</sub>)(CO)] was formed quantitatively.

### 7.2.13 Preparation of *trans*-[Ru(acac)<sub>2</sub>(PCy<sub>3</sub>)(CO)]

A suspension of [Ru(acac)<sub>2</sub>(PCy<sub>3</sub>)<sub>2</sub>] (200 mg, 0.23 mmol) was stirred in benzene (10 mL) under a CO atmosphere (1 bar) and within 30 minutes, a clear orange solution had formed; the solvent was evaporated to almost dryness. The yellow residue was stirred with pentane (5 mL) and the solution was then reduced to *ca.* 2 mL in volume. A yellow solid was filtered from the solution and washed with a small amount of pentane (2 mL). 101mg of *trans*-[Ru(acac)<sub>2</sub>(PCy<sub>3</sub>)(CO)] was isolated (72%).

The yellow solid *trans*-[Ru(acac)<sub>2</sub>(PCy<sub>3</sub>)(CO)] also appears to be stable towards air, but like *trans*-[Ru(acac)<sub>2</sub>(PPr<sup>i</sup><sub>3</sub>)(CO)] after several months the solid has a green tinge. The complex is readily soluble in THF, benzene and toluene.

Microanalysis (Found: C, 57.08; H, 7.66; P, 4.62%. C<sub>29</sub>H<sub>47</sub>O<sub>5</sub>PRu requires C, 57.31; H, 7.79; P, 5.10%). IR (KBr): ν(CO) 1950 cm<sup>-1</sup>; ν(acac) 1572 and 1510 cm<sup>-1</sup>. NMR (C<sub>6</sub>D<sub>6</sub>): δ<sub>H</sub> (300 MHz) 5.09 [2H, C(O)CH]; 2.30 - 1.50, 1.40 - 1.05 [33H, br m, P(C<sub>6</sub>H<sub>11</sub>)<sub>3</sub>]; 1.73 [12H, C(O)CH<sub>3</sub>]. δ<sub>C</sub> (75.43 MHz) 206.8 [d, J<sub>PC</sub> = 120 Hz, C≡O]; 188.9 [C(O)CH<sub>3</sub>]; 100.6 [C(O)CH]; 33.3 [d, J<sub>PC</sub> = 10 Hz, PCH(CH<sub>2</sub>)<sub>5</sub>]; 29.1, 28.6 (d, J<sub>PC</sub> = 8.8 Hz), 27.1 [PCH(CH<sub>2</sub>)<sub>5</sub>]; 27.0 [C(O)CH<sub>3</sub>]. δ<sub>P</sub> (121.5 MHz) +8.4 (s).

A solution of *cis*-[Ru(acac)<sub>2</sub>(η<sup>2</sup>-C<sub>2</sub>H<sub>4</sub>)(PCy<sub>3</sub>)] (20 mg, 0.04 mmol) in C<sub>6</sub>D<sub>6</sub> (ca. 0.4 mL) was made up under a CO atmosphere (1 bar) overnight. The <sup>1</sup>H and <sup>31</sup>P{<sup>1</sup>H} NMR spectra were checked periodically over several hours; they showed the quantitative formation of *trans*-[Ru(acac)<sub>2</sub>(PCy<sub>3</sub>)(CO)].

#### 7.2.14 Preparation of *cis*-[Ru(acac)<sub>2</sub>(PPr<sup>i</sup><sub>3</sub>)(CO)]

A solution of *trans*-[Ru(acac)<sub>2</sub>(PPr<sup>i</sup><sub>3</sub>)(CO)] (150 mg, 0.31 mmol) was prepared in benzene (10 mL) and refluxed for 1 hour during which the colour of the solution had faded. The solvent was evaporated almost to dryness and *n*-pentane (ca. 2 mL) was added to the yellow residue. The light yellow solution was cooled to -20 °C for two days. The light yellow crystalline solid *cis*-[Ru(acac)<sub>2</sub>(PPr<sup>i</sup><sub>3</sub>)(CO)] was isolated by filtration (85 mg, 57%) and washed with cold *n*-pentane.

It is stable in air for several weeks and is readily soluble in aromatic solvents.

Microanalysis (Found: C, 49.20; H, 6.90; P, 6.03%. C<sub>20</sub>H<sub>35</sub>O<sub>5</sub>PRu requires C, 49.27; H, 7.24; P, 6.35%). IR (KBr): ν(CO) 1928 cm<sup>-1</sup>; ν(acac) 1588, 1573 and 1516 cm<sup>-1</sup>. NMR (C<sub>6</sub>D<sub>6</sub>): δ<sub>H</sub> (300 MHz) 5.34, 5.16 [1 H each, both s, C(O)CH]; 2.25 [3 H, m PCHCH<sub>3</sub>]; 1.91, 1.85, 1.79, 1.71 [3 H each, all s, C(O)CH<sub>3</sub>]; 1.25, 1.13 (9 H each, both dd, J<sub>PH</sub> = 13 Hz, J<sub>HH</sub> = 7.0 Hz, PCHCH<sub>3</sub>). δ<sub>C</sub> (75.43 MHz) 209.4 [d, J<sub>PC</sub> = 20 Hz, C≡O]; 189.1, 187.8, 186.6, 186.0 [C(O)CH<sub>3</sub>]; 100.2, 99.1 [C(O)CH]; 28.0, 27.8, 27.7, 27.2 [C(O)CH<sub>3</sub>]; 24.7 [d, J<sub>PC</sub> = 22 Hz, PCHCH<sub>3</sub>]; 19.4, 18.8 [PCHCH<sub>3</sub>]. δ<sub>P</sub> (121.5 MHz) +61.5 (s).

### 7.2.15 Preparation of *cis*-[Ru(acac)<sub>2</sub>(PCy<sub>3</sub>)(CO)]

A solution of *trans*-[Ru(acac)<sub>2</sub>(PCy<sub>3</sub>)(CO)] (200 mg, 0.33 mmol) was prepared in benzene (10 mL) and refluxed for 1 hour during which the colour of the solution became paler. The solvent was evaporated almost to dryness and *n*-pentane (*ca.* 3 mL) was added to the yellow residue. A light yellow solid was formed after stirring the solution overnight and isolated (123 mg, 62%) after filtration.

The light yellow solid *cis*-[Ru(acac)<sub>2</sub>(PCy<sub>3</sub>)(CO)] stable in air for several weeks and is readily soluble in aromatic solvents.

Microanalysis (Found: C, 57.21; H, 7.87; P, 4.87%. C<sub>29</sub>H<sub>47</sub>O<sub>5</sub>PRu requires C, 57.31; H, 7.79; P, 5.10%). IR (KBr):  $\nu(\text{CO})$  1944 cm<sup>-1</sup>;  $\nu(\text{acac})$  1589, 1575 and 1520 cm<sup>-1</sup>. NMR (C<sub>6</sub>D<sub>6</sub>):  $\delta_{\text{H}}$  (300 MHz) 5.40, 5.17 [1H each, both s, C(O)CH]; 2.30 - 2.10, 2.00 - 1.50, 1.30 - 1.10 [33H, br m, P(C<sub>6</sub>H<sub>11</sub>)<sub>3</sub>]; 1.98, 1.86, 1.86, .173 [3H each, all s, C(O)CH<sub>3</sub>].  $\delta_{\text{C}}$  (75.43 MHz) 209.6 [d,  $J_{\text{PC}} = 18$  Hz, C≡O]; 189.0, 187.9, 186.4, 186.0 [C(O)CH<sub>3</sub>]; 100.3, 99.2 [C(O)CH]; 35.1 [d,  $J_{\text{PC}} = 21$  Hz, PCH(CH<sub>2</sub>)<sub>5</sub>]; 29.5, 29.0 (d,  $J_{\text{PC}} = 2$  Hz), 28.4 (d,  $J_{\text{PC}} = 3$  Hz), 28.2 (d,  $J_{\text{PC}} = 2$  Hz), 27.0 [PCH(CH<sub>2</sub>)<sub>5</sub>]; 28.1, 27.9, 27.8 (d,  $J_{\text{PC}} = 5.4$  Hz), 27.3 [C(O)CH<sub>3</sub>].  $\delta_{\text{P}}$  (121.5 MHz) +52.3 (s).

### 7.2.16 Preparation of *cis*-[Ru(acac)<sub>2</sub>(PPr<sup>*i*</sup>)<sub>3</sub>](=C=C(H)Ph)]

A sample of *cis*-[Ru(acac)<sub>2</sub>(PPr<sup>*i*</sup>)<sub>2</sub>] (38 mg, 0.06 mmol) was dissolved in C<sub>6</sub>D<sub>6</sub> (*ca.* 0.4 mL) and PhC≡CH (10  $\mu$ L, 0.09 mmol) was added via microsyringe. The reaction mixture was allowed to stand at room temperature. The <sup>31</sup>P{<sup>1</sup>H} NMR spectrum was checked periodically and showed quantitative formation of *cis*-[Ru(acac)<sub>2</sub>(PPr<sup>*i*</sup>)<sub>3</sub>](=C=C(H)Ph)] [ $\delta$ [<sup>31</sup>P{<sup>1</sup>H}]] +54.3 (s)] [literature value of +53.8 (s)]<sup>14</sup> after two days. No intermediates were detected during the course of the reaction.

A solution of *cis*-[Ru(acac)<sub>2</sub>(η<sup>2</sup>-C<sub>2</sub>H<sub>4</sub>)(PPr<sup>*i*</sup><sub>3</sub>)] (20 mg, 0.04 mmol) in C<sub>6</sub>D<sub>6</sub> (ca. 0.4 mL) and PhC≡CH (10 μL, 0.09 mmol) was added via micro-syringe. The reaction mixture allowed to stand at room temperature. After two days the <sup>31</sup>P{<sup>1</sup>H} NMR spectrum showed that *cis*-[Ru(acac)<sub>2</sub>(PPr<sup>*i*</sup><sub>3</sub>)](=C=C(H)Ph)] had formed quantitatively. No intermediates were detected during the course of the reaction. This compound has been previously prepared<sup>14</sup> by treating *cis*-[Ru(acac)<sub>2</sub>(PPr<sup>*i*</sup><sub>3</sub>)<sub>2</sub>] with PhC≡CH in hot benzene.

### 7.2.17 Preparation of *cis*-[Ru(acac)<sub>2</sub>(PPr<sup>*i*</sup><sub>3</sub>)](=C=C(H)SiMe<sub>3</sub>)]

To a solution of *cis*-[Ru(acac)<sub>2</sub>(PPr<sup>*i*</sup><sub>3</sub>)<sub>2</sub>] (99 mg, 0.16 mmol) in benzene (8 mL), Me<sub>3</sub>SiC≡CH (ca. 65 μL, 0.46 mmol) was added via gas-tight syringe and the reaction mixture was refluxed for 1 hour. After allowing the solution to cool to room temperature, the solvent was removed *in vacuo* leaving a sticky red residue. The red residue was dissolved in n-hexane and after 2 weeks at -10 °C, 50 mg of the red solid *cis*-[Ru(acac)<sub>2</sub>(PPr<sup>*i*</sup><sub>3</sub>)](=C=C(H)SiCH<sub>3</sub>)<sub>3</sub>] was isolated (56%).

The compound is stable to air for several weeks but prolonged exposure leads to the formation of *trans*-[Ru(acac)<sub>2</sub>(PPr<sup>*i*</sup><sub>3</sub>)(CO)], probably due to reaction with oxygen. The compound is readily soluble in benzene or toluene but insoluble in methanol.

Microanalysis: (Found: C, 51.91; H, 8.40; P, 5.57%. C<sub>24</sub>H<sub>45</sub>O<sub>4</sub>PRuSi requires C, 51.68; H, 8.13, P, 5.55%). IR (KBr): ν(C=C) 1610 cm<sup>-1</sup>; ν(acac) 1589 and 1519 cm<sup>-1</sup>. NMR (C<sub>6</sub>D<sub>6</sub>): δ<sub>H</sub> (300 MHz) 5.35, 5.20 [1 H each, s, CHC(O)]; 3.67 [1 H, d, J<sub>PH</sub> = 4.2 Hz, Ru=C=C(H)Si(CH<sub>3</sub>)<sub>3</sub>]; 2.45 [3 H, m, PCHCH<sub>3</sub>]; 1.94 [6 H, s, C(O)CH<sub>3</sub>]; 1.84, 1.79 [3 H each, s, C(O)CH<sub>3</sub>]; 1.29, 1.21 (9 H each, both dd, J<sub>PH</sub> = 12.9 Hz, J<sub>HH</sub> = 7.4 Hz, PCHCH<sub>3</sub>). δ<sub>C</sub> (75.43 MHz) 338.5 [d, J<sub>PC</sub> 19.0 Hz, Ru=C=C]; 188.3,

187.6, 186.8, 184.7 [ $\underline{\text{C}}(\text{O})\text{CH}_3$ ]; 100.2, 99.5 [ $\text{C}(\text{O})\underline{\text{C}}\text{H}$ ]; 93.0 [ $\text{Ru}=\text{C}=\underline{\text{C}}\text{HSi}$ ]; 28.6, 28.5, 28.4, 27.7 [ $\text{C}(\text{O})\underline{\text{C}}\text{H}_3$ ]; 24.9 (d,  $J_{\text{PC}} = 22$  Hz,  $\text{P}\underline{\text{C}}\text{HCH}_3$ ); 19.7, 19.4 [ $\text{PCH}\underline{\text{C}}\text{H}_3$ ]; 2.3 [ $\text{Si}(\underline{\text{C}}\text{H}_3)_3$ ];  $\delta_{\text{P}}$  (121.5 MHz) +56.9 (s).

### 7.2.18 Preparation of *cis*-[Ru(acac)<sub>2</sub>(PPr<sup>*i*</sup>)<sub>2</sub>(=C=C(H)Bu<sup>*t*</sup>)]

A solution of *cis*-[Ru(acac)<sub>2</sub>(PPr<sup>*i*</sup>)<sub>2</sub>] (205 mg, 0.33 mmol) in benzene (10 mL) was refluxed in the presence of Bu<sup>*t*</sup>C≡CH (41 μL, 0.33 mmol) for 1 hour. The solution was evaporated almost to dryness leaving a red residue. The red residue was dissolved in the minimum amount of n-hexane (*ca.* 1 mL) and the resulting solution was chromatographed on neutral alumina (Activity III) with n-hexane. The red fraction eluted with n-hexane was discarded. Ether was then used to eluate the red band on the top of the column. The ether was then removed *in vacuo* and a small amount of n-hexane was added. The solution was cooled in dry ice/ethanol and 115 mg of red crystals were collected (yield 64.2%).

The solid *cis*-[Ru(acac)<sub>2</sub>(PPr<sup>*i*</sup>)<sub>2</sub>(=C=C(H)Bu<sup>*t*</sup>)] appears to be stable to air for several weeks but prolonged exposure also leads to the formation of *trans*-[Ru(acac)<sub>2</sub>(PPr<sup>*i*</sup>)<sub>2</sub>(CO)]. The red complex is readily soluble in benzene or toluene but insoluble in methanol.

Microanalysis: (Found: C, 55.08; H, 7.73; P, 5.52%. C<sub>25</sub>H<sub>45</sub>O<sub>4</sub>PRu requires C, 55.47; H, 8.31, P, 5.72%). IR (C<sub>6</sub>H<sub>6</sub>):  $\nu(\text{C}=\text{C})$  1638 cm<sup>-1</sup>;  $\nu(\text{acac})$  1580 and 1514 cm<sup>-1</sup>. NMR (C<sub>6</sub>D<sub>6</sub>):  $\delta_{\text{H}}$  (300 MHz) 5.35, 5.18 [1 H, C(O) $\underline{\text{C}}\text{H}$ ]; 4.11 [1 H, d,  $J_{\text{PH}} = 4.0$  Hz, Ru=C=C( $\underline{\text{H}}$ )C(CH<sub>3</sub>)<sub>3</sub>]; 2.47 [3 H, m, P $\underline{\text{C}}\text{HCH}_3$ ]; 1.97, 1.93, 1.80, 1.77 [3 H each, all s, C(O) $\underline{\text{C}}\text{H}_3$ ]; 1.29, 1.21 (9 H each, both dd,  $J_{\text{PH}} = 12.9$  Hz,  $J_{\text{HH}} = 7.2$  Hz, P $\underline{\text{C}}\text{HCH}_3$ ).  $\delta_{\text{C}}$  (75.43 MHz) 356.4 [d,  $J_{\text{PC}} = 20.0$  Hz, Ru= $\underline{\text{C}}=\text{C}(\text{H})\text{C}(\text{CH}_3)_3$ ]; 188.3, 187.6, 186.8, 184.7 [ $\underline{\text{C}}(\text{O})\text{CH}_3$ ], 121.2 [=C= $\underline{\text{C}}(\text{H})\text{C}(\text{CH}_3)_3$ ]; 99.7, 98.8 [ $\text{C}(\text{O})\underline{\text{C}}\text{H}$ ]; 33.1

[=C=C(H)C(CH<sub>3</sub>)<sub>3</sub>]; 30.1 [=C=C(H)C(CH<sub>3</sub>)<sub>3</sub>]; 28.0, 27.1, 24.6, 24.3 [C(O)CH<sub>3</sub>]; 24.5 (d,  $J_{PC} = 22. \text{ Hz}$ , PCHCH<sub>3</sub>); 19.3, 18.9 [PCHCH<sub>3</sub>].  $\delta_P$  (121.5 MHz) +55.5 (s).

### 7.2.19 Attempted reaction of HC≡CCO<sub>2</sub>Me with *cis*-[Ru(acac)<sub>2</sub>(PPr<sup>*i*</sup>)<sub>2</sub>]

A sample of *cis*-[Ru(acac)<sub>2</sub>(PPr<sup>*i*</sup>)<sub>2</sub>] (131 mg, 0.21 mmol) was dissolved in benzene (5 mL) and HC≡CCO<sub>2</sub>CH<sub>3</sub> (19 μL, 0.21 mmol) was added via syringe. The mixture was then refluxed for 2 hours. The <sup>31</sup>P{<sup>1</sup>H} NMR spectrum of the reaction mixture indicated that no reaction had taken place.

### 7.2.20 Attempted reaction of PhC≡CPh with *cis*-[Ru(acac)<sub>2</sub>(PPr<sup>*i*</sup>)<sub>2</sub>]

A mixture of *cis*-[Ru(acac)<sub>2</sub>(PPr<sup>*i*</sup>)<sub>2</sub>] (33 mg, 0.05 mmol) and PhC≡CPh (90 mg, 0.50 mmol) in C<sub>6</sub>D<sub>6</sub> (ca. 0.4 mL) was heated to 80 °C for two hours. <sup>31</sup>P{<sup>1</sup>H} NMR spectroscopy of the reaction mixture indicated that no reaction had taken place.

### 7.2.21 Attempted reaction of 3-hexyne with *cis*-[Ru(acac)<sub>2</sub>(PPr<sup>*i*</sup>)<sub>2</sub>]

A mixture of *cis*-[Ru(acac)<sub>2</sub>(PPr<sup>*i*</sup>)<sub>2</sub>] (15 mg, 0.02 mmol) and CH<sub>3</sub>CH<sub>2</sub>C≡CCH<sub>2</sub>CH<sub>3</sub> (10 μL, 0.09 mmol) in C<sub>6</sub>D<sub>6</sub> (ca. 0.4 mL) was heated to 80 °C for two hours. <sup>31</sup>P{<sup>1</sup>H} NMR spectroscopy of the reaction mixture indicated that no reaction had taken place.

### 7.2.22 Attempted reaction of 3-hexyne with *cis*-[Ru(acac)<sub>2</sub>(η<sup>2</sup>-C<sub>2</sub>H<sub>4</sub>)(PCy<sub>3</sub>)]

A solution of *cis*-[Ru(acac)<sub>2</sub>(η<sup>2</sup>-C<sub>2</sub>H<sub>4</sub>)(PCy<sub>3</sub>)] (31 mg, 0.05 mmol) in C<sub>6</sub>D<sub>6</sub> (ca. 0.4 mL) was mixed with excess 3-hexyne at room temperature. There was no detectable reaction at room temperature after one day or heating to 80 °C for one hour by <sup>31</sup>P{<sup>1</sup>H} NMR spectroscopy.

### 7.2.23 Attempted reaction of 2-butyne with *cis*-[Ru(acac)<sub>2</sub>(η<sup>2</sup>-C<sub>2</sub>H<sub>4</sub>)(PPr<sup>i</sup><sub>3</sub>)]

A solution of *cis*-[Ru(acac)<sub>2</sub>(η<sup>2</sup>-C<sub>2</sub>H<sub>4</sub>)(PCy<sub>3</sub>)] (28 mg, 0.06 mmol) in C<sub>6</sub>D<sub>6</sub> (ca. 0.4 mL) was mixed with excess 2-butyne at room temperature. There was no detectable reaction at room temperature after heating to 55 °C for three hours by <sup>31</sup>P{<sup>1</sup>H} NMR spectroscopy.

### 7.2.24 Synthesis of *cis*-[Ru(acac)<sub>2</sub>(PCy<sub>3</sub>)(SbPh<sub>3</sub>)]

A solution of SbPh<sub>3</sub> (115 mg, 0.33 mmol) in toluene (10 mL) was added dropwise to a solution of *cis*-[Ru(acac)<sub>2</sub>(η<sup>2</sup>-C<sub>2</sub>H<sub>4</sub>)(PCy<sub>3</sub>)] (200 mg, 0.33 mmol) and the mixture was stirred overnight at room temperature. An orange residue was obtained after the solvent had been removed *in vacuo*. The addition of n-pentane (ca. 10 mL) to the residue and subsequent magnetic stirring resulted in the formation of an orange micro-crystalline solid. The solid was isolated after filtration and washing with small amounts of n-hexane (256 mg, 83%).

The orange solid *cis*-[Ru(acac)<sub>2</sub>(PCy<sub>3</sub>)(SbPh<sub>3</sub>)] appears to be air-stable and is readily soluble in aromatic solvents.

Microanalysis (Found: C, 58.85; H 6.68; P 3.13%. C<sub>46</sub>H<sub>46</sub>O<sub>4</sub>PRuSb requires C, 59.21; H 6.70; P 3.32%). IR (KBr): ν(acac) 1568 and 1510 cm<sup>-1</sup>. NMR (C<sub>6</sub>D<sub>6</sub>): δ<sub>H</sub> (300 MHz) 7.80-7.77 [6 H, m, *o*-SbC<sub>6</sub>H<sub>5</sub>]; 7.13-7.06 [9 H, m, *m*- and *p*-SbC<sub>6</sub>H<sub>5</sub>]; 5.46, 5.02 [1 H each, s, C(O)CH]; 2.30 - 1.00 [33 H, br m, PC<sub>6</sub>H<sub>11</sub>]; 2.00, 1.93, 1.80, 1.68 [3 H each, s, C(O)CH<sub>3</sub>]. δ<sub>C</sub> (75.43 MHz) 186.8, 186.2, 184.7, 184.0 [C(O)CH<sub>3</sub>]; 137.1 [SbC<sub>6</sub>H<sub>5</sub>]; 136.5 [*ipso*-SbC<sub>6</sub>H<sub>5</sub>]; 129.0, 128.4 [SbC<sub>6</sub>H<sub>5</sub>]; 100.4, 99.6 [C(O)CH]; 38.8 (d, J<sub>PC</sub> = 19 Hz, PCH(CH<sub>2</sub>)<sub>5</sub>); 29.8 (s), 29.1 (s), 28.6 (d, J<sub>PC</sub> = 4 Hz), 28.5 (d, J<sub>PC</sub> = 4 Hz), 27.4 (s) [PCH(CH<sub>2</sub>)<sub>5</sub>]; 28.0<sub>4</sub>, 28.0<sub>0</sub>, 27.9 [all s, C(O)CH<sub>3</sub>]. δ<sub>P</sub> (121.5 MHz) +53.5 (s).



A mixture of *cis*-[Ru(acac)<sub>2</sub>(η<sup>2</sup>-C<sub>2</sub>H<sub>4</sub>)(SbPh<sub>3</sub>)] (18 mg, 0.03 mmol) and PCy<sub>3</sub> (8 mg, 0.03 mmol) in C<sub>6</sub>D<sub>6</sub> was left for three days at *ca.* 25 °C with quantitative formation of *cis*-[Ru(acac)<sub>2</sub>(PCy<sub>3</sub>)(SbPh<sub>3</sub>)] by <sup>1</sup>H and <sup>31</sup>P{<sup>1</sup>H} NMR spectroscopy.

#### 7.2.25 Attempted reaction of CO with *cis*-[Ru(acac)<sub>2</sub>(η<sup>2</sup>-C<sub>2</sub>H<sub>4</sub>)(SbPh<sub>3</sub>)]

A solution of *cis*-[Ru(acac)<sub>2</sub>(η<sup>2</sup>-C<sub>2</sub>H<sub>4</sub>)(SbPh<sub>3</sub>)] (170 mg, 0.25 mmol) in benzene (10 mL) was placed under CO (2 - 3 bar) behind a safety shield and stirred for 3 days. <sup>1</sup>H NMR spectroscopy and IR spectroscopy indicated that the replacement of C<sub>2</sub>H<sub>4</sub> was not occurring at a detectable level.

#### 7.2.26 Attempted reaction of PCy<sub>3</sub> with *cis*-[Ru(acac)<sub>2</sub>(η<sup>2</sup>-C<sub>2</sub>H<sub>4</sub>)(NH<sub>3</sub>)]

A solution of *cis*-[Ru(acac)<sub>2</sub>(η<sup>2</sup>-C<sub>2</sub>H<sub>4</sub>)(NH<sub>3</sub>)] (41 mg, 0.12 mmol) in C<sub>6</sub>D<sub>6</sub> (*ca.* 0.4 mL) was treated with PCy<sub>3</sub> (11 mg, 0.04 mmol) and any reaction monitored by <sup>31</sup>P{<sup>1</sup>H} NMR spectroscopy. There was no detectable reaction after one week at room temperature.

#### 7.2.27 Reaction of dinitrogen with *cis*-[Ru(acac)<sub>2</sub>(η<sup>2</sup>-C<sub>2</sub>H<sub>4</sub>)(PPr<sup>*i*</sup><sub>3</sub>)] to give *cis*- [[Ru(acac)<sub>2</sub>(PPr<sup>*i*</sup><sub>3</sub>)]<sub>2</sub>(μ-N<sub>2</sub>)

Benzene (10 mL) was added to *cis*-[Ru(acac)<sub>2</sub>(η<sup>2</sup>-C<sub>2</sub>H<sub>4</sub>)(PPr<sup>*i*</sup><sub>3</sub>)] (167 mg, 0.34 mmol) under an industrial grade dihydrogen (H<sub>2</sub>) atmosphere (1 bar) in a medium pressure vessel. The dihydrogen probably contains at least 100 ppm N<sub>2</sub> (specified in Grade 3.8 High Purity which contains 100 ppm). The H<sub>2</sub> pressure was increased (3 bar) and the yellow solution heated to 60 °C for two days. After allowing the solution to cool to room temperature and reducing the H<sub>2</sub> pressure (1 bar), the solution was cannulated into a Schlenk

flask under a H<sub>2</sub> atmosphere and the solvent removed *in vacuo*. A yellow residue was isolated and a small amount of n-pentane was added forming a yellow solution. The flask was then cooled to -20 °C for two days during which yellow crystals formed. These crystals were isolated (149 mg, 92%) after filtration under an argon atmosphere and washed with small aliquots of cold n-pentane. They were identified by X-ray crystallography as the yellow binuclear dinitrogen complex *cis*-[Ru(acac)<sub>2</sub>(PPr<sup>i</sup><sub>3</sub>)<sub>2</sub>(μ-N<sub>2</sub>)].

It may be handled for short periods in air but was stored under an argon atmosphere. It forms stable, air-sensitive solutions in benzene or toluene but decomposes in CH<sub>2</sub>Cl<sub>2</sub> to form an unidentified red complex. Exposure of the yellow benzene solutions to air results in a green solution which also has not been identified.

Microanalysis (Found: C, 48.07; H 7.61; N 2.63%. C<sub>38</sub>H<sub>70</sub>O<sub>8</sub>P<sub>2</sub>Ru<sub>2</sub> requires C, 48.19; H, 7.45; N, 2.96%). IR (KBr): ν(acac) 1582 and 1512 cm<sup>-1</sup>. Raman (solid): ν(N≡N) 2087 cm<sup>-1</sup>. NMR (C<sub>6</sub>D<sub>6</sub>): δ<sub>H</sub> (300 MHz) (major isomer) 5.33, 5.26 [1 H each, both s, C(O)CH]; 2.47 [6 H, m, PCHCH<sub>3</sub>]; 2.03, 1.85, 1.83, 1.81 [3 H each, all s, C(O)CH<sub>3</sub>]; 1.40, 1.29 [9 H each, both dd J<sub>PC</sub> = 12.5 Hz, J<sub>PH</sub> = 7.5 Hz, PCHCH<sub>3</sub>]; (minor isomer) 5.35, 5.29 [1 H each, both s, C(O)CH]; 2.47 [6 H, m, PCHCH<sub>3</sub>]; 2.08, 1.87, 1.80 [3 H each, all s, C(O)CH<sub>3</sub>]; 1.40, 1.29 [9 H each, both dd J<sub>PC</sub> = 12.5 Hz, J<sub>PH</sub> = 7.5 Hz, PCHCH<sub>3</sub>]; δ<sub>C</sub> (75.43 MHz) major isomer 187.5, 186.4, 185.7, 184.6 [all s, C(O)CH<sub>3</sub>]; 100.3, 98.5 [both s, C(O)CH]; 24.6 (d, J<sub>PC</sub> = 20 Hz, PCHCH<sub>3</sub>); 28.3 (d, J<sub>PC</sub> = 5.6 Hz), 27.8 (s), 27.6 (s), 27.2 (s) [C(O)CH<sub>3</sub>]; 19.5, 19.2 [both s, PCHCH<sub>3</sub>]; minor isomer 187.6, 185.8, 184.5 [all s, C(O)CH<sub>3</sub>]; 100.3, 98.6 [both s, C(O)CH]; 24.6 (d, J<sub>PC</sub> = 20 Hz, PCHCH<sub>3</sub>); 28.4 (d, J<sub>PC</sub> = 5.6 Hz), 27.6 (s), 27.2 (s), [C(O)CH<sub>3</sub>]; 19.4, 19.1 [both s, PCHCH<sub>3</sub>]; δ<sub>P</sub> (121.5 MHz) major isomer +60.6 (s); minor isomer +60.5 (s). E<sub>1/2</sub>(Ru<sup>3+/2+</sup>): +0.30 and +0.90 V (ca. -50 °C).

7.2.28 Attempted oxidation of *trans*-[Ru(acac)<sub>2</sub>(η<sup>2</sup>-C<sub>2</sub>H<sub>4</sub>)(NH<sub>3</sub>)] with  
[Cp<sub>2</sub>Fe]PF<sub>6</sub>

A solution of *trans*-[Ru(acac)<sub>2</sub>(η<sup>2</sup>-C<sub>2</sub>H<sub>4</sub>)(NH<sub>3</sub>)] (36 mg, 0.10 mmol) in CH<sub>2</sub>Cl<sub>2</sub> (2 mL) at *ca.* 20 °C was mixed with [Cp<sub>2</sub>Fe]PF<sub>6</sub> (31 mg, 0.09 mmol). Within 5 minutes, the solution had turned initially green and finally purple. The solvent was removed *in vacuo* and n-pentane added. An unidentified mauve solid (25 mg) was isolated. Cyclic voltammogram traces indicated that Cp<sub>2</sub>Fe, [Ru(acac)<sub>3</sub>] and an unidentified compound were present.

7.2.29 Oxidation of *trans*-[Ru(acac)<sub>2</sub>(η<sup>2</sup>-C<sub>2</sub>H<sub>4</sub>)(NH<sub>3</sub>)] with AgPF<sub>6</sub>

A solution of *trans*-[Ru(acac)<sub>2</sub>(η<sup>2</sup>-C<sub>2</sub>H<sub>4</sub>)(NH<sub>3</sub>)] (105 mg, 0.31 mmol) in CH<sub>2</sub>Cl<sub>2</sub> (10 mL) was cooled to *ca.* -70 °C before the addition of AgPF<sub>6</sub> (105 mg, 0.41 mmol). After stirring for one hour at -70 °C, the deep blue solution was filtered through Celite (in a dry ice chilled column) and evaporated *in vacuo* resulting in a blue residue. A blue solid, believed to be *trans*-[Ru<sup>III</sup>(acac)<sub>2</sub>(η<sup>2</sup>-C<sub>2</sub>H<sub>4</sub>)(NH<sub>3</sub>)]PF<sub>6</sub> (see Chapter 3), was isolated (115 mg, 70%) after stirring the residue with cold ether for two hours. Over a period of two weeks at -20 °C, the solid changed colour from blue to purple and finally red.

7.2.30 Oxidation of *cis*-[Ru(acac)<sub>2</sub>(η<sup>2</sup>-C<sub>8</sub>H<sub>14</sub>)(SbPh<sub>3</sub>)] with AgPF<sub>6</sub>

AgPF<sub>6</sub> (165 mg, 0.65 mmol) was added to a chilled solution (-70 °C) of *cis*-[Ru(acac)<sub>2</sub>(η<sup>2</sup>-C<sub>8</sub>H<sub>14</sub>)(SbPh<sub>3</sub>)]<sup>8</sup> (330 mg, 0.43 mmol) in CH<sub>2</sub>Cl<sub>2</sub> (10 mL) and the mixture was allowed to stir for one hour, during which a blue solution formed. The mixture was filtered through Celite (in a dry ice chilled column) and the solvent was removed *in vacuo* to leave a blue residue. A blue solid, believed to be *cis*-[Ru<sup>III</sup>(acac)<sub>2</sub>(η<sup>2</sup>-C<sub>8</sub>H<sub>14</sub>)(SbPh<sub>3</sub>)]PF<sub>6</sub> (see Chapter

3), was isolated (316 mg, 80%) after stirring in cold ether for two hours. The blue solid appears to be stable when exposed to air at room temperature as a solid for several months.

Microanalysis (Found: C, 46.27; H, 4.84; P, 3.33; Ag, 1.60.  $C_{38}H_{36}F_6O_4P_3Ru \cdot 0.1(AgPF_6)$  requires C, 46.35; H, 4.65; P, 3.65; Ag, 1.16). IR (KBr):  $\nu(\text{acac})$  1552 and 1518  $\text{cm}^{-1}$ ;  $\nu([\text{PF}_6])$  840  $\text{cm}^{-1}$ .  $E_{1/2}(\text{Ru}^{3+/2+})$ : +0.48 V (ca. -45 °C)

### 7.2.31 Reaction of $C_5H_5N$ with $\text{cis-}[Ru(\text{acac})_2(o\text{-PhC}\equiv\text{CC}_6\text{H}_4\text{NMe}_2)][\text{PF}_6]$

To a violet solution of  $\text{cis-}[Ru(\text{acac})_2(o\text{-PhC}\equiv\text{CC}_6\text{H}_4\text{NMe}_2)][\text{PF}_6]$  (154 mg, 0.23 mmol) in  $\text{CH}_2\text{Cl}_2$  (15 mL), neat  $C_5H_5N$  (38  $\mu\text{L}$ , 0.47 mmol) was added via microsyringe resulting in an almost immediate colour change to red. After stirring for 3 hours, the solvent was evaporated until a concentrated solution was obtained and then layered with n-hexane (ca. 10 mL). Red crystals identified as

$\text{cis-}(E)\text{-}[Ru^{\text{III}}(\text{acac})_2\{o\text{-Me}_2\text{NC}_6\text{H}_4\text{C}=\text{C}(\text{NC}_5\text{H}_5)\text{Ph}\}][\text{PF}_6]$  by X-ray crystallography (see Chapter 3) were filtered from the colourless solution. The yield was 128 mg (74%).

Microanalysis (Found: C, 48.20; H, 4.52; N, 3.59%.  $C_{31}H_{34}F_6N_2O_4PRu$  requires C, 50.00; H, 4.60; N, 3.76%). IR (KBr):  $\nu(\text{acac})$  1569 and 1519  $\text{cm}^{-1}$ ;  $\nu(\text{PF}_6)$  841 and 558  $\text{cm}^{-1}$ .  $E_{1/2}(\text{Ru}^{3+/2+})$ : -0.50 V.

### 7.2.32 Reaction of $\text{NEt}_2\text{H}$ with $\text{cis-}[Ru(\text{acac})_2(o\text{-PhC}\equiv\text{CC}_6\text{H}_4\text{NMe}_2)][\text{PF}_6]$

To a violet solution of  $\text{cis-}[Ru(\text{acac})_2(o\text{-PhC}\equiv\text{CC}_6\text{H}_4\text{NMe}_2)][\text{PF}_6]$  (67 mg, 0.10 mmol) in  $\text{CH}_2\text{Cl}_2$  (ca. 3 mL), neat  $\text{NEt}_2\text{H}$  (35  $\mu\text{L}$ , 0.34 mmol) was added via micro-syringe causing an immediate colour change to deep red. After stirring for at least one hour, the solution was concentrated *in vacuo*

and layered with n-hexane (ca. 5 mL). Blackish red crystalline material of the complex  $cis\text{-}[\text{Ru}^{\text{III}}(\text{acac})_2(o\text{-Me}_2\text{NC}_6\text{H}_4\text{C}(\text{H})\text{C}=\text{N}(\text{C}_2\text{H}_5)_2)\text{Ph}][\text{PF}_6]$  was isolated by filtration (39 mg, 48%).

An acceptable analysis was not obtained, carbon and hydrogen percentages being consistently low. Possible contaminants may include  $\text{CH}_2\text{Cl}_2$ .

Microanalysis (Found: C, 44.33; H, 4.90; N, 3.79%.  $\text{C}_{26}\text{H}_{31}\text{F}_6\text{N}_2\text{O}_5\text{PRu}$  requires C, 48.78; H, 5.46; N, 3.79%). IR (KBr):  $\nu(\text{acac})$  1547 and 1518  $\text{cm}^{-1}$ ;  $\nu(\text{PF}_6)$  842 and 557  $\text{cm}^{-1}$ .

### 7.2.33 Reaction of $\text{H}_2\text{O}$ with $cis\text{-}[\text{Ru}(\text{acac})_2(o\text{-PhC}\equiv\text{CC}_6\text{H}_4\text{NMe}_2)][\text{PF}_6]$

Deoxygenated distilled water (101  $\mu\text{L}$ ) was added via microsyringe to a violet solution of  $cis\text{-}[\text{Ru}(\text{acac})_2(o\text{-PhC}\equiv\text{CC}_6\text{H}_4\text{NMe}_2)][\text{PF}_6]$  (257 mg, 0.39 mmol) in THF (40 mL). After stirring overnight, the solution was red. The solution was concentrated *in vacuo* and layered with n-hexane which afforded a sticky red residue. A red crystalline solid was isolated after stirring rapidly with dry ether for 30 minutes. Red crystals of  $cis\text{-}[\text{Ru}^{\text{III}}(\text{acac})_2\{o\text{-Me}_2\text{NC}_6\text{H}_4\text{C}(\text{O})\text{CH}_2\text{Ph}\}][\text{PF}_6]$  were identified by X-ray crystallography after dissolving the solid in  $\text{CH}_2\text{Cl}_2$  and the solution was carefully layered with n-hexane (181 mg, 69 %).

Microanalysis (Found: C, 45.21; H, 4.42; N, 2.29; P, 4.81.  $\text{C}_{26}\text{H}_{31}\text{F}_6\text{NO}_5\text{PRu}$  requires C, 45.68; H, 4.57; N, 2.05; P, 4.53). IR (KBr):  $\nu(\text{C}=\text{O})$  1594  $\text{cm}^{-1}$ ;  $\nu(\text{acac})$  1523  $\text{cm}^{-1}$ ;  $\nu(\text{PF}_6)$  843 and 558  $\text{cm}^{-1}$ .  $E_{1/2}(\text{Ru}^{3+}/2^+)$  (*vs* Ag/AgCl): 0.00 V.

### 7.2.34 Reaction of PPh<sub>3</sub> with *cis*-[Ru(acac)<sub>2</sub>(*o*-PhC≡CC<sub>6</sub>H<sub>4</sub>NMe<sub>2</sub>)] [PF<sub>6</sub>]

Excess PPh<sub>3</sub> (290 mg, 1.11 mmol) was added to a violet solution of *cis*-[Ru(acac)<sub>2</sub>(*o*-PhC≡CC<sub>6</sub>H<sub>4</sub>NMe<sub>2</sub>)] [PF<sub>6</sub>] (218 mg, 0.33 mmol) in CH<sub>2</sub>Cl<sub>2</sub> (15 mL) resulting in a red solution within 5 minutes. After 3 hours the solution was evaporated leaving a sticky red residue. This residue was rapidly stirred in Et<sub>2</sub>O to afford a red crystalline material (180 mg) was isolated after filtration. Crystals suitable for X-ray crystallography were not isolated.

Microanalysis (Found: C, 55.67; H 4.75; N 1.58. C<sub>44</sub>H<sub>44</sub>F<sub>6</sub>NO<sub>4</sub>P<sub>2</sub>Ru requires C, 56.96; H 4.78; N 1.51, C<sub>44</sub>H<sub>44</sub>F<sub>6</sub>NO<sub>5</sub>P<sub>2</sub>Ru requires C, 55.99; H 4.70; N 1.48). IR (KBr): ν(acac) 1567 and 1517 cm<sup>-1</sup>; ν(PF<sub>6</sub>) 841 and 558 cm<sup>-1</sup>. E<sub>1/2</sub>(Ru<sup>3+/2+</sup>) (*vs* Ag/AgCl): -0.46 V.

### 7.2.35 Reaction of dry MeOH with *cis*-[Ru(acac)<sub>2</sub>(*o*-PhC≡CC<sub>6</sub>H<sub>4</sub>NMe<sub>2</sub>)] [PF<sub>6</sub>]

Dry methanol (*ca.* 5mL) was added via syringe to a violet solution of *cis*-[Ru(acac)<sub>2</sub>(*o*-PhC≡CC<sub>6</sub>H<sub>4</sub>NMe<sub>2</sub>)] [PF<sub>6</sub>] (160 mg, 0.24 mmol) in THF (10 mL). After stirring for one hour, the solution was red. The solution was concentrated *in vacuo* and dry ether added, from which a red crystalline solid (144 mg) was isolated after stirring rapidly for 30 minutes. Although X-ray crystals were not isolated, the product is believed to be an 1:1 adduct of MeOH per ruthenium cation.

An acceptable elemental analysis could not be obtained, carbon and hydrogen percentages being consistently low.

Microanalysis (Found: C, 42.20; H, 4.20; N, 2.01. C<sub>27</sub>H<sub>33</sub>F<sub>6</sub>NO<sub>5</sub>PRu requires C, 46.49; H, 4.77; N, 2.01). IR (KBr): ν(CO) 1632 cm<sup>-1</sup>; ν(acac) 1564 and 1523 cm<sup>-1</sup>; ν(PF<sub>6</sub>) 843 and 558 cm<sup>-1</sup>.

### 7.2.36 Reaction of PPh<sub>3</sub> with *cis*-[Ru(acac)<sub>2</sub>(*o*-H<sub>2</sub>C=C(H)C<sub>6</sub>H<sub>4</sub>NMe<sub>2</sub>)] [PF<sub>6</sub>]

Excess PPh<sub>3</sub> (193 mg, 0.74 mmol) was added to a blue solution of *cis*-[Ru(acac)<sub>2</sub>(*o*-H<sub>2</sub>C=C(H)C<sub>6</sub>H<sub>4</sub>NMe<sub>2</sub>)] [PF<sub>6</sub>] (133 mg, 0.22 mmol) in CH<sub>2</sub>Cl<sub>2</sub> (15 mL) resulting in a red solution within 5 minutes. After 1.5 hours the solution was evaporated leaving a sticky red residue. This red residue was stirred rapidly in Et<sub>2</sub>O to afford a red crystalline solid (156 mg, 56%) after filtration. Crystals suitable for X-ray crystallography were grown from a CH<sub>2</sub>Cl<sub>2</sub>/n-hexane solution exposed to air.

This reaction was repeated several times; in all cases the <sup>31</sup>P{<sup>1</sup>H} NMR spectrum showed the presence of [PO<sub>2</sub>F<sub>2</sub>]<sup>-</sup>, which may account for the poor elemental analysis of the isolated compound.

Microanalysis (Found: C, 50.63; H 4.33; N 1.31. C<sub>38</sub>H<sub>42</sub>F<sub>6</sub>NO<sub>4</sub>P<sub>2</sub>Ru requires C, 53.46; H 4.96; N 1.64). IR (KBr): ν(acac) 1549 and 1520 cm<sup>-1</sup>; ν(PF<sub>6</sub>) 840 and 558 cm<sup>-1</sup>. E<sub>1/2</sub>(Ru<sup>3+</sup>/2+) (vs Ag/AgCl): -0.46 V.

Microanalysis (Found: C, 57.38; H 4.95; N 1.38; P 4.62. C<sub>38</sub>H<sub>42</sub>BF<sub>4</sub>NO<sub>4</sub>PRu requires C, 57.37; H 5.32; N 1.76; P 3.89). IR (KBr): ν(acac) 1551 and 1516 cm<sup>-1</sup>; ν(BF<sub>4</sub>) 1056 and 520 cm<sup>-1</sup>.

### 7.2.37 Preparation of *trans*-[Ru(acac)<sub>2</sub>(Ph<sub>2</sub>PC≡CH)<sub>2</sub>]

A clear solution of *cis*-[Ru(acac)<sub>2</sub>(η<sup>2</sup>-C<sub>2</sub>H<sub>4</sub>)<sub>2</sub>] (prepared from 260 mg [Ru(acac)<sub>3</sub>], 0.65 mmol) in THF (20 mL) was stirred with Ph<sub>2</sub>PC≡CCH (275 mg, 1.31 mmol) for one hour, within 5 minutes of mixing, a fine orange precipitate had formed. An orange solid was isolated after evaporating the mixture to dryness and washing with n-hexane 3 times (ca. 10 mL). 357 mg (79%) of *trans*-[Ru(acac)<sub>2</sub>(Ph<sub>2</sub>PC≡CH)<sub>2</sub>] was isolated after filtration and air-

dried. A small amount of the orange solid was recrystallised from  $\text{CH}_2\text{Cl}_2$  and n-pentane was vapour diffused into the solution resulting in large orange crystals.

The orange complex *trans*- $[\text{Ru}(\text{acac})_2(\text{Ph}_2\text{PC}\equiv\text{CH})_2]$  is very stable towards air as a solid; the solid is insoluble in benzene, toluene, n-hexane, diethyl-ether but is readily soluble in  $\text{CH}_2\text{Cl}_2$  and  $\text{C}_6\text{H}_5\text{Cl}$  forming air-stable solutions.

Microanalysis (Found: C, 63.31; H 4.97; P 8.68%.  $\text{C}_{38}\text{H}_{36}\text{O}_4\text{P}_2\text{Ru}$  requires C, 63.42; H 5.04; P 8.61%). IR (KBr):  $\nu(\text{C}\equiv\text{C})$  2035  $\text{cm}^{-1}$ ;  $\nu(\text{acac})$  1568 and 1511  $\text{cm}^{-1}$ . NMR ( $\text{CD}_2\text{Cl}_2$ ):  $\delta_{\text{H}}$  (300 MHz) 7.73-7.66 [8 H, m, *o*- $\text{PC}_6\text{H}_5$ ]; 7.36-7.26 [12 H, m, *m*- and *p*- $\text{PC}_6\text{H}_5$ ]; 4.36 [2 H, s,  $\text{CHCH}_3$ ]; 3.49 [1 H, t,  $J_{\text{PH}} = 2.4$  Hz,  $\equiv\text{CCH}$ ]; 1.39 [12 H, s,  $\text{C}(\text{O})\text{CH}_3$ ];  $\delta_{\text{C}}$  (75.43 MHz) 185.5 [s,  $\underline{\text{C}}(\text{O})\text{CH}_3$ ]; 132.7 [t,  $J_{\text{PC}} = 6.6$  Hz, *o*- $\underline{\text{C}}_6\text{H}_5$ ]; 132.0 [t,  $J_{\text{PC}} = 20$  Hz, *ipso*- $\underline{\text{C}}_6\text{H}_5$ ]; 129.6 [s, *p*- $\underline{\text{C}}_6\text{H}_5$ ]; 128.1 [t,  $J_{\text{PC}} = 4.5$  Hz, *m*- $\underline{\text{C}}_6\text{H}_5$ ]; 100.3 [ $\text{C}(\text{O})\underline{\text{C}}\text{H}$ ]; 97.7 [d,  $J_{\text{PC}} = 4.2$  Hz,  $-\text{C}\equiv\underline{\text{C}}\text{H}$ ]; 79.0 (t,  $J_{\text{PC}} = 30$  Hz,  $-\underline{\text{C}}\equiv\text{CH}$ ]; 27.6 [s,  $\text{C}(\text{O})\underline{\text{C}}\text{H}_3$ ];  $\delta_{\text{P}}$  (121.5 MHz) +21.9 (s).  $E_{1/2}(\text{Ru}^{3+/2+})$ : +0.16 V.

### 7.2.38 Preparation of *trans*- $[\text{Ru}(\text{acac})_2(\text{Ph}_2\text{PC}\equiv\text{CMe})_2]$

A solution of *cis*- $[\text{Ru}(\text{acac})_2(\eta^2\text{-C}_2\text{H}_4)_2]$  (prepared from 260 mg  $[\text{Ru}(\text{acac})_3]$ , 0.65 mmol) in THF (20 mL) was stirred with  $\text{Ph}_2\text{PC}\equiv\text{CCCH}_3$  (305 mg, 1.36 mmol) for one hour during which a fine orange precipitate formed. An orange solid was isolated after removing the solvent *in vacuo* and washed with n-hexane 3 times (*ca.* 10 mL). 482 mg of the orange solid *trans*- $[\text{Ru}(\text{acac})_2(\text{Ph}_2\text{PC}\equiv\text{CCH}_3)_2]$  was isolated (98% yield). The solid was recrystallised from the vapour diffusion of n-pentane into an orange  $\text{CH}_2\text{Cl}_2$  solution resulting in the isolation of orange crystals suitable for X-ray diffraction studies.



The orange solid *trans*-[Ru(acac)<sub>2</sub>(Ph<sub>2</sub>PC≡CCH<sub>3</sub>)<sub>2</sub>] has similar physical properties to those described for *trans*-[Ru(acac)<sub>2</sub>(Ph<sub>2</sub>PC≡CH)<sub>2</sub>]

Microanalysis (Found: C, 63.98; H 5.61; P 8.41%. C<sub>40</sub>H<sub>40</sub>O<sub>4</sub>P<sub>2</sub>Ru requires C, 64.25; H 5.39; P 8.28%). IR (KBr): ν(C≡C) 2198 cm<sup>-1</sup>; ν(acac) 1568 and 1512 cm<sup>-1</sup>. NMR (CD<sub>2</sub>Cl<sub>2</sub>): δ<sub>H</sub> (300 MHz) 7.77-7.71 [8 H, m, *o*-PC<sub>6</sub>H<sub>5</sub>]; 7.37-7.32 [12 H, m, *m*- and *p*-PC<sub>6</sub>H<sub>5</sub>]; 4.43 [2 H, s, CHCH<sub>3</sub>]; 2.20 [6 H, s, -C≡CCH<sub>3</sub>]; 1.42 [12 H, s, C(O)CH<sub>3</sub>]. δ<sub>C</sub> (75.43 MHz) 185.6 [s, C(O)CH<sub>3</sub>]; 133.5 [t, J<sub>PC</sub> = 20 Hz, *ipso*-PC<sub>6</sub>H<sub>5</sub>]; 132.7 [t, J<sub>PC</sub> = 6.3 Hz, *o*-PC<sub>6</sub>H<sub>5</sub>]; 129.2 [s, *p*PC<sub>6</sub>H<sub>5</sub>]; 127.9 [t, J<sub>PC</sub> = 4.3 Hz, *m*PC<sub>6</sub>H<sub>5</sub>]; 107.5 [s, -C≡CCH<sub>3</sub>]; 99.9 [C(O)CH]; 72.4 [t J<sub>PC</sub> = 36 Hz, -C≡CCH<sub>3</sub>]; 27.4 [s, C(O)CH<sub>3</sub>], 6.0 [s, -C≡CCH<sub>3</sub>]; δ<sub>P</sub> (121.5 MHz) +21.9 (s). E<sub>1/2</sub>(Ru<sup>3+/2+</sup>): +0.08 V.

### 7.2.39 Preparation of *trans*-[Ru(acac)<sub>2</sub>(Ph<sub>2</sub>PC≡CPh)<sub>2</sub>]

A solution of *cis*-[Ru(acac)<sub>2</sub>(η<sup>2</sup>-C<sub>2</sub>H<sub>4</sub>)<sub>2</sub>] (208 mg [Ru(acac)<sub>3</sub>], 0.52 mmol) in THF (16 ml) was stirred with Ph<sub>2</sub>PC≡CPh (300 mg, 1.05 mmol) for one hour during which an orange solid formed. The solvent was removed *in vacuo* to leave an orange solid which was washed with n-pentane (*ca.* 20 mL) and isolated via filtration. The solid was washed a further two times with n-pentane (*ca.* 10 mL). The mass of the isolated material was 278 mg (61%).

The orange solid *trans*-[Ru(acac)<sub>2</sub>(Ph<sub>2</sub>PC≡CPh)<sub>2</sub>] has similar physical properties to those described for *trans*-[Ru(acac)<sub>2</sub>(Ph<sub>2</sub>PC≡CH)<sub>2</sub>].

Microanalysis (Found: C, 68.67; H 5.22; P 7.00%. C<sub>50</sub>H<sub>44</sub>O<sub>4</sub>P<sub>2</sub>Ru requires C, 68.88; H 5.09; P 7.10%). IR (KBr): ν(C≡C) 2172 cm<sup>-1</sup>; ν(acac) 1567 and 1512 cm<sup>-1</sup>. NMR (CD<sub>2</sub>Cl<sub>2</sub>): δ<sub>H</sub> (300 MHz) 7.84 - 7.30 [30 H, m, C<sub>6</sub>H<sub>5</sub>]; 4.50 [2 H, s, CHCH<sub>3</sub>]; 1.37 [12 H, s, C(O)CH<sub>3</sub>]. δ<sub>C</sub> (75.43 MHz) 186.0 [s, C(O)CH<sub>3</sub>]; 132.9 [t, J<sub>PC</sub> = 6.5 Hz, *ipso*-PC<sub>6</sub>H<sub>5</sub>]; 132.1 [s, *ipso*-C<sub>6</sub>H<sub>5</sub>]; 129.6 [s, C<sub>6</sub>H<sub>5</sub>]; 129.5 [s, C<sub>6</sub>H<sub>5</sub>]; 128.8 [s, C<sub>6</sub>H<sub>5</sub>];

128.1 [t,  $J_{PC} = 4.3$  Hz,  $mPC_6H_5$ ]; 108.9 [m,  $-C\equiv C-Ph$ ]; 100.3 [s,  $C(O)CH$ ], 83.6 [m,  $-C\equiv C-Ph$ ]; 27.5 [s,  $C(O)CH_3$ ];  $\delta_P$  (121.5 MHz) +22.1 (s).  $E_{1/2}(Ru^{3+/2+})$ : +0.12V.

#### 7.2.40 Preparation of *trans*-[Ru(acac)<sub>2</sub>(Ph<sub>2</sub>PC≡CPh<sub>2</sub>)<sub>n</sub>]

Solid Ph<sub>2</sub>PC≡CPh<sub>2</sub> (400 mg, 1.01 mmol) was added to a THF solution of *cis*-[Ru(acac)<sub>2</sub>(η<sup>2</sup>-C<sub>8</sub>H<sub>14</sub>)<sub>2</sub>] (200 mg [Ru(acac)<sub>3</sub>], 0.51 mmol) and the mixture was stirred overnight, during which time an orange solid formed. The solid was isolated after filtration (325 mg) and washed several times with n-hexane. Free Ph<sub>2</sub>PC≡CPh<sub>2</sub> was detected in the supernatant by <sup>31</sup>P{<sup>1</sup>H} NMR spectroscopy but no attempt was made to determine the amount present.

The isolated solid is insoluble in THF, benzene, toluene, CH<sub>2</sub>Cl<sub>2</sub> and C<sub>6</sub>H<sub>5</sub>Cl and could not, therefore, be purified by recrystallization. The properties are suggestive of an oligomeric structure *trans*-[Ru(acac)<sub>2</sub>(Ph<sub>2</sub>PC≡CPh<sub>2</sub>)<sub>n</sub>].

Microanalysis (Found: C, 64.24; H 4.95. C<sub>36</sub>H<sub>34</sub>O<sub>4</sub>P<sub>2</sub>Ru requires C, 62.33; H 4.94). IR (KBr): ν(acac) 1564 and 1510 cm<sup>-1</sup>.

#### 7.2.41 Preparation of *cis*-[Ru(acac)<sub>2</sub>(Ph<sub>2</sub>PC≡CMe)<sub>2</sub>]

An orange solution of *trans*-[Ru(acac)<sub>2</sub>(Ph<sub>2</sub>PC≡CCH<sub>3</sub>)<sub>2</sub>] (232 mg, 0.31 mmol) in C<sub>6</sub>H<sub>5</sub>Cl (5 mL) was refluxed for 1 hour, during which time a colour change from orange to yellow occurred. A yellow residue was obtained after the solvent was removed *in vacuo*. The residue was dissolved in CH<sub>2</sub>Cl<sub>2</sub> (2 mL) forming a yellow solution and n-hexane (25 mL) was carefully poured into the flask. A yellow micro-crystalline solid was obtained the following day which was filtered and washed with n-hexane (*ca.* 5 mL). 151 mg of the bright yellow solid *cis*-[Ru(acac)<sub>2</sub>(Ph<sub>2</sub>PC≡CCH<sub>3</sub>)<sub>2</sub>] was isolated (65%).

It is very stable towards air and is readily soluble in benzene, toluene,  $\text{CH}_2\text{Cl}_2$  and  $\text{C}_6\text{H}_5\text{Cl}$  forming yellow air-stable solutions.

Microanalysis (Found: C, 64.54; H 5.43; P 8.33%.  $\text{C}_{40}\text{H}_{40}\text{O}_4\text{P}_2\text{Ru}$  requires C, 64.25; H 5.39; P 8.28%). IR (KBr):  $\nu(\text{C}\equiv\text{C})$  2200  $\text{cm}^{-1}$ ;  $\nu(\text{acac})$  1574 and 1514  $\text{cm}^{-1}$ . NMR ( $\text{CD}_2\text{Cl}_2$ ):  $\delta_{\text{H}}$  (300 MHz) 7.90 - 7.00 [40 H, m,  $\text{C}_6\text{H}_5$ ]; 7.59 - 7.53 [4 H, m,  $\text{C}_6\text{H}_5$ ]; 7.25 - 7.08 [12 H, m,  $\text{C}_6\text{H}_5$ ]; 5.33 [2 H, s,  $\text{C}(\text{O})\text{CH}$ ]; 2.07, 1.32 [6 H each, both s,  $\text{C}(\text{O})\text{CH}_3$ ]; 2.02 [6 H, t,  $J_{\text{PH}} = 1.2$  Hz,  $-\text{C}\equiv\text{CCH}_3$ ].  $\delta_{\text{C}}$  (75.43 MHz) 187.2, 185.4 [both s,  $\text{C}(\text{O})\text{CH}_3$ ]; 137.5 [t,  $J_{\text{PC}} = 26$  Hz, *ipso*- $\text{C}_6\text{H}_5$ ]; 136.7 [t,  $J_{\text{PC}} = 22$  Hz, *ipso*- $\text{C}_6\text{H}_5$ ]; 132.5 [t,  $J_{\text{PC}} = 5.5$  Hz, *o*- $\text{C}_6\text{H}_5$ ]; 132.1 [t,  $J_{\text{PC}} = 5.5$  Hz, *o*- $\text{C}_6\text{H}_5$ ]; 128.7 [s, *p*- $\text{C}_6\text{H}_5$ ]; 127.6 [t,  $J_{\text{PC}} = 5$  Hz, *m*- $\text{C}_6\text{H}_5$ ]; 127.2 [t,  $J_{\text{PC}} = 5$  Hz, *m*- $\text{C}_6\text{H}_5$ ]; 107.9 [t,  $J_{\text{PC}} = 5.5$  Hz,  $-\text{C}\equiv\text{CCH}_3$ ]; 99.5 [s,  $\text{C}(\text{O})\text{CH}$ ]; 72.8 (a symmetrical six line multiplet, spacing between lines 17.6, 38.4, 6.9, 37.0 and 18.7 Hz,  $-\text{C}\equiv\text{CCH}_3$ ); 28.6, 27.2 [both s,  $\text{C}(\text{O})\text{CH}_3$ ]; 5.8 [s,  $-\text{C}\equiv\text{CCH}_3$ ].  $\delta_{\text{P}}$  (121.5 MHz) +39.9 (s).  $E_{1/2}(\text{Ru}^{3+/2+})$  (*vs* Ag/AgCl): +0.19 V.

#### 7.2.42 Preparation of *cis*- $[\text{Ru}(\text{acac})_2(\text{Ph}_2\text{PC}\equiv\text{CPh})_2]$

A solution of *trans*- $[\text{Ru}(\text{acac})_2(\text{Ph}_2\text{PC}\equiv\text{CPh})_2]$  (120 mg, 0.14 mmol) in  $\text{C}_6\text{H}_5\text{Cl}$  (20 mL) was refluxed for one hour during which time the colour changed from orange to yellow. The solvent was evaporated leaving a yellow residue from which a yellow solid formed after stirring with n-hexane (10 mL). The solid was filtered and washed with n-hexane (*ca.* 5 mL). The yield was 80 mg (67%).

The yellow solid *cis*- $[\text{Ru}(\text{acac})_2(\text{Ph}_2\text{PC}\equiv\text{CPh})_2]$  has similar physical properties to those described for *cis*- $[\text{Ru}(\text{acac})_2(\text{Ph}_2\text{PC}\equiv\text{CCH}_3)_2]$ .

Microanalysis (Found: C, 67.74; H 5.08.  $\text{C}_{50}\text{H}_{44}\text{O}_4\text{P}_2\text{Ru}$  requires C, 68.88; H 5.09). IR (KBr):  $\nu(\text{C}\equiv\text{C})$  2171  $\text{cm}^{-1}$ ;  $\nu(\text{acac})$  1574 and 1515  $\text{cm}^{-1}$ . NMR ( $\text{CD}_2\text{Cl}_2$ ):

$\delta_{\text{H}}$  (300 MHz) 7.94 - 7.08 [30 H, m,  $\text{C}_6\text{H}_5$ ], 5.23 [2 H,  $\text{C}(\text{O})\text{CH}$ ], 2.02, 1.38 [12 H,  $\text{C}(\text{O})\text{CH}_3$ ].  $\delta_{\text{C}}$  (75.43 MHz) 187.3, 185.4 [ $\text{C}(\text{O})\text{CH}_3$ ]; 137.2 [t,  $J_{\text{PC}} = 26$  Hz, *ipso*- $\text{C}_6\text{H}_5$ ]; 136.7 [t,  $J_{\text{PC}} = 23$  Hz, *ipso*- $\text{C}_6\text{H}_5$ ]; 132.5 [t,  $J_{\text{PC}} = 5.5$  Hz, *o*- $\text{C}_6\text{H}_5$ ]; 132.0 [s, *o*- $\text{C}_6\text{H}_5$ ]; 132.0 [s, *o*- $\text{C}_6\text{H}_5$ ]; 131.9 [t,  $J_{\text{PC}} = 5.5$  Hz, *o*- $\text{C}_6\text{H}_5$ ]; 129.5 [s, *o*- $\text{C}_6\text{H}_5$ ]; 128.9 [s, *p*- $\text{C}_6\text{H}_5$ ]; 128.8 [s, *p*- $\text{C}_6\text{H}_5$ ]; 127.7 (t,  $J_{\text{PC}} = 5$  Hz, *m*- $\text{C}_6\text{H}_5$ ); 109.09 [t,  $J_{\text{PC}} = 5$  Hz,  $-\text{C}\equiv\text{CPh}$ ]; 99.5 [s,  $\text{C}(\text{O})\text{CH}$ ]; 84.3 [a symmetrical six line multiplet, spacing between lines 18.6, 34.0, 7.7, 34.0 and 17.6 Hz,  $-\text{C}\equiv\text{CCH}_3$ ]; 28.6, 27.2 [both s,  $\text{C}(\text{O})\text{CH}_3$ ].  $\delta_{\text{P}}$  (121.5 MHz) +40.3 (s).  $E_{1/2}(\text{Ru}^{3+/2+})$ : +0.49 V.

### 7.2.43 Preparation of *cis*- $\{[\text{Ru}(\text{acac})_2(\text{Ph}_2\text{PC}\equiv\text{CPh}_2)]_2\}$

A suspension of the oligomeric material *trans*- $[\text{Ru}(\text{acac})_2(\text{Ph}_2\text{PC}\equiv\text{CPh}_2)]_n$  (157 mg; 0.11 mmol) in  $\text{C}_6\text{H}_5\text{Cl}$  (20 mL) was heated to *ca.* 150 °C for 3 hours, during which time a clear yellow solution formed. After cooling the solution, the solvent was removed *in vacuo* leaving a yellow residue which was dissolved in a small amount of  $\text{CH}_2\text{Cl}_2$  and layered with *n*-hexane (20 mL). 63 mg (40%) of the yellow *cis*-isomer was isolated after filtration and washed with *n*-hexane.

The isolated air-stable yellow solid is readily soluble in  $\text{CH}_2\text{Cl}_2$ ,  $\text{C}_6\text{H}_5\text{Cl}$  and also forms yellow air-stable solutions.

Microanalysis (Found: C, 61.18; H 4.95%.  $\text{C}_{72}\text{H}_{68}\text{O}_8\text{P}_4\text{Ru}_2$  requires C, 62.33; H 4.95%). IR (KBr):  $\nu(\text{acac})$  1573 and 1514  $\text{cm}^{-1}$ . Raman (solid):  $\nu(\text{C}\equiv\text{C})$  2131  $\text{cm}^{-1}$ . NMR ( $\text{CD}_2\text{Cl}_2$ ):  $\delta_{\text{H}}$  (300 MHz) 8.16 - 8.10 [16 H, m,  $\text{C}_6\text{H}_5$ ]; 7.25 - 6.99 [14 H, m,  $\text{C}_6\text{H}_5$ ]; 5.02 [2 H,  $\text{C}(\text{O})\text{CH}$ ]; 1.65, 1.45 [12 H,  $\text{C}(\text{O})\text{CH}_3$ ].  $\delta_{\text{C}}$  (75.43 MHz) 187.4, 184.6 [ $\text{C}(\text{O})\text{CH}_3$ ]; 135.9 [t,  $J_{\text{PC}} = 24$  Hz, *ipso*- $\text{C}_6\text{H}_5$ ]; 135.4 [t,  $J_{\text{PC}} = 5.5$  Hz, *o*- $\text{C}_6\text{H}_5$ ]; 133.9 [t,  $J_{\text{PC}} = 24$  Hz, *ipso*- $\text{C}_6\text{H}_5$ ]; 132.0 [t,  $J_{\text{PC}} = 5.2$  Hz, *o*- $\text{C}_6\text{H}_5$ ]; 129.6 [s, *p*- $\text{C}_6\text{H}_5$ ]; 128.6 [s, *p*- $\text{C}_6\text{H}_5$ ]; 127.6 [t,  $J_{\text{PC}} = 4$  Hz, *m*- $\text{C}_6\text{H}_5$ ]; 127.5 [t,  $J_{\text{PC}} = 4$  Hz, *m*- $\text{C}_6\text{H}_5$ ]; 104.8 [a symmetrical six line multiplet, spacing between lines 19.0, 30.8, 7.7,

27.0 and 19.2 Hz,  $-\text{C}\equiv\text{CPh}_2$ ]; 99.6 [s,  $\text{C}(\text{O})\underline{\text{C}}\text{H}$ ]; 27.7, 27.6 [both s,  $\text{C}(\text{O})\underline{\text{C}}\text{H}_3$ ].  $\delta_{\text{P}}$  (121.5 MHz) +43.1 (s).  $E_{1/2}(\text{Ru}^{3+/2+})$ : +0.60 and +0.90 V.

#### 7.2.44 Preparation of *trans*-[Ru(acac)<sub>2</sub>(Ph<sub>2</sub>PC≡CH)<sub>2</sub>][PF<sub>6</sub>]

The addition of AgPF<sub>6</sub> (50 mg, 0.20 mmol) to a solution of *trans*-[Ru(acac)<sub>2</sub>(Ph<sub>2</sub>PC≡CH)<sub>2</sub>] (100 mg, 0.14 mmol) in CH<sub>2</sub>Cl<sub>2</sub> (10 mL) resulted in immediate change in colour from orange to blue-green, a grey metallic mirror forming on the flask. The solution was stirred for 30 minutes and filtered through Celite. The solvent was removed *in vacuo* leaving a green solid which was dissolved in a small amount of CH<sub>2</sub>Cl<sub>2</sub> and carefully layered with n-pentane. 96 mg (89%) of the green crystalline solid *trans*-[Ru(acac)<sub>2</sub>(Ph<sub>2</sub>PC≡CH)<sub>2</sub>][PF<sub>6</sub>] was isolated.

It is stable towards air and is insoluble in benzene and ether but is readily soluble in CH<sub>2</sub>Cl<sub>2</sub> forming air-stable green solutions.

Microanalysis (Found: C, 50.52; H 4.11; P 10.40%. C<sub>38</sub>H<sub>36</sub>F<sub>6</sub>O<sub>4</sub>P<sub>3</sub>Ru.0.5(CH<sub>2</sub>Cl<sub>2</sub>) requires C, 50.98; H 4.11; P 10.24%). IR (KBr):  $\nu(\text{C}\equiv\text{C})$  2059 cm<sup>-1</sup>;  $\nu(\text{acac})$  1538 and 1520 cm<sup>-1</sup>;  $\nu(\text{PF}_6)$  841 cm<sup>-1</sup>.  $E_{1/2}(\text{Ru}^{3+/2+})$ : +0.16 V.

#### 7.2.45 Preparation of *trans*-[Ru(acac)<sub>2</sub>(Ph<sub>2</sub>PC≡CCMe)<sub>2</sub>][PF<sub>6</sub>]

The addition of AgPF<sub>6</sub> (52 mg, 0.21 mmol) to an orange solution of *trans*-[Ru(acac)<sub>2</sub>(Ph<sub>2</sub>PC≡CCH<sub>3</sub>)<sub>2</sub>] (65 mg, 0.09 mmol) in CH<sub>2</sub>Cl<sub>2</sub> (5 mL) resulted in a immediate colour change to a green and a grey solid formed. The reaction was stirred for 90 minutes before filtrating through Celite and the removal of the solvent *in vacuo* resulted in a green residue. A small amount of CH<sub>2</sub>Cl<sub>2</sub> was added to dissolve the residue and layered with n-pentane (*ca.* 5 mL). The solution was then stirred for 1 minute and the

solution allowed to stand. The green solid settled to the bottom of the flask leaving a pale orange solution. The solution was decanted off and the above procedure was repeated until the solution was colourless. The green solid was dissolved in  $\text{CH}_2\text{Cl}_2$  (ca. 2 mL) and n-pentane (ca. 10 mL) was carefully layered onto the green solution, which was left to stand overnight. 70 mg (90%) of the green crystalline solid *trans*- $[\text{Ru}(\text{acac})_2(\text{Ph}_2\text{PC}\equiv\text{CCH}_3)_2][\text{PF}_6]$  had formed with some X-ray quality green crystals.

The green crystalline solid *trans*- $[\text{Ru}(\text{acac})_2(\text{Ph}_2\text{PC}\equiv\text{CCH}_3)_2][\text{PF}_6]$  has similar physical properties to those found for *trans*- $[\text{Ru}(\text{acac})_2(\text{Ph}_2\text{PC}\equiv\text{CH})_2][\text{PF}_6]$ .

Microanalysis (Found: C, 53.61; H 4.55; P, 10.71%).  $\text{C}_{40}\text{H}_{40}\text{F}_6\text{O}_4\text{P}_3\text{Ru}$  requires C, 53.82; H 4.52; P, 10.41%. IR (KBr):  $\nu(\text{C}\equiv\text{C})$  2201  $\text{cm}^{-1}$ ;  $\nu(\text{acac})$  1520  $\text{cm}^{-1}$ ;  $\nu([\text{PF}_6])$  840  $\text{cm}^{-1}$ .  $E_{1/2}(\text{Ru}^{3+/2+})$ : +0.09 V.

## 7.3 References

- (1) Armarego, W. L. F.; Perrin, D. D. *Purification of Laboratory Chemicals*; 4th ed.; Butterworth Heinemann: 1996.
- (2) Brauer, G. *Handbook of Preparative Chemistry*; Academic: New York, 1965; Vol. 2, p 1806.
- (3) Gordon, J. G.; O'Connor, M. J.; Holm, R. H. *Inorg. Chim. Acta* **1971**, *5*, 381.
- (4) Earley, J. E.; Base, R. N.; Berrie, B. H. *Inorg. Chem.* **1983**, *22*, 1836.
- (5) Knowles, T. S.; Howlin, B. J.; Jones, J. R.; Povey, D. C.; Amodio, C. A. *Polyhedron* **1993**, *12*, 2921.
- (6) Knowles, T. S.; Howells, M. E.; Howlin, B. J.; Smith, G. W.; Amodio, C. A. *Polyhedron* **1994**, *13*, 2197.
- (7) Brauer, G. *Handbuch der Präparativen Anorganischen Chemie*; Ferdinand Enke Verlag: Stuttgart, 1981, p 1845.
- (8) Bennett, M. A.; Chung, G.; Hockless, D. C. R.; Neumann, H.; Willis, A. C. *J. Chem. Soc., Dalton Trans.* **1999**, 3451.
- (9) Bennett, M. A.; Heath, G. A.; Hockless, D. C. R.; Kovacic, I.; Willis, A. *C. J. Am. Chem. Soc.* **1998**, *120*, 932.
- (10) Bennett, M. A.; Heath, G. A.; Hockless, D. C. R.; Kovacic, I.; Willis, A. *C. Organometallics* **1998**, *17*, 5867.
- (11) Charrier, C.; Chodkiewicz, W.; Cadiot, P. *Bull. Soc. Chim. Fr.* **1966**, 1002.
- (12) Carty, A. J.; Hota, N. K.; Ng, T. W.; Patel, H. A.; O'Connor, T. J. *Can. J. Chem.* **1971**, *49*, 2706.
- (13) Duff, C. M.; Heath, G. A. *Inorg. Chem.* **1991**, *30*, 2528.
- (14) Grünwald, G.; Laubender, M.; Wolf, J.; Werner, H. *J. Chem. Soc., Dalton Trans.* **1998**, 833.

# *Appendices*



**Table A.1.1:** Crystallographic and refinement data for *cis*-[Ru(acac)<sub>2</sub>(η<sup>2</sup>-C<sub>2</sub>H<sub>4</sub>)<sub>2</sub>] at 200 K.

<b>Crystal Data</b>	
Empirical Formula	C <sub>14</sub> H <sub>22</sub> O <sub>4</sub> Ru
Formula Weight	355.40
Crystal Colour, Habit	yellow, plate
Crystal Dimensions	0.20 x 0.20 x 0.10 mm
Crystal System	triclinic
Lattice Type	Primitive
Lattice Parameters	a = 7.6278(2) Å b = 8.9725(4) Å c = 12.5027(5) Å α = 76.719(2) ° β = 74.620(2) ° γ = 70.659(2) ° V = 766.78(3) Å <sup>3</sup>
Space Group	P $\bar{1}$ (#2)
Z value	2
D <sub>calc</sub>	1.535 g/cm <sup>3</sup>
F <sub>000</sub>	364.00
μ(MoKα)	10.27 cm <sup>-1</sup>
<b>Intensity Measurements</b>	
diffractometer	Nonius KappaCD
Radiation	MoKα (λ = 0.71069 Å) graphite monochromated
Detector Aperture	65 mm x 65 mm
Data Images	2.00°/frame; 20 sec/°
Detector Position	25.00 mm
2θ <sub>max</sub>	55.1°
No. of Reflections Measured	Total: 8834 Unique: 3476 (R <sub>int</sub> = 0.028)
Corrections	Lorentz-polarization Absorption (trans. Factors: 0.905 - 0.845)

**Table A.1.1 (cont):** Crystallographic and refinement data for *cis*-[Ru(acac)<sub>2</sub>(η<sup>2</sup>-C<sub>2</sub>H<sub>4</sub>)<sub>2</sub>] at 200 K.

<b>Structure Solution and Refinement</b>	
Structure Solution	Patterson Methods (DIRDIF92 PATTY)
Refinement	Full-Matrix least squares
Function Minimized	$\sum w( F_o  -  F_c )^2$
Least Squares Weights	$w = [\sigma_c^2(F_o) + 0.25p^2F_o^2]^{-1}$
p-factor	0.040
Anamalous Dispersion	All non-hydrogen atoms
No. Observations (I>2.0σ(I))	3285
No. of variables	196
Reflection/Parameter Rotation	16.76
Residuals: R; Rw	0.025; 0.035
Goodness of Fit Indicator	1.23
Max Shift/Error in Final Cycle	<0.01
Max peak in Final Diff. Map	0.44 e <sup>-</sup> /Å <sup>3</sup>
Min peak in Final Diff Map	-0.96 e <sup>-</sup> /Å <sup>3</sup>

**Table A.1.2:** Interatomic distances (Å) and angles (°) involving non-hydrogen atoms of the molecular structure of *cis*-[Ru(acac)<sub>2</sub>(η<sup>2</sup>-C<sub>2</sub>H<sub>4</sub>)<sub>2</sub>] at 200 K.

Ru(1)-O(1)	2.080(1)	Ru(1)-O(2)	2.068(1)
Ru(1)-O(3)	2.061(1)	Ru(1)-O(4)	2.055(1)
Ru(1)-C(11)	2.205(2)	Ru(1)-C(12)	2.209(2)
Ru(1)-C(13)	2.212(2)	Ru(1)-C(14)	2.183(2)
O(1)-C(2)	1.270(2)	O(2)-C(4)	1.264(2)
O(3)-C(7)	1.272(3)	O(4)-C(9)	1.273(3)
C(1)-C(2)	1.506(3)	C(2)-C(3)	1.396(3)
C(3)-C(4)	1.391(3)	C(4)-C(5)	1.509(3)
C(6)-C(7)	1.506(3)	C(7)-C(8)	1.396(3)
C(8)-C(9)	1.403(3)	C(9)-C(10)	1.507(3)
C(11)-C(12)	1.370(3)	C(13)-C(14)	1.353(4)
C(11)-H(15)	0.90(3)	C(11)-H(16)	0.89(3)
C(12)-H(17)	0.98(2)	C(12)-H(18)	0.90(3)
C(13)-H(19)	0.88(3)	C(13)-H(20)	1.04(3)
C(14)-H(21)	0.98(3)	C(14)-H(22)	0.95(3)
O(1)-Ru(1)-O(2)	90.32(6)	O(1)-Ru(1)-O(3)	85.87(6)
O(1)-Ru(1)-O(4)	170.05(5)	O(1)-Ru(1)-C(11)	111.64(7)
O(1)-Ru(1)-C(12)	75.63(7)	O(1)-Ru(1)-C(13)	98.47(8)
O(1)-Ru(1)-C(14)	85.18(8)	O(2)-Ru(1)-O(3)	81.56(6)

**Table A.1.2 (cont):** *Interatomic distances (Å) and angles (°) involving non-hydrogen atoms of the molecular structure of  $\text{cis-[Ru(acac)}_2(\eta^2\text{-C}_2\text{H}_4)_2]$  at 200 K.*

O(2)-Ru(1)-O(4)	79.86(6)	O(2)-Ru(1)-C(11)	152.77(8)
O(2)-Ru(1)-C(12)	160.95	O(2)-Ru(1)-C(13)	112.26(8)
O(2)-Ru(1)-C(14)	79.25(8)	O(3)-Ru(1)-O(4)	94.21(6)
O(3)-Ru(1)-C(11)	84.11(7)	O(3)-Ru(1)-C(12)	84.60(8)
O(3)-Ru(1)-C(13)	165.35(8)	O(3)-Ru(1)-C(14)	158.74(9)
O(4)-Ru(1)-C(11)	78.24(7)	O(4)-Ru(1)-C(12)	114.29(7)
O(4)-Ru(1)-C(13)	83.92(8)	O(4)-Ru(1)-C(14)	91.35(8)
C(11)-Ru(1)-C(12)	36.17(8)	C(11)-Ru(1)-C(13)	81.28(9)
C(11)-Ru(1)-C(14)	117.13(9)	C(12)-Ru(1)-C(13)	83.0(1)
C(12)-Ru(1)-C(14)	111.66(9)	C(13)-Ru(1)-C(14)	35.85(9)
Ru(1)-O(1)-C(2)	124.0(1)	Ru(1)-O(2)-C(4)	124.4(1)
Ru(1)-O(3)-C(7)	121.4(1)	Ru(1)-O(4)-C(9)	121.6(1)
O(1)-C(2)-C(1)	114.9(2)	O(1)-C(2)-C(3)	126.6(2)
C(1)-C(2)-C(3)	118.4(2)	C(2)-C(3)-C(4)	127.2(2)
O(2)-C(4)-C(3)	126.4(2)	O(2)-C(4)-C(5)	114.5(2)
O(3)-C(7)-C(8)	127.2(2)	C(6)-C(7)-C(8)	118.5(2)
C(7)-C(8)-C(9)	128.3(2)	O(4)-C(9)-C(8)	126.9(2)
O(4)-C(9)-C(10)	114.3(2)	C(8)-C(9)-C(10)	118.7(2)
Ru(1)-C(11)-C(12)	72.1(1)	Ru(1)-C(12)-C(11)	71.7(1)
Ru(1)-C(13)-C(14)	70.9(1)	Ru(1)-C(14)-C(13)	73.2(1)
Ru(1)-C(11)-H(15)	103(2)	Ru(1)-C(11)-H(16)	108(2)
C(12)-C(11)-H(15)	121(2)	C(12)-C(11)-H(16)	123(2)
H(15)-C(11)-H(16)	115(2)	Ru(1)-C(12)-H(17)	103(1)
Ru(1)-C(12)-H(18)	110(2)	C(11)-C(12)-H(17)	121(2)
C(11)-C(12)-H(18)	120(2)	H(17)-C(12)-H(18)	117(2)
Ru(1)-C(13)-H(19)	105(2)	Ru(1)-C(13)-H(20)	116(1)
C(14)-C(13)-H(19)	117(2)	C(14)-C(13)-H(20)	126(2)
H(19)-C(13)-H(20)	112(2)	Ru(1)-C(14)-H(21)	101(2)
Ru(1)-C(14)-H(22)	109(2)	C(13)-C(14)-H(21)	123(2)
C(13)-C(14)-H(22)	118(2)	H(21)-C(14)-H(22)	117(2)

**Table A.2.1:** Crystallographic and refinement data for *trans*-[Ru(acac)<sub>2</sub>(η<sup>2</sup>-C<sub>2</sub>H<sub>4</sub>)(C<sub>5</sub>H<sub>5</sub>N)].

<b>Crystal Data</b>	
Empirical Formula	C <sub>17</sub> H <sub>23</sub> NO <sub>4</sub> Ru
Formula Weight	406.44
Crystal Colour, Habit	orange, plate
Crystal Dimensions	0.27 × 0.19 × 0.08 mm
Crystal System	monoclinic
Lattice Type	Primitive
No. of Reflections Used for Unit Cell Determination (2θ range)	23 (109.2 - 109.8°)
Omega Scan Peak Width at Half-height	0.31°
Lattice Parameters	a = 8.340(1) Å b = 17.307(1) Å c = 13.026(1) Å β = 99.324(9)° V = 1855.3(3) Å <sup>3</sup>
Space Group	P2 <sub>1</sub> /n (#14)
Z value	4
D <sub>calc</sub>	1.455 g/cm <sup>3</sup>
F <sub>000</sub>	832.00
μ(MoKα)	71.42 cm <sup>-1</sup>
<b>Intensity Measurements</b>	
diffractometer	Rigaku AFC6R
Radiation	CuKα (λ = 1.54178 Å) graphite monochromated
Take-off Angle	6.0°
Detector Aperture	9 mm horizontal 7.0 mm vertical
Crystal to Detector Distance	400 mm
Voltage, Current	50 kV, 180 mA
Temperature	-30.0 °C
Scan Type	ω-2θ
Scan Rate	16.0°/min (in ω) (up to 4 scans)
Scan Width	(1.20 + 0.30 tan θ)°
2θ <sub>max</sub>	120.1°
No. of Reflections Measured	Total: 5970 Unique: 2761 (R <sub>int</sub> = 0.044)
Corrections	Lorentz-polarization Absorption (trans. Factors: 0.2791 - 0.5797)

**Table A.2.1 (cont):** Crystallographic and refinement data for *trans*-[Ru(acac)<sub>2</sub>(η<sup>2</sup>-C<sub>2</sub>H<sub>4</sub>)(C<sub>5</sub>H<sub>5</sub>N)].

<b>Structure Solution and Refinement</b>	
Structure Solution	Direct Methods (SIR92)
Refinement	Full-Matrix least squares
Function Minimized	$\sum w( F_o  -  F_c )^2$
Least Squares Weights	$w = [\sigma_c^2(F_o) + 0.25p^2F_o^2]^{-1}$
p-factor	0.0200
Anomalous Dispersion	All non-hydrogen atoms
No. Observations (I>2.0σ(I))	2551
No. of variables	227
Reflection/Parameter Rotation	11.24
Residuals: R; R <sub>w</sub>	0.028; 0.031
Goodness of Fit Indicator	1.83
Max Shift/Error in Final Cycle	0.02
Max peak in Final Diff. Map	0.71 e <sup>-</sup> /Å <sup>3</sup>
Min peak in Final Diff Map	-0.58 e <sup>-</sup> /Å <sup>3</sup>

**Table A.2.2:** Interatomic distances (Å) and angles (°) involving non-hydrogen atoms of the molecular structure of *trans*-[Ru(acac)<sub>2</sub>(η<sup>2</sup>-C<sub>2</sub>H<sub>4</sub>)(C<sub>5</sub>H<sub>5</sub>N)].

Ru(1)-O(1)	2.054(2)	Ru(1)-O(2)	2.046(2)
Ru(1)-O(3)	2.063(2)	Ru(1)-O(4)	2.051(2)
Ru(1)-N(1)	2.095(3)	Ru(1)-C(110)	2.171(5)
Ru(1)-C(111)	2.164(8)*	Ru(1)-C(120)	2.179(5)
Ru(1)-C(121)	2.179(7)*	O(1)-C(2)	1.262(4)
O(2)-C(4)	1.265(4)	O(3)-C(7)	1.270(4)
O(4)-C(9)	1.278(4)	N(1)-C(13)	1.337(4)
N(1)-C(17)	1.344(4)	C(1)-C(2)	1.514(5)
C(2)-C(3)	1.399(5)	C(3)-C(4)	1.389(5)
C(4)-C(5)	1.505(5)	C(6)-C(7)	1.516(5)
C(7)-C(8)	1.396(5)	C(8)-C(9)	1.387(4)
C(9)-C(10)	1.514(5)	C(13)-C(14)	1.375(5)
C(14)-C(15)	1.367(5)	C(15)-C(16)	1.361(5)
C(16)-C(17)	1.372(5)	C(110)-C(111)	0.73(2)
C(110)-C(120)	1.35(1)	C(111)-C(121)	1.39(3)

\* restrained during refinement

**Table A.2.2 (cont):** Interatomic distances (Å) and angles (°) involving non-hydrogen atoms of the molecular structure of *trans*-[Ru(acac)<sub>2</sub>(η<sup>2</sup>-C<sub>2</sub>H<sub>4</sub>)(C<sub>5</sub>H<sub>5</sub>N)].

O(1)-Ru(1)-O(2)	93.58(9)	O(1)-Ru(1)-O(3)	169.72(9)
O(1)-Ru(1)-O(4)	85.65(9)	O(1)-Ru(1)-C(11)	83.96(9)
O(1)-Ru(1)-C(110)	112.8(2)	O(1)-Ru(1)-C(111)	98.0(5)
O(1)-Ru(1)-C(120)	76.7(2)	O(1)-Ru(1)-O(121)	96.6(4)
O(2)-Ru(1)-O(3)	86.76(8)	O(2)-Ru(1)-O(4)	176.22(9)
O(2)-Ru(1)-N(1)	88.0(1)	O(2)-Ru(1)-C(110)	91.9(2)
O(2)-Ru(1)-C(111)	105.8(5)	O(2)-Ru(1)-C(120)	93.4(2)
O(2)-Ru(1)-C(121)	68.7(5)	O(3)-Ru(1)-O(4)	93.34(8)
O(3)-Ru(1)-N(1)	85.78(9)	O(3)-Ru(1)-C(110)	77.4(2)
O(3)-Ru(1)-C(111)	91.8(5)	O(3)-Ru(1)-C(120)	113.6(2)
O(3)-Ru(1)-C(121)	93.4(4)	O(3)-Ru(1)-N(1)	88.2(1)
O(4)-Ru(1)-C(110)	91.8(2)	O(4)-Ru(1)-C(111)	77.9(5)
O(4)-Ru(1)-C(120)	90.0(2)	O(4)-Ru(1)-C(121)	115.1(5)
N(1)-Ru(1)-C(110)	163.2(2)	N(1)-Ru(1)-C(111)	165.8(5)
N(1)-Ru(1)-C(120)	160.6(2)	N(1)-Ru(1)-C(121)	115.1(5)
C(110)-Ru(1)- C(120)	36.1(3)	C(111)-Ru(1)- C(121)	37.3(7)
Ru(1)-O(1)-C(2)	122.4(2)	Ru(1)-O(2)-C(4)	122.2(2)
Ru(1)-O(3)-C(7)	122.6(2)	Ru(1)-O(4)-C(9)	122.2(2)
Ru(1)-N(1)-C(13)	121.3(2)	Ru(1)-N(1)-C(17)	121.7(2)
C(13)-N(1)-C(17)	117.0(3)	O(1)-C(2)-C(1)	114.3(4)
O(1)-C(2)-C(3)	126.4(3)	C(1)-C(2)-C(3)	119.2(3)
C(2)-C(3)-C(4)	128.4(3)	O(2)-C(4)-C(3)	126.9(4)
O(2)-C(4)-C(5)	114.3(3)	C(3)-C(4)-C(5)	118.8(3)
O(3)-C(7)-C(6)	115.2(3)	O(3)-C(7)-C(8)	126.2(3)
C(6)-C(7)-C(8)	118.6(3)	C(7)-C(8)-C(9)	128.8(3)
O(4)-C(9)-C(8)	126.8(3)	O(4)-C(9)-C(10)	114.4(3)
C(8)-C(9)-C(10)	118.9(4)	N(1)-C(13)-C(14)	123.1(3)
C(13)-C(14)-C(15)	118.9(4)	C(14)-C(15)-C(16)	122.5(3)
C(15)-C(16)-C(17)	119.7(3)	N(1)-C(17)-C(16)	122.5(3)
Ru(1)-C(110)- C(120)	72.3(3)	Ru(1)-C(111)- C(121)	72.0(6)
Ru(1)-C(120)- C(110)	71.6(3)	Ru(1)-C(121)- C(111)	70.7(5)

**Table A.3.1:** Crystallographic and refinement data for *cis*-[Ru(acac)<sub>2</sub>(η<sup>2</sup>-C<sub>2</sub>H<sub>4</sub>)(NH<sub>3</sub>)].

<b>Crystal Data</b>	
Empirical Formula	C <sub>12</sub> H <sub>21</sub> NO <sub>4</sub> Ru
Formula Weight	344.37
Crystal Colour, Habit	orange, plate
Crystal Dimensions	0.38 x 0.29 x 0.08 mm
Crystal System	monoclinic
Lattice Type	Primitive
No. of Reflections Used for Unit Cell Determination (2θ range)	25 (49.7 - 54.8°)
Omega Scan Peak Width at Half-height	0.33°
Lattice Parameters	a = 11.869(3) Å b = 10.400(4) Å c = 12.247(2) Å β = 203.26(1)° V = 1471.5(5) Å <sup>3</sup>
Space Group	P2 <sub>1</sub> /n (#14)
Z value	4
D <sub>calc</sub>	1.554 g/cm <sup>3</sup>
F <sub>000</sub>	704.00
μ(MoKα)	10.49 cm <sup>-1</sup>
<b>Intensity Measurements</b>	
diffractometer	Rigaku AFC6S
Radiation	CuKα (λ = 0.71069 Å) graphite monochromated
Take-off Angle	6.0°
Detector Aperture	7.0 mm horizontal 7.0 mm vertical
Crystal to Detector Distance	200 mm
Voltage, Current	50 kV, 30 mA
Temperature	23.0 °C
Scan Type	ω-2θ
Scan Rate	4.0°/min (in ω) (up to 4 scans)
Scan Width	(1.20 + 0.34 tan θ)°
2θ <sub>max</sub>	55.1°
No. of Reflections Measured	Total: 3755 Unique: 3589 (R <sub>int</sub> = 0.012)
Corrections	Lorentz-polarization Absorption (trans. Factors: 0.7525 - 0.9196)

**Table A.3.1 (cont):** Crystallographic and refinement data for *cis*-[Ru(acac)<sub>2</sub>( $\eta^2$ -C<sub>2</sub>H<sub>4</sub>)(NH<sub>3</sub>)].

<b>Structure Solution and Refinement</b>	
Structure Solution	Direct Methods (SIR92)
Refinement	Full-Matrix least squares
Function Minimized	$\sum w( F_o  -  F_c )^2$
Least Squares Weights	$w = [\sigma_c^2(F_o) + 0.25p^2F_o^2]^{-1}$
p-factor	0.0200
Anomalous Dispersion	All non-hydrogen atoms
No. Observations ( $I > 2.0\sigma(I)$ )	2713
No. of variables	226
Reflection/Parameter Rotation	12.00
Residuals: R; R <sub>w</sub>	0.021; 0.022
Goodness of Fit Indicator	1.33
Max Shift/Error in Final Cycle	0.08
Max peak in Final Diff. Map	0.28 e <sup>-</sup> /Å <sup>3</sup>
Min peak in Final Diff. Map	-0.30 e <sup>-</sup> /Å <sup>3</sup>

**Table A.3.2:** Interatomic distances (Å) and angles (°) involving non-hydrogen atoms of the molecular structure of *cis*-[Ru(acac)<sub>2</sub>( $\eta^2$ -C<sub>2</sub>H<sub>4</sub>)(NH<sub>3</sub>)].

Ru(1)-O(1)	2.052(2)	Ru(1)-O(2)	2.066(2)
Ru(1)-O(3)	2.048(2)	Ru(1)-O(4)	2.092(2)
Ru(1)-N(1)	2.108(2)	Ru(1)-C(11)	2.147(3)
Ru(1)-C(12)	2.151(3)	O(1)-C(2)	1.275(3)
O(2)-C(4)	1.272(3)	O(3)-C(7)	1.264(3)
O(4)-C(9)	1.275(3)	C(1)-C(2)	1.499(3)
C(2)-C(3)	1.272(3)	C(3)-C(4)	1.389(3)
C(4)-C(5)	1.507(4)	C(6)-C(7)	1.503(3)
C(7)-C(8)	1.409(3)	C(8)-C(9)	1.396(3)
C(9)-C(10)	1.500(4)	C(11)-C(12)	1.356(4)
C(11)-H(18)	0.94(3)	C(11)-H(19)	1.06(3)
C(12)-H(20)	0.96(3)	C(12)-H(21)	0.97(3)
O(1)-Ru(1)-O(2)	93.07(6)	O(1)-Ru(1)-O(3)	176.67(6)
O(1)-Ru(1)-O(4)	88.28(6)	O(1)-Ru(1)-N(1)	89.74(8)
O(1)-Ru(1)-C(11)	89.87(9)	O(1)-Ru(1)-C(12)	90.05(9)
O(2)-Ru(1)-O(3)	90.18(6)	O(2)-Ru(1)-O(4)	83.68(6)
O(2)-Ru(1)-N(1)	165.43(8)	O(2)-Ru(1)-C(11)	78.30(9)
O(2)-Ru(1)-C(12)	115.02(9)	O(3)-Ru(1)-O(4)	92.79(6)
O(3)-Ru(1)-N(1)	87.29(7)	O(3)-Ru(1)-C(11)	90.09(9)
O(3)-Ru(1)-C(12)	87.93(9)	O(4)-Ru(1)-N(1)	82.12(8)



**Table A.3.2 (cont):** Interatomic distances (Å) and angles (°) involving non-hydrogen atoms of the molecular structure of *cis*-[Ru(acac)<sub>2</sub>(η<sup>2</sup>-C<sub>2</sub>H<sub>4</sub>)(NH<sub>3</sub>)].

O(4)-Ru(1)-C(11)	161.75(9)	O(4)-Ru(1)-C(12)	161.29(9)
N(1)-Ru(1)-C(11)	116.0(1)	N(1)-Ru(1)-C(12)	79.2(1)
C(11)-Ru(1)-C(12)	36.8(1)	Ru(1)-O(1)-C(2)	122.9(1)
Ru(1)-O(2)-C(4)	122.0(2)	Ru(1)-O(3)-C(7)	123.7(1)
Ru(1)-O(4)-C(9)	121.9(1)	O(1)-C(2)-C(1)	115.3(2)
O(1)-C(2)-C(3)	126.1(2)	C(1)-C(2)-C(3)	118.6(2)
C(2)-C(3)-C(4)	128.8(2)	O(2)-C(4)-C(3)	126.9(2)
O(2)-C(4)-C(5)	114.5(2)	C(3)-C(4)-C(5)	118.6(2)
O(3)-C(7)-C(6)	114.9(2)	O(3)-C(7)-C(8)	126.0(2)
C(6)-C(7)-C(8)	119.1(2)	C(7)-C(8)-C(9)	128.7(2)
O(4)-C(9)-C(8)	126.6(2)	O(4)-C(9)-C(10)	115.2(2)
C(8)-C(9)-C(10)	118.3(2)	Ru(1)-C(11)-C(12)	71.8(2)
Ru(1)-C(12)-C(11)	71.4(2)	Ru(1)-C(11)-H(18)	110(2)
Ru(1)-C(11)-H(19)	110(2)	C(12)-C(11)-H(18)	121(2)
C(12)-C(11)-H(19)	119(1)	H(18)-C(11)-H(19)	115(2)
Ru(1)-C(12)-H(20)	113(2)	Ru(1)-C(12)-H(21)	109(2)
C(11)-C(12)-H(20)	125(2)	C(11)-C(12)-H(21)	118(2)
H(20)-C(12)-H(21)	111(3)		

**Table A.4.1:** Crystallographic and refinement data for *cis*-[Ru(acac)<sub>2</sub>(η<sup>2</sup>-C<sub>2</sub>H<sub>4</sub>)(PP*r*<sub>3</sub>)].

<b>Crystal Data</b>	
Empirical Formula	C <sub>21</sub> H <sub>39</sub> O <sub>4</sub> PRu
Formula Weight	487.58
Crystal Colour, Habit	orange, wedge
Crystal Dimensions	0.30 × 0.16 × 0.10 mm
Crystal System	triclinic
Lattice Type	Primitive
No. of Reflections Used for Unit Cell	24 (104.5 - 109.4°)
Determination (2θ range)	
Omega Scan Peak Width at Half-height	0.33°
Lattice Parameters	a = 9.747(1) Å b = 15.645(2) Å c = 17.270(2) Å α = 66.391(7)° β = 81.03(1)° γ = 89.79(1)° V = 2378.5(5) Å <sup>3</sup>
Space Group	P $\bar{1}$ (#2)
Z value	4
D <sub>calc</sub>	1.362 g/cm <sup>3</sup>
F <sub>000</sub>	1024.00
μ(MoKα)	62.70 cm <sup>-1</sup>

**Table A.4.1 (cont):** Crystallographic and refinement data for *cis*-[Ru(acac)<sub>2</sub>(η<sup>2</sup>-C<sub>2</sub>H<sub>4</sub>)(PPr<sup>i</sup><sub>3</sub>)].

<b>Intensity Measurements</b>	
diffractometer	Rigaku AFC6R
Radiation	CuKα (λ = 1.5178 Å) graphite monochromated
Take-off Angle	6.0°
Detector Aperture	9.0 mm horizontal 7.0 mm vertical
Crystal to Detector Distance	400 mm
Voltage, Current	50 kV, 180 mA
Temperature	-30.0 °C
Scan Type	ω-2θ
Scan Rate	32.0°/min (in ω) (up to 4 scans)
Scan Width	(1.20 + 0.30 tan θ)°
2θ <sub>max</sub>	120.1°
No. of Reflections Measured	Total: 7548 Unique: 7064 (R <sub>int</sub> = 0.045)
Corrections	Lorentz-polarization Absorption (trans. Factors: 0.3566 - 0.5408) Decay (1.41% decline)
<b>Structure Solution and Refinement</b>	
Structure Solution	Direct Methods (SIR92)
Refinement	Full-Matrix least squares
Function Minimized	Σw( Fo  -  Fc ) <sup>2</sup>
Least Squares Weights	w = [σ <sub>c</sub> <sup>2</sup> (Fo) + 0.25p <sup>2</sup> Fo <sup>2</sup> ] <sup>-1</sup>
p-factor	0.020
Anomalous Dispersion	All non-hydrogen atoms
No. Observations (I > 2.0σ(I))	5865
No. of variables	511
Reflection/Parameter Rotation	11.48
Residuals: R; Rw	0.036; 0.044
Goodness of Fit Indicator	1.88
Max Shift/Error in Final Cycle	0.03
Max peak in Final Diff. Map	0.78 e <sup>-</sup> /Å <sup>3</sup>
Min peak in Final Diff Map	-0.74 e <sup>-</sup> /Å <sup>3</sup>

**Table A.4.2:** Interatomic distances (Å) and angles (°) involving non-hydrogen atoms of the molecular structures of *cis*-[Ru(acac)<sub>2</sub>(η<sup>2</sup>-C<sub>2</sub>H<sub>4</sub>)(PPr<sup>i</sup><sub>3</sub>)] (ethene hydrogen atoms included).

Ru(1)-P(1)	2.321(1)	Ru(1)-O(1)	2.079(3)
Ru(1)-O(2)	2.077(3)	Ru(1)-O(3)	2.071(3)
Ru(1)-O(4)	2.094(3)	Ru(1)-C(11)	2.172(5)
Ru(1)-C(12)	2.181(5)	Ru(2)-P(2)	2.322(1)
Ru(2)-O(5)	2.082(3)	Ru(2)-O(6)	2.079(3)
Ru(2)-O(7)	2.064(3)	Ru(2)-O(8)	2.089(3)
Ru(2)-C(32)	2.180(6)	Ru(2)-C(33)	2.185(5)
P(1)-C(13)	1.864(5)	P(1)-C(16)	1.866(5)
P(1)-C(19)	1.867(5)	P(2)-C(34)	1.869(5)
P(2)-C(37)	1.877(5)	P(2)-C(40)	1.867(5)
O(1)-C(2)	1.279(6)	O(2)-C(4)	1.269(5)
O(3)-C(7)	1.278(5)	O(4)-C(9)	1.264(5)
O(5)-C(23)	1.274(5)	O(6)-C(25)	1.279(5)
O(7)-C(28)	1.273(5)	O(8)-C(30)	1.257(6)
C(1)-C(2)	1.513(7)	C(2)-C(3)	1.381(7)
C(3)-C(4)	1.394(7)	C(4)-C(5)	1.505(7)
C(6)-C(7)	1.504(7)	C(7)-C(8)	1.389(7)
C(8)-C(9)	1.404(7)	C(9)-C(10)	1.500(7)
C(11)-C(12)	1.350(9)	C(13)-C(14)	1.508(7)
C(13)-C(15)	1.532(7)	C(16)-C(17)	1.530(7)
C(16)-C(18)	1.515(8)	C(19)-C(20)	1.525(7)
C(19)-C(21)	1.516(7)	C(22)-C(23)	1.497(7)
C(23)-C(24)	1.389(7)	C(24)-C(25)	1.392(6)
C(25)-C(26)	1.501(7)	C(27)-C(28)	1.509(7)
C(28)-C(29)	1.388(7)	C(29)-C(30)	1.404(7)
C(30)-C(31)	1.499(7)	C(32)-C(33)	1.350(9)
C(34)-C(35)	1.495(8)	C(34)-C(36)	1.526(7)
C(37)-C(38)	1.536(7)	C(37)-C(39)	1.517(8)
C(40)-C(41)	1.521(8)	C(40)-C(42)	1.517(7)
C(11)-H(1)	1.00(6)	C(11)-H(2)	0.87(6)
C(12)-H(3)	0.91(5)	C(12)-H(4)	0.88(6)
C(32)-H(5)	0.97(6)	C(32)-H(6)	0.92(6)
C(33)-H(7)	0.89(5)	C(33)-H(8)	1.08(5)
P(1)-Ru(1)-O(1)	95.68(9)	P(1)-Ru(1)-O(2)	91.63(9)
P(1)-Ru(1)-O(3)	90.70(9)	P(1)-Ru(1)-O(4)	175.9(1)
P(1)-Ru(1)-C(11)	99.7(2)	P(1)-Ru(1)-C(12)	91.3(2)

**Table A.4.2 (cont):** Interatomic distances (Å) and angles (°) involving non-hydrogen atoms of the molecular structure of *cis*-[Ru(acac)<sub>2</sub>(η<sup>2</sup>-C<sub>2</sub>H<sub>4</sub>)(PPri<sub>3</sub>)].

O(1)-Ru(1)-O(2)	89.1(1)	O(1)-Ru(1)-O(3)	167.4(1)
O(1)-Ru(1)-O(4)	81.4(1)	O(1)-Ru(1)-C(11)	111.2(2)
O(1)-Ru(1)-C(12)	77.3(2)	O(2)-Ru(1)-O(3)	79.9(1)
O(2)-Ru(1)-O(4)	85.4(1)	O(2)-Ru(1)-C(11)	155.3(2)
O(2)-Ru(1)-C(12)	166.3(2)	O(3)-Ru(1)-O(4)	91.6(1)
O(3)-Ru(1)-C(11)	78.2(2)	O(3)-Ru(1)-C(12)	113.4(2)
O(4)-Ru(1)-C(11)	84.1(2)	O(4)-Ru(1)-C(12)	90.9(2)
C(11)-Ru(1)-C(12)	36.1(2)	P(2)-Ru(2)-O(5)	95.93(9)
P(2)-Ru(2)-O(6)	91.14(9)	P(2)-Ru(2)-O(7)	90.48(9)
P(2)-Ru(2)-O(8)	175.01(9)	P(2)-Ru(2)-C(32)	100.5(2)
P(2)-Ru(2)-C(33)	91.0(2)	O(5)-Ru(2)-O(6)	89.5(1)
O(5)-Ru(2)-O(7)	168.1(1)	O(5)-Ru(2)-O(8)	81.4(1)
O(5)-Ru(2)-C(32)	110.2(2)	O(5)-Ru(2)-C(33)	76.9(2)
O(6)-Ru(2)-O(7)	80.3(1)	O(6)-Ru(2)-O(8)	84.7(1)
O(6)-Ru(2)-C(32)	155.6(2)	O(6)-Ru(2)-C(33)	166.4(2)
O(7)-Ru(2)-O(8)	91.5(1)	O(7)-Ru(2)-C(32)	78.3(2)
O(7)-Ru(2)-C(33)	113.1(2)	O(8)-Ru(2)-C(32)	84.4(2)
O(8)-Ru(2)-C(33)	92.5(2)	C(32)-Ru(2)-C(33)	36.0(2)
Ru(1)-P(1)-C(13)	112.4(2)	Ru(1)-P(1)-C(16)	117.2(2)
Ru(1)-P(1)-C(19)	115.1(2)	C(13)-P(1)-C(16)	100.5(2)
C(13)-P(1)-C(19)	108.5(2)	C(16)-P(1)-C(19)	101.7(2)
Ru(2)-P(2)-C(34)	112.7(2)	Ru(2)-P(2)-C(37)	116.7(2)
Ru(2)-P(2)-C(40)	115.4(2)	C(34)-P(2)-C(37)	100.3(2)
C(34)-P(2)-C(40)	108.3(2)	C(37)-P(2)-C(40)	101.9(2)
Ru(1)-O(1)-C(2)	123.6(3)	Ru(1)-O(2)-C(4)	125.3(3)
Ru(1)-O(3)-C(7)	122.7(3)	Ru(1)-O(4)-C(9)	124.0(3)
Ru(2)-O(5)-C(23)	123.9(3)	Ru(2)-O(6)-C(25)	124.3(3)
Ru(2)-O(7)-C(28)	123.2(3)	Ru(2)-O(8)-C(30)	124.2(3)
O(1)-C(2)-C(1)	113.4(4)	O(1)-C(2)-C(3)	127.1(4)
C(1)-C(2)-C(3)	119.5(5)	C(2)-C(3)-C(4)	126.8(5)
O(2)-C(4)-C(3)	125.7(4)	O(2)-C(4)-C(5)	114.9(4)
C(3)-C(4)-C(5)	119.4(4)	O(3)-C(7)-C(6)	113.6(4)
O(3)-C(7)-C(8)	127.6(5)	C(6)-C(7)-C(8)	118.8(4)
C(7)-C(8)-C(9)	128.1(5)	O(4)-C(9)-C(8)	125.7(5)
O(4)-C(9)-C(10)	115.6(5)	C(8)-C(9)-C(10)	118.6(5)
Ru(1)-C(11)-C(12)	72.3(3)	Ru(1)-C(12)-C(11)	71.6(3)
P(1)-C(13)-C(14)	114.5(4)	P(1)-C(13)-C(15)	117.1(3)
C(14)-C(13)-C(15)	109.4(4)	P(1)-C(16)-C(17)	113.0(4)

**Table A.4.2 (cont):** *Interatomic distances (Å) and angles (°) involving non-hydrogen atoms of the molecular structure of  $\text{cis-[Ru(acac)}_2(\eta^2\text{-C}_2\text{H}_4)(\text{PPr}^i_3)]$ .*

P(1)-C(16)-C(18)	113.5(4)	C(17)-C(16)-C(18)	110.1(5)
P(1)-C(19)-C(20)	113.5(4)	P(1)-C(19)-C(21)	117.6(4)
C(20)-C(19)-C(21)	109.2(5)	O(5)-C(23)-C(22)	114.8(4)
O(5)-C(23)-C(24)	126.5(4)	C(22)-C(23)-C(24)	118.7(4)
C(23)-C(24)-C(25)	127.1(4)	O(6)-C(25)-C(24)	126.2(4)
O(6)-C(25)-C(26)	114.9(4)	C(24)-C(25)-C(26)	119.0(4)
O(7)-C(28)-C(27)	113.9(4)	O(7)-C(28)-C(29)	126.9(5)
C(27)-C(28)-C(29)	119.2(5)	C(28)-C(29)-C(30)	128.6(5)
O(8)-C(30)-C(29)	125.4(5)	O(8)-C(30)-C(31)	115.8(5)
C(29)-C(30)-C(31)	118.8(5)	Ru(2)-C(32)-C(33)	72.2(3)
Ru(2)-C(33)-C(32)	71.8(3)	P(2)-C(34)-C(35)	114.6(4)
P(2)-C(34)-C(36)	117.4(4)	C(35)-C(34)-C(36)	108.8(5)
P(2)-C(37)-C(38)	111.6(4)	P(2)-C(37)-C(39)	112.9(4)
C(38)-C(37)-C(39)	110.4(5)	P(2)-C(40)-C(41)	112.8(4)
P(2)-C(40)-C(42)	118.0(4)	C(41)-C(40)-C(42)	109.3(5)
Ru(1)-C(11)-H(1)	115(4)	Ru(1)-C(11)-H(2)	99(4)
C(12)-C(11)-H(1)	117(4)	C(12)-C(11)-H(2)	114(4)
H(1)-C(11)-H(2)	125(6)	Ru(1)-C(12)-H(3)	113(4)
Ru(1)-C(12)-H(4)	105(4)	C(11)-C(12)-H(3)	117(4)
C(11)-C(12)-H(4)	111(4)	H(3)-C(12)-H(4)	126(5)
Ru(2)-C(32)-H(5)	108(4)	Ru(2)-C(32)-H(6)	97(4)
C(33)-C(32)-H(5)	112(4)	C(33)-C(32)-H(6)	109(4)
H(5)-C(32)-H(6)	137(5)	Ru(2)-C(33)-H(7)	122(4)
Ru(2)-C(33)-H(8)	102(3)	C(32)-C(33)-H(7)	123(4)
C(32)-C(33)-H(8)	102(3)	H(7)-C(33)-H(8)	117(5)

**Table A.5.1:** *Crystallographic and refinement data for cis-[Ru(acac)<sub>2</sub>(η<sup>2</sup>-C<sub>2</sub>H<sub>4</sub>)(PCy<sub>3</sub>)].*

Crystal Data	
Empirical Formula	C <sub>30</sub> H <sub>51</sub> O <sub>4</sub> PRu
Formula Weight	607.78
Crystal Colour, Habit	orange, triangular fragment
Crystal Dimensions	0.50 x 0.30 x 0.18 mm
Crystal System	monoclinic
Lattice Type	Primitive
No. of Reflections Used for Unit Cell Determination (2θ range)	24 (104.5 - 109.4°)
Omega Scan Peak Width at Half-height	0.33°
Lattice Parameters	a = 13.699(4) Å b = 11.780(4) Å c = 19.130(3) Å β = 82.94(2)° V = 3076(2) Å <sup>3</sup>
Space Group	P2 <sub>1</sub> /c (#14)
Z value	4
D <sub>calc</sub>	1.31 g/cm <sup>3</sup>
F <sub>000</sub>	1283.00
μ(MoKα)	62.70 cm <sup>-1</sup>

**Table A.5.1 (cont):** Crystallographic and refinement data for *cis*-[Ru(acac)<sub>2</sub>(η<sup>2</sup>-C<sub>2</sub>H<sub>4</sub>)(PCy<sub>3</sub>)].

<b>Intensity Measurements</b>	
diffractometer	Rigaku AFC6S
Radiation	MoKα (λ = 0.7107 Å)
	graphite monochromated
Take-off Angle	6.0°
Detector Aperture	9.0 mm horizontal 7.0 mm vertical
Crystal to Detector Distance	400 mm
Voltage, Current	50 kV, 180 mA
Temperature	23.2 °C
Scan Type	ω-2θ
Scan Rate	4.0°/min (in ω) (up to 5 scans)
Scan Width	(0.80 + 0.34 tan θ)°
2θ <sub>max</sub>	120.1°
No. of Reflections Measured	Total: 5995
	Unique: 5743 (R <sub>int</sub> = 0.050)
Corrections	Lorentz-polarization Absorption (trans. Factors: 0.3566 - 0.5408) Decay (-0.47% decline)
<b>Structure Solution and Refinement</b>	
Structure Solution	Direct Methods (SIR92)
Refinement	Full-Matrix least squares
Function Minimized	Σw( F <sub>o</sub>   -  F <sub>c</sub>  ) <sup>2</sup>
Least Squares Weights	w = [σ <sub>c</sub> <sup>2</sup> (F <sub>o</sub> ) + 0.25p <sup>2</sup> F <sub>o</sub> <sup>2</sup> ] <sup>-1</sup>
p-factor	0.020
Anomalous Dispersion	All non-hydrogen atoms
No. Observations (I > 2.0σ(I))	5865
No. of variables	511
Reflection/Parameter Rotation	11.48
Residuals: R; R <sub>w</sub>	0.036; 0.044
Goodness of Fit Indicator	1.88
Max Shift/Error in Final Cycle	0.03
Max peak in Final Diff. Map	0.78 e <sup>-</sup> /Å <sup>3</sup>
Min peak in Final Diff Map	-0.74 e <sup>-</sup> /Å <sup>3</sup>



**Table A.5.2:** Interatomic distances (Å) and angles (°) involving non-hydrogen atoms of the molecular structure of *cis*-[Ru(acac)<sub>2</sub>(η<sup>2</sup>-C<sub>2</sub>H<sub>4</sub>)(PCy<sub>3</sub>)].

Ru(1)-P(1)	2.356(7)	Ru(1)-O(1)	2.06(2)
Ru(1)-O(2)	2.10(2)	Ru(1)-O(3)	2.07(2)
Ru(1)-O(4)	2.074(18)	Ru(1)-C(110)	2.167(2)
Ru(1)-C(111)	2.151(2)	Ru(1)-C(120)	2.190(2)
Ru(1)-C(121)	2.148(2)	P(1)-C(13)	1.87(3)
P(1)-C(19)	1.87(3)	P(1)-C(25)	1.88(3)
O(1)-C(2)	1.27(4)	O(2)-C(4)	1.27(4)
O(3)-C(9)	1.27(4)	O(4)-C(7)	1.27(4)
C(1)-C(2)	1.52(5)	C(2)-C(3)	1.38(5)
C(3)-C(4)	1.39(5)	C(4)-C(5)	1.50(5)
C(6)-C(7)	1.51(4)	C(7)-C(8)	1.39(5)
C(8)-C(9)	1.40(5)	C(9)-C(10)	1.50(5)
C(13)-C(14)	1.53(4)	C(13)-C(18)	1.54(4)
C(14)-C(15)	1.52(5)	C(15)-C(16)	1.51(6)
C(16)-C(17)	1.52(5)	C(17)-C(18)	1.52(4)
C(19)-C(20)	1.54(4)	C(19)-C(24)	1.54(4)
C(20)-C(21)	1.53(4)	C(21)-C(22)	1.51(5)
C(22)-C(23)	1.51(5)	C(23)-C(24)	1.52(4)
C(25)-C(26)	1.52(4)	C(25)-C(30)	1.52(4)
C(26)-C(27)	1.52(4)	C(27)-C(28)	1.50(5)
C(28)-C(29)	1.50(5)	C(29)-C(30)	1.53(4)
C(110)-C(111)*	1.00	C(110)-C(120)*	1.34
C(110)-C(121)*	0.99	C(111)-C(120)*	1.10
C(111)-C(121)*	1.36	C(120)-C(121)*	0.74

\*) restrained during refinement and thus no estimated standard deviations are reported.

**Table A.6.1:** Crystallographic and refinement data for *trans*-[Ru(acac)<sub>2</sub>(PCy<sub>3</sub>)<sub>2</sub>] at 200 K.

<b>Crystal Data</b>	
Empirical Formula	C <sub>46</sub> H <sub>80</sub> O <sub>4</sub> P <sub>2</sub> Ru
Formula Weight	860.16
Crystal Colour, Habit	Brown, plate
Crystal Dimensions	-
Crystal System	Monoclinic
Lattice Type	
Lattice Parameters	a = 9.56650(10) Å b = 17.8085(3) Å c = 13.6210(2) Å α = 90.00 ° β = 109.4660(10) ° γ = 90.00 ° V = 2187.90(5) Å <sup>3</sup>
Space Group	P2 <sub>1</sub> /n
Z value	2
D <sub>calc</sub>	1.306 g/cm <sup>3</sup>
F <sub>000</sub>	924
μ(MoKα)	0.47 cm <sup>-1</sup>
<b>Intensity Measurements</b>	
diffractometer	Nonius KappaCD
Radiation	MoKα (λ = 0.71073 Å) graphite monochromated
Detector Aperture	65 mm x 65 mm
Data Images	2.00°/frame; 20 sec/°
Detector Position	25.00 mm
2θ <sub>max</sub>	66.3°
No. of Reflections Measured	Total: 45663 Unique: 8233 (R <sub>int</sub> = 0.047)
Corrections	Lorentz-polarization Absorption (trans. Factors: 0.977 - 0.892)

**Table A.6.1 (cont):** Crystallographic and refinement data for *trans*-[Ru(acac)<sub>2</sub>(PCy<sub>3</sub>)<sub>2</sub>] at 200 K.

<b>Structure Solution and Refinement</b>	
Structure Solution	Patterson Methods (DIRDIF92 PATTY)
Refinement	Full-Matrix least squares
Function Minimized	$\sum w( F_o  -  F_c )^2$
Least Squares Weights	$w = [\sigma_c^2(F_o) + 0.25p^2F_o^2]^{-1}$
p-factor	0.040
Anomalous Dispersion	All non-hydrogen atoms
No. Observations (I>3.0σ(I))	5902
No. of variables	241
Reflection/Parameter Rotation	24.49
Residuals: R; Rw	0.038; 0.061
Goodness of Fit Indicator	1.475
Max Shift/Error in Final Cycle	<0.01
Max peak in Final Diff. Map	0.46 e <sup>-</sup> /Å <sup>3</sup>
Min peak in Final Diff. Map	-1.35 e <sup>-</sup> /Å <sup>3</sup>

**Table A.6.2:** Interatomic distances (Å) and angles (°) involving non-hydrogen atoms of the molecular structure of *trans*-[Ru(acac)<sub>2</sub>(PCy<sub>3</sub>)<sub>2</sub>] at 200 K.

Ru(1)-P(1)	2.4268(3)	Ru(1)-O(1)	2.0707(10)
Ru(1)-O(2)	2.0646(10)		
P(1)-C(6)	1.8680(10)	P(1)-C(12)	1.8880(10)
P(1)-C(18)	1.8640(10)	O(1)-C(2)	1.271(2)
O(2)-C(4)	1.276(2)	C(1)-C(2)	1.507(2)
C(2)-C(3)	1.401(2)	C(3)-C(4)	1.398(2)
C(4)-C(5)	1.511(2)	C(6)-C(7)	1.528(2)
C(6)-C(11)	1.537(2)	C(7)-C(8)	1.532(2)
C(8)-C(9)	1.523(2)	C(9)-C(10)	1.516(2)
C(10)-C(11)	1.531(2)	C(12)-C(13)	1.543(2)
C(12)-C(17)	1.542(2)	C(13)-C(14)	1.528(2)
C(14)-C(15)	1.517(2)	C(15)-C(16)	1.528(2)
C(16)-C(17)	1.524(2)	C(18)-C(19)	1.534(2)
C(18)-C(23)	1.541(2)	C(19)-C(20)	1.529(2)
C(20)-C(21)	1.522(2)	C(21)-C(22)	1.519(2)
C(22)-C(23)	1.529(2)		
P(1)-Ru(1)-P(1) <sup>a</sup>	180.0	P(1)-Ru(1)-O(1)	91.0(1)
P(1)-Ru(1)-O(1) <sup>a</sup>	89.0(1)	P(1)-Ru(1)-O(2)	91.1(1)
P(1)-Ru(1)-O(2) <sup>a</sup>	88.9(1)	P(1) <sup>a</sup> -Ru(1)-O(1)	91.0(1)

**Table A.6.2 (cont):** Interatomic distances (Å) and angles (°) involving non-hydrogen atoms of the molecular structure of *trans*-[Ru(acac)<sub>2</sub>(PCy<sub>3</sub>)<sub>2</sub>] at 200 K.

P(1) <sup>a</sup> -Ru(1)-O(2)	88.9(1)	P(1) <sup>a</sup> -Ru(1)-O(2) <sup>a</sup>	91.1(1)
O(1)-Ru(1)-O(1) <sup>a</sup>	180.0	O(1)-Ru(1)-O(2)	91.9(1)
O(1)-Ru(1)-O(2) <sup>a</sup>	88.1(1)	O(1) <sup>a</sup> -Ru(1)-O(2)	88.1(1)
O(1) <sup>a</sup> -Ru(1)-O(2) <sup>a</sup>	91.9(1)	O(2)-Ru(1)-O(2) <sup>a</sup>	180.0
Ru(1)-P(1)-C(6)	116.9(1)	Ru(1)-P(1)-C(12)	113.8(1)
Ru(1)-P(1)-C(18)	113.9(1)	Ru(1)-P(1)-C(6)	116.9(1)
Ru(1)-P(1)-C(12)	113.8(1)	Ru(1)-P(1)-C(18)	113.9(1)
C(6)-P(1)-C(12)	100.5(1)	C(6)-P(1)-C(18)	101.8(1)
C(12)-P(1)-C(18)	108.4(1)	Ru(1)-O(1)-C(2)	123.7(1)
Ru(1)-O(2)-C(4)	123.3(1)	O(1)-C(2)-C(1)	115.5(2)
O(1)-C(2)-C(3)	126.2(2)	C(1)-C(2)-C(3)	118.3(2)
C(2)-C(3)-C(4)	127.7(2)	O(2)-C(4)-C(3)	126.9(2)
O(2)-C(4)-C(5)	115.0(2)	C(3)-C(4)-C(5)	118.1(2)
P(1)-C(6)-C(7)	116.9(2)	P(1)-C(6)-C(11)	110.3(1)
C(7)-C(6)-C(11)	110.4(2)	C(6)-C(7)-C(8)	110.2(2)
C(7)-C(8)-C(9)	111.5(2)	C(8)-C(9)-C(10)	111.1(2)
C(9)-C(10)-C(11)	111.5(2)	C(6)-C(11)-C(10)	110.5(2)
P(1)-C(12)-C(13)	118.6(1)	P(1)-C(12)-C(17)	113.9(1)
C(13)-C(12)-C(17)	107.7(2)	C(12)-C(13)-C(14)	111.0(2)
C(13)-C(14)-C(15)	112.7(2)	C(14)-C(15)-C(16)	110.9(2)
C(15)-C(16)-C(17)	110.6(2)	C(12)-C(17)-C(16)	111.5(2)
P(1)-C(18)-C(19)	116.4(1)	P(1)-C(18)-C(23)	114.3(1)
C(19)-C(18)-C(23)	109.9(2)	C(18)-C(19)-C(20)	110.6(2)
C(19)-C(20)-C(21)	111.2(2)	C(20)-C(21)-C(22)	110.8(2)
C(21)-C(22)-C(23)	111.6(2)	C(18)-C(23)-C(22)	110.7(2)

**Table A.7.1:** Crystallographic and refinement data for *cis*-[Ru(acac)<sub>2</sub>(PPr<sup>i</sup><sub>3</sub>)<sub>2</sub>].

<b>Crystal Data</b>	
Empirical Formula	C <sub>28</sub> H <sub>56</sub> O <sub>4</sub> P <sub>2</sub> Ru
Formula Weight	619.77
Crystal Colour, Habit	orange, block
Crystal Dimensions	0.22 x 0.18 x 0.15 mm
Crystal System	monoclinic
Lattice Type	Primitive
No. of Reflections Used for Unit Cell Determination (2 $\theta$ range)	25 (106.6 - 109.8°)
Omega Scan Peak Width at Half-height	0.30°
Lattice Parameters	a = 10.660(3) Å b = 19.825(3) Å c = 15.504(3) Å $\beta$ = 98.89(2)° V = 3237(1) Å <sup>3</sup>
Space Group	P2 <sub>1</sub> /n (#14)
Z value	4
D <sub>calc</sub>	1.272 g/cm <sup>3</sup>
F <sub>000</sub>	1320.00
$\mu$ (MoK $\alpha$ )	50.76 cm <sup>-1</sup>
<b>Intensity Measurements</b>	
diffractometer	Rigaku AFC6R
Radiation	CuK $\alpha$ ( $\lambda$ = 1.5178 Å) graphite monochromated
Take-off Angle	6.0°
Detector Aperture	9.0 mm horizontal 7.0 mm vertical
Crystal to Detector Distance	400 mm
Voltage, Current	50 kV, 180 mA
Temperature	-80.0 °C
Scan Type	$\omega$ -2 $\theta$
Scan Rate	16.0°/min (in $\omega$ ) (up to 4 scans)
Scan Width	(1.00 + 0.30 tan $\theta$ )°
2 $\theta$ <sub>max</sub>	120.1°
No. of Reflections Measured	Total: 6272 Unique: 4813 ( $R_{int}$ = 0.026)
Corrections	Lorentz-polarization Absorption (trans. Factors: 0.4638 - 0.5780) Secondary Extinction (coefficient: 1.52(6) x 10 <sup>-6</sup> )

**Table A.7.1 (cont):** Crystallographic and refinement data for *cis*-[Ru(acac)<sub>2</sub>(PPri<sub>3</sub>)<sub>2</sub>].**Structure Solution and Refinement**

Structure Solution	Direct Methods (SIR92)
Refinement	Full-Matrix least squares
Function Minimized	$\sum w( F_o  -  F_c )^2$
Least Squares Weights	$w = [\sigma_c^2(F_o) + 0.25p^2F_o^2]^{-1}$
p-factor	0.030
Anomalous Dispersion	All non-hydrogen atoms
No. Observations (I>2.0σ(I))	4295
No. of variables	317
Reflection/Parameter Rotation	13.55
Residuals: R; Rw	0.028; 0.034
Goodness of Fit Indicator	1.71
Max Shift/Error in Final Cycle	0.03
Max peak in Final Diff. Map	0.275 e <sup>-</sup> /Å <sup>3</sup>
Min peak in Final Diff Map	-0.52 e <sup>-</sup> /Å <sup>3</sup>

**Table A.7.2:** Interatomic distances (Å) and angles (°) involving non-hydrogen atoms of the molecular structure of *cis*-[Ru(acac)<sub>2</sub>(PPri<sub>3</sub>)<sub>2</sub>].

Ru(1)-P(1)	2.3525(9)	Ru(1)-P(2)	2.3467(8)
Ru(1)-O(1)	2.068(2)	Ru(1)-O(2)	2.088(2)
Ru(1)-O(3)	2.059(2)	Ru(1)-O(4)	2.104(2)
P(1)-C(11)	1.873(3)	P(1)-C(14)	1.886(3)
P(1)-C(17)	1.863(3)	P(2)-C(20)	1.878(3)
P(2)-C(23)	1.884(3)	P(2)-C(26)	1.874(3)
O(1)-C(2)	1.276(4)	O(2)-C(4)	1.274(4)
O(3)-C(7)	1.276(4)	O(4)-C(9)	1.272(4)
C(1)-C(2)	1.501(5)	C(2)-C(3)	1.395(5)
C(3)-C(4)	1.380(5)	C(4)-C(5)	1.513(4)
C(6)-C(7)	1.505(4)	C(7)-C(8)	1.395(4)
C(8)-C(9)	1.383(4)	C(9)-C(10)	1.518(4)
C(11)-C(12)	1.532(5)	C(11)-C(13)	1.538(4)
C(14)-C(15)	1.532(5)	C(14)-C(16)	1.543(4)
C(17)-C(18)	1.540(4)	C(17)-C(19)	1.530(4)
C(20)-C(21)	1.528(4)	C(20)-C(22)	1.533(4)
C(23)-C(24)	1.528(5)	C(23)-C(25)	1.540(4)
C(26)-C(27)	1.523(5)	C(26)-C(28)	1.527(4)

**Table A.7.2 (cont):** Interatomic distances (Å) and angles (°) involving non-hydrogen atoms of the molecular structure of *cis*-[Ru(acac)<sub>2</sub>(PPr<sup>i</sup><sub>3</sub>)<sub>2</sub>].

P(1)-Ru(1)-P(2)	105.42(3)	P(1)-Ru(1)-O(1)	90.20(6)
R(1)-Ru(1)-O(2)	167.23(6)	P(1)-Ru(1)-O(3)	93.86(6)
P(1)-Ru(1)-O(4)	87.57(6)	P(2)-Ru(1)-O(1)	94.43(6)
P(2)-Ru(1)-O(2)	87.25(6)	P(2)-Ru(1)-O(3)	88.73(6)
P(2)-Ru(1)-O(4)	167.01(6)	O(1)-Ru(1)-O(2)	90.46(8)
O(1)-Ru(1)-O(3)	174.02(7)	O(1)-Ru(1)-O(4)	85.28(8)
O(2)-Ru(1)-O(3)	84.62(8)	O(2)-Ru(1)-O(4)	79.77(8)
O(3)-Ru(1)-O(4)	90.50(8)	Ru(1)-P(1)-C(11)	118.7(1)
Ru(1)-P(1)-C(14)	110.6(1)	Ru(1)-P(1)-C(17)	118.8(1)
C(11)-P(1)-C(14)	106.7(1)	C(11)-P(1)-C(17)	101.2(1)
C(14)-P(1)-C(17)	98.4(1)	Ru(1)-P(2)-C(20)	117.9(1)
Ru(1)-P(2)-C(23)	110.3(1)	Ru(1)-P(2)-C(26)	119.3(1)
C(20)-P(2)-C(23)	106.2(1)	C(20)-P(2)-C(26)	101.9(1)
C(23)-P(2)-C(26)	99.0(1)	Ru(1)-O(1)-C(2)	123.8(2)
Ru(1)-O(2)-C(4)	123.5(2)	Ru(1)-O(3)-C(7)	124.0(2)
Ru(1)-O(4)-C(9)	122.2(2)	O(1)-C(2)-C(1)	114.6(3)
O(1)-C(2)-C(3)	126.3(3)	C(1)-C(2)-C(3)	119.1(3)
C(2)-C(3)-C(4)	127.9(3)	O(2)-C(4)-C(3)	126.5(3)
O(2)-C(4)-C(5)	113.6(3)	C(3)-C(4)-C(5)	119.9(3)
O(3)-C(7)-C(6)	114.2(3)	O(3)-C(7)-C(8)	126.4(3)
C(6)-C(7)-C(8)	119.5(3)	C(7)-C(8)-C(9)	127.4(3)
O(4)-C(9)-C(8)	127.3(3)	O(4)-C(9)-C(10)	114.4(3)
C(8)-C(9)-C(10)	118.3(3)	P(1)-C(11)-C(12)	111.0(2)
P(1)-C(11)-C(13)	118.5(2)	C(12)-C(11)-C(13)	109.5(3)
P(1)-C(14)-C(15)	116.9(2)	P(1)-C(14)-C(16)	115.9(2)
C(15)-C(14)-C(16)	109.7(3)	P(1)-C(17)-C(18)	112.0(2)
P(1)-C(17)-C(19)	114.6(2)	C(18)-C(17)-C(19)	109.5(3)
P(2)-C(20)-C(21)	111.6(2)	P(2)-C(20)-C(22)	118.7(2)
C(21)-C(20)-C(22)	109.4(3)	P(2)-C(23)-C(24)	117.3(2)
P(2)-C(23)-C(25)	115.5(2)	C(24)-C(23)-C(25)	109.2(3)
P(2)-C(26)-C(27)	112.4(2)	P(2)-C(26)-C(28)	113.7(2)
C(27)-C(26)-C(28)	109.7(3)		

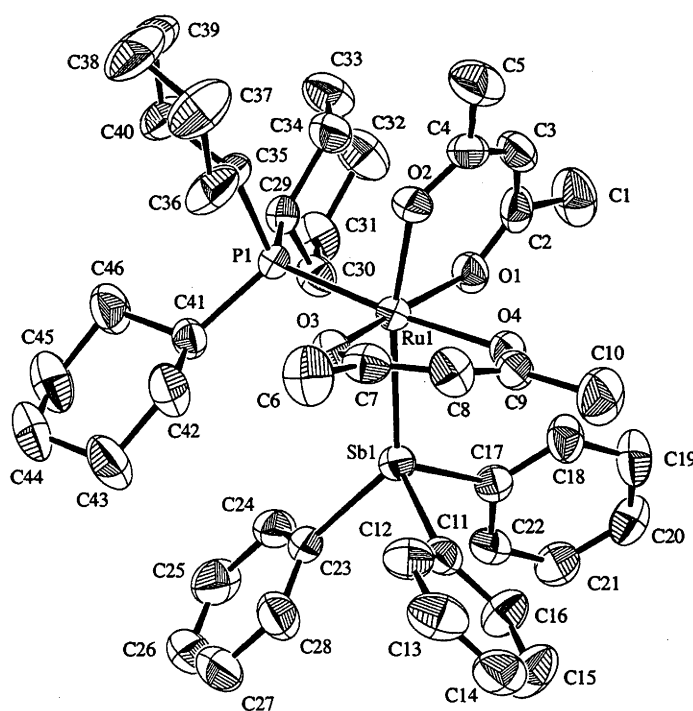
**Table A.8.1:** Crystallographic and refinement data for *cis*-[Ru(acac)<sub>2</sub>(PCy<sub>3</sub>)(SbPh<sub>3</sub>)].

<b>Crystal Data</b>	
Empirical Formula	C <sub>46</sub> H <sub>62</sub> O <sub>4</sub> PRuSb
Formula Weight	932.79
Crystal Colour, Habit	orange, platelet
Crystal Dimensions	0.19 x 0.18 x 0.08 mm
Crystal System	triclinic
Lattice Type	Primitive
No. of Reflections Used for Unit Cell Determination (2 $\theta$ range)	25 (29.1 - 32.0°)
Lattice Parameters	a = 12.220(3) Å b = 12.829(3) Å c = 14.693(3) Å $\alpha$ = 86.39(2)° $\beta$ = 73.90(2)° $\gamma$ = 89.43(2)° V = 2208.6(9) Å <sup>3</sup>
Space Group	P $\bar{1}$ (#2)
Z value	2
D <sub>calc</sub>	1.403 g/cm <sup>3</sup>
F <sub>000</sub>	960.00
$\mu$ (MoK $\alpha$ )	10.29 cm <sup>-1</sup>
<b>Intensity Measurements</b>	
diffractometer	Philips PW1100/20
Radiation	MoK $\alpha$ ( $\lambda$ = 0.71069 Å) graphite monochromated
Take-off Angle	3.0°
Detector Aperture	3.4 mm horizontal 3.4 mm vertical
Crystal to Detector Distance	195 mm
Voltage, Current	50 kV, 30 mA
Temperature	20.0 °C
Scan Type	$\omega$ -2 $\theta$
Scan Rate	2.0°/min (in $\omega$ )
Scan Width	(1.00 + 0.35 tan $\theta$ )°
2 $\theta$ <sub>max</sub>	52.2°
No. of Reflections Measured	Total: 8691 Unique: 8690 (R <sub>int</sub> = 0.022)
Corrections	Lorentz-polarization Absorption (trans. Factors: 0.922 - 0.801)



**Table A.8.1 (cont):** Crystallographic and refinement data for *cis*-[Ru(acac)<sub>2</sub>(PCy<sub>3</sub>)(SbPh<sub>3</sub>)].**Structure Solution and Refinement**

Structure Solution	Direct Methods (SIR92)
Refinement	Full-Matrix least squares
Function Minimized	$\sum w( F_o  -  F_c )^2$
Least Squares Weights	$w = [\sigma_c^2(F_o) + 0.25p^2F_o^2]^{-1}$
p-factor	0.020
Anomalous Dispersion	All non-hydrogen atoms
No. Observations ( $I > 2.0\sigma(I)$ )	5927
No. of variables	478
Reflection/Parameter Rotation	12.40
Residuals: R; R <sub>w</sub>	0.045; 0.036
Goodness of Fit Indicator	1.22
Max Shift/Error in Final Cycle	0.02
Max peak in Final Diff. Map	0.51 e <sup>-</sup> /Å <sup>3</sup>
Min peak in Final Diff. Map	-0.56 e <sup>-</sup> /Å <sup>3</sup>

**Figure A.8.1:** ORTEP diagram of the molecular structure of *cis*-[Ru(acac)<sub>2</sub>(PCy<sub>3</sub>)(SbPh<sub>3</sub>)].**Table A.8.2:** Interatomic distances (Å) and angles (°) involving non-hydrogen atoms of the molecular structure of *cis*-[Ru(acac)<sub>2</sub>(PCy<sub>3</sub>)(SbPh<sub>3</sub>)].

Sb(1)-Ru(1)	2.5847(5)	Sb(1)-C(11)	2.151(5)
Sb(1)-C(17)	2.135(5)	Sb(1)-C(23)	2.156(5)
Ru(1)-P(1)	2.309(1)	Ru(1)-O(1)	2.059(3)

**Table A.8.2 (cont):** Interatomic distances (Å) and angles (°) involving non-hydrogen atoms of the molecular structure of *cis*-[Ru(acac)<sub>2</sub>(PCy<sub>3</sub>)(SbPh<sub>3</sub>)].

Ru(1)-O(2)	2.058(3)	Ru(1)-O(3)	2.059(3)
Ru(1)-O(2)	2.058(3)	Ru(1)-O(3)	2.059(3)
Ru(1)-O(4)	2.121(3)	P(1)-C(29)	1.865(5)
P(1)-C(35)	1.858(5)	P(1)-C(41)	1.873(5)
O(1)-C(2)	1.265(6)	O(2)-C(4)	1.271(6)
O(3)-C(7)	1.277(6)	O(4)-C(9)	1.267(6)
C(1)-C(2)	1.511(7)	C(2)-C(3)	1.382(8)
C(3)-C(4)	1.383(7)	C(4)-C(5)	1.506(8)
C(6)-C(7)	1.507(7)	C(7)-C(8)	1.384(7)
C(8)-C(9)	1.387(7)	C(9)-C(10)	1.523(7)
C(11)-C(12)	1.364(7)	C(11)-C(16)	1.380(7)
C(12)-C(13)	1.388(8)	C(13)-C(14)	1.357(9)
C(14)-C(15)	1.357(9)	C(15)-C(16)	1.377(8)
C(17)-C(18)	1.377(7)	C(17)-C(22)	1.383(7)
C(18)-C(19)	1.400(7)	C(19)-C(20)	1.362(7)
C(20)-C(21)	1.363(7)	C(21)-C(22)	1.373(7)
C(23)-C(24)	1.377(7)	C(23)-C(28)	1.383(7)
C(24)-C(25)	1.388(7)	C(25)-C(26)	1.367(9)
C(26)-C(27)	1.355(9)	C(27)-C(28)	1.391(8)
C(29)-C(30)	1.529(7)	C(29)-C(34)	1.534(7)
C(30)-C(31)	1.521(7)	C(31)-C(32)	1.514(8)
C(32)-C(33)	1.507(9)	C(33)-C(34)	1.525(8)
C(35)-C(36)	1.521(8)	C(35)-C(40)	1.530(7)
C(36)-C(37)	1.533(9)	C(37)-C(38)	1.511(9)
C(38)-C(39)	1.502(9)	C(39)-C(40)	1.513(8)
C(41)-C(42)	1.522(7)	C(41)-C(46)	1.513(7)
C(42)-C(43)	1.525(8)	C(43)-C(44)	1.503(8)
C(44)-C(45)	1.499(8)	C(45)-C(46)	1.530(8)
Ru(1)-Sb(1)-C(11)	11.2(1)	Ru(1)-Sb(1)-C(17)	115.1(1)
Ru(1)-Sb(1)-C(23)	133.9(1)	C(11)-Sb(1)-C(17)	95.5(2)
C(11)-Sb(1)-C(23)	95.6(2)	C(17)-Sb(1)-C(23)	98.1(2)
Sb(1)-Ru(1)-P(1)	100.20(4)	Sb(1)-Ru(1)-O(1)	88.6(1)
Sb(1)-Ru(1)-O(2)	167.42(9)	Sb(1)-Ru(1)-O(3)	94.93(9)
Sb(1)-Ru(1)-O(4)	84.09(9)	P(1)-Ru(1)-O(1)	95.2(1)
P(1)-Ru(1)-O(2)	92.3(1)	P(1)-Ru(1)-O(3)	91.7(1)
O(1)-Ru(1)-O(3)	171.6(1)	O(1)-Ru(1)-O(4)	82.9(1)
O(2)-Ru(1)-O(3)	83.2(1)	O(2)-Ru(1)-O(4)	83.5(1)
O(3)-Ru(1)-O(4)	89.9(1)	Ru(1)-P(1)-C(29)	116.8(2)

**Table A.8.2 (cont):** Interatomic distances (Å) and angles (°) involving non-hydrogen atoms of the molecular structure of *cis*-[Ru(acac)<sub>2</sub>(PCy<sub>3</sub>)(SbPh<sub>3</sub>)].

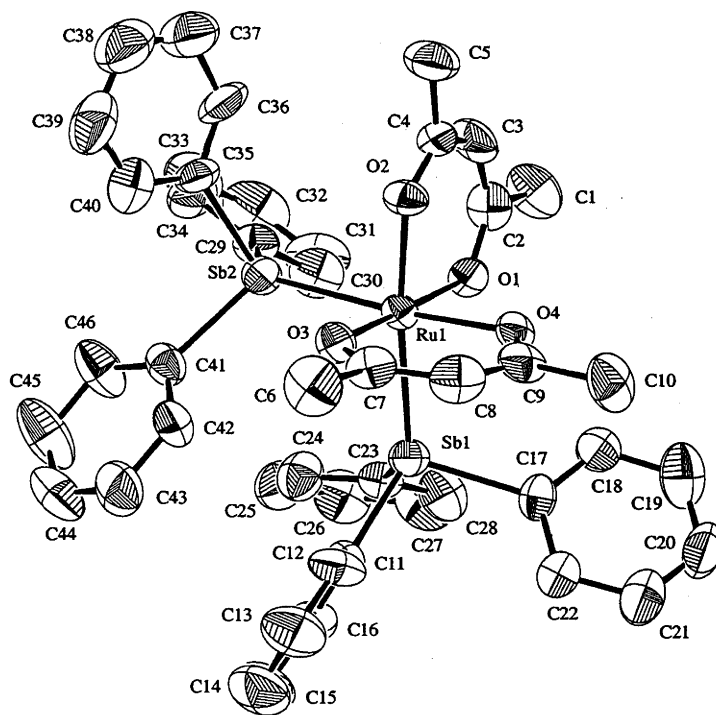
Ru(1)-P(1)-C(35)	111.3(2)	Ru(1)-P(1)-C(41)	116.8(2)
C(29)-P(1)-C(35)	101.1(2)	C(29)-P(1)-C(41)	101.0(2)
C(35)-P(1)-C(41)	108.3(2)	Ru(1)-O(1)-C(2)	122.4(4)
Ru(1)-O(2)-C(4)	123.1(4)	Ru(1)-O(3)-C(7)	123.6(3)
Ru(1)-O(4)-C(9)	123.0(3)	O(1)-C(2)-C(1)	113.6(6)
O(1)-C(2)-C(3)	127.5(5)	C(1)-C(2)-C(3)	118.9(6)
C(2)-C(3)-C(4)	127.4(5)	O(2)-C(4)-C(3)	126.6(5)
O(2)-C(4)-C(5)	114.2(5)	C(3)-C(4)-C(5)	119.2(5)
O(3)-C(7)-C(6)	114.0(5)	O(3)-C(7)-C(8)	127.0(5)
C(6)-C(7)-C(8)	118.8(5)	C(7)-C(8)-C(9)	127.1(5)
O(4)-C(9)-C(8)	126.9(5)	O(4)-C(9)-C(10)	115.2(5)
C(8)-C(9)-C(10)	117.8(5)	Sb(1)-C(11)-C(12)	119.4(4)
Sb(1)-C(11)-C(16)	121.9(4)	C(12)-C(11)-C(16)	118.7(5)
C(11)-C(12)-C(13)	120.8(6)	C(12)-C(13)-C(14)	119.8(6)
C(13)-C(14)-C(15)	119.9(6)	C(14)-C(15)-C(16)	120.8(6)
C(11)-C(16)-C(15)	120.0(6)	Sb(1)-C(17)-C(18)	117.6(4)
Sb(1)-C(17)-C(22)	123.2(4)	C(18)-C(17)-C(22)	118.7(5)
C(17)-C(18)-C(19)	119.6(5)	C(18)-C(19)-C(20)	120.8(5)
C(19)-C(20)-C(21)	119.5(5)	C(20)-C(21)-C(22)	120.6(5)
C(17)-C(22)-C(21)	120.9(5)	Sb(1)-C(23)-C(24)	121.3(4)
Sb(1)-C(23)-C(28)	120.0(4)	C(24)-C(23)-C(28)	118.7(5)
C(23)-C(24)-C(25)	120.8(5)	C(24)-C(25)-C(26)	119.8(6)
C(25)-C(26)-C(27)	120.0(6)	C(26)-C(27)-C(28)	120.8(6)
C(23)-C(28)-C(27)	119.8(6)	P(1)-C(29)-C(30)	113.5(4)
P(1)-C(29)-C(34)	114.2(4)	C(30)-C(29)-C(34)	109.7(4)
C(29)-C(30)-C(31)	112.0(5)	C(30)-C(31)-C(32)	112.3(5)
C(31)-C(32)-C(33)	111.3(5)	C(32)-C(33)-C(34)	111.8(5)
C(29)-C(34)-C(33)	111.6(5)	P(1)-C(35)-C(36)	115.3(4)
P(1)-C(35)-C(40)	119.2(4)	C(36)-C(35)-C(40)	108.5(5)
C(35)-C(36)-C(37)	111.1(5)	C(36)-C(37)-C(38)	111.6(6)
C(37)-C(38)-C(39)	111.3(6)	C(38)-C(39)-C(40)	111.9(6)
C(35)-C(40)-C(39)	110.9(5)	P(1)-C(41)-C(42)	113.4(4)
P(1)-C(41)-C(46)	119.2(4)	C(42)-C(41)-C(46)	109.4(4)
C(41)-C(42)-C(43)	113.0(5)	C(42)-C(43)-C(44)	112.4(6)
C(43)-C(44)-C(45)	110.3(5)	C(44)-C(45)-C(46)	112.4(5)
C(41)-C(46)-C(45)	112.0(5)		

Table A.9.1: Crystallographic and refinement data for *cis*-[Ru(acac)<sub>2</sub>(SbPh<sub>3</sub>)<sub>2</sub>].

<b>Crystal Data</b>	
Empirical Formula	C <sub>46</sub> H <sub>44</sub> O <sub>4</sub> RuSb <sub>2</sub>
Formula Weight	1005.42
Crystal Colour, Habit	yellow, plate
Crystal Dimensions	0.44 x 0.20 x 0.05 mm
Crystal System	triclinic
Lattice Type	Primitive
No. of Reflections Used for Unit Cell Determination (2θ range)	21 (18.2 - 23.4°)
Lattice Parameters	a = 10.810(4) Å b = 11.414(6) Å c = 18.170(6) Å α = 74.89(4)° β = 87.06(4)° γ = 79.56(3)° V = 2129(2) Å <sup>3</sup>
Space Group	P $\bar{1}$ (#2)
Z value	2
D <sub>calc</sub>	1.569 g/cm <sup>3</sup>
F <sub>000</sub>	996.00
μ(MoKα)	16.49 cm <sup>-1</sup>
<b>Intensity Measurements</b>	
diffractometer	Philips PW1100/20
Radiation	MoKα (λ = 0.71069 Å) graphite monochromated
Take-off Angle	2.8°
Detector Aperture	3.4 mm horizontal 3.4 mm vertical
Crystal to Detector Distance	195 mm
Voltage, Current	50 kV, 25 mA
Temperature	23.0 °C
Scan Type	ω-2θ
Scan Rate	3.0°/min (in ω)
Scan Width	(1.10 + 0.34 tan θ)°
2θ <sub>max</sub>	52.0°
No. of Reflections Measured	Total: 8349
Corrections	Lorentz-polarization Absorption (trans. Factors: 0.718 - 0.922)

**Table A.9.1 (cont):** Crystallographic and refinement data for *cis*-[Ru(acac)<sub>2</sub>(SbPh<sub>3</sub>)<sub>2</sub>].

Structure Solution and Refinement	
Structure Solution	Direct Methods (SHELXS86)
Refinement	Full-Matrix least squares
Function Minimized	$\sum w( F_o  -  F_c )^2$
Least Squares Weights	$w = [\sigma_c^2(F_o) + 0.25p^2F_o^2]^{-1}$
p-factor	0.02
Anomalous Dispersion	All non-hydrogen atoms
No. Observations ( $I > 2.0\sigma(I)$ )	4480
No. of variables	478
Reflection/Parameter Rotation	9.37
Residuals: R; Rw	0.048; 0.043
Goodness of Fit Indicator	1.41
Max Shift/Error in Final Cycle	0.01
Max peak in Final Diff. Map	0.94 e <sup>-</sup> /Å <sup>3</sup>
Min peak in Final Diff. Map	-0.69 e <sup>-</sup> /Å <sup>3</sup>

**Figure A.9.1:** ORTEP diagram of the structure *cis*-[Ru(acac)<sub>2</sub>(SbPh<sub>3</sub>)<sub>2</sub>].

**Table A.9.2:** Interatomic distances (Å) and angles (°) involving non-hydrogen atoms of the molecular structure of *cis*-[Ru(acac)<sub>2</sub>(SbPh<sub>3</sub>)<sub>2</sub>].

Sb(1)-Ru(1)	2.571(1)	Sb(1)-C(11)	2.163(9)
Sb(1)-C(17)	2.135(9)	Sb(1)-C(23)	2.132(9)
Sb(2)-Ru(1)	2.543(1)	Sb(2)-C(29)	2.132(9)
Sb(2)-C(35)	2.133(9)	Sb(2)-C(41)	2.141(9)
Ru(1)-O(1)	2.052(6)	Ru(1)-O(2)	2.067(6)
Ru(1)-O(3)	2.057(6)	Ru(1)-O(4)	2.063(6)
O(1)-C(2)	1.25(1)	O(2)-C(4)	1.27(1)
O(3)-C(7)	1.27(1)	O(4)-C(9)	1.27(1)
C(1)-C(2)	1.50(1)	C(2)-C(3)	1.39(1)
C(3)-C(4)	1.40(1)	C(4)-C(5)	1.51(1)
C(6)-C(7)	1.51(1)	C(7)-C(8)	1.38(1)
C(8)-C(9)	1.39(1)	C(9)-C(10)	1.51(1)
C(11)-C(12)	1.36(1)	C(11)-C(16)	1.39(1)
C(12)-C(13)	1.39(1)	C(13)-C(14)	1.36(2)
C(14)-C(15)	1.36(2)	C(15)-C(16)	1.39(1)
C(17)-C(18)	1.35(1)	C(17)-C(22)	1.41(1)
C(18)-C(19)	1.41(1)	C(19)-C(20)	1.37(2)
C(20)-C(21)	1.34(2)	C(21)-C(22)	1.40(1)
C(23)-C(24)	1.36(1)	C(23)-C(28)	1.39(1)
C(24)-C(25)	1.40(1)	C(25)-C(26)	1.34(1)
C(26)-C(27)	1.37(2)	C(27)-C(28)	1.36(1)
C(29)-C(30)	1.37(1)	C(29)-C(32)	1.35(2)
C(32)-C(33)	1.37(2)	C(33)-C(34)	1.40(2)
C(35)-C(36)	1.32(1)	C(35)-C(40)	1.39(1)
C(36)-C(37)	1.41(2)	C(37)-C(38)	1.37(2)
C(38)-C(39)	1.40(2)	C(39)-C(40)	1.35(2)
C(41)-C(42)	1.38(1)	C(41)-C(46)	1.37(1)
C(42)-C(43)	1.38(1)	C(43)-C(44)	1.33(2)
C(44)-C(45)	1.37(2)	C(45)-C(46)	1.39(1)
Ru(1)-Sb(1)-C(11)	125.1(3)	Ru(1)-Sb(1)-C(17)	109.1(3)
Ru(1)-Sb(1)-C(23)	118.9(2)	C(11)-Sb(1)-C(17)	101.5(4)
C(11)-Sb(1)-C(23)	98.3(4)	C(17)-Sb(1)-C(23)	100.1(4)
Ru(1)-Sb(1)-C(29)	121.0(3)	Ru(1)-Sb(2)-C(35)	115.4(3)
Ru(1)-Sb(2)-C(41)	116.3(3)	C(29)-Sb(2)-C(35)	100.3(4)
C(29)-Sb(2)-C(41)	100.7(4)	C(35)-Sb(2)-C(41)	99.6(4)
Sb(1)-Ru(1)-Sb(2)	96.89(3)	Sb(1)-Ru(1)-O(1)	87.4(2)
Sb(1)-Ru(1)-O(2)	173.2(2)	Sb(1)-Ru(1)-O(3)	94.7(2)
Sb(1)-Ru(1)-O(4)	87.4(2)	Sb(2)-Ru(1)-O(1)	92.4(2)

**Table A.9.2 (cont):** Interatomic distances (Å) and angles (°) involving non-hydrogen atoms of the molecular structure of *cis*-[Ru(acac)<sub>2</sub>(SbPh<sub>3</sub>)<sub>2</sub>].

Sb(2)-Ru(1)-O(2)	89.9(2)	Sb(2)-Ru(1)-O(3)	89.2(2)
Sb(2)-Ru(1)-O(4)	175.4(2)	O(1)-Ru(1)-O(2)	92.3(2)
O(1)-Ru(1)-O(3)	177.1(3)	O(1)-Ru(1)-O(4)	86.3(2)
O(2)-Ru(1)-O(3)	85.4(2)	O(2)-Ru(1)-O(4)	85.8(2)
O(3)-Ru(1)-O(4)	91.9(2)	Ru(1)-O(1)-C(2)	123.8(6)
Ru(1)-O(2)-C(4)	123.0(6)	Ru(1)-O(3)-C(7)	123.5(6)
Ru(1)-O(4)-C(9)	122.8(6)	O(1)-C(2)-C(1)	116(1)
O(1)-C(2)-C(3)	125.9(9)	C(1)-C(2)-C(3)	118(1)
C(2)-C(3)-C(4)	129.0(9)	O(2)-C(4)-C(3)	125.6(9)
O(2)-C(4)-C(5)	114.5(9)	C(3)-C(4)-C(5)	119.9(9)
O(3)-C(7)-C(6)	115(1)	O(3)-C(7)-C(8)	126.5(9)
C(6)-C(7)-C(8)	118(1)	C(7)-C(8)-C(9)	128(1)
O(4)-C(9)-C(8)	127(1)	O(4)-C(9)-C(10)	114(1)
C(8)-C(9)-C(10)	119(1)	Sb(1)-C(11)-C(12)	119.6(8)
Sb(1)-C(11)-C(16)	121.3(8)	C(12)-C(11)-C(16)	119.0(9)
C(11)-C(12)-C(13)	121(1)	C(12)-C(13)-C(14)	120(1)
C(13)-C(14)-C(15)	120(1)	C(14)-C(15)-C(16)	121(1)
C(11)-C(16)-C(15)	119(1)	Sb(1)-C(17)-C(18)	120.2(8)
Sb(1)-C(17)-C(22)	120.5(8)	C(18)-C(17)-C(22)	119(1)
C(17)-C(18)-C(19)	121(1)	C(18)-C(19)-C(20)	120(1)
C(19)-C(20)-C(21)	119(1)	C(20)-C(21)-C(22)	122(1)
C(17)-C(22)-C(21)	118(1)	Sb(1)-C(23)-C(24)	120.3(8)
Sb(1)-C(23)-C(28)	122.7(8)	C(24)-C(23)-C(28)	116.9(9)
C(23)-C(24)-C(25)	122(1)	C(24)-C(25)-C(26)	119(1)
C(25)-C(26)-C(27)	122(1)	C(26)-C(27)-C(28)	119(1)
C(23)-C(28)-C(27)	122(1)	Sb(2)-C(29)-C(30)	118.3(8)
Sb(2)-C(29)-C(34)	122.8(8)	C(30)-C(29)-C(34)	119(1)
C(29)-C(30)-C(31)	123(1)	C(30)-C(31)-C(32)	118(1)
C(31)-C(32)-C(33)	122(1)	C(32)-C(33)-C(34)	120(1)
C(29)-C(34)-C(33)	118(1)	Sb(2)-C(35)-C(36)	119.4(9)
Sb(2)-C(35)-C(40)	122.1(8)	C(36)-C(35)-C(40)	118(1)
C(35)-C(36)-C(37)	123(1)	C(36)-C(37)-C(38)	118(1)
C(37)-C(38)-C(39)	120(1)	C(38)-C(39)-C(40)	119(1)
C(35)-C(40)-C(39)	122(1)	Sb(2)-C(41)-C(42)	117.4(8)
Sb(2)-C(41)-C(46)	124.0(8)	C(42)-C(41)-C(46)	118(1)
C(41)-C(42)-C(43)	121(1)	C(42)-C(43)-C(44)	120(1)
C(43)-C(44)-C(45)	120(1)	C(44)-C(45)-C(46)	120(1)
C(41)-C(46)-C(45)	120(1)		

**Table A.10.1:** Crystallographic and refinement data for *cis*- $[[Ru(acac)_2(PPr^i_3)]_2(\mu-N_2)].C_6H_{14}$  at 200 K.

<b>Crystal Data</b>	
Empirical Formula	$C_{44}H_{84}N_2O_8P_2Ru_2$
Formula Weight	1033.24
Crystal Colour, Habit	orange, block
Crystal Dimensions	0.20 x 0.10 x 0.10 mm
Crystal System	monoclinic
Lattice Type	C-centered
Lattice Parameters	$a = 20.087(1) \text{ \AA}$ $b = 14.562(1) \text{ \AA}$ $c = 18.065(1) \text{ \AA}$ $\beta = 106.538(4)^\circ$ $V = 5065.5(5) \text{ \AA}^3$
Space Group	P2/c (#15)
Z value	4
$D_{calc}$	$1.355 \text{ g/cm}^3$
$F_{000}$	2176.00
$\mu(\text{MoK}\alpha)$	$7.07 \text{ cm}^{-1}$
<b>Intensity Measurements</b>	
diffractometer	Nonius KappaCD
Radiation	MoK $\alpha$ ( $\lambda = 0.71069 \text{ \AA}$ ) graphite monochromated
Detector Aperture	65 mm x 65 mm
Data Images	1.9°/frame; 30 sec/°
Detector Position	25.00 mm
$2\theta_{max}$	55.1°
No. of Reflections Measured	Total: 9739 Unique: 5751 ( $R_{int} = 0.051$ )
Corrections	Lorentz-polarization



**Table A.10.1 (cont):** Crystallographic and refinement data for *cis*- $[[Ru(acac)_2(PPri_3)]_2(\mu-N_2)].C_6H_{14}$  at 200 K.**Structure Solution and Refinement**

Structure Solution	Patterson Methods (DIRDIF92 PATTY)
Refinement	Full-Matrix least squares
Function Minimized	$\sum w( F_o  -  F_c )^2$
Least Squares Weights	$w = [\sigma_c^2(F_o) + 0.25p^2F_o^2]^{-1}$
p-factor	0.040
Anomalous Dispersion	All non-hydrogen atoms
No. Observations ( $I > 2.0\sigma(I)$ )	3093
No. of variables	254
Reflection/Parameter Rotation	12.18
Residuals: R; Rw	0.050; 0.059
Goodness of Fit Indicator	1.44
Max Shift/Error in Final Cycle	0.01
Max peak in Final Diff. Map	$0.62 e^-/\text{\AA}^3$
Min peak in Final Diff Map	$-0.55 e^-/\text{\AA}^3$

**Table A.10.2:** Interatomic distances ( $\text{\AA}$ ) and angles ( $^\circ$ ) involving non-hydrogen atoms of the molecular structure of *cis*- $[[Ru(acac)_2(PPri_3)]_2(\mu-N_2)].C_6H_{14}$  at 200 K.

Ru(1)-P(1)	2.312(2)	Ru(1)-O(1)	2.046(4)
Ru(1)-O(2)	2.035(4)	Ru(1)-O(3)	2.050(4)
Ru(1)-O(4)	2.107(4)	Ru(1)-N(1)	1.919(4)
P(1)-C(11)	1.855(7)	P(1)-C(14)	1.871(9)
P(1)-C(17)	1.88(1)	P(1)-C(17a)	1.91(2)
O(1)-C(2)	1.268(7)	O(2)-C(4)	1.273(7)
O(3)-C(7)	1.281(7)	O(4)-C(9)	1.272(7)
N(1)-N(1) <sup>a</sup>	1.135(8)	C(1)-C(2)	1.502(9)
C(2)-C(3)	1.382(9)	C(3)-C(4)	1.397(9)
C(4)-C(5)	1.496(9)	C(6)-C(7)	1.487(9)
C(7)-C(8)	1.389(9)	C(8)-C(9)	1.394(9)
C(9)-C(10)	1.512(9)	C(11)-C(12)	1.53(1)
C(11)-C(13)	1.53(1)	C(14)-C(15)	1.52(1)
C(14)-C(16)	1.53(1)	C(17)-C(18)	1.60(2)
C(17)-C(19)	1.49(2)	C(17a)-C(19a)	1.54(3)
C(31)-C(32)	1.354(9)*	C(32)-C(33)	1.351(9)*
C(33)-C(34)	1.346(9)*	C(34)-C(35)	1.348(9)*
C(35)-C(36)	1.345(9)*		

**Table A.10.2 (cont):** Interatomic distances (Å) and angles (°) involving non-hydrogen atoms of the molecular structure of *cis*-[Ru(acac)<sub>2</sub>(PPr<sub>3</sub>)<sub>2</sub>(μ-N<sub>2</sub>)]·C<sub>6</sub>H<sub>14</sub>at 200 K.

P(1)-Ru(1)-O(1)	96.0(1)	P(1)-Ru(1)-O(2)	92.3(1)
P(1)-Ru(1)-O(3)	90.2(1)	P(1)-Ru(1)-O(4)	177.9(1)
P(1)-Ru(1)-N(1)	92.6(1)	O(1)-Ru(1)-O(2)	92.4(2)
O(1)-Ru(1)-O(3)	173.8(2)	O(1)-Ru(1)-O(4)	82.5(2)
O(1)-Ru(1)-N(1)	90.3(2)	O(2)-Ru(1)-O(3)	86.8(1)
O(2)-Ru(1)-O(4)	86.4(1)	O(2)-Ru(1)-N(1)	174.2(2)
O(3)-Ru(1)-O(4)	91.3(2)	O(3)-Ru(1)-N(1)	90.0(2)
O(4)-Ru(1)-N(1)	88.9(2)	Ru(1)-P(1)-C(11)	112.8(3)
Ru(1)-P(1)-C(14)	116.4(3)	Ru(1)-P(1)-C(17)	110.8(4)
Ru(1)-P(1)-C(17a)	119.7(6)	C(11)-P(1)-C(14)	101.8(4)
C(11)-P(1)-C(17)	117.9(5)	C(11)-P(1)-C(17a)	93.6(7)
C(14)-P(1)-C(17)	96.0(5)	C(14)-P(1)-C(17a)	108.9(7)
Ru(1)-O(1)-C(2)	122.3(4)		
Ru(1)-O(2)-C(4)	123.3(4)	Ru(1)-O(3)-C(7)	124.7(4)
Ru(1)-O(4)-C(9)	122.4(4)	Ru(1)-N(1)-N(1) <sup>a</sup>	174.2(4)
O(1)-C(2)-C(1)	114.4(6)	O(1)-C(2)-C(3)	127.1(6)
C(1)-C(2)-C(3)	118.4(6)	C(2)-C(3)-C(4)	127.4(6)
O(2)-C(4)-C(3)	126.1(5)	O(2)-C(4)-C(5)	114.7(6)
C(3)-C(4)-C(5)	119.2(6)	O(3)-C(7)-C(6)	114.0(6)
O(3)-C(7)-C(8)	125.5(6)	C(6)-C(7)-C(8)	120.5(6)
C(7)-C(8)-C(9)	128.7(6)	O(4)-C(9)-C(8)	126.8(6)
O(4)-C(9)-C(10)	115.2(6)	C(8)-C(9)-C(10)	118.0(6)
P(1)-C(11)-C(12)	117.1(6)	P(1)-C(11)-C(13)	114.5(6)
C(12)-C(11)-C(13)	109.9(7)	P(1)-C(14)-C(15)	111.6(6)
P(1)-C(14)-C(16)	110.4(7)	C(15)-C(14)-C(16)	112.9(9)
P(1)-C(17)-C(18)	108.8(8)	P(1)-C(17)-C(19)	118.5(9)
C(18)-C(17)-C(19)	114(1)	P(1)-C(17a)-C(18)	119(1)
P(1)-C(17a)-C(19a)	122(2)	C(18)-C(17a)- C(19a)	118(2)
C(32)-C(31)-C(35)	57(2)	C(31)-C(32)-C(33)	108(3)*
C(32)-C(33)-C(34)	112(3)*	C(33)-C(34)-C(35)	114(3)*
C(34)-C(35)-C(36)	111(3)*		

a) Indicates atom generated by the symmetry operation (2-x, y, 3/2 - z);

\*) Restrained during refinement.

**Table A.11.1:** Crystallographic and refinement data for

$\overline{cis-[Ru(acac)_2(o-Me_2NC_6H_4C=C(NC_5H_5)Ph)] [PF_6]_2 \cdot (CH_3)_2CO}$ .

**Crystal Data**

Empirical Formula	C <sub>34</sub> H <sub>40</sub> F <sub>6</sub> N <sub>2</sub> O <sub>5</sub> PRu
Formula Weight	683.57
Crystal Colour, Habit	brown, block
Crystal Dimensions	0.34 x 0.28 x 0.16 mm
Crystal System	monoclinic
Lattice Type	Primitive
No. of Reflections used for Unit Cell Determination (2 $\theta$ range)	20 (12.1 - 20.0°)
Omega Scan Peak Width at Half-height	0.33°
Lattice Parameters	a = 7.711(7) Å b = 18.807(3) Å c = 20.903(4) Å $\beta$ = 100.99(3) ° V = 2976(3) Å <sup>3</sup>
Space Group	P2 <sub>1</sub> /n (#14)
Z value	4
D <sub>calc</sub>	1.526 g/cm <sup>3</sup>
F <sub>000</sub>	1388.00
$\mu$ (MoK $\alpha$ )	6.39 cm <sup>-1</sup>
<b>Intensity Measurements</b>	
diffractometer	Rigaku AFC6S
Radiation	MoK $\alpha$ ( $\lambda$ = 0.71069 Å) graphite monochromated
Take-off Angle	6.0°
Detector Aperture	3.5 mm horizontal 3.5 mm vertical
Crystal to Detector Distance	200 mm
Temperature	23.0 °C
Scan Type	$\omega$ -2 $\theta$
Scan Rate	4.0°/min (in $\omega$ ) (up to 4 scans)
Scan Width	(0.80 + 0.34 tan $\theta$ )°
2 $\theta_{max}$	50.1°
No. of Reflections Measured	Total: 5877 Unique: 5448 ( $R_{int}$ = 0.032)
Corrections	Lorentz-polarization Absorption (trans. Factors: 0.9535 - 1.0000)

**Table A.11.1 (cont):** Crystallographic and refinement data for

*cis*-[Ru(acac)<sub>2</sub>(*o*-Me<sub>2</sub>NC<sub>6</sub>H<sub>4</sub>C=C(NC<sub>5</sub>H<sub>5</sub>)Ph)][PF<sub>6</sub>].

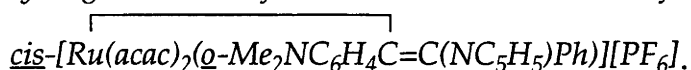
**Structure Solution and Refinement**

Structure Solution	Direct Methods (SIR92)
Refinement	Full-Matrix least squares
Function Minimized	$\sum w( F_o  -  F_c )^2$
Least Squares Weights	$w = [\sigma_c^2(F_o) + 0.25p^2F_o^2]^{-1}$
p-factor	0.050
Anomalous Dispersion	All non-hydrogen atoms
No. Observations ( $I > 2.0\sigma(I)$ )	2626
No. of variables	347
Reflection/Parameter Rotation	7.57
Residuals: R; Rw	0.058; 0.051
Goodness of Fit Indicator	2.54
Max Shift/Error in Final Cycle	0.05
Max peak in Final Diff. Map	1.13 e <sup>-</sup> /Å <sup>3</sup>
Min peak in Final Diff Map	-0.65 e <sup>-</sup> /Å <sup>3</sup>

**Table A.11.2:** Interatomic distances (Å) and angles (°) involving non-hydrogen atoms of the molecular structure of

*cis*-[Ru(acac)<sub>2</sub>(*o*-Me<sub>2</sub>NC<sub>6</sub>H<sub>4</sub>C=C(NC<sub>5</sub>H<sub>5</sub>)Ph)][PF<sub>6</sub>].

Ru(1)-O(1)	2.116(5)	Ru(1)-O(2)	2.018(5)
Ru(1)-O(3)	2.018(5)	Ru(1)-O(4)	2.002(5)
Ru(1)-N(1)	2.152(5)	Ru(1)-C(7)	2.031(7)
P(1)-F(1)	1.452(8)	P(1)-F(2)	1.48(1)
P(1)-F(3)	1.491(7)	P(1)-F(4)	1.454(9)
P(1)-F(5)	1.428(9)	P(1)-F(6)	1.543(7)
O(1)-C(23)	1.268(9)	O(2)-C(25)	1.287(8)
O(3)-C(28)	1.270(8)	O(4)-C(30)	1.265(8)
O(5)-C(32)	1.12(2)	N(1)-C(1)	1.468(8)
N(1)-C(15)	1.481(9)	N(1)-C(16)	1.489(9)
N(2)-C(8)	1.488(8)	N(2)-C(17)	1.329(9)
N(2)-C(21)	1.344(9)	C(1)-C(2)	1.376(9)
C(1)-C(6)	1.391(9)	C(2)-C(3)	1.38(1)
C(3)-C(4)	1.37(1)	C(4)-C(5)	1.36(1)
C(5)-C(6)	1.401(9)	C(6)-C(7)	1.494(9)
C(7)-C(8)	1.348(9)	C(8)-C(9)	1.475(9)
C(9)-C(10)	1.396(9)	C(9)-C(14)	1.39(1)
C(10)-C(11)	1.37(1)	C(11)-C(12)	1.38(1)

**Table A.11.2 (cont):** Interatomic distances (Å) and angles (°) involving non-hydrogen atoms of the molecular structure of

C(12)-C(13)	1.37(1)	C(13)-C(14)	1.39(1)
C(17)-C(18)	1.38(1)	C(18)-C(19)	1.36(1)
C(19)-C(20)	1.37(1)	C(20)-C(21)	1.37(1)
C(22)-C(23)	1.50(1)	C(23)-C(24)	1.40(1)
C(24)-C(25)	1.40(1)	C(25)-C(26)	1.50(1)
C(27)-C(28)	1.52(1)	C(28)-C(29)	1.38(1)
C(29)-C(30)	1.39(1)	C(30)-C(31)	1.50(1)
C(32)-C(33)	1.48(4)	C(32)-C(34)	1.32(3)
O(1)-Ru(1)-O(2)	89.4(2)	O(1)-Ru(1)-O(3)	84.2(2)
O(1)-Ru(1)-O(4)	90.5(2)	O(1)-Ru(1)-N(1)	91.7(2)
O(1)-Ru(1)-C(7)	171.8(2)	O(2)-Ru(1)-O(3)	86.7(2)
O(2)-Ru(1)-O(4)	178.1(2)	O(2)-Ru(1)-N(1)	95.2(2)
O(2)-Ru(1)-C(7)	87.4(2)	O(3)-Ru(1)-O(4)	91.4(2)
O(3)-Ru(1)-N(1)	175.5(2)	O(3)-Ru(1)-C(7)	103.1(2)
O(4)-Ru(1)-N(1)	86.7(2)	O(4)-Ru(1)-C(7)	92.9(2)
N(1)-Ru(1)-C(7)	81.1(2)	F(1)-P(1)-F(2)	89.1(8)
F(1)-P(1)-F(3)	94.3(2)	F(1)-P(1)-F(4)	178(1)
F(1)-P(1)-F(5)	91.4(9)	F(1)-P(1)-F(6)	88.3(5)
F(2)-P(1)-F(3)	95.4(7)	F(2)-P(1)-F(4)	92.4(9)
F(2)-P(1)-F(5)	179.0(7)	F(2)-P(1)-F(6)	93.7(5)
F(3)-P(1)-F(4)	86.8(6)	F(3)-P(1)-F(5)	83.8(6)
F(3)-P(1)-F(6)	177.2(6)	F(4)-P(1)-F(5)	87.0(7)
F(4)-P(1)-F(6)	90.7(5)	F(5)-P(1)-F(6)	97.1(7)
Ru(1)-O(1)-C(23)	122.7(5)	Ru(1)-O(2)-C(25)	124.1(5)
Ru(1)-O(3)-C(28)	121.5(5)	Ru(1)-O(4)-C(30)	123.5(5)
Ru(1)-N(1)-C(1)	106.8(4)	Ru(1)-N(1)-C(15)	111.4(5)
Ru(1)-N(1)-C(16)	109.6(4)	C(1)-N(1)-C(15)	109.2(6)
C(1)-N(1)-C(16)	111.2(6)	C(15)-N(1)-C(16)	108.5(6)
C(8)-N(2)-C(17)	120.6(6)	C(8)-N(2)-C(21)	118.9(6)
C(17)-N(2)-C(21)	120.4(7)	N(1)-C(1)-C(2)	121.2(7)
N(1)-C(1)-C(6)	117.0(6)	C(2)-C(1)-C(6)	121.8(7)
C(1)-C(2)-C(3)	118.7(7)	C(2)-C(3)-C(4)	121.0(7)
C(3)-C(4)-C(5)	119.9(7)	C(4)-C(5)-C(6)	121.3(7)
C(1)-C(6)-C(5)	117.2(6)	C(1)-C(6)-C(7)	116.4(6)
C(5)-C(6)-C(7)	126.2(7)	Ru(1)-C(7)-C(6)	110.0(5)
Ru(1)-C(7)-C(8)	128.4(5)	C(6)-C(7)-C(8)	121.0(6)

**Table A.11.2 (cont):** Interatomic distances (Å) and angles (°) involving non-hydrogen atoms of the molecular structure of
$$\overbrace{cis-[Ru(acac)_2(o-Me_2NC_6H_4C=C(NC_5H_5)Ph)]}^{[PF_6]}$$

N(2)-C(8)-C(7)	116.1(6)	N(2)-C(8)-C(9)	110.5(6)
C(7)-C(8)-C(9)	133.4(6)	C(8)-C(9)-C(10)	121.5(7)
C(8)-C(9)-C(14)	122.1(7)	C(10)-C(9)-C(14)	116.4(7)
C(9)-C(10)-C(11)	121.5(7)	C(10)-C(11)-C(12)	121.3(8)
C(11)-C(12)-C(13)	118.2(8)	C(12)-C(13)-C(14)	120.6(8)
C(9)-C(14)-C(13)	121.9(8)	N(2)-C(17)-C(18)	120.4(8)
C(17)-C(18)-C(19)	119.4(8)	C(18)-C(19)-C(20)	119.8(8)
C(19)-C(20)-C(21)	118.9(8)	N(2)-C(21)-C(20)	121.0(7)
O(1)-C(23)-C(22)	115.1(8)	O(1)-C(23)-C(24)	125.5(7)
C(22)-C(23)-C(24)	119.4(8)	C(23)-C(24)-C(25)	126.8(7)
O(2)-C(25)-C(24)	126.0(7)	O(2)-C(25)-C(26)	116.1(7)
C(24)-C(25)-C(26)	117.9(7)	O(3)-C(28)-C(27)	113.1(7)
O(3)-C(28)-C(29)	126.8(7)	C(27)-C(28)-C(29)	120.1(8)
C(28)-C(29)-C(30)	125.7(7)	O(4)-C(30)-C(29)	125.8(7)
O(4)-C(30)-C(31)	115.8(7)	C(29)-C(30)-C(31)	118.3(7)
O(5)-C(32)-C(33)	118(4)	O(5)-C(32)-C(34)	137(4)
C(33)-C(32)-C(34)	102(3)		

**Table A.12.1:** Crystallographic and refinement data for
$$\overline{\text{cis-[Ru}^{\text{III}}(\text{acac})_2(\text{o-Me}_2\text{NC}_6\text{H}_4\text{C(H)-C(=NEt}_2\text{)Ph)]}[\text{PF}_6\text{]}}$$
**Crystal Data**

Empirical Formula	C <sub>30</sub> H <sub>40</sub> F <sub>6</sub> N <sub>2</sub> O <sub>4</sub> PRu
Formula Weight	738.69
Crystal Colour, Habit	black, block
Crystal Dimensions	0.63 x 0.20 x 0.20 mm
Crystal System	monoclinic
Lattice Type	Primitive
No. of Reflections used for Unit Cell Determination (2 $\theta$ range)	25 (43.1 - 46.5°)
Omega Scan Peak Width at Half-height	0.35°
Lattice Parameters	a = 9.965(3) Å b = 21.604(4) Å c = 15.417(2) Å $\beta$ = 100.26(1) ° V = 3266(1) Å <sup>3</sup>
Space Group	P2 <sub>1</sub> /c (#14)
Z value	4
D <sub>calc</sub>	1.502 g/cm <sup>3</sup>
F <sub>000</sub>	1516.00
$\mu$ (MoK $\alpha$ )	5.86 cm <sup>-1</sup>
<b>Intensity Measurements</b>	
diffractometer	Rigaku AFC6S
Radiation	MoK $\alpha$ ( $\lambda$ = 0.71069 Å) graphite monochromated
Take-off Angle	6.0°
Detector Aperture	4.0 mm horizontal 4.0 mm vertical
Crystal to Detector Distance	200 mm
Temperature	23.0 °C
Scan Type	$\omega$ -2 $\theta$
Scan Rate	8.0°/min (in $\omega$ ) (up to 4 scans)
Scan Width	(1.10 + 0.34 tan $\theta$ )°
2 $\theta_{max}$	55.1°
No. of Reflections Measured	Total: 8160 Unique: 7729 (R <sub>int</sub> = 0.020)
Corrections	Lorentz-polarization Absorption (trans. Factors: 0.8714 - 0.9172)

**Table A.12.1 (cont):** Crystallographic and refinement data for

$\overline{\text{cis-[Ru}^{\text{III}}(\text{acac})_2(\text{o-Me}_2\text{NC}_6\text{H}_4\text{C(H)-C(=NEt}_2\text{)Ph)]PF}_6\text{]}$ .

**Structure Solution and Refinement**

Structure Solution	Direct Methods (SIR92)
Refinement	Full-Matrix least squares
Function Minimized	$\sum w( F_o  -  F_c )^2$
Least Squares Weights	$w = [\sigma_c^2(F_o) + 0.25p^2F_o^2]^{-1}$
p-factor	0.020
Anamalous Dispersion	All non-hydrogen atoms
No. Observations ( $I > 2.0\sigma(I)$ )	4652
No. of variables	517
Reflection/Parameter Rotation	9.00
Residuals: R; Rw	0.033; 0.035
Goodness of Fit Indicator	1.42
Max Shift/Error in Final Cycle	0.07
Max peak in Final Diff. Map	$0.46 \text{ e}^-/\text{\AA}^3$
Min peak in Final Diff Map	$-0.31 \text{ e}^-/\text{\AA}^3$

**Table A.12.2:** Interatomic distances ( $\text{\AA}$ ) and angles ( $^\circ$ ) involving non-hydrogen atoms of the molecular structure of

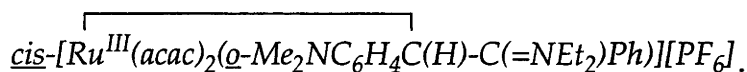
$\overline{\text{cis-[Ru}^{\text{III}}(\text{acac})_2(\text{o-Me}_2\text{NC}_6\text{H}_4\text{C(H)-C(=NEt}_2\text{)Ph)]PF}_6\text{]}$ .

Ru(1)-O(1)	2.081(2)	Ru(1)-O(2)	2.004(2)
Ru(1)-O(3)	2.019(2)	Ru(1)-O(4)	1.990(2)
Ru(1)-N(1)	2.181(3)	Ru(1)-C(8)	2.194(3)
P(1)-F(1)	1.568(3)	P(1)-F(2)	1.577(3)
P(1)-F(3)	1.564(3)	P(1)-F(4)	1.582(3)
P(1)-F(5)	1.549(3)	P(1)-F(6)	1.579(3)
O(1)-C(22)	1.280(4)	O(2)-C(24)	1.286(4)
O(3)-C(27)	1.266(4)	O(4)-C(29)	1.279(5)
N(1)-C(1)	1.472(4)	N(1)-C(15)	1.498(5)
N(1)-C(16)	1.503(5)	N(2)-C(19)	1.483(4)
C(1)-C(2)	1.383(5)	C(1)-C(6)	1.397(4)
C(2)-C(3)	1.383(5)	C(3)-C(4)	1.360(6)
C(4)-C(5)	1.377(5)	C(5)-C(6)	1.392(4)
C(6)-C(7)	1.495(4)	C(7)-C(8)	1.426(4)
C(8)-C(9)	1.500(4)	C(9)-C(10)	1.390(5)
C(9)-C(14)	1.392(5)	C(10)-C(11)	1.381(5)
C(11)-C(12)	1.370(6)	C(12)-C(13)	1.369(6)

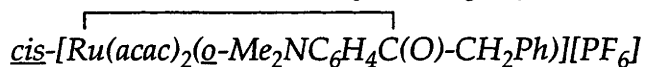


**Table A.12.2 (cont):** Interatomic distances (Å) and angles (°) involving non-hydrogen atoms of the molecular structure of
$$\overline{\text{cis-[Ru}^{\text{III}}(\text{acac})_2(\text{O-Me}_2\text{NC}_6\text{H}_4\text{C(H)-C(=NEt}_2\text{)Ph)]PF}_6\text{]}}$$

C(13)-C(14)	1.392(5)	C(17)-C(18)	1.503(6)
C(19)-C(20)	1.512(6)	C(21)-C(22)	1.510(6)
C(22)-C(23)	1.380(5)	C(23)-C(24)	1.379(5)
C(24)-C(25)	1.502(5)	C(26)-C(27)	1.497(6)
C(27)-C(28)	1.400(6)	C(28)-C(29)	1.377(6)
C(29)-C(30)	1.499(7)		
O(1)-Ru(1)-O(2)	89.47(9)	O(1)-Ru(1)-O(3)	88.43(9)
O(1)-Ru(1)-O(4)	90.1(1)	O(1)-Ru(1)-N(1)	88.9(1)
O(1)-Ru(1)-C(8)	173.1(1)	O(2)-Ru(1)-O(3)	88.28(9)
O(2)-Ru(1)-O(4)	179.5(1)	O(2)-Ru(1)-N(1)	93.4(1)
O(2)-Ru(1)-C(8)	87.9(1)	O(3)-Ru(1)-O(4)	92.0(1)
O(3)-Ru(1)-N(1)	176.9(1)	O(3)-Ru(1)-C(8)	85.1(1)
O(4)-Ru(1)-N(1)	86.3(1)	O(4)-Ru(1)-C(8)	92.6(1)
N(1)-Ru(1)-C(8)	97.5(1)	F(1)-P(1)-F(2)	89.0(2)
F(1)-P(1)-F(3)	91.8(2)	F(1)-P(1)-F(4)	178.5(2)
F(1)-P(1)-F(5)	91.4(2)	F(1)-P(1)-F(6)	89.0(2)
F(2)-P(1)-F(3)	89.7(2)	F(2)-P(1)-F(4)	89.6(2)
F(2)-P(1)-F(5)	179.4(2)	F(2)-P(1)-F(6)	88.7(2)
F(3)-P(1)-F(4)	88.8(2)	F(3)-P(1)-F(5)	90.7(2)
F(3)-P(1)-F(6)	178.2(2)	F(4)-P(1)-F(5)	89.9(2)
F(4)-P(1)-F(6)	90.4(2)	F(5)-P(1)-F(6)	90.9(2)
Ru(1)-O(1)-C(22)	124.7(2)	Ru(1)-O(2)-C(24)	126.8(2)
Ru(1)-O(3)-C(27)	124.3(3)	Ru(1)-O(4)-C(29)	125.1(3)
Ru(1)-N(1)-C(1)	114.6(2)	Ru(1)-N(1)-C(15)	109.8(2)
Ru(1)-N(1)-C(16)	108.1(3)	C(1)-N(1)-C(15)	107.1(3)
C(1)-N(1)-C(16)	110.8(3)	C(15)-N(1)-C(16)	106.1(3)
C(7)-N(2)-C(17)	123.5(3)	C(7)-N(2)-C(19)	121.9(3)
C(17)-N(2)-C(19)	114.3(3)	N(1)-C(1)-C(2)	121.9(3)
N(1)-C(1)-C(6)	119.0(3)	C(2)-C(1)-C(6)	119.1(3)
C(1)-C(2)-C(3)	120.4(4)	C(2)-C(3)-C(4)	121.0(4)
C(3)-C(4)-C(5)	119.6(4)	C(4)-C(5)-C(6)	120.6(4)
C(1)-C(6)-C(5)	119.4(3)	C(1)-C(6)-C(7)	122.7(3)
C(5)-C(6)-C(7)	117.5(3)	N(2)-C(7)-C(6)	118.1(3)
N(2)-C(7)-C(8)	122.7(3)	C(6)-C(7)-C(8)	119.2(3)
Ru(1)-C(8)-C(7)	95.5(2)	Ru(1)-C(8)-C(9)	113.9(2)
C(7)-C(8)-C(9)	123.7(3)	C(8)-C(9)-C(10)	126.4(3)

**Table A.12.2 (cont):** Interatomic distances (Å) and angles (°) involving non-hydrogen atoms of the molecular structure of

C(8)-C(9)-C(14)	116.4(3)	C(10)-C(9)-C(14)	117.1(3)
C(9)-C(10)-C(11)	121.1(4)	C(10)-C(11)-C(12)	121.2(4)
C(11)-C(12)-C(13)	118.7(4)	C(12)-C(13)-C(14)	120.8(4)
C(9)-C(14)-C(13)	121.0(4)	N(2)-C(17)-C(18)	112.8(3)
N(2)-C(19)-C(20)	112.3(3)	O(1)-C(22)-C(21)	114.7(4)
O(1)-C(22)-C(23)	125.6(3)	C(21)-C(22)-C(23)	119.7(4)
C(22)-C(23)-C(24)	127.1(4)	O(2)-C(24)-C(23)	125.4(4)
O(2)-C(24)-C(25)	113.9(3)	C(23)-C(24)-C(25)	120.6(3)
O(3)-C(27)-C(26)	115.6(4)	O(3)-C(27)-C(28)	125.7(4)
C(26)-C(27)-C(28)	118.7(4)	C(27)-C(28)-C(29)	126.9(4)
O(4)-C(29)-C(28)	125.5(4)	O(4)-C(29)-C(30)	114.1(5)
C(28)-C(29)-C(30)	120.4(5)		

**Table A.13.1:** Crystallographic and refinement data for**Crystal Data**

Empirical Formula	C <sub>26</sub> H <sub>31</sub> F <sub>6</sub> NO <sub>5</sub> PRu
Formula Weight	683.57
Crystal Colour, Habit	brown, block
Crystal Dimensions	0.34 x 0.28 x 0.16 mm
Crystal System	monoclinic
Lattice Type	Primitive
No. of Reflections used for Unit Cell Determination (2θ range)	20 (12.1 - 20.0°)
Omega Scan Peak Width at Half-height	0.33°
Lattice Parameters	a = 7.711(7) Å b = 18.807(3) Å c = 20.903(4) Å β = 100.99(3) ° V = 2976(3) Å <sup>3</sup>
Space Group	P2 <sub>1</sub> /n (#14)
Z value	4
D <sub>calc</sub>	1.526 g/cm <sup>3</sup>
F <sub>000</sub>	1388.00
μ(MoKα)	6.39 cm <sup>-1</sup>

**Table A.13.1 (cont): Crystallographic and refinement data for**

cis-[Ru(acac)<sub>2</sub>(*o*-Me<sub>2</sub>NC<sub>6</sub>H<sub>4</sub>C(O)-CH<sub>2</sub>Ph)][PF<sub>6</sub>].

**Intensity Measurements**

diffractometer	Rigaku AFC6S
Radiation	MoK $\alpha$ ( $\lambda = 0.71069$ Å) graphite monochromated
Take-off Angle	6.0°
Detector Aperture	3.5 mm horizontal 3.5 mm vertical
Crystal to Detector Distance	200 mm
Temperature	23.0 °C
Scan Type	$\omega$ -2 $\theta$
Scan Rate	4.0°/min (in $\omega$ ) (up to 4 scans)
Scan Width	(0.80 + 0.34 tan $\theta$ )°
$2\theta_{max}$	50.1°
No. of Reflections Measured	Total: 5877 Unique: 5448 ( $R_{int} = 0.032$ )
Corrections	Lorentz-polarization Absorption (trans. Factors: 0.9535 - 1.0000)

**Structure Solution and Refinement**

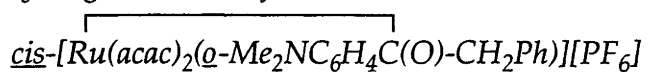
Structure Solution	Direct Methods (SIR92)
Refinement	Full-Matrix least squares
Function Minimized	$\sum w( F_o  -  F_c )^2$
Least Squares Weights	$w = [\sigma_c^2(F_o) + 0.25p^2F_o^2]^{-1}$
p-factor	0.050
Anomalous Dispersion	All non-hydrogen atoms
No. Observations ( $I > 2.0\sigma(I)$ )	2626
No. of variables	347
Reflection/Parameter Rotation	7.57
Residuals: R; R <sub>w</sub>	0.058; 0.051
Goodness of Fit Indicator	2.54
Max Shift/Error in Final Cycle	0.05
Max peak in Final Diff. Map	1.13 e <sup>-</sup> /Å <sup>3</sup>
Min peak in Final Diff Map	-0.65 e <sup>-</sup> /Å <sup>3</sup>

**Table A.13.2:** Interatomic distances (Å) and angles (°) involving non-hydrogen atoms of the molecular structure of
$$\text{cis-[Ru(acac)}_2(\text{o-Me}_2\text{NC}_6\text{H}_4\text{C(O)-CH}_2\text{Ph)]}[\text{PF}_6]$$

Ru(1)-O(1)	1.978(7)	Ru(1)-O(2)	2.003(6)
Ru(1)-O(3)	1.989(7)	Ru(1)-O(4)	1.995(7)
Ru(1)-O(5)	2.016(7)	Ru(1)-N(1)	2.148(9)
P(1)-F(1)	1.54(1)	P(1)-F(2)	1.53(1)
P(1)-F(3)	1.61(2)	P(1)-F(3')	1.59(2)
P(1)-F(4)	1.56(2)	P(1)-F(4')	1.56(3)
P(1)-F(5)	1.59(2)	P(1)-F(5')	1.60(2)
P(1)-F(6)	1.52(3)	P(1)-F(6')	1.63(2)
F(3)-F(3')	0.95(3)	F(3)-F(6')	1.63(3)
F(3')-F(4)	1.48(2)	F(4)-F(4')	1.06(3)
F(4')-F(5)	1.43(3)	F(5)-F(5')	1.15(2)
F(5')-F(6)	1.38(3)	F(6)-F(6')	1.02(3)
O(1)-C(18)	1.27(1)	O(2)-C(20)	1.26(1)
O(3)-C(23)	1.26(1)	O(4)-C(25)	1.26(1)
O(5)-C(7)	1.24(1)	N(1)-C(1)	1.48(1)
N(1)-C(15)	1.48(1)	N(1)-C(16)	1.50(1)
C(1)-C(2)	1.35(1)	C(1)-C(6)	1.44(1)
C(2)-C(3)	1.39(2)	C(3)-C(4)	1.35(2)
C(4)-C(5)	1.34(2)	C(5)-C(6)	1.39(2)
C(6)-C(7)	1.46(2)	C(7)-C(8)	1.53(1)
C(8)-C(9)	1.49(2)	C(9)-C(10)	1.36(2)
C(9)-C(14)	1.37(2)	C(10)-C(11)	1.39(2)
C(11)-C(12)	1.34(3)	C(12)-C(13)	1.33(4)
C(13)-C(14)	1.43(3)	C(17)-C(18)	1.48(1)
C(18)-C(19)	1.40(1)	C(19)-C(20)	1.39(1)
C(20)-C(21)	1.51(1)	C(22)-C(23)	1.50(1)
C(23)-C(24)	1.40(1)	C(24)-C(25)	1.39(1)
C(25)-C(26)	1.50(1)		
O(1)-Ru(1)-O(2)	92.2(3)	O(1)-Ru(1)-O(3)	89.0(3)
O(1)-Ru(1)-O(4)	86.8(3)	O(1)-Ru(1)-O(5)	174.8(3)
O(1)-Ru(1)-N(1)	99.0(3)	O(2)-Ru(1)-O(3)	90.1(3)
O(2)-Ru(1)-O(4)	177.0(3)	O(2)-Ru(1)-O(5)	92.0(3)
O(2)-Ru(1)-N(1)	87.1(3)	O(3)-Ru(1)-O(4)	92.7(3)
O(3)-Ru(1)-O(5)	87.8(3)	O(3)-Ru(1)-N(1)	171.6(3)
O(4)-Ru(1)-O(5)	89.2(3)	O(4)-Ru(1)-N(1)	90.2(3)
O(5)-Ru(1)-N(1)	84.3(3)	F(1)-P(1)-F(2)	179.1(6)

**Table A.13.2 (cont):** Interatomic distances (Å) and angles (°) involving non-hydrogen atoms of the molecular structure of
$$\overbrace{cis-[Ru(acac)_2(o-Me_2NC_6H_4C(O)-CH_2Ph)] [PF_6]}$$

F(1)-P(1)-F(3)	82.6(9)	F(1)-P(1)-F(3')	93.4(8)
F(1)-P(1)-F(4)	89.7(7)	F(1)-P(1)-F(4')	85(1)
F(1)-P(1)-F(5)	95.5(7)	F(1)-P(1)-F(5')	86.2(7)
F(1)-P(1)-F(6)	78(1)	F(1)-P(1)-F(6')	103.7(8)
F(2)-P(1)-F(3)	98.1(9)	F(2)-P(1)-F(3')	87.4(8)
F(2)-P(1)-F(4)	90.9(7)	F(2)-P(1)-F(4')	95(1)
F(2)-P(1)-F(5)	83.9(7)	F(2)-P(1)-F(5')	93.0(7)
F(2)-P(1)-F(6)	101(1)	F(2)-P(1)-F(6')	76.2(7)
F(3)-P(1)-F(3')	34.4(9)	F(3)-P(1)-F(4)	89(1)
F(3)-P(1)-F(4')	127(1)	F(3)-P(1)-F(5)	178(1)
F(3)-P(1)-F(5')	136(1)	F(3)-P(1)-F(6)	84(1)
F(3)-P(1)-F(6')	60.6(9)	F(3')-P(1)-F(4)	56.3(8)
F(3')-P(1)-F(4')	96(1)	F(3')-P(1)-F(5)	147(1)
F(3')-P(1)-F(5')	170(1)	F(3')-P(1)-F(6)	118(1)
F(3')-P(1)-F(6')	89(1)	F(4)-P(1)-F(4')	40(1)
F(4)-P(1)-F(5)	92(1)	F(4)-P(1)-F(5')	133(1)
F(4)-P(1)-F(6)	167(1)	F(4)-P(1)-F(6')	144(1)
F(4')-P(1)-F(5)	54(1)	F(4')-P(1)-F(5')	94(1)
F(4')-P(1)-F(6)	143(2)	F(4')-P(1)-F(6')	170(1)
F(5)-P(1)-F(5')	42.1(7)	F(5)-P(1)-F(6)	95(1)
F(5)-P(1)-F(6')	119(1)	F(5')-P(1)-F(6)	53(1)
F(5')-P(1)-F(6')	82(1)	F(6)-P(1)-F(6')	37(1)
P(1)-F(3)-F(3')	71(2)	P(1)-F(3)-F(6')	60(1)
F(3')-F(3)-F(6')	119(3)	P(1)-F(3')-F(3)	74(2)
P(1)-F(3')-F(4)	61(1)	F(3)-F(3')-F(4)	131(3)
P(1)-F(4)-F(3')	63(1)	P(1)-F(4)-F(4')	71(2)
F(3')-F(4)-F(4')	133(3)	P(1)-F(4')-F(4)	70(2)
P(1)-F(4')-F(5)	64(1)	F(4)-F(4')-F(5)	131(3)
P(1)-F(5)-F(4')	62(1)	P(1)-F(5)-F(5')	69(1)
F(4')-F(5)-F(5')	127(2)	P(1)-F(5')-F(5)	69(1)
P(1)-F(5')-F(6)	61(1)	F(5)-F(5')-F(6)	130(2)
P(1)-F(6)-F(5')	67(1)	P(1)-F(6)-F(6')	77(2)
F(5')-F(6)-F(6')	122(3)	P(1)-F(6')-F(3)	59(1)
P(1)-F(6')-F(6)	66(2)	F(3)-F(6')-F(6)	102(3)
Ru(1)-O(1)-C(18)	124.5(6)	Ru(1)-O(2)-C(20)	124.3(6)
Ru(1)-O(3)-C(23)	123.8(7)	Ru(1)-O(4)-C(25)	125.0(7)
Ru(1)-O(5)-C(7)	130.0(8)	Ru(1)-N(1)-C(1)	109.6(6)

**Table A.13.2 (cont):** Interatomic distances (Å) and angles (°) involving non-hydrogen atoms of the molecular structure of

Ru(1)-N(1)-C(15)	108.3(7)	Ru(1)-N(1)-C(16)	111.9(7)
C(1)-N(1)-C(15)	112.1(9)	C(1)-N(1)-C(16)	108.6(9)
C(15)-N(1)-C(16)	106.4(9)	N(1)-C(1)-C(2)	121(1)
N(1)-C(1)-C(6)	120(1)	C(2)-C(1)-C(6)	119(1)
C(1)-C(2)-C(3)	121(1)	C(2)-C(3)-C(4)	121(1)
C(3)-C(4)-C(5)	120(1)	C(4)-C(5)-C(6)	123(1)
C(1)-C(6)-C(5)	117(1)	C(1)-C(6)-C(7)	123(1)
C(5)-C(6)-C(7)	120(1)	O(5)-C(7)-C(6)	122(1)
O(5)-C(7)-C(8)	115(1)	C(6)-C(7)-C(8)	123(1)
C(7)-C(8)-C(9)	114(1)	C(8)-C(9)-C(10)	121(2)
C(8)-C(9)-C(14)	122(2)	C(10)-C(9)-C(14)	117(2)
C(9)-C(10)-C(11)	124(2)	C(10)-C(11)-C(12)	114(3)
C(11)-C(12)-C(13)	128(4)	C(12)-C(13)-C(14)	115(3)
C(9)-C(14)-C(13)	121(2)	O(1)-C(18)-C(17)	115(1)
O(1)-C(18)-C(19)	125(1)	C(17)-C(18)-C(19)	120(1)
C(18)-C(19)-C(20)	127(1)	O(2)-C(20)-C(19)	125(1)
O(2)-C(20)-C(21)	115(1)	C(19)-C(20)-C(21)	120(1)
O(3)-C(23)-C(22)	115(1)	O(3)-C(23)-C(24)	126(1)
C(22)-C(23)-C(24)	119(1)	C(23)-C(24)-C(25)	126(1)
O(4)-C(25)-C(24)	125(1)	O(4)-C(25)-C(26)	116(1)
C(24)-C(25)-C(26)	119(1)		

**Table A.14.1:** Crystallographic and refinement data for
$$\text{cis-}[Ru(acac)_2(\text{O-Me}_2\text{NC}_6\text{H}_4\text{C(O)-CHPh}_3)]\text{[PF}_6\text{]}.$$
**Crystal Data**

Empirical Formula	$\text{C}_{38}\text{H}_{40}\text{F}_6\text{NO}_5\text{P}_2\text{Ru}$
Formula Weight	867.75
Crystal Colour, Habit	red, plate
Crystal Dimensions	0.40 x 0.29 x 0.07 mm
Crystal System	monoclinic
Lattice Type	Primitive
No. of Reflections used for Unit Cell Determination ( $2\theta$ range)	25 (32.0 - 36.9°)
Omega Scan Peak Width at Half-height	0.34°
Lattice Parameters	$a = 12.127(1) \text{ \AA}$ $b = 12.397(1) \text{ \AA}$ $c = 26.463(3) \text{ \AA}$ $\beta = 101.712(9)^\circ$ $V = 3895.4(7) \text{ \AA}^3$
Space Group	$P2_1/c$ (#14)
Z value	4
$D_{\text{calc}}$	1.479 g/cm <sup>3</sup>
$F_{000}$	1772.00
$\mu(\text{MoK}\alpha)$	5.56 cm <sup>-1</sup>

**Intensity Measurements**

diffractometer	Rigaku AFC6S
Radiation	MoK $\alpha$ ( $\lambda = 0.71069 \text{ \AA}$ ) graphite monochromated
Take-off Angle	6.0°
Detector Aperture	4.0 mm horizontal 4.0 mm vertical
Crystal to Detector Distance	200 mm
Voltage, Current	50 kV, 30 mA
Temperature	23.0 °C
Scan Type	$\omega$
Scan Rate	4.0°/min (in $\omega$ ) (up to 4 scans)
Scan Width	(1.20 + 0.34 tan $\theta$ )°
$2\theta_{\text{max}}$	55.1°
No. of Reflections Measured	Total: 9869 Unique: 9432 ( $R_{\text{int}} = 0.031$ )
Corrections	Lorentz-polarization Absorption (trans. Factors: 0.8974 - 0.9613)

**Table A.14.1 (cont): Crystallographic and refinement data for*****cis*-[Ru(acac)<sub>2</sub>(*o*-Me<sub>2</sub>NC<sub>6</sub>H<sub>4</sub>C(O)-CHPh<sub>3</sub>)]PF<sub>6</sub>].****Structure Solution and Refinement**

Structure Solution	Direct Methods (SIR92)
Refinement	Full-Matrix least squares
Function Minimized	$\sum w( F_o  -  F_c )^2$
Least Squares Weights	$w = [\sigma_c^2(F_o) + 0.25p^2F_o^2]^{-1}$
p-factor	0.020
Anomalous Dispersion	All non-hydrogen atoms
No. Observations (I>2.0σ(I))	4858
No. of variables	481
Reflection/Parameter Rotation	10.10
Residuals: R; Rw	0.044; 0.046
Goodness of Fit Indicator	1.53
Max Shift/Error in Final Cycle	0.02
Max peak in Final Diff. Map	0.47 e <sup>-</sup> /Å <sup>3</sup>
Min peak in Final Diff Map	-0.56 e <sup>-</sup> /Å <sup>3</sup>

**Table A.14.2: Interatomic distances (Å) and angles (°) involving non-hydrogen atoms of the molecular structure of*****cis*-[Ru(acac)<sub>2</sub>(*o*-Me<sub>2</sub>NC<sub>6</sub>H<sub>4</sub>C(O)-CHPh<sub>3</sub>)]PF<sub>6</sub>].**

Ru(1)-O(1)	1.999(3)	Ru(1)-O(2)	1.996(3)
Ru(1)-O(3)	1.999(3)	Ru(1)-O(4)	2.043(3)
Ru(1)-N(1)	2.204(4)	Ru(1)-C(20)	2.160(4)
P(1)-C(20)	1.794(5)	P(1)-C(21)	1.799(5)
P(1)-C(27)	1.814(5)	P(1)-C(33)	1.795(5)
P(2)-F(1)	1.430(5)	P(2)-F(2)	1.545(5)
P(2)-F(3)	1.519(6)	P(2)-F(4)	1.576(6)
P(2)-F(5)	1.514(6)	P(2)-F(6)	1.516(5)
O(1)-C(1)	1.286(6)	O(2)-C(4)	1.288(6)
O(3)-C(6)	1.293(6)	O(4)-C(9)	1.277(6)
O(5)-C(19)	1.227(5)	N(1)-C(11)	1.502(6)
N(1)-C(12)	1.502(6)	N(1)-C(13)	1.477(6)
C(1)-C(2)	1.498(8)	C(1)-C(3)	1.388(8)
C(3)-C(4)	1.393(7)	C(4)-C(5)	1.501(7)
C(6)-C(7)	1.490(7)	C(6)-C(8)	1.393(7)
C(8)-C(9)	1.373(8)	C(9)-C(10)	1.498(7)
C(13)-C(14)	1.392(7)	C(13)-C(18)	1.381(6)
C(14)-C(15)	1.371(9)	C(15)-C(16)	1.370(9)



**Table A.14.2 (cont):** Interatomic distances (Å) and angles (°) involving non-hydrogen atoms of the molecular structure of
$$\overbrace{cis-[Ru(acac)_2(o-Me_2NC_6H_4C(O)-CHPh_3)]PF_6]}$$

C(16)-C(17)	1.363(8)	C(17)-C(18)	1.388(6)
C(18)-C(19)	1.494(6)	C(19)-C(20)	1.459(6)
C(21)-C(22)	1.386(7)	C(21)-C(26)	1.382(7)
C(22)-C(23)	1.381(7)	C(23)-C(24)	1.362(9)
C(24)-C(25)	1.35(1)	C(25)-C(26)	1.393(8)
C(27)-C(28)	1.370(7)	C(27)-C(32)	1.382(7)
C(28)-C(29)	1.387(7)	C(29)-C(30)	1.373(8)
C(30)-C(31)	1.352(9)	C(31)-C(32)	1.379(8)
C(33)-C(34)	1.382(7)	C(33)-C(38)	1.371(7)
C(34)-C(35)	1.384(7)	C(35)-C(36)	1.360(9)
C(36)-C(37)	1.34(1)	C(37)-C(38)	1.386(9)
O(1)-Ru(1)-O(2)	90.3(1)	O(1)-Ru(1)-O(3)	88.1(1)
O(1)-Ru(1)-O(4)	85.5(1)	O(1)-Ru(1)-N(1)	174.3(1)
O(1)-Ru(1)-C(20)	92.3(2)	O(2)-Ru(1)-O(3)	177.2(1)
O(2)-Ru(1)-O(4)	86.3(1)	O(2)-Ru(1)-N(1)	92.0(1)
O(2)-Ru(1)-C(20)	95.8(2)	O(3)-Ru(1)-O(4)	91.2(1)
O(3)-Ru(1)-N(1)	89.4(1)	O(3)-Ru(1)-C(20)	86.6(2)
O(4)-Ru(1)-N(1)	89.4(1)	O(4)-Ru(1)-C(20)	177.0(2)
N(1)-Ru(1)-C(20)	92.6(2)	C(20)-P(1)-C(21)	108.4(2)
C(20)-P(1)-C(27)	108.4(2)	C(20)-P(1)-C(33)	119.0(2)
C(21)-P(1)-C(27)	105.6(2)	C(21)-P(1)-C(33)	106.1(2)
C(27)-P(1)-C(33)	108.6(2)	F(1)-P(2)-F(2)	93.3(4)
F(1)-P(2)-F(3)	95.9(5)	F(1)-P(2)-F(4)	179.3(5)
F(1)-P(2)-F(5)	90.6(5)	F(1)-P(2)-F(6)	92.6(5)
F(2)-P(2)-F(3)	87.0(4)	F(2)-P(2)-F(4)	86.0(4)
F(2)-P(2)-F(5)	175.9(4)	F(2)-P(2)-F(6)	90.4(4)
F(3)-P(2)-F(4)	84.2(4)	F(3)-P(2)-F(5)	93.5(4)
F(3)-P(2)-F(6)	171.2(4)	F(4)-P(2)-F(5)	90.0(4)
F(4)-P(2)-F(6)	87.3(4)	F(5)-P(2)-F(6)	88.6(4)
Ru(1)-O(1)-C(1)	122.5(3)	Ru(1)-O(2)-C(4)	122.0(3)
Ru(1)-O(3)-C(6)	122.5(3)	Ru(1)-O(4)-C(9)	121.7(3)
Ru(1)-N(1)-C(11)	107.1(3)	Ru(1)-N(1)-C(12)	106.9(3)
Ru(1)-N(1)-C(13)	118.9(3)	C(11)-N(1)-C(12)	106.8(4)
C(11)-N(1)-C(13)	106.6(4)	C(12)-N(1)-C(13)	109.9(4)
O(1)-C(1)-C(2)	114.9(6)	O(1)-C(1)-C(3)	125.0(5)
C(2)-C(1)-C(3)	120.1(6)	C(1)-C(3)-C(4)	125.5(5)

**Table A.14.2 (cont):** Interatomic distances (Å) and angles (°) involving non-hydrogen atoms of the molecular structure of
$$\overbrace{cis-[Ru(acac)_2(o-Me_2NC_6H_4C(O)-CHPh_3)]} [PF_6].$$

O(2)-C(4)-C(3)	125.4(5)	O(2)-C(4)-C(5)	114.9(5)
C(3)-C(4)-C(5)	119.7(5)	O(3)-C(6)-C(7)	114.2(5)
O(3)-C(6)-C(8)	125.8(5)	C(7)-C(6)-C(8)	120.0(5)
C(6)-C(8)-C(9)	126.8(5)	O(4)-C(9)-C(8)	125.8(5)
O(4)-C(9)-C(10)	114.6(5)	C(8)-C(9)-C(10)	119.6(5)
N(1)-C(13)-C(14)	120.8(5)	N(1)-C(13)-C(18)	119.6(4)
C(14)-C(13)-C(18)	118.9(5)	C(13)-C(14)-C(15)	120.2(6)
C(14)-C(15)-C(16)	121.0(6)	C(15)-C(16)-C(17)	119.1(6)
C(16)-C(17)-C(18)	121.3(5)	C(13)-C(18)-C(17)	119.5(5)
C(13)-C(18)-C(19)	123.8(4)	C(17)-C(18)-C(19)	116.7(5)
O(5)-C(19)-C(18)	119.5(4)	O(5)-C(19)-C(20)	123.8(5)
C(18)-C(19)-C(20)	116.5(4)	Ru(1)-C(20)-P(1)	124.0(2)
Ru(1)-C(20)-C(19)	100.0(3)	P(1)-C(20)-C(19)	111.5(3)
P(1)-C(21)-C(22)	118.7(4)	P(1)-C(21)-C(26)	123.4(4)
C(22)-C(21)-C(26)	117.9(5)	C(21)-C(22)-C(23)	121.4(5)
C(22)-C(23)-C(24)	118.9(6)	C(23)-C(24)-C(25)	121.4(6)
C(24)-C(25)-C(26)	120.0(6)	C(21)-C(26)-C(25)	120.2(6)
P(1)-C(27)-C(28)	121.5(4)	P(1)-C(27)-C(32)	119.5(4)
C(28)-C(27)-C(932)	118.9(5)	C(27)-C(28)-C(29)	120.3(5)
C(28)-C(29)-C(30)	120.0(6)	C(29)-C(30)-C(31)	120.0(6)
C(30)-C(31)-C(32)	120.4(6)	C(27)-C(32)-C(31)	120.4(6)
P(1)-C(33)-C(34)	121.3(4)	P(1)-C(33)-C(38)	119.2(4)
C(34)-C(33)-C(38)	118.9(5)	C(33)-C(34)-C(35)	120.6(5)
C(34)-C(35)-C(36)	119.3(6)	C(35)-C(36)-C(37)	120.8(7)
C(36)-C(37)-C(38)	120.8(7)	C(33)-C(38)-C(37)	119.6(6)

**Table A.15.1:** Crystallographic and refinement data for *trans*- $[Ru(acac)_2(Ph_2PC\equiv CMe)_2].2CH_2Cl_2$ .

<b>Crystal Data</b>	
Empirical Formula	$C_{42}H_{44}Cl_4O_4P_2Ru$
Formula Weight	917.64
Crystal Colour, Habit	orange, block
Crystal Dimensions	0.20 x 0.12 x 0.10 mm
Crystal System	triclinic
Lattice Type	Primitive
Lattice Parameters	$a = 10.247(1) \text{ \AA}$ $b = 11.045(3) \text{ \AA}$ $c = 11.720(2) \text{ \AA}$ $\alpha = 117.21(2)^\circ$ $\beta = 94.27(2)^\circ$ $\gamma = 107.61(1)^\circ$ $V = 1088.3(5) \text{ \AA}^3$
Space Group	$P \bar{1} (\#2)$
Z value	1
$D_{calc}$	$1.400 \text{ g/cm}^3$
$F_{000}$	470.00
$\mu(\text{MoK}\alpha)$	$63.16 \text{ cm}^{-1}$
<b>Intensity Measurements</b>	
diffractometer	Rigaku AFC6R
Radiation	$\text{CuK}\alpha (\lambda = 1.54178 \text{ \AA})$ graphite monochromated
Take-off Angle	$6.0^\circ$
Detector Aperture	7.0 mm horizontal 7.0 mm vertical
Crystal to Detector Distance	400 mm
Voltage, Current	180kV, 50mA
Temperature	$-80.0^\circ \text{C}$
Scan Type	$\omega$ - $2\theta$
Scan Rate	$32.0^\circ/\text{min}$ (in $\omega$ ) (up to 4 scans)
Scan Width	$(1.42 + 0.30 \tan \theta)$
$2\theta_{max}$	$120.0^\circ$
No. of Reflections Measured	Total: 3425 Unique: 3241 ( $R_{int} = 0.039$ )
Corrections	Lorentz-polarization Absorption (trans. factors: 0.4566 - 0.6079)

**Table A.15.1 (cont): Crystallographic and refinement data for *trans*-[Ru(acac)<sub>2</sub>(Ph<sub>2</sub>PC≡CMe)<sub>2</sub>].2CH<sub>2</sub>Cl<sub>2</sub>.**

<b>Structure Solution and Refinement</b>	
Structure Solution	Direct Methods (SIR92)
Refinement	Full-Matrix least squares
Function Minimized	$\sum w( F_o  -  F_c )^2$
Least Squares Weights	$w = [\sigma_c^2(F_o) + 0.25p^2F_o^2]^{-1}$
p-factor	0.020
Anomalous Dispersion	All non-hydrogen atoms
No. Observations (I>2.0σ(I))	3026
No. of variables	307
Reflection/Parameter Rotation	9.86
Residuals: R; Rw	0.028; 0.035
Goodness of Fit Indicator	1.63
Max Shift/Error in Final Cycle	0.04
Max peak in Final Diff. Map	0.49 e <sup>-</sup> /Å <sup>3</sup>
Min peak in Final Diff Map	-0.43 e <sup>-</sup> /Å <sup>3</sup>

**Table A.15.2: Interatomic distances (Å) and angles (°) involving non-hydrogen atoms of the molecular structure of *trans*-[Ru(acac)<sub>2</sub>(Ph<sub>2</sub>PC≡CMe)<sub>2</sub>].2CH<sub>2</sub>Cl<sub>2</sub>.**

Ru(1)-P(1)	2.3330(7)	Ru(1)-O(1)	2.060(2)
Ru(1)-O(2)	2.063(2)		
CL(1)-C(21)	1.739(5)	Cl(2)-C(21)	1.742(5)
P(1)-C(6)	1.760(3)	P(1)-C(9)	1.835(3)
P(1)-C(15)	1.827(3)	O(1)-C(2)	1.281(3)
O(2)-C(4)	1.277(3)	C(1)-C(2)	1.502(4)
C(2)-C(3)	1.388(4)	C(3)-C(4)	1.393(4)
C(4)-C(5)	1.511(4)	C(6)-C(7)	1.185(4)
C(7)-C(8)	1.458(5)	C(9)-C(10)	1.376(4)
C(9)-C(14)	1.392(4)	C(10)-C(11)	1.404(5)
C(11)-C(12)	1.372(7)	C(12)-C(13)	1.356(6)
C(13)-C(14)	1.388(5)	C(15)-C(16)	1.378(4)
C(15)-C(20)	1.402(4)	C(16)-C(17)	1.375(5)
C(17)-C(18)	1.382(7)	C(18)-C(19)	1.368(7)
C(19)-C(20)	1.391(5)		
P(1)-Ru(1)-P(1) <sup>a</sup>	180.0	P(1)-Ru(1)-O(1)	88.73(6)
P(1)-Ru(1)-O(1) <sup>a</sup>	91.27(6)	P(1)-Ru(1)-O(2)	90.22(6)
P(1)-Ru(1)-O(2) <sup>a</sup>	89.78(6)	O(1)-Ru(1)-O(1) <sup>a</sup>	180.0
O(1)-Ru(1)-O(2)	93.34(7)	O(1)-Ru(1)-O(2) <sup>a</sup>	86.66(7)
O(2)-Ru(1)-O(2) <sup>a</sup>	180.0	Ru(1)-P(1)-C(6)	114.8(1)

**Table A.15.2 (cont):** Interatomic distances (Å) and angles (°) involving non-hydrogen atoms of the molecular structure of *trans-**[Ru(acac)<sub>2</sub>(Ph<sub>2</sub>PC≡CMe<sub>2</sub>)]·2CH<sub>2</sub>Cl<sub>2</sub>.*

Ru(1)-P(1)-C(9)	113.34(9)	Ru(1)-P(1)-C(15)	117.7(1)
C(6)-P(1)-C(9)	102.6(1)	C(6)-P(1)-C(15)	103.1(1)
C(9)-P(1)-C(15)	103.5(1)	Ru(1)-O(1)-C(2)	122.2(2)
Ru(1)-O(2)-C(4)	121.2(2)	O(1)-C(2)-C(1)	114.9(3)
O(1)-C(2)-C(3)	126.1(3)	C(1)-C(2)-C(3)	119.0(3)
C(2)-C(3)-C(4)	128.7(3)	O(2)-C(4)-C(3)	127.2(3)
O(2)-C(4)-C(5)	114.0(3)	C(3)-C(4)-C(5)	118.7(3)
P(1)-C(6)-C(7)	174.5(3)	C(6)-C(7)-C(98)	179.6(4)
P(1)-C(9)-C(10)	121.1(3)	P(1)-C(9)-C(14)	119.3(2)
C(10)-C(9)-C(14)	119.4(3)	C(9)-C(10)-C(11)	119.8(4)
C(100-C(11)-C(12)	119.7(4)	C(11)-C(12)-C(13)	120.9(4)
C(12)-C(13)-C(14)	120.2(4)	C(9)-C(14)-C(13)	120.0(4)
P(1)-C(15)-C(16)	118.3(2)	P(1)-C(15)-C(20)	122.3(3)
C(916)-C(915)-C(20)	119.3(3)	C(15)-C(16)-C(17)	120.8(4)
C(16)-C(17)-C(18)	120.1(4)	C(17)-C(18)-C(19)	119.9(4)
C(18)-C(19)-C(20)	120.8(4)	C(15)-C(20)-C(19)	119.1(4)
Cl(1)-C(21)-Cl(2)	112.5(2)		

**Table A.16.1:** Crystallographic and refinement data for *cis-*  
*[Ru(acac)<sub>2</sub>(Ph<sub>2</sub>PC≡CMe<sub>2</sub>)]·0.5CH<sub>2</sub>Cl<sub>2</sub>.***Crystal Data**

Empirical Formula	C <sub>81</sub> H <sub>82</sub> Cl <sub>2</sub> O <sub>8</sub> P <sub>4</sub> Ru <sub>2</sub>
Formula Weight	1580.48
Crystal Colour, Habit	yellow, hexagonal prism
Crystal Dimensions	0.52 x 0.24 x 0.16 mm
Crystal System	triclinic
Lattice Type	Primitive
Lattice Parameters	a = 16.417(4) Å b = 16.469(6) Å c = 18.975(4) Å α = 65.46(2) ° β = 66.17(2) ° γ = 60.76(2) ° V = 60.76(2) Å <sup>3</sup>
Space Group	P $\bar{1}$ (#2)
Z value	2
D <sub>calc</sub>	1.340 g/cm <sup>3</sup>
F <sub>000</sub>	1628.00
μ(MoKα)	5.88 cm <sup>-1</sup>

**Table A.16.1 (cont):** Crystallographic and refinement data for *cis*- $[Ru(acac)_2(Ph_2PC\equiv CMe)_2].0.5CH_2Cl_2$ .

<b>Intensity Measurements</b>	
diffractometer	Rigaku AFC6S
Radiation	CuK $\alpha$ ( $\lambda = 0.71069 \text{ \AA}$ ) graphite monochromated
Take-off Angle	6.0°
Detector Aperture	5.0 mm horizontal 4.0 mm vertical
Crystal to Detector Distance	200 mm
Voltage, Current	50kV, 30mA
Temperature	23.0 °C
Scan Type	$\omega$ -2 $\theta$
Scan Rate	8.0°/min (in $\omega$ ) (up to 4 scans)
Scan Width	(1.10 + 0.34 tan $\theta$ )
2 $\theta_{\max}$	55.1 °
No. of Reflections Measured	Total: 18715 Unique: 18081 ( $R_{int} = 0.030$ )
Corrections	Lorentz-polarization Absorption (trans. factors: 0.8823 - 0.9179) Decay (11.82% decline)
<b>Structure Solution and Refinement</b>	
Structure Solution	Direct Methods (SIR92)
Refinement	Full-Matrix least squares
Function Minimized	$\sum w( F_o  -  F_c )^2$
Least Squares Weights	$w = [\sigma_c^2(F_o) + 0.25p^2F_o^2]^{-1}$
p-factor	0.0200
Anamalous Dispersion	All non-hydrogen atoms
No. Observations ( $I > 2.0\sigma(I)$ )	9045
No. of variables	876
Reflection/Parameter Rotation	10.33
Residuals: R; Rw	0.042; 0.044
Goodness of Fit Indicator	1.54
Max Shift/Error in Final Cycle	0.03
Max peak in Final Diff. Map	0.70 e <sup>-</sup> /Å <sup>3</sup>
Min peak in Final Diff Map	-0.54 e <sup>-</sup> /Å <sup>3</sup>

**Table A.16.2:** Interatomic distances (Å) and angles (°) involving non-hydrogen atoms of the molecular structures of *cis*-[Ru(acac)<sub>2</sub>(Ph<sub>2</sub>PC≡CMe)<sub>2</sub>].0.5CH<sub>2</sub>Cl<sub>2</sub>.

Ru(1)-P(1)	2.249(1)	Ru(1)-P(2)	2.265(1)
Ru(1)-O(1)	2.063(3)	Ru(1)-O(2)	2.088(3)
Ru(1)-O(3)	2.059(3)	Ru(1)-O(4)	2.098(3)
Ru(2)-P(3)	2.259(1)	Ru(2)-P(4)	2.254(2)
Ru(2)-O(5)	2.056(3)	Ru(2)-O(6)	2.095(3)
Ru(2)-O(7)	2.069(3)	Ru(2)-O(8)	2.104(4)
Cl(1)-C(81)	1.687(8)	Cl(21)-C(81)	1.621(8)
P(1)-C(11)	1.768(5)		
P(1)-C(14)	1.834(5)	P(1)-C(20)	1.831(5)
P(2)-C(26)	1.770(5)	P(2)-C(29)	1.840(5)
P(2)-C(35)	1.840(5)	P(3)-C(54)	1.840(6)
P(3)-C(60)	1.846(6)	P(3)-C(511)	1.77(1)
P(3)-C(512)	1.79(2)	P(4)-C(66)	1.770(5)
P(4)-C(69)	1.842(5)	P(4)-C(75)	1.835(5)
O(1)-C(2)	1.282(6)	O(2)-C(4)	1.249(6)
O(3)-C(7)	1.271(5)	O(4)-C(9)	1.271(5)
O(5)-C(42)	1.267(5)	O(6)-C(44)	1.268(6)
O(7)-C(47)	1.265(6)	O(8)-C(49)	1.254(6)
C(1)-C(2)	1.511(7)	C(2)-C(3)	1.390(8)
C(3)-C(4)	1.398(8)	C(4)-C(5)	1.507(8)
C(6)-C(7)	1.510(7)	C(7)-C(8)	1.382(7)
C(8)-C(9)	1.387(7)	C(9)-C(10)	1.514(7)
C(11)-C(12)	1.183(6)	C(12)-C(13)	1.458(7)
C(14)-C(15)	1.386(7)	C(14)-C(19)	1.381(7)
C(15)-C(16)	1.394(7)	C(16)-C(17)	1.372(8)
C(17)-C(18)	1.354(8)	C(18)-C(19)	1.375(7)
C(20)-C(21)	1.387(7)	C(20)-C(25)	1.373(7)
C(21)-C(22)	1.387(8)	C(22)-C(23)	1.372(9)
C(23)-C(24)	1.355(9)	C(24)-C(25)	1.379(7)
C(26)-C(27)	1.180(6)	C(27)-C(28)	1.470(7)
C(29)-C(30)	1.386(7)	C(29)-C(34)	1.385(7)
C(30)-C(31)	1.376(8)	C(31)-C(32)	1.362(9)
C(32)-C(33)	1.354(9)	C(33)-C(34)	1.383(8)
C(35)-C(36)	1.391(6)	C(35)-C(40)	1.379(6)
C(36)-C(37)	1.381(7)	C(37)-C(38)	1.365(7)
C(38)-C(39)	1.366(7)	C(39)-C(40)	1.379(7)
C(41)-C(42)	1.501(7)	C(42)-C(43)	1.388(7)
C(43)-C(44)	1.390(7)	C(44)-C(45)	1.510(7)

**Table A.16.2 (cont):** Interatomic distances (Å) and angles (°) involving non-hydrogen atoms of the molecular structure of *cis*-[[Ru(acac)<sub>2</sub>(Ph<sub>2</sub>PC≡CMe)<sub>2</sub>].0.5CH<sub>2</sub>Cl<sub>2</sub>.

C(46)-C(47)	1.515(7)	C(47)-C(48)	1.383(8)
C(48)-C(49)	1.402(8)	C(49)-C(50)	1.504(8)
C(54)-C(55)	1.365(8)	C(54)-C(59)	1.394(7)
C(55)-C(56)	1.395(8)	C(56)-C(57)	1.344(9)
C(57)-C(58)	1.35(1)	C(58)-C(59)	1.385(9)
C(60)-C(61)	1.377(8)	C(60)-C(65)	1.391(8)
C(61)-C(62)	1.390(8)	C(62)-C(32)	1.37(1)
C(63)-C(64)	1.35(1)	C(64)-C(65)	1.383(9)
C(66)-C(67)	1.177(6)	C(67)-C(68)	1.450(7)
C(69)-C(70)	1.388(7)	C(69)-C(74)	1.379(7)
C(70)-C(71)	1.381(7)	C(71)-C(72)	1.372(8)
C(72)-C(73)	1.362(8)	C(73)-C(74)	1.377(7)
C(75)-C(76)	1.374(7)	C(75)-C(80)	1.375(7)
C(76)-C(77)	1.390(8)	C(77)-C(78)	1.351(9)
C(78)-C(79)	1.351(8)	C(79)-C(80)	1.382(7)
C(511)-C(521)	1.18(2)	C(512)-C(522)	1.20(2)
C(521)-C(531)	1.53(2)	C(522)-C(532)	1.53(2)
P(1)-Ru(1)-P(2)	94.20(5)	P(1)-Ru(1)-O(1)	91.3(1)
P(1)-Ru(1)-O(2)	174.3(1)	P(1)-Ru(1)-O(3)	93.5(1)
P(1)-Ru(1)-O(4)	90.1(1)	P(2)-Ru(1)-O(1)	89.91(9)
P(2)-Ru(1)-O(2)	91.0(1)	P(2)-Ru(1)-O(3)	92.82(9)
P(2)-Ru(1)-O(4)	174.2(1)	O(1)-Ru(1)-O(2)	91.2(1)
O(1)-Ru(1)-O(3)	174.3(1)	O(1)-Ru(1)-O(4)	86.0(1)
O(2)-Ru(1)-O(3)	83.8(1)	O(2)-Ru(1)-O(4)	85.0(1)
O(3)-Ru(1)-O(4)	90.9(1)	P(3)-Ru(2)-P(4)	94.30(5)
P(3)-Ru(2)-O(5)	90.6(1)	P(3)-Ru(2)-O(6)	176.8(1)
P(3)-Ru(2)-O(7)	92.0(1)	P(3)-Ru(2)-O(8)	92.6(1)
P(4)-Ru(2)-O(5)	92.4(1)	P(4)-Ru(2)-O(6)	88.8(1)
P(4)-Ru(2)-O(7)	91.8(1)	P(4)-Ru(2)-O(8)	172.8(1)
O(5)-Ru(2)-O(6)	90.0(1)	O(5)-Ru(2)-O(7)	174.9(1)
O(5)-Ru(2)-O(8)	85.5(1)	O(6)-Ru(2)-O(7)	87.2(1)
O(6)-Ru(2)-O(8)	84.3(1)	O(7)-Ru(2)-O(8)	89.9(1)
Ru(1)-P(1)-C(11)	115.6(2)		
Ru(1)-P(1)-C(14)	116.5(2)	Ru(1)-P(1)-C(20)	118.0(2)
C(11)-P(1)-C(14)	100.9(2)	C(11)-P(1)-C(20)	102.3(2)
C(14)-P(1)-C(20)	100.8(2)	Ru(1)-P(2)-C(26)	115.4(2)
Ru(1)-P(2)-C(29)	114.4(2)	Ru(1)-P(2)-C(35)	121.0(2)



**Table A.16.2 (cont):** Interatomic distances (Å) and angles (°) involving non-hydrogen atoms of the molecular structure of *cis*-[Ru(acac)<sub>2</sub>(Ph<sub>2</sub>PC≡CMe)<sub>2</sub>]0.5CH<sub>2</sub>Cl<sub>2</sub>.

C(26)-P(2)-C(29)	108.2(2)	C(26)-P(2)-C(35)	102.3(2)
C(29)-P(2)-C(35)	100.0(2)	Ru(2)-P(3)-C(54)	115.5(2)
Ru(2)-P(3)-C(60)	118.7(2)	Ru(2)-P(3)-C(511)	116.6(4)
Ru(2)-P(3)-C(512)	115.4(5)	C(54)-P(3)-C(60)	100.6(2)
C(54)-P(3)-C(511)	93.5(6)	C(54)-P(3)-C(512)	108.1(6)
C(60)-P(3)-C(511)	108.1(6)	C(60)-P(3)-C(512)	95.9(6)
Ru(2)-P(4)-C(66)	115.8(2)		
Ru(2)-P(4)-C(69)	115.0(2)	Ru(2)-P(4)-C(75)	120.6(2)
C(66)-P(4)-C(69)	101.6(2)	C(66)-P(4)-C(75)	1007.(2)
C(69)-P(4)-C(75)	100.2(2)	Ru(1)-O(1)-C(2)	122.0(4)
Ru(1)-O(2)-C(4)	123.3(4)	Ru(1)-O(3)-C(7)	124.2(3)
Ru(1)-O(4)-C(9)	122.5(3)	Ru(2)-O(5)-C(42)	124.3(3)
Ru(2)-O(6)-C(44)	122.5(3)	Ru(2)-O(7)-C(47)	123.5(4)
Ru(2)-O(8)-C(49)	123.8(4)	O(1)-C(2)-C(1)	113.5(6)
O(1)-C(2)-C(3)	127.0(5)	C(1)-C(2)-C(3)	119.5(6)
C(2)-C(3)-C(4)	127.8(5)	O(2)-C(4)-C(3)	126.0(5)
O(2)-C(4)-C(5)	115.8(6)	C(3)-C(4)-C(5)	118.2(6)
O(3)-C(7)-C(6)	113.9(5)	O(3)-C(7)-C(8)	126.6(5)
C(6)-C(7)-C(8)	119.5(5)	C(7)-C(8)-C(9)	127.8(5)
O(4)-C(9)-C(8)	126.9(5)	O(4)-C(9)-C(10)	114.5(5)
C(8)-C(9)-C(10)	118.5(5)	P(1)-C(11)-C(12)	175.8(5)
C(11)-C(12)-C(13)	178.8(6)	P(1)-C(14)-C(15)	119.3(4)
P(1)-C(14)-C(19)	121.9(4)	C(15)-C(14)-C(19)	118.6(5)
C(14)-C(15)-C(16)	119.2(5)	C(15)-C(16)-C(17)	121.4(6)
C(16)-C(17)-C(18)	118.9(6)	C(17)-C(18)-C(19)	121.1(6)
C(14)-C(19)-C(18)	120.9(6)	P(1)-C(20)-C(21)	119.2(4)
P(1)-C(20)-C(25)	122.2(4)	C(21)-C(20)-C(25)	118.4(5)
C(20)-C(21)-C(22)	120.1(6)	C(21)-C(22)-C(23)	119.9(6)
C(22)-C(23)-C(24)	120.5(6)	C(23)-C(24)-C(25)	119.8(6)
C(20)-C(25)-C(24)	121.3(6)	P(2)-C(26)-C(27)	176.4(5)
C(26)-C(27)-C(28)	178.9(6)	P(2)-C(29)-C(30)	118.1(4)
P(2)-C(29)-C(34)	123.4(4)	C(30)-C(29)-C(34)	118.5(5)
C(29)-C(30)-C(31)	120.0(6)	C(30)-C(31)-C(32)	120.8(7)
C(31)-C(32)-C(33)	119.8(7)	C(32)-C(33)-C(34)	120.6(6)
C(29)-C(34)-C(33)	120.2(6)	P(2)-C(35)-C(36)	118.6(4)
P(2)-C(35)-C(40)	122.6(4)	C(36)-C(35)-C(40)	118.7(5)
C(35)-C(36)-C(37)	120.2(5)	C(36)-C(37)-C(38)	120.2(5)
C(37)-C(38)-C(39)	120.2(5)	C(38)-C(39)-C(40)	120.2(5)

**Table A.16.2 (cont):** Interatomic distances (Å) and angles (°) involving non-hydrogen atoms of the molecular structure of *cis*-[Ru(acac)<sub>2</sub>(Ph<sub>2</sub>PC≡CMe)<sub>2</sub>].0.5CH<sub>2</sub>Cl<sub>2</sub>.

C(35)-C(40)-C(39)	120.5(5)	O(5)-C(42)-C(41)	114.2(5)
O(5)-C(42)-C(43)	126.2(5)	C(41)-C(42)-C(43)	119.6(5)
C(42)-C(43)-C(44)	127.4(5)	O(6)-C(44)-C(43)	126.3(5)
O(6)-C(44)-C(45)	115.0(5)	C(43)-C(44)-C(45)	118.7(5)
O(7)-C(47)-C(46)	113.4(6)	O(7)-C(47)-C(48)	127.7(5)
C(46)-C(47)-C(48)	118.9(6)	C(47)-C(48)-C(49)	127.0(5)
O(8)-C(49)-C(48)	126.0(6)	O(8)-C(49)-C(50)	115.5(6)
C(48)-C(49)-C(50)	118.5(5)	P(3)-C(54)-C(55)	119.3(4)
P(3)-C(54)-C(59)	122.4(5)	C(55)-C(54)-C(59)	118.3(6)
C(54)-C(55)-C(56)	120.5(6)	C(55)-C(56)-C(57)	120.2(7)
C(56)-C(57)-C(58)	120.7(7)	C(57)-C(58)-C(59)	120.1(7)
C(54)-C(59)-C(58)	120.2(7)	P(3)-C(60)-C(61)	117.5(5)
P(3)-C(60)-C(65)	124.1(5)	C(61)-C(60)-C(65)	118.4(6)
C(60)-C(61)-C(62)	119.9(7)	C(61)-C(62)-C(63)	120.9(8)
C(62)-C(63)-C(64)	119.4(8)	C(63)-C(64)-C(65)	120.9(8)
C(60)-C(65)-C(64)	120.4(7)	P(4)-C(66)-C(67)	177.2(5)
C(66)-C(67)-C(68)	179.4(7)	P(4)-C(69)-C(70)	119.0(4)
P(4)-C(69)-C(74)	122.4(4)	C(70)-C(69)-C(74)	118.6(5)
C(69)-C(70)-C(71)	120.4(5)	C(70)-C(71)-C(72)	119.9(6)
C(71)-C(72)-C(73)	120.2(6)	C(72)-C(73)-C(74)	120.2(6)
C(69)-C(74)-C(73)	120.7(5)	P(4)-C(75)-C(76)	119.3(4)
P(4)-C(75)-C(80)	122.3(4)	C(76)-C(75)-C(80)	118.2(5)
C(75)-C(76)-C(77)	120.2(6)	C(76)-C(77)-C(78)	120.2(7)
C(77)-C(78)-C(79)	120.5(6)	C(78)-C(79)-C(80)	119.9(6)
C(75)-C(80)-C(79)	121.0(6)	Cl(1)-C(81)-Cl(2)	117.2(5)
P(3)-C(511)-C(521)	173(1)	P(3)-C(512)-C(522)	173(2)
C(511)-C(521)- C(531)	177(2)	C(512)-C(522)- C(532)	180(2)

**Table A.17.1:** Crystallographic and refinement data for *trans*- $[Ru(acac)_2(Ph_2PC\equiv CMe)_2][PF_6].2CH_2Cl_2$ .

<b>Crystal Data</b>	
Empirical Formula	$C_{42}H_{44}Cl_4F_6O_4P_3Ru$
Formula Weight	1062.60
Crystal Colour, Habit	green, rhomboid
Crystal Dimensions	0.08 × 0.07 × 0.07 mm
Crystal System	triclinic
Lattice Type	Primitive
Omega Scan Peak Width at Half-Height	0.29°
Lattice Parameters	$a = 9.7900(9) \text{ \AA}$ $b = 11.1192(8) \text{ \AA}$ $c = 11.1518(9) \text{ \AA}$ $\alpha = 104.946(6)^\circ$ $\beta = 93.248(7)^\circ$ $\gamma = 97.520(7)^\circ$ $V = 1157.6(2) \text{ \AA}^3$
Space Group	$P \bar{1} (\#2)$
Z value	1
$D_{calc}$	1.524 g/cm <sup>3</sup>
$F_{000}$	539.00
$\mu(\text{MoK}\alpha)$	64.07 cm <sup>-1</sup>
<b>Intensity Measurements</b>	
diffractometer	Rigaku AFC6R
Radiation	CuK $\alpha$ ( $\lambda = 1.54178 \text{ \AA}$ ) graphite monochromated
Take-off Angle	6.0°
Detector Aperture	7.0 mm horizontal 7.0 mm vertical
Crystal to Detector Distance	400 mm
Voltage, Current	180kV, 50mA
Temperature	-80.0 °C
Scan Type	$\omega$ -2 $\theta$
Scan Rate	32.0°/min (in $\omega$ ) (up to 4 scans)
Scan Width	(1.30 + 0.30 tan $\theta$ )
$2\theta_{max}$	120.1°
No. of Reflections Measured	Total: 3678 Unique: 3443 ( $R_{int} = 0.031$ )
Corrections	Lorentz-polarization Absorption (trans. factors: 0.5183 - 0.7.467) Decay (2.62% decline)

**Table A.17.1 (cont):** Crystallographic and refinement data for *trans*-[Ru(acac)<sub>2</sub>(Ph<sub>2</sub>PC≡CMe)<sub>2</sub>][PF<sub>6</sub>].2CH<sub>2</sub>Cl<sub>2</sub>.

Structure Solution and Refinement	
Structure Solution	Direct Methods (SIR92)
Refinement	Full-Matrix least squares
Function Minimized	$\sum w( F_o  -  F_c )^2$
Least Squares Weights	$w = [\sigma_c^2(F_o) + 0.25p^2F_o^2]^{-1}$
p-factor	0.020
Anomalous Dispersion	All non-hydrogen atoms
No. Observations (I>2.0σ(I))	2737
No. of variables	340
Reflection/Parameter Rotation	8.05
Residuals: R; Rw	0.036; 0.041
Goodness of Fit Indicator	1.36
Max Shift/Error in Final Cycle	0.09
Max peak in Final Diff. Map	0.55 e <sup>-</sup> /Å <sup>3</sup>
Min peak in Final Diff Map	-0.46 e <sup>-</sup> /Å <sup>3</sup>

**Table A.17.2:** Interatomic distances (Å) and angles (°) involving non-hydrogen atoms of the molecular structures of *trans*-[Ru(acac)<sub>2</sub>(Ph<sub>2</sub>PC≡CMe)<sub>2</sub>][PF<sub>6</sub>].2CH<sub>2</sub>Cl<sub>2</sub>.

Ru(1)-P(1)	2.393(1)	Ru(1)-O(1)	2.011(3)
Ru(1)-O(2)	2.003(3)	Cl(1)-C(21)	1.756(6)
Cl(2)-C(21)	1.760(6)	P(1)-C(6)	1.753(5)
P(1)-C(9)	1.826(4)	P(1)-C(15)	1.816(4)
P(2)-F(1)	1.595(3)	P(2)-F(2)	1.597(3)
P(2)-F(3)	1.597(3)	O(1)-C(2)	1.280(5)
O(2)-C(4)	1.281(5)	C(1)-C(2)	1.503(6)
C(2)-C(3)	1.394(6)	C(3)-C(4)	1.403(6)
C(4)-C(5)	1.490(6)	C(6)-C(7)	1.185(6)
C(7)-C(8)	1.451(7)	C(9)-C(10)	1.395(6)
C(9)-C(14)	1.388(6)	C(10)-C(11)	1.372(7)
C(11)-C(12)	1.378(8)	C(12)-C(13)	1.374(8)
C(13)-C(14)	1.381(7)	C(15)-C(16)	1.395(6)
C(15)-C(20)	1.400(6)	C(16)-C(17)	1.383(6)
C(17)-C(18)	1.369(7)	C(18)-C(19)	1.371(8)
C(19)-C(20)	1.376(7)		
P(1)-Ru(1)-P(1) <sup>a</sup>	180.0	P(1)-Ru(1)-O(1)	89.64(8)
P(1)-Ru(1)-O(1) <sup>a</sup>	90.36(8)	P(1)-Ru(1)-O(2)	88.88(9)
P(1)-Ru(1)-O(2) <sup>a</sup>	91.12(9)	O(1)-Ru(1)-O(1) <sup>a</sup>	180.0

**Table A.17.2 (cont):** Interatomic distances (Å) and angles (°) involving non-hydrogen atoms of the molecular structure of *trans*-[Ru(acac)<sub>2</sub>(Ph<sub>2</sub>PC≡CMe)<sub>2</sub>][PF<sub>6</sub>].2CH<sub>2</sub>Cl<sub>2</sub>.

O(1)-Ru(1)-O(2)	90.3(1)	O(1)-Ru(1)-O(2) <sup>a</sup>	89.7(1)
O(2)-Ru(1)-O(2) <sup>a</sup>	180.0	Ru(1)-P(1)-C(6)	114.6(2)
Ru(1)-P(1)-C(9)	113.1(1)	Ru(1)-P(1)-C(15)	113.8(1)
C(6)-P(1)-C(9)	103.2(2)	C(6)-P(1)-C(15)	104.7(2)
C(9)-P(1)-C(15)	106.4(2)	F(1)-P(2)-F(1) <sup>a</sup>	180.0
F(1)-P(2)-F(2)	89.4(2)	F(1)-P(2)-F(2) <sup>a</sup>	90.6(2)
F(1)-P(2)-F(3)	89.9(2)	F(1)-P(2)-F(3) <sup>a</sup>	90.1(2)
F(2)-P(2)-F(2) <sup>a</sup>	180.0	F(2)-P(2)-F(3)	89.5(2)
F(2)-P(2)-F(3) <sup>a</sup>	90.5(2)	F(3)-P(2)-F(3) <sup>a</sup>	180.0
Ru(1)-O(1)-C(2)	122.9(3)	Ru(1)-O(2)-C(4)	124.2(3)
O(1)-C(2)-C(1)	114.8(4)	O(1)-C(2)-C(3)	125.5(4)
C(1)-C(2)-C(3)	119.6(4)	C(2)-C(3)-C(4)	125.8(4)
O(2)-C(4)-C(3)	124.3(4)	O(2)-C(4)-C(5)	115.2(4)
C(3)-C(4)-C(5)	120.4(4)	P(1)-C(6)-C(7)	178.9(5)
C(6)-C(7)-C(8)	179.3(6)	P(1)-C(9)-C(10)	119.4(4)
P(1)-C(9)-C(14)	121.9(4)	C(10)-C(9)-C(14)	118.6(4)
C(9)-C(10)-C(11)	120.6(5)	C(10)-C(11)-C(12)	120.2(5)
C(11)-C(12)-C(13)	120.0(5)	C(12)-C(13)-C(14)	120.3(5)
C(9)-C(14)-C(13)	120.4(5)	P(1)-C(15)-C(16)	118.1(3)
P(1)-C(15)-C(20)	122.6(4)	C(16)-C(15)-C(20)	119.3(4)
C(15)-C(16)-C(17)	120.0(4)	C(16)-C(17)-C(18)	120.1(5)
C(17)-C(18)-C(19)	120.2(5)	C(18)-C(19)-C(20)	121.1(5)
C(15)-C(20)-C(19)	119.2(5)	Cl(1)-C(21)-Cl(2)	110.9(3)

a) Atom generated by the symmetry operation (1-x, 1-y, 1-z)